

Multilevel Optimisation of Laminated Composite Thin-walled Structures Using Isogeometric Analysis

SHUANG QU*

*SHANDONG JIANZHU UNIVERSITY

ABSTRACT

Due to the heterogeneity of CAD and CAE system, the general finite element analysis method cannot calculate the local mechanical response of the structure with high precision during the process of optimizing complex structures. The Isogeometric Analysis will be applied to the optimisation of complex structures, and the problem will be simplified by using multilevel approach. Based on the Isogeometric Analysis, the research will involve three major contents: the design model construction and mesh subdivision research, research of structure analysis method and development of the corresponding software, research of multilevel optimisation method and development of the corresponding software. The aim of this research is to apply the Isogeometric Analysis to the multilevel optimisation design, and to set up a multilevel optimisation design system for the laminated composite thin-walled structures. The achievements of the research will open up a new direction for the application of the Isogeometric Analysis in the field of structural optimisation, and at the same time, it will provide a new design method with high efficiency and high safety for the industrial design of thin-walled structures.

Low-Dimensional Reduced-Order Models for Statistical Response and Uncertainty Quantification in Turbulent Systems

Di Qi^{*}, Andrew Majda^{**}

^{*}Courant Institute, New York University, ^{**}Courant Institute, New York University

ABSTRACT

A low-dimensional reduced-order statistical closure model is developed for quantifying the uncertainty in statistical sensitivity and intermittency in principal model directions with largest variability in high-dimensional turbulent system. Imperfect model sensitivity is improved through a recent mathematical strategy for calibrating model errors in a training phase, where information theory and linear statistical response theory are combined in a systematic fashion to achieve the optimal model performance. The idea in the reduced-order method is from a self-consistent mathematical framework for general systems with quadratic nonlinearity, where crucial high-order statistics are approximated by a systematic model calibration procedure. Model efficiency is improved through additional damping and noise corrections to replace the expensive energy-conserving nonlinear interactions. Model errors due to the imperfect nonlinear approximation are corrected by tuning the model parameters using linear response theory with an information metric in a training phase before prediction. A statistical energy principle is adopted to introduce a global scaling factor in characterizing the higher-order moments in a consistent way to improve model sensitivity. Stringent models of barotropic and baroclinic turbulence are used to display the feasibility of the reduced-order methods. It is demonstrated that crucial principal statistical quantities in mean and variance in the most important large scales can be captured with accuracy and efficiency using the reduced-order model in various dynamical regimes of the flow field with distinct statistical structures.

A Computational Study on Colloidal Gold-Nanoparticle Interaction with Ultra-short Pulse Laser

Dong Qian^{*}, Mohammad Rezaul Karim^{**}, Xiuying Li^{***}, Jaona Randrianalisoa^{****}, Zhenpeng Qin^{*****}

^{*}University of Texas at Dallas, ^{**}University of Texas at Dallas, ^{***}University of Texas at Dallas, ^{****}University of Reims Champagne-Ardenne, ^{*****}University of Texas at Dallas

ABSTRACT

With the recent advances in laser-based manufacturing, there is a continuing interest in exploring the fundamental mechanisms of laser-material interaction to improve the performance of diverse engineering applications. The unique spatial and temporal profiles of lasers provide a wide range of capabilities for material processing and device fabrication. In this talk, we present a computational study on the responses of colloidal plasmonic vesicles subjected to ultra-short pulse laser. The plasmonic vesicle consists of multiple nanocrystals on a liposome surface or within a polymer coating and provides an important class of template for biomedical applications such as drug delivery, ultrasensitive bio-sensing and imaging. To capture the key mechanisms, a multiphysics computational framework that couples the electric field with molecular dynamics simulation has been established. The simulation demonstrates that the responses of the nanoparticles depend strongly on the laser intensity, the inter-particle distance and water-particle interaction. This study identifies key factors responsible for the observed nanoparticle transformation and the significant role of water in the inter-particle interactions. The presentation concludes with validation against the experiment and perspectives on applications.

Topology Optimization of Self-supporting Support Structures for Additive Manufacturing

Xiaoping Qian^{*}, Francesco Mezzadri^{**}, Vladimir Bouriakov^{***}

^{*}UW-Madison, ^{**}UW-Madison, ^{***}UW-Madison

ABSTRACT

In this research, we formulate the generation of support structures for additive manufacturing as a topology optimization problem. We have formulated the problem as a compliance minimization that presents analogies with compliance minimization of bridges and of roof supports, with, however, a difference in the setting of zero-displacement boundary conditions. This difference fosters a comparison with transmissible loads which, together with other mechanical considerations, helps explaining why the computed structures are generally self-supporting. Compared with usual geometric considerations based support structure design, this formulation affords mechanistic meaning to the computed support structures. We show the generality of the procedure by computing supports for a variety of parts in both two and three dimensions, including a complex model of the mascot of the University of Wisconsin-Madison. The resulting support structures have also been 3D printed, demonstrating that the computed designs can successfully be used as supports. Moreover, a comparison with supports generated by existing software shows that the computed structures indeed employ less material than other approaches currently used.

Study of Numerical Model for Stress Corrosion of Bioabsorbable Zinc Alloy Stent

Aike Qiao^{*}, Zihao Li^{**}, Xinyang Cui^{***}, Kun Peng^{****}

^{*}Beijing University of Technology, ^{**}Beijing University of Technology, ^{***}Beijing University of Technology,
^{****}Beijing University of Technology

ABSTRACT

Background The use of biodegradable stents for interventional treatment of coronary heart disease has become a hot research. Iron and magnesium and their alloys were considered as bioabsorbable stent materials during the last decade. However, zinc alloy exhibits a suitable degradation performance and become the hot research in bioabsorbable stent. The numerical model for stress corrosion of the zinc alloy is not clear at present. The present work aims to establish a elementary numerical model for stress corrosion of a new zinc alloy Zn-5Al-1Mg. Method First finite element method (FEM) was used to simulate the stent expansion in an idealized coronary stenosis model, and to obtain the max Mises stress. According to the formula: $\sigma = (1-D)\sigma_0$, $D = 0$, when the material is undamaged and $D = 1$ when it is completely damaged and loses its ability to sustain loads. Once D reaches a critical value D_{cr} , the element "fails", and then it is deleted. A uniaxial stress stretching of the model is a simple and convenient model for stress corrosion simulation of different biodegradable materials. Thus, a simple stress damage model of Zn-5Al-1Mg alloy is established according to the stress corrosion equation in the literature. The uniaxial stress stretching of the model is performed, and the stress of stretching is the max Mises stress of the FEM. A subroutine was developed in ABAQUS to mimic the stress corrosion process. Results Stress corrosion started when the equivalent stress reaches 50% of the yield stress. After the beginning of stress corrosion, it is obvious that the damage factor shows an increasing trend. The time unit of the model was 220. The increasing trend is becoming steeper and steeper. After reaching the set damage factor and the time unit was 247, it will not change and the element was deleted in the model. Conclusion This study presents a numerical modeling approach to describe the stress corrosion of Zn-5Al-1Mg through a phenomenological model. In the future work, the pulsation force will be added to the model according to the pulsation of the blood vessel, and the stress corrosion of the model can be observed. Then, the stress corrosion model can be applied to the stent expansion idealized stenosis vessel model to calculate the stress corrosion of the material of the stent in complex geometry and complex contact. Acknowledgement: Science and Technology of Beijing Municipal Education Commission and Beijing Natural Science Foundation (KZ201710005007).

Characterizing Elastic Turbulence in Channel Flows at Low Reynolds Number

Boyang Qin*, Paulo Arratia**

*University of Pennsylvania, **University of Pennsylvania

ABSTRACT

In this talk, the flow of a viscoelastic fluid is experimentally investigated using particle velocimetry methods in a microfluidic device. The device is a long and straight microchannel that is 100- μm wide and deep; the channel has a short 3-mm region that contains a linear array of cylinders (perturbation region) followed by a 3-cm long and straight region (parallel shear region). We find that, both in the wake of the cylinders and far downstream in the parallel shear region, the flow is excited over a broad range of frequencies and wavelengths. Dye injection experiments and pressure tap measurements show enhanced mixing and increased flow resistance in the parallel shear region. These key flow features are consistent with those characterizing elastic turbulence at low Re . In the wake of the cylinder, we find that the decay in velocity temporal and spatial spectra is approximately -2.7 and -3.0, respectively. However, the decay of the initial elastic turbulence around the cylinders is followed by a growth downstream in the straight region. The emergence of distinct flow characteristics both in time and space suggests a new type of elastic turbulence, markedly different from that near the curved cylinders.

Predicting Residual Stress and Deflection in an Eulerian Frame by Extended Finite Element Method

Xiaoliang Qin*

*Onfea Computing LLC

ABSTRACT

The moving laser heat in the metal additive manufacturing results in residual stresses and distortion, which can cause the crack, warpage, and delamination of the 3d printed part. Residual stress and distortion have been predicted using the Lagrangian formulation. A fully coupled thermal-mechanical transient simulation for an additive manufacturing process using a Lagrangian frame is computational costive. The moving heat problem can be treated as a quasi-steady state process in an Eulerian reference frame for some cases. In a quasi-steady state Eulerian analysis, the process can be solved within one time increment. Thus the computational cost and time spent on large time increment in a Lagrangian transient analysis can be saved. This paper is a continuation and extension of earlier work of Dr. Qin and Dr. Michaleris [1] [2]. In our previous work, the elasto-viscoplastic Eulerian formulation with four unknown fields (velocity, stress, deformation gradient and internal variable) is developed to predict residual stress and strain from the Eulerian frame. The formulation is shown to be able to accurately predict residual stress for Friction Stir Welding. However, this method cannot predict the deflection of the material, it is because the velocity is used as the primary unknown in the Eulerian reference frame. In this work, an additional unknown field is introduced to denote the signed distance from the free surface of the deformed material. Level set evolution equation is used to track the material surface deformation. Extended Finite Element Method (XFEM) is implemented to integrate the elements which are split by the signed distance function in the Eulerian frame. The Newton-Raphson method is used to solve this five fields formulation implicitly. The formulation is implemented in an in-house code. Two numerical examples are implemented to verify the accuracy of the direct equilibrium Eulerian formulation. Reference [1] Xiaoliang Qin and P. Michaleris. Thermo-Elasto-Visco-Plastic Modeling of Friction Stir Welding. *Science and Technology in Welding*, 14(7): 640-649, 2009. [2] Xiaoliang Qin and P. Michaleris. Eulerian Elasto-Visco-Plastic Formulations for Residual Stress Prediction. *International Journal for Numerical Methods in Engineering*, 77(5): 634-663, 2009.

Computation on Effective Elastic Properties of Flexible Chiral Honeycomb Cores

Kepeng Qiu^{*}, Zhi Wang^{**}

^{*}Northwestern Polytechnical University, ^{**}Northwestern Polytechnical University

ABSTRACT

Cellular materials are widely applied in various fields due to their high stiffness-to-weight ratio and designable features [1], particularly for lightweight aircraft structures. And cellular materials are known to have properties: structures and mechanisms [2]. Therefore, one may design structures with cellular materials while controlling stiffness and flexibility [3]. The application of flexible honeycomb materials to morphing aircraft, the development of which has become a subject of great interest in recent years, is of particular relevance, due to their low density and low in-plane and high out-of-plane stiffness. Flexible chiral honeycomb cores generally exhibit nonlinear elastic properties due to the large geometric deformation. To rapidly and efficiently analyze the mechanical properties of chiral honeycomb sandwich structures, it is standard to replace the actual core structure in analyses with a homogenized core material presenting reasonably equivalent elastic properties. As such, a convenient and efficient method is required to evaluate the equivalent elastic properties of flexible chiral honeycomb cores. Here we develop analytical expressions based on a deformable cantilever beam under the large deformation. Firstly, the Euler-Bernoulli beam theory and micropolar theory are used to calculate the effective elastic modulus under the small deformation. The aim is to analyze the deflection characteristic of chiral honeycombs during the effective calculation. On that basis, the equivalence expressions are improved by including the stretching deformations of the chiral honeycomb structure on an infinitesimal section of a unit cell. Finite element analysis is subsequently performed for two examples of flexible chiral honeycomb cores. Equivalent results indicate that the analytical expressions under consideration of the geometric nonlinearity are more suitable to flexible chiral honeycomb cores under conditions of high strain and low elastic modulus. **ACKNOWLEDGMENTS** This work is supported by the National Natural Science Foundation of China (11772258). **REFERENCES** [1] L.J. Gibson, M.F. Ashby, Cellular Solids: Structure and Properties, 2nd ed., Cambridge University Press, Cambridge, 1997. [2] H. Heo, J. Ju, D.M. Kim. Compliant cellular structures: Application to a passive morphing airfoil. *Composite Structures*, 2013, 106: 560-569. [3] I. K. Kuder, A.F. Arrieta, W.E. Raither, P. Ermanni. Variable stiffness material and structural concepts for morphing applications. *Progress in Aerospace Sciences*, 2013 63: 33-55.

Modeling Rolling Contact Problems in Mining Industry

Xiangjun Qiu*

*Metso Minerals

ABSTRACT

Rolling contact is a phenomenon, which exists in industries in various form, such as tire to road contact rolling, idler to conveyor indentation rolling, metal sheet to mill plastic rolling, ore to ore or ore to steel ball comminution rolling in various mills and etc.. Accurate modeling of the rolling contact problems, such as rolling resistance, contact stresses, standing waves and comminution, in industrial applications is of significant scientific and economic value. This presentation focus on the modeling of rolling mechanisms in two types of industrial contact rolling problems: viscoelastic contact rolling and comminution contact rolling. The viscoelastic rolling contact problem is characterized as a thin layer of rubber material involved in contact rolling process, in which rolling resistance and standing wave are of primary concerns. The comminution rolling contact problem is characterized as geomaterial (ore) breakage in a rolling contact cycle, in which particle breakage efficiency is of primary concern. It is demonstrated that both types of rolling contact problems can be accurately modeled, the rolling processes can be numerically simulated, and the modeling tools have been successfully integrated into engineering design and/or optimization process. In the presentation, several examples are given to show the modeling based design and optimization process in mining industry.

Puncture Mechanics of Soft Membranes with Large Deformation

Shaoxing Qu^{*}, Junjie Liu^{**}

^{*}Zhejiang University, China, ^{**}Zhejiang University, China

ABSTRACT

Soft elastic membrane structures are widely used in biological and engineering application, owing to their ability of spanning relatively large areas despite low weight. Usually, large local deformation can be induced by indentation of rigid solids on the soft elastic membranes. The indentation of the soft elastic membrane structure is followed by puncture when continuously indented by a rigid solid, which is one of the primary failure modes for membrane structures. However, the puncture of soft elastic membrane is not so well understood compared with the indentation of elastic membranes such as metallic thin films. The main challenges in puncture are the difficulties to obtain the large local deformation around the rigid indenter and to set up the failure criteria for puncture. We study the puncture of silicone rubber membrane by rigid cylindrical indenters both experimentally and theoretically, focusing on the effects of indenter size, prestretch of the membrane, and contact friction between the soft elastic membrane and the rigid indenter. In the experiment, cylindrical steel indenters with various radius are adopted to puncture the prestretched silicone rubber membranes. Puncturing force-displacement relationship, as well as the deformation configurations, of the silicone rubber membrane are obtained. It is also observed that the membrane is punctured along the corner of the cylindrical indenter and a circular hole is left at the center of the membrane. The analytical model based on continuum mechanics is developed to predict the puncture behavior of the membrane observed in experiment. Gent model is used to describe the elasticity and the stiffening effect of the silicone rubber material. The deformed membrane of three distinct regions is considered as an out-of-plane axisymmetric configuration. There is no contact between membrane and the indenter in region I, while the membrane contacts with the indenter along its side surface in region II. In region III, the membrane contacts with the indenter along its fact tip surface. We adopt the Coulomb friction law to descript the contact friction behavior between the membrane and the indenter. The governing equations and boundary conditions for each region are developed for the membrane. Analytical results show that the punctured membrane fails accompanied with large deformation near the indenter tip. The first invariant of the right Cauchy-Green deformation tensor is adopted to characterize the rupture of the membrane. Once it reaches a critical value, the membrane is punctured. In this study, the analytical results agree well with the experimental observations.

IFMM-Preconditioning for 2D Stokes Flow in Porous Media

Bryan Quaife^{*}, Pieter Coulier^{**}, Eric Darve^{***}

^{*}Florida State University, ^{**}Velo3D, ^{***}Stanford University

ABSTRACT

We consider a boundary integral equation (BIE) formulation of the two-dimensional Stokes equations in a porous geometry. While BIEs are well-suited for resolving the complex geometry, they lead to a dense linear system of equations that is computationally expensive to solve. A fast multipole accelerated iterative method is possible, but for complex geometries, many iterations are required. Therefore, we apply the inverse fast multipole method (IFMM), which is based on the framework of H^2 matrices, to precondition the linear system. We examine the effect of the preconditioners tolerance and compare its efficacy with a block-diagonal preconditioner on several geometries.

A Partitioned and a Monolithic Approach to Fluid-Composite Structure Interaction

Annalisa Quaini^{*}, Davide Forti^{**}, Martina Bukac^{***}, Suncica Canic^{****}, Simone Deparis^{*****}

^{*}University of Houston, ^{**}Ecole Polytechnique Federale de Lausanne, ^{***}University of Notre Dame, ^{****}University of Houston, ^{*****}Ecole Polytechnique Federale de Lausanne

ABSTRACT

We study a nonlinear fluid-structure interaction (FSI) problem between an incompressible, viscous fluid and a composite elastic structure consisting of two layers: a thin layer (membrane) in direct contact with the fluid, and a thick layer (linearly elastic structure) sitting on top of the thin layer. The coupling between the fluid and structure, and the coupling between the two structures is achieved via the kinematic and dynamic coupling conditions modeling no-slip and balance of forces, respectively. The coupling is evaluated at the moving fluid-structure interface with mass, i.e., the thin structure. To solve this nonlinear moving-boundary problem in 2D a partitioned approach based on Lie&amp;apos;s operator splitting was developed, while a monolithic method was used for 3D problems. Both methods are combined with an Arbitrary Lagrangian-Eulerian (ALE) approach to deal with the motion of the fluid domain. This class of problems and its generalizations are important in e.g., modeling FSI between blood flow and arterial walls, which are known to be composed of several different layers, each with different mechanical characteristics and thickness. By using this model we show how multi-layered structure of arterial walls influences the pressure wave propagation in arterial walls, and how the presence of atheroma and the presence of a vascular device called a stent, influence intramural strain distribution throughout different layers of the arterial wall.

A PGD-based Numerical Microscope for Evaluating Processing-induced Defects on Composites Structural Performances: Towards a Macroscopic Data-based Hybrid Modeling

Giacomo Quaranta^{*}, Emmanuelle Abisset-Chavanne^{**}, Anaïs Barasinski^{***}, Jean Louis Duval^{****}, Francisco Chinesta^{*****}

^{*}ESI Group Chair at Ecole Centrale de Nantes, ^{**}ESI Group Chair at Ecole Centrale de Nantes, ^{***}Ecole Centrale de Nantes, ^{****}ESI Group, ^{*****}ESI Group Chair at ENSAM ParisTech

ABSTRACT

Composites structures exhibit deviations from nominal conditions considered for determining structural performances. These deviations come from both, the intermediate material (e.g. pre-impregnated tapes or plies) and the final part processing. Thus, pre-impregnated plies sometimes exhibit fluctuations in the reinforcement distribution, irregularities at the surface level, where a non-negligible roughness on the fiber and matrix distribution is observed, as well as impregnation defects that results in micro-cavities with different shapes and sizes located inside the ply. When processing these pre-impregnated plies or tapes, the process exacerbates some of the existing defects, creating inter-ply polymer layers (where the concentration of fibers is almost negligible) with its own roughness, micro-cavities at the ply interfaces, or gaps between contiguous tapes originated during their placement or even discontinuities originated when during the placement tapes break and process re-starts. High fidelity calculations can be performed at the ply and defect level thanks to the use of the space separated representation characteristic of PGD-based solvers, constituting a sort of numerical microscope that zooms defect effects, in order to evaluate the parametric effect of each defect in both static and dynamic loadings, and their associated mechanical performances. Finally, if macroscopic models coming from nominal designs exhibit too large deviations with respect to the ones incorporating defects and deviations existing in real parts, and because creating enriched models that include details at the fine scale is too difficult, data-based models assimilating static and dynamical mechanical responses could be included and added to the nominal model to better describe the real part and consequently guarantee model predictability, without renouncing to a fully-macroscopic description. References 1) B. Bognet, A. Leygue, F. Chinesta, A. Poitou, F. Bordeu. "Advanced simulation of models defined in plate geometries: 3D solutions with 2D computational complexity". *Computer Methods in Applied Mechanics and Engineering*, 201, 1-12, 2012. 2) F. Chinesta, A. Leygue, F. Bordeu, J.V. Aguado, E. Cueto, D. Gonzalez, I. Alfaro, A. Ammar, A. Huerta. "Parametric PGD based computational vademecum for efficient design, optimization and control". *Archives of Computational Methods in Engineering*, 20/1, 31-59, 2013.

Application of a Strain-based Formulation of PDS-FEM for the Simulation of Dynamic Crack Propagation

Lionel Quaranta^{*}, Lalith Wijerathne^{**}, Tomoo Okinaka^{***}, Muneo Hori^{****}

^{*}University of Tokyo, ^{**}Earthquake Research Institute, Tokyo, ^{***}Kindai University, ^{****}Earthquake Research Institute, Tokyo

ABSTRACT

We present an application of a strain-momentum based Hamiltonian to dynamic crack propagation, using PDS-FEM [1] as the numerical method. While Lagrangian based formulations are widely used in continuum mechanics, the existing applications of Hamiltonian in continuum mechanics are based on the displacement and momentum variables. In this work, we consider a strain-momentum based Hamiltonian. Our objective is to compare the traditional displacement-momentum form with the strain-momentum form regarding numerical accuracy and computational cost. By developing a strain-based formulation of the dynamic Hamiltonian system in the PDS-FEM frame, and using adapted symplectic time integration, we derive a numerical method which reproduces accurately the dynamic crack propagation with a relatively low computational effort. Symplectic time integrators have the advantage of ensuring the symplectic character of the flow of local variables, and variational integrators ensure in particular the conservation of total momentum throughout the computation, and the average conservation of the total energy. This participates to an improved accuracy and stability for long-time integration. PDS-FEM is used as the numerical technique due to its simple and numerically efficient crack treatment. The PDS-FEM implementation is verified by comparing with analytical solutions, and validated by comparing with dynamic mode-I crack propagation and resulting photoelastic fringe patterns captured with a 1Mfps camera. Our preliminary results show that this method is successful in reproducing the crack patterns observed experimentally for standard 2D and 3D problems, especially for mode I cracks, as well as the variation of the stress distribution around the crack tip during the propagation. A further objective will be to extend this approach to simulate the generation of crack under high strain rates, in particular shockwave induced rupture, and use it to design an accurate damage prediction method for full-scale civil infrastructures after extreme events such as hypothetical near field super-shear earthquakes. Keywords: dynamic crack propagation, Hamiltonian, symplectic algorithms, PDS-FEM, photoelasticity [1] Hori, M., Oguni, K., Sakaguchi, H., (2005) Proposal of FEM implemented with particle discretization scheme for analysis of failure phenomena, J. of Mech. and Phys. of Solids, 53 681–703.

Numerical Experiments on the Convergence Properties of State-based Peridynamic Laws and Influence Functions in Two-Dimensional Problems

Alejandro Queiruga*, George Moridis**

*Lawrence Berkeley National Lab, **Lawrence Berkeley National Lab

ABSTRACT

Peridynamics is widely used as the theoretical basis for numerical studies of fracture evolution, propagation, and behavior. While the theory has been shown to converge to continuum mechanics in the theoretical limit, its behavior as a discrete numerical approximation with respect to classic problems has been largely neglected in the literature. We present the results published in Queiruga and Moridis, 2017 in which standard analytical solutions were used to thoroughly test the numerical accuracy and rate of convergence of the spatial discretization obtained by peridynamics. We analyze the accuracy and rate of convergence of three different peridynamic constitutive responses: of these, two involve a state-based dilation, and the third is based on the estimation of the deformation gradient. The peridynamic influence function is also varied in each of the constitutive responses. The methods are tested using classical results from mechanics for uniaxial compression, isotropic compression, and simple shear, as well as Westergaard's solution for a pressurized thin crack. The two dilation-based peridynamic constitutive responses are found to only converge to one of the constant-strain solutions, while the deformation gradient-based law converges in all cases with certain influence functions. We show that a cubic influence function is the best choice of those considered in all methods. Only the deformation gradient-based model converges to the classic solutions for all three linear deformation problems, but is less accurate than the dilation-based models for the thin crack problem because of instabilities.

Phase Conservative, Monolithic Level-Set Method for Multiphase Flow

Manuel Quezada de Luna*, Dmitri Kuzmin**, Christopher Kees***

*Us Army ERDC-CHL, **TU Dortmund, ***US Army ERDC-CHL

ABSTRACT

In fluid mechanics the interaction of fluids with distinguishable material properties (e.g. water and air) is referred as multiphase flow. This problem is important due to its wide range of applications. In this work we consider two-phase incompressible flow and concentrate on the representation and time evolution of the interface. There is an extensive list of methods to treat material interfaces. Popular choices include the volume of fluid and level set techniques. We propose a novel level-set like methodology for multiphase flow that preserves the initial mass of each phase. The model combines ideas from the volume of fluid and level set methods by solving a non-linear conservation law for a regularized Heaviside of the (distance function) level-set. This guarantees conservation of the volume enclosed by the zero level-set. The equation is regularized by a consistent term that assures a non-singular Jacobian. In addition, the regularization term penalizes deviations from the distance function. The result is a nonlinear monolithic model for a phase conservative level-set where the level-set is given by the distance function. The continuous model is monolithic; meaning that only one equation is needed, doesn't require any post-processing like: numerical stabilization, re-distancing, artificial compression, flux limiting and others, all of which are commonly used in either level-set or volume of fluid methods. In addition, we have only one parameter that controls the strength of regularization/penalization in the model. We start the presentation reviewing the main ingredients of this model: 1) a conservative level-set method by [1], which combines a distanced, non-conservative level-set method with the volume of fluid method via a non-linear correction and 2) elliptic re-distancing by [2]. Afterwards, we manipulate the conservative level-set method by [1] to motivate our formulation. We present a first model which we then modify to resolve some difficulties. Finally, we present a full discretization given by continuous Galerkin Finite Elements in space and a high-order Implicit-Explicit time integration. We demonstrate the behavior of this model by solving different benchmark problems in the literature of level-set methods. Then, we present results of this model coupled with a Navier-Stokes solver to simulate water-air interaction problems in two and three dimensions. [1] C.E. Kees, I. Akkerman, M.W. Farthing, and Y. Bazilevs. A conservative level set method suitable for variable-order approximations and unstructured meshes. *Journal of Computational Physics*. [2] C. Basting and D. Kuzmin. A minimization-based finite element formulation for interface-preserving level set reinitialization. *Computing*.

Approximation of the Weakly Symmetric Elasticity Problem on Quadrilaterals

Thiago Quinelato^{*}, Abimael Loula^{**}, Maicon Correa^{***}, Todd Arbogast^{****}

^{*}LabMeC - University of Campinas, ^{**}National Laboratory for Scientific Computing, ^{***}University of Campinas,
^{****}The University of Texas at Austin

ABSTRACT

A family of stable finite element spaces for the mixed $H(\text{div})$ -conforming formulation for elasticity is introduced. These spaces are shown to be suitable for quadrilateral meshes and are based on the satisfaction in the variational sense of the symmetry condition on the stress tensor. The main contribution is that the convergence order for the stress field in the $H(\text{div})$ -norm is the same as the one for displacements in the L_2 -norm, even on non-affine quadrilateral elements. The approximation strategy is based on the combination of ABF spaces (Arnold, Boffi, and Falk, 2005) with polynomials on quadrilateral meshes, resulting in a formulation that is locking-free under both compressible and incompressible regimes. Numerical experiments are used to confirm the analysis and to illustrate the stability of the approximation. References: D. N. Arnold, D. Boffi, and R. S. Falk. Quadrilateral $H(\text{div})$ finite elements. SIAM J. Numer. Anal., 42(6):2429-2451, 2005.

Automatic Constructions of Patient-specific Finite Element Models, Study of the Load Bypass Induced by TKR Implant Placement

Jean-Baptiste RENAULT*, Sébastien PARRATTE**, Patrick CHABRAND***

*1. Aix-Marseille University, France; 2. APHM, Institute for Locomotion, France, **1. Aix-Marseille University, France; 2. APHM, Institute for Locomotion, France, ***1. Aix-Marseille University, France; 2. APHM, Institute for Locomotion, France

ABSTRACT

Introduction Historically, total knee replacement (TKR) has been performed by placing the implants in a 90° position relative to the “mechanical” axis but this concept has been recently challenged [1]. TKR failure has several non-exclusive modalities, aseptic loosening could be initiated by stress shielding. Tibial implants generally have a stem, but they might cause load bypass [2]. In this study, we investigate if the stem position relative to the tibial cortical shell could explain the load bypass better than the implant frontal orientation. Materials and Methods 15 Varus-aligned tibias were segmented from QCT (MIMICS®). An in-house MATLAB® algorithm automatically selected and placed the implants in 7 different angular configurations. The 105 automatically created finite elements models comprised of the tibia, the implant and a 1.5mm thick cement layer, materials were assumed linear elastic isotropic. Bone elasticity modulus was mapped from QCT and parts meshed with quadratic tetrahedron. The distal tibia was fully constrained and several load cases, representative of daily activities, were applied on the implant. Surface interactions between parts were modeled as cohesive. The centrality of the stem was defined as the ratio of the minimal over average distance between the stem tip and tibia surfaces, and the load bypass by the percentage of axial force transiting by the stem tip. Results Centrality explains most of the load bypass variance ($R^2 = 0.54$, $p < 0.001$), while the linear relation between the Valgus angle and the load bypass was low ($R^2 = 0.002$, NS). The load transiting through the stem tip ranged from 10 to 27% of the total axial load applied to the implant. General and intra-subject linear regressions agreed: increasing centrality resulting in lower load bypass in both case. Discussion Those results can be explained by an increase in rigidity caused by a structural effect, the closer to the cortical shell the stiffer, and a trabecular bone heterogeneity effect, its stiffness increases as getting closer to the cortical shell. Conclusion Our preliminary results suggest that stem centrality is a good predictor of stem tip loading. Those results could partly explain the discrepancies between post-op alignment and functional outcome, and give a potential cause for the pain associated with malrotation of the tibial implant [3]. References [1] Parratte et al., JBJS Am. 92:2143-9, 2010. [2] Au et al., J Biomech. 40:1410-6, 2007 [3] Nicoll et al., JBJS Br. 92-B:1238-44, 2010.

A Gaussian Surrogate Model for Complex Manufacturing Processes

Jean-Christophe ROUX*, Rémi LACROIX**, Vincent ROBIN***, Eric FEULVARCH****

*Univ Lyon, ENISE, LTDS, UMR 5513 CNRS, **ESI Group, ***Electricité de France R&D, ****Univ Lyon, ENISE, LTDS, UMR 5513 CNRS

ABSTRACT

A surrogate model is developed for the mechanical analysis of complex manufacturing processes, involving non-linear, strongly coupled and time-consuming models. The objective is to build a simple and fast model for calculating mechanical quantities (e.g. residual stresses) as a function of the dimensions, material properties, process parameters and so on. This model is based on numerical experiments which are made of costly multi-physical finite element simulations and it is built by means of a full factorial design of experiments technique. The main interest of this model is that: - it is entirely numerical, - it has the ability to calculate results for the mechanical analysis in a multi-physical context, - it is based on Gaussian processes [1] used as a regression technique in non-linear structural mechanics. This Gaussian surrogate model is first applied to the computation of residual stresses induced by orbital multi-pass TIG welding of metal pipes [2]. The analysis of variance (ANOVA) is used to attest the great influence of the input parameters and the classical polynomial approach and the Gaussian process are compared for calculating the residual hoop stresses. Experience shows that the Gaussian process can be very successful for non-linear multiphysical welding applications. Then Gaussian processes are used as a surrogate model in fractures mechanics to predict the structure behavior according to the inputs parameters. Since Gaussian processes and their results quality are fully specified by the use of parametrized covariance functions, a discussion is held on the choice and construction of such functions, as well as on the values of their hyperparameters and approaches for these parameters estimations. References [1] C.E. Rasmussen, C.K.I. Williams. Gaussian processes for machine learning. MIT Press, 2006. [2] L. Portelette, J.-C. Roux, V. Robin, E. Feulvarch, A Gaussian surrogate model for residual stresses induced by orbital multi-pass TIG welding, Computers & Structures, Vol. 183, 27-37, 2017 <https://doi.org/10.1016/j.compstruc.2017.01.009>.

Micromechanical Modeling of the Fracture of Nacre-like Alumina Using a Discrete Approach

Kaoutar Radi^{*}, David Jauffres^{**}, Christophe L Martin^{***}

^{*}Univ. Grenoble Alpes, CNRS, Institute of Engineering Univ. Grenoble Alpes, SIMaP, F-38000 Grenoble, France,

^{**}Univ. Grenoble Alpes, CNRS, Institute of Engineering Univ. Grenoble Alpes, SIMaP, F-38000 Grenoble, France,

^{***}Univ. Grenoble Alpes, CNRS, Institute of Engineering Univ. Grenoble Alpes, SIMaP, F-38000 Grenoble, France

ABSTRACT

Ceramics exhibit an unmatched combination of high stiffness and strength, which makes them a suitable choice for high stress and/or high temperature applications. However, their brittleness limits their use for a wide range of applications. Interestingly, several damage-resistant materials that include ceramics are used for structural purposes in nature. Nacre is the perfect example of nature's design of damage-resistant materials. Due to its complex hierarchical "brick and mortar" structure, nacre can achieve high strength and toughness simultaneously. In this context, a new bio-inspired material, nacre-like alumina, was designed from brittle constituents arranged as brick and mortar (Bouville 2014). The intrinsic and extrinsic toughening mechanisms in this material are still poorly understood. A better insight on the reinforcement mechanisms and on the microstructure/properties relationships together with microstructural optimization are paramount for this new class of materials. Using Discrete Element Modeling (DEM) which is a very suitable method to model cracks and topological modifications in materials made from brittle components (Jauffres 2012), we have developed a pseudo-3D numerical model to study the influence of the microstructural key parameters (the aspect ratio of bricks, the thickness of the mortar and their relative strength and stiffness) on fracture and crack propagation of nacre-like alumina. We account for both intrinsic and extrinsic reinforcement mechanisms, which improves on previous models (elastic/elasto-plastic) that only consider intrinsic reinforcement. Compared to previous numerical models, the increase of fracture resistance as the crack propagates due to crack bridging is studied. The model is calibrated on both elasticity and fracture for the bricks and the mortar, which are modeled by a packing of spherical discrete particles. The model is validated against the analytical model of Barthelat (Barthelat 2014) on a 2D periodic unit cell of an idealized brick and mortar geometry. Depending on the overlap region, the bricks volume fraction and the strength of the mortar, we are able to retrieve two failure modes, mortar failure and bricks failure. We determine the parameters that prevent bricks failure and control the failure mode. Building on this validated model, an example of a realistic microstructure encompassing a few hundred platelets is created to investigate crack propagation, extrinsic reinforcement mechanisms such as crack bridging and to show the rising R-curve. Bouville, & al, (2014), Nature Materials. Barthelat, (2014), Journal of the Mechanics and Physics of Solids. Jauffres & al, (2012), Acta Materialia.

Advances in the Application of Discontinuous Galerkin Methods to Material and Structural Failure

Raul Radovitzky^{*}, Brandon Talamini^{**}, Bianca Giovanardi^{***}, Anwar Koshakji^{****}

^{*}MIT, ^{**}MIT, ^{***}MIT, ^{****}MIT

ABSTRACT

In this talk, I will discuss progress in the application of discontinuous Galerkin methods to material and structural failure. Topics will include: large-scale simulation of shell structures, challenges and approaches in describing quasi-static crack propagation, and the development of a scalable algorithm to describe hydraulic fracture in three dimensions.

Multiscale Modeling of Carbon Fiber/Carbon Nanotube/Epoxy Hybrid Composites: Comparison of Epoxy Matrices

Matthew Radue^{*}, Gregory Odegard^{**}

^{*}Michigan Technological University, Houghton, MI 49931, USA, ^{**}Michigan Technological University, Houghton, MI 49931, USA

ABSTRACT

The growing usage of carbon fiber (CF) composites attests to the demand of stiff-yet-lightweight materials. However, these composites presently demonstrate some weaknesses that limit their applicability: low compressive strength, susceptibility to delamination upon impact, and low thermal conductivity. It is conjectured that the inclusion of nanoparticles in the matrix may address these issues collectively. The noteworthy mechanical and thermal properties of carbon nanotubes (CNTs) make these nanoparticles attractive candidates for enhancing the deficiencies of traditional CF composites. Some studies have sought to understand what matrix characteristics promote good CNT-matrix interaction, showing that CNTs have a greater reinforcing effect on more ductile epoxies compared to stiff epoxies. Despite the important knowledge that has been gained, it is still unclear how the functionality of the epoxy (i.e., di-functional, tri-functional, tetra-functional) influences the CNT-matrix interaction and the overall elastic properties of CF/CNT/epoxy hybrid composites. The objective of this study is to employ Molecular Dynamics (MD) to compare the interfacial and mechanical response of three different crosslinked epoxy systems on the molecular level. A micromechanics approach is then utilized to predict the effective properties of realistic CNT/epoxy nanocomposites and CF/CNT/epoxy hybrid composites. At each step, the dissimilarities due to the three matrices are identified. The MD results demonstrate that the strength of the CNT-epoxy interaction correlates with the epoxy's ability to conform to the CNT and closely pack around it. Analysis of the interface and interphase region revealed that the tetra-functional epoxy did not adhere well to CNT (as compared to the other epoxies), which was detrimental to the stiffness of the MD model. However, the tri-functional resin paired with CNT outperforms the other models with respect to stiffness. The multiscale model was used to determine whether the excellent properties of the CNT/tri-functional resin MD model ultimately translate into a superior nanocomposite at the bulk level. The results indicate the tri-functional epoxy does indeed deliver the highest modulus nanocomposite and CF/CNT/epoxy hybrid composites for high CNT loadings. However, for CNT concentrations up to 5 wt%, the tri- and tetra-functional epoxies are expected to result in composites with comparable stiffness. For CNT composites with even higher concentrations, the tri-functional epoxy is more promising because of the combination of good bulk stiffness and strong interaction with CNT.

Analysis of Reliability of Levees against Slope Instability Using FLAC3D and an Adaptive Kriging-Based Monte Carlo Simulation Method

Mehrzad Rahimi^{*}, Zeyu Wang^{**}, Abdollah Shafieezadeh^{***}, Dylan Wood^{****}, Ethan J. Kubatko^{*****}

^{*}The Ohio State University, ^{**}The Ohio State University, ^{***}The Ohio State University, ^{****}The Ohio State University, ^{*****}The Ohio State University

ABSTRACT

Over 100,000 miles of levees in the United States protect communities from storm surge. Analysis of reliability of these systems against surge hazard is critical to determine the likelihood of failures and develop cost-effective risk mitigation solutions. Instability along with external erosion, internal erosion, and hydraulic failure are considered as primary failure processes of levees. Levee instability, in particular, occurs when the sum of destabilizing forces exceeds the resistance to failure on a failure surface. This type of failure can manifest in the form of shallow or deep sliding along the shear surface within the embankment in the waterside or landside of levees. Many former investigations used factor of safety evaluated through strength reduction method as the limit state function to evaluate the reliability of levees. In this approach, material strengths of levees are continually reduced by strength reduction factors until failure is reached. A primary shortcoming of this approach is that the same strength reduction factor is applied to all soil properties that affect the shear strength of soil in order to bring the slope to the state of instability [1]. Moreover, the factor of safety determined using this approach does not necessarily correspond to a shear surface that can lead to collapse of the slope and hence levee breach. To address these limitations in this study, limiting equilibrium states of the model are identified as an assembly of grid points in critical zones of levee embankments with rate of displacement increase higher than a critical threshold. Numerical analyses of levees to determine the rate of increase in displacement of various points in embankments are conducted in finite difference platform of FLAC3D. A new reliability analysis technique called REAK is used here to analyze the probability of failure of levees with respect to embankment instability. REAK employs Kriging surrogate modeling for adaptive and strategic sampling of random variables to generate most effective training points for model refinement. This feature significantly reduces the high computational demand for failure probability analyses of systems with complex numerical models. Results indicate the high efficiency of the proposed procedure for reliability analysis of levees and potentially for other geotechnical structures. 1. Li, D. Q., Xiao, T., Cao, Z. J., Phoon, K. K., &&&& Zhou, C. B. (2016). Efficient and consistent reliability analysis of soil slope stability using both limit equilibrium analysis and finite element analysis. Applied Mathematical Modelling, 40(9), 5216-5229.

Parallel, Contact-aware Simulations of Concentrated Stokesian Suspensions in 3D

Abtin Rahimian^{*}, Libin Lu^{**}, Denis Zorin^{***}

^{*}University of Colorado Boulder, ^{**}New York University, ^{***}New York University

ABSTRACT

We present an efficient, accurate, robust, and parallel-scalable method for simulation of dense suspensions of deformable and rigid particles immersed in Stokesian fluid in three dimensions. We use a well-established boundary integral formulation for the problem as the foundation of our approach. This type of formulation, with a high-order spatial discretization and an implicit and adaptive time discretization, have been shown to be able to handle complex interactions between particles with high accuracy. Yet, for suspensions with high volume fractions, very small time-steps or expensive implicit solves as well as a large number of discretization points are required to avoid non-physical contact and intersections between particles, leading to infinite forces and numerical instability. Our method maintains the accuracy of previous methods at a significantly lower cost for dense suspensions. The key idea is to ensure interference-free configuration by introducing explicit contact constraints into the system. While such constraints are unnecessary in the formulation, in the discrete form of the problem, they make it possible to eliminate catastrophic loss of accuracy by preventing contact explicitly. Introducing contact constraints results in a significant increase in stable time-step size for explicit time-stepping, and a reduction in the number of points adequate for stability.

AllQuad, a New Automatic High Quality 3D Quadrilateral Mesher

Robert Rainsberger^{*}, John Rogers^{**}

^{*}XYZ Scientific Applications, Inc., ^{**}XYZ Scientific Applications, Inc.

ABSTRACT

A new automatic 3D multi-block structured all quadrilateral mesh generation algorithm for arbitrary composite surfaces with non-self intersecting boundaries is described in this paper. It can be used to form shell element meshes or to form the boundary mesh for an automatic 3D multi-block structured all hexahedral mesh generator under development. The surfaces can have any number of holes. First, the surfaces are sewn together to form one polygonal surface approximating the composite surface. Nodes are selected along the boundaries. Nearly geodesic 3D curves connect critical points on the boundary, dividing the polygonal surface into nearly convex patches. One of sixty templates is chosen to mesh each patch. Finally, the composite mesh is smoothed on the actual surfaces. This method is designed to maintain element quality while minimizing the number of irregular nodes. Examples are given.

Hidden Physics Models: Machine Learning of Nonlinear Partial Differential Equations

Maziar Raissi^{*}, Paris Perdikaris^{**}, George Karniadakis^{***}

^{*}Brown University, ^{**}University of Pennsylvania, ^{***}Brown University

ABSTRACT

A grand challenge with great opportunities is to develop a coherent framework that enables blending conservation laws, physical principles, and/or phenomenological behaviours expressed by differential equations with the vast data sets available in many fields of engineering, science, and technology. At the intersection of probabilistic machine learning, deep learning, and scientific computations, this work is pursuing the overall vision to establish promising new directions for harnessing the long-standing developments of classical methods in applied mathematics and mathematical physics to design learning machines with the ability to operate in complex domains without requiring large quantities of data. To materialize this vision, this work is exploring two complimentary directions: (1) designing data-efficient learning machines capable of leveraging the underlying laws of physics, expressed by time dependent and non-linear differential equations, to extract patterns from high-dimensional data generated from experiments, and (2) designing novel numerical algorithms that can seamlessly blend equations and noisy multi-fidelity data, infer latent quantities of interest (e.g., the solution to a differential equation), and naturally quantify uncertainty in computations. The latter is aligned in spirit with the emerging field of probabilistic numerics.

A Monolithic Constraint-Based Approach for Handling Fluid-Solid Interaction Problems via Smoothed Particle Hydrodynamics

Milad Rakhsha^{*}, Arman Pazouki^{**}, Radu Serban^{***}, Dan Negrut^{****}

^{*}University of Wisconsin-Madison, ^{**}California State University, ^{***}University of Wisconsin-Madison, ^{****}University of Wisconsin-Madison

ABSTRACT

We present a meshless discretization of Navier-Stokes equations that draws on a differential-algebraic equation (DAE) formulation and results in a monolithic coupling between the fluid and solid phases. The methodology is particularly attractive when dealing with Fluid-Solid Interaction (FSI) problems containing a large number of bodies whose dynamics are governed by kinematic constraints, friction, and contact. In this approach, the dynamics of the fluid phase is resolved by Smoothed Particle Hydrodynamics (SPH) and is formulated as a set of DAEs. Particularly, the mass conservation is satisfied by enforcing bilateral constraints on the density of SPH markers at the velocity level, which consequently ensures a divergence-free velocity field. Moreover, our formulation for DEAs prevents drift from incompressibility condition at the position level. Therefore, both the constant-density and the divergence-free velocity conditions are naturally satisfied with the current methodology; this is particularly an advantage of the current methodology compared to the conventional projection-based methods where special care is required to satisfy both conditions simultaneously (Hu and Adams, *Journal of Computational Physics*, 2007, Mitsuteru Asai et al., *Journal of Applied Mathematics*, 2012). Overall, the solution to the fluid-solid interaction problem is cast as a Cone Complementarity Problem (CCP), which is posed as the first-order optimality condition of a convex quadratic optimization problem with conic constraints. We use a Nesterov-type method, Accelerated Projected Gradient Descent (APGD), to efficiently solve the optimization problem at every time-step. We present numerical results demonstrating the scalability and accuracy of the current approach for three test studies (dam break, incompressibility, sloshing). Furthermore, we demonstrate the capability of the current method when dealing with real world problems such as tracked-vehicle fording simulation. In conclusion, the resulting FSI solution is both fast and scalable. It is fast owing to the semi-implicit and monolithic nature of the approach that results in two-orders of magnitude larger time steps compared to an explicit SPH approach. It is scalable owing to its reliance on a matrix-free iterative solver for the solution of the underlying optimization problem. [1] X. Y. Hu and N. A. Adams. An incompressible multi-phase SPH method. *Journal of Computational Physics*, 227(1):264-278, Nov 10, 2007. [2] Mitsuteru Asai, Abdelraheem M Aly, Yoshimi Sonoda, and Yuzuru Sakai. A stabilized incompressible sph method by relaxing the density invariance condition. *Journal of Applied Mathematics*, 2012.

A Finite Temperature Quasicontinuum analysis of Recrystallization of Amorphous Silicon

Amuthan Arunkumar Ramabathiran*

*Indian Institute of Technology Bombay

ABSTRACT

The recrystallization of amorphous silicon plays an important role in many technological applications, most notably in microelectronics in the context of device miniaturization. A variety of computational and experimental studies of recrystallization have been carried out in the past by investigating the amorphous/crystalline (a/c) interface and measuring the rate of recrystallization. In this work, a new strategy to extend the quasicontinuum method for non-crystalline solids is proposed, and subsequently utilized to study the recrystallization process in pure Si. In particular, the temperature dependence of the a/c interface velocity and the atomistic mechanisms operative during recrystallization are investigated. The recrystallization of amorphous silicon is also numerically interesting from the point of view of the quasicontinuum method since the fraction of silicon atoms in amorphous form is significant in comparison with that in crystalline form. As a first step, a study of the recrystallization process using a previously developed finite temperature extension of the quasicontinuum method, in conjunction with an adaptive coarse-graining strategy that tracks all the atoms in the amorphous region and only those atoms in the crystalline region that are near the a/c phase boundary, is presented and validated using molecular dynamics simulations. The validated quasicontinuum model subsequently serves as a useful benchmark to test new ideas related to the extension of the quasicontinuum method for non-crystalline solids. One possible extension of the quasicontinuum method for amorphous materials is proposed in this work via a statistical algorithm based on the local atomic neighborhood. In the context of the recrystallization study, the statistical nature of the method results in a probability distribution for the a/c interface growth rate. Convergence studies of the recrystallization rate distribution according to the proposed algorithm and detailed comparisons with both numerical and experimental data are presented to highlight the usefulness of the proposed coarse-graining technique for studying non-crystalline solids. Limitations of the current approach and promising ideas that refine and extend this framework will also be discussed.

High-order Chimera Method Based on Moving Least Squares for Fluid-Structure Interaction

Luis Ramirez*, Xesús Nogueira**, Pablo Ouro***, Fermín Navarrina****

*Grupo de Métodos Numéricos en Ingeniería (GMNI), E.T.S.I. Caminos, Canales y Puertos Universidade da Coruña, Campus Elviña, 15171, A Coruña, Spain, **Grupo de Métodos Numéricos en Ingeniería (GMNI), E.T.S.I. Caminos, Canales y Puertos Universidade da Coruña, Campus Elviña, 15171, A Coruña, Spain,

***Hydro-Environmental Research Centre, School of Engineering, Cardiff University, The Parade, Cardiff, UK,

****Grupo de Métodos Numéricos en Ingeniería (GMNI), E.T.S.I. Caminos, Canales y Puertos Universidade da Coruña, Campus Elviña, 15171, A Coruña, Spain

ABSTRACT

The Chimera/overset approach is widely used in the numerical simulation of flows involving moving bodies. In this approach, first used by Steger et al. in 1983 [1], the domain is subdivided into a set of overlapping grids, which provide flexible grid adaptation, the ability to handle complex geometries and the relative motion of bodies in dynamic simulations. In this work a higher-order (> 2) accurate finite volume method [2,3] for the resolution of the Euler/Navier-Stokes equations on Chimera grids is presented. The formulation is based on the use of Moving Least Squares (MLS) approximations [4] for transmission of information between the overlapped grids [5]. The accuracy and performance of the proposed method is demonstrated by solving different benchmark problems. An example of fluid structure interaction using this method is shown with the application of the proposed scheme to the computation of a Vertical Axis Turbine. REFERENCES [1] Steger, J., Dougherty, F., Benek, J., "A Chimera Grid Scheme", ASME, Mini-Symposium on Advances in Grid Generation, Houston, June 1982. [2] Cueto-Felgueroso, L., Colominas, I., Nogueira, X., Navarrina, F., Casteleiro, M., "Finite volume solvers and Moving Least-Squares approximations for the compressible Navier-Stokes equations on unstructured grids", Computer Methods in Applied Mechanics and Engineering, 196 :4712-4736, 2007. [3] X. Nogueira, L. Ramirez, S. Khelladi, J.C. Chassaing, I. Colominas, "A high-order density-based finite volume method for the computation of all-speed flows". Computer Methods in Applied Mechanics and Engineering, 298, 229–251, 2016. [4] Lancaster, P., Salkauskas, K., "Surfaces generated by moving least squares methods", Mathematics of Computation 37, 155: 141-158, 1981. [5] L. Ramirez, C. Foulquié, X. Nogueira, S. Khelladi, J.C. Chassaing, I. Colominas, New high-resolution preserving sliding mesh techniques for higher-order finite volume schemes. Computers & Fluids, vol 118, 114–130, 2015.

A Multicomplex Finite Element Approach for Curvilinear Progressive Fracture

Daniel Ramirez Tamayo^{*}, Harry Millwater^{**}, Arturo Montoya^{***}

^{*}The University of Texas at San Antonio, ^{**}The University of Texas at San Antonio, ^{***}The University of Texas at San Antonio

ABSTRACT

A unique, curvilinear fracture algorithm for simulating crack growth has been developed based on the complex variable finite element method, ZFEM. ZFEM has the capability of computing arbitrary-order derivatives of a structure's response variable under a single finite element run. In previous publications [1-2], ZFEM analyses of first order have been used to conduct fracture mechanics analyses undergoing different loading conditions such as thermal, mechanical and mixed mode. The energy release rate, a critical fracture parameter, has been computed as the first order derivative of the strain energy with respect to the crack size. In this study, higher order derivatives of the strain energy with respect to the crack size are obtained by expanding ZFEM to multicomplex algebras. The proposed crack progression methodology consists of constructing an arbitrary order Taylor series approximation of the strain energy as a function of crack propagation. This Taylor series is formed by the high order derivatives that are obtained from the multicomplex finite element analyses. Using this local energy response function, a curvilinear crack path is predicted along the maximum energy release rate direction. The approach was tested by comparing the crack path measured by Miranda et al. [3] on a homogeneous steel specimen with a hole to the results provided by the proposed approach. The crack path predictions were performed for response functions constructed with different derivative orders, 1 to 4. The numerical results were in excellent agreement with the experimental paths. Nonetheless, fewer crack path increments were required when higher order derivatives were considered. This method offers significant advantages over traditional methods models that predict a curved crack path using several small linear crack increments. ZFEM curvilinear capabilities yield to higher accuracies and require less simulation steps. References [1] Millwater, H., Wagner, D., Baines, A., Montoya, A., 2016. A virtual crack extension method to compute energy release rates using a complex-valued finite element method. *Engineering Fracture Mechanics* 162, 95–111. [2] Daniel Ramirez Tamayo, Arturo Montoya, Harry Millwater, A Virtual Crack Extension Method for Thermoelastic Fracture using a Complex-variable Finite Element Method, *Engineering Fracture Mechanics*, 2017. [3] A.C.O. Miranda, M.A. Meggiolaro, J.T.P. Castro, L.F. Martha, and T.N. Bittencourt. Fatigue life and crack path predictions in generic 2d structural components. *Engineering Fracture Mechanics*, 70(10):1259 – 1279, 2003.

Hierarchic Isogeometric Shell Formulations Intrinsically Avoiding Locking

Ekkehard Ramm^{*}, Bastian Oesterle^{**}, Renate Sachse^{***}, Manfred Bischoff^{****}

^{*}University of Stuttgart, Germany, ^{**}University of Stuttgart, Germany, ^{***}University of Stuttgart, Germany,
^{****}University of Stuttgart, Germany

ABSTRACT

The contribution addresses novel concepts emerging on the basis of Isogeometric Analyses (IGA) offering smooth function spaces (as NURBS) with higher inter-element continuity. They allow avoiding locking phenomena a priori on the theory level before discretization. IGA easily satisfies C1-continuity Kirchhoff-Love (KL) finite elements with low order trial functions. These results are taken as basic building block for a Reissner-Mindlin (RM) model. Instead of introducing total rotations as primal variables modified parametrizations in a sense of hierarchic formulations are chosen superimposing the transverse shear parts in an incremental way. Since the function spaces of these extra parts are separated from the KL basis the formulation is completely free from shear locking independent of the kind of discretization. Two different parametrizations are described. In the first concept [1] both transverse shear components are introduced as hierarchic (incremental) rotations superimposed on the KL-rotations, which in turn depend per definition on the mid-plane displacements. Since it turned out that the shear stress resultants still show a tendency to oscillate due to an unbalance in spaces, a second concept [2] is proposed, in which the two displacement fractions responsible for the transverse shear are superimposed as hierarchic displacement parameters to the total displacements. This leads to a shear deformable, rotation-free isogeometric shell formulation intrinsically free of shear locking showing excellent performance for shear stress resultants. Both formulations have been extended into the geometrically non-linear regime [3]. In the majority of practically relevant cases the transverse shear rotations can be assumed to be small. Thus, this linearized part can be added hierarchically to the fully non-linear KL shell model following the same additive procedure as in the case of small rotations, avoiding the cumbersome treatment of large rotations, for instance using Rodrigues parameters. A corresponding primal formulation to avoid membrane locking is still a challenge. Therefore, this defect has been remedied by applying either mixed formulations, or we resort directly to the Discrete Strain Gap (DSG) method. [1] R. Echter, B. Oesterle, M. Bischoff, A hierarchic family of isogeometric shell finite elements, *Comput. Methods Appl. Mech. Engrg.* 254 (2013) 170-180. [2] B. Oesterle, E. Ramm, M. Bischoff, A shear deformable, rotation-free isogeometric shell formulation, *Comput. Methods Appl. Mech. Engrg.* 307 (2016) 235-255. [3] B. Oesterle, R. Sachse, E. Ramm, M. Bischoff. Hierarchic isogeometric large rotation shell elements including linearized transverse shear, *Comput. Methods Appl. Mech. Engrg.* 321 (2017) 383-405.

Evolution of Shell Formulations - from Love to IGA

Ekkehard Ramm*, Manfred Bischoff**

*University of Stuttgart, Germany, **University of Stuttgart, Germany

ABSTRACT

The contribution gives a brief outline how shell formulations evolved in the last 130 years. It starts with the seminal paper of A.E.H. Love published in 1888 [1]. The subsequent period was concentrating on finding analytical solutions known at that time from mathematical physics like Euler or Bessel ODEs or applying corresponding energy expressions. Thus, Love's general equations were specialized to specific rotational or translational shells or to subclasses like deep and shallow shells; in addition minor terms were neglected simplifying the analysis. This period until the mid of the 20th century was of utmost importance for understanding the physical behavior of these delicate structures. In addition, first steps into the non-linear regime were made, in particular investigating buckling phenomena (von Karman, Koiter et al.). Beginning of the second half of the 20th century shell theories were extended and refined in many ways. Further mechanical effects were added to the basic formulation such as transverse shear deformations, higher order kinematics, heterogeneous layout across the thickness as well as geometrical and material nonlinearities, again mostly for simplified models. The potential for concrete analyses dramatically changed after the advent of modern computers and the rapid developments of numerical solution schemes, above all the finite element method. In the first decade, the C1-continuity requirement for the (Kirchhoff-) Love (KL) model was a major challenge, so that around 1970 versions with C0-continuity applying the so-called Reissner-Mindlin (RM) kinematics including transverse shear deformations were favored. Due to locking problems, innumerable un-locking schemes were proposed. In this period, shell problems in the entire spectrum of the computational environment have been investigated in the non-linear, multi-scale, multi-physics regime including multilayer and solid shell models. When in 2005 Hughes and co-workers introduced the Isogeometric Analysis it was soon recognized that low order NURBS (or subdivision) discretizations allow satisfying the continuity requirement for KL shells. Starting from this model recently hierarchic shell formulations were developed which intrinsically avoid geometrical locking problems on the theory level [2]; these formulations utilize hierarchic rotations or displacements in the sense of a re-parametrization of primary variables. [1] A.E.H. Love, The Small Free Vibrations and Deformation of a Thin Elastic Shell, Phil. Trans. R. Soc., 1888, 179A , 491-546. [2] B. Oesterle, E. Ramm, M. Bischoff, A shear deformable, rotation-free isogeometric shell formulation, Comput. Methods Appl. Mech. Engrg. 307 (2016) 235-255.

Using Micro-computed Tomography for Image-based Material Testing of Particulate Composites to Quantify Microscale Damage

Katherine Ramos*, Karel Matouš**

*University of Notre Dame, **University of Notre Dame

ABSTRACT

Understanding the mechanical behavior that arises from the heterogeneity at different length scales of natural and synthetic heterogeneous materials is essential. X-ray micro-computed tomography (micro-CT) has become a popular method in the materials science community for nondestructive analysis of the internal microstructure in these complex materials. In particular, this technology allows in situ analysis of materials under mechanical loading. The power of this experimental technique is enhanced through detailed statistical analysis of the evolution of various structural features through robust image processing strategies at various stages of loading. In this work, we develop an image-based material testing approach using micro-CT to understand the influence of microstructure and local damage phenomenon on the effective mechanical response of rubber-glass bead composites. Furthermore, a nondestructive, three-dimensional image-based analysis protocol which provides high fidelity of sample testing and data assessment has been established. An investigation was performed on various microstructure compositions of silicone rubber reinforced with silica particles. In situ compression experiments were used to study how the microscale damage (void creation from debonding) develops and evolves in the context of four primary studies: i) effect of particle volume fraction ii) effect of particle diameter iii) local damage phenomena and its evolution (incremental loading/unloading) and iv) effect of surface treatments on bonding characteristics. We use image analysis tools to quantify damage in the composites through calculations of void volume fractions and void size distributions. Additionally, we exploit the ability to directly examine the material's microstructure before and after loading to determine multiscale linking and evolution of fields when assessing the damage. The rich data analysis collected from the various experimental studies offers an understanding of the complex phenomena attributing to the material's response to loading including the mechanical and morphological response of non-linear viscoelastic materials subjected to uniaxial compression. In addition to the fundamental understanding, these experiments serve as validation data sets for multi-scale modeling approaches. In particular, the analysis will serve as a foundation in the development of better constitutive theories for Finite Element Analysis (FEA) of these heterogeneous microstructures. Focus is placed on the development of non-linear viscoelastic constitutive models with damage/debonding for these complex heterogeneous systems. This analysis and framework yields new insight of these composite materials required for the optimal material design. Additionally, the thorough and reliable experimental and image processing framework established supplements existing image-based modeling techniques substantially.

Topology Optimized Functionally Graded Structures for Impact Applications

Francisco Ramírez-Gil*, Esteban Foronda-Obando**, Wilfredo Montealegre-Rubio***

*Universidad Nacional de Colombia, **Universidad Nacional de Colombia, ***Universidad Nacional de Colombia

ABSTRACT

Functionally graded materials (FGM) are a kind of composites in which the microstructure, composition, porosity or other characteristics is changed continuously through one or more directions allowing a smooth variation of properties over the volume [Miyamoto et al., 1999]. In particular, the concept of FGM can be used for impact applications where the material is designed at macroscopic level with varying stiffness from the surface to the core looking for the best relation of parameters to enhance the energy absorption [Ramírez-Gil et al., 2016]. Although there are several options to design impact-resistant FGMs, in this research the density of the material of a rectangular plate is changed by controlling its porosity throughout its thickness. This approach is commonly used by nature in structures subjected to impact such as bones, teeth, horns, bird beaks and wood [McKittrick et al., 2010]. The topology optimization method (TOM) is used herein for optimal generation of the holes (size, shape, location, and the number of pores) by discretizing the plate in several layers, allowing each of them to have a different thickness and volume fraction constraint in order to achieve a functionally graded structure. Commercial software, LS-TaSC in conjunction with LS-DYNA, is used to get the topologies. The impact is assessed with the explicit finite element software and the model considers an elastoplastic material behavior at sub-ordnance velocity. Several patterns of holes are obtained and compared to a solid plate in terms of weight and energy absorption capability. The results show that it is possible to design the pattern of holes reducing the weight of the plate without having a substantial detriment on its structural response, which can be useful in applications where the weight is a priority. Finally, further research should be developed so that this design technique can be applied to components subjected to more complex impact phenomena produced by medium- and high-velocity impacts. References • Miyamoto et al., Functionally Graded Materials. Design, Processing and Applications. Springer, 1999. • Ramírez-Gil et al., "Optimization of functionally graded materials considering dynamical analysis," in Advanced Structured Materials, Springer, 205–237, 2016. • McKittrick et al., Energy absorbent natural materials and bioinspired design strategies: A review. Materials Science and Engineering C, 30(3), 331-342, 2010.

Concurrent Optimization of Topology and Distributed Transverse Isotropy for 3D Structures

Narindra Ranaivomiarana^{*}, Dimitri Bettebghor^{**}, François-Xavier Irisarri^{***}, Boris Desmorat^{****}

^{*}Onera, Chatillon, France, ^{**}Onera, Chatillon, France, ^{***}Onera, Chatillon, France, ^{****}Sorbonne Universite, Centre Nationale de la Recherche Scientifique, UMR7190, Institut Jean le Rond d'Alembert, Paris, France

ABSTRACT

This research project is funded by STELIA Aerospace. Reducing weight and costs of structures is crucial for aeronautic industry. Thus, great effort is placed in the development of new methodologies for mass minimization. Topology optimization is a relevant method on the rise. It consists of determining the best shape of structural components or the best layout of structures for a given bulk and predefined loadings. Most of the works in the field deals with isotropic materials, especially metallic ones. However, composites are increasingly used to lighten structures. These materials give new degrees of freedom for the optimization as it is possible to tailor the material anisotropy through the fiber orientations. Composite structures design and optimization is classically performed with fixed predefined shapes, most of the time derived from the preexisting metallic parts. Nevertheless, such a practice is questionable since the material anisotropy influences the optimal shape. The aim of the present project is to bridge the gap between topology optimization and composite optimization by developing an innovative method for simultaneous topology and anisotropy optimization of three dimensional structures. In the present paper, transversely isotropic materials are used. This work generalizes previous work by the authors about compliance minimization with a maximal volume constraint in two dimensions. The problem is solved numerically with an optimality criteria algorithm. The algorithm iterates between local minimizations in each element with fixed stress and re-actualization of the stress field with fixed design variables using finite element analysis. The material distribution is parameterized by a continuous density variable, penalized with the SIMP method (Solid Isotropic Method Penalization). The distributed anisotropy is parameterized using elasticity tensor invariants by change of frame. In two dimensions, the polar invariants are used. In three dimensions, significant work has been done to identify the adequate invariants and to solve the local minimizations. The results show that the optimal orientation of the transversely isotropic material is in the same direction as the highest absolute eigenvalue of the stress tensor's deviator. The optimal values of anisotropic invariants are found with explicit expressions. The developed method is applied on academic and industrial test cases. Compared with sequential optimization results where the shape is first optimized with a fixed isotropic material and then the material distribution is optimized with the obtained shape, the simultaneous optimization leads to a stiffer optimal design with a different shape.

A Comparison of Viscoelastic Level Set Formulations: Property Averaging versus Equation Averaging

Rekha Rao^{*}, Weston Ortiz^{**}

^{*}Sandia National Laboratories, ^{**}University of New Mexico

ABSTRACT

In this work, we extend a finite element, Newtonian, level set implementation to viscoelastic flow, where a separate stress tensor must be solved in addition to the velocity and pressure. We investigate formulations where one fluid is viscoelastic and the other is Newtonian. We look at two viscoelastic level set (VE-LS) approaches; one based on the traditional property averaging common in level set implementations and the other using an equation averaging approach for the polymeric extra stress tensor. The viscoelastic equations are discretized using DEVSS-G method with LBB elements for the velocity and pressure spaces and bilinear interpolation for the stress and velocity gradient space. A Phan-Thien-Tanner (PTT) exponential constitutive equation is used to describe the viscoelastic response. Surface tension forces play a key role in many two-phase and immiscible fluid problems, especially in microfluidic flows where capillary forces can become dominant. For level set implementations, surface tension implementations can be plagued by parasitic currents. We investigate and compare multiple methods for reducing parasitic currents. The approaches are benchmarked against an arbitrary-Lagrangian-Eulerian (ALE) implementation for viscoelastic die swell into a Newtonian gas phase and a Newtonian droplet in a viscoelastic fluid traveling through a microfluidic constriction. In general, we have found that the results are better using equation averaging, though this is a costlier algorithm. ^{*}Sandia National Laboratories is a multi mission laboratory managed and operated by National Technology and Engineering Solutions of Sandia, LLC., a wholly owned subsidiary of Honeywell International, Inc., for the U.S. Department of Energy's National Nuclear Security Administration under contract DE-NA0003525.

Temporal Decomposition Strategies for Long-horizon Dynamic Optimization

Vishwas Rao*, Mihai Anitescu**

*Argonne National Laboratory, **Argonne National Laboratory

ABSTRACT

In this work, we investigate a temporal decomposition approach to long-horizon dynamic optimization problems. The problems are discrete-time, time-dependent and with box constraints on the control variables. These problems typically arise as optimal planning problems in electrical power industry for transmission or generation expansion. Planning analysis for these problems involves a production cost model (PCM). A PCM simulates the operation of generation and transmission systems by solving a nonlinear constrained optimal control problem for each time-interval in order to arrive at a least-cost solution to meet the energy demands. Many studies require simulating a PCM on an hourly scale for 1-20 years under different scenarios and this would mean that the number of time-intervals exceed 100,000. Additionally, each time interval involves tens of thousands of state and control variables, making the solution to a PCM a computationally expensive proposition. In this study, we propose an approximate temporal decomposition using overlapping time-intervals for approximate temporal decomposition of long-horizon dynamic optimization problem. The proposed approach opens up avenues to expose temporal-parallelism and hence creates an opportunity for faster computation. We demonstrate the effectiveness of this approach for Alternative Current Optimal Power Flow (ACOPF) and Security Constrained ACOPF (SCACOPF).

On the Formulation of Dissipative Path-Following Constraints in the Embedded Finite Element Method

Giuseppe Rastello*, Francesco Riccardi**, Benjamin Richard***

*DEN - Service d'études mécaniques et thermiques (SEMT), CEA, Université Paris-Saclay, France, **LMT, ENS Cachan, CNRS, Université Paris-Saclay, France, ***DEN - Service d'études mécaniques et thermiques (SEMT), CEA, Université Paris-Saclay, France

ABSTRACT

The present contribution aims to investigate the formulation of dissipative path-following constraints [1] within the Embedded Finite Element Method (E-FEM) [2,3] framework. According to this approach, cracking is described by distinguishing between a global problem (where the displacement field is regular) and a finite set of local problems driving the response of element-wise defined strong discontinuities. At the embedded discontinuity level, a discrete traction-separation law describes the interaction between the crack surfaces. Furthermore, traction-continuity conditions ensure that each finite element crossed by the discontinuity line/surface satisfies the momentum balance equation. The localization and propagation of cracks often lead, however, to unstable structural responses characterized by snap-backs. Path-following procedures allow overcoming these instabilities. Accordingly, the equilibrium problem is augmented by an additional global unknown (the loading factor) which should comply with a dedicated equation: the path-following constraint equation. Thanks to the enhanced kinematic description provided by the E-FEM, this contribution shows that it is possible to formulate constraint equations where the controlled quantities are directly related to the dissipation process occurring at the strong discontinuity level. Several dissipative path-following constraints and their numerical implementation (based on an operator-splitting method) are illustrated. Simple two-dimensional quasi-static simulations, involving unstable structural responses characterized by multiple snap-backs, are presented. A comparison with some well-known path-following constraints used in non-linear finite element simulations is also established. This allows illustrating the main features of the proposed methods, as well as their effectiveness in controlling embedded discontinuity finite element simulations of failure in solids. [1] De Borst, R., Crisfield, M.A., Remmers, J.J.C, Verhoosel, C.V., *Nonlinear finite element analysis of solids and structures*. John Wiley & Sons (2012). [2] Oliver, J., *Modeling strong discontinuities in solid mechanics via strain softening constitutive equations. Part-2: Numerical Simulation*, *International Journal for Numerical Methods in Engineering*, 39, 3601-3623 (1996). [3] Linder, C., Armero, F., *Finite elements with embedded strong discontinuities for the modeling of failure in solids*, *International Journal for Numerical Methods in Engineering*, 72, 1391-1433 (2007).

Multiscale Model of Cooling after Cold Forging Based on the Solution of Diffusion Equation in the Micro Scale

Lukasz Rauch^{*}, Krzysztof Bzowski^{**}, Marek Wilkus^{***}

^{*}AGH University of Science and Technology, ^{**}AGH University of Science and Technology, ^{***}AGH University of Science and Technology

ABSTRACT

The structure and final properties of forgings after the thermo-mechanical treatment are a result of all operations, including the heating of the charge material itself, forging and controlled cooling. Performing the heat treatment of the forging during cooling, using the heat of the forging, is the main challenge today. Therefore, for the design of the process with the heat treatment directly after hot forging it is necessary to possess precise information on the whole process, which is possible to be acquired by applying modern numerical modelling methods. Development of the multiscale model of this process was the main objective of the paper. The common approach is to connect finite element (FE) model in the macro scale with mean field model (e.g. JMAK) in the micro scale. However, information supplied by this approach is constrained to the phase composition in the final product. On the other hand, the properties of the product depend on some additional parameters such as morphology of phases and distribution of carbon and alloying elements in each phase. Therefore, a new approach was proposed in which FE code in macro scale is connected with the FE solution of the diffusion equation in the micro scale. The latter is described in Authors earlier publications [1]. In this solution level set method was used to control motion of the interphase. New position of the interface in each time step was determined by the mass balance, interphase mobility and interphase curvature. Connection of the micro model with the FE model of the forging process is computationally costly. Therefore, searching for a balance between predictive capabilities of the model and computing costs was the next objective of the work. Possibilities of decreasing the computing costs while the accuracy of the model remains on a reasonable level were considered [2]. Distributed computing was applied. Results of simulation including distribution of microstructural features in the volume of the forging is the main output of the paper. Acknowledgement: The work is financed in TECHMATSTRATEG1/348491/10/NCBR/2017 project by NCBiR. References 1. Pernach M., Bzowski K., Pietrzyk M., Numerical modelling of phase transformation in DP steel after hot rolling and laminar cooling, International Journal for Multiscale Computational Engineering, 12, 2014, 397–410.. 2. Rauch L., Kuziak R., Pietrzyk M., From high accuracy to high efficiency in simulations of processing of Dual-Phase steels, Metallurgical and Materials Transactions B, 45B, 2014, 497-506.

Patient-specific Models of Tricuspid Valves Based on Healthy Human Heart Explants

Manuel Rausch^{*}, William Meador^{**}, Chen Shen^{***}, Marcin Malinowski^{****}, Tomasz Jazwiec^{*****}, Tomasz Timek^{*****}

^{*}University of Texas at Austin, ^{**}University of Texas at Austin, ^{***}University of Texas at Austin, ^{****}Spectrum Health, ^{*****}Spectrum Health, ^{*****}Spectrum Health

ABSTRACT

Functional tricuspid regurgitation (FTR), i.e., a leaking tricuspid valve (TV) due to valve extrinsic causes, is a significant source of morbidity and mortality [1]. Our treatment options are currently suboptimal with a large number of patients exhibiting signs of recurrence within few years after surgery. Little is known about the mechanics of the TV, in health or disease, which may be impairing our ability to devise better treatment strategies for FTR and improve our current clinical standard. Toward a deeper understanding of the mechanics of the TV, we are setting out to develop detailed computational models of healthy human valves. We inform these models with in-situ experiments of healthy human hearts that were rejected from transplantation and with in-vitro experiments of the matched tissue samples. Specifically, we use sonomicrometry to determine the in-situ shape of the TV annulus in a beating human heart temporarily maintained in an organ preservation system. Upon termination of the experiments, we perform histo-mechanical analyses of the valve leaflets and chordae tendineae of the same valves to extract the mechanical properties of these tissues, their microstructural composition, and their geometry. Subsequently, we merge the matched sonomicrometry data with the mechanical, histological, and geometric data to build the first, patient-specific, finite element models of healthy human hearts. Additionally, we include chordae tendineae in our models whose origin and insertion sites are identified based on tissue samples. Using the non-linear, implicit finite method, we simulate the opening and closing behavior of the TV during one full cardiac cycle. To this end, we impose Dirichlet boundary conditions, which we derive from our in-vivo sonomicrometry data, to the annular geometry of our patient-specific models of the TV. In addition, we impose the in-situ measured transvalvular pressure to the ventricular surface of the valve's three-leaflets. The TV shows a complex closing behavior, with a Y-shaped coaptation line that originates from its three distinct leaflets. Naturally, the leaflet stresses are largest during peak systole and smallest during diastole with the belly regions showing maximal stresses. Moving forward, we will employ these models to virtually test and optimize different treatment strategies for FTR. Our main focus will be on the shape of annuloplasty devices, the current gold-standard treatment of FTR. In conclusion, we developed a first patient-specific model of the TV and tested the feasibility of our combined in-situ/in-vitro experimental/computational framework. References [1] Rausch et al. Ann Biomed Eng, 2017

Patient-Specific Drug Elution Simulations in Stented Coronary Arteries Using a Combined Experimental-Numerical Scheme

Atefeh Razavi^{*}, John LaDisa^{**}, Harkamaljot Kandail^{***}

^{*}Marquette University, ^{**}Marquette University/Medical College of Wisconsin, ^{***}Eindhoven University of Technology

ABSTRACT

Cardiovascular disease (CVD) is a major cause of death worldwide. For example, about 92M Americans (28%) have CVD, a heart attack happens every 34 seconds, and someone dies from a coronary artery event every ~1 minute(1). Drug eluting stents (DES) have revolutionized CVD treatment, but restenosis forces >200,000 repeat coronary interventions in the US annually(2). Remodeling occurs after stenting, which causes changes in local coronary artery geometry and adverse hemodynamics on the wall. For bare metal stents it is known that adverse wall shear stress (WSS) is associated with restenosis, and can be improved through stent design. For DES, however, the details of how WSS-related parameters may impact restenosis are not known since many studies lack realistic representations for arterial geometry and hemodynamics due to limitations of the imaging or modeling methods, material properties of the coronary plaque, drug characteristics and/or biological reaction terms. The objective of the current study is to develop a combined experimental-numerical scheme leading to the most realistic study of hemodynamics after coronary artery DES implantation to date. Limited literature on drug and plaque properties prevents the implementation of realistic conditions in coronary artery DES simulations. To address this issue, stress-strain curves, diffusion coefficients, and reaction terms are determined using human coronary arteries with atherosclerotic plaques classified using the modified American Heart Association (AHA) criteria after patient-specific geometry is reconstructed from optical coherence and computed tomography(3). Experimentally derived nominal stress-strain curves are used to calibrate ABAQUS' isotropic hyperelastic material models. Diffusion coefficients are obtained by measuring drug concentration at various coronary artery locations. Binding capacity and equilibrium dissociation values are extracted from these measurements and bulk drug solution to identify biological reaction terms. Empirical values are then applied to the deformed artery geometry in FlowVision (Capvidia, Belgium) to conduct patient-specific simulations of drug-elution patterns for ultimate use in identifying patients at greater risk of restenosis. This approach also addresses challenges from minuscule faces that present in complex patient-specific DES models through the use of an improved cut-cell method within FlowVision, thereby extending the scheme to a cohort of DES patient models with malposition between the stent and artery. This work is expected to result in the most detailed characterization of plaque properties to date for use in more realistic patient-specific simulations of coronary artery DES. 1. Go et al. *Circulation*. 2013;127:e6-e245 2. Garg et al. *JACC*. 2010;56:S1-42 3. Ellwein et al. *Cardiovasc Eng Tech*. 2011;2(3): 212-7

Isogeometric Simulation of Structures: Recent Advances with a Focus on Composites

Alessandro Reali*

*University of Pavia

ABSTRACT

Tom Hughes is surely one of the most talented and influential researchers in the history of Computational Mechanics, given the incredible quality and quantity of fundamental contributions he was able to give to all aspects of this field. The latest of them, Isogeometric Analysis, has established itself as one of the hottest topics in Computational Mechanics despite its relatively young age, attracting a huge interest from many researchers around the world, testified by the exponentially growing number of related papers, talks, and citations. In this presentation, after a brief introduction on Isogeometric Analysis, I will review some of the new possibilities that this family of methods has allowed to develop in the context of structural simulation techniques. I will finally focus on a novel approach for composite structures, which takes advantage of the accuracy and high-regularity properties of Isogeometric Analysis to build a cost-effective stress recovery procedure based on equilibrium in strong form.

Analytical and Numerical Investigations of Locking in Transversely Isotropic Elasticity

Daya Reddy*, Faraniaina Rasolofoson**, Beverley Grieshaber***

*University of Cape Town, **University of Cape Town, ***University of Cape Town

ABSTRACT

For isotropic materials the concept of volumetric locking in the context of low-order finite element approximations is well understood, and a variety of effective remedies exist: for example, the use of mixed methods, discontinuous Galerkin (DG) methods, or selective underintegration. Corresponding studies have been carried out, to a limited extent, to determine conditions under which locking related to inextensibility occurs, in small- and large-deformation contexts [1,2] The models treated in these works are of an isotropic material, with inextensibility imposed as a constraint. The present work is concerned with transversely isotropic linear elastic materials, which are characterized by 5 material parameters [3]. The behaviour under limiting conditions of near-incompressibility and near-inextensibility are investigated. It is shown both through numerical examples and an analysis of finite element approximations that locking behaviour for low-order elements depends critically on the degree of anisotropy of the material, that is, on the ratio of Young's moduli and Poisson ratios for the directions parallel and transverse to the direction characterizing transverse isotropy. In addition to conforming finite element approximations, the use of DG approximations is also pursued: for these, it is shown that behaviour is locking-free. References 1. Auricchio F., Scalet G. and Wriggers P. Fibre-reinforced materials: finite elements for the treatment of the inextensibility constraint. *Compute. Mech.* (2017) 60:905:922. 2. Wriggers P., Schröder J. and Auricchio F. Finite element formulations for large strain anisotropic material with inextensible fibers. *Adv Model Simul Eng Sci* (2016) 3(1):25. 3. Spencer, A.J.M. The formulation of constitutive equations for anisotropic solids. In *Mechanical Behavior of Anisotropic Solids* (J. P. Boehler, ed.) Martinus Nijhoff Publishers, The Hague (1982) 2–26.

Mathematical Modelling of Drug Delivery to the Targeted Organs through Bio-Absorbable Nanoparticles

J V Ramana Reddy*, Dasari Srikanth**, Sint Sundar***

*Indian Institute of Technology Madras, **Defence Institute of Advanced Technology, ***Indian Institute of Technology

ABSTRACT

It is proposed to control the thermal and concentration dispersion from drug-coated nanoparticles in the blood flow. It is assumed that the temperature sensitive drug is coated on the surface of the bio-absorbable nanoparticles. The mixture of blood together with the nanoparticle is modelled as nano-polar fluid. The formulation is useful to understand the impact of the deformation of the blood components on hemodynamics. The physiological pressure gradient caused due to the cardiac cycle, and the flexible arterial wall is also incorporated in the model. To make the model more realistic, the hematocrit has been considered along with the variable viscosity in the blood flow model. The resultant highly non-linear coupled modelled governing equations of flow are simulated by the Marker and Cell along with the suitable choice of the boundary and initial conditions. The numerical stability is also checked with the desired accuracy. The rate and the amount of drug release are controlled by the temperature provided by the catheter in the targeted region. The influence of various parameters which are arising out of the fluid and geometry considered on the physiological blood flow characteristics are computed numerically. The mathematical understanding of the drug release and blood flow through stenosed tapered arteries with flexible walls is having direct applications in lessening the adverse effects caused due to the medication, helps in designing the pharmaceutical drug, deemed to be a great help in the treatment of vascular diseases, and also the biomedical engineers.

Microscale Multiphysical Modeling of Tool Steels and Cast Irons

Konstantin Redkin^{*}, Christopher Hrizo^{**}, Isaac Garcia^{***}

^{*}WHEMCO Inc, ^{**}WHEMCO Inc, ^{***}University of Pittsburgh

ABSTRACT

Applied image-based 2D finite element modeling approach was developed to simulate microscale multiphysical behavior of highly alloyed steels and cast irons, which are used as the rolls' materials for cold and hot rolling mill applications. Combined image processing, advanced materials characterization techniques, thermodynamic-kinetics modeling and finite element analysis enabled one to simulate microscale deformation and heat transfer phenomena of considered microstructures. A fundamental understanding of composite-like materials' behavior will be shown and discussed, leading to more comprehensive materials engineering for industrial scale applications.

Data Mining for Electromechanical and Phase Change Properties of Over 1000 2D Materials

Evan Reed*

*Stanford University

ABSTRACT

We have utilized data mining approaches to elucidate over 1000 2D materials and several hundred 3D materials consisting of van der Waals bonded 1D subcomponents, or molecular wires. We find that hundreds of these 2D materials have the potential to exhibit observable piezoelectric effects, representing a new class of piezoelectrics. Another subset of these materials has the potential to exhibit structural changes under a variety of external stimuli including electrostatic gating. I will discuss calculations of phase diagrams, recent experimental results demonstrating the predicted electrostatic gating phase change effect, and potential phase change applications for these materials. We find that the nature of mechanical constraint has a significant impact on the phase diagram.

Uncertainty Quantification of the Performance of Seismic Waveguides through Reduced Order Model Interpolation

Heather Reed^{*}, Alex Kelly^{**}, Jeffrey Cipolla^{***}, Andrew Shakalis^{****}

^{*}Thornton Tomasetti – Weidlinger Applied Science, ^{**}Thornton Tomasetti – Weidlinger Applied Science,
^{***}Thornton Tomasetti – Weidlinger Applied Science, ^{****}Thornton Tomasetti – Weidlinger Applied Science

ABSTRACT

In seismic applications, incident waves are redirected, causing them to avoid a structure in their path of normal incidence. Seismic cloaking enables 'hiding' a structure through the selection or construction of a material that has specific waveguide properties. The material and mechanical properties required to achieve the cloaking effects are not found in nature, and therefore heterogeneous materials (metamaterials) are fabricated by gradually layering manufactured unit cell microstructures, resulting in a (usually smooth) variation of properties. Advances in additive manufacturing (i.e. 3D printing) have enabled these complex metamaterials to be fabricated relatively quickly, compared to conventional manufacturing methods. Metamaterials, however, present challenges in optimization for any desired waveguide effect. Homogenization methods, which assume Cartesian symmetry, are a staple in metamaterial design, but these only approximate a feasible optimum. Moreover, total reliance on homogenized continuum models provides no information about the actual cloak performance, and presents problems in functionally graded applications. To overcome this, a full field, explicit time domain finite element simulation of the wave propagation is required in the cloaking design process, resulting in a computationally expensive cloak optimization problem. Another challenge in the design of such waveguides stems from the uncertainty in the manufacturing process. Additive manufacturing is notorious for generating highly variable component properties. As the design process heavily depends on these metamaterial base properties, the uncertainty surrounding those properties must be quantified and accounted for in the simulation. A Monte Carlo analysis enables determination of the cloak performance uncertainty by integrating over the base material parameter space. However, because each evaluation of the integral entails evaluating the costly finite element model, a projection-based reduced order model (ROM) is leveraged to drastically decrease the deterministic model computational time. A ROM adaptation procedure is implemented, where projection-based ROMs are seen as points on a Riemannian manifold and are tracked and interpolated during the sampling process from a database of precomputed ROMs [1]. This approach ensures that an appropriate ROM is used for the model evaluation in every region of the parameter space, thus leading to computational savings while conserving sufficient accuracy. [1] Amsallem, David; Cortial, Julien; Carlberg, Kevin; Farhat, Charbel. A method for interpolating on manifolds structural dynamics reduced-order models. International Journal for Numerical Methods in Engineering Vol. 80, Iss. 9, (Nov 26, 2009): 1241-58.

Proper Orthogonal Decomposition (POD) Combined with Hierarchical Tensor Approximation (HTA) in the Context of Uncertain Parameters

Stefanie Reese^{*}, Steffen Kastian^{**}, Dieter Moser^{***}, Lars Grasedyck^{****}

^{*}RWTH Aachen, Germany, ^{**}RWTH Aachen, Germany, ^{***}RWTH Aachen, Germany, ^{****}RWTH Aachen, Germany

ABSTRACT

The evaluation of robustness and reliability of realistic structures in the presence of polymorphic uncertainty involves numerical simulations with a very high number of degrees-of-freedom, as well as a high number of parameters. Some of these parameters are certain in the way that they are a priori known. However, most of the parameters are uncertain, since they are based on incomplete information or imprecise measurements. To account for this uncertainty it is necessary to observe the high dimensional parameterspace. Therefore, a huge amount of simulation is required. In this context a method of model order reduction is used to reduce the cost of each simulation. In the present contribution, the POD [1] is chosen for this purpose. In order to get accurate results by means of the POD method it is essential to find proper projection matrices. The goal of the present contribution is to significantly improve the accuracy and efficiency of the existing POD method by developing adaptive projection matrices during the simulation. A moderate number of quantities of interest can be found in most technical problems. This could be for example the maximum displacement or the maximum stress in a deformed object. For several uncertain parameters the number of possible combinations of different parameters can be very high. The HTA [2] is a very good candidate to overcome this issue. The HTA needs several precalculations which can be speeded up by combining it with the POD method. In the next step the HTA can be used for uncertainty quantifications. This includes the calculation of the average, maximum and minimum value of the quantity of interest. [1] A. Radermacher, S. Reese, 2016. POD-based model reduction with empirical interpolation applied to nonlinear elasticity, *International Journal for Numerical Methods in Engineering*, 107 (6), 477--495 [2] L. Grasedyck, R. Kriemann, C.Löbber, A. Nägel, G. Wittum, K. Xylouris, 2015. Parallel tensor sampling in the hierarchical Tucker format, *Computing and Visualization in Science*, 17 (2), 67--78.

Three-Dimensional Large Deformation Micromorphic Elastostatics with Microstructural Linkage and Comparison to Micropolar Elastostatics

Richard Requeiro*, Farhad Shahabi**, Volkan Isbuga***

*University of Colorado Boulder, **University of Colorado Boulder, ***Hasan Kalyoncu University

ABSTRACT

A three-dimensional (3D), large deformation, finite element analysis (FEA) framework accounting for material micro-structure is presented for micromorphic continuum mechanics. A fundamental assumption of the theory is that material micro-structure satisfies the governing equations of classical continuum mechanics within a "micro-element." The micro-element deformation with respect to a mass-centered macroscopic continuum point (called a "macro-element") is governed by an independent micro-deformation tensor. Assuming that proper constitutive models may be formulated, and material parameters calibrated, the theory may fill the gap between microstructural and macroscopic continuum length scales. The aim of the paper is to provide insight into micromorphic continuum mechanics, including the linkage between micro- and macro-element deformation, through numerical examples comparing static micromorphic and micropolar elasticity, while investigating the effects of boundary conditions which will influence the "length-scale effect." A 3D large deformation FEA framework for materially-linear isotropic micromorphic elastic materials is developed and applied to illustrate the effects of independent microstructural deformation on the macroscopic micromorphic and micropolar continuum-scale responses.

A Materials Scientists View of Crystal Plasticity -- The OOF Project

Andrew Reid^{*}, Shahriyar Keshavarz^{**}, Stephen Langer^{***}

^{*}NIST, ^{**}NIST / Theiss Research, ^{***}NIST

ABSTRACT

The OOF software tool, developed at the National Institute of Standards and Technology, is designed to allow users with a materials science background to quickly and flexibly assess the behavior of possibly complex microstructures, using as inputs an image of the microstructure, and the constitutive properties of the phases making up the system. Users do not have to be experts in the relevant physics, nor in the underlying Finite Element mathematics, in order to undertake useful explorations of structure-property relationships. As initially constructed, the software was principally focussed on solving problems that are easily posed as partial differential equations, including nonlinear and time-dependent PDEs. This covers a large fraction of materials problems, but is ultimately not sufficient to solve interesting problems in solid mechanics. A current development focus for this tool is the incorporation of crystal plasticity into the tool. Efforts so far have proven to be a useful exercise in testing the extensibility of the code, as well as in abstracting the large space of crystal plastic constitutive rules and techniques into categories of use and interest to our materials. This talk will focus on the progress to date in incorporating crystal plasticity into the OOF code, as well as related projects which have arisen from a materials-focused approach to crystal plasticity, including some potentially useful statistical approaches.

Expressing the Differences in Code Optimizations between Intel Knights Landing and NEC SX-ACE Processors

Thorsten Reimann^{*}, Hiroyuki Takizawa^{**}, Kazuhiko Komatsu^{***}, Takashi Soga^{****}, Ryusuke Egawa^{*****}, Akihiro Musa^{*****}, Hiroaki Kobayashi^{*****}

^{*}Technische Universität Darmstadt, ^{**}Tohoku University, ^{***}Tohoku University, ^{****}Tohoku University, ^{*****}Tohoku University, ^{*****}Tohoku University, ^{*****}Tohoku University

ABSTRACT

The latest processor of the Intel Xeon Phi architecture, called Knights Landing (KNL), has AVX-512 instructions for efficiently executing “vectorizable” loops, and one might hence consider that it is a kind of vector processors. However, code optimizations for KNL could be different from those for orthodox vector processors. This work thus discusses the differences in code optimizations between orthodox vector computing systems and KNL. In this case study, an incompressible flow solver, FASTEST, is optimized for a vector computing system, NEC SX-ACE. In addition to restructuring its kernel loops to help compiler’s vectorization, we employ the wavefront reordering for increasing the vector length of the most time-consuming kernel, called the SIPSOL kernel. That is, the FASTEST code is optimized so that it can achieve a higher performance on the SX-ACE system. Then, the KNL performance for the optimized FASTEST code is evaluated to discuss the similarities and differences in code optimizations between KNL and SX-ACE. The performance evaluation results show that code optimizations for KNL have certainly some similarities with those for vector computing systems such as SX-ACE, which mainly focus on increasing the lengths of innermost loops. However, some optimization techniques for SX-ACE obviously have negative impacts on the KNL performance. The wavefront reordering can increase the innermost loop length, and hence significantly improve the performance on the SX-ACE system. On the other hand, it also causes irregular memory access patterns and results in a higher cache miss ratio, leading to the KNL performance degradation. Accordingly, different processor architectures often require different code optimization techniques. Finally, we use the Xevolver code transformation framework to express system-specific code optimizations as user-defined code transformations. By using some custom code transformation rules, we can transform the original FASTEST code in different ways, depending on the target system, i.e., KNL or SX-ACE. As a result, we can achieve not only high performance but also high performance portability across different systems without maintaining multiple versions of a kernel for each system. In the case where a kernel already has multiple versions, each of which is optimized for a different system, Xevolver allows users to even simplify the kernel by preserving only one version and removing the others. The removed versions can be generated by transforming the remaining one if a rule for the code transformation is properly defined. Maintaining only a single version of each kernel is beneficial to keep the whole code tractable.

The Local Cohesive Zone Method for Efficient Modelling of Delamination in Large Composite Structures Under Low Velocity Impact

Johannes Reiner*, Reza Vaziri**

*The University of British Columbia, **The University of British Columbia

ABSTRACT

Damage tolerance is an advantageous characteristic of composite materials. Computational models for structural design solutions need to consider interlaminar delamination in composite laminates in order to represent their behavior more realistically and utilize their full potential and weight saving benefits. Within Finite Element Analysis (FEA), the Cohesive Zone Method (CZM) is a common tool to simulate initiation and growth of interlaminar cracks. Detailed modelling of pre-inserted interconnecting cohesive elements between different plies is required to accurately capture the mechanics of separation of plies. This leads to high modelling complexity and computational cost. Hence, such models are not feasible to use in large-scale industrial applications. The Local Cohesive Zone Method (LCZ) [1] is a novel computational concept to adaptively insert cohesive elements only within local regions where interlaminar delamination has the potential to initiate. Computational cost is significantly reduced which makes the method applicable to large-scale composite structures. LCZ is verified and validated against composite structures in Mode I, Mode II and Mixed-Mode fracture tests [1] as well as under axial crushing and transverse impact loading [2]. We are presenting the latest modifications and applications of LCZ with regards to low velocity impact simulations of automotive carbon fiber reinforced composite structures. Implemented in the commercial FE solver LS-DYNA, interlaminar damage in LCZ is combined with intralaminar continuum damage models to account for matrix and fiber damage. Results are compared with conventional interlaminar modelling techniques using pre-inserted cohesive elements. References: [1] Shor, O., & Vaziri, R. (2015). Adaptive insertion of cohesive elements for simulation of delamination in laminated composite materials. *Engineering Fracture Mechanics*, 146, 121-138. doi:<http://dx.doi.org/10.1016/j.engfracmech.2015.07.044> [2] Shor, O., & Vaziri, R. (2017). Application of the Local Cohesive Zone Method to Numerical Simulation of Composite Structures under Impact Loading. *Engineering Fracture Mechanics*, 104, 127-149. doi: <https://doi.org/10.1016/j.ijimpeng.2017.01.022>

Damage Analysis of Shells Using a Consistent Anisotropic Puck-based Damage Model for Laminated Fiber-reinforced Composites

José Reinoso^{*}, Giuseppe Catalanotti^{**}, Ana Vallecillos-Portillo^{***}, Antonio Blázquez^{****},
Federico París^{*****}, Pedro P. Camanho^{*****}

^{*}Universidad de Sevilla, ^{**}Queen's University Belfast, ^{***}Universidad de Sevilla, ^{****}Universidad de Sevilla,
^{*****}Universidad de Sevilla, ^{*****}Universidade do Porto

ABSTRACT

The engineering use of carbon and glass fiber-reinforced polymer (CFRP and GFRP, respectively) composites has significantly increased in the last three decades. This tendency is especially relevant in aerospace and aeronautical components, whereby their superior material properties in terms of their specific stiffness and strength ratios play a central role. The exploitation of the load bearing capacities of such materials requires a comprehensive understanding of the different damage mechanisms that characterize their mechanical performance. On the basis of composite laminates, damage events can be arranged into two principal categories: (i) interlaminar failure (delamination), and (ii) intralaminar failure. From the computational point of view, FEM has been the most popular method to develop computational models that allows triggering this inelastic response upon failure. In this contribution, a novel anisotropic damage criterion for intralaminar damage in laminated fiber-reinforced composites using the 3D-version of the Puck failure criterion is presented [1]. This failure theory distinguishes between inter-fibre fracture (IFF) and fibre fracture (FF) which are accounted for through the definition of the corresponding set of damage variables. The current model specifically complies with the thermodynamic consistency by means of exploiting the additive decomposition of the Helmholtz free-energy function [2]. Additionally, the model endows: (i) an energetic-based evolution for the corresponding damage variables and (ii) the derivation of the consistent tangent operator to be integrated into a nonlinear FE solution scheme. Derived from its 3D character, the proposed model is integrated into a solid shell element to model intralaminar damaged in thin-walled structures. The solid shell formulation herein used relies in the mixed-enhanced formulation. Finally, the proposed model is assessed by means of several examples, exhibiting an excellent accuracy with respect to experimental data. References [1] Puck, A., Schürmann, H. Failure analysis of frp laminates by means of physically based phenomenological models. *Compos Sci Technol*, 62:1633–1662, 2002. [2] Reinoso, J, Catalanotti, G., Blázquez, A., Areias, P, París, F., Camanho, P.P. A consistent anisotropic damage model for laminated fiber-reinforced composites using the 3D-version of the Puck failure criterion. *Int. J. Solids and Structures*, 126-127:37-53, 2017.

Adaptive Curvilinear Meshing

Jean-François Remacle^{*}, Amaury Johnen^{**}, ruili zhang^{***}

^{*}Université catholique de Louvain, ^{**}Université catholique de Louvain, ^{***}Université catholique de Louvain

ABSTRACT

Assume a unit square $(x,y) \in [0,1] \times [0,1]$ and a smooth function $f(x,y)$ defined on the square. The question we want to address is the following: is it possible to compute the P^2 mesh with N triangles that minimizes the approximation error? Note of course that the elements of our optimized mesh have the freedom to be curved. In this talk, we present a way to generate such a mesh.

Ductile Rupture under Cyclic Loadings conditions

Al Mahdi Remmal*, Jean-Baptiste Leblond**, Stephane Marie***

*Framatome - Sorbonne Université, Faculté des Sciences et Ingénierie (formerly Université Pierre et Marie Curie), CNRS, UMR 7190, Institut Jean Le Rond d'Alembert, **Sorbonne Université, Faculté des Sciences et Ingénierie (formerly Université Pierre et Marie Curie), CNRS, UMR 7190, Institut Jean Le Rond d'Alembert, ***Framatome

ABSTRACT

It is known that for ductile porous materials, cyclic loadings lead to lower fracture strains than monotone ones. This reduction of ductility probably arises from an effect called "ratcheting of the porosity" [1] that consists of a continued increase of the mean porosity during each cycle with the number of cycles. Finite element based micromechanical simulations [2] confirmed this interpretation. Recently [3], the authors proposed a Gurson-type "layer model" better fit than Gurson's original one, which does not predict the ratcheting of the porosity, for the description of the ductile behavior under cyclic loading conditions. A very good agreement was obtained between the results of the micromechanical simulations and the model predictions for a rigid-hardenable material. Yet, the ratcheting of the porosity is a consequence of both hardening and elasticity; and the theory of sequential limit analysis used [3] in order to get the "layer model" is strictly applicable in the absence of elasticity. Based on an expression of the porosity rate accounting for elasticity, a proposal is made to improve the new model with regard to elasticity. This proposal is assessed through comparison of its predictions with the results of micromechanical simulations and with the results of tests on notched tensile and Compact Tensions specimens subjected to cyclic loadings. [1] P. Gilles, B. Jullien and G. Mottet. Analysis of cyclic effects on ductile tearing strength by a local approach of fracture, *Advances in Fracture/Damage Models for the Analysis of Engineering Problems*, ASME Publication AMD - Vol. 137, pp. 269-284, 1992. [2] J. Devaux, M. Gologanu, J.B. Leblond and G. Perrin. On continued void growth in ductile metals subjected to cyclic loadings, *Proceedings of IUTAM Symposium on Nonlinear Analysis of Fracture*, Cambridge, GB, J. Willis, ed., Kluwer, pp. 299-310, 1997. [3] L. Morin, J.C. Michel, and J.B. Leblond. "A Gurson-type layer model for ductile porous solids with isotropic and kinematic hardening." *International Journal of Solids and Structures* 118 (2017): 167-178.

Study on Hydraulic Concrete Cracking Criterion in Smearred Crack Numerical Model

Qingwen Ren^{*}, Yajuan Yin^{**}

^{*}Hohai University, ^{**}Hohai University

ABSTRACT

The representative volume element (RVE) is defined as the smallest volume element, but sufficiently large to represent the effective properties of a composite at a large scale. It plays an important role in the study of concrete properties. Meanwhile, the RVE size determination itself is an issue that needs further study. Primarily, the RVE itself can be the measured object in laboratory testing of the macroscopic properties of material. Another advantage of RVE is related to the mechanistic modelling of concrete mixtures. Recently, the calculation meso-mechanical model has drawn more and more attention from the community of concrete mechanics, in an effort to establish the relationship between meso-structure and macro-mechanical properties when studying the failure of heterogeneous materials, which involves the two dimensions of meso and macro scales. For the first time, the problem of determining RVE size based on several factors is regarded as a multi-objective decision-making problem. A new method of entropy weight–grey correlation model is proposed, by comprehensively considering the influence of coarse aggregate content, aggregate average particle size and aggregate fineness modulus. A two-dimensional concrete aggregate specimen, randomly generated by numerical simulation with aggregate size of 5–20 mm, is taken as a case study, and the RVE size is determined as 6–7 times the maximum aggregate size. Then the finite-element method is used to verify its mechanical properties. This new method has an advantage of less dependency on variable data over the traditional method, indicating a wider range of applicability. Additionally, the model is applied to determine the RVE size of three-dimensional concrete, which is similar to two-dimensional concrete. It provides a new comprehensive insight for the study of concrete RVE size, which could also be extended to apply to the RVE determination of other composite materials. Acknowledgements: The financial supports provided by the National Natural Science Foundation of China (51739006)

Modeling and Simulation of Moving Contact Lines in Multi-phase Fluids

Weiqing Ren*

*National University of Singapore and IHPC

ABSTRACT

Contact line forms when a fluid interface intersects with a solid wall. The moving contact line problem is a classical problem in fluid mechanics. The difficulty stems from the fact that the classical Navier-Stokes equation with no-slip boundary condition predicts a non-physical singularity at the contact line with infinite rate of energy dissipation. Many modified continuum models have been proposed to overcome this difficulty. Though they all succeed in removing the singularity, it is not clear whether they describe the real physics near the contact line region. In this talk, we will discuss how the continuum theory, molecular dynamics and the more recently developed multiscale techniques can be combined to give us a better understanding of the fundamental physics of the moving contact line and formulate simple and effective models. We also illustrate how this model can be used to analyze the behavior of the apparent contact angle, hysteresis and other important physical problems for the moving contact line. [1] W. Ren, P. H. Trinh and W. E, On the distinguished limits of the Navier slip model of the moving contact line problem, *J. Fluid Mech.* vol 772, 107-126 (2015) [2] W. Ren, D. Hu and W. E, Continuum models for the contact line problem, *Phys. Fluids*, vol 22, 102103 (2010) [3] W. Ren and W. E, Boundary conditions for the moving contact line problem, *Phys. Fluids*, vol 19, 022101 (2007)

High-Fidelity T-Spline Based Isogeometric Analysis for 3D Complex Structures

Xiang Ren^{*}, Yongjie Jessica Zhang^{**}, Jim Lua^{***}, Xiaodong Wei^{****}

^{*}Global Engineering & Materials, Inc., ^{**}Carnegie Mellon University, ^{***}Global Engineering & Materials, Inc.,
^{****}Carnegie Mellon University

ABSTRACT

Isogeometric analysis (IGA) has shown its attractive feature recently for integrating a Finite Element Analysis (FEA) and Computer Aided Design (CAD) into a single unified process. For stress analysts, it is common practice to convert a spline/NURBS based CAD model to polynomial based finite element mesh for analysis. However, for complex geometries such as optimized 3D printing objects, it is known that smooth curvature cannot be exactly reserved by the discretized finite element mesh. As a consequence the simulation results can either be imprecise due to the geometric misrepresentation or a great larger number of degrees of freedom is needed to achieve a convergent solution. As such, T-spline based 3D IGA is developed by us to fill the gap. A 3D CAD geometry is first automatically converted to a T-spline control mesh, and then converted to analysis suitable T-spline elements for a high fidelity analysis. With unified and higher order T-spline basis functions selected for the geometry representation, FEA is directly conducted on the smooth CAD geometry without loss of any key design details. By taking advantage of the Bézier transformation, FEA is conducted by implementing IGA via customization of Abaqus' user-defined elements (UELs). To further enhance the IGA analysis capability without strong reliance on the generation of an analysis suitable T-spline for the entire geometry, a hybrid "T-spline and finite element" modeling approach is developed to preserve the smooth surface geometry of a complex 3D object. To accurately prescribe boundary conditions for an IGA solution domain, special algorithms are implemented for mapping both Cauchy and Dirichlet type boundary conditions from a physical boundary to the control points. A suite of numerical examples are selected to demonstrate the accuracy and rate of convergence for the stress response prediction of complex 3D components.

Phantom Paired Elements Approach for Matrix Cracking and Segmented Cohesive Interface for Failure Prediction of Composite Laminates

Xiang Ren^{*}, Xiaodong Cui^{**}, Jim Lua^{***}

^{*}Global Engineering and Materials, Inc., ^{**}Global Engineering and Materials, Inc., ^{***}Global Engineering and Materials, Inc.

ABSTRACT

Modeling and characterization of discrete damage and interaction of matrix cracks and interface delamination have received growing interests for the failure analysis of composite structures due to its ability to capture mechanisms of energy dissipation associated with crack and delamination failure progression. Fracture mechanics based approaches coupled with a kinematic description of discrete cracks have been extensively developed based on XFEM, RXFEM, AFEM, floating node, or phantom paired elements approaches. A key problem that has not been well addressed is an accurate characterization of the interaction of matrix cracks and interface delamination when matrix cracks of different orientations from the top or bottom ply intersect a ply interface, namely the 'segmented cohesive interface'. The bridging forces (Mode I & Mode II) applied by a segmented cohesive interface on the surfaces of matrix cracks located on the top or bottom side of the interface are essential not only in capturing the stiffness but also the dissipated energy of the cracked layer system (cracked ply bonded by segmented cohesive interface). In the literature, a superimposed approach based on a cohesive interface cut by matrix cracks from its top and bottom was used and the combined bridging effects were characterized via an average approach assuming an equal contribution from the cracked interface from its top and bottom side. In order to better characterize the bridging effect of the segmented cohesive interface, an energy based phantom paired elements approach is developed for the cracked layer system to describe kinematic admissible displacement discontinuities without introducing a conforming mesh. A subdomain energy superposition is used to determine the overall response of the segmented cohesive interface influenced by its top and bottom side. A verification study is performed to examine its validity and effects of segmented cohesive interface using an Abaqus model of a conforming mesh for a given cracked configuration. Application examples are used next to demonstrate the proposed method for the discrete damage characterization and failure prediction driven by the evolution of matrix cracking, interface delamination, and their synergistic effect.

An Unbiased Nitsche's Formulation for Frictional Contact and Self-contact : Numerical Integration Aspects

Yves Renard^{*}, Franz Chouly^{**}, Rabii Mlika^{***}

^{*}INSA-Lyon, ^{**}Université de Franche Comté, ^{***}INSA-Lyon

ABSTRACT

In this work, we present a formulation of frictional contact between two elastic bodies based on Nitsche's method. Nitsche's method was adapted for unilateral contact in [1]. It aims to treat the interface conditions in a weak sense, thanks to a stabilized consistent term. At first, we introduce the study carried out in the small strain framework for an unbiased version of the method. The non-distinction between a master surface and a slave one will allow the method to be more generic and directly applicable to the self-contact problem. The restrictive framework of small strain and Tresca friction allowed us to obtain theoretical results on the consistency and convergence of the method (see [2]). Our Nitsche's method is then extended to the large strain case more relevant for industrial applications and situations of self-contact. The method is formulated for an hyper-elastic material and declines in the two versions: biased and unbiased. As in [1], we describe a class of methods through a generalization parameter γ . Particular variants have different properties from a numerical point of view, in terms of accuracy and robustness. To prove the accuracy of the method for large deformations, we provide several validation tests (Taylor patch test, elastic half ring, cross tubes ...). The description of the method and all the results are detailed in [3]. The presentation will focus on the influence of numerical quadrature on the accuracy and convergence of the method. This study covers a comparison of several integration rules (element-based, segment-based, non-symmetric integration) proposed in the literature for other integral methods. References [1] F. Chouly, P. Hild, and Y. Renard. Symmetric and non-symmetric variants of Nitsche's method for contact problems in elasticity: theory and numerical experiments. *Mathematics of Computation*, 84:1089–1112, 2015. [2] F. Chouly, R. Mlika, and Y. Renard. An unbiased Nitsche's approximation of the frictional contact between two elastic structures. To appear in *Numerische Mathematik*, Available on HAL as hal-01240068, 2016. [3] R. Mlika, Y. Renard, and F. Chouly. An unbiased Nitsche's formulation of large deformation frictional contact and self-contact. *Computer Methods in Applied Mechanics and Engineering*, 325(Supplement C):265 – 288, 2017.

Discontinuous Galerkin Material Point Method for Hyperbolic Problems in Solid Mechanics

Adrien Renaud^{*}, Laurent Stainier^{**}, Thomas Heuzé^{***}

^{*}Ecole Centrale of Nantes, ^{**}Ecole Centrale of Nantes, ^{***}Ecole Centrale of Nantes

ABSTRACT

A wide variety of physical problems in solid mechanics, such as impact on structures or high-speed forming techniques, involve waves propagating in solids submitted to large strains. The Material Point Method is now well established as an effective tool for dealing with finite deformations due to the use of particles that can move in an arbitrary Eulerian grid. However, the MPM can be viewed as an extension of classical Finite Element Method with moving quadrature points and therefore inherits the high frequency noise introduced in the vicinity of discontinuities by classical time integrators. Oscillations are troublesome for tracking the paths of waves in order to accurately assess residual stresses and strains. On the other hand, Discontinuous Galerkin methods are based on discontinuous shape functions across element boundaries and allow the use of efficient tools to accurately track waves fronts. First, the DG approximation permits to introduce the characteristic structure of the solution of hyperbolic problems within a Finite Element scheme through the computation of interface fluxes. Second, numerical strategies developed for Finite Volume methods can be employed so as to build Total Variation Bounded or Total Variation Diminishing in the Means finite element schemes. The purpose of this work is to extend the MPM to the DG framework in order to accurately capture both continuous and discontinuous waves. The resulting Discontinuous Galerkin Material Point Method uses the same space discretization than that of the MPM with an arbitrary computational grid supporting the DG approximation. Interface fluxes arising in the weak form of a system of conservation laws, written element-by-element on the reference configuration, are computed by means of an approximate Riemann solver. As for MPM, projection steps are required since particles carry all the fields of the problem while discrete equations are solved at nodes. A von Neumann stability analysis shows that the DGMPM can be used with a less restrictive Courant condition compared to that of the MPM and the DGFEM. In particular, a special space discretization yields the optimal CFL condition. This method is illustrated and compared to the original MPM and a developed analytical solution on one-dimensional problems, and to the classical FEM for two-dimensional ones. D. Sulsky, Z. Chen, H. L. Schreyer, A particle method for history-dependent materials, *Computer methods in applied mechanics and engineering* 118 (1-2) (1994) 179–196. B. Cockburn, Discontinuous galerkin methods for convection-dominated problems, *High-order methods for computational physics*, Springer, 1999, pp. 69–224.

Multiscale Strategy for Modelling the Mechanical Performance of Hook and Loop Fasteners Based On a Detachment Process Zone Model: Mode I

Vanessa Restrepo*, Pablo Zavattieri**, Chris Gallant***

*Purdue University, **Purdue University, ***Velcro USA Inc

ABSTRACT

Inspired by the natural mechanism of burdock burr seed, George de Mestral created a provisional and reversible closure system based on hooks and loops fasteners. The mechanics and physics involved in the detachment process of the hook and loop fastener are complex but present an excellent opportunity for the development of novel modelling strategies. A multiscale mechanical model that can capture the right mechanics of the hook and loop mating was developed through a bottom-up approach. The main dissipative mechanisms, the deformation and failure modes, and relevant length scales were explicitly incorporated into a high-fidelity micromechanical model of a Representative Hook and Loop Element (RHLE). An algorithm generates the fibrous surface taking into account the random variation on the geometric parameters of the material. The mechanical behaviour of polypropylene microfibers was characterized by a tensile set of experimental data and ESEM imaging. Subsequently, a macroscopic model was developed, where the length scale at which the entire specimen in the peel test is modelled explicitly. The information obtained from the RHLE model is bridged with the macroscopic model through a User-defined cohesive model (Park et al., 2009) inside the Detachment Process Zone (DPZ). Experimental and numerical peel tests were created to validate the accuracy of the multiscale model. The model accurately captures the mechanical performance of the fastening joint given a geometrical description and material information of the hooks and loops. Therefore, the computational model facilitates the design process and predictions allowing for quick changes and tests in the design parameters and virtually testing the performance of the new fasteners. Keywords: multiscale model, computational model, detachment process zone, hook and loop fasteners. Park, K., Paulino, G.H., Roesler, J.R., 2009. A unified potential-based cohesive model of mixed-mode fracture. *J. Mech. Phys. Solids* 57, 891–908. <https://doi.org/10.1016/j.jmps.2008.10.003>

Cementitious Composites Based on Bismuth Oxide Nanoparticles for X-ray Shielding

Luciana Restuccia^{*}, A. Favero^{**}, Giuseppe Ferro^{***}, Pravin Jagdale^{****}

^{*}Politecnico di Torino, ^{**}Politecnico di Torino, ^{***}Politecnico di Torino, ^{****}Politecnico di Torino

ABSTRACT

In this research work, a new kind of composite produced with the addition of Bismuth oxide nanoparticles has been investigated, to enhance the x-ray shielding properties of cement-based materials. Bismuth - a cheap, non-toxic and biocompatible element, characterized by having a high atomic number Z ($Z=83$) - has been used as additive by considering different percentages of addition (1%, 5% and 10% with respect the weight of cement for each composition). The experimental activity was focused on the preparation of cement-paste samples with and without addition of bismuth oxide nanoparticles. Water deionized and Portland-Limestone Cement (CEM II/B-LL 32,5 R) were used with a w/c ratio equal to 0.50. X-ray shielding effectiveness has been investigated by using a CT-Scanner for medical tomography: samples have been exposed to the ionising radiations afterwards the 28 days curing time for the complete cement hydration. Through the processing of the data acquired by the CT scanner it has been possible to appreciate the good reactivity of the new cement composites. The radio-opacity of the samples is directly related to the content of bismuth oxide nanoparticles: the higher the percentage, the opaquer they are. Furthermore, by analysing the averages of measurable ROI data for single slice (distance per slice: 4/10 mm), it has been possible evaluate the good homogeneous distribution of bismuth oxide nanoparticles added for each batch. The shielding properties shown by the experimental samples during the tests allow to state that bismuth can be used as a "smart" nanomaterial in cement-based composites, thanks to its chemical-physical properties and above all its non-hazardousness and its low cost.

Preconditioning for HDG and EDG: Stokes Problem

Sander Rhebergen*, Garth Wells**

*University of Waterloo, **University of Cambridge

ABSTRACT

In this talk we introduce optimal preconditioners for linear systems that arise from discretizing the Stokes problem by hybridizable and embedded discontinuous Galerkin finite element methods. This talk presents an initial step towards preconditioning space-time hybrid finite element methods for the Navier-Stokes equations. Recently we introduced hybrid finite element methods for the Stokes problem which were constructed such that the approximate velocity field is pointwise divergence free and $H(\text{div})$ -conforming [1]. The interesting aspect of these hybrid methods is that the discretization is pressure-robust, compatible with discontinuous Galerkin discretizations of transport equations and, in the case of the Navier-Stokes problem, our method is locally conservative and energy stable [2]. These properties are achieved by introducing a Lagrange multiplier to enforce normal continuity of the velocity field across facets and a Lagrange multiplier to penalize the fact that the approximate velocity field is not in H^1 . Typical of hybrid methods is that it is possible to eliminate element degrees of freedom from the linear system so that the Lagrange multipliers are the only globally coupled degrees of freedom. This static condensation significantly reduces the size of the discrete problem. This talk focusses on optimal preconditioners of these statically condensed linear systems. [1] S. Rhebergen and G.N. Wells, Analysis of a hybridized/interface stabilized finite element method for the Stokes equations. *SIAM J. Numer. Anal.*, Vol. 55/4, pp. 1982-2003, 2017. <https://doi.org/10.1137/16M1083839> [2] S. Rhebergen and G.N. Wells, A hybridizable discontinuous Galerkin method for the Navier-Stokes equations with pointwise divergence-free velocity field, 2017. Submitted. <http://arxiv.org/abs/1704.07569>

A Multi-Fidelity Approach for Aircraft Aero-Structural Optimization

Sergio Ricci^{*}, Alessandro De Gaspari^{**}

^{*}Politecnico di Milano, ^{**}Politecnico di Milano

ABSTRACT

The need for more efficient aircraft, coupled with a request for a significant reduction of the environmental impact, is driving the design of new. Despite the development of new numerical procedures and methods, as well the availability of more powerful computational tools, the development of a fully integrated Aero-structural optimization still represents a challenging goal. Martins in [1] presents a comprehensive overview of the current multidisciplinary design-optimization. The paper presents a multi-fidelity aero-structural design and optimization framework for the optimal design of aircraft wings taking into account the combination of aerodynamic and structural goals. The framework is mainly based on in-house developed tools that are combined in a weak but efficient way. In our case we adopted a typical conceptual design tool, named NeCASS, for the global analysis and aeroelastic optimization of the free flying full flexible aircraft. The structural model adopted is based on a stick representation of the structural components while the aerodynamic model is based on the classical VLM and DLM approaches. While this level of fidelity is usually enough at conceptual design level, this is not true in case of more detailed aero-structural indices have to be included into the optimization loop. For this reason, two different fidelity enhancements are included. The first one concerns the structural model, i.e. for each configuration analyzed a detailed wingbox is generated and optimized externally using the Nastran SOL200. The second fidelity enhancement includes a 2.5D module able to estimate the total Drag starting from the inviscid calculation. The aero-structural coupling is weakly defined by imposing the deformed shape resulting from the aeroelastic trimmed configuration on the aerodynamic mesh used for the Drag estimation. The obtained procedure is driven by a DOE engine to sample the design space that includes also geometrical design variables such as the aspect ratio and the swept angle. The results of the DOE analysis are used for a multi objectives optimization able to offer to the designer a Pareto front on which pick up the most promising configuration. The results concerning an application example will be included in the final paper. [1] Joaquim R. R. A. Martins and Andrew B. Lambe. "Multidisciplinary Design Optimization: A Survey of Architectures", AIAA Journal, Vol. 51, No. 9 (2013), pp. 2049-2075.

Fluid Forces Acting on a Confined Oscillating Cylinder

Guillaume Ricciardi*

*CEA Cadaracge

ABSTRACT

Earthquakes can irreversibly damage nuclear power plants especially in the core, where the nuclear fuel assemblies containing enriched uranium dioxide have to be particularly resistant. Before building a nuclear power plant, it is necessary to make sure that the core will resist the worst possible earthquake conditions liable to occur at the reactor site. Therefore, safety measures are required to insure the drop of control rods and that the core is cooled when the fuel assembly spacer grids strike each other during seismic excitation of a Pressurized Water Reactors. A way to insure these two criteria is to prevent the spacer grids from buckling. Engineers need special tools for designing and maintaining reactor cores. The reactor core made of fuel assemblies is subjected to an axial water flow to cool the reactor. The flow strongly modifies the dynamical behaviour of the fuel assemblies which is made of cylinders; therefore the identification of the fluid forces is important to provide a relevant modelling of the fuel assemblies' behaviour. It is proposed in this paper to perform turbulent CFD of a cylinder in a confined flow accounting for moving boundaries. An ALE method is used for the moving boundaries and a k epsilon model is applied for the turbulence. The Reynolds number is about 50 000. Dynamic simulations are compared the steady simulation with an inclination of the cylinder. Simulations are made for various flow velocities and inclinations. Results are compared to literature and experimental results.

A Continuum Mechanical Bi-scale PDE-ODE Multiphase Model for Alloy Solidification Processes Including Columnar to Equiaxed Transition (CET)

Tim Ricken^{*}, Lukas Moj^{**}, Carla Henning^{***}

^{*}University of Stuttgart, ^{**}University of Stuttgart, ^{***}University of Stuttgart

ABSTRACT

ABSTRACT: Numerical hot working process simulations have gained significant importance for steel making industries in order to improve manufacturing. Hence, a thermal driven, bi-phasic, two-scale model consisting of a macro and a micro scale for describing thermo-mechanical loading as well as the physics of solidification is presented. A special focus will be given on the description of the columnar to equiaxed transition (CET). Macro-Scale: At macro level, the solid and liquid phases represent the steel physical states based on the theory of porous media (TPM) , cf. DE BOER [2000]. Following the concept of volume fraction, a local, discrete, spatial resolving of the phases is not required. The steel mechanical properties are strongly temperature dependent. Therefore, finite plasticity superimposed by a secondary power creep law as well as finite viscoelasticity are utilized for the solid and the liquid phase, respectively. One temporal and place dependent temperature field for both phases without any interface energy exchange is assumed This macro-level description leads to a coupled partial differential equation (PDE) system. Micro-Scale: On micro-scale, the solidification behavior is described by a coupled ordinary differential equation (ODE) system based on a diffusion-driven dendrite growth model cf. WANG & BECKERMANN [1993]. This process description enables tracking of the transition between columnar and equiaxed dendritic growth (CET), and the influence of solute diffusion on the solidification progression. The strong coupling between volume fractions and concentrations of the alloying element considers the ejection of atoms from the crystal lattice and the associated change in solidification temperature range. Example: This two scale PDE-ODE approach has been already successfully applied from our group. This process description enables tracking of the transition between columnar and equiaxed dendritic growth (CET), and the influence of solute diffusion on the solidification progression. The strong coupling between volume fractions and concentrations of the alloying element considers the ejection of atoms from the crystal lattice and the associated change in solidification temperature range. By means of significant examples, the model approaches and the scale coupling will be presented, as well as pro and cons will be discussed. REFERENCES: de Boer, R. 2000, "Theory of Porous Media", Springer, New York. Wang, C.Y., and Beckermann, C. (1993), "A Multiphase Solute Diffusion Model for Dendritic Alloy Solidification," Metall. Trans. A, Vol. 24A, pp. 2787-2802.

Data Analytics Using Canonical Correlation Analysis and Monte Carlo Simulation

Jeffrey Rickman*

*Lehigh University

ABSTRACT

We describe the use of correlation analyses, coupled with Monte Carlo simulation, to solve data-intensive problems in materials science and engineering. With this approach, one can identify important, possibly non-linear, relationships among materials processing variables and properties, thereby reducing the dimensionality of large data spaces. We demonstrate the utility of our approach by considering two applications, namely 1.) determining the interdependence of processing and microstructural variables associated with doped polycrystalline aluminas, and 2.) relating microstructural descriptors to the electrical and optoelectronic properties of thin-film solar cells. Finally, we describe how this approach facilitates experimental planning and process control.

Small Changes with Large Impact: Developing Multiscale Models to Understand How Chemical Structure Impacts the Performance of Organic Semiconductors

Chad Risko*

*University of Kentucky

ABSTRACT

Semiconducting materials derived from organic, π -conjugated molecules or polymers have drawn the attention of materials chemists for decades because of the potential to modulate material (opto)electronic properties through well-established synthetic chemistry methods. Unfortunately, materials design remains highly Edisonian, due to limited knowledge of the intimate relationships that connect chemical composition and molecular architecture, materials processing, and the solid-state packing arrangements that determine material performance. We seek to address these connections through the development and application of multiscale, theoretical materials chemistry approaches that build upon principles from organic and physical chemistry, condensed matter physics, and materials science. In this presentation, we will focus on how these models can reveal the striking influence of seemingly modest changes in chemical structure on the processing and solid-state packing of organic semiconducting active layers and resulting materials characteristics. The chemical insight developed through these investigations is beginning to refine and offer novel design paradigms essential to the development of next generation organic semiconducting active layers, and is opening new pathways for in silico materials development.

Stochastic Modelling of Hysteretic Bit-Rock Interaction for Torsional Vibrations of a Drill-String

Thiago Ritto*, Fabio Real**, Anas Batou***, Christophe Desceliers****

*UFRJ, **INMETRO, ***University of Liverpool, ****Université Paris-Est

ABSTRACT

This paper aims at constructing a stochastic model for the hysteretic behaviour of the nonlinear bit-rock interaction of a drillstring under torsional vibrations, based on field data. The proposed model takes into account the fluctuations of the stick-slip oscillations and the hysteretic effect observed during the drilling process. Two nonstationary random processes are taken into account in this work, reproducing the high-frequency (added to the mean torque curve) and the low-frequency (multiplied to the mean torque curve) fluctuations, in order to represent the variation of the fluctuations with the bit speed, and the variations of independent stick-slip cycles respectively. The parameters of the proposed model for nominal hysteretic nonlinear torque are identified cycle by cycle with the least square method, in order to calculate the average parameters for the global nominal model. The coefficient of variation and the correlation length of high-frequency fluctuations are obtained for the stick-slip cycles as a part of the added stochastic fluctuations. Then, correlation length and one parameter that depends on the standard-deviation are identified to construct the low-frequency fluctuations over the independent stick-slip cycles. A nonlinear function of the bit speed is proposed, completing the model for the added fluctuations. Finally, independent trajectories of the proposed stochastic model are generated and used to simulate the stochastic response of the drillstring torsional dynamics in presence of random bit-rock interaction. The numerical results are compared with field data obtained from a 5km drillstring. Ritto, T. G., Soize, C., Sampaio, R., 2009, Nonlinear dynamics of a drill-string with uncertain model of the bit-rock interaction. *International Journal of NonLinear Mechanics*, vol. 44, no. 8, pp. 865-876. Ritto, T. G.; Aguiar, R.R. ; Hbaieb, S. . Validation of a drill string dynamical model and torsional stability. *Meccanica*, v. 52, p. 2959-2967, 2017.

Leveraging GPUs and the Multiple-Program Multiple-Data (MPMD) Computing Model to Enable Material-Aware Topology Optimization

Joshua Robbins^{*}, Miguel Aguilo^{**}, Thomas Voth^{***}, Brett Clark^{****}

^{*}Sandia National Laboratories, ^{**}Sandia National Laboratories, ^{***}Sandia National Laboratories, ^{****}Sandia National Laboratories

ABSTRACT

Additive Manufacturing (AM) expands the engineering design space by enabling creation of freeform geometries that can be driven by performance requirements rather than manufacturing constraints. Widespread adoption of this technology has been slow due to limitations in printed material quality and accompanying difficulties in part qualification. The most common approach in overcoming this qualification challenge is to pursue improvements in AM processes and resulting material quality. Alternatively, material imperfections can be incorporated into the design optimization problem so that designs are robust to deviations from the ideal material, thereby enabling the use of AM technology “as-is”. This presentation will cover the development of optimization based design tools that facilitate component qualification by accounting for AM material quality in the optimization process. By composing objectives that reflect details of the as-printed material, designs can be computed that i) use existing, well characterized AM processes, and ii) meet essential performance requirements. These tools use the multiple-program multiple-data (MPMD) computing model to distribute the evaluation of solutions, objectives, and gradients to available computing resources – including GPUs. Details of the formulation and implementation will be presented along with example applications that demonstrate our approach.

OceanMesh2D: A MATLAB Toolbox for 2-D Finite Element Mesh Development for Coastal Circulation Problems

Keith Roberts^{*}, Joannes Westerink^{**}, William Pringle^{***}

^{*}University of Notre Dame, ^{**}University of Notre Dame, ^{***}University of Notre Dame

ABSTRACT

Often, the most laborious process of geophysical finite-element type numerical simulations involve designing a “good” mesh that captures the features of interest adequately. Many times, the mesh is developed tediously through trial-and-error within a graphical user interface. This is undesirable because 1) it is not reproducible, 2) the development process is not objective, and 3) it frequently requires topological adjustments to ensure numerical stability and to correct flow conveyance. We present a toolbox written with an object oriented programming style in MATLAB to eliminate 1) and 2) and significantly reduce 3), the frequency of post-development adjustments to the mesh. The toolbox can construct large (> 5 million vertices), high quality and objectively built meshes in short computational times (< 1 hours) on an ordinary desktop machine. The mesh resolution is based on objective edge length functions that are derived from digital elevation models (DEMs). The mesh generation algorithm is based on the work of DistMesh2D (Persson and Strang, 2004) but with many improvements for quality solutions in large domains with irregular coastlines. Edge length functions determine how much resolution certain topographic length scales receive based on the following considerations: nodes per wavelength of the dominant tidal species nodes per topographic slope nodes to resolve geometrically complex nearshore features high resolution in deep-draft channels which funnel fluid flow. The edge length function is checked and adjusted to prevent CFL violations and for steep-transitions in mesh resolution. Additionally, the ability to design floodplain meshes where logic based wetting and drying severely limits numerical stability is considered. We illustrate the capabilities of the OceanMesh2D with some mesh sensitivity experiments using the Advanced CIRCulation (Luettich and Westerink 1991) model. The results motivate the selection of parameters used for the edge length function, which improve the objectivity in the mesh development process. In general, we show that meshes created with OceanMesh2D have fewer vertices than meshes developed by hand but have a comparably higher resolution nearshore Luettich, Rick, Westerink, Joannes, Scheffner, N.W.: (1991). ADCIRC: an advanced three-dimensional circulation model for shelves, coasts and estuaries. Coast. Eng. Res. Ct., US Army Engs. Wtrways. Experiment Station, Vicksburg, MS Report 1: Theory and Methodology of ADCIRC-2DDI and ADCIRC-3DL. Persson, Per Olof, Strang Gilbert (2004): A Simple Mesh Generator in MATLAB. SIAM Review, vol. 46 (2), pp. 329-345.

Camellia for DPG and Other Finite Element Methods: New(er) Capabilities and Plans

Nathan V. Roberts*, Brendan Keith**

*Sandia National Laboratories, **University of Texas at Austin

ABSTRACT

Camellia is a finite element library intended to facilitate rapid development of computationally efficient, hp-adaptive finite element solvers, starting with support for DPG. In the last couple of years, Camellia has gained several capabilities relevant to DPG and other high-order finite element methods. Among these, Camellia now supports discretizations involving C^0 continuous field variables, DPG* methods, and a platform for customized adaptive mesh refinement strategies, including goal-oriented strategies. In this talk, we will discuss these capabilities, including a new suite of tools for a posteriori error estimation with DPG* methods and some nascent work relating to running on next-generation platforms using Kokkos. [1] B. Keith and A. Vaziri Astaneh and L. Demkowicz. "Goal-oriented adaptive mesh refinement for non-symmetric functional settings." arXiv:1711.01996 [math.NA], 2017. [2] N. V. Roberts. "Camellia v1.0 Manual: Part I." Technical Report ANL/ALCF-16/3, Argonne National Laboratories, 2016.

Combination of Discrete and Finite Element Methods for Coupled Electrochemical-Mechanical Simulations of Lithium-Ion Battery Electrodes

Scott Roberts^{*}, Ishan Srivastava^{**}, Bradley Trembacki^{***}, Mark Ferraro^{****}, Jeremy Lechman^{*****}, David Noble^{*****}

^{*}Sandia National Laboratories, ^{**}Sandia National Laboratories, ^{***}Sandia National Laboratories, ^{****}Sandia National Laboratories, ^{*****}Sandia National Laboratories, ^{*****}Sandia National Laboratories

ABSTRACT

Discrete Element Methods (DEM) are a useful tool for capturing rheological behaviors of granular materials, such as those that arise during lithium-ion battery manufacturing processes, including coating and calendaring. We have extended the LAMMPS DEM simulator to realistically simulate the manufacturing of battery electrodes using experimentally-measured particle size distributions, physical particle interaction models of contact and cohesion, and realistic mechanical stresses introduced during manufacturing. This simulator has been used to create large mesostructures of NMC cathode particles at a wide variety of calendaring stresses. We will discuss these mesostructures and validate them against experimental data where available. The DEM-generated mesostructures are then fed into Finite Element Method (FEM) simulations of electrode performance, utilizing the Conformal Decomposition Finite Element Method (CDFEM) to efficiently create computable meshes of a large number of particles. We analyze the impact of manufacturing processes on relevant electrode-scale effective properties, such as electrical, ionic, and thermal conductivities. Sandia National Laboratories is a multi-mission laboratory managed and operated by National Technology and Engineering Solutions of Sandia, LLC., a wholly owned subsidiary of Honeywell International, Inc., for the U.S. Department of Energy's National Nuclear Security Administration under contract DE-NA0003525. Unclassified Unlimited Release: SAND2018-0016A.

The Role of Inter-constituent Mechanical Interaction in Left Ventricular Mechanics

Sara Roccabianca^{*}, Marissa Grobbel^{**}, Shavik Sheikh Mohammad^{***}, Stephanie Watts^{****}, Lik Chuan Lee^{*****}

^{*}Michigan State University, ^{**}Michigan State University, ^{***}Michigan State University, ^{****}Michigan State University, ^{*****}Michigan State University

ABSTRACT

Intro: Mechanical behavior of myocardial tissue is influenced primarily by two key constituents: myocytes and collagen fibers. These two constituents are often assumed to not be interacting mechanically in the tissue. However, an interaction between collagen fibers and myocytes may greatly influence the overall mechanical behavior of the myocardium. To better understand this interaction, opening angle tests were performed on intact left ventricular (LV) tissue and its isolated constituents. A constrained mixture with inter-constituent mechanical interaction (CMMI) modeling framework was then used to interpret experimental results. Methods: Ring-shaped tissue samples were extracted from LVs of healthy adult male rats. These samples were separated equally into three test groups: intact tissue, isolated myocytes, and isolated collagen fibers. Myocytes and collagen fibers were isolated through treatment with collagenase, and decellularization, respectively. We performed classical opening angle experiments [1] to quantify the contribution of the two constituents to overall LV residual stress. The CMMI modeling framework used was based on weighted strain energy function. Inter-constituent mechanical interaction in this framework was described by two parameters α_m and α_c that are, respectively, associated with the myocytes and collagen fibers stretch/compression when interacting mechanically. If the interaction is negligible, the CMMI framework should be able to predict the experimental opening angle without any interaction (i.e. $\alpha_m = \alpha_c = 1$). Results: Opening angles measured from the isolated collagen fibers ($106.45 \pm 23.02^\circ$) and isolated myocytes ($21.00 \pm 4.37^\circ$) were significantly higher and lower than the intact tissue ($57.88 \pm 12.29^\circ$), respectively. The traditional constrained mixture framework (i.e. no inter-constituent interaction) greatly overestimated the experimental opening angle. However, the experimental results were reproducible using the CMMI framework and introducing interaction described by the range of values from $\alpha_m = 0.1$ and $\alpha_c \leq 1.42$ to $\alpha_m = 0.9$ and $\alpha_c = 0.94$. Discussion: Results of the opening angle experiments allude to the idea that the collagen fibers are the key contributor to residual stress in the LV. Additionally, the traditional constrained mixture modeling framework was unable to reproduce the experimental results of this study without introducing some form of mechanical interaction between the collagen fibers and myocytes (CMMI). This interaction between constituents in intact cardiac tissue may greatly influence LV mechanics. References [1] Omens and Fung, Circ. Res., vol. 66, pp. 37-45, 1990.

SEPARATION OF MULTIPLE NATURAL FREQUENCIES IN TOPOLOGY OPTIMIZATION

Gustavo C. Rodrigues*, Ederval S. Lisboa*, João B. D. Moreira*, Fernanda B. Link* and
Walter J. P. Casas*

*Department of Mechanical Engineering, Federal University of Rio Grande do Sul
Rua Sarmiento Leite 425, 90050-170
Porto Alegre, Rio Grande do Sul, Brazil
www.ufrgs.br

Key Words: Frequency gaps, Natural frequencies, Topology optimization, Multiobjective Optimization.

Abstract. *In order to avoid mechanical resonance in vibrating structures, it is necessary to design said structures so that their natural frequencies do not coincide with their operational frequencies. Therefore, a machine with multiple modes of operation would need to avoid all of its resonant frequencies in each mode. As such, optimization algorithms can be used to search for a structural layout that maximizes the intervals between the different separated frequencies. This paper aims to accomplish the simultaneous separation of multiple distinct natural frequencies for various structures through the Bi-directional Evolutionary Structural Optimization (BESO) method of topology optimization. Introducing a set of variables representing the equipment's operational frequencies, the BESO algorithm is used to maximize the gap between the superior and inferior frequencies of said variables. As the separation of one pair of eigenfrequencies often affects the remaining eigenfrequencies of a structure, it is necessary to adopt a multi-objective formulation for the optimization problem. Therefore, to scalarize said problem the weighed sum method, where additional frequency intervals are added to the objective function, is utilized. The proposed method was implemented in the MATLAB programming environment and applied in examples of biclamped, unilaterally clamped and simply supported beams found in the literature. It is expected that different weighing coefficients within the optimization process result in varying frequency gaps in the final topologies. The resulting layouts and associated frequency gaps for each system are then presented. The results obtained by the proposed method demonstrate its applicability and efficiency for each case, and it is also shown that general Pareto frontiers for each analyzed system's frequency gaps can be inferred utilizing the resulting topologies.*

1. INTRODUCTION

Topology optimization techniques have become frequently used tools to aid designers and engineers when developing new products. Certain specifications, however, may come to impose limits on a product's natural frequencies, with the goal of avoiding structural mechanical resonance and failure modes. For instance, if a structure will be subjected to two

different known frequencies, the structure's natural frequencies would have to be as distant as possible from these entry frequencies. As such, it is of interest to study topological optimization procedures to develop band-gap structures.

The ESO method (*evolutionary structural optimization*) was first presented in 1993^[1], where in a given project domain, discretized by a fine grid, elements which contribute the least to the overall stiffness of a load-bearing structure are gradually removed, until a desired optimum is reached for the topology. The method was later rewritten^[2] utilizing the elemental deformation energy criteria, in an attempt to maximize structural stiffness. The method was further refined into bidirectional ESO (BESO)^[3], where materials can be added in regions with high stress, and removed in regions with low stress, typically implemented through the addition and removal of elements from the finite element method (FEM), meaning that elements that were removed in some previous iteration of the process can return in later iterations.

The method became very popular among structural optimization researchers, as can be seen in the literature^{[4] [5] [6]}. This method is well established and has evolved to more complex versions^[7], such as bidirectional ESO (BESO)^[4]; the multi-objective version based on fixed elements (MESO)^[8], the genetic ESO method (GESO)^[9]; the version for analysis of fluid-structure systems (BEFSO)^[10]; smoothing ESO (SESO)^[11], which applies a smoothing technique during the removal of inefficient elements from the grid, and the Evolutionary Topology Optimization method (ETO)^[12], capable of generating a smooth and clear boundary shape, in contrast with BESO's zigzagging outline, are just some of the various works found in the literature based on the general principles of the ESO method.

Optimization processes can be classified according to the number of objective functions as mono- or multi-objective problems. Although mono-objective type optimization problems are more widely researched, multi-objective type problems are closer to real problems faced in an engineering context. Unlike a typical mono-objective optimization problem, multi-objective problems do not necessarily have a solution that simultaneously minimizes or maximizes all the desired objective functions. Rather, different objectives can often conflict with each other, and the optimal parameters of one objective do not achieve the optimum of other objectives^[13].

According to the literature^{[14] [15]}, the solution to the multi-criteria problem is known as a Pareto optimum (or a non-inferior solution). For these multi-objective problems, the Pareto frontier of the entire design space is the most valuable tool a designer can have to select the most appropriate designs. Originally, the Pareto frontier is defined as the set of all solutions for which no other solution is better in all objectives^[16].

The ESO method was expanded for multi-criteria analysis on the design of structures with the objective of maximizing the fundamental frequency and minimizing flexibility, simultaneously^[17]. Furthermore, a multi-objective criterion for the optimization of a three-dimensional structure of a thermal protection system (TPS) was developed, in order to concurrently maximize the natural frequency, and minimize thermal stresses^[18].

Refining the BESO method through the implementation of a technique for adaptive removal of alternate and singular elements, propose the multi-objective optimization of frequency-stiffness was proposed ^[19], obtaining structures free from the checkerboard pattern problem.

Many solution algorithms attempt to combine all of the multi-objective functions in a single scalar objective using a weighted sum. The weighted sum is a simple, straightforward approximation to the solutions of the multi-objective optimization problem, employing a linear combination of different objectives, conflicting or not, aided by weights relative to the importance of an objective in relation to another.

This work aims to develop a multi-objective evolutionary structural optimization algorithm for structures with multiple band-gaps. First, section 2 introduces a theoretical foundation of the frequency optimization problem focused on frequency separation. Section 3 presents the proposed algorithm and its implementation concerning different natural frequency intervals. Section 4 presents the numerical procedures and tests realized utilizing the developed code in MATLAB, alongside the resulting Pareto sets from different weights. Finally, section 5 presents the results and conclusions regarding the implemented method.

2. THEORETICAL FOUNDATION

There are different mathematical techniques to define the multi-objective function and choose the optimal vector of variables which satisfies said objectives. Some of the most traditional techniques among them are weighted sum methods and compromise programming. We chose the weighted sum method due to its simplicity and ease of implementation.

The weighted sum method is an approximation for the multi-objective function that implements a linear combination of the different conflicting objectives, aided by artificial weights which measure the relative importance of one objective to another. As read in the literature ^[20], the aggregated objective function to be minimized is a combination of different performance indices, where the conflicting objectives are aggregated on a single function. For a given function A , which represents the separation between any two consecutive adjacent frequencies, we can define the optimization problem as:

$$\text{Maximize : } A\Lambda_{inf} + B\Lambda_{sup} \quad (1.1)$$

$$\text{Such that: } (\mathbf{K} - \omega_k^2 \mathbf{M}) \mathbf{u}_k = \mathbf{0} \quad (1.2)$$

$$V_f - \sum_{i=1}^{N_{elements}} x_i V_i = 0 \quad (1.3)$$

$$x_i = 1 \text{ or } x_{min} \quad (1.4)$$

$$A + B = 1 \quad (1.5)$$

where A can be obtained by equation (2), following from the equations previously presented in early papers^[21] as

$$\Lambda = \sum_{j=n}^m \frac{1}{(\omega_{n_j}^2 - \omega_0^2)} + \sum_{j=1}^{n-1} \frac{1}{(\omega_0^2 - \omega_{n_j}^2)} \quad (2)$$

where ω_0 represents an intermediary frequency between the n th natural frequency and its consecutive. The derivative of equation (2) in relation to a project variable x_i , may be expressed by Equation (3), which represents the function's sensitivity α .

$$\alpha = \left[\sum_{j=n}^{n_{freq}} \frac{1}{(\omega_{n_j}^2 - \omega_0^2)} \right]^{-2} \sum_{j=n}^{n_{freq}} \frac{1}{(\omega_{n_j}^2 - \omega_0^2)} \mathbf{u}_j^T \left(\frac{1 - x_{min}}{1 - x_{min}^p} x_i^{p-1} [K^0] - \frac{\omega_{n_j}^2}{p} [M^0] \right) \mathbf{u}_j + \left[\sum_{j=1}^{n-1} \frac{1}{(\omega_0^2 - \omega_{n_j}^2)} \right]^{-2} \sum_{j=1}^{n-1} \frac{1}{(\omega_0^2 - \omega_{n_j}^2)} \mathbf{u}_j^T \left(\frac{1 - x_{min}}{1 - x_{min}^p} x_i^{p-1} [K^0] - \frac{\omega_{n_j}^2}{p} [M^0] \right) \mathbf{u}_j \quad (3)$$

where x_{min} is a chosen minimum non-zero value for the design variable, p is the penalization factor, K^0 is the elemental stiffness matrix, M^0 is the elemental mass matrix, \mathbf{u}_j is the j -th eigenmode and n_{freq} is the chosen number of natural frequencies added to the function.

3. ALGORITHM AND METHODOLOGY

The BESO algorithm is a method of topology optimization based on iteratively removing or adding selected material according to a chosen criterion, according to the objective function. Originally developed for structural stiffness optimization, it was further adapted for multiple material, periodicity constraints and frequency optimization objectives^[5], proving to be a versatile and adaptive algorithm. This work implements a variation of the BESO algorithm, which is detailed in flowchart form in Figure 1.

In traditional frequency separation procedures, two frequencies are statically chosen at the beginning of the procedure, with an intermediary frequency between them, to be separated. It is expected that said frequencies do not fall when the volume fraction reaches lower than a certain threshold. However, this can be disruptive to the overall process as it is common that during an optimization run the chosen frequencies may be significantly altered from their initial values, potentially rising or falling below or above the intermediary frequency. This causes their separation to cease being an adequate distance metric for the entry frequency, and therefore we propose to consider the current upper and lower natural frequencies in any iteration, thus shifting the focus to the chosen intermediary frequency.

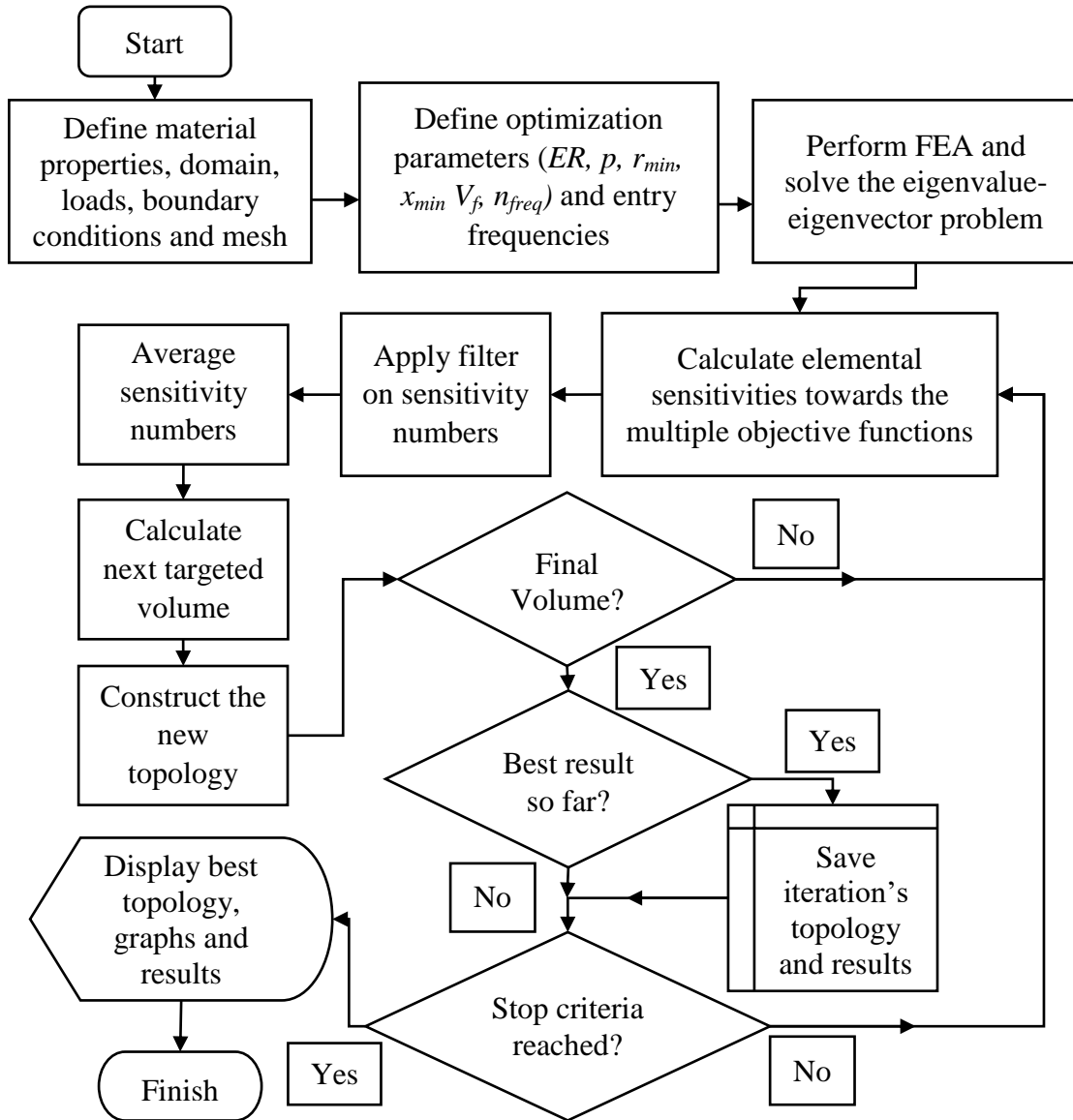


Figure 1. Flowchart of the proposed algorithm used in this work.

The algorithm used in this work adopted two further changes to the traditional BESO method: first, the adoption of a connectivity check between key structural elements (such as mass or support boundary conditions) and second, the selection of “best overall result” as the final structure. The first change is because in the examples chosen, we verified experimentally that if, during the optimization process, a structure loses integrity (for instance, a bi-clamped beam is separated in two) during any iteration, further iterations often do not remedy this

flaw, and the final iteration still presents this error. As such, in some cases we found it useful to stop the algorithm in the first iteration in which structural integrity is lost, and consider only the past iterations in the final procedure. The second change is due to instabilities in the final process. Due to the chosen objective function, the structure's natural frequencies can change wildly and sometimes unpredictably during a run, often to the detriment of the chosen objective. Therefore, it can be more interesting to consider only the best result, here defined as the topology with the highest obtained value S given by the weighted sum of the direct gaps related to the two entry frequencies, as given in equation (4)

$$S = A(\omega_{upper}^{inf} - \omega_{lower}^{inf}) + B(\omega_{upper}^{sup} - \omega_{lower}^{sup}) \quad (4)$$

in which $\omega_{upper}^{inf} - \omega_{lower}^{inf}$ refers to the separation between the closest higher and lower natural frequencies to the lower entry frequency, $\omega_{upper}^{sup} - \omega_{lower}^{sup}$ is the corresponding separation to the higher entry frequency, and A and B are the weights in Eq. (1.1) and (1.5).

4. NUMERICAL EXAMPLES

To analyze and test the proposed method, three key structure examples were chosen. For each case, we obtain the general Pareto frontier for the chosen parameters varying the weights from 0 to 1, as well as an example resulting topology and its natural frequencies along the iterations.

4.1 Simply supported beam

Following ^[22], a simply supported beam at both ends with dimensions of 10 m × 1 m × 1 m, as illustrated in Fig. 2, is studied. The material's Young's modulus is assumed to be $E = 10$ MPa, the density $\rho = 1$ kg/m³, and Poisson's ratio of $\nu = 0.3$.

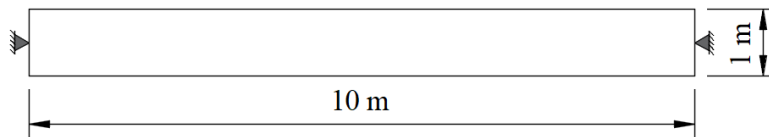


Figure 2 – Representation of the simply supported beam studied.

In this example, there are two entry frequencies, equal to 80 Hz and 390 Hz, respectively. The first entry frequency's sensitivity is calculated taking into account all the frequencies below it, and the first two immediately superior frequencies, while the second entry frequency's sensitivity is calculated taking into account all the natural frequencies below it, and all the natural frequencies above it, up to n_{freq} , here equal to 30. For a final volume V_f of

80%, the BESO process was carried out with $ER=4\%$, $p=6$, $r_{min}=4$ elements, $x_{min}=10^{-3}$ and $\tau=0.1\%$ with linearly varying weights. Figure 3a presents the topology with highest objective function value, while Figure 3b is its graph evolution in the optimization run and figure 3c presents the optimal solutions for different weights.

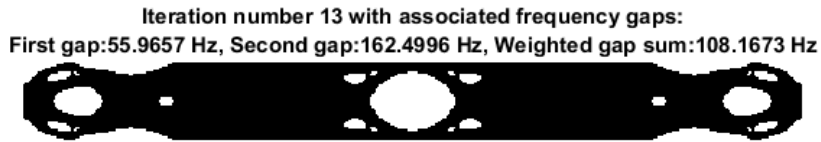


Figure 3a – Topology with the best weighted gap sum obtained in the optimization with weights $A=0.49$, and $B=0.51$.

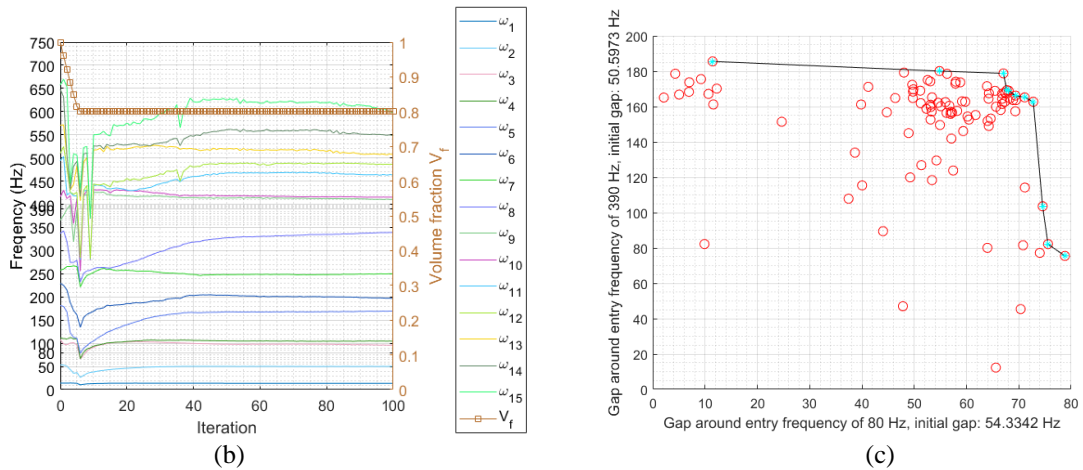


Figure 3b - Evolution of the natural frequencies for weights $A=0.49$ and $B=0.51$, and Figure 3c – Resulting data set obtained by varying the objective function’s weights with points in the Pareto frontier.

4.2 Cantilever beam

For this case, a clamped $8\text{ m} \times 4\text{ m}$ beam with 1 m thickness, taken from [23] and seen in Fig. 4, is used. The material properties are elastic modulus $E = 10\text{ GPa}$, density $\rho = 1000\text{ kg/m}^3$ and Poisson’s ratio $\nu = 0.3$, with a concentrated mass M of 16000 kg . The two entry frequencies are 100 and 300 Hz considering the same frequencies as the previous case, and the final volume was set as 60% . The parameters used are $ER=5\%$, $p=5$, $r_{min}=2.5$ elements, $x_{min}=10^{-3}$ and $\tau=0.1\%$.

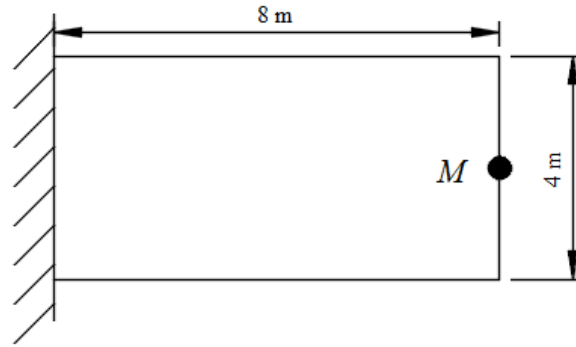


Figure 4 – Representation of the cantilever beam used.

Figure 5a contains the optimized topology for weights $A=0.3$ and $B=0.7$, with its evolution detailed in figure 5b. The resulting Pareto set for these parameters is shown in figure 5c.

Iteration number 34 with associated frequency gaps:
 First gap:77.1414 Hz, Second gap:93.3807 Hz, Weighted gap sum:88.5089 Hz

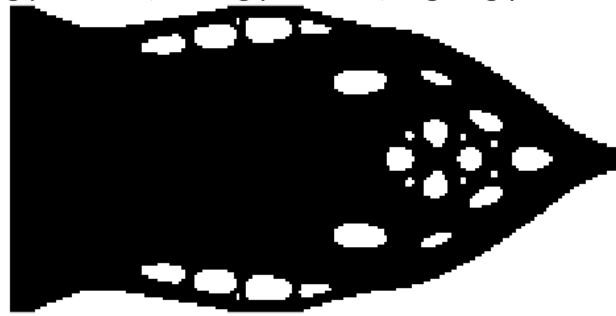


Figure 5a – Topology with the best weighted gap sum obtained in the optimization with weights $A=0.3$, and $B=0.7$.

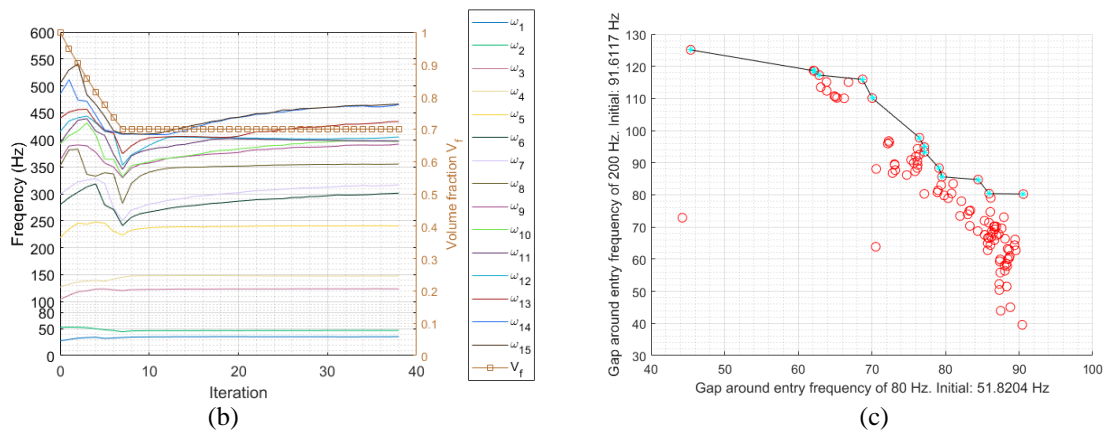


Figure 5b - Evolution of the natural frequencies for weights $A=0.3$ and $B=0.7$, and Figure 5c – Resulting data set obtained by varying the objective function’s weights with points in the Pareto frontier.

4.3 Biclamped beam

Finally, a biclamped beam with dimensions $8\text{ m} \times 1\text{ m}$ and thickness 0.001 m , based on [24] is tested, as in Figure 6. The material properties are elastic modulus $E = 10\text{ MPa}$, density $\rho = 1\text{ kg/m}^3$ and Poisson's ratio $\nu = 0.3$, with a concentrated mass M of 4 kg . The two entry frequencies are 100 and 300 Hz taking into account the same frequencies as the other two cases, and the final volume was set as 60% . The parameters used are $ER=4\%$, $p=6$, $r_{min}=4$ elements, $x_{min}=10^{-3}$ and $\tau=0.1\%$

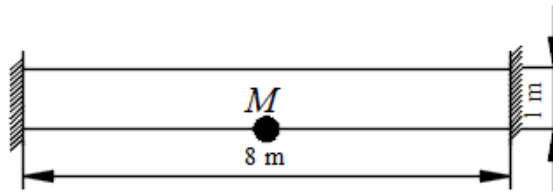


Figure 6 – Representation of the cantilever beam used.

Figure 7a contains the optimized topology for weights $A=0.26$ and $B=0.74$, with its evolution detailed in Figure 7b. The resulting Pareto set for these parameters is shown in Figure 7c.

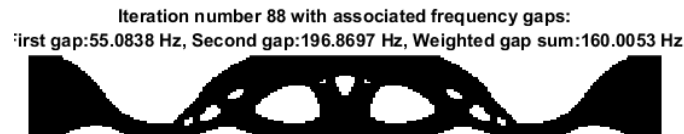


Figure 7a – Topology with the best weighted gap sum obtained in the optimization with weights $A=0.26$, and $B=0.74$.

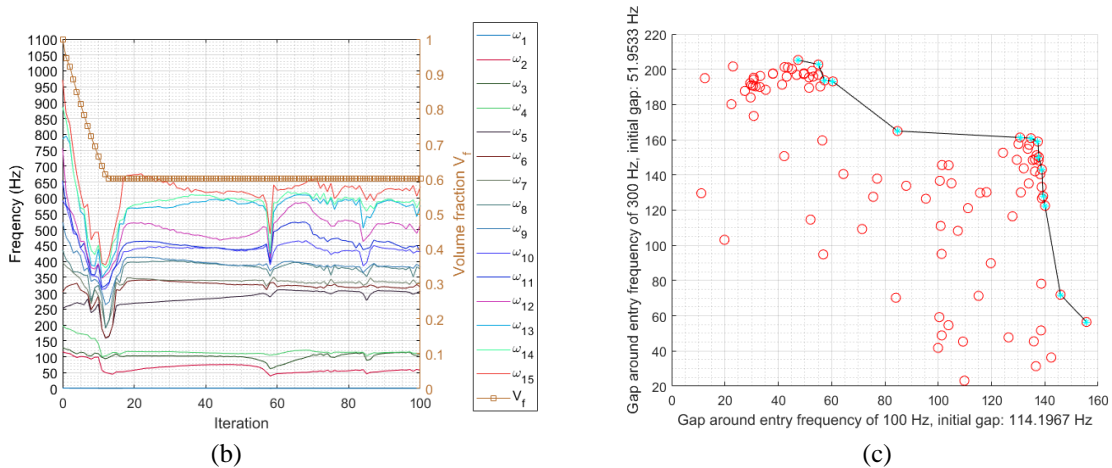


Figure 7b - Evolution of the natural frequencies for weights $A=0.26$ and $B=0.74$, and Figure 7c – Resulting data set obtained by varying the objective function's weights with points in the Pareto frontier.

5. CONCLUSIONS

In this work, the BESO algorithm was applied to the concurrent separation of multiple natural frequencies within a structure given two entry frequencies. The objective function is the maximization of two frequency gaps, utilizing a multi-objective separation function which prioritizes the closest natural frequencies. For each iteration, the closest natural frequencies are re-evaluated and taken into account for the objective function and its sensitivity, thus shifting the focus towards the entry intermediary frequencies. Some numerical examples of topology optimization of 2D structures are carried out, obtaining the algorithm's optimal results in each case.

From the results obtained it is clear that, although extra cautions were taken into obtaining the best possible results from the implemented algorithm, it is still very unstable and may not actually converge to the desired optimum, even if it is capable of optimizing the natural frequency gaps in a structure. It is theorized that this is due to gap optimization objectives not being strictly conflicting, and because the chosen objective function is non-linear, thus being influenced unevenly by higher and lower frequencies. Furthermore, the scalarized weighing method proved to a poor choice to obtain the Pareto set, as it gives unevenly spaced points on its frontier.

6. REFERENCES

- [1] Xie, Y. M.; Steven, G. P. A simple evolutionary procedure for structural optimization. *Comp. & Struct.* (1993) 49: 885–896.
- [2] Chu, D. N.; Xie, Y. M.; Hira, A. and Steven, G. P. Evolutionary structural optimization for problems with stiffness constraints. *Finite Element Analysis*, (1996) 21:239–251.
- [3] Querin, O. M.; Steven, G. P.; Xie Y. M. Evolutionary structural optimisation (ESO) using a bidirectional algorithm. *Eng. Comp.* (1998) 15:1031–1048.
- [4] Huang, X. and Xie, Y. M. Convergent and mesh-independent solutions for the bidirectional evolutionary structural optimization method, *Finite Elements in Analysis and Design*, (2007) 43:1039–1049.
- [5] Huang, X. and Xie, Y. M. *Evolutionary Topology Optimization of Continuum Structures: Methods and Applications*. John Wiley & Sons Ltd. (2010a).
- [6] Huang, X. and Xie, Y. M. A further review of ESO type methods for topology optimization. *Struct. Multidiscip. Opt.* (2010b) 41:671-683.
- [7] Picelli, R. *Otimização Estrutural Evolucionária usando malhas hexagonais*, Masters Dissertation in Mechanical Engineering. Universidade Estadual de Campinas, (2011).

- [8] Tanskanen, P. A multiobjective and fixed elements based modification of the evolutionary structural optimization method. *Comp. Meth. App. Mech. and Engng.* (2006) 196:76–90.
- [9] Liu, X.; Yi, W.; Li, Q. S. and Shen, P. Genetic evolutionary structural optimization. *J. Const. Steel Research*, (2008) 64:305–311.
- [10] Vicente, W. M. *Otimização Topológica Evolucionária Aplicada a Sistemas Elasto-Acústicos*, Thesis (Doctorate in Mechanical Engineering). Universidade Estadual de Campinas, (2013).
- [11] Almeida, V. S.; Simonetti, H. L. and de Assis das Neves, F. Optimal topology selection for 2D structures with stress constraints via Smooth Evolutionary Structural Optimization, *Rev. Int. Mét. Num. Cál. Dsño. Ing.* (2014) 30:69–76.
- [12] Da, D.; Xia, L. and Li, G. Evolutionary topology optimization of continuum structures with smooth boundary representation. *Struct. Multidiscip. Opt.* (2018) 57:2143-2159.
- [13] Yang, X. H. *Engineering Optimization - An Introduction with Metaheuristic Applications*. John Wiley & Sons, (2010).
- [14] Carmichael, D. G. Computation of Pareto Optima in Structural Design, *Int. J. Num. Meth. Engng.* (1980) 15:925–952,
- [15] Koski, J. Multicriterion Structural Optimization. *Opt. Large Struct. Systems.* (1994) 231:793-804.
- [16] Pareto, V. *Cour deconomie politique*. Librairie Droz-Geneve (1964).
- [17] Proos, K. A.; Steven, G. P.; Querin, O. M. and Xie, Y. M. Stiffness and inertia multicriteria evolutionary structural optimisation. *Eng. Comp.* (2001) 18:1031-1054.
- [18] Kim, W. Y. and Grandhi, R. V. Multiobjective evolutionary structural optimization using combined static/ dynamic control parameters. *AIAA Journal.* (2006) 44:794-802.
- [19] Zuo, Z. X.; Xie, Y. M.; Huang, X. An improved bi-directional evolutionary topology optimization method for frequencies. *Int. J. Struct. Stab. & Dynm.* (2010) 10:55 – 75.
- [20] Messac, A. and Mullur, A. A. *Optimization of Structural & Mechanical Systems*. World Scientific (2007).
- [21] Ma, Z.-D., Cheng, H.-C. and Kikuchi, N. Structural design for obtaining desired eigenfrequencies by using the topology and shape optimization method. *Comp. Systems Engng.* (1994) 5:77-89.

[22] Lopes, H. N., Pavanello, R. and Mahfoud, J. Topology Optimization for the Maximization of Frequency Separation Margin. VI Int. Symposium on Solid Mech – MecSol 2017 (Conference paper).

[23] Zheng, J., Long, S. and Li, G. Topology optimization of free vibrating continuum structures based on the element free Galerkin method. *Struct. Multidisc. Optim.* (2012) 45:119-127.

[24] Du, J. and Olhoff, N. Topological design of freely vibrating continuum structures for maximum values of simple and multiple eigenfrequencies and frequency gaps. *Struct. Multidisc. Optim.* (2007) 34:91-110.

Multi-Scale Analysis of Second-Order Effects at Finite Strains

Igor Rodrigues Lopes*, Francisco Andrade Pires**

*DeMec, Faculdade de Engenharia da Universidade do Porto, **DeMec, Faculdade de Engenharia da
Universidade do Porto

ABSTRACT

Multi-scale analyses are of utmost importance in order to understand the micro-scale mechanisms that influence the macroscopic material behaviour. Materials which are heterogeneous at a certain spatial scale may be modelled by a Representative Volume Element (RVE), where phenomena arising at the micro-scale due to a macro-scale loading may be analysed in detail, accounting for the effect of material heterogeneities. Computational analysis of RVEs behaviour are usually performed considering only the linear part of the macroscopic loading, e.g. by means of the insertion of a deformation gradient. However, in some applications, it may be interesting to include second-order effects through the macroscopic second-order displacement gradient [1,2]. In the present contribution, details on the implementation of a computational framework to analyse RVEs under second-order loadings are presented. Numerical simulations are performed in order to analyse the effects of including the second-order component of the macro-scale loading on RVEs representing materials with heterogeneous microstructures. Keywords: Multi-Scale, Heterogeneous materials, Second-order effects, Finite strain, Finite element method. References: [1] V.G. Kouznetsova, M.G.D. Geers and W.A.M. Brekelmans, Multi-scale constitutive modelling of heterogeneous materials with a gradient-enhanced computational homogenization scheme. *Int. J. Numer. Meth. Eng.*, Vol. 54, pp. 1235-1260, 2002. [2] D.J. Luscher, D.L. McDowell and C.A. Bronkhorst, A second gradient theoretical framework for hierarchical multiscale modeling of materials. *Int. J. Plast.*, Vol. 26, pp. 1248-1275, 2010.

Simulations of Rayleigh Bubble Collapse Near a Soft Object

Mauro Rodriguez*, Eric Johnsen**

*University of Michigan, Ann Arbor, **University of Michigan, Ann Arbor

ABSTRACT

Understanding the mechanics of bubble dynamics and shock wave propagation in viscoelastic media is important for various biomedical applications, particularly in the context of cavitation-induced damage. The application of interest is histotripsy, a therapeutic ultrasound treatment that uses high-amplitude (100 MPa peak positive pressure, -25 MPa peak negative pressure) and high-frequency (MHz) ultrasound waves to destroy tissue. The local/transient pressure changes lead to the formation of cavitation bubbles that grow and violently collapse, thus producing shock waves that propagate in the surroundings. Although not fully understood, the damage mechanism induced on the nearby object combines the effect of the incoming pulses and cavitation (bubble oscillation and collapse) produced by the high tension. In such problems, the constitutive models describing the soft material are non-trivial and include effects such as (nonlinear) elasticity, history (relaxation effects) and viscosity. Thus, the influence of the shock on the material and the response of the material to the shock are poorly understood. Understanding these mechanisms will provide invaluable insights to the further the development of histotripsy as a therapy tool for treating malignant tissues. To simulate this phenomenon, an in-house, solution-adaptive, high-order accurate shock- and interface-capturing method is used to solve the 3D equations for conservation of mass, momentum, energy in a Eulerian framework [1]. This method incorporates evolution equations for the elastic stresses and stress relaxation variables to solve multi-component flows including Zener-like viscoelastic media [2]. In this approach, the evolution equations are evaluated by taking the Lie objective time derivative of the constitutive relation that models the material of interest using strain rates. In the principal contributions to the field, a 3D canonical problem is considered which involves the Rayleigh collapse of a vapor bubble in a liquid next to a viscoelastic or elastic medium of a certain thickness. Using these simulations, scaling relations for the maximum pressures and temperatures produced during this process will be presented for different initial stand-off distances and shear moduli of the soft object. This research was supported in part by NSF grant CBET 1253157 and the Ford Foundation Dissertation Fellowship. [1] S. Alahyari Beig and E. Johnsen, Maintaining interface equilibrium conditions in compressible multiphase flows using interface capturing, *J. Comput. Phys.* 302 (2015) 548-566. [2] M. Rodriguez, E. Johnsen, A high-order accurate, finite-difference approach for numerical simulations of shocks interacting with interfaces between fluids and linear viscoelastic materials. In preparation. (2018)

Estimation of Material Coefficients for an Idealized Model of the Human Abdominal Aorta

Miguel Rodriguez*, Shawn Shadden**

*University of California, Berkeley, **University of California, Berkeley

ABSTRACT

The finite element method (FEM) has been used extensively to study the mechanics of arterial and cardiac tissue [1]. Magnetic resonance and computed tomography imaging techniques enable the extraction of a patient's cardiovascular geometry, which is then used to carry out patient-specific simulations. In most studies, the material coefficients required by constitutive equations are obtained through ex vivo patient-averaged material testing. For clinical applications however — and due to substantial patient variation in material properties — there exists a need for a patient-specific in vivo method to obtain these coefficients. We present a variational data assimilation (4DVar) technique applied to an idealized model of arterial walls. Before applying 4DVar techniques to patient data, we validate our framework using a thick-walled cylinder modeled as a neo-Hookean material. First, to produce a synthetic observation data set, a forward simulation of the time-dependent loading of the inner wall of the cylinder is carried out with known material coefficients, and the results are recorded. To test the robustness of this technique, white noise is added to the observation data. Then, material coefficient values different from those used to generate the observation data are fed to the 4DVar framework as the initial guess for the coefficients that are to be recovered. The forward problem is solved with this initial guess, and the gradient of the objective function quantifying the misfit between the simulation and observations with respect to the material coefficients is used to iteratively update the coefficient values. Preliminary results using the 4DVar framework show that the material coefficient simulation values are recovered within a 20% error of those used to produce the artificial observation data set with a signal-to-noise ratio as low as 2.25. Future work will focus on using different constitutive equations, as well as study the effect of adding regularization terms to the objective function. Developing and validating this framework will provide an automated technique for tuning simulations to specific patients, and in turn bring cardiovascular biomechanics closer to the clinical setting. 1. Holzapfel, Gerhard A. et al., Proc. R. Soc., 2010.

Dynamic Recrystallization and Adiabatic Shear Localization

José Rodríguez-Martínez^{*}, Guadalupe Vadillo^{**}, Daniel Rittel^{***}, Ramón Zaera^{****}, José Fernández-Sáez^{*****}

^{*}University Carlos III of Madrid, ^{**}University Carlos III of Madrid, ^{***}Technion, ^{****}University Carlos III of Madrid, ^{*****}University Carlos III of Madrid

ABSTRACT

It has recently been reported that, in alloys exhibiting early dynamic recrystallization (DRX), the onset of adiabatic shear bands (ASB) is primarily related to microstructural transformations, instead of the commonly assumed thermal softening mechanism, as shown by Rittel et al. (2008) and Osovski et al. (2012). Further, the dominant role of microstructural softening in the necking process of dynamically stretching rods showing DRX has been verified using linear stability analysis and finite element simulations by Rodríguez-Martínez et al. (2015). With the aim of extending this coupled methodology to shear conditions, this paper presents an analytical solution to the related problem of ASB in a material that undergoes both twinning and dynamic recrystallization. A special prescription of the initial and loading conditions precludes wave propagation in the specimen which retains nevertheless its inertia, allowing for a clear separation of material versus structural effects on the localization process. A parametric study, performed on the constants of the constitutive model, permits the identification of their relative role in the onset of the dynamic instability. The main outcome of the analysis confirms the strong destabilizing effect played by the development of DRX, consistently with the former statement regarding ASB, and contributes to rationalize the observations of other authors. We have also shown that the amount of DRX influences the width of the shear band, and the separation between shear bands in multiple shear band problems. Rittel, D., Landau, P., Venkert, A., 2008. Dynamic recrystallization as a potential cause for adiabatic shear failure. *Phys. Rev. Lett.* 101, 165501. Osovski, S., Rittel, D., Landau, P., Venkert, A., 2012b. Microstructural effects on adiabatic shear band formation. *Scr. Mater.* 66, 9–12. Rodríguez-Martínez, J.A., Vadillo, G., Zaera, R., Fernández-Sáez, J., Rittel, D., 2014. An analysis of microstructural and thermal softening effects in dynamic necking. *Mech. Mater.* 80B, 298-310.

TWO-SCALE MODELLING OF LARGE-DEFORMING FLUID-SATURATED POROUS MEDIA: RATE FORMULATION AND HOMOGENIZATION CONCEPT

EDUARD ROHAN*, VLADIMÍR LUKEŠ†

* Department of Mechanics, Faculty of Applied Sciences,
University of West Bohemia, Univerzitní 8, Pilsen, Czech Republic
rohan@kme.zcu.cz

† New Technologies for the Information Society, Faculty of Applied Sciences,
University of West Bohemia, Univerzitní 8, Pilsen, Czech Republic
lukes@kme.zcu.cz

Keywords: Porous media, Homogenization, Biot model, Updated Lagrangian formulation

Abstract: The paper deals with the homogenization of the locally periodic Biot medium subject to large deformation. As the main outcome, a consistent two-scale incremental scheme is derived, leading to a variant of the FE-square computational approach. A particular three compartment topology of the representative volume featured by large contrasts in the permeability is considered.

1 INTRODUCTION

Behaviour of the fluid-saturated porous media (FSPM) at finite strains has been studied within the mixture theories and also using the macroscopic phenomenological approach [1, 4]. The fluid retention in unsaturated media is so far not well understood in the context of deterministic models, a number of publications involve this phenomenon in computational models [5]. In any case, in this paper we consider only porous media with one phase fluids saturating the pores. In the context of homogenization, the FSPM has been treated *e.g.* in [12] At the pore level, the mechanical model describes interactions of an elastic, or hyperelastic skeleton and a compressible viscous fluid, see [8, 6] where the updated Lagrangian formulations has been employed. As an alternative, the ALE formulation provides some advantages [2]. Macroscopic treatment of the FSPM using the incremental updated Lagrangian formulations was reported in [13], the dynamic behaviour is confined to an approximation of the inertia effects associated with the relative fluid-solid motion so that the model is convenient for describing quasistatic loading of large-deforming porous structures.

In the present paper, we consider quasistatic loading of a FSPM medium with periodic heterogeneities related to the poroelastic and permeability coefficients of the Biot-Darcy model. More-

over, the double porosity structures are considered as an extension of the models developed by the homogenization to treat small deforming media, see [10]. At the macro-level, the computational algorithm is consistent with linearization of the residual formulation in the Eulerian framework, such that the incremental scheme (for a given time step) uses the updated Lagrangian approach. The equilibrium equation and the mass conservation expressed in the spatial configuration are differentiated using the material derivative with respect to a convection velocity field.

This yields linearized equations to which the homogenization can be applied, assuming locally periodic structures graded continuously at the macroscopic scale, cf. [8]. This allows us to establish the effective medium properties involved in the incremental formulation using the homogenization based on asymptotic analysis w.r.t the microstructure scale. In this way, modified poroelastic coefficients can be computed for given updated configurations, as in the linear case, cf. [9]. The proposed two-scale incremental formulation provides a basis for enrichment of the model by multiphysics effects, such as transport of electrolytes. The model is implemented in the SfePy code. A numerical example is presented.

2 PROBLEM FORMULATION AT THE MESOSCOPIC SCALE

In this section we introduce the residual formulation of the problem for a large deforming poroelastic medium with large contrast in the permeability coefficients. The initial configuration is associated with material coordinates X_i , $i = 1, 2, 3$ and with domain Ω_0 . The spatial (current) configuration at time t is associated with spatial coordinates x_i and with domain $\Omega(t)$. The deformation gradient $F_{ij} = \delta_{ij} + \partial u_i / \partial X_j$ is introduced using the displacement fields.

2.1 Weak formulations

The boundary conditions are prescribed on the boundary consisting of disjoint parts; two decompositions are considered: $\partial\Omega = \partial_u\Omega \cup \partial_\sigma\Omega$, where $\partial_u\Omega \cap \partial_\sigma\Omega = \emptyset$, and $\partial\Omega = \partial_p\Omega \cup \partial_w\Omega$, where $\partial_p\Omega \cap \partial_w\Omega = \emptyset$. This decompositions is reflected by the admissibility sets and corresponding linear spaces employed in the weak formulation,

$$\begin{aligned} V(t) &= \{\mathbf{v} \mid \mathbf{v} = \mathbf{u}^\partial \text{ on } \partial_u\Omega(t) \subset \partial\Omega(t)\}, \\ Q(t) &= \{q \mid q = p^\partial \text{ on } \partial_p\Omega(t) \subset \partial\Omega(t)\}, \\ V_0(t) &= \{\mathbf{v} \mid \mathbf{v} = 0 \text{ on } \partial_u\Omega(t) \subset \partial\Omega(t)\}, \\ Q_0(t) &= \{q \mid q = 0 \text{ on } \partial_p\Omega(t) \subset \partial\Omega(t)\}. \end{aligned} \tag{1}$$

The true (Cauchy) stress for the incompressible poroelastic medium $\boldsymbol{\sigma} = \boldsymbol{\sigma}^{\text{eff}} - p\mathbf{I}$ consists of the effective strain-dependent part $\boldsymbol{\sigma}^{\text{eff}}$, and the pore fluid pressure part $-p\mathbf{I}$. The state of the poroelastic medium is obtained as a solution of the nonlinear residual equation,

$$\Phi_t((\mathbf{u}, p); (\mathbf{v}, q)) = 0 \quad \forall (\mathbf{v}, q) \in V_0(t) \times Q_0(t), \tag{2}$$

consisting of the equilibrium equation and the Darcy flow driven balance of the fluid content,

$$\begin{aligned}\Phi_t((\mathbf{u}, p); (\mathbf{v}, 0)) &= \int_{\Omega(t)} \boldsymbol{\sigma} : \nabla \mathbf{v} - \int_{\Omega(t)} \rho \mathbf{b} \cdot \mathbf{v} \quad \forall V_0(t), \\ \Phi_t((\mathbf{u}, p); (0, q)) &= \int_{\Omega(t)} (\nabla \cdot \dot{\mathbf{u}} q + \mathbf{K} \nabla p \cdot \nabla q) - \mathcal{J}_t(q) \quad \forall q \in Q_0(t),\end{aligned}\tag{3}$$

where $\dot{\mathbf{u}}$ is the skeleton (local) velocity, $\mathbf{K} = (K_{ij})$ is the permeability, \mathcal{J}_t is the fluid mass source/sink, ρ is the solid density and \mathbf{b} represents volume forces per mass. The linearization (2) involves the state increments $(\delta \mathbf{u}, \delta p)$; the following problem is subject to the homogenization, as described below: Given $(\bar{\mathbf{u}}, \bar{p})$ at time $t > 0$, compute a new state (\mathbf{u}, p) at time $t + \delta t$ such that

$$\Phi_{t+\delta t}((\mathbf{u}, p); (\mathbf{v}, q)) \approx \Phi_t((\bar{\mathbf{u}}, \bar{p}); (\mathbf{v}, q)) + \delta \Phi_t((\bar{\mathbf{u}}, \bar{p}); (\mathbf{v}, q)) \circ (\delta \mathbf{u}, \delta p, \delta t \mathcal{V}),\tag{4}$$

where $\delta \Phi_t((\bar{\mathbf{u}}, \bar{p}); (\mathbf{v}, q)) \circ (\delta \mathbf{u}, \delta p, \delta t \mathcal{V})$ is the increment due to the material derivative associated with convected field \mathcal{V} ,

$$\begin{aligned}\mathbf{u} &= \bar{\mathbf{u}} + \delta \mathbf{u}, \quad p = \bar{p} + \delta p, \\ \text{where } \delta \mathbf{u} &= \dot{\mathbf{u}} \delta t, \quad \delta p = \dot{p} \delta t, \\ \Omega(t + \delta t) &= \Omega(t) + \delta t \{\mathcal{V}\}_{\Omega(t)}\end{aligned}\tag{5}$$

By differentiating $\boldsymbol{\sigma} = J^{-1} \mathbf{F} \mathbf{S} \mathbf{F}^T$ where \mathbf{S} is the 2nd Piola-Kirchhoff stress, $J = \det \mathbf{F}$ and \mathbf{F} is the deformation gradient, $F_{ij} = \delta_{ij} + \partial u_i / \partial X_j$, the Lie derivative of $\boldsymbol{\sigma}$ is obtained.

2.2 Time discretization

The time derivatives are approximated by backward differences $\delta \mathbf{u}^k = \mathbf{u}^k - \mathbf{u}^{k-1}$,

$$\begin{aligned}\dot{\mathbf{u}}(t_k) &\approx (\mathbf{u}^k - \mathbf{u}^{k-1}) / \delta t = \delta \mathbf{u}^k / \delta t, \\ \ddot{\mathbf{u}}(t_k) &\approx (\delta \mathbf{u}^k - \delta \mathbf{u}^{k-1}) / (\delta t)^2 = (\mathbf{u}^k - 2\mathbf{u}^{k-1} + \mathbf{u}^{k-2}) / (\delta t)^2.\end{aligned}\tag{6}$$

The convection velocity field can be approximated by the backward, or forward difference of the displacements. We shall employ the following notation:

$$\begin{aligned}\delta \mathbf{u}^{k+1} &\mapsto \mathbf{u}, \quad \delta p^{k+1} \mapsto p, \\ \delta \mathbf{u}^k &\mapsto \bar{\mathbf{u}}, \quad \delta p^k \mapsto \bar{p}, \\ p^k &= \hat{p}.\end{aligned}\tag{7}$$

The incremental subproblem is imposed in the actual spatial configuration represented by domain $\Omega_k = \Omega$. Further abbreviated $\mathbb{D}^{\text{eff}}(t_k) = \mathbb{D}^{\text{eff}}$, $\boldsymbol{\sigma}^{\text{eff}}(t_k) = \boldsymbol{\sigma}^{\text{eff}}$, $\delta \mathbf{b}^{k+1} = \delta \mathbf{b}$.

To simplify notation, we shall introduce some further notation:

$$\begin{aligned}
 \mathbf{I} &= (\delta_{ij}) , & (\mathbf{I})_{ij} &= \delta_{ij} , \\
 \mathbb{I} &= (\delta_{jl}\delta_{ik}) , & (\mathbb{I})_{ijkl} &= \delta_{jl}\delta_{ik} , \\
 \mathbf{B}^T(\mathbf{v}) &= (\mathbf{I} \otimes \mathbf{I} - \mathbb{I})\nabla\mathbf{v} , \\
 \mathbf{H}(\mathbf{v}) &= (\nabla \cdot \mathbf{v})\mathbf{K} - \mathbf{K}(\nabla\mathbf{v})^T - (\nabla\mathbf{v})\mathbf{K}^T .
 \end{aligned} \tag{8}$$

Note that $\mathbf{H}(\mathbf{v})$ is symmetric for any symmetric \mathbf{K} , whereas $\mathbf{B}^T(\mathbf{v})$ is non-symmetric in general; using the latter tensor we can simply write

$$\begin{aligned}
 (\nabla \cdot \mathbf{v})(\nabla \cdot \bar{\mathbf{u}}) - \nabla\mathbf{v}\nabla\bar{\mathbf{u}} : \mathbf{I} &= (\nabla\bar{\mathbf{u}})^T : (\mathbf{I} \otimes \mathbf{I} - \mathbb{I})\nabla\mathbf{v} = (\nabla\mathbf{v})^T : (\mathbf{I} \otimes \mathbf{I} - \mathbb{I})\nabla\bar{\mathbf{u}} \\
 &= \mathbf{B}(\mathbf{v}) : \nabla\bar{\mathbf{u}} = \mathbf{B}^T(\bar{\mathbf{u}}) : (\nabla\mathbf{v})^T = \mathbf{B}(\bar{\mathbf{u}}) : \nabla\mathbf{v} .
 \end{aligned} \tag{9}$$

Using notation (8), the general incremental formulation (4) yields the linear subproblem: Find $(\mathbf{u}, p) \in \delta V(t_{k+1}) \times \delta Q(t_{k+1})$ which satisfy

$$\begin{aligned}
 &\int_{\Omega} \mathbb{D}^{\text{eff}} e(\mathbf{u}) : e(\mathbf{v}) + \int_{\Omega} \boldsymbol{\sigma}^{\text{eff}} : \nabla\mathbf{v}(\nabla\mathbf{u})^T - \int_{\Omega} \hat{p}\mathbf{B}(\mathbf{u}) : \nabla\mathbf{v} - \int_{\Omega} p\mathbf{B}(\bar{\mathbf{u}}) : \nabla\mathbf{v} - \int_{\Omega} p\nabla \cdot \mathbf{v} \\
 &= - \int_{\Omega} (\boldsymbol{\sigma}^k : \nabla\mathbf{v} - \rho\mathbf{b}^{k+1} \cdot \mathbf{v})
 \end{aligned} \tag{10}$$

for all $\mathbf{v} \in V_0(t_k)$ and

$$\begin{aligned}
 &\int_{\Omega} q\mathbf{B}(\bar{\mathbf{u}}) : \nabla\mathbf{u} + \int_{\Omega} q\nabla \cdot \mathbf{u} + \delta t \int_{\Omega} (\mathbf{K} + \mathbf{H}(\bar{\mathbf{u}})) \nabla p \cdot \nabla q \\
 &= \delta t \mathcal{J}^{k+1}(q) - \delta t \int_{\Omega} (\mathbf{K} + \mathbf{H}(\bar{\mathbf{u}}) + \delta\mathbf{K}) \nabla\hat{p} \cdot \nabla q ,
 \end{aligned} \tag{11}$$

for all $q \in Q_0(t_k)$.

3 HOMOGENIZATION

We consider a reference configuration generated as a periodic lattice by repeating the representative cell \hat{Y} . By virtue of the unfolding operation, the coordinates can be split into the macroscopic parts denoted by x and the local (microscopic) parts, denoted by y . As the consequence of the finite deformation and the incremental formulation, an updated configuration is established in terms of the locally representative periodic deformed cell.

3.1 Locally periodic microstructures

Using a diffeomorphic mapping $\mathcal{F}^\varepsilon \in C^1(\hat{\Omega}; \mathbb{R}^3)$ we may introduce ‘‘locally periodic microstructure’’. For the location $x \in \Omega(t)$, there exists $\hat{x}^0 \in \Omega(0)$

$$x - \hat{x} = \mathcal{F}^\varepsilon(y^0, \hat{x}^0) , \quad \text{and} \quad Y^\varepsilon(\hat{x}) = \mathcal{F}^\varepsilon(\hat{Y}, \hat{x}^0) , \tag{12}$$

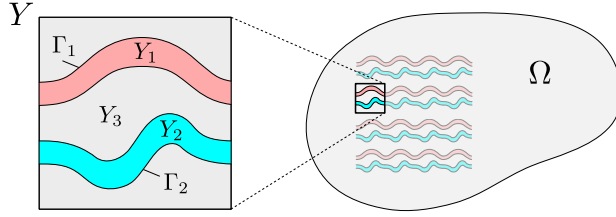


Figure 1: The representative cell with three porous compartments.

where \hat{x} is the spatial position of the cell central position $\hat{x}^0 \in \Omega(0)$ in the initial configuration. By $Y(\hat{x}) = \varepsilon^{-1}Y^\varepsilon(\hat{x})$ we denote the rescaled (but not necessarily unit) local reference cell representing the locally periodic microstructure, see Fig. 2. We recall that ε determines the ratio between the macro- and microscopic scales, the latter represented by the cell $Y(\hat{x})$; for $y, y' \in Y(\hat{x})$ the corresponding point $x, x' \in Y^\varepsilon(\hat{x})$ is given by $x - x' = \varepsilon(y - y')$. Evidently with ε getting smaller the number of cells Y^ε which cover any fixed subdomain of Ω increases. In this process any two adjacent cells, or those which are close enough, become almost identical. Thereby, in the limit case $\varepsilon \rightarrow 0$, each “macroscopic” point x is associated with the microstructure formed by periodic array of cells, which are defined as the Y -periodic translation of the representative cell $Y(\hat{x})$.

By Y we now abbreviate the local spatial reference cell $\varepsilon^{-1}Y^\varepsilon$ defined above in (12), without writing explicitly the macroscopic location. Since our interests are in porous media with large contrasts in the permeability coefficients, we shall introduce the following decomposition of Y into the sectors of primary and dual porosities.

Let Y_α , for $\alpha = 1, 2$ be mutually disconnected subdomains of Y with Lipschitz boundary, then Y_3 forms the complement (see Fig. 1)

$$Y_3 \equiv Y \setminus \bigcup_{\alpha=1,2} \overline{Y_\alpha}, \quad (13)$$

$$\text{interface } 3\text{-}\alpha: \quad \Gamma_\alpha = \partial_3 Y_\alpha = \partial_\alpha Y_3 \equiv \overline{Y_\alpha} \cap \overline{Y_3}.$$

Furthermore, we require that $\partial Y \cap \partial Y_k \neq \emptyset$, so that the all domains Ω_k^ε , $k = 1, 2, 3$ generated by repeating the cells εY_k are connected.

The parts of the periodic boundary will be denoted (interface k - k) by

$$\partial_k Y = \partial_k Y_k \equiv \overline{Y_k} \cap \partial Y, \quad k = 1, 2, 3.$$

The material parameters in deformed configuration depend on the deformation gradient $F_{ij}^\varepsilon(x)$. To define them in the local reference cell, we use the unfolding operation, [3], For the sake of brevity, we shall consider couples (y, x) implicitly matching, such that $y - \hat{y} = \varepsilon^{-1}(x - \hat{x})$. In the spatial configuration we introduce the permeability parameters, as follows:

$$K_{ij}^\varepsilon(x) = \begin{cases} \tilde{K}_{ij}^\alpha(x, y) & y \in Y_\alpha, \alpha = 1, 2, \\ \varepsilon^2 \tilde{K}_{ij}^3(x, y) & y \in Y_3. \end{cases} \quad (14)$$

We emphasize, that the scaling by ε^2 the permeability coefficients in the “matrix” compartment leads to the *double porosity* effect. Obviously, tensors \tilde{K}_{ij} are depend on the material deformation and should be modified from one time level to the next one using \tilde{F} .

3.2 Asymptotic expansions and decomposition of two-scale functions

This paper only summarizes those results which enable to construct a computational algorithm. In particular, the characteristic responses are introduced which allow for splitting the dependence of the two-scale responses describing the heterogeneous medium on the macroscopic fields (strain and pressures) and on the local microscopic configuration. With reference to the simplified notation (7), in the context of the incremental formulation we introduce truncated expansions of the time step increments,

$$\begin{aligned} \mathbf{u}^\varepsilon(x) &= \mathbf{u}^0(x) + \varepsilon \mathbf{u}^1(x, y) + O(\varepsilon^2), \\ p^\varepsilon(x) &= \sum_{\alpha=1,2} \chi_\alpha(y) (p_\alpha^0(x) + \varepsilon p_\alpha^1(x, y) + O(\varepsilon^2)) + \chi_3(y) (\tilde{p}_3(x, y) + O(\varepsilon)). \end{aligned} \quad (15)$$

Upon substituting (15) into (10)-(11) and passing to the limit $\varepsilon \rightarrow 0$, the limit two-scale equations of the weak formulation are obtained. Due to the linearity of these equations, we may introduce the following splits,

$$\begin{aligned} \mathbf{u}^1 &= \omega^{ij} \partial_j^x u_i^0 + \sum_{\alpha=1,2} \omega^\alpha p_\alpha^0 + \mathbf{u}^P \\ p_3 &= \pi^{ij} \partial_j^x u_i^0 + \sum_{\alpha=1,2} \pi^\alpha p_\alpha^0 + p_3^P, \\ p_\alpha^1 &= \eta_\alpha^k \partial_k^x p_\alpha^0 + p_\alpha^P, \end{aligned} \quad (16)$$

where ω , π and η are characteristic responses. Although these responses are governed by equations reflecting the local current configuration, so-called particular responses \mathbf{u}^P and p_k^P , $k = 1, 2, 3$ must be computed in addition, depending on the local actual stresses and pressures.

3.3 Microscopic local problems

These problems are established in terms of bilinear and linear forms (depending on a vector field parameter $\bar{\mathbf{v}}$) which involve the tangent elastic operator,

$$\mathbb{A} = \mathbb{D}^{\text{eff}} + \boldsymbol{\sigma}^{\text{eff}} \otimes \mathbf{I} - \hat{p}(\mathbf{I} \otimes \mathbf{I} - \mathbb{I}), \quad A_{ijkl} = D_{ijkl}^{\text{eff}} + \sigma_{ik}^{\text{eff}} \delta_{jl} - \hat{p}(\delta_{ij} \delta_{kl} - \delta_{ik} \delta_{jl}), \quad (17)$$

and further tensors depending on a two-scale vector fields $\bar{\mathbf{v}} = (\bar{\mathbf{v}}^0, \bar{\mathbf{v}}^1)$,

$$\begin{aligned} \tilde{\mathbf{B}}^T(\bar{\mathbf{v}}) &= (\mathbf{I} \otimes \mathbf{I} - \mathbb{I})(\nabla_x \bar{\mathbf{v}}^0 + \nabla_y \bar{\mathbf{v}}^1), \\ \tilde{\mathbf{H}}^k(\bar{\mathbf{v}}) &= (\nabla_x \cdot \bar{\mathbf{v}}^0 + \nabla_y \cdot \bar{\mathbf{v}}^1) \tilde{\mathbf{K}}^k - \tilde{\mathbf{K}}^k (\nabla_x \bar{\mathbf{v}}^0 + \nabla_y \bar{\mathbf{v}}^1)^T - (\nabla_x \bar{\mathbf{v}}^0 + \nabla_y \bar{\mathbf{v}}^1) (\tilde{\mathbf{K}}^k)^T, \end{aligned} \quad (18)$$

defined for $k = 1, 2, 3$, the subdomain index.

The following bilinear and linear forms (depending on a vector field parameter $\bar{\mathbf{u}}$) will be employed:

$$\begin{aligned}
 b_{Y_k}(\bar{\mathbf{u}}; q, \mathbf{u}) &= \int_{Y_k} q [\tilde{\mathbf{B}}(\bar{\mathbf{u}}) + \mathbf{I}] : \nabla_y \mathbf{u}, \quad k = 1, 2, 3, \\
 c_{Y_k}(\bar{\mathbf{u}}; p, q) &= \int_{Y_k} [\tilde{\mathbf{K}}^k + \tilde{\mathbf{H}}^k(\bar{\mathbf{u}})] : \nabla_y p \cdot \nabla_y q, \quad k = 1, 2, 3, \\
 a_Y(\mathbf{u}, \mathbf{v}) &= \int_Y \mathbb{A} \nabla_y \mathbf{u} : \nabla_y \mathbf{v}, \\
 d_{Y_\beta}(p, q) &= \int_{Y_\beta} \delta \tilde{\mathbf{K}}^\beta \nabla_y p \cdot \nabla_y q, \quad \beta = 1, 2, 3, \\
 g_3^\alpha(\bar{\mathbf{u}}; p) &= \int_{\Gamma_\alpha} (\tilde{\mathbf{K}}^3 + \tilde{\mathbf{H}}(\bar{\mathbf{u}})) \nabla_y p \cdot \mathbf{n}^3 \, dS_y.
 \end{aligned} \tag{19}$$

It should be noted, that all integrals over Y , or its sub-parts are defined in the reference deformed configuration $\varepsilon^{-1}Y^\varepsilon(\hat{x})$, see (12).

As announced above, the two-scale split (16) employed in the limit problem arising from (10)-(11) enables to extract autonomous local problems for the characteristic responses $\boldsymbol{\omega}$, π and η . The following problems associated with the poroelasticity in the whole cell Y and perfusion in the dual porosity Y_3 must be resolved for a given time step increment Δt .

1. Find $(\boldsymbol{\omega}^{ij}, \pi^{ij}) \in \mathbf{H}_\#^1(Y) \times H_{\#0}^1(Y_3)$ such that

$$\begin{aligned}
 a_Y(\boldsymbol{\omega}^{ij} + \mathbf{\Pi}^{ij}, \mathbf{v}) - b_{Y_3}(\bar{\mathbf{u}}; \pi^{ij}, \mathbf{v}) &= 0, \quad \forall \mathbf{v} \in \mathbf{H}_\#^1(Y), \\
 b_{Y_3}(\bar{\mathbf{u}}; q, \boldsymbol{\omega}^{ij} + \mathbf{\Pi}^{ij}) + \Delta t c_{Y_3}(\bar{\mathbf{u}}; \pi^{ij}, q) &= 0, \quad \forall q \in H_{\#0}^1(Y_3).
 \end{aligned} \tag{20}$$

2. Find $(\boldsymbol{\omega}^\alpha, \pi^\alpha) \in \mathbf{H}_\#^1(Y) \times H_{\#0}^1(Y_3)$ such that

$$\begin{aligned}
 a_Y(\boldsymbol{\omega}^\alpha, \mathbf{v}) - b_{Y_3}(\bar{\mathbf{u}}; \pi^\alpha, \mathbf{v}) &= b_{Y_\alpha}(\bar{\mathbf{u}}; 1, \mathbf{v}), \quad \forall \mathbf{v} \in \mathbf{H}_\#^1(Y), \\
 b_{Y_3}(\bar{\mathbf{u}}; q, \boldsymbol{\omega}^\alpha) + \Delta t c_{Y_3}(\bar{\mathbf{u}}; \pi^\alpha, q) &= 0, \quad \forall q \in H_{\#0}^1(Y_3),
 \end{aligned} \tag{21}$$

where (in the sense of traces) $\pi^\alpha = \delta_{\alpha\beta}$ on $\partial_\beta Y_3 = \Gamma_\beta$.

3. Find $(\mathbf{u}^P, p_3^P) \in \mathbf{H}_\#^1(Y) \times H_{\#0}^1(Y_3)$, the particular response to the current reference state, such that

$$\begin{aligned}
 a_Y(\mathbf{u}^P, \mathbf{v}) - b_{Y_3}(\bar{\mathbf{u}}; p_3^P, \mathbf{v}) &= -\langle \hat{\boldsymbol{\sigma}}^{\text{tot}}, \nabla_y \mathbf{v} \rangle_Y, \quad \forall \mathbf{v} \in \mathbf{H}_\#^1(Y), \\
 b_{Y_3}(\bar{\mathbf{u}}; q, \mathbf{u}^P) + \Delta t c_{Y_3}(\bar{\mathbf{u}}; p_3^P, q) &= -\Delta t (c_{Y_3}(\bar{\mathbf{u}}; \hat{p}_3, q) + d_{Y_3}(\hat{p}_3, q)), \quad \forall q \in H_{\#0}^1(Y_3),
 \end{aligned} \tag{22}$$

The two channels ($\alpha = 1, 2$) are related to the following microscopic problems:

1. The channel flow correctors: Find $\eta_\alpha^k \in H_{\#}^1(Y_\alpha)$ such that

$$c_{Y_\alpha}(\bar{\mathbf{u}}; \eta_\alpha^k + y_k, q) = 0, \quad \forall q \in H_{\#}^1(Y_\alpha). \quad (23)$$

2. The particular response for the current load response: Find $p_\alpha^P \in H_{\#}^1(Y_\alpha)$, $\alpha = 1, 2$, such that

$$c_{Y_\alpha}(\bar{\mathbf{u}}; p_\alpha^P, q) = d_{Y_\alpha}(\hat{P}_\alpha, q) - c_{Y_\alpha}(\bar{\mathbf{u}}; \hat{P}_\alpha, q), \quad \forall q \in H_{\#}^1(Y_\alpha), \quad (24)$$

where $\hat{P}_\alpha = \mathbf{y} \cdot \nabla_x \hat{p}_\alpha^0 + \hat{p}_\alpha^1$.

3.4 Homogenized coefficients and the macroscopic model

Let us consider the limit two-scale equations of the weak formulation tested by macroscopic fields, namely by the displacements \mathbf{v}^0 and the two pressures q_β^0 , $\beta = 1, 2$ associated with the channel pressure increments p_α^0 . In these equations involving the two-scale functions integrated over local reference cells $Y(x)$, due to the decomposed forms (16), we can identify the following homogenized coefficients.

- The viscoelastic incremental tensor, $\mathcal{D} = (\mathcal{D}_{ijkl})$,

$$\mathcal{D}_{ijkl} = |Y|^{-1} [a_Y(\boldsymbol{\omega}^{kl} + \boldsymbol{\Pi}^{kl}, \boldsymbol{\omega}^{ij} + \boldsymbol{\Pi}^{ij}) + \Delta t c_{Y_3}(\bar{\mathbf{u}}; \pi^{kl}, \pi^{ij})]. \quad (25)$$

- The Biot poroelasticity tensor, $\mathcal{B} = (\mathcal{B}_{ij})$,

$$\mathcal{B}_{ij}^\alpha = |Y|^{-1} [b_{Y_3}(\bar{\mathbf{u}}; \pi^\alpha, \boldsymbol{\Pi}^{ij}) + b_{Y_\alpha}(\bar{\mathbf{u}}; 1, \boldsymbol{\Pi}^{ij}) - a_Y(\boldsymbol{\omega}^\alpha, \boldsymbol{\Pi}^{ij})]. \quad (26)$$

- The averaged stress, $\mathcal{S}^{\text{tot}} = (S_{ij}^{\text{tot}})$,

$$S_{ij}^{\text{tot}} = |Y|^{-1} \int_Y \hat{\boldsymbol{\sigma}}^{\text{tot}}. \quad (27)$$

- The retardation stress, $\mathcal{Q} = (Q_{ij})$,

$$Q_{ij} = |Y|^{-1} [b_{Y_3}(\bar{\mathbf{u}}; p_3^P, \boldsymbol{\Pi}^{ij}) - a_Y(\mathbf{u}^P, \boldsymbol{\Pi}^{ij})]. \quad (28)$$

- The effective channel permeability, $\mathcal{C} = (\mathcal{C}_{ij})$,

$$\mathcal{C}_{ij}^\beta = |Y|^{-1} c_{Y_\beta}(\bar{\mathbf{u}}; \eta^i + y_i, \eta^j + y_j). \quad (29)$$

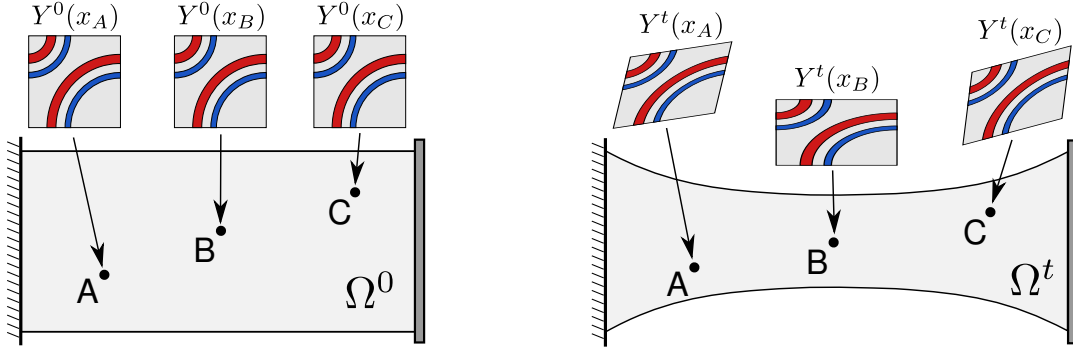


Figure 2: Schematic view of the deformed macroscopic specimen and of the local microstructures.

- The adjoint Biot poroelasticity tensor, $\mathcal{R} = (\mathcal{R}_{ij})$,

$$\mathcal{R}_{ij}^\alpha = |Y|^{-1} [b_{Y_\alpha}(\bar{\mathbf{u}}; 1, \boldsymbol{\omega}^{ij} + \boldsymbol{\Pi}^{ij}) + \Delta t g_3^\alpha(\bar{\mathbf{u}}, \pi^{ij})] . \quad (30)$$

- The perfusion coefficient,

$$\mathcal{G}_\beta^\alpha = |Y|^{-1} [g_3^\alpha(\bar{\mathbf{u}}, \pi^\beta) + (\Delta t)^{-1} b_{Y_\alpha}(\bar{\mathbf{u}}; 1, \boldsymbol{\omega}^\beta)] . \quad (31)$$

- The effective discharge due to deformation of the reference state; there are two coefficients:

$$\begin{aligned} \zeta_\alpha^{\text{eff}} &= (\Delta t |Y|)^{-1} b_{Y_\alpha}(\bar{\mathbf{u}}; 1, \mathbf{u}^P) + |Y|^{-1} g_3^\alpha(\bar{\mathbf{u}}, p_3^P + \hat{p}_3) + \int_{Y_\alpha} \delta \tilde{\mathbf{K}}^3 \nabla_y \hat{p}_3 \cdot \mathbf{n}^3 \, dS_y , \\ \gamma_\alpha^{k, \text{eff}} &= |Y|^{-1} [c_{Y_\alpha}(\bar{\mathbf{u}}; \mathbf{y} \cdot \nabla_x \hat{p}_\alpha^0 + \hat{p}_\alpha^1, y_k) + d_{Y_\alpha}(\mathbf{y} \cdot \nabla_x \hat{p}_\alpha^0 + \hat{p}_\alpha^1, y_k) + c_{Y_\alpha}(\bar{\mathbf{u}}; p_\alpha^P, y_k)] . \end{aligned} \quad (32)$$

In the above expressions, the boundary integrals on the interface Γ_β^3 , $\beta = 1, 2$, can be computed using the residual form expression, which yields

$$\begin{aligned} g_3^\beta(\bar{\mathbf{u}}, \pi^\alpha) &= (\Delta t)^{-1} b_{Y_3}(\bar{\mathbf{u}}; \pi^\beta, \boldsymbol{\omega}^\alpha) + c_{Y_3}(\bar{\mathbf{u}}; \pi^\alpha, \pi^\beta) , \\ g_3^\beta(\bar{\mathbf{u}}, p_3^P + \hat{p}_3) &= (\Delta t)^{-1} b_{Y_3}(\bar{\mathbf{u}}; \pi^\beta, \mathbf{u}^P) + c_{Y_3}(\bar{\mathbf{u}}; p_3^P + \hat{p}_3, \pi^\beta) + d_{Y_3}(\hat{p}_3, \pi^\beta) . \end{aligned} \quad (33)$$

Moreover, the symmetry expression $\mathcal{B}^\alpha = \mathcal{R}^\alpha$ can be proved, $\alpha = 1, 2$.

Macroscopic equations On substituting the corresponding expressions of the homogenized coefficients in the limit problem arising from (10)-(11) by the homogenized coefficients, equations

of the macroscopic incremental problem are obtained which involve the increments \mathbf{u}, p_α ,

$$\begin{aligned} \int_{\Omega} \left(\mathbf{D} \nabla_x \mathbf{u} - \sum_{\alpha} p_{\alpha} \mathbf{B}^{\alpha} \right) : \nabla_x \mathbf{v} &= L^{\text{new}}(\mathbf{v}) + \int_{\Omega} (\mathbf{Q} - \mathbf{S}^{\text{tot}}) : \nabla_x \mathbf{v} , \\ \int_{\Omega} q_{\beta} \left(\mathbf{B}^{\beta} : \nabla_x \mathbf{u} + \Delta t \sum_{\alpha} \mathcal{G}_{\alpha}^{\beta} p_{\alpha} \right) &+ \Delta t \int_{\Omega} \mathbf{c}^{\beta} \nabla_x p_{\beta} \cdot \nabla_x q_{\beta} = -\Delta t \int_{\Omega} (\zeta_{\beta}^{\text{eff}} q_{\beta} + \gamma_{\beta}^{\text{eff}} \cdot \nabla_x q_{\beta}) . \end{aligned} \quad (34)$$

where $\beta = 1, 2$ and $L^{\text{new}}(\mathbf{v})$ is the functional defined by the volume and surface traction forces at time $t + \Delta t$. Boundary conditions for the two pressure increments can be introduced for a generalized decomposition of $\partial\Omega$. In particular, p_{α} can be prescribed on $\partial_{p,\alpha}\Omega \subset \partial\Omega$, whereas there is no relationship between $\partial_{p,1}\Omega$ and $\partial_{p,2}\Omega$; they can be disjoint or can overlap. This requires to establish two admissibility sets Q^{α} , $\alpha = 1, 2$ and, correspondingly, two spaces Q_0^{α} .

Incremental algorithm At each time level t , the reference two-scale configuration is established for a given FE discretization, so that at selected points $\hat{x}^k \in \Omega(t)$, $k = 1, 2, \dots$ (associated with the Gaussian quadrature points) the local problems (20)-(24) are solved. Consequently, the effective coefficients (25)-(32) are evaluated to constitute the macroscopic subproblem: Given the reference state, domain Ω and the microscopic configuration at time t , for the new load (associated with time $t + \Delta t$) find $(\mathbf{u}, p_1, p_2) \in V(\Omega) \times Q^1(\Omega) \times Q^2(\Omega)$ such that (34) holds for all test fields $(\mathbf{v}, q_1, q_2) \in V_0(\Omega) \times Q_0^1(\Omega) \times Q_0^2(\Omega)$. With the time increment computed from (34), the local configurations are updated in analogy with the procedure described in [8], cf. [7].

4 NUMERICAL ILLUSTRATION AND CONCLUSIONS

The two-scale model of the double porosity large deforming poroelastic medium has been implemented in the in-house developed SfePy code which is well suited for this kind of modelling. To illustrate capabilities of the homogenized model, we consider a 2D example with topology of the channels depicted in Fig. 1. It is not possible to provide periodic lattices with domains Ω_k^{ε} being simply connected for each $k = 1, 2, 3$. As the consequence, the homogenized permeabilities \mathbf{C}^{β} are rank-one, so that they must be regularized by adding a very small isotropic tensor. The macroscopic domain Ω is rectangular. On two opposite edges of $\partial\Omega$ the Dirichlet boundary conditions are prescribed which mimic that the structure is being stretched in the x_1 direction; the ramp-and-hold test is applied. The whole boundary $\partial\Omega$ is impermeable. Therefore, the fluid is being redistributed in the structure as the mere consequence of the deformation. The viscous effects captured by the retardation stress \mathbf{Q}^{ε} are associated with the flow between the double porosity.

The proposed model describes behaviour of the Biot medium featured by the double porosity. The topology of the microstructure with two conductive channels leads to the two macroscopic pressure fields. For the linear case of small deformation, in [9], an analogous model of the periodic Biot medium with large contrast permeability was considered to describe tissue perfusion.

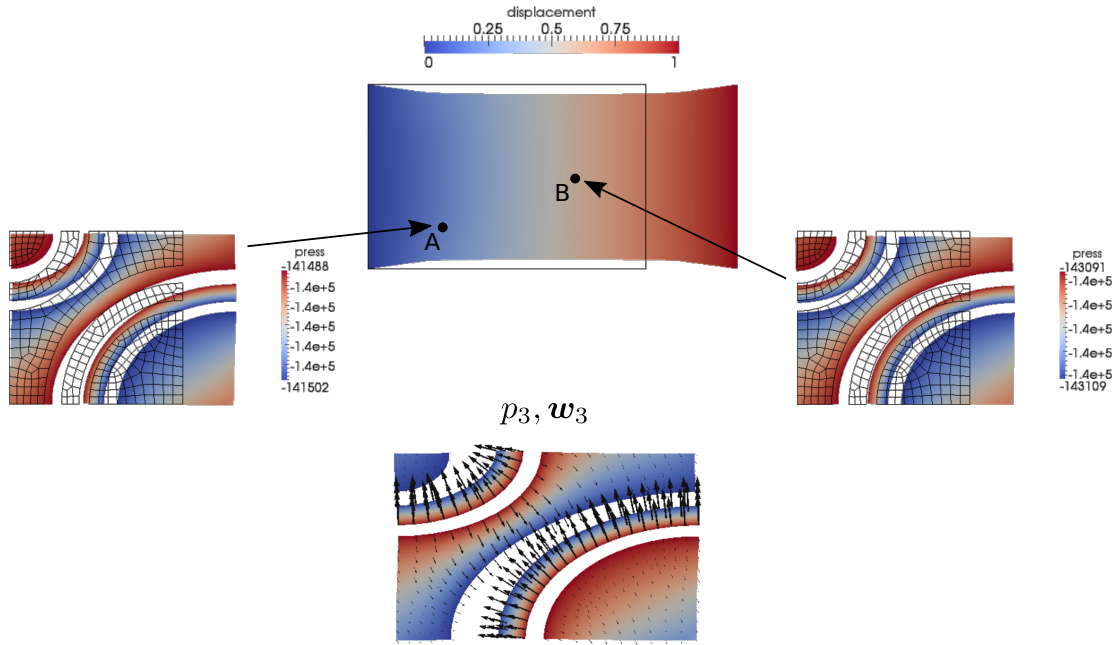


Figure 3: Macroscopic response of the deformation and displayed local reconstructions of the flow and pressure in the double porosity compartments Y_3 .

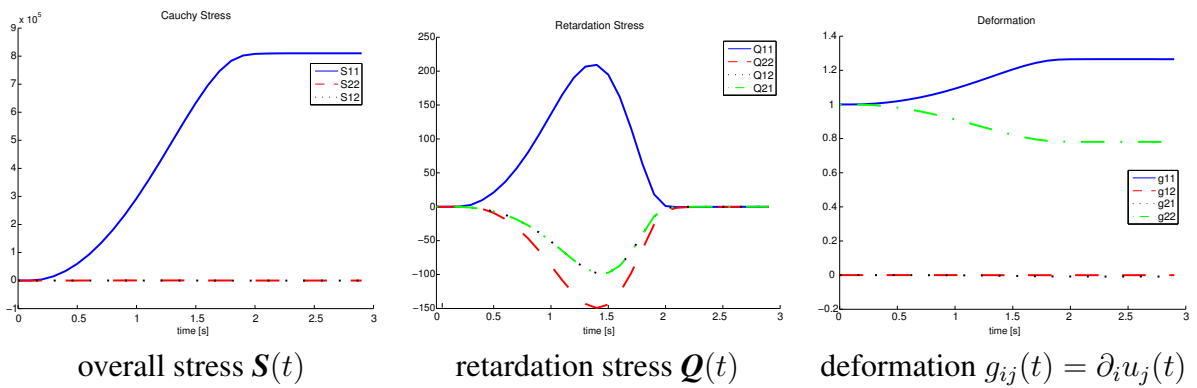


Figure 4: Macroscopic response computed at point B (see Fig. 3) in the time interval of the test

ACKNOWLEDGMENTS

The research and the participation in the conference was supported in part by the grant project GACR 16-03823S and by the the project LO 1506 of the Czech Ministry of Education, Youth and Sports.

REFERENCES

- [1] Biot, M. A. Variational Lagrangian-thermodynamics of non isothermal finite strain. mechanics of porous solid and thermomolecular diffusion. *Int J Solids Struct*, (1977) 13: 579–597.
- [2] Brown, D.L., Popov, P. and Efendiev, F. Effective equations for fluid-structure interaction with applications to poroelasticity. *Applicable Analysis*. (2014) 93: 771-790
- [3] Cioranescu, D., Damlamian, A., and Griso, G. The periodic unfolding method in homogenization, *SIAM Journal on Mathematical Analysis* (2008) 40: 1585–1620.
- [4] Coussy, O. *Poromechanics*. John Wiley & Sons, 2004.
- [5] Meroi, E. A. Schrefler, B. A. and Zienkiewicz, O. C. Large strain static and dynamic semisaturated soil behaviour. *Int J Numer Anal Met*, (1995) 19: 81–106.
- [6] Rohan, E. Sensitivity strategies in modelling heterogeneous media undergoing finite deformation. *Math Comput Simulat*, (2003)61): 261–270..
- [7] Rohan E. Modeling large-deformation-induced microflow in soft biological tissues. *Theoretical and Computational Fluid Dynamics* (2006) 20:251-276
- [8] Rohan, E., Cimrman, R., and Lukeš, V. Numerical modelling and homogenized constitutive law of large deforming fluid saturated heterogeneous solids *Computers and Structures* (2006)84:1095–1114
- [9] Rohan, E. and Cimrman, R. Two-scale modelling of tissue perfusion problem using homogenization of dual porous media. *Int. J. Multiscale Comput. Eng.*, (2010)8: 81–102.
- [10] Rohan, E., Naili, S., Cimrman, R. and Lemaire, T. Multiscale modeling of a fluid saturated medium with double porosity: Relevance to the compact bone. *J. Mech. Phys. Solids*, (2012) 60: 857–881.
- [11] Rohan, E. and Lukeš, V. On modelling nonlinear phenomena in deforming heterogeneous media using homogenization and sensitivity analysis concepts. *Appl Math Comput*, (2015)267:583–595.
- [12] Rohan, E., Naili, S., and Lemaire, T. Double porosity in fluid-saturated elastic media: deriving effective parameters by hierarchical homogenization of static problem. *Continuum Mech Thermodyn*, (2015)28: 1263–1293.
- [13] Rohan, E. and Lukeš, V. Modelling large-deforming fluid-saturated porous media using an Eulerian incremental formulation. *Advances in Engineering Software* (2017)113: 84–95.

On Size Effects Emerging in Pattern-Transforming Elastomeric Metamaterials

Ondrej Rokos^{*}, Maqsood Ameen^{**}, Ron H. J. Peerlings^{***}, Marc G. D. Geers^{****}

^{*}Eindhoven University of Technology, ^{**}Eindhoven University of Technology, ^{***}Eindhoven University of Technology, ^{****}Eindhoven University of Technology

ABSTRACT

Cellular and foam-like materials have been successfully used in many engineering applications over decades due to their attractive overall properties such as light weight, high specific stiffness, or good ability to absorb impact. These properties result mainly from a particular arrangement of the base material in the underlying microstructural morphology, which nowadays can be controlled by means of additive manufacturing. Properties of such designed materials can range from a significant dependence of stiffness on overall deformation to more exotic ones, such as negative Poisson's ratio. In general, the entire class of materials with designed microstructures is usually referred to as mechanically tunable metamaterials, because their apparent properties cannot be observed in nature. It is of high engineering interest to design materials with specific effective properties, and to manufacture microstructures that are optimal with respect to their target application. To this end, an efficient homogenization procedure capable of accurate predictions of the mechanical response of mechanically tunable metamaterials needs to be provided. In the present study, we examine systematically and quantitatively size effects occurring in elastomeric voided metamaterial over a wide range of scale ratios, providing thus a solid basis for the development of advanced homogenization schemes. The elastomer under consideration follows the Mooney-Rivlin type of constitutive law, and its microstructural morphology consists of a periodic arrangement of circular holes. The resulting material exhibits an auxetic effect due to microstructural instabilities, followed by a rotational transformation of rigid islands positioned between individual holes. The effective behavior is obtained by considering an entire family of microstructures shifted randomly relative to specimen's geometry, making subsequently use of ensemble averaging. The ensemble averaged, homogenized response is shown to exhibit strong size effects, emerging either from boundary layers or steep strain gradients, which in certain parts of the specimen restrict the underlying kinematic microstructural mechanism that otherwise establishes long-range arrangements in the microstructure. Such long-range arrangements, and mainly their spatial variations, are one of the great challenges of homogenization theory. Based on the numerical solutions provided, first steps in enriching FE2 computational homogenization scheme capable of capturing these (size) effects will be discussed. Acknowledgement: The research leading to these results has received funding from the European Research Council under the European Union's Seventh Framework Programme (FP7/2007-2013) / ERC grant agreement no. [339392].

A New Workflow for an Experimental Testing and Simulation of Osteosynthesis Systems for Tibial Fractures

Michael Roland*, Thorsten Tjardes**, Bertil Bouillon***, Stefan Diebels****

*Saarland University, **Cologne Merheim Medical Center, ***Cologne Merheim Medical Center, ****Saarland University

ABSTRACT

A personalized approach to fracture therapy necessitates the integration of knowledge and techniques from mechanics, orthopedic trauma surgery and computer science. Merging the relevant knowledge of these disciplines can lead to the development of less invasive, individually tailored treatment approaches comprising the surgical technique and the implant used. Focusing on the case of distal tibia fractures, a new setup for a more realistic experimental testing of osteosynthesis systems is presented. Therefore, the experimental workflow is organized as follows: (1) starting point is a testing device to produce predefined tibia fractures, (2) the fractured lower extremities will be treated by an orthopedic trauma surgeon and (3) tested in a second testing device simulating the forces acting during a normal step forward. The experiments are realized with artificial bones from Sawbone as well as with fresh frozen human cadaveric specimen. During the first step of the workflow, the main goal is the repeatability of the fractures with respect to the applied forces and moments. Before the procedure starts, computed tomography scans of the bones are performed and are used as basis for the simulations. After the fracture is produced, an orthopedic trauma surgeon treats the lower extremity with an osteosynthesis locking plate and a second computed tomography scan is executed to enhance the computational model. Thereafter, in the last step of the testing workflow, the treated tibia is clamped in the second testing device and a mechanical loading scenario is applied on the bone-implant-system. The loading scenario is based on the OrthoLoad database and is calibrated by the subject-specific data of the human cadaveric specimen. During the test, stresses and strains are gained via a high-speed camera system combined with digital image correlation and several pressure and force measurements. This workflow allows a more realistic testing of tibia implants and gives information about the mechanical behavior of the fracture gap, like the interfragmentary move. The whole procedure is also simulated based on the performed tomograms. Therefore, the image stacks are segmented, the material parameters are assigned and passed to a meshing procedure. After that, finite element simulations are executed with respect to the testing parameters and protocols in order to validate and to verify the simulation process. Here, the investigation of the simulations is focused on the best possible match of the experiments and the achieved results.

Highly Scalable End-to-end Parallel Framework for Coupled Multi-scale and Multi-physics Fluid Dynamics

Sabine Roller^{*}, Harald Klimach^{**}, Daniel F. Harlacher^{***}

^{*}University of Siegen, Simulation Techniques and Scientific Computing, ^{**}University of Siegen, Simulation Techniques and Scientific Computing, ^{***}University of Siegen, Center for Information and Media Technology

ABSTRACT

This contribution is concerned with software engineering for HPC applications in engineering with a focus on multi-physics simulations such as fluid-acoustics, fluid-structure or fluid-electromagnetics applications. Our goals are easy usability, high maintainability, easy portability and of course high performance with high scalability, even when changing the characteristics of the application and/or the system. Usability is a key property to any application as it sets the bounds on the efficiency the user can work with it. But for developing new applications, also code maintainability is an important issue. In the context of multi-physics simulations, this introduces a conflict of objectives, considering modularity and encapsulation on the one hand, and integration and interaction on the other. With the focus on these objectives, we develop the APES simulation framework, consisting of a common core to handle meshes, modularized solvers, and additional helper tools for preprocessing, post-processing, steering and evaluation. The implementation of all parts ensures high scalability and good load balancing, allowing for workflows that are parallel from the very beginning to the final step. We call this the end-to-end-parallelization. Software engineering for the entire framework development guarantees for maintainability as well as feature development with the focus on efficiency, as any chain is only as strong as its weakest element. In this contribution, we will present an overview of the APES framework, show some software engineering principles like regular regression checks, and automatic code documentation, but also applications of different complexity together with the impacts on performance and load balancing. References: Roller S. et al. (2011): An Adaptable Simulation Framework Based on a Linearized Octree. In: Resch M., Wang X., Bez W., Focht E., Kobayashi H., Roller S. (eds) High Performance Computing on Vector Systems 2011. Springer, Berlin, Heidelberg Harlacher D.F., Klimach H., Roller S. (2015): Experiences in Developing HPC Software with Portable Efficiency. In: Resch M., Bez W., Focht E., Kobayashi H., Patel N. (eds) Sustained Simulation Performance 2014. Springer, Cham

Additive Manufacturing Inspired Computation

Anthony Rollett^{*}, Christopher Kantzos^{**}, Joseph Pauza^{***}, Tugce Ozturk^{****}, Ross
Cunningham^{*****}

^{*}Carnegie Mellon Univ., ^{**}Carnegie Mellon Univ., ^{***}Carnegie Mellon Univ., ^{****}Carnegie Mellon Univ.,
^{*****}Carnegie Mellon Univ.

ABSTRACT

Representative 3D synthetic microstructures were generated in Dream.3D, based on the characteristics of additively manufactured (AM) Ti-6Al-4V, and the input structures were modified for features of interest. The sensitivity to microstructure was quantified by performing full field simulations using a spectral elasto-viscoplastic code that uses parallelized fast Fourier Transforms (FFTs) and Hierarchical Data Format (HDF) for input/output. The strongest effect was related to volume fraction of the alpha phase. Texture in the original deposit produced anisotropy although this is mitigated by the multiplicity of variants that occurs in the beta to alpha transformation. To investigate the effect of surface roughness, computed tomography scans from AM samples made from two different size powders were used in the same elasto-plastic FFT code with isotropic properties. Near-surface voids and low points in the surface dominated the hot spots in stress. Subtle differences in hot spot character between von Mises stress and triaxiality were noted. These results were consistent with experimentally determined variations in fatigue life as a function of near-surface porosity in AM parts. The grain-scale microstructure of AM parts is well known to be sensitive to variations in processing conditions such as power, scan speed and hatch spacing. These variations are explored with the Monte Carlo ssparks code. Preliminary efforts are described to add the capability to simulate the preferred <100> growth direction in solidification of cubic materials.

Simulation of Dilute and Dense Non-Spherical Particle Laden Flows: Movement and Orientation Behaviour

Miguel A. Romero-Valle*, Hermann Nirschl**, Christoph Goniva***

*BASF SE, **Karlsruhe Institute of Technology, ***DCS Computing GmbH

ABSTRACT

The fast advancement of existing and new functional material systems, where particulate morphology differs from traditional systems (e.g. fibres, flakes, ...), demands technical know-how on the processing of non-spherical particles in liquid media. There are few to no technical relevant tools available for the prediction of such particulate systems, specifically when particle-particle interactions and particle orientation are relevant, making development of such processes time consuming and expensive. Therefore, a tool is needed to support process design and further understand non-spherical systems. On this work, a novel approach for the calculation of drag forces and drag induced torques for non-spherical particles in the context of CFD-DEM coupling (Kloss, Goniva, Hager, Amberger, & Pirker, 2012) is presented. The approach is inspired by Stokesian Dynamics for the computation of drag forces and torques (Joung, 2006) when using the multi-sphere method for the representation of non-spherical particles (Kruggel-Emden, Rickelt, Wirtz, & Scherer, 2008). In each multi-sphere particle, individual spheres of the multi-sphere clump have a hydrodynamic contribution to the multi-sphere drag force depending on the flow conditions that the sphere experiences, which in turn induces a torque on the multi-sphere representation. To consider the hydrodynamic proximity of the spheres within the multi-sphere clump, one computes the individual sphere contributions using Stokes's drag law and an Oseen type tensor, both which in a Stokesian Dynamics context are used to compute the mobility matrix of a particle suspension system. The method is validated for single rigid fibre particles in shear flow using an analytical solution given by an adaptation of Jeffery's orbits. Preliminary results show promise for dilute and semi-dilute rigid fibre suspensions, where a tapered channel is simulated and compared to experimental data. Potential relevant applications are discussed and evaluated.

Joung, C. G. (2006). Dynamic simulation of arbitrarily shaped particles in shear flow. *Rheologica Acta*, 46(1), 143–152. <https://doi.org/10.1007/s00397-006-0110-6>

Kloss, C., Goniva, C., Hager, A., Amberger, S., & Pirker, S. (2012). Models , algorithms and validation for opensource DEM and CFD-DEM. *Pcfd*, 12, 140–152. <https://doi.org/10.1504/PCFD.2012.047457>

Kruggel-Emden, H., Rickelt, S., Wirtz, S., & Scherer, V. (2008). A study on the validity of the multi-sphere Discrete Element Method. *Powder Technology*, 188(2), 153–165. <https://doi.org/10.1016/j.powtec.2008.04.037>

Estimation of Modeling Errors in Local Quantities of Interest in the Elastostatic Analysis of Heterogeneous Solids

Albert Romkes*, Justin King**

*South Dakota School of Mines & Technology, **South Dakota School of Mines & Technology

ABSTRACT

We consider the analysis of the mechanics of multiphase composite materials, exhibiting complex microstructure with highly oscillatory material properties. It is generally prohibitive to numerically resolve all the features in the microstructure. Classical approaches have therefore focused on methods of homogenization, generally based on the assumption that the microstructure of the media is periodic, or on techniques for determining effective properties of representative volume elements. These averaged material models cannot account for local micromechanical effects that are critical factors in the initiation and evolution of failure mechanisms. To resolve this issue, Oden et al. [1] developed the Goal-Oriented Adaptive Modeling (GOAM) method. It represents an adaptive multi-scale modeling method based on control of modeling errors in a local quantity of interest of the material response, specified by the analyst. The GOAM method starts the analysis with an initial model of homogenized properties that are obtained via the classical averaging techniques. The homogeneous surrogate model is then enhanced in an iterative process of including the material microstructure in a local area surrounding the quantity of interest that increases in size with every iteration step. A critical element in the GOAM method is the ability to accurately estimate the modeling error. Currently, this is established by providing a residual-based a posteriori error estimator. It involves solving for a global influence function, related to the quantity of interest, and subsequently computing global integrals of governing residual functionals. Unfortunately, in the case of multiphase composite materials, this estimation process can be computationally prohibitive, again due to the complexity of the microstructure. We therefore propose a technique for local, goal-oriented estimation of the modeling error that resolves this computational issue. It is a continued effort by the authors in recent years and based on a local variational approach. It requires computing influence functions and residual integrals which are strictly local and can be computed at low computational cost and at high numerical accuracy. We introduce this approach for the linear elastostatic analysis of multiphase composites and the investigation of linear local quantities of interest. References: [1] J. T. Oden, S. Prudhomme, A. Romkes, P. Bauman. Multi-scale modeling of physical phenomena: Adaptive control of models. *SIAM J. Sc. Comp.*, Vol. 28 (6), 2359-2389, 2006. [2] A. Romkes, T. C. Moody. Local Goal-Oriented Estimation of Modeling Error for Multi-Scale Modeling of Heterogeneous Elastic Materials. *Int. J. Comp. Meth. Eng. Sc. Mech.*, Vol. 8 (4), 201--209, 2007.

Hamiltonian-based Buckling Analysis of Double-layered Orthotropic Nanoplate Systems Subjected to In-plane Magnetic Field

Dalun Rong^{*}, Zengbo Lian^{**}, Junhai Fan^{***}, Xinsheng Xu^{****}

^{*}State Key Laboratory of Structure Analysis of Industrial Equipment, International Research Center for Computational Mechanics, Dalian University of Technology, ^{**}State Key Laboratory of Structure Analysis of Industrial Equipment, International Research Center for Computational Mechanics, Dalian University of Technology, ^{***}State Key Laboratory of Structure Analysis of Industrial Equipment, International Research Center for Computational Mechanics, Dalian University of Technology, ^{****}State Key Laboratory of Structure Analysis of Industrial Equipment, International Research Center for Computational Mechanics, Dalian University of Technology

ABSTRACT

Due to the exceptional thermal, electrical, mechanical and magnetic properties, nanoscale structures have wide applications in nanoelectro-mechanical systems (NEMS). The double-layered orthotropic nanoplate system (DLNS) with magnetic effects is one of the fundamental components in the manufacture of high frequency and high sensitivity NEMS resonant magnetic field sensors. Therefore, a thorough understanding of the DLNS is of considerable importance for the design and fabrication of such sensors. However, the existing theoretical studies were concentrated on the DLNS with Levy-type boundaries. Exact solutions for dynamic behaviors of the DLNS with non Levy-type boundaries were rarely mentioned. Therefore, this paper aims to present an analytical symplectic method to find the exact solutions of buckling of the DLNS with two opposite edges clamped subjected to in-plane magnetic field based on Eringen's nonlocal theory. In the symplectic space, a new total unknown vector is introduced to establish the Hamiltonian system, so that the governing equations of biaxial buckling in the Lagrangian system are converted into its Hamiltonian dual form by a rigorous way. The governing equation of Hamiltonian system is reduced to a set of one-order ordinary differential equations instead of a high-order differential governing equation. Therefore, the method of separation of variables and the expansion of eigenfunctions are available to solve the governing equation and to derive the exact solution. For the Levy-type edges, the analytical critical buckling load equations are derived, and buckling mode shapes are expressed in terms of the total unknown vectors. Based on the obtained exact solution, DLNS with two opposite edges clamped are investigated by symplectic superposition technique. Closed-form solutions of the original problems are achieved by superposition of the exact solution from the fundamental subproblems. Comparisons validate the efficiency and accuracy of the proposed method. The comprehensive numerical examples demonstrate the effects of nonlocal parameters, boundary conditions, stiffness parameters, and magnetic field on the buckling behaviors of the nanoplate systems. This paper presents an analytical solution to nanoplate systems with two opposite edges clamped which can serve the design and fabrication of NEMS.

Topology Optimization Design of Broadband Elastic Hyperbolic Metamaterial

Junjie Rong^{*}, Wenjing Ye^{**}

^{*}The Hong Kong University of Science and Technology, ^{**}The Hong Kong University of Science and Technology

ABSTRACT

Metamaterials with delicately engineered architectures have been attracting considerable attention because of their unique properties and/or capabilities for wave manipulation. One such an example is metamaterials with hyperbolic dispersion, which have many promising applications such as negative refraction, partial focusing and super-resolution imaging [1]. However, compared with their acoustic and electromagnetic counterparts, the design of elastic hyperbolic metamaterials is more challenging due to the presence of both longitudinal and transverse waves [2]. In this talk, we present a computational approach for designing elastic hyperbolic metamaterial with a broad operation frequency band. A design formulation based on topology optimization is constructed and solved by a gradient-based optimizer. The material is designed to achieve the desired dispersion with a complete band gap in one direction and a single propagating state in the other direction. Proper constraints are imposed to avoid multiple mode interactions in the designed frequency band. Because the structural worthiness could be hampered by the perforation introduced in the design, the static effective modulus is incorporated into the optimization algorithm as a constraint in order to maintain a certain level of stiffness. Using the proposed optimization formulation, our designed metamaterial exhibits hyperbolic dispersion over a broad relative frequency range of 77%. Partial focusing and imaging with a super-resolution up to 0.25 times wavelength are also demonstrated. The developed approach could be extended to the design of other metamaterials with any desired dispersion. References: [1] Alexander Poddubny, Ivan Iorsh, Pavel Belov, Yuri Kivshar. Hyperbolic metamaterials. *Nature Photonics*, 7: 948-957, 2013. [2] Joo Hwan Oh, Hong Min Seung, Yoon Young Kim. A truly hyperbolic elastic metamaterial lens. *Applied Physics Letters*, 104: 073503, 2014.

The Effect of Shear Properties of Anterior Cruciate Ligament and of Patellar Tendon Grafts on Whole-Knee Biomechanics

Ryan Rosario*, Ellen Arruda**, Rhima Coleman***

*University of Michigan, **University of Michigan, ***University of Michigan

ABSTRACT

Finite element (FE) models of the knee are used to study how joint injury and repair affect joint kinematics and tissue mechanics. Ligaments are transversely isotropic, non-linear poro-viscoelastic materials. Typically, ligament material models are fit to uniaxial tension data along the predominant fiber direction (axial) and, less commonly, uniaxial tension data orthogonal to the fiber direction (transverse). Transversely isotropic material models can have excellent fit to axial and transverse data yet predict very different shear responses. These differences in shear behavior result in differences in tissue deformation and joint kinematics in whole joint models. In this study, the transversely isotropic freely-jointed eight-chain and the Holzapfel-Gasser-Ogden models were used to describe ACL behavior in a previously validated whole-knee FE model [1]. Material properties of the ACL were fitted to axial and transverse data with applied constraints to result in 3 shear response levels. Axial compression of the joint and anterior tibial shear were simulated. The same procedure was repeated for the patellar tendon. Under 800 N of axial compression, simulations showed that low shear stiffness resulted in the least overall joint motion in terms of knee flexion, external tibial rotation, and anterior tibial displacement, and mid shear stiffness resulted in the most. The high shear stiffness ACL model resulted in lowest maximum compression in the femoral articular cartilage. The mid shear stiffness model resulted in the highest maximum compression (12.1%). Differing shear properties can cause a 3.0° difference in external tibial rotation and a 1.0 mm difference in anterior tibial displacement under 800 N of axial compression. Small differences in joint kinematics can shift the location of maximum deformation in cartilage, potentially leading to the initiation and progression of osteoarthritis in cartilage [2]. Thus, to most accurately model the behavior of the knee in response to physical loads, material models of ligaments should also be well-fit to shear behavior. References: [1] Marchi B.C., et al., (2016). Biomech Model Mechanobiol. [2] Andriacchi T.P., et al., (2009). J Bone Joint Surg.

On the Application of Embedded Solution Techniques for the Solution of Computational Wind Engineering Problems

Riccardo Rossi^{*}, Ruben Zorrilla^{**}, Pooyan Dadvand^{***}, Roland Wuechner^{****}, Antonia Larese^{*****}, Jordi Cotela^{*****}

^{*}UPC, CIMNE, ^{**}UPC, CIMNE, ^{***}CIMNE, ^{****}TUM, ^{*****}CIMNE, ^{*****}TUM

ABSTRACT

Computational Wind Engineering (CWE) focuses on the assessment of the wind flow around structures. The simulation of city-scale problems is challenging due to the sheer size of the problem as well as due to the geometrical complexity of the problem. Current work combines a body fitted discretization of the surface with an embedded approach, employed in the simulation of the city buildings.

Locally-Implicit DG-FEM for Moment-Closure Approximations of Plasma

James Rossmanith*

*Iowa State University

ABSTRACT

In many applications broadly of interest to modern science, the dynamics of gas and plasma can be simulated using either kinetic or fluid models. Kinetic models are valid over most of the spatial and temporal scales that are of physical relevance in many application problems; however, they are computationally expensive due to the high-dimensionality of phase space. Fluid models typically have a more limited range of validity, but are generally computationally more tractable than kinetic models. One critical aspect of fluid models is the question of what assumptions to make in order to close the fluid model (i.e., what assumptions can we make about the microscale physics that will allow us to not explicitly resolve these scales). In principle, if the moment-closures are sufficiently information-dense, they allow fluid models to accurately capture important non-equilibrium dynamics. Determining such closures that also produce systems of well-posed partial differential equations is an ongoing area of research. In this work, we develop a class of high-order discontinuous Galerkin finite element methods (DG-FEM) for solving fluid models with various moment-closure approximations. The proposed methods are in the class of locally-implicit DG-FEM, which are built using a predictor-corrector approach. In particular, the predictor is a locally implicit spacetime method (i.e., the predictor is something like a block-Jacobi update for a fully implicit spacetime DG method). The corrector is an explicit method that uses the spacetime reconstructed solution from the predictor step. We develop limiters that guarantee that at each quadrature point the solution remains realizable. The schemes developed in this work are applied to a variety of moment-closures, including quadrature-based moment closures (QMOM) and ϕ -divergence moment closures. The resulting numerical methods are applied to several standard numerical tests in one dimension for both gas and plasma dynamics problems. These tests are used as benchmarks to verify and assess the accuracy and robustness of the method.

Application of Residual Strength Study to Improve Concrete Constitutive Models

Michael Roth^{*}, George Vankirk^{**}, Andreas Frank^{***}

^{*}US Army Engineer Research and Development Center, ^{**}US Army Engineer Research and Development Center,
^{***}US Army Engineer Research and Development Center

ABSTRACT

Impact and blast effects in geomaterials like concrete and soil is an area of important research interest for the U.S. Department of Defense. Events of specific interest include projectile penetration, shaped-charge penetration, and close-in explosive detonation, which involve a spectrum of challenging material behaviors and failure modes. Due to the events' high-rate impulsive nature, large deformations and material failure must be accurately represented; accurate representation of material behavior in the near and far-field regions from the event is especially critical to achieve reliable modeling results. The constitutive model must capture the high-rate, high-pressure mechanics occurring near a penetrator nose or explosive detonation that dominate the initial penetration and cavity formation. The model must also accurately represent shock-induced far-field effects such as brittle tensile failure and material heave, which dominate overall failure at the structural scale. Over the past decade technologies have evolved for this class of problems, with emphasis in areas like phenomenologically advanced material models to accurately predict material damage, failure, and residual strength. The proposed presentation will detail the results of a study on residual strength of a high-performance concrete. In this study, the residual unconfined compressive strength of a high-performance concrete ($f'_c \sim 130$ MPa) was investigated by using samples that were pre-loaded to specific states of triaxial confinement. The samples were first subjected to specified stress-strain paths corresponding to pure hydrostatic compression and uniaxial strain in compression. Both the hydrostatic compression and uniaxial strain tests were performed at low- and high-pressure levels under controlled conditions to prevent reaching the material failure limit. Once the samples were tested through either hydrostatic compression or uniaxial strain, they were recovered and subjected to unconfined compression until failure. Data from these samples were compared to the unconfined compressive strength of pristine samples from the same concrete batch. Residual strength was determined through a comparison of these values and as a means to quantify damage induced (both with and without shear) by the specified stress-strain paths. Applications of these data are discussed for future improvements to concrete constitutive models commonly used at the U.S. Army Engineer Research and Development Center to simulate dynamic events. Permission to publish was granted by Director, Geotechnical and Structures Laboratory.

Molecular Mobility in Driven Monomeric and Polymeric Glasses

Joerg Rottler*

*University of British Columbia

ABSTRACT

Glasses form when their structural relaxation time exceeds the experimentally accessible observation timescales, and the material falls out of equilibrium. However, relaxation speeds up greatly as soon as the glass is being deformed. The relaxation time is an important internal state variable in many theories of amorphous plastic flow, and can be measured with dynamic light scattering or fluorescence spectroscopy techniques. In this talk, we show with molecular simulations that in monomeric supercooled liquids and glasses that are plastically flowing at a constant shear stress while being deformed with fixed strain rate, the microscopic structural relaxation time equals a macroscopic "Maxwell time" that is proportional to the ratio of shear stress and strain rate. The equality holds for all rheological regimes from temperatures above the glass transition all the way to the athermal limit, and arises from the competing effects of elastic loading and viscous dissipation. In macromolecular (polymeric) glasses, however, the stress decouples from the Maxwell time and the relaxation time is in fact further reduced even through the stress rises during glassy strain hardening. Comprehensive expressions are developed that predict the accelerated dynamics during active deformation in terms of all relevant deformation variables.

Nanoindentation in Studying Mechanical Properties of Organic-rich Shale

Mo Rouainia^{*}, Majid Goodarzi^{**}, Andy Aplin^{***}

^{*}Newcastle University, ^{**}Newcastle University, ^{***}Durham University

ABSTRACT

Shale, or mudstone, is the most common sedimentary rock. It is a heterogeneous, multi-mineralic natural composite consisting of clay mineral aggregates, organic matter, and variable quantities of minerals such as quartz, calcite, and feldspar. Determination of the mechanical response of shales through experimental procedures is a challenge due to their heterogeneity and the practical difficulties of retrieving good-quality core samples. Therefore, in recent years extensive research has been directed at developing alternative approaches for the mechanical characterisation of shale rocks [1,2,3,4,5]. In this paper, several well-characterised shale samples have been subjected to indentation tests using different indenters in order to generate various stress-strain paths under controlled load conditions set at 500mN. Numerical modelling has been undertaken to back-calculate the plastic response of the shale samples using load-displacement curves obtained from indentation tests. Inverse analysis of the indentation tests was conducted by assuming only two material parameters, angle of friction and cohesion. The reduced modulus was derived from unloading curves and the value of Poisson's ratio dilation and contact friction were assumed. Issues related to indentation testing such as loading and unloading rate, tip shape and creep behaviour were studied. The capabilities and limitations of this test applied to shale rock were further clarified. References [1] Bennett K.C., Berla L.A., Nix W.D., Borja R.I. 2015. Instrumented nanoindentation and 3D mechanistic modeling of a shale at multiple scales. *Acta Geotechnica*, 10, 1-14. [2] Bobko C., Ulm F.J. 2008. The nano-mechanical morphology of shale. *Mechanics of Material*, 40, 318-337. [3] Goodarzi M., Rouainia M., Aplin A.C. 2016. Numerical evaluation of mean-field homogenisation methods for predicting shale elastic response. *Computational Geosciences*, Volume 20(5), 1109–1122 [4] Goodarzi M., Rouainia M., Aplin A.C. Cubillas P., de Block M. 2017. Predicting the elastic response of organic-rich shale using nanoscale measurements and homogenisation methods. *Geophysical Prospecting*, 65, 1597–1614. [5] Ortega J.A., Ulm F.J., Abousleiman Y. 2010. The effect of particle shape and grain-scale properties of shale: A micromechanics approach. *International Journal of Numerical and Analytical Method in Geomechanics* 34, 1124-1156.

Multi-scale Simulation of Seismic Wave Propagation

Varvara Roubtsova*, Mohamed Chekired**

*Hydro-Quebec (IREQ), **Hydro-Quebec (IREQ)

ABSTRACT

A numerical simulation of seismic wave propagation through the soils is an important part for the prediction of earthquake damage. The soils are a complex granular media with pore channels filled with water. The parameters of soils such as granulometry, density, shape of particles, etc. determine a capability to transmit and dissipate the seismic waves. On the other hand, the reflected wave at boundaries conditions between two soils must take into account. Furthermore, the soils characteristics vary under periodic loads up to critical state namely liquefaction. Liquefaction is a phenomenon whereby saturated soils lose strength. Finally a complex state is takes place in the soils because of interaction of p-waves (pressure primary waves) and s-waves (shear secondary waves) during earthquake. Simulations of the seismic wave propagation were carried out with Virtual Laboratory SiGran developed in Research Institute of Hydro-Quebec (IREQ). These codes are a bulk-parallel and can be run on GPU-devices. Smoothed Particle Hydrodynamics (SPH) method was used to model seismic waves at a macro level. At this level, the problem is described by the multiphysics continuum mechanics equations with the special rheological soil laws. The particles movement and their interactions with an increasing pore pressure and a water motion into pore channels under seismic loads determine a soil behavior during earthquake. The soils micro characteristics were modeled by coupling Discrete Element Method (DEM) with Marker And Cell (MAC) method. This coupling simulates the wet granular media as a matrix of particles with a free space (pore channels) filled with water. The information will be transferred from the micro level to a macro level by establishing of the rheological law. These codes were tested for many theoretical and physical problems. The possibilities of Virtual Laboratory will be presented.

Fluid Driven Discrete Cracks via 2D FDEM

Esteban Rougier*, Zhou Lei**, Antonio Munjiza***, Earl Knight****

*Los Alamos National Laboratory, **Los Alamos National Laboratory, ***University of Split, ****Los Alamos National Laboratory

ABSTRACT

In recent years the coupling of rock mechanics to fluid flow has become a critical topic for understanding the performance of energy systems including the production of unconventional oil and gas (e.g. hydraulic fracturing) where fluids are used to create fractures to increase the permeability of formations. On the rock mechanics modelling side the combined finite-discrete element method (FDEM) has become a tool of choice for simulations of complex fracture problems. In this work we combine our FDEM implementation with a novel fluid solver using an Integrated Solid Fluid (ISF) solver approach in order to simulate the key mechanisms that control fluid driven cracks. The main innovative aspects of the ISF solver are: the use of the same spatial discretization to describe the behavior of the solid (i.e., rock medium) and the fluid, the use of the same time step for both phases (solid and fluid); and the independence of the size of the critical time step with the fracture opening. This last point is extremely important because it means that the ISF simulations can use very fine meshes around areas of interest, such as a borehole, without penalizing the computational cost as fractures propagate (i.e., open) and the fluid flows through them. This paper presents a series of benchmark cases. The results shown in this work clearly demonstrate that the ISF approach is able to reproduce analytical results for fluid flow through a single crack. In addition, this approach is also able to reproduce analytical results for the problem of a fluid flow driven single crack propagation. The results shown also demonstrate that the same approach is robust enough to deal with complex fracture patterns and complex geometries; the obtained fluid driven fracture patterns in the vicinity of a borehole presented in this paper certainly stands to the scrutiny of human visual perception.

Size Dependent Crystal Plasticity Model Incorporating Strain-rate Effect and Temperature Dependence

Anish Roy^{*}, Qiang Liu^{**}, Vadim Silberschmidt^{***}, Ka Ho Pang^{****}

^{*}Loughborough University, ^{**}Loughborough University, ^{***}Loughborough University, ^{****}Loughborough University

ABSTRACT

Size-dependent crystal plasticity of metal single crystals is investigated using the finite-element method based on a phenomenological crystal-plasticity model, incorporating both first-order and second-order effects. The first-order effect is independent of the nature of the loading state and described by three phenomenological relationships based on experimental results. The second-order effect is considered in terms of storage of geometrically necessary dislocations, affected significantly by the loading state. The modelling approach is shown to capture the influence of loading conditions on the sample size effect observed in compression and bending experiments. The model accounts dislocation slip and twinning on different crystallographic systems. Special attention is paid to a strain-rate effect and temperature dependence in the constitutive description employed in the model. The model is extended for use in polycrystalline materials. Several case studies are performed to demonstrate the effect of strain-rates – as an example – micro scratching experiments are performed which are then used to first calibrate and then predict the effect of machining speeds on the structural integrity of the component.

Optimized Schwarz Methods for Time-Harmonic Elastodynamic Problems

Anthony Royer^{*}, Christophe Geuzaine^{**}, Vanessa Mattesi^{***}, Steven Roman^{****}

^{*}Université de Liège, ^{**}Université de Liège, ^{***}Université de Liège, ^{****}Université de Liège

ABSTRACT

Solving wave propagation problems in heterogeneous media is computationally challenging, especially in the high-frequency regime where discretizing the domain at the scale of the (small) wavelength leads to the solution of very large systems of equations. In the time-harmonic case (i.e. in Fourier space), recent progress has been made for acoustic and electro-magnetic wave problems, where quasi-optimal Schwarz domain decomposition methods have been proposed [1, 2, 3]. In this contribution we extend these results to the case of elastic waves, where we compare transmission conditions based either on Padé-localized approximations of the exact freespace Dirichlet-to-Neumann map, or on the use of perfectly matched layers. References [1] Y. Boubendir, X. Antoine, and C. Geuzaine. A quasi-optimal non-overlapping domain decomposition algorithm for the helmholtz equation. *Journal of Computational Physics*, 231(2):262–280, 2012. [2] M. El Bouajaji, B.Thierry, X. Antoine, and C. Geuzaine. A quasi-optimal domain decomposition algorithm for the time-harmonic maxwell’s equations. *Journal of Computational Physics*, 294:38–57, 2015. [3] B. Thierry, A.Vion, S. Tournier, M. El Bouajaji, D. Colignon, N. Marsic, X. Antoine, and C. Geuzaine. Getddm: an open framework for testing optimized schwarz methods for time-harmonic wave problems. *Computer Physics Communications*, 203:309–330, June 2016.

Galerkin-RB-POD Reduced Order Methods: State of the Art and Perspectives with Focus on Parametric Computational Fluid Dynamics

Gianluigi Rozza*

*SISSA, International School for Advanced Studies, Trieste, Italy, Mathematics Area, mathLab

ABSTRACT

We provide the state of the art of Reduced Order Methods (ROM) for parametric Partial Differential Equations (PDEs), and we focus on some perspectives in their current trends and developments, with a special interest in parametric problems arising in Computational Fluid Dynamics (CFD). Systems modelled by PDEs are depending by several complex parameters in need of being reduced, even before the computational phase in a pre-processing step, in order to reduce parameter space. Efficient parametrizations (random inputs, geometry, physics) are very important to be able to properly address an offline-online decoupling of the computational procedures and to allow competitive computational performances. Current ROM developments in CFD include: a better use of stable high fidelity methods, considering also spectral element method, to enhance the quality of the reduced model too; more efficient sampling techniques to reduce the number of the basis functions, retained as snapshots, as well as the dimension of online systems; the improvements of the certification of accuracy based on residual based error bounds and of the stability factors, as well as the the guarantee of the stability of the approximation with proper space enrichments. For nonlinear systems, also the investigation on bifurcations of parametric solutions are crucial and they may be obtained thanks to a reduced eigenvalue analysis of the linearised operator. All the previous aspects are very important in CFD problems to be able to focus in real time on complex parametric industrial and biomedical flow problems, or even in a control flow setting, and to couple viscous flows -velocity, pressure, as well as thermal field - with a structural field or a porous medium, thus requiring also an efficient reduced parametric treatment of interfaces between different physics. Model flow problems will focus on few benchmark cases in a time-dependent framework, as well as on simple fluid-structure interaction problems. Further examples of applications will be delivered concerning shape optimisation applied to industrial problems. This work has been developed in collaboration with my research team in the framework of ERC AROMA-CFD, FARE-X-AROMA, HEaD, SOPHYA and PRELICA projects.

Local Yield Stress Analysis of Simulated Cu₆₄Zr₃₆ Bulk Metallic Glass

Dihui Ruan^{*}, Chris Rycroft^{**}, Sylvain Patinet^{***}, Michael Shields^{****}, Michael Falk^{*****}

^{*}Johns Hopkins University, ^{**}Harvard University, ^{***}Laboratoire PMMH, ESPCI, ^{****}Johns Hopkins University,
^{*****}Johns Hopkins University

ABSTRACT

The 'Local Yield Stress' (LYS) method is applied to an atomistic model of an as-quenched Cu₆₄Zr₃₆ metallic glass by shearing local regions of the glass along various orientations. By probing the structure in local shear modes, the LYS method measures the local yield stress as the minimum incremental stress require to trigger the onset of a plastic instability. This analysis is then utilized to identify the population of 'Shear Transformation Zones' (STZs), defined as local atomic clusters that rearrange cooperatively when the material is subjected to shear. These STZs are present in the as-quenched material structure. The population of STZs is correlated with the plastic events observed during a molecular dynamics simulation in which the glass is subjected to shear at the boundaries in order to assess the predictive capability and persistence of the derived STZ population while the material undergoes deformation.

A SIMPLE TECHNIQUE TO AVOID ACCURACY LOSS IN HIGHER ORDER FINITE-ELEMENT SIMULATIONS IN CURVED DOMAINS

VITORIANO RUAS*

* ∂ Alembert, Sorbonne Université - Campus de Jussieu
Couloir 55-65, 4^{ème} étage. 4 place Jussieu. 75005 Paris, France
and CNPq research grant holder, PUC-Rio, Brazil
ruas.vitoriano@gmail.com

Key words: Curved domain, Finite element, Hermite, Higher order, Simplex, Straight-edged.

Abstract. The isoparametric version of the finite element method for meshes consisting of curved triangles or tetrahedrons is widely employed to solve second order partial differential equations posed in curved domains. It allows to recover optimal approximation properties that hold for elements of order greater than one in the energy norm for polytopic domains. However so far it has mostly been applied to Lagrange interpolations. Even in this case it requires the manipulation of rational functions and the systematic use of numerical integration. Moreover natural isoparametric versions of other types of finite elements are still incipient, if not unavailable. We consider a simple alternative to deal with Dirichlet boundary conditions that bypasses these drawbacks, without eroding qualitative approximation properties. Applications involving prescribed values of an unknown field but also normal-component or normal-derivative degrees of freedom, illustrate the wide scope and the potential of the new technique.

1 INTRODUCTION

Among a few known techniques the isoparametric version of the finite element method (cf. [1]) for meshes consisting of curved triangles or tetrahedrons is the one most widely employed to solve partial differential equations with essential conditions prescribed on curved boundaries. It allows recovering optimal approximation properties that hold for elements of order greater than one in the energy norm for polytopic domains. However, besides a greater geometric complexity, this method requires the manipulation of rational functions and the use of numerical integration. We consider a simple alternative to deal with essential - that is, Dirichlet boundary

conditions that bypasses these drawbacks, without eroding qualitative approximation properties. Moreover, in contrast to other methods such as the isoparametric version of the finite element method, our technique is universal, for it applies to different types of degrees of freedom, such as normal components of vector or tensor fields. Actually the idea behind it was first disclosed during the talk given by the author on a Hermite method with normal-derivative degrees of freedom at ICNAAM - the International Conference of Numerical Analysis and Applied Mathematics -, which was held in Rhodes, Greece, in September 2016. Later on this work was published in the form of article [2]. In the present work we first recall the main principle the new technique is based upon, by taking as a model the solution of the Poisson equation with quadratic Lagrange finite elements. A detailed description thereof in both the two- and the three-dimensional case can be found in the open access article [3] and references therein. Then we show that the new method extends very naturally to both classical elasticity systems and viscous incompressible flow equations. This forms a basis for technique's application to the finite-element modeling of both fluid flow and solid-body deformation. In the particular case of the Stokes system, for instance, we show that the new method can be combined with any velocity-pressure pairing of global order greater than one. As an illustration we consider the classical Taylor-Hood (cf. [4]) and the Crouzeix-Raviart method, for which examples are given in two-dimension space. Some simulations of deformations of solid bodies of curved shape using our technique in connection with quadratic Lagrange finite elements are also supplied (see also [5]).

2 METHOD'S SHORT DESCRIPTION

First of all it is important to recall that the technique under consideration is aimed at interpolating Dirichlet conditions prescribed on curvilinear boundaries of bi- or tridimensional computational domains. It can provide a significant cost reduction of finite-element simulations in pure CFD or in Structural Calculus, as long as the method in use is of order greater than one. In this respect we can take as an example the popular Taylor-Hood method to solve the incompressible Navier-Stokes equations in a region delimited by two deformable excentric cylinders, both rotating with given angular velocities. The precision of this second order method to simulate the flow of an incompressible viscous fluid in such a domain will be considerably eroded, in case it is simply approximated by the polygon formed by the union of the straight-edged triangles, when a standard mesh is used. A classical solution to overcome such an accuracy loss is to employ the isoparametric version of the finite element method to represent the velocity of the fluid, which requires the use of elements with parabolic edges to approximate boundary portions. However, besides obvious geometric complications, this technique transforms the original local polynomial shape-functions into rational functions. Handling such functions can become a delicate issue. This is because the use of numerical integration is inevitable to compute the matrices inherent to the simulation, and the right choice of a quadrature rule is not always very clear. For all those reasons our method provides an efficient

efficient alternative, since it avoids the use of curved elements and handles only polynomial shape- and test-functions, thereby allowing for exact integration without any qualitative loss, as compared to the isoparametric technique.

Our method's guiding principle can be well understood in the framework of the finite-element solution of the following model-problem. Let us consider the Laplace equation $\Delta u = 0$ in a smooth curved plane domain Ω , with Dirichlet conditions $u=g$ on its boundary Γ , where g is assumed to be sufficiently smooth as well. Suppose that classical Lagrange finite elements are used to solve this problem, based on a straight-edged triangular mesh, in association with continuous functions which are a polynomial of degree less than or equal to k in each triangle.

Suppose again that Ω is approximated by the polygon Ω_h with boundary Γ_h , formed by the union of the triangles of a mesh with maximum edge-length equal to h . If the values of g at the nodes on Γ_h different from vertexes are taken from points on Γ close to them, it is well-known that, whatever $k > 1$, the error of the approximation of u in the energy norm will be an $O(h^{1.5})$ (see e.g. [6]), instead of the $O(h^k)$ one could hope for with this kind of interpolation. With the new technique it suffices to substitute the Lagrangian nodes in the interior of the edges contained in Γ_h , by nodes on Γ located nearby. The choice of the latter nodes is very wide, since anyway integration remains restricted to the triangles that form the polygon Ω_h . We further observe that the test-functions are not defined in this manner, but rather in the usual way for Lagrange finite elements. This is one of the main advantages of our method. In short this procedure allows generating approximations of optimal order k in the energy norm. A rigorous analysis of this property in both 2D and 3D can be found in two *arXiv* papers cited in [3].

A possible construction of the nodes located on Γ pertaining to the new method, generically denoted by P , is illustrated in Figure 1 for $k=3$.

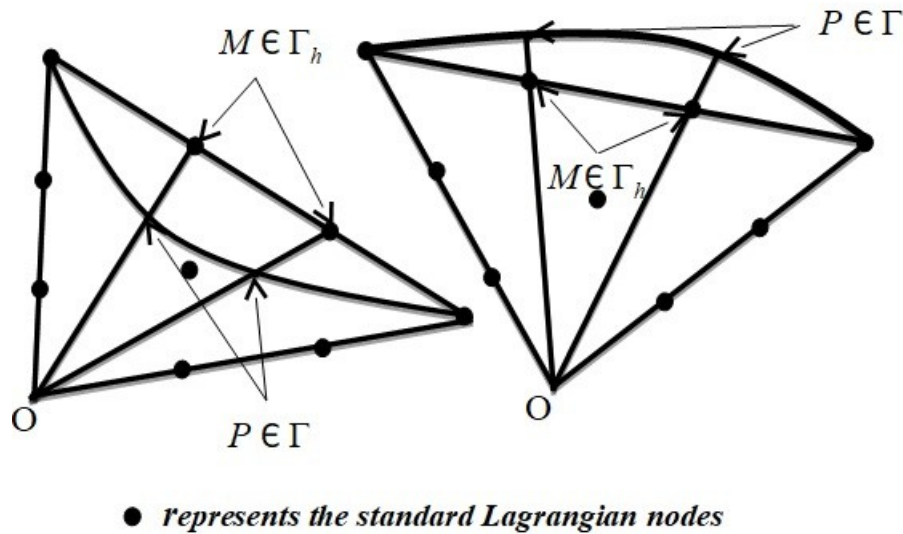


Figure 1- Lagrangian nodes $M \in \Gamma_h$ for $k=3$ and corresponding nodes $P \in \Gamma$ for typical boundary triangles

3 AN EXAMPLE WITH DEGREES OF FREEDOM OF THE NORMAL TYPE

In this section we apply the principles described in Section 2 to a finite element method based on Hermite interpolation incorporating degrees of freedom of the normal-derivative type. The aim is to show that, in contrast to classical methods to handle Dirichlet conditions for second order boundary-value problems posed in curved domains, the technique studied in this work is as universal as can be. For this purpose we solve a model-problem using a variant of the classical Raviart-Thomas mixed finite element of the lowest order [7], commonly known as RT_0 . This variant studied in author's work [8] among other papers of his, is to be employed in the framework of variational formulations mimicking corresponding mixed formulations. A Hermite interpolation with discontinuous piecewise quadratic functions allows for better accuracy of an approximate unknown field in the mean-square sense, as compared to the RT_0 finite element, though at equivalent cost. Solution's gradients in turn, are identically represented.

Suppose that we wish to determine the deflection u of an elastic membrane occupying a smooth plane domain Ω with edge Γ , under the action of a force density f perpendicular to its plane. It is well-known that this problem is governed by the Poisson equation $-c \Delta u = f$ in Ω , supplemented with appropriate boundary conditions, where c is a constant accounting for the mechanical properties of the material the membrane is made of. We consider that a portion Γ_0 of membrane's edge is kept fixed, that is, the essential boundary condition $u = 0$ holds on Γ_0 . On the other hand we assume zero traction on the complementary portion Γ_1 of Γ , which corresponds to the natural boundary condition $\partial u / \partial n = 0$ on Γ_1 , where $\partial u(\cdot) / \partial n$ denotes the outer normal derivative along Γ .

In order to solve this problem with our method, we first recast it in mixed form, by introducing the auxiliary field $\mathbf{p} = \text{grad } u$, which satisfies $\text{div } \mathbf{p} = -c^{-1}f$. The underlying mixed variational form writes: Find (\mathbf{p}, u) in $\mathbf{Q} \times W$ such that

$$\int_{\Omega} (v \text{div } \mathbf{p} + \mathbf{p} \cdot \mathbf{q} + u \text{div } \mathbf{q}) d\mathbf{x} = -c^{-1} \int_{\Omega} f v d\mathbf{x} \text{ for all } (\mathbf{q}, v) \text{ in } \mathbf{Q} \times W, \quad (1)$$

where W is the space of integrable functions in Ω (i.e. $W = L^2(\Omega)$), and \mathbf{Q} is a subspace of the space of vector fields which are square integrable in Ω , and whose divergence is also square-integrable in Ω , that is, the space $\mathbf{H}(\text{div}, \Omega)$ (cf. [7]). More precisely \mathbf{Q} is the subspace of $\mathbf{H}(\text{div}, \Omega)$ consisting of fields \mathbf{q} whose component $\mathbf{q} \cdot \mathbf{n}$ vanishes on Γ_1 , where \mathbf{n} is the outer normal vector to Γ .

It is important to recall that in the framework of formulation (1) the condition $\mathbf{p} \cdot \mathbf{n} = 0$ on Γ_1 is to be treated as an essential (Dirichlet) boundary condition, while the prescribed deflection $u = 0$ on Γ_0 is regarded as a natural (Neumann) boundary condition.

We actually solved a toy-problem with an empty Γ_0 . This requires taking an f satisfying the condition $\int_{\Omega} f d\mathbf{x} = 0$, and in this case u is defined up to an additive constant.

Now let \mathbf{T}_h be a mesh consisting of triangles with maximum edge length equal to h , satisfying the usual compatibility conditions (cf. [1]). Here again we denote by Ω_h the union of the triangles in \mathbf{T}_h and by Γ_h the boundary of this polygon. We define two subspaces \mathbf{Q}_h and W_h associated with \mathbf{T}_h , which are discrete counterparts of \mathbf{Q} and W . We recall that the Raviart-Thomas mixed method RT_0 consists of choosing W_h to be the space of functions which are constant in each triangle of the mesh. \mathbf{Q}_h in turn is the subspace of \mathbf{Q} consisting of fields of the form $a\mathbf{x} + \mathbf{b}$ in each triangle, where a is a real coefficient and \mathbf{b} is a vector of \mathbf{R}^2 , whose normal component is continuous on the edges of the elements in \mathbf{T}_h .

As for the Hermite variant of RT_0 , an approximation u_h of u is searched for in a space V_h defined as follows: In each triangle T of \mathbf{T}_h a function v in V_h is of the form $a\mathbf{x}^2/2 + \mathbf{b} \cdot \mathbf{x} + e$ where a and e are real coefficients and \mathbf{b} is a vector of \mathbf{R}^2 . Then, like the flux variable \mathbf{p} in the RT_0 method, the gradient of v is of the form $a\mathbf{x} + \mathbf{b}$ and its normal component along an edge is constant according to [7]. We require that this normal component of every v in V_h along a mesh edge be single valued if the edge is common to two triangles in the mesh, or to vanish if the edge is contained in Γ , in order to prescribe the zero traction condition on the edge of the membrane. Then following [8], we recast the finite-element counterpart of the mixed formulation (1) in the following variational form: Find u_h in V_h such that,

$$\sum_{T \in \mathbf{T}_h} \left[\int_T (v \Delta u_h + \text{grad } u_h \cdot \text{grad } v + u_h \Delta v) d\mathbf{x} \right] = -c^{-1} \int_{\Omega_h} f v d\mathbf{x} \quad \text{for all } v \text{ in } V_h. \quad (2)$$

Owing to these continuity requirements the local construction of functions in V_h must rely upon Hermite interpolation. Actually the degrees of freedom of V_h are precisely the (constant) normal derivatives along the edges, besides the function mean values in the elements of the mesh (cf. [8]). Since this method represents the gradient of the unknown field in the same way as the RT_0 mixed method, both methods differ only in the (discontinuous) representation of the deflection itself. Indeed in each triangle it is a linear function enriched with a quadratic term in the case of the Hermite method, whereas it is just constant for the mixed method. As long as Ω is a polygon, the Hermite variant of RT_0 described above is a second order method in the mean-square sense (cf. [8]), in contrast to the mixed method, which is just of the first order in the same sense.

Here we endeavor to show that, unless u_h is searched for in a suitable space U_h different from V_h such a property no longer holds, and moreover a substantial accuracy loss occurs in case Ω is a curved domain

Our choice of U_h is a space defined in the same way as V_h , except for elements in the subset of \mathbf{S}_h of \mathbf{T}_h consisting of triangles having an edge in Γ_h upon which a zero normal derivative condition must be enforced. However instead of enforcing this condition along such an edge, we require that the first order derivative of a function in U_h in the direction normal to it vanish along the tangent to the boundary at the intersection with it of the line joining the mid-point of this edge to the opposite vertex. This means that for each triangle in \mathbf{S}_h we pick up

the normal derivative where it is prescribed, that is, on the neighboring portion of the true boundary. This is precisely the counterpart of the Hermite finite element under study, for the technique designed to treat Dirichlet boundary conditions with Lagrange finite elements described in Section 2.

We next proceed to the numerical solution of our model-problem, taking $c = 1$ and Ω to be the ellipse with semi-axes equal to 0.5 and 1.0. We consider a manufactured exact solution given by $u(x,y) = (x^2/8+y^2/32-x^4/4-y^4/64-x^2y^2/8)$, f being defined accordingly. For symmetry reasons the computational domain is a quarter ellipse. We assess the convergence rates to the exact solution for three different approaches, namely, the classical RT_0 method, its Hermite variant taking $U_h=V_h$ and the latter combined with our method to approximate Dirichlet boundary conditions on curved boundaries. The meshes employed in these computations, indexed by an integer M with $h=1/M$, are the transformation of a uniform mesh of the unit square into the mesh of the quarter ellipse, by letting polar coordinates play the role of cartesian coordinates.

From the error evolution measured in the mean-square norm, it turned out that the power of h in the corresponding **OACR** is roughly 1, 1.8 and 2, respectively, where the acronym **OACR** stands for observed asymptotic convergence rate. We refer to Table 1 for such data. Moreover we checked the evolution as the mesh is refined of numerical solution's maximum absolute value at the centroids of the elements in the mesh. The **OACR** in this sense is roughly an $O(h^2)$ for the three methods. Nevertheless it is noteworthy that the accuracy of the boundary-modified Hermite variant of RT_0 in this respect is considerably improved, even for the coarser meshes, taking into account that the maximum absolute value of the exact solution is 1.56250, up to the fifth decimal. This comparison is illustrated in Figure 2.

All these results indicate that the modification in order to enforce on the true boundary the normal derivative boundary condition, with the Hermite variant of RT_0 , is indeed necessary whenever Ω is a curved domain. Indeed in doing so one takes the same advantage thereof in terms of accuracy enhancement, as in the case of polygonal domains (cf. [8]).

$M \rightarrow$	8	16	32	64	128	OACR
$h \rightarrow$	0.01250000	0.00625000	0.00312500	0.00156250	0.00078125	\downarrow
Raviart-Thomas mixed method RT_0	0.53435×10^{-3}	0.20712×10^{-3}	0.90368×10^{-4}	0.42781×10^{-4}	0.21005×10^{-4}	$O(h^{-1.0})$
Hermite variant of RT_0 ($U_h=V_h$)	0.32559×10^{-3}	0.99666×10^{-4}	0.29191×10^{-4}	0.83411×10^{-5}	0.24152×10^{-5}	$O(h^{-1.8})$
Modified Hermite variant of RT_0	0.18500×10^{-3}	0.48191×10^{-4}	0.12493×10^{-4}	0.32565×10^{-5}	0.82059×10^{-6}	$O(h^{-2.0})$

Table 1 - Absolute errors of the solution to a toy-problem in an ellipse in the mean-square norm

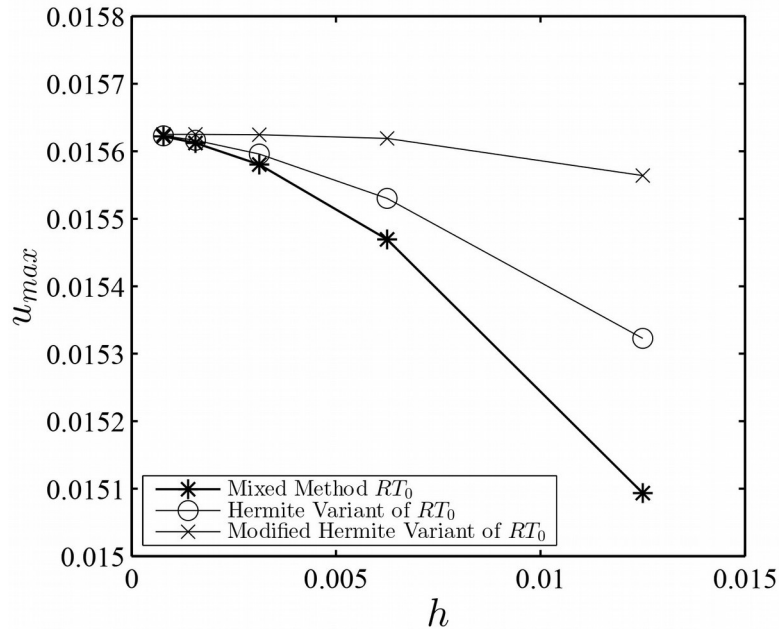


Figure 2 - Approximate solution's maximum absolute value u_{max} at the centroids of the elements

CONCLUSION

From the numerous experiments carried out so far with the new method to take into account Dirichlet boundary conditions prescribed on smooth curved boundaries, it is possible to assert that it is a simple, reliable and accurate tool to allow for higher order finite-element modeling. Moreover, as shown in this work, it is a universal technique, for it applies to different types of interpolations and degrees of freedom, and not only to those based only on function values, such as Lagrange finite elements.

To summarize we highlight the main features of the new method :

- Only polynomial local test- and shape-functions are employed;
- Curved domains are approximated by polytopes consisting of straight-edged N -simplexes;
- The method is universal, as far as degrees of freedom and interpolation types are concerned;
- Akin to classical techniques, optimal arbitrary order is attained;
- No numerical integration is necessary to compute element matrices;
- Implementation is simple and straightforward;
- The method is well-suited to adaptivity and the p -version of the finite element method;
- The multigrid or the h -version of the finite element method is not difficult to implement.

ACKNOWLEDGEMENT

The author gratefully acknowledges the financial support provided by CNPq through grant number 307996/2008-5. He is also thankful to his colleague Marco Antonio Silva Ramos for the diligent support in the preparation of this extended abstract.

REFERENCES

- [1] Zienkiewicz, O.C. and Taylor, R.L. The Finite Element Method. McGraw Hill, Vol. I., (1989), Vol. II., (1991).
- [2] Ruas, V. and Silva Ramos, M.A. A Hermite finite element method for Maxwell's equations. Applied Mathematics and Information Sciences, (2018) 12-2 : 271–283.
- [3] Ruas, V. Variational formulations yielding high-order finite-element solutions in smooth domains without curved elements. Journal of Applied Mathematics and Physics, (2017) 5-11: DOI:10.4236/jamp.2017.511174.
- [4] -,-. Accuracy enhancement for non-isoparametric finite-element simulations in curved domains; application to fluid flow. Computer and Mathematics with Applications, to appear.
- [5] -,-. Optimal Calculation of Solid-Body Deformations with Prescribed Degrees of Freedom over Smooth Boundaries. In: Advanced Structured Materials, H. Altenbach et al. Eds., Magdeburg, Springer International Publishing, Vol.1 (2018), 695–704.
- [6] Ciarlet, P.G., The Finite Element Method for Elliptic Problems, North-Holland, 1978.
- [7] Raviart, P.A. and Thomas, J.M. Mixed Finite Element Methods for Second Order Elliptic Problems, Lecture Notes in Mathematics, Springer Verlag, (1977) 292-315.
- [8] Ruas, V. Hermite finite elements for second order boundary value problems with sharp gradient discontinuities, Journal of Computational and Applied Mathematics, (2013) 246 : 234-242.

A Diffuse Interface Framework for Modelling the Evolution of Multi-cell Aggregates as a Soft Packing Problem

Shiva Rudraraju^{*}, Krishna Garikipati^{**}, Jiahao Jiang^{***}, Debabrata Auddya^{****}, Tugba Topal^{*****}, Luis Villa Diaz^{*****}

^{*}University of Wisconsin Madison, ^{**}University of Michigan Ann Arbor, ^{***}University of Michigan Ann Arbor,
^{****}University of Michigan Ann Arbor, ^{*****}University of Michigan Ann Arbor, ^{*****}Oakland University

ABSTRACT

We present a model for cell growth, division and packing under soft constraints that arise from the deformability of the cells as well as of a membrane that encloses them. Our treatment falls within the framework of diffuse interface methods, under which each cell is represented by a scalar phase field and the zero level set of the phase field represents the cell membrane. One crucial element in the treatment is the definition of a free energy density function that models cell-cell contact and adhesion. In order to properly represent cell packing and the associated free energy, we include a simplified representation of the anisotropic mechanical response of the underlying cytoskeleton and cell membrane through appropriate penalization of the cell shape change. Numerical examples are presented to demonstrate the evolution of multi-cell clusters, and the total free energy of the clusters as a consequence of growth, division and packing.

Instabilities in Magnetorheological Elastomers with Periodically Distributed Magnetizable Particles

Stephan Rudykh*, Artemii Godhkoderia**

*Technion, **Technion

ABSTRACT

We investigate the magneto-mechanical behavior of magnetorheological elastomers (MRE) undergoing large deformations subjected to magnetic fields. These magnetoactive materials can change their mechanical properties and develop large deformations when subjected to a magnetic field. We focus on the role of microstructures in the overall performance and stability of the deformable magnetoactive composites. We examine the coupled behavior of the active composites with (i) periodically and (ii) randomly distributed magnetizable particles embedded in soft matrix [3], and (iii) periodic laminates and anisotropic structured composites with chain like structures [2]. We identify the key parameters governing the magneto-mechanical couplings. We find that even very similar microstructures, such as periodic composites with hexagonal and rectangular representative volume elements (RVE), exhibit very different behavior in terms of actuation, and effective properties [3]. Next, we investigate the magnetomechanical instabilities [1] that may develop at different length-scales. Here, we focus on the so called macroscopic or long-wave magnetomechanical instabilities to obtain estimates of the onset of magnetomechanical instabilities. We explore the role of external magnetic fields, microstructure parameters, and phase properties on the onset of magneto-mechanical instabilities. To this end, we develop a finite element based code, which allows us to obtain the primary solution for various RVEs subjected to finite deformation and magnetic field ; moreover, the critical condition for the onset of macroscopic instability. By making use of the numerical tool, we identify the unstable domains for MRE composites with periodically distributed circular and elliptical inclusions embedded in a soft matrix. We use the isotropic Langevin model for magnetic behavior, to account for the initial (linear) susceptibility and saturation magnetization of the magnetoactive inclusions. We analyze the influence of the applied magnetic field and finite strains, as well as particle shape and material properties, on the stability of the MRE composites. We find that the stable and unstable domains can be significantly tuned by the applied magnetic field, depending on deformation, microstructure and magnetic properties of the inclusions such as initial susceptibility and saturation magnetization. REFERENCES: [1] Stability of magnetoactive composites with periodic microstructures undergoing finite strains in the presence of a magnetic field. Composites B 128:19-29 (2017) [2] Stability of Anisotropic Magnetorheological Elastomers in Finite Deformations : A Micromechanical Approach. J. Mech. Phys. Solids 61:949-967 (2013) [3] Magnetoactive elastomers with periodic and random microstructures. Int. J. Solids Struct. 51:3012-3024 (2014)

Mechanical Loading Maintains Bone Mass in vivo in Osteolytic Multiple Myeloma

Maximilian Rummler^{*}, Fani Ziouti^{**}, Anne Seliger^{***}, Maureen Lynch^{****}, Bettina Willie^{*****},
Franziska Jundt^{*****}

^{*}Research Centre, Shriners Hospital for Children-Canada, Department of Pediatric Surgery, McGill University, Montreal, Canada, ^{**}Medizinische Klinik und Poliklinik II-Hämatologie/Onkologie, Universitätsklinikum Würzburg, Germany, ^{***}Julius Wolff Institut, Charite- Universitätsmedizin Berlin, Germany, ^{****}University of Massachusetts, Amherst, USA, ^{*****}Research Centre, Shriners Hospital for Children-Canada, Department of Pediatric Surgery, McGill University, Montreal, Canada, ^{*****}Medizinische Klinik und Poliklinik II-Hämatologie/Onkologie, Universitätsklinikum Würzburg, Germany

ABSTRACT

Multiple myeloma (MM) is an incurable plasma cell derived neoplasia, leading to pathological osteoclast activity resulting in increased bone resorption. Treating MM bone disease is a major goal in MM therapy. We hypothesized, that loading would maintain bone mass in a mouse model of MM. The left tibiae of 40, 10wk old female BALB/c mice were either a) PBS injected, b) MOPC315.BM cell injected (2), or c) not injected. 14 days after injection, 25 mice (n = 7-10/treatment) underwent 3 wks of in vivo tibial loading (3) (left limb, right limb nonloaded), with the remaining 15 mice (n = 6 PBS, n = 9 tumor) serving as nonloaded controls. In vivo microCT was performed at day 0, 5, 10, 15 and 20 of loading, at proximal metaphysis and midshaft. Cortical and trabecular parameters were measured. An ANOVA assessed the effects of treatment, loading, and limb. After 20 days of loading, metaphyseal cortical bone formation (CtTh, CtAr, TAr, CtAr/TtAr, CtvTMD) was significantly greater and cortical porosity (CtPo) was lower compared to nonloaded right limbs and nonloaded groups. All right limbs had similar increases in cortical parameters over 20 days, indicating no systemic effects present. Left limbs of tumor-injected loaded group had +41% cortical thickness, while left limbs of tumor-injected nonloaded group increased by 1%. In conclusion, these data indicate mechanical loading can maintain bone mass in this model of MM. 1) Lynch et al. JBMR 2013, 2) Hofgaard et al. PLoS One 2012, 3) Willie et al. Bone 2013

Computational Design and Fabrication of Foams for Actuators and Dampers in Robots

Daniela Rus^{*}, Jeffrey Lipton^{**}, Robert MacCurdy^{***}

^{*}MIT CSAIL, ^{**}MIT CSAIL, ^{***}UC Boulder

ABSTRACT

Computationally designing and 3D printing foam will be an important tool for the on-demand design and fabrication of robots. Impact protection and vibration isolation are important factors in robot design. In the past researchers and engineers have used foams as padding, vibration isolators, actuators, and as structural elements in robotic systems. With the explosion of soft robotics as a field, foams are increasingly becoming an integral element of robot design. Traditionally foams and other damping materials are available only in bulk or molded form. 3D Printing foams allows roboticists to produce custom shapes and distributions of material properties, enabling the rapid design and fabrication of robots. Methods of 3D printing foams work at three layers of the design and fabrication process: explicit geometry, print process control, and material blending. Explicit geometry methods rely on 3D representations of each cell and pore to be printed. Print process methods change the fabrication process to induce a porous foamed structure. For example, inducing viscous thread instability in direct write 3D printing generates open celled foams with controllable stiffness and pore size (1). Blending methods rely on two or more materials that are brought together before or during printing process (2). Researchers have used these foam-printing methods to make high force actuators, low force actuators and viscoelastic dampers. The foam actuators combined elastomers with phase change material. The high force actuators are made of printed wax-silicone blends and are capable of producing over 4.5 kN of blocked force (3). The lower force actuators combine silicone with ethanol. The viscoelastic dampers were closed cell foams of un-curing liquid encapsulated in a UV-curing acrylate elastomer. Varying the relative concentration of the un-curing liquid can adjust the elastic and damping modulus of the material over one order of magnitude. Engineers can programmatically control the shape and material properties produced using the empirical models of material properties. In this talk, we will discuss how these methods work and how they can be integrated into computation design systems for robots to produce actuators, dampers, and materials that change stiffness. References 1. 3D printing variable stiffness foams using viscous thread instability. Lipton, Jeffrey and Lipson, Hod. 2016, Scientific Reports, Vol. 6. 2. Printable programmable viscoelastic materials for robots. Lipton, Jeffrey I, et al. 2016, Intelligent Robotics and Systems, pp. 2628-2635. 3. Electrically Actuated Hydraulic Solids. Lipton, Jeffrey I, et al. 10, s.l. : Advanced Engineering Materials, 2016, Vol. 18. 10.1002/adem.201600271.

Pore-scale Computation of the Effective Diffusion and Hydrodynamic Dispersion in Inhomogeneous Porous Media

Héctor Rusinque*, Gunther Brenner**

*PhD Candidate, **Dr. Professor

ABSTRACT

In this study, a method for the quantification of effective diffusive and convective mass transport in porous media is presented. Engineering approaches to describe mass transport are based on averaged quantities such as effective diffusion coefficients to consider the diffusion inhibition due to the structure of the porous medium or the hydrodynamic dispersion coefficient in the transport is additionally determined by overlapping convection and diffusion. Here, the combined use of the Lattice-Boltzmann method and the lagrangian random-walk particle tracking method offers the possibility to accurately describe the transport phenomena at a pore scale. From the data obtained, effective parameters can be determined as needed in engineering models. This simulation approach requires a pore-scale reconstruction of the porous medium, resulting in the necessity of exceptional computational resources, such as those provided by supercomputers to perform pore-scale simulations. In the presentation, the method will be described and verified by means of known solutions, e.g. for the Taylor Aris dispersion. Based on this, the effective diffusion and hydrodynamic dispersion in beds of spherical and irregular particles are analyzed and effective parameters for the description of the mass transport are discussed. The focus is on packing in confined spaces with an inhomogeneous porosity distribution near the wall and porous media with designed transport pores.

The Virtual Element Method for Curved Domains

Alessandro Russo^{*}, Lourenco Beirao da Veiga^{**}, Giuseppe Vacca^{***}

^{*}University of Milano-Bicocca, ^{**}University of Milano-Bicocca, ^{***}University of Milano-Bicocca

ABSTRACT

In this talk I will present the first results about the investigation of the Virtual Element Method in the presence of curved elements. We consider the case of a fixed curved boundary in two dimensions, as it happens in the approximation of problems posed on a curved domain or with a curved interface. We show that the proposed Curved Virtual Elements lead to an optimal rate of convergence, independently of the shape of the curved edges.

Contribution to Multiscale Modelling of Additive Manufacturing: Selective Laser Melting

Romain Ruysse^{*}, Andrea Barbarulo^{**}, Hachmi Ben Dhia^{***}

^{*}CentraleSupélec, Université Paris Saclay, ^{**}CentraleSupélec, Université Paris Saclay, ^{***}CentraleSupélec, Université Paris Saclay

ABSTRACT

Additive Manufacturing refers to all processes creating parts by adding material from a numerical model. Those methods present several important advantages by making possible the creation of parts with complex shapes impossible to obtain with classical processes. However, although their utilization is expanding fastly for twenty years, their application remains marginal because of the lack of scientific and technical control of the process. Produced parts may not respect the specifications and the numerical simulations are a preferential way to determine key parameters for dimensioning. Several processes exist and we chose to focus on the Selective Laser Melting (SLM) process, wich is difficult to master due to the complexity of physical phenomena taking place during parts fabrication . The aim of this paper is to model the SLM by taking into account these several physical scales, and to this end, the multiscale Arlequin framework is especially suited for this problematic thanks to its great flexibility [1][2]. Indeed, this technique allowed to decompose our analysis by considering different scale levels. Firstly, a micro scale in the area under the laser have been used, to modelize precisely its heat inflow. A second zone has been modelled at mesoscopic scale for considering the phase changing phenomena thanks to the Latent Heat Source Method. The movement of this two domains, allows to modelize the microscopic material addition. Then, other scales (coarser at macroscale) are progressively and incrementally introduced during the process evolution as the laser and the high thermal gradients move far away from the previous layers. Moreover, we present a particular Model Order Reduction method infered by our simulations that leads to drastic reduction of computational costs. [1] Ben Dhia.H, Comptes Rendus de l'Académie des Sciences Series IIB Mechanics Physics Astronomy, 1998, Multiscale mechanical problems: the Arlequin Method. [2] Ben Dhia.H, International Journal for Multiscale Computational Engineering, 2008, Further Insights by Theoretical Investigations of the Multiscale Arlequin Method.

Topological and Localized Modes in Quasiperiodic Structures

Massimo Ruzzene*

*Georgia Institute of Technology

ABSTRACT

Phononic crystals and acoustic metamaterials are periodic structures that have drawn much attention to the engineering and physics communities due to their numerous applications in passive vibration and noise control. Topology concepts originally developed in electronics have recently inspired a number of applications in photonics and phononics. Many of these concepts rely on the existence of topological properties that lead to edge modes or interface wave modes. In this context, this paper explores quasiperiodicity, which has been the subject of extensive research in the fields of crystallography and photonics, as related to continuous quasiperiodic elastic structures. The objective is to find topological modes, such as localized modes in one-dimensional and two-dimensional quasiperiodic systems. These can be as interesting if not more useful than the interface modes that are found in periodic structures, as the quasiperiodicity framework provides a consistent methodology that leads to interfaces, which may be topologically protected. The concept is first illustrated for simple 1D quasiperiodic spring-mass chain that exhibits localized modes, introducing the mechanical analogues to the Harper models previously found in photonics. Next, the study investigates arrays of coupled rods, as analogues of a recent experiment conducted with a quasiperiodic photonic lattice designed to robustly transfer energy from one boundary to another. Finally, the investigation of plate structures with quasiperiodic arrangements of lumped masses and resonators are presented as structural components which support a variety of localized modes and that are suitable for the experimental characterization of the waveguiding behavior of these configurations.

Modeling Plasticity of FCC/BCC Micro-pillars Using Dislocation Dynamics

Ill Ryu*

*UT-Dallas

ABSTRACT

From the recent micro-pillar experiments, it is now known that the flow stress of metallic micro-pillars increases with decreasing sample size with and without the strain gradient by geometrically necessary dislocations. To understand size dependent plasticity, several models have been proposed, but the role of the dislocation sources in submicron sample is still under debate. In the present study, we make a three-dimensional, dislocation dynamics model to study collective dislocation behavior under tension/torsion in FCC/BCC micro-pillars. We follow both the evolution of the dislocation structure and the corresponding stress-strain relation. Our simulation results show the evident size effect and the effect of cross slip and clear Bauschinger effect, which appear to be good agreement with experimental results.

On the Fracture Strength Measurement of Polycrystalline Graphene Using Nanoindentation

Seunghwa Ryu^{*}, Sangryun Lee^{**}, Dongwoo Sohn^{***}, Jihoon Han^{****}

^{*}Korea Advanced Institute of Science and Technology, ^{**}Korea Advanced Institute of Science and Technology,
^{***}Korea Maritime and Ocean University, ^{****}Korea Advanced Institute of Science and Technology

ABSTRACT

The strength of pristine graphene and its grain boundaries (GBs) are mainly measured by nano-indentation with a spherical tip due to the difficulty of conducting uniaxial tensile tests. However, we recently showed that the fracture forces from the spherical indenter cannot be directly mapped onto the uniaxial strength. In this paper, employing a series of molecular dynamics simulations combined with a fracture mechanics analysis, we demonstrate that the fracture force from cylindrical indenters can be directly mapped onto the strength of graphene under uniaxial tension. Under indentation with cylindrical tips or uniaxial tension, the rupture of graphene sheets that have GBs with a low-tilt angle occurs simultaneously with the onset of crack nucleation at the GBs. On the contrary, when indented by a spherical indenter tip, the graphene sheets sustain the indentation loads until the crack size becomes comparable to the tip radius. Furthermore, the results show that estimating the strength with a cylindrical indenter is not very sensitive to the indentation site as well as angular misalignments that can be caused by human error or the limitations of the apparatus. We provide a detailed theoretical analysis on the crack growth based on the fracture mechanics. Our work presents the feasibility of obtaining the tensile strength from nanoindentation experiments, which may suggest a new standard to measure the tensile strength of graphene and related two-dimensional materials.

Gradient-based Optimization with the Cartesian Grid Finite Element Method (cgFEM)

Juan José Ródenas^{*}, Onofre Marco^{**}, Enrique Nadal^{***}, Francisco Javier Fuenmayor^{****},
Manuel Tur^{*****}

^{*}Research Centre in Mechanical Engineering (CIIM). Universitat Politècnica de València, ^{**}Laboratori de Càlcul Numèric (LaCàN). Universitat Politècnica de Catalunya, ^{***}Research Centre in Mechanical Engineering (CIIM). Universitat Politècnica de València, ^{****}Research Centre in Mechanical Engineering (CIIM). Universitat Politècnica de València, ^{*****}Research Centre in Mechanical Engineering (CIIM). Universitat Politècnica de València

ABSTRACT

This paper presents how an immersed boundary method, namely, the Cartesian grid Finite Element Method (cgFEM) described for the 2D case in [1], can be used to enhance the performance of gradient-based 3D shape optimization processes. To do this, we first developed a technique to perform the shape sensitivity analysis (SSA), used to evaluate the gradients required by the optimization algorithm, within the cgFEM framework [2]. This included a tailored evaluation of the design velocity field required by the SSA and the consideration of Dirichlet boundary conditions in non-fitted meshes. We then used the hierarchical Cartesian structure to improve the efficiency of the analysis of each geometry, as this structure allows for trivial data sharing between similar entities (including the exchange of information between different geometries) or for an optimal system matrix reordering, among other benefits. Finally, we developed a projection technique[3] based on [4] to directly create the h-adapted meshes required by each geometry to obtain the prescribed accuracy, thus eliminating the need to perform a full h-adaptive iteration for each geometry, consequently, improving the performance of the optimization algorithm. The numerical results obtained show the accuracy of the shape sensitivity analysis, its adequate behaviour in the cgFEM context, and a considerable improvement in the efficiency of the shape optimization algorithm. REFERENCES [1] E Nadal, JJ Ródenas, J Albelda, M Tur, JE Tarancón, FJ Fuenmayor. Efficient Finite Element Methodology Based on Cartesian Grids: Application to Structural Shape Optimization. Abstract and Applied Analysis 2013, Article ID 953786, 19 pages (2013). [2] O Marco, JJ Ródenas, FJ Fuenmayor, M Tur. An extension of shape sensitivity analysis to an immersed boundary method based on Cartesian grids Computational Mechanics. <https://doi.org/10.1007/s00466-017-1522-0> (2017) [3] O Marco, JJ Ródenas, J Albelda, E Nadal, M Tur. Structural shape optimization using Cartesian grids and automatic h-adaptive mesh projection. Structural and Multidisciplinary Optimization. <https://doi.org/10.1007/s00158-017-1875-1> (2017) [4] G Bugada, JJ Ródenas, E Oñate. An integration of a low-cost adaptive remeshing strategy in the solution of structural shape optimization problems using evolutionary algorithms. Computers & Structures (86)1563 – 1578 (2008). Acknowledgements: The financial support to this work of Generalitat Valenciana (PROMETEO/2016/007) and the Spanish Ministerio de Economía, Industria y Competitividad (DPI2017-89816-R) is greatly acknowledged.

Modelling the Musculoskeletal System - A Two-muscle Upper Arm Model

Oliver Röhrle^{*}, Michael Sprenger^{**}, Julian Valentin^{***}, Dirk Pflüger^{****}

^{*}University of Stuttgart, ^{**}University of Stuttgart, ^{***}University of Stuttgart, ^{****}University of Stuttgart

ABSTRACT

Investigating the interplay between muscular activity and motion is the basis to improve our understanding of healthy or diseased musculoskeletal systems. To be able to analyze the musculoskeletal systems, computational models are employed. Albeit some severe modeling assumptions, almost all existing musculoskeletal system simulations appeal to multi-body simulation frameworks. Although continuum-mechanical musculoskeletal system models can compensate for some of these limitations, they are essentially not considered due to their computational complexity and cost. Based on the two-muscle upper arm musculoskeletal framework proposed in [1] an efficient and for multi-muscle musculoskeletal system feasible modelling framework, in which the exerted skeletal muscle forces are computed using three-dimensional, continuum-mechanical skeletal muscle models and in which muscle activations are determined based on a constraint optimization problem, is proposed. In [1], the framework was limited to determine the state of activation of one of the two muscle or the positions of the bones based on the level of activation of both muscles. Now, a fully activation-driven musculoskeletal system model is feasible. Numerical feasibility is achieved by computing sparse grid surrogates with hierarchical B-splines. Adaptive sparse grid refinement further reduces the computational effort. The choice of B-splines allows the use of all existing gradient-based optimization techniques without further numerical approximation. To demonstrate this, we show several different test scenarios in which the upper limb model consisting of the elbow joint, the biceps and triceps brachii and an external load is subjected to different optimization criteria. In addition to the numerical framework, appropriate constitutive laws for the active behavior of the skeletal muscle tissue are needed. The presentation will conclude with an outlook on how one can extend this method to musculoskeletal systems with three or more muscles. [1] Röhrle O., Sprenger M., and Schmitt S. A two-muscle, continuum-mechanical forward simulation of the upper limb. *Biomechanics and Modeling in Mechanobiology*. 2017, 16(3), p. 743-762.

High-Order Time Stepping in Partitioned Fluid-Structure Interaction with Black-Box Solvers

Benjamin R uth*, Benjamin Uekermann**, Miriam Mehl***, Hans-Joachim Bungartz****

*Technical University of Munich, **Technical University of Munich, ***University of Stuttgart, ****Technical University of Munich

ABSTRACT

Fluid-structure interaction problems are solved by applying either the monolithic or the partitioned approach [1]. While the monolithic approach usually provides more stable solutions, the partitioned approach has many advantages from a software engineering perspective as, for example, the reuse of well-tested existing solvers (participants) in a black-box fashion. However, this typically results in a degradation of time stepping to first order if applied in the standard way [2] - even if the used solvers are of higher order. In this talk, the convergence order of time-stepping for a simple 1D model problem is investigated. In our partitioned approach, the solvers are considered as black-boxes: Only nodal data at the wet interface between the fluid and the structure region is exchanged between the solvers. The aforementioned effect of order degradation is reproduced for state-of-the-art explicit (weak) and implicit (strong) coupling. Finally, an order conserving coupling scheme is introduced. This scheme allows to couple participants using arbitrary time stepping schemes and differing temporal meshes. Here, dense output is used to construct high-order local interpolants between the timesteps at low cost. Waveform relaxation iteratively improves the approximative, time-continuous solution at the boundary and windowing techniques are used to allow non-matching temporal discretization. In the future, we plan to implement this mechanism in the open source coupling library preCICE [3] to be able to solve complex multi-scale-multi-physics scenarios, such as turbulent fluid-structure interaction or fluid-structure-acoustics interaction. Currently, very small time steps are needed in this area due to degradation of convergence order and stability properties of the time-stepping scheme if a partitioned approach is in use. References [1] C Michler et al. "A Monolithic Approach to Fluid-Structure Interaction". In: Comput. Fluids (2004) [2] C. Farhat and M. Lesoinne. "Two efficient staggered algorithms for the serial and parallel solution of three-dimensional nonlinear transient aeroelastic problems". In: Comput. Methods Appl. Mech. Eng. (2000) [3] Hans-Joachim Bungartz et al. "preCICE - A fully parallel library for multi-physics surface coupling". In: Comput. Fluids (2016)

Analysis of Anisotropic Elastic Wave Field Using Boundary Element Method with Far- Field Approximation

Takahiro SAITOH^{*}, Takashi ONODERA^{**}, Akira FURUKAWA^{***}, Sohichi HIROSE^{****}

^{*}Gunma University, ^{**}Gunma University, ^{***}Tokyo Institute of Technology, ^{****}Tokyo Institute of Technology

ABSTRACT

A new boundary element method (BEM) with far field approximation is presented for the elastodynamic problems of general anisotropy. The BEM has been developed as an effective and accurate numerical approach for wave propagation problems. However, the BEM for general anisotropic elastic solids still remains to be improved [1]. The fundamental solution for general anisotropic elastodynamics was developed by Wang and Achenbach [2]. The fundamental solution used in the BEM for anisotropic elastodynamic problems can be expressed by the sum of the static and dynamic part. The static part can be obtained by the closed form. However, the dynamic part of the fundamental solution cannot be obtained by the closed form and involves the numerical integration over a unit circle for 2-D and a unit sphere for 3-D problems. The evaluation of the numerical integration for them is very time consuming. Therefore, the most important key of the BEM analysis for general anisotropic elastodynamic problems is how to save the computational cost for the numerical integrations. Therefore, in this research, a far field approximation of the fundamental solution for general anisotropic elastodynamic problems is developed. The far-field approximation can be derived by using the stationary phase method. The far-field approximated fundamental solution has no integration over a unit circle for 2-D and a unit sphere for 3-D problems. Therefore, the development of the far-field approximated fundamental solution for BEM for general anisotropic elastodynamics can contribute to the reduction of the computational cost. In addition, parallel computing techniques, such as OpenMP, and MPI (Message Passing Interface) are utilized with the help of the supercomputer of Kyoto University for more reduction of the computational time. The numerical evaluation for the proposed far-field fundamental solution has been implemented and tested with numerical examples. The problems of elastic wave scattering by a cavity in general anisotropic elastodynamics are solved to validate the BEM with the proposed far-field approximation.

Low Impact Cratering on Granular Beds Under Low Gravity

Lucas SARDO^{*}, Florian Thuillet^{**}, Patrick Michel^{***}, Elie Hachem^{****}, Rudy Valette^{*****}

^{*}Center for Material Forming (CEMEF), MINES ParisTech, PSL Research University, France, ^{**}Lagrange Laboratory, University of Nice Sophia Antipolis, CNRS, Observatoire de la Côte d'Azur, France, ^{***}Lagrange Laboratory, University of Nice Sophia Antipolis, CNRS, Observatoire de la Côte d'Azur, France, ^{****}Center for Material Forming (CEMEF), MINES ParisTech, PSL Research University, France, ^{*****}Center for Material Forming (CEMEF), MINES ParisTech, PSL Research University, France

ABSTRACT

In the context of asteroid material sampling, landers are sent on the asteroid surface, which is made of regolith, that can be considered at first approximation as a granular bed. An important question is to understand the physics that governs the penetration of the lander in the granular bed, for a given impact velocity. For slow impact-induced flows on frictional non-cohesive granular beds on Earth, the soil behaves like a yield-stress fluid, where the yield-stress increases linearly with (depth induced) static pressure, and this rheology governs the penetration flow. However, for vanishing gravity, as encountered on asteroids, one expects dynamic (impact) pressure to dominate the penetration flow dynamics. In this paper, we model regolith as a $\mu(i)$ granular continuum fluid and propose both dimensional analysis and numerical simulations to identify asymptotic and coupled regimes for penetration of an impacting sphere from Earth to vanishing gravities. We find a penetration that scales quasi linearly with impact velocity for Earth gravity, that switch to sublinear for low enough gravities. The role of bed layer thickness and elasticity will be discussed and compared to discrete simulations.

New Unsymmetric Finite Elements Based on Analytical Trial Solutions Insensitive to Severe Mesh-Distortion

Yan SHANG*

*State Key Laboratory of Mechanics and Control of Mechanical Structures, College of Aerospace Engineering,
Nanjing University of Aeronautics and Astronautics, Nanjing 210016, China

ABSTRACT

The unsymmetric FEM is a very promising technique to produce finite elements with good numerical accuracies and high tolerances to mesh distortions. In this work, new high-performance unsymmetric quadrilateral element models are developed for analysis of the plane problems and Mindlin-Reissner plate problems within the framework of the so-called improved unsymmetric formulae, which is characterized by directly adopting a reasonable self-equilibrium stress field to be the element's trial functions. This stress field is obtained based on the analytical trial solutions of related problems and the quasi-conforming technique, thus can a priori satisfy the governing equations. Extensive numerical tests reveal that these new elements exhibit excellent capabilities for predicting results of both displacement and stress. In particular, they can still work very well in severely distorted meshes even when the element shapes deteriorate into concave quadrangle or degenerated triangle.

Simulation Analysis of the Optimal Position of Elastic Fixation for the Lumbar Spine

HONGFANG SONG*, QI LI**, ZHICHENG LIU***

*Capital Medical University, Beijing 100069, China, **Capital Medical University, Beijing 100069, China, ***Capital Medical University, Beijing 100069, China

ABSTRACT

The elastic dynamic fixation device COFLEX is approved to be an effective approach for the treatment of lumbar spine. What is the influence of different implantation depths on the motion of adjacent segments? This is still an open problem. The objective of the present work is to investigate the optimal position of elastic fixation COFLEX, and to provide the basis for clinical operation. The lumbar L1-L5 vertebral model was reconstructed based on CT images of volunteers. The intervertebral disc and nucleus pulposus model were established according to the upper and lower vertebral body by using CAD tools. The main ligaments of the control lumbar movement were added according to the anatomical structure, including the anterior longitudinal ligament, the posterior longitudinal ligament, the yellow ligament, the ligaments of the spine, the ligament of the transverse process, and the articulationes zygapophysiales ligament. The segments L3 - L4 were selected as the surgical segments. The complete group and the damage group models were constructed respectively. The 3d geometric structure of COFLEX was established by using laser scanning technique. Then 3 groups of models were built according to the depth from the U top of COFLEX to endorachis, and the different depths are 10 mm, 5 mm and 0 mm respectively. ABAQUS software was used to numerically analyze the movement of models under the flexion, left-right side bending and left-right rotation. The similarities to the complete group of motion variation range in the six motion states are in the descending order as 0 mm group, 5 mm group, 10 mm group and damaged instable group. In other words, the closer is the distance between the U top of COFLEX and endorachis, the closer is the variation range of lumbar vertebrae and adjacent segment to the complete group, while the difference in the instable group is the largest. Whether for the surgical segments or the overall lumbar spine, the closer is the U top of COFLEX to endorachis, the closer is the motion to the complete group. This indicates that COFLEX implanting close to the spine demonstrates good postoperative performance this good motion effect close to the complete spine. This phenomena is consistent with the experimental results. The elastic fixation device can be implanted as close to the dura as possible without injuring the nerve. Key words: lumbar spine; Elastic fixation; COFLEX; Finite element analysis; References 1?Divya V. Ambati, MS et al. Bilateral pedicle screw fixation provides superior biomechanical stability in transforaminal lumbar interbody fusion: a finite element study. The spine journal, available online 28 June 2014. 2?ZU Dan, HAI Yong, YUN Cai, et al.Adjacent segment range of motion after different insertion depth of lumbar interspinous dynamic stabilization device(Coflex): a biomechanical study. Chinese Journal of Spine and Spinal Cord, 2014, 24(10): 933-937. Acknowledgement: Project of Science and Technology of Beijing Municipal Education Commission (KM201410025012), Beijing Natural Science Foundation (7112056) Email?songhf@ccmu.edu.cn *corresponding, zcliu@ccmu.edu.cn

Roles of Length and Time Scales in Phase Transition Paradigm Shift

Qingping SUN*

*Hong Kong Univ. of Sci. & Tech.

ABSTRACT

Roles of Length and Time Scales in Phase Transition Paradigm Shift Qingping SUN¹, Mingpeng LI² ¹ Hong Kong University of Science and Technology, Hong Kong, China ² Wuhan University, China We report recent advances in the experimental and theoretical study of effects of material internal length scales (grain size, grain boundary and phase boundary) and time scales (loading time and heat conduction time) on the phase transition responses of NiTi polycrystalline shape memory alloy (SMA). For length scale effect [1-3], it is shown that, with grain size reduction, the energy of the elastic non-transformable grain boundary will gradually become dominant in the phase transition process and eventually bring fundamental changes of the deformation behaviors: breakdown of two-phase coexistence and vanishing of superelastic hysteresis dissipation. Such effects of length scale reduction originates from the large increase in the area-to-volume ratios of the interfaces (grain boundary and phase boundary) in the polycrystal, which provides a theoretical base to improve and control the performance of the existing NiTi SMA by grain size engineering. For the effects of time scales, it is shown that competition of physical processes (phase transition and heat transfer) with different time scales brings the emergence of a new length scale in the experimental observed domain patterns. Nucleation and growth of new phase, two-phase coexistence and the hysteresis dissipation are the key signatures of the first-order phase transition in materials and are widely used as the basic paradigms. It is shown that with the grain size reduction and/or loading time reduction, many unusual phenomena and properties will emerge, which not only open up new possibilities in the application but also lead to new paradigm building and shift in modelling and understanding. References [1] Li, M. P. and Q. P. Sun, "Nanoscale phase transition behavior of shape memory alloys — Closed form solution of 1D effective modelling", *J. Mech. Phys. Solids*, 110 (2018) 21–37. [2] Sun Q. P., A. Ahadi, Li M. P. and Chen M. X, "Effects of Grain Size on Phase Transition Behavior of Nanocrystalline Shape Memory Alloys", *Science China Technological Sciences*, 2014, 57: 671–679. [3] Aslan, A and Q. P. Sun, "Stress hysteresis and temperature dependence of phase transition stress in nanostructured NiTi—Effects of grain size", *Applied Physics Letters* 103, 021902 (2013).

Fluid/Solid Coupling for the Simulation of SLM Process

Yassine Saadlaoui^{*}, Jean-Michel Bergheau^{**}, Alexandre Delache^{***}, Eric Feulvarch^{****},
Jean-Baptiste Leblond^{*****}

^{*}Univ. Lyon, ENISE, ^{**}Univ. Lyon, ENISE, ^{***}LMFA UMR, ^{****}Univ. Lyon, ENISE, ^{*****}UPMC, Université Paris-6

ABSTRACT

Selective Laser Melting is among the additive manufacturing processes most used. It is one of the Powder Bed Fusion AM processes that consists in producing fully functional metal parts presenting high mechanical properties. The large use of SLM process and the need to improve and better control this process ability have led to the development of several numerical simulation approaches, which may provide valuable assistance to study the process's effects on the final parts. During SLM, the material undergoes thermal cycles which lead to state changes and fluid flows in molten pool. These fluid flows are related to the strong thermal gradient and caused by the effects of surface tension "Marangoni and curvature effects". This dynamic in molten pool can affect the temperature field distribution, the morphology of the molten zone and the generated stress field. Therefore, in order to reproduce as possible the physical phenomena occurring during the SLM process, it is very important to take into account the fluid flows during numerical simulation. Additionally, the type of coupling between fluid and solid computations is very important during the numerical simulation. Generally, a weak coupling is used to relate these computations. In this context, the aim of this work is to propose a new method to simulate the interaction between fluid flows and solid deformations. In first step, a new approach was developed, it consists to take into account the dynamic in molten pool through the two effects of surface tension (including both the "curvature effect" and the "Marangoni effect") and floatability. Additionally, the free surface was considered using an ALE method. To validate these methods, two numerical tests were used. Thereafter, two simulations of SLM were carried out, the first is a thermal computation without fluid flows and the second is a thermal-fluid computation with dynamic in molten pool. Finally, the authors have studied the effect of fluid flows on temperature evolution and weld pool morphology. The comparison of results between these two simulations shows a great influence of fluid flows on temperature and molten pool morphology. In second step, a new coupling strategy is developed to simulate the thermo-fluid flows and the solid-state stress field at each computing time step. The aim is to estimate residual stresses and distortions, in order to obtain final proprieties of SLM parts.

ICME Design of High Performance Ni-based and High-Entropy Turbine Alloys

James Saal^{*}, Jiadong Gong^{**}, Ricardo Komai^{***}, Greg Olson^{****}

^{*}QuesTek Innovations LLC, ^{**}QuesTek Innovations LLC, ^{***}QuesTek Innovations LLC, ^{****}QuesTek Innovations LLC / Northwestern University

ABSTRACT

Integrated Computational Materials Engineering (ICME) tools are being developed at QuesTek Innovations for the design of high-performance alloys for turbine blades, specifically (1) a highly castable yet creep-resistant low-Re Ni-based superalloy and (2) high entropy alloys (HEAs) for extreme environments. The integration of various CALPHAD calculations such as phase-equilibria, solidification pathways, diffusion fields, and precipitation behavior form an important foundation for designing high-performance alloys. Using internally developed processing-structure-property models and a parametric design platform integrated with both commercial and proprietary thermodynamic/mobility databases, QuesTek designed a novel low-Re castable SX Ni-based superalloy for blade applications. Select design criteria includes nominally 60% volume fraction of γ' , slight negative misfit between γ and γ' at 1000-1100°C, minimized propensity for TCP formation, and ability to be solution treatable without incipient melting, in addition to the processing and property objectives previously mentioned. The resulting design, termed QTSX, possesses an optimized combination of the processing constraints and property criteria specific for the blade application. HEAs, particularly those containing refractory elements, have the potential to surpass Ni-based superalloy performance in blade applications by enabling higher operating temperature. In addition to commercial CALPHAD databases, QuesTek is utilizing an internally developed database based on experimental data as well as exhaustive high-throughput density functional theory (DFT) calculations. Novel HEA compositions have been identified and experimentally verified by lab-scale alloy synthesis and characterization. A processing-structure-property framework has been created, and ongoing work focuses on the design of HEAs for high-temperature stability, strength, oxidation resistance, ductility, and creep resistance.

Virtual Element Method Approach for 2D Fracture Mechanics Problems

Elio Sacco^{*}, Edoardo Artioli^{**}, Sonia Marfia^{***}

^{*}, University of Naples Federico II, Naples, Italy, ^{**}University of Rome Tor Vergata, Rome, Italy, ^{***}University of Cassino and Southern Lazio, Cassino, Italy

ABSTRACT

The object of the present work is the development of an innovative methodology for 2D fracture mechanics problems based on the Virtual Element Method (VEM). The VEM is a new technology for the approximation of partial differential equations, which can be interpreted as an evolution of modern mimetic finite difference schemes, and which shares the same variational background of the finite element method. The main feature of the VEM is the possibility to construct an accurate Galerkin scheme with the flexibility to deal with highly general polygonal/polyhedral meshes, including “hanging vertices” and non-convex shapes, retaining the conformity of the method, i.e. the property to build an approximated solution which shares the same regularity features as the analytical solution of the problem under consideration [1,2]. In many interesting cases, this means that the discrete solution is continuous across adjacent elements. Owing to the powerful features of the VEM in relation with mesh generation and enhanced topological tools, the analysis will point to assessing accuracy and efficiency in the aforementioned computational fracture mechanics problem presenting a comparison with more established techniques [3]. In particular, the analysis will point out some interesting issues made possible using the innovative method, which are more cumbersome when resorting to standard FEM, namely the easiness of fracturing and segmenting existing elements whenever a fracturing path crosses them. Based on a wide variety of material models and fracture domain setups, an extensive numerical campaign will show the efficiency and accuracy of the proposed methodology which can then be seen as a powerful alternative classical methods. References [1] L. Beirão da Veiga, F. Brezzi, A. Cangiani, G. Manzini, L. D. Marini, and A. Russo, Basic principles of virtual element methods, *Math. Models Methods Appl. Sci.* 23 (2013), no. 1, 199–214. [2] E. Artioli, L. Beirão da Veiga, C. Lovadina, and E. Sacco, Arbitrary order 2D virtual elements for polygonal meshes: Part I, elastic problem, *Computational Mechanics* (2017), doi:10.1007/s00466–017–1404–5. [3] Moës, Nicolas; Dolbow, John; Belytschko, Ted (1999). “A finite element method for crack growth without remeshing”. *International Journal for Numerical Methods in Engineering*. 46 (1): 131–150.

Investigating the Role of Interventricular Interdependence in Development of Right Heart Failure during LVAD Support: A Finite-element Methods-based Approach

Kevin L. Sack*, Thomas Franz**, Daniel Burkhoff***, Julius Guccione****

*University of California, San Francisco, USA, **University of Cape Town, South Africa, ***Columbia University, USA, ****University of California, San Francisco, USA

ABSTRACT

Patients with end-stage heart failure have limited treatment options and an extremely poor prognosis. The use of left ventricular assistance devices (LVADs) as a therapy offers much needed mechanical assistance to the left ventricle (LV) of these patients. However right heart failure, a substantial related adverse effect, occurs in 10-40% of LVAD patients, shortening their long-term morbidity and mortality [1]. Although the potential implications of ventricular interactions on right ventricle (RV) function during LVAD support are well appreciated, due to the mechanical complexity involved, no study has yet proven, in any setting, that LV unloading and septal shift can actually lead to RV failure. Computational modeling is well suited to investigate and elucidate the individual contributions of these primary hemodynamic factors. To investigate this LV-RV interdependence, we extend on our previous work [2] by introducing a patient-specific finite-element model of dilated chronic heart failure. This model consists of coupled subsystems describing ventricular wall mechanics and lumped circulatory fluid flow. The material parameters were calibrated using patient-specific clinical data, producing a realistic mechanical surrogate of the failing in vivo heart that predicts its dynamic strain and stress throughout the cardiac cycle. The coupled model of lumped circulatory flow was modified to include additional fluid exchanges between the LV and the systemic circuit, which simulate ventricular assistance. These incorporate experimentally recorded flow data for the HeartMate II LVAD a commonly used LVAD operating between 8k– 12k RPM. Our findings show that LVAD operation reduces myofiber stress in the LV (14.6 ± 8.0 vs. 5.26 ± 5.86 kPa) (no intervention vs. 12k RPM LVAD) and, to a lesser extent, RV free wall, while increasing leftward septal-shift with increased operating-speeds. These improvements were achieved with secondary, potentially negative effects on the interventricular septum which showed that LVAD support introduces unnatural bending of the septum and with it, increased localized stress regions. LVAD operation unloads the LV significantly and shifts the RV pressure-volume-loop toward larger volumes and pressures (19.5 vs. 24.1 mmHg) (no intervention vs. 12k RPM LVAD); a consequence of RV-LV interactions and increased flow to the systemic circuit. References 1. Hayek, S., et al., Assessment of right ventricular function in left ventricular assist device candidates. *Circulation: Cardiovascular Imaging*, 2014. 7(2): p. 379-389. 2. Sack, K.L., et al., Partial LVAD restores ventricular outputs and normalizes LV but not RV stress distributions in the acutely failing heart in silico. *Int J Artif Organs*, 2016. 39(8): p. 421-430.

On the 3D Mechanical Properties of Passive Myocardium Using a Novel Numerical-experimental Inverse Modeling Approach

Michael Sacks^{*}, David Li^{**}, Reza Avaz^{***}

^{*}University of Texas at Austin, ^{**}University of Texas at Austin, ^{***}University of Texas at Austin

ABSTRACT

Recent studies have demonstrated the utility of the injection of biomaterials into the heart infarct region as bulking agents. Despite promising initial success, optimization of the mechanical characteristics and injection patterns of these polymers is limited by a lack of biomechanical knowledge of the remodeling events that occur as a result of MI and physical support by the injectate. We employed a novel 3D integrated numerical/experimental approach to apply 3D deformations to single soft tissue specimens, for characterizing the stress-strain response of non-contracting, healthy, drained LV myocardium. We developed an optimal set of displacement paths based on the full 3D deformation gradient tensor. We also performed studies on specimens injected with dual-crosslinked hyaluronic acid (HA)-based hydrogels. Diffusion tensor MRI was used to determine the local 3D orientation of myofibers. We then utilized an inverse finite element (FE) simulation of the experimental configuration embedded in a parameter optimization scheme for estimation of the SEDF parameters. Notable features of this approach include: (i) enhanced determinability and predictive capability of the estimated parameters following an optimal design of experiments, (ii) accurate simulation of the experimental setup and transmural variation of local fiber directions in the FE environment, and (iii) application of all displacement paths to a single specimen. Our results indicated that, in contrast to the common approach of conducting pre-selected tests and choosing an SEDF a posteriori, the optimal design of experiments integrated with a chosen SEDF and full 3D kinematics, leads to a more robust characterization of the mechanical behavior of myocardium. Resulting responses showed clearly nonlinear, fairly anisotropic, and slightly hysteretic behavior of the viable myocardium. We also confirmed detectable stiffening in mechanical behavior for samples injected with the HA hydrogel, which was also noted to stiffen the tissue anisotropically. To our knowledge, this work is the first of its kind on the robust fully 3D modeling of the tissue-level mechanical properties of viable myocardium. We found that the inclusion of optimal design of experiments was critical in our inverse model to minimize the dependence of the estimated values of the SEDF constants on the applied boundary conditions, and therefore to improve the predictive capability of the SEDF to capture the behavior of the myocardium under general in-vivo loading conditions. The results from this study will guide the development of a robust, clinically relevant organ-level model of injection therapies for the optimization of minimally invasive treatment of the post-MI heart.

A Macro-micro Modeling Approach to Determine In-situ Heart Valve Interstitial Cell Contractile Behaviors in Native and Synthetic Environments

Michael Sacks*

*University of Texas at Austin

ABSTRACT

Mechanical forces are known to regulate valve interstitial cell (VIC) functional state by modulating their biosynthetic activity, translating to differences in tissue composition and structure, and potentially leading to valve dysfunction. VICs can change phenotype dynamically; in diseased valves VICs switch to a myofibroblast-like phenotype and become contractile. Activated VICs display prominent SMA stress fibers and an increase in ECM remodeling. Yet, while advances have been made toward the understanding of VIC behavior ex-situ, the VIC biomechanical state in its native extracellular matrix (ECM) remains largely unknown. We hypothesize that improved descriptions of VIC biomechanical state in-situ, obtained using a macro-micro modeling approach, will provide deeper insight into VIC interactions with the surrounding ECM, revealing important changes resulting from pathological state, and possibly informing pharmaceutical therapies. To achieve this, a novel integrated numerical-experimental framework to estimate VIC mechanobiological state in-situ was developed. Flexural deformation of intact valve leaflets was used to quantify the effects of VIC stiffness and contraction at the tissue level. In addition to being a relevant deformation mode of the cardiac cycle, flexure is highly sensitive to layer-specific changes in VIC biomechanics. As a first step, a tissue-level bilayer model that accurately captures the bidirectional flexural response of AV intact layers was developed. Next, tissue micromorphology was incorporated in a macro-micro scale framework to simulate layer-specific VIC-ECM interactions. The macro-micro AV model enabled the estimation of changes in effective VIC stiffness and contraction in-situ that are otherwise grossly inaccessible through experimental approaches alone. While the use of native tissues provided much insight, we also utilized 3-D hydrogel encapsulation, which is an increasingly popular technique for studying VICs. Specifically, we employed poly(ethylene glycol) (PEG) gels to encapsulate VICs and study their mechanical response to the surrounding hydrogel stiffness and to varying levels of adhesion availability. Cell contraction was elicited through chemical treatments and the resulting mechanical properties of the constructs were measured through end-loading flexural deformation testing. We applied the downscale model, which was improved by 3D stress fiber visualization. The resulting cell force levels were comparable to native in-situ results. Overall, the developed numerical-experimental methodology can be used to obtain VIC properties in-situ. Most importantly, this approach can lead to further understanding of VIC-ECM mechanical coupling under various pathophysiological conditions and the investigation of possible treatment strategies targeting the myofibroblast phenotype characteristic of early signs of valvular disease.

Coupling Crystal-Plasticity Phase Field and Extended Finite Element Methods for Efficient Modeling of Fatigue Crack Initiation and Propagation

Alireza Sadeghirad^{*}, Kasra Momeni^{**}, Yanzhou Ji^{***}, Xiang Ren^{****}, Long-Qing Chen^{*****}, Jim Lua^{*****}

^{*}Global Engineering and Materials, Inc., ^{**}The Pennsylvania State University; Louisiana Tech University, ^{***}The Pennsylvania State University, ^{****}Global Engineering and Materials, Inc., ^{*****}The Pennsylvania State University, ^{*****}Global Engineering and Materials, Inc.

ABSTRACT

To model fatigue crack initiation and short crack within a grain or across grains, understanding behavior of the crack at microstructural level, considering the effects of crack size, shape, grain boundaries, and other microstructural features, is required. For this purpose, we integrated the phase field (PF) approach and the crystal plasticity (CP) theory following our recent coupling technique in the framework of the fast Fourier transform (FFT). Advantages of this coupled method include: (1) the PF and CP models are seamlessly coupled since both models use the FFT algorithm and (2) the spectral FFT formulation greatly reduce the computation cost at acceptable accuracy levels. We employed the coupled method to characterize realistic microstructures based on the electron backscatter diffraction (EBSD) data, and predict the fatigue micro-crack initiation using a microstructure-based failure model. The remaining issue is that the computational cost, associated with micro-mechanics simulation of crack initiation and propagation, is prohibitively large for length scales greater than a few millimeters. Noting that the effects of microstructural features are profound mainly for fatigue crack initiation and short-crack growth in metals justifies application of much more efficient linear elastic fracture mechanics (LEFM) modeling techniques for simulation of long-crack growth, e.g. the extended finite element method (XFEM). We developed a multiscale technique for unified fatigue crack initiation and propagation modeling in metallic alloys by combining two simulation techniques: (1) the coupled FFT-PF/CP method at micro-scale to simulate fatigue crack initiation taking into account the important microstructural features, and (2) the XFEM method at macro-scale to simulate fatigue long-crack growth. The motivation for this coupled modeling technique is to take advantage of the strengths of each method to physics-based predictions. A sequential coupling has been accomplished where the hot spots at each cyclic loading increment are determined using the XFEM model. The associated stress/strain values are then passed to the unit-cell PF model for accurate physics-based microstructure modeling and prediction of plasticity induced crack initiation. The accurate micromechanics model predicts the number of cycles for the crack initiation and the analytical crack growth models will be employed to propagate the initiated crack by the appropriate length to be inserted in the FE mesh. Finally, the XFEM method will be employed for the final stage of long crack growth prediction. Some numerical examples demonstrate the effectiveness of the proposed multiscale method.

Computational Modeling of the Intracellular Retrograde Flow During Cell Migration

Pablo Saez^{*}, Saskia Loosveldt^{**}, Kiran Sagar^{***}, Paris Mulye^{****}

^{*}Universitat Politecnica de Catalunya, ^{**}Universitat Politecnica de Catalunya, ^{***}École centrale de Nantes, ^{****}École centrale de Nantes

ABSTRACT

Actin dynamic is a key player in cell motility and migration [1]. Understanding the actin turnover at different spatial and temporal scales is of profound relevance in biology because it is involved in fundamental biological processes, e.g. in embryogenesis or wound healing. The retrograde flow protrudes the leading edge; one of the main exploratory mechanisms in the cell migration. The continuous flow of cellular components moves backward from the leading edge to the rear of the cell. This retrograde flow is conditioned by the actin polymerization against the plasma membrane and pushing forces exerted by myosin motors. Actin monomers polymerize rapidly after a period of slow nucleation. The resulting actin filaments undergo a complex reaction while forming and disassembling, providing a pool of new actin monomer [1]. Experimental cell biology has made the greatest progresses in understanding the actin turnover cycle and in the dynamic of the retrograde flow. Mathematical theories and computational models are highly reliable, low-cost and reliable tools to foster new insights and answer open questions in cellular motility. Complete mathematical models have also been proposed however the computational modeling of the cell migration has not been still extensively developed in literature. Pollard and co-workers [2] established the mathematical foundations of actin polymerization and depolymerization. Mogilner and coworkers, among many others, moved the field further with complete mathematical models [3]. Today, many question remain open in field of cell motility and migration. In this work, we have adopted a model of the main mechanisms involved in the dynamic of the retrograde flow and developed a fully coupled finite element model. We have focused on fast motile cells where the protrusion and the retrograde flow are steady during migration. We have reproduced some experimental results in literature. Furthermore, we modeled a number of flow responses under the effect of the manipulation of different assembly and disassembly rates. Using standard numerical techniques to solve complex models of actin turnover and cell motility opens tremendous opportunities in the understanding of cell migration. [1] T. D. Pollard and J. A Cooper. Actin, a central player in cell shape and movement. *Science*, 326(5957):1208–12, 2009. [2] T. D. Pollard. Rate constants for the reactions of ATP- and ADP-actin with the ends of actin filaments. *J. Cell Biol.*, 103(6):2747, 1986. [3] A. Mogilner and L. Edelstein-Keshet. Regulation of actin dynamics in rapidly moving cells: a quantitative analysis. *Biophys. J.*, 83(3):1237–1258, 2002.

MultiscaleHub: A Web-enabled Platform for Multiscale Modeling and Analysis of Materials

Masoud Safdari*, Jacob Fish**

*Illinois Rocstar LLC, **Columbia University

ABSTRACT

In the current work, we present design, formulation, and prototyping of MultiscaleHub, a web-enabled platform for multiscale modeling and analysis of materials and chemistry. MultiscaleHub's design was performed based on previously published similar works. An established framework for multiscale discrete-to-continuum coupling was adopted in the formulation of MultiscaleHub. To simplify future development, a modular, extensible, and object-oriented structure was designed and implemented for MultiscaleHub. In the current form, the package provides general-purpose methods, data structure, tools and algorithms for encapsulating uniscale solvers, multiscale coupling, and analysis. A pair of open source atomistic and continuum computational physics solvers were selected and coupled together with MultiscaleHub. The preliminary capabilities of the package in solving multiscale structural and thermal problems were demonstrated using a series of illustrative examples and case studies. A web module and interface were designed and implemented for MultiscaleHub to providing Internet access to the package. The feasibility of delivering MultiscaleHub tools and capabilities on the web was demonstrated using a battery of preliminary example problems.

Machine Learning Materials Physics: Homogenization of Computed Martensitic Microstructures by Deep Neural Networks

Koki Sagiyama^{*}, Krishna Garikipati^{**}

^{*}University of Michigan, ^{**}University of Michigan

ABSTRACT

In this work, we study deep neural networks as a paradigm for abstracting the complexity of martensitic microstructures. This investigation is part of a larger exploration of the roles of machine learning in materials physics. The martensitic microstructures in our study are obtained by direct numerical simulations in three dimensions, based on non-convex elastic free energy functions. This model is regularized by Toupin's theory of gradient elasticity at finite strains. The computations use Isogeometric Analysis for the high-order continuity of spline basis functions, and fully resolve the laminae of martensitic variants [1,2]. The effective elastic response of the martensitic microstructures is explored to generate training data for standard deep neural network (DNN) representations of the constitutive relations. With the Lagrange strain components as features, we train DNNs for both: the nonlinear stress-strain response and the elastic free energy density function. Questions of symmetry representations and constitutive theory are addressed in the context of the DNNs. Finally, in order to accommodate arbitrary martensitic microstructures, we consider extensions of the feature vector to include microstructural variables. [1] Sagiyama, K., Garikipati, K., Unconditionally stable, second-order schemes for gradient-regularized, non-convex, finite-strain elasticity modeling martensitic phase transformations. (in review). [2] Sagiyama, K., Rudraraju, S., Garikipati, K., A numerical study of branching and stability of solutions to three-dimensional martensitic phase transformations using gradient-regularized, non-convex, finite strain elasticity. arXiv:1701.04564 (2017).

Euler-Lagrange Prediction of Aerosol Particle Transport and Deposition in Terminal Airways

Suvash Saha^{*}, Mohammad Islam^{**}

^{*}School of Mechanical and Mechatronic Engineering, Faculty of Engineering and Information Technology, University of Technology Sydney, Ultimo NSW 2007, Australia, ^{**}School of Mechanical and Mechatronic Engineering, Faculty of Engineering and Information Technology, University of Technology Sydney, Ultimo NSW 2007, Australia

ABSTRACT

The knowledge of the complex aerosol transport procedure through the human respiratory system is important for dosimetry and respiratory health effects analysis. The studies over the last few decades have improved the understanding of the aerosol particle transport in the extra-thoracic and upper airways. However, almost all of the studies have predicted the particle transport and deposition for non-realistic anatomical model. A detail and complete prediction of the pharmaceutical aerosol transport and deposition in the terminal bronchioles of a large-scale whole lung model is still unknown. This study considered a large-scale realistic anatomical model to predict the deposition pattern in the terminal airways. High-resolution CT-DiCom images are used to construct the realistic anatomical model. Finite volume based ANSYS Fluent (18) solver is used to simulate the particle transport and deposition in the terminal airways. The micro-particle deposition pattern shows a new deposition hot spot for the realistic model, which could help the targeted drug delivery in the respiratory airways. The nanoparticle transport and deposition are also investigated for the large-scale model. The numerical study showed different deposition hot spot for different lobes. The deposition efficiency in the different lobes is different for different flow rates, which could help with the health risk assessment of respiratory diseases and eventually could help the targeted drug delivery system

A High Resolution Multiscale Model to Study Drug-induced Arrhythmias

Francisco Sahli Costabal*, Jiang Yao**, Ellen Kuhl***

*Stanford University, **Dassault Systemes Simulia Corp, ***Stanford University

ABSTRACT

Drugs often have undesired side effects. In the heart, they can induce lethal arrhythmias such as torsades de pointes. The risk evaluation of a new compound is costly and can take a long time, which often hinders the development of new drugs. Here we establish a high resolution, multiscale computational model to quickly assess the cardiac toxicity of new and existing drugs. The input of the model is the drug-specific current block from single cell electrophysiology; the output is the spatio-temporal activation profile and the associated electrocardiogram. We demonstrate the potential of our model for a low risk drug, ranolazine, and a high risk drug, quinidine: For ranolazine, our model predicts a prolonged QT interval of 19.4% compared to baseline and a regular sinus rhythm at 60.15 beats per minute. For quinidine, our model predicts a prolonged QT interval of 78.4% and a spontaneous development of torsades de pointes both in the activation profile and in the electrocardiogram. Our model reveals the mechanisms by which electrophysiological abnormalities propagate across the spatio-temporal scales, from specific channel blockage, via altered single cell action potentials and prolonged QT intervals, to the spontaneous emergence of ventricular tachycardia in the form of torsades de pointes. Our model could have important implications for researchers, regulatory agencies, and pharmaceutical companies on rationalizing safe drug development and reducing the time-to-market of new drugs.

Adaptive Construction of Locally Anisotropic Spectral Discretization for Stochastic PDEs

Onkar Sahni^{*}, Joseph Lapierre^{**}, Vignesh Srinivasaragavan^{***}, Jason Li^{****}

^{*}Rensselaer Polytechnic Institute, ^{**}Rensselaer Polytechnic Institute, ^{***}Rensselaer Polytechnic Institute,
^{****}Rensselaer Polytechnic Institute

ABSTRACT

Many multi-physics stochastic problems of interest exhibit anisotropic behavior in that some stochastic directions are more prominent than others. Furthermore, this behavior changes in a local fashion in the physical space. For example, in a local physical region, only a few stochastic directions have significant influence on the solution while the remaining majority of stochastic directions have zero to marginal influence. However, in a different physical region, other stochastic directions show significance. Such problems can be efficiently resolved by employing anisotropic adaptivity as not all stochastic directions require the same level of resolution to control the discretization error. In this presentation we will focus on the formulation and application of an anisotropic adaptive approach for stochastic PDEs with uncertain input data. In this approach, we employ finite element basis in the physical domain and spectral basis (based on generalized polynomial chaos) in the stochastic domain. Our approach is based on the variational multiscale (VMS) method for this basis setting. In the VMS method, the effect of missing/fine scales on resolved/coarse scales is modeled as an algebraic approximation within each element using the strong-form residual and a stochastic stabilization parameter. In addition, a model term of a similar form is derived to estimate the error in the numerical solution in a local/element-wise fashion. Variance-based sensitivity analysis is applied on the element-wise error to devise an anisotropic indicator. This anisotropic indicator is used in conjunction with the estimated measure of the local error to adaptively control the order of the spectral basis in each dimension of the stochastic space independently, resulting in anisotropic stochastic adaptivity. In summary, our approach is designed for the adaptive construction of locally anisotropic spectral discretizations for stochastic PDEs. We demonstrate the effectiveness of our approach on multiple example cases including transport problems where locally in the physical space the stochastic behavior is anisotropic.

Smart Constrained Layer Damping Analysis of Laminated Plates by Meshfree Method

Soumya Sahoo*

*Indian Institute of Technology, Kharagpur-721302, India

ABSTRACT

In this article, the performance of advanced piezoelectric composite (PZC) based smart constrained layer damping (SCLD) treatment is analysed in controlling vibration of laminated composite plates. The overall structure is comprised of a substrate laminated plate integrated with a viscoelastic layer and a piezoelectric composite layer attached partially or fully at the top surface of the plate. A mesh free (FE) model is formulated based on the element free Galerkin method to study the dynamic behaviour of the laminated composite plates with regular and irregular shaped SCLD treatments within the framework of a first order layer wise displacement field theory. Both symmetric cross-ply and antisymmetric angle-ply laminated plates are considered for the numerical analysis. It is observed that SCLD treatment significantly improves the active damping properties of the substrate plate. The numerical results also reveal that the performance of irregular shaped SCLD patches are more effective in controlling vibration of the laminated composite plates than the regular rectangular ones. Keywords: SCLD, vibration analysis, element free galerkin method, composite structure, laminated plate, layerwise plate theory

An Arbitrary Lagrangian--Eulerian Finite Element Formulation for Lipid Membranes

Amaresh Sahu^{*}, Yannick Omar^{**}, Roger Sauer^{***}, Kranthi Mandadapu^{****}

^{*}UC Berkeley, ^{**}RWTH Aachen University, ^{***}RWTH Aachen University, ^{****}UC Berkeley

ABSTRACT

Biological membranes comprised of lipids and proteins make up the boundary of the cell, as well as the boundaries of internal organelles such as the nucleus, endoplasmic reticulum, and Golgi complex. Lipid membranes, however, pose significant modeling challenges because they bend elastically out-of-plane yet flow in-plane as a two-dimensional fluid. In this work, we present the continuum mechanical equations of motion of an arbitrarily curved and deforming lipid bilayer. We then provide the theory underlying a novel arbitrary Lagrangian--Eulerian description of evolving two-dimensional surfaces, in which the in-plane and out-of-plane behavior can be treated differently. Finally, we demonstrate the utility of this description within an isogeometric finite element framework with C^1 -continuous basis functions. We apply the framework to study membrane shapes during endocytosis, and discuss how our framework can model large in-plane flows and their coupling to out-of-plane deformations.

Thermo-Mechanical Modelling of HTP Process: Prediction of Martensite Formation in Pearlitic Rail Steel

Loïc Saint-Aimé*, Aurélien Saulot**, Frédéric Lebon***, Grégory Antoni****

*IRT Railenium / INSA-Lyon / LaMCoS, **INSA-Lyon / LaMCoS, ***Université de Provence / LMA, ****Université de Provence / LMA

ABSTRACT

For about twenty years, some rails of railway network have been affected by a phenomenon called Tribological Surface Transformation (TST). These TSTs correspond to a permanent, quasi-surfacic solid-solid phase transformation, e.g. pearlitic-martensitic transformations. They are characterized by the formation of a thin white layer progressively appearing, in proportion to the number of loading cycles, on the near-surface of the rail. In the worst cases, and for a number of cycles depending on both the material and the loading, TSTs can eventually lead to the emergence of a crack, due to strong strain incompatibilities between the quasi-surfacic, "white phase" (e.g. martensite) and the volumetric, "bulk" phase (e.g. pearlite). Initially attributed to flash temperatures generated by frictional heating at the contact zone, followed by subsequent quenching, several studies have shown that the temperature increase is often too low to explain these phase transformations. Thus it is not unrealistic to assume that TSTs could result from a thermo-mechanical coupling; this is actually the main assumption underlying our study. In order to describe these TSTs, we propose a thermo-mechanical model based on previous work [Leblond et al. (1989)] for Transformation Induced Plasticity (TRIP), which, however, are here extended for a thermo-mechanical coupling, relevant for TSTs, to be taken into account. Under rolling contact loading, rails are subjected to significant hydrostatic pressure simultaneously with shearing stress that could induce material transformations. With the aim to reproduce similar loading conditions High Pressure Torsion (HPT) experiments were conducted on the standard rail grade R260. Our purpose was to quantitatively assess load parameters (i.e., high pressure, shear and/or temperature) that could lead to WEL development. Therefore, these experimental data were used to calibrate the phenomenological thermo-mechanical model. Simulation of the HPT process has been the subject of a few studies with focus on the material behaviour and plastic flow as well as stress state and contact conditions between the sample and the anvils. However, the focus was on prediction of volume changes during phase transformation and the associated strain hardening. Hence the HPT process was simulated with the commercial FE software ABAQUS using an axi-symmetric model of the sample whose the material behaviour has been implemented as user material subroutines (UMAT). Good agreement between simulations and experimentally obtained stress-strain curves was achieved. Otherwise, the model was able to predict the emergence and progress of TSTs near the contact areas where the thermo-mechanical loading is applied.

Plastic Deformation Behavior in Nano-sized Metallic Wires Subjected to Drawing Process: Molecular Dynamics Simulation

Ken-ichi Saitoh^{*}, Kosuke Oda^{**}, Koki Yoshida^{***}, Tomohiro Sato^{****}, Masanori Takuma^{*****},
Yoshimasa Takahashi^{*****}

^{*}Kansai University, Faculty of Engineering Science, ^{**}Kansai University, Graduate School of Engineering(Student),
^{***}Kansai University, Graduate School of Engineering(Student), ^{****}Kansai University, Faculty of Engineering
Science, ^{*****}Kansai University, Faculty of Engineering Science, ^{*****}Kansai University, Faculty of Engineering
Science

ABSTRACT

The process of nano-sized wiredrawing is investigated by using molecular dynamics (MD) simulation in this study. Recently, in industrial wiredrawing process, a diameter of wire is going smaller and smaller such down to just several micrometers. It is supposed that this leads to a future demand of thin wire and an adequate mechanical process to produce it. The authors have constructed novel computation models of wiredrawing, in which a single wire has axisymmetric shape and is just a several nanometers in dimension (i.e. nano-sized wire). In those material models, a perfectly rigid or flexible die is attached to the wire so that the wire is smoothly drawn through it and is deformed to be thinner one. In MD simulations, all equations of motion for each atoms are solved numerically by using an interatomic potential which reproduces the needed properties for the simulated material. A many-body (EAM or MEAM method) and pairwise potential, both for pure iron (alpha-Fe) and iron-carbon binary (for pearlitic steel) systems, are adopted in this study. From MD results of the wiredrawing, we capture the dislocation mechanism inherent to nano-sized wire. According to crystalline orientations of drawing, the behavior of nucleated dislocations is quite different. We clarify that not only von Mises equivalent stress but also regional hydrostatic stress takes large effect on nucleation and subsequent motion of dislocations. We will also discuss an idea of aging status of each atom which is actually the history of atomistic and plastic stress or strain. By pearlite steel wire model, it is realized that the ferrite-cementite interface effectively offers high-speed paths for carbon atoms to diffuse from cementite to ferrite (it is called cementite decomposition in real system). It is observed that, when carbons diffuse, both ferrite and cementite crystals undergoes effectively microscopic plastic deformation, i.e. emission, movement, interaction and annihilation of many dislocations, as well as phase transition.

Technology of AI Aided Development for Electronic Devices

Akira Sakai^{*}, Tomo Kaniwa^{**}, Nobuyoshi Yamaoka^{***}, Serban Georgescu^{****}, Makoto Sakairi^{*****}

^{*}Fujitsu Advanced Technologies, ^{**}Fujitsu Advanced Technologies, ^{***}Fujitsu Advanced Technologies, ^{****}Fujitsu Laboratories of Europe, ^{*****}Fujitsu Advanced Technologies

ABSTRACT

Artificial Intelligence (AI) in the form of deep learning has made rapid progress during this decade and it started to influence a broad spectrum of technologies. We consider that “extended CAE technology” includes not only conventional CAD & simulation technology but also AI. This presentation introduces three concrete examples of our contributions to extended CAE technology. (1) Predicting the number of substrate layers. Due to the recent progress in miniaturization and high performance of electronic devices, the number of necessary substrate layers has been increasing. However, predicting the number of necessary substrate layers largely relies on the skill of engineers. To make this task simple for everyone, we have developed a technology to predict the number of layers of the substrate by using Support Vector Machine (SVM), a machine learning technique. Furthermore, we confirmed that the required number of layers of the substrate can be correctly predicted with the probability of 96% by using this technology. (2) Component recognition of a 3D-object in a CAD system. 3D-CAD is frequently used in designing of electronic devices. However, there are cases where the labels for identifying the components are not attached making it necessary to manually check the components with defects. We have developed a technique to classify the 3D-components by recognizing them with 2D images to identify unlabeled components. By using this technology, we have achieved a probability of 96% in finding screw components. (3) Optimization technique combining AI and a genetic algorithm. The application of optimization technology to electronic device design has been actively discussed. However, optimization algorithms, including genetic ones, require hundreds of simulations, making it difficult to apply them in practice. One example of such problems is the optimization of the hole positions on the server. This belongs to the class of combinatorial optimization problems, which are regarded as the most difficult in the field. To solve this problem, we have developed method to accelerate the convergence of genetic algorithms by giving prerequisite knowledge using AI which leads to a reduction of the number of simulations. Finally, we are going to introduce the future prospects gained from our experiences.

Discrete Element Simulation for Industrial Applications

Mikio Sakai*

*The University of Tokyo

ABSTRACT

Abstract The discrete element method (DEM) is widely used in the simulations of industrial granular and multi-phase flows. Very recently, an innovative approach was developed by my group, where the DEM, computational fluid dynamics (CFD), signed distance functions [1], immersed boundary method [2] and coarse grain model [3] were employed. This approach makes it possible to simulate several complex and large-scale systems easily, e.g., a fluidized bed [3], die-filling for fine particles [4] and a wet ball milling [5]. This is because scaling law model can simulate an enormous number of particles with low calculation cost and because the arbitrary shape wall can be created by a simple algorithm. Adequacy of this approach was shown through the validation tests. References [1] Y. Shigeto, M. Sakai, "Arbitrary-shaped wall boundary modeling based on signed distance functions for granular flow simulations," Chem. Eng. J., 231, 464-476 (2013) [2] X. Sun, M. Sakai, "Immersed boundary method with artificial density in pressure equation for modelling flows confined by wall boundaries," J. Chem. Eng. Jpn., 50, 161-169 (2017) [3] M. Sakai, M. Abe, Y. Shigeto, S. Mizutani, H. Takahashi, A. Vire, J.R. Percival, J. Xiang, C.C. Pain, "Verification and validation of a coarse grain model of the DEM in a bubbling fluidized bed," Chem. Eng. J., 244, 33-43 (2014) [4] H. Yao, Y. Mori, K. Takabatake, X. Sun, M. Sakai, "Numerical investigation on the influence of air flow in a die filling process," J. Taiwan Inst. Chem. Eng. (accepted) [5] M. Sakai, "How should the discrete element method be applied in industrial systems?: A review," KONA Powder and Particle Journal, 33, 169-178 (2016)

Three-dimensional Phase-field Simulations during Directional Solidification of a Binary Alloy Considering Thermal-solutal Convection

Shinji Sakane^{*}, Tomohiro Takaki^{**}, Munekazu Ohno^{***}, Yasushi Shibuta^{****}, Takayuki Aoki^{*****}

^{*}Kyoto Institute of Technology, ^{**}Kyoto Institute of Technology, ^{***}Hokkaido University, ^{****}The University of Tokyo, ^{*****}Tokyo Institute of Technology

ABSTRACT

In terrestrial solidification of an alloy, a thermal-solutal convection inevitably occurs due to a liquid density difference caused by the special distribution of temperature and solute concentration in liquid. However, the thermal-solutal convection is usually not considered in simulations for predicting a solidification microstructure, because it needs large computational cost. Depending on the solidification conditions, the thermal-solutal convection greatly influences on the interdendritic microsegregation, dendrite fragmentation, and dendrite morphology. Therefore, for numerically evaluating the effects of thermal-solutal convection on the solidification microstructures, it is essential to enable a simulation taking into account all fields which occur during solidification, such as solute concentration, thermal field, and flow field. In this study, we develop a parallel computing code using multiple graphic processing units (GPU) to accelerate the phase-field simulations for dendrite growth of a binary alloy taking solute, thermal, and fluid fields into account. Then, the parallel efficiency and computational cost are evaluated for conditions with and without thermal and fluid fields. Moreover, we investigate the effects of thermal and fluid fields on the dendrite morphology and microsegregation during directional solidification of a binary alloy. Because these simulations become large-scale, the simulations are performed using the GPU supercomputer TSUBAME3.0 at Tokyo Institute of Technology.

Multiscale Stochastic Stress Analysis of FRP with a Successive Sensitivity Analysis Considering Randomness in Multi Fibers Location

Sei-Ichiro Sakata*, Takuro Sakamoto**

*Kindai University, **Graduate School of Kindai University

ABSTRACT

In this presentation, a multiscale stochastic stress analysis of composites considering microscopic geometrical randomness (location variation of inclusions) is discussed for estimation of the probabilistic properties of the maximum microscopic stresses. One of the reasons on uncertainty in an apparent strength of a composite material is randomness in microstructure. In particular, random variation of location of inclusions will have a large influence on its microscopic stress distribution, even if the influence on the homogenized elastic property is not so large [1]. For this problem, the Monte-Carlo simulation (MC) is one of standard approached, but because of some reasons, for instance computational costs, bias, or unclerness between the random variables and the responses, an effective computational method is needed. In particular, for the purpose of V&V or reliability-based optimization, non-MC method should be developed. For this purpose, from theoretical simplicity, the first, second or successive perturbation based approach is one of the attractive approaches. In previous reports, however, only one or two fibers variation were considered, and applicability of the perturbation-based approach to the problems was discussed [1]. These methods will be expensive and difficult to be applicable to a problem considering geometrical random variation when the number of random variables is large. From this background, a successive sensitivity analysis based approach is developed in this study. In this paper, random location variations of 3x3 fibers in a unit cell of a unidirectional fiber reinforced composite are considered as a first example, and the CV of the microscopic maximum stress is analyzed. For this problem, applicability of the proposed approach is discussed. In addition, the proposed approach is applied to a problem considering a unit cell including more fibers for a general case. As a numerical example, the proposed method is applied to the multiscale stochastic stress analysis of a unidirectional fiber reinforced composite plate under a tensile uniform load along transverse direction, and validity and effectiveness of the proposed method are discussed with comparison of the results of MC. [1] S. Sakata and I. Torigoe, "Multiscale Stochastic Stress Analysis for Randomness of Fiber Arrangement in Fiber Reinforced Composite Material", the proceedings of WCCM XI, 2014

Meso-mechanical Embedded Discontinuity Finite Element Modelling of Concrete Fracture Processes under Dynamic Loading

Timo Saksala*

*Tampere University of Technology, Tampere, Finland

ABSTRACT

This paper deals with numerical modelling of concrete fracture under dynamic loading. For this end, a 2D meso-mechanical model based on embedded discontinuity finite elements was developed. The aggregates are represented by polygons obtained by shrinking of Voronoi cells. The matrix, i.e. the mortar, and its failure are described by CST elements with three pre-embedded (before the analysis) discontinuities oriented parallel to the element edges. This approach is similar to the cohesive zone elements with the advantage of no need to double the nodes in the mesh since the embedded discontinuities are element-internal. The aggregates, also meshed with the CST elements, may fracture in mode-I and, consequently, a single discontinuity is embedded parallel to the first principal direction in the failing element inside an aggregate. The effect of the interfacial transition zone between the aggregates and the mortar matrix can be accounted for, to some extent, by lowering the strength of the elements in a narrow strip around the aggregates. The rate sensitivity is accommodated by adding a linear viscosity term to the static strength of an element. The finite element formulation of discontinuity kinematics is based on the enhanced assumed strains concept where the enhanced modes (variations of the crack opening displacement) are constructed in the strain space, orthogonal to the stress field. This formulation, with the CST element, results in a simple implementation where no crack length nor its exact location inside the element appears. Moreover, the multiple discontinuity approach alleviates, to some extent, the crack locking and spreading problems typical to low-order elements with embedded discontinuities. This kind of approach has two sources of heterogeneity. The first is the polygonal aggregates generated by shrinking of random seed Voronoi cells. The second source is the underlying non-structural CST mesh with (more or less) quasi-random triangle side orientations. As the finite elements representing the mortar have pre-embedded discontinuities parallel to the element sides, the strengths of the elements are quasi-random as well with respect to loading, say uniaxial compression for example. In the numerical examples, the performance of the model is demonstrated in uniaxial tension and compressive test simulations. The influence of the main parameters on the model behavior is tested. Finally, the dynamic Brazilian disc test is simulated. These simulations demonstrate that this kind of modelling approach is capable of capturing the salient features concrete under the various loading conditions.

Ocular Mathematical Virtual Simulator: A Hemodynamical and Biomechanical Study towards Clinical Applications

Lorenzo Sala^{*}, Christophe Prud'Homme^{**}, Giovanna Guidoboni^{***}, Marcela Szopos^{****}

^{*}IRMA UMR 7501, Université de Strasbourg, Strasbourg, France, ^{**}IRMA UMR 7501, Université de Strasbourg, Strasbourg, France, ^{***}Mizzou, University of Missouri, Columbia (MO), USA, ^{****}IRMA UMR 7501, Université de Strasbourg, Strasbourg, France

ABSTRACT

We present the development of a mathematical virtual simulator to model the interplay of biomechanics and hemodynamics in the human eye. This model provides a multiscale view of ocular physiology, in particular it simulates (i) the blood circulation in the retinal vasculature and the central retinal vessels via a circuit-based model, (ii) the blood perfusion within the lamina cribrosa via a porous-media model, and (iii) the biomechanical behavior of cornea, sclera, choroid, retina and lamina cribrosa via an isotropic linear elasticity system. Parts (ii) and (iii) within the lamina cribrosa are mathematically described by poro-elastic equations[1], whereas the coupling between the three-dimensional(3D) systems and the lumped-parameter circuit is achieved by employing an energy-preserving method in the spirit of [2]. To numerically solve the overall system, we implemented step (i) in OpenModelica and steps (ii) and (iii) in the multiphysics open-source platform Feel++ [3]. The 3D problem is solved by adopting a Hybridizable Discontinuous Galerkin (HDG) method, taking advantage of static condensation within the high performance computing environment developed in Feel++. In the present work, we aim to contribute to a better understanding of ocular neurodegenerative disease - in particular glaucoma, which is the second main condition that leads to blindness - in the context of biomedical research. Starting from clinically-measurable inputs of blood pressure, intraocular pressure and cerebrospinal fluid, the proposed virtual simulator is able to predict the main hemodynamical and biomechanical aspects of significant ocular components. In particular the model illustrates the spatial distribution of blood within the ocular tissues and the local displacement of the lamina cribrosa, which plays a crucial role in the pathogenesis of glaucoma. In addition, novel clinically relevant patient-specific insights can be obtained with respect to the central retinal vessels and other tissues of the eye included in the model. We envision this virtual simulator as a promising non-invasive clinical investigation tool in the biomedical context, after completion of thorough validation against experimental and clinical data. References: [1] Causin P et al. A poroelastic model for the perfusion of the lamina cribrosa in the optic nerve head. *Mathematical biosciences*. 2014. [2] Carichino L et al. Energy-based operator splitting approach for the time discretization of coupled systems of partial and ordinary differential equations for fluid flows: the Stokes case. *Journal of Computational Physics*. Submitted. [3] Sala L et al. An implementation of HDG methods with Feel++. Application to problems with integral boundary condition. In preparation.

Prestress Induced Phase Transitions In Tensegrity-Based Metamaterials

Hossein Salahshoor^{*}, Raj Kumar Pal^{**}, Julian Rimoli^{***}

^{*}Georgia Institute of Technology, ^{**}Georgia Institute of Technology, ^{***}Georgia Institute of Technology

ABSTRACT

Pre-stressing the cables of tensegrity structures is a widespread practice for enhancing their stability and mechanical properties. We chose a three dimensional tensegrity lattice [1] and have studied material symmetry phase transitions induced by varying the cable prestress. We studied several combinations of prestress cases and a vast regime of prestress values for each case. In each prestress scenario, we compute the effective elasticity tensor through a homogenization scheme. By examining the eigenspaces of the homogenized elasticity tensor, we study the material symmetries of the tensegrity lattice and characterize the effects of cable prestressing on it. We demonstrate symmetry breaking and phase transitions, occurring solely due to prestressing the members of our lattice. We observed several phase transitions including cubic to tetragonal and tetragonal to orthotropic and vice-verses. We also show that under a certain prestress condition, where the finite lattice exhibits orthotropic symmetry, we obtain tetragonal symmetry for the infinite lattice. This discrepancy in symmetries of the finite and infinite lattice is due to surface effects in finite size and the nonsymmorphic nature of the tensegrity lattice. Consequently, unlike the crystalline materials where surface effects increases the symmetries [2], we found a class of metamaterials where surface effects leads to symmetry reduction. [1] J. J. Rimoli, R. K. Pal, Mechanical response of 3-dimensional tensegrity lattices, *Composites Part B: Engineering* 115 (2017) 30{42. [2] P. Ayyub, V. Palkar, S. Chattopadhyay, M. Multani, Effect of crystal size reduction on lattice symmetry and cooperative properties, *Physical Review B* 51 (9) (1995) 6135.

Modeling of Crystal Plasticity by Using a Non-convex Energy Based on $GL(2, Z)$ Invariance

Oguz Umut Salman^{*}, Giovanni Zanzotto^{**}, Lev Truskinovsky^{***}, Roberta Baggio^{****}

^{*}CNRS/Paris 13, ^{**}Padova University, ^{***}CNRS/ESPCI, ^{****}ESPCI/Paris 13

ABSTRACT

For micro- and nano-sized samples, dislocation-mediated crystal plasticity is radically different from that described by classical engineering theories. At the microscale, plasticity evolves in a disordered manner through a sequence of intermittent events involving collective motion of dislocations and their interaction with each other and with existing lattice defects. Detailed mathematical modeling of these processes remains a major challenge in materials science. We present a mesoscopic post-DDD approach which involves constructing a coarse-grained non-convex energy invariant under the full symmetry group of lattices - such as $GL(2, Z)$ in the 2-d case. The model is thus informed by the inherent structure of the material, and is largely free of arbitrariness when dealing with the fast topological changes in dislocation configurations such as nucleation, annihilation, interaction with obstacles/other phases and with various other entanglements. We will also present an efficient numerical solver for the resulting equations.

A Phase Field Approach for Solid-state Dewetting

Marco Salvalaglio^{*}, Axel Voigt^{**}, Rainer Backofen^{***}

^{*}TU Dresden, ^{**}TU Dresden, ^{***}TU Dresden

ABSTRACT

We consider a practical numerical scheme for a phase field approximation for surface diffusion to simulate solid-state dewetting phenomena. The scheme is based on a combined convexity splitting approach and a Rosenbrock method and uses a model with improved accuracy. We discuss modeling approaches to incorporate contact angles and show large scale simulations in comparison with experiments.

Optimization of Carbon Black Polymer Composite Microstructure for Rupture Resistance

Bingbing San^{*}, Haim Waisman^{**}

^{*}Hohai University, ^{**}Columbia University

ABSTRACT

In this manuscript, we study the optimal location of Carbon Black (CB) particle inclusions in a natural rubber (NR) matrix with the objective to maximize the rupture resistance of such polymer composites. Hyperelasticity is used to model the rubber matrix and stiff inclusions and the phase field method is used to model the fracture accounting for large deformation kinematics. A genetic algorithm is employed to solve the inverse problem in which three parameters are proposed as optimization objective, including maximum peak force, maximum deformation at failure-point and maximum fracture energy at failure-point. Two kinds of optimization variables, continuous and discrete variables, are adopted to describe the location of particles and several numerical examples are carried out to provide insight into the optimal locations for different objectives. The main conclusions from our studies are as follows: (i) location of particles has only a slight influence on the hardening part, but significantly affects the softening part after the peak force is reached; (ii) with the increase of particle numbers, the optimal position closet to notch is not changed, while other optimal position varies due to the inter-particle interactions; (iii) the location of particles does not change the overall crack propagation path; (iv) the fracture energy at failure-point is the most appropriate quantity to evaluate the effect of particle locations and yields most significant optimization results.

Influence of Microstructural Evolutions on Macroscopic Mechanical Behaviour of Cementitious Materials

Julien Sanahuja^{*}, Shun Huang^{**}, Luc Dormieux^{***}, Benoit Bary^{****}, Eric Lemarchand^{*****}

^{*}Edf lab Les Renardieres, ^{**}Edf lab Les Renardieres, ^{***}Ecole des Ponts ParisTech, ^{****}Den-Secr, CEA, Universite Paris-Saclay, ^{*****}Ecole des Ponts ParisTech

ABSTRACT

Civil engineering facilities are, as any concrete structure, subject to ageing phenomena in association with environmental conditions, operating conditions and potential internal pathologies. Structure analysis and computations require relevant material constitutive models. The latter must integrate the influence of degradation, damage and ageing mechanisms. Such mechanisms often occur in pore space, or more generally at a much lower scale than the structure scale. This contribution examines the mechanisms associated to chemical processes. Through dissolution and precipitation, the latter induce progressive evolutions of microstructure. In turn, this microstructural evolution yields variations of the mechanical behaviour. Microstructure changes are thus the key linking the chemical processes occurring at lower scales to the mechanical behavior at the structure scale. To bridge the scales, micromechanics represents an appealing tool. Cementitious materials are the focus of this contribution, investigating both precipitation (due to hydration) and dissolution (due to leaching or hydration) mechanisms, and also elastic and creep behaviours. As far as upscaling is concerned, mean-field homogenization is used to benefit from its efficient computations. More precisely, when the considered behaviour does not involve time, such as elasticity, homogenization techniques can be readily used, on a time by time basis, to estimate the evolution of effective properties. But when the behaviour is intrinsically time-dependent, such as creep, modelling is much more involved as two processes coexist: microstructure evolution and the time-dependent individual behaviour of phases. The last part of this contribution proposes to take advantage of recent developments in micromechanics to investigate the influence of time-dependent microstructure changes, due to hydration, on the effective ageing viscoelastic behaviour of concrete. Model predictions are compared to experimental basic creep responses on VeRCoRs concrete loaded at various ages, and with a creep recovery experiment.

PDE-Constrained Optimization Framework and Inverse Design of Mechanical Metamaterials for Vibration Control

Clay Sanders^{*}, Timothy Walsh^{**}, Wilkins Aquino^{***}

^{*}Duke University, ^{**}Sandia National Laboratories, ^{***}Duke University

ABSTRACT

Harsh shock and vibration environments are commonly encountered in engineering applications involving dynamic loading. Acoustic/elastic metamaterials are showing significant potential as candidates for controlling wave propagation and isolating sensitive structural components. However, these materials have complex microstructures that must be properly designed to achieve their desired properties. In this talk we will present PDE-constrained, time and frequency-domain strategies for inverse design of elastic/acoustic metamaterials. A frequency-domain approach is typically the desirable strategy when designing band-gap or notch filter materials, whereas a time-domain strategy may be advantageous in a transient shock environment. For the frequency-domain optimization, a Modified Error in Constitutive Equation (MECE) objective function will be compared with the least squares counterpart in terms of effectiveness for designing a band-gap material. For the time-domain, a transient optimization formulation will be presented and demonstrated on a vibration isolation problem. Numerical examples will be presented on a variety of structural and acoustic cloaking scenarios. Sandia National Laboratories is a multimission laboratory managed and operated by National Technology and Engineering Solutions of Sandia, LLC., a wholly owned subsidiary of Honeywell International, Inc., for the U.S. Department of Energy's National Nuclear Security Administration. With main facilities in Albuquerque, N.M., and Livermore, C.A., Sandia has major R&D responsibilities in national security, energy and environmental technologies, and economic competitiveness.

Influence of Stress Triaxiality on Fracture Ductility for Stereolithography

Anjali Sandip*, Ravi Kiran Yellavajjala**

*University of North Dakota, **North Dakota State University

ABSTRACT

Stress triaxiality is one of the most important factors that controls fracture ductility [1]. The objective of this study was to investigate the influence of stress triaxiality on fracture ductility for specimens' printed using stereolithography. Dog bone shape specimens were printed using Formlabs® Form 2 Desktop SLA 3D printer. The specimens were built layer by layer with the help of this 3D printer. Each layer of liquid photopolymer is solidified through a computer-controlled ultraviolet (UV) light source with a laser spot size of 140 μm [1, 2]. A photopolymer resin supplied by the manufacturer which comprised of a proprietary mix of Methacrylated oligomers, Methacrylated monomer, photo initiators and trace amount of pigments and additives was used for printing the specimens. The length of the specimens was 92.06 mm and the width of the specimens in the gage length portion was 6 mm. Uniaxial tensile tests were conducted on 3D printed specimens. Numerical simulations of the uniaxial tensile tests were performed using the commercial finite element code, ABAQUS. Material properties of 3D printed specimens were calibrated using Abaqus/Isight. The stress triaxiality distribution in the critical cross section at a displacement corresponding to fracture displacement was evaluated. The maximum and average stress triaxialities at the critical cross section was recorded. Triaxiality versus equivalent strain to fracture was plotted for the tested specimens. The results indicate a strong dependence of fracture ductility on stress triaxiality for the 3D printed specimens investigated in this study. References: [1]. Bao, Y., & Wierzbicki, T. (2004). On fracture locus in the equivalent strain and stress triaxiality space. *International Journal of Mechanical Sciences*, 46(1), 81-98. [2]. Melchels, F. P., Feijen, J., & Grijpma, D. W. (2010). A review on stereolithography and its applications in biomedical engineering. *Biomaterials*, 31(24), 6121-6130. [3]. Crivello, J. V., & Reichmanis, E. (2013). Photopolymer materials and processes for advanced technologies. *Chemistry of Materials*, 26(1), 533-548.

Isogeometric Analysis and the k-refinement

Giancarlo Sangalli*

*Universita` di Pavia

ABSTRACT

k-refinement is one of the many great innovations proposed and promoted by Prof. Thomas J.R. Hughes. It has been described as one of the key features of isogeometric analysis, "a new, more efficient, higher-order concept", in the seminal work [1]. The idea of using high-degree and continuity splines (or NURBS, etc.) as a basis for a new high-order method appeared very promising from the beginning, and received confirmations from the next developments. k-refinement leads to several advantages: higher accuracy per degree-of-freedom, improved spectral accuracy, the possibility of structure-preserving smooth discretizations are the most interesting features that have been studied actively in the community. At the same time, the k-refinement brings significant challenges at the computational level: using standard finite element routines, its computational cost grows with respect to the degree, making degree raising computationally expensive. However, it has been understood recently that k-refinement is in fact superior from the point of view of computational efficiency, with respect to low-degree isogeometric discretizations, thanks to a proper code design that goes beyond standard finite element technology. I report the results obtained in collaboration with Mattia Tani, in [2]. In the proposed framework the k-refinement significantly improves not only the accuracy, but also the accuracy-to-computation-time ratio. The novelty is a matrix-free strategy, which is first used in this context but is well-known for other high-order methods. Matrix-free implementation speeds up matrix operations, and, perhaps even more important, greatly reduces memory consumption. Our strategy also employs the recently proposed weighted quadrature, which is an ad-hoc strategy to compute the integrals of the Galerkin system. The other key ingredient is a preconditioner based on the Fast Diagonalization method, an old idea to solve Sylvester-like equations. Numerical tests show that the new implementation is faster than the standard one (where the main cost is the matrix formation by standard Gaussian quadrature) even for low degree. But the main point is that, with the new approach, k-refinement leads to orders of magnitude faster execution, given a target accuracy. This is applicable to realistic differential problems, but its effectiveness will depend on the preconditioner stage, which is as always problem-dependent. [1] T.J.R.Hughes, J.A.Cottrell, Y.Bazilevs, Isogeometric analysis: CAD, finite elements, NURBS, exact geometry and mesh refinement, CMAME Volume 194, Issues 39–41, 1 October 2005, Pages 4135-4195 [2] G. Sangalli, M. Tani, Matrix-free isogeometric analysis: the computationally efficient k-method, arXiv:1712.08565

Utilizing Machine Learning and a Data-Driven Approach to Identify the Fatigue Crack Driving Force in Polycrystalline Materials

Michael Sangid^{*}, Andrea Rovinelli^{**}, Henry Proudhon^{***}, Ricardo Lebensohn^{****}, Wolfgang Ludwig^{*****}

^{*}Purdue University, ^{**}Purdue University, ^{***}Mines ParisTech, ^{****}Los Alamos National Lab, ^{*****}University of Lyon

ABSTRACT

Identifying the short crack driving force of polycrystalline engineering alloys is critical to correlate the inherent microstructure variability and the uncertainty in the short crack growth behavior observed during stage I fatigue crack growth. Due to recent experimental advancements, data of a short crack propagating at the relevant length scale is available via phase and diffraction contrast tomography. To compute the micromechanical fields not available from the experiment, crystal plasticity simulations are performed. Results of the experiment and simulations are combined in a single dataset and sampled utilizing non-local mining technique. Sampled data is analyzed using a machine learning Bayesian Network framework to identify statically relevant correlations between state variables, microstructure features, location of the crack front, and experimentally observed growth rate, in order to postulate a data-driven, non-parametric short crack driving force.

The Mechanics of Random Origami

Christian Santangelo*

*UMass Amherst

ABSTRACT

Origami is a new framework for the design of complex three-dimensional structures from an initially flat sheet or film, but has also been proposed as a way to fabricate mechanical metamaterials, which have effective mechanical response that is controlled by the material's architecture. In an origami structure, a fixed network of hinges along which the structure can be bent span a series of vertices. In this talk, I will discuss the interaction between origami geometry and the mechanical response of the folded structure. As I will discuss, the configuration space of an origami structure is characterized by an exponential number of distinct branches meeting at a bifurcation. Away from this, the dimension of the configuration space scales with the perimeter of the structure, allowing the rational design of mechanical response in these structures.

Effect of Topography on the Power Production and Wake Recovery of a Wind Turbine

Christian Santoni^{*}, Umberto Ciri^{**}, Stefano Leonardi^{***}

^{*}The University of Texas at Dallas, ^{**}The University of Texas at Dallas, ^{***}The University of Texas at Dallas

ABSTRACT

The performance of on-shore wind farms is largely affected the local topography of the region. Orographic features can induce velocity fluctuations that can be detrimental for the power production and increase fatigue loads. To address how the topography affects wind turbine power production and wake, Large Eddy simulations of a wind turbine located in a ridged terrain are performed. The hills are described by a sinusoidal wave. Two different amplitudes are considered, $0.10D$ and $0.05D$, where D is the rotor diameter. The wavelength is kept constant to $3D$. We investigate the effect of the position of the turbine within the domain by placing the turbine in the cavity and the crest of the hills and in a flat terrain downstream from the topography. Precursor simulations of a ridged topography are performed to obtain a fully developed flow to provide as an inflow condition. The numerical code is based on a finite difference scheme with a fractional step and a Runge-Kutta, providing a second order accuracy in space and time. It combines the immersed boundary method to model the tower, nacelle, and the topography with the actuator line method to represent the aerodynamic loads of the blades. It has been validated for surface roughness [1, 2] and turbine simulations [3]. Preliminary results show that fluctuations in the power production is not dependent on the location of the turbine with respect to the wavy wall but rather on the height of the ridges. Additionally, topography generated turbulence increases the entrainment of high momentum flow into the wake of the turbine increasing the recovery. This may be positive aspects considering wind farm configurations, because could mitigate wake interactions. References [1] Leonardi S, Orlandi P, Smalley RJ, Djenidi L and Antonia RA. Direct numerical simulations of turbulent channel flow with transverse square bars on one wall. *Journal of Fluid Mechanics* 2003; 491: 229-238. [2] Burattini P, Leonardi S, Orlandi P and Antonia RA. Comparison between experiments and direct numerical simulations in a channel flow with roughness on one wall. *Journal of Fluid Mechanics* 2008; 600: 403-426. [3] Santoni C, Carrasquillo K, Arenas-Navarro I and Leonardi S. Effect of tower and nacelle on the flow past a wind turbine. *Wind Energy*. 2017;20:1927–1939.

A Nonlinear Multiscale Method for Solving Incompressible Flow Problems

Isaac Santos^{*}, Riedson Baptista^{**}, Sérgio Bento^{***}, Leonardo Lima^{****}, Paulo Barbosa^{****},
Lucia Catabriga^{*****}

^{*}Federal University of Espírito Santo, ^{**}Federal University of Espírito Santo, ^{***}Federal University of Espírito Santo,
^{****}Federal Institute of Espírito Santo, ^{*****}Federal University of Espírito Santo, ^{*****}Federal University of Espírito
Santo

ABSTRACT

In this work we present a nonlinear variational multiscale method for solving incompressible flow problems with equal-order elements (P1/P1). The method is based on a two-level decomposition of the approximation space and consists of adding a residual-based nonlinear operator to the enriched Galerkin formulation, following a similar strategy of the methods presented in [1] for scalar advection-diffusion equation and in [2], [3] for compressible flow. The artificial viscosity acts adaptively in all scales of the discretization as a numerical stabilization and as a shock capturing scheme. In order to reduce the computational cost typical of two-scale methods, the subgrid scale space is defined using bubble functions whose degrees of freedom are locally eliminated in favor of the degrees of freedom that live on the resolved scales. Performance and accuracy comparisons with the streamline-upwind/Petrov-Galerkin (SUPG) formulation combined with the pressure stabilizing/Petrov-Galerkin (PSPG) method and shock capturing operators are conducted based on 2D benchmark problems.

Three-dimensional Fracture Analysis Using Scaled Boundary Polyhedral Elements

Albert Artha Saputra*, Ean Tat Ooi**, Chongmin Song***

*University of New South Wales, **Federation University Australia, ***University of New South Wales

ABSTRACT

A novel formulation based on scaled boundary finite element method is employed to construct a polyhedral element that can have an arbitrary number of planar faces. Each polygonal face can also be made up of an arbitrary number of vertices. Within each polyhedron, a volumetric scaling centre is chosen where the whole boundary is visible. Likewise, a surface scaling centre on each polygonal face is also selected such that it is able to see the whole perimeter of the polygon. Scaling in two scaled boundary coordinates is performed based on the two types of scaling centres. The displacements on each polygonal face are interpolated using the scaled boundary surface shape functions that are derived based on the boundary lines of the polygonal face [1]. These surface displacements are then scaled towards the volumetric scaling centre. Essentially, the dimension of the problem reduces by two, hence leaving the polyhedron to only be described by line elements (one-dimensional elements). Along the two scaling direction, analytical integration could be performed. This new formulation also enables the polyhedron to be constructed with arbitrary element order for each line. In the fracture analysis performed, the scaling centres of the polyhedron elements can be placed along the crack lines that allow the stress singularity of arbitrary order to be captured analytically [2]. The stress intensity factors can be simply extracted from the singular stress solution without a priori knowledge of the singularity order. Octree meshes [3] are also utilised such that smaller elements are placed around the crack that can transition quickly to larger elements for the other regions of the model. Keywords: three-dimensional, stress intensity factor, polyhedral element, scaled boundary finite element method, octree mesh References [1] Chiong, I., Ooi, E. T., Song, C., & Tin?Loi, F. (2014). Scaled boundary polygons with application to fracture analysis of functionally graded materials. *International Journal for Numerical Methods in Engineering*, 98(8), 562-589. [2] Saputra, A. A., Birk, C., & Song, C. (2015). Computation of three-dimensional fracture parameters at interface cracks and notches by the scaled boundary finite element method. *Engineering Fracture Mechanics*, 148, 213-242. [3] Saputra, A., Talebi, H., Tran, D., Birk, C., & Song, C. (2017). Automatic image?based stress analysis by the scaled boundary finite element method. *International Journal for Numerical Methods in Engineering*, 109(5), 697-738.

Mechanics of Pressure Ulcer: Application of Particle Based Methods

Sohan Sarangi*, Tetsu Uesaka**

*Department of Chemical Engineering, Mid Sweden University, **Department of Chemical Engineering, Mid Sweden University

ABSTRACT

Pressure ulcer is a silent epidemic in many of the developed countries. Elderly patients with limited mobility are particularly vulnerable to pressure ulcers (PUs). Although pressure is undoubtedly involved in PUs, there have not been good understandings of what mechanical environments induce complex bio-chemical reactions that leads to PUs. Factors related to the mechanical environment include the type of stresses, stress histories, damage evolutions, human body geometries and boundary conditions (e.g., bed mattress, clothes, diapers), for example. In order to model the specific features of PU problems, we have used particle-based methods. The human body model is based on the 3D reconstruction of a real human model from Visual Human Project. First, bones are modeled as a system of rigid bodies using Discrete Element Method (DEM). Bone joints can undergo rotations with the use of "ghost joint". Muscles, fat and skin are modeled as Smoothed Particle Hydrodynamics (SPH) particles, that follow a Mooney-Rivlin type hyperelastic constitutive equation with different material constants. We modified an open-source SPH code, "PySPH", in order to allow hyperelasticity, contact interactions, and DEM coupling. Validations have been made for cases of uniaxial tensile tests, multi-phase coupling, and stress concentrations around a hole. As the first step, we have performed the stress analysis of the whole human body which is lying in the bed. Unlike previous works using finite element method (FEM) with immobile bones, we have allowed complex joint movements with a multilayer discretization of human body. For interactions between bones and muscles, and also between skin and bed mattress (or diaper), the newly implemented contact model has been used. The results predicted the most vulnerable locations to the occurrence of pressure ulcer in the body, which are consistent to the clinical observations. We have also investigated the effect of friction coefficient (COF) between skin and underlying layer (e.g., diaper). The COF was varied from 0.3 to 1.3, the latter of which corresponds to wet skin case. The maximum shear and maximum compressive stresses were obtained on skin, fat and muscle layers. Increasing COF increased both maximum shear and principal compressive stresses, very much in the same way. Stresses on the fat region tended to flatten out for higher friction coefficient, but stresses on the muscle layer continued to increase with increasing friction. The implication of these results to damage evolution needs to be further investigated.

A Hybrid FE-FV Framework for Modeling Crack Propagation in Saturated Porous Media

Juan Michael Sargado^{*}, Eirik Keilegavlen^{**}, Inga Berre^{***}, Jan Martin Nordbotten^{****}

^{*}University of Bergen, ^{**}University of Bergen, ^{***}University of Bergen, ^{****}University of Bergen

ABSTRACT

Fluid driven fracture propagation in porous media has gained considerable attention in recent years due to its relevance to several important modern day applications. These include hydraulic fracturing of gas shales and the stimulation of enhanced geothermal systems, in which pressurized fluid is injected into the crack network to create or open up existing fractures, thereby improving the overall flow property of the reservoir. In this study, we develop a hybrid approach for solving the Biot poroelasticity equations coupled to a phase-field model for brittle fracture propagation. We begin by monolithically coupling a finite element approximation of stress equilibrium to a control volume form of the fluid mass balance. This subsystem is further coupled iteratively to a finite volume description of the phase-field evolution equation using an alternate minimization scheme. In particular, we leverage recent results dealing on alternative degradation functions that minimize spurious loss of stiffness in the mechanical response prior to fracture. Flow within open fractures is assumed to be of Poiseuille type, and it can be shown that accurately accounting for this additional flow can lead to mesh size constraints that are much more stringent than those coming from the phase-field equation. Performance of the proposed model is investigated by solving various numerical examples ranging from classical benchmarks to more sophisticated configurations.

Embedded Model Error Representation in Computational Models

Khachik Sargsyan^{*}, Xun Huan^{**}, Habib Najm^{***}

^{*}Sandia National Laboratories, ^{**}Sandia National Laboratories, ^{***}Sandia National Laboratories

ABSTRACT

Parameter calibration often assumes the computational model can replicate the true physical mechanism behind data generation. In practice, however, computational models rely on parameterizations, assumptions, and constitutive relations that entail significant model structural error. Ignoring such model errors can lead to overconfident calibrations and poor predictive capability, even when high-quality data are used for calibration. It is thus crucial to quantify and propagate uncertainty due to model error, and to differentiate it from parametric uncertainty and data noise. Traditional approaches accommodate model error through discrepancy terms that are only available for model output quantities used for calibration, and generally do not preserve physical constraints in subsequent predictions. The ability to extrapolate to other predictive quantities and to retain certain physical properties (e.g. conservation principles, positivity constraints) is often required in physical science and engineering applications. We develop a stochastically embedded model correction approach that enables these qualities, and illustrate computational methods for Bayesian inference of the correction terms together with model parameters [3]. Representing the correction terms using polynomial chaos expansions, the new formulation becomes a density estimation problem [1], and allows efficient quantification, propagation, and decomposition of uncertainty that includes contributions from data noise, parameter posterior uncertainty, and model error. The framework provides principled tools for the analyst, e.g. to examine the utility of corrections to specific suspect model components, and to identify the model components where model improvements are relevant for agreement with the data. We demonstrate the key strengths of this method on realistic engineering applications, including climate models, chemical kinetics [1, 3], and reacting flow simulations from a supersonic jet engine design [2].

Evaluation of Maximum Entropy Moment Closures for Predicting Radiative Heat Transfer Phenomena

Joaquim Sarr*, Clinton Groth**

*University of Toronto, **University of Toronto

ABSTRACT

This study considers an evaluation of moment closures based on the principle of maximization of entropy for providing approximate solutions to the radiative heat transfer equation (RTE). Several representative tests cases in both one- and two-dimensions are considered whereby the predictions of the maximum-entropy closures are compared to those of the discrete ordinates method (DOM) as well as the more commonly used spherical harmonics solutions in terms of both accuracy and computational cost. More specifically, the present analysis is concerned with the lower-order approximations of the hierarchy of the maximum-entropy closures, namely the M1 and M2 closures and, for comparison purposes, the P1 and P3 spherical-harmonic closures are also considered. The discrete governing equations resulting from the application of a Godunov-type finite-volume method with anisotropic mesh refinement (AMR) to the system of moment equations in each case are solved using an inexact Newton method in which a generalized minimal residual (GMRES) technique is used to solve the linear system at each step of the Newton method. The proposed finite-volume method uses limited piecewise-linear solution reconstruction and Riemann solvers to evaluate the fluxes of the moments. The potential of the M 1 and M2 closures is explored and discussed for a range of problems involving radiative heat transfer in gray media.

EARTHQUAKE RESPONSE ANALYSIS OF NON-STRUCTURAL MEMBERS OF BUILDING BY USING THE LARGE-SCALE PARALLEL CALCULATION METHOD

TOMOHARU SARUWATARI*, YASUYOSHI UMEZU^{†1}, YOSHITAKA USHIO^{†2},
LYU ZHILUN^{†3}, YASUYUKI NAGANO^{†4}

* JSOL Corporation

Tosabori Daibiru Bldg. 2-2-4 Tosabori, Nishi-ku, Osaka 550-0001, JAPAN

E-mail: saruwatari.tom@jsol.co.jp

^{†1} JSOL Corporation

Tosabori Daibiru Bldg. 2-2-4 Tosabori, Nishi-ku, Osaka 550-0001, JAPAN

E-mail: umezu.yasu@jsol.co.jp

^{†2} University of Hyogo

7-1-28, Minatojima-Minamimachi, Chuo-ku, Kobe 650-0047, Japan

E-mail: sb16q001@sim.u-hyogo.ac.jp

^{†3} University of Hyogo

7-1-28, Minatojima-Minamimachi, Chuo-ku, Kobe 650-0047, Japan

E-mail: sb15v003@sim.u-hyogo.ac.jp

^{†4} University of Hyogo

7-1-28, Minatojima-Minamimachi, Chuo-ku, Kobe 650-0047, Japan

E-mail: nagano@sim.u-hyogo.ac.jp

Key words: earthquake, non-structural members, Large-scale FEM, LS-DYNA.

Abstract. In large-scale earthquake disasters, it is reported that there were many serious damages of the non-structural members, such as ceilings and claddings, of the facilities with large space such as gymnasiums and assembly halls.

The technical standard for preventive measures against falling off is provided for the ceiling of the building, but it is applied only to prevent the damages caused by rare earthquake (middle-scale) at which the behavior of the ceiling can be predicted to some extent. In order to this problem, it is necessary to study the structure system after having clarified the behavior of the ceiling suspended from the building structure at the time of the extremely rare earthquake (large-scale earthquake).

To realize this, they need the analyzing methods to evaluate precisely the response of non-structural members according to the precisely predicted response data of the building structure against earthquake.

This study, making the suspended ceilings applied to large span structures as an example, prepares the detailed structural analysis models created by modeling the shape of the structural members through as faithfully following to the real one as possible, and tries to obtain the extremely precise earthquake response of the structures by means of large-scale parallel calculation.

In the future, it is aimed to evaluate the behavior of a whole building through piling of the results of the earthquake response of the ceilings by making as the boundary conditions the responses obtained by extremely precise analysis of the structure to which the ceilings are connected.

1 INTRODUCTION

In Japan, many cases of ceiling collapse and falling-down caused by earthquake was reported. For extremely rare earthquakes, it is necessary to study the real phenomenon in detail from the viewpoint of securing safety and evacuation plan at the time of earthquake^[7]. In this research, in order to solve these problems, we tried to analyze nonlinear dynamic transient response by a large scale parallel computer for a general suspended ceiling system used in Japan and to reproduce the behavior in detail.

2 NUMERICAL SIMULATION METHOD

Based on the use of large scale parallel computing environment, explicit non-linear dynamic response analysis was adopted. For software, LS-DYNA R 9.0.2 (double precision version) developed by Livermore Software Technology Corporation was used. We used the supercomputer system of the University of Hyogo for the calculator and parallel calculation by 160 to 320 parallel was carried out.

2.1 Finite element modeling

Modeling with BEAM elements and spring elements is often applied in FEM analysis because standard shape of channel sections are used for the parts that compose the suspended ceilings^[1]. These modeling methods have good accuracy with respect to elastic deformation, easy expression of rupture, and low calculation cost. However, it is difficult to express precision and complex destruction mode for nonlinear behavior at large deformation. On the other hand, if the shape of a member is precisely expressed by FE-MESH using the SHELL element or SOLID element, it is possible to express the nonlinear behavior due to buckling and yield, and to reproduce the failure mode accurately.

2.2 Finite element method

Explicit non-linear dynamic response analysis method is used for numerical calculation, and the software is DYNA R9.0.2 double precision version made by Livermore Software Technology

Corporation. This software, as its characteristics, has many non-linear material models, can precisely analyze non-linear large deformation and so on. Also, using the contact algorithm installed, it is possible to accurately analyze the change of the stress transmission mechanism due to contact and separation between parts at large deformation, and it is possible to express the phenomenon of collapse and damage with higher precision.

3 UNIT MODEL SIMULATION

In order to investigate the characteristics of the ceiling unit, static characteristic analysis and dynamic seismic response analysis were carried out. As for the suspended ceiling system, type 25, which is specified in the Japanese Industrial Standard JIS, was used [2, 3, 4].

3.1 Model Overview

Fig.1 shows a schematic diagram of a suspended ceiling model. In order to accurately express the shape of each part, all metal parts except the suspension rod were modeled with shell elements. The mesh pitch was based on 10 mm. The gypsum board and the rock wool board on the ceiling surface were modeled as one and the physical properties were determined so that the mass was equivalent. The mesh pitch was 100 mm.

The information specified in JIS for material property, and the elastic-plastic material model (*MAT_PIECEWISE_LINEAR_PLASTICITY) [9, 10] installed in the software for material model were used. Table.1 shows a list of material properties of the model.

Like the actual ceiling system, the suspension mechanism was expressed only by the contact between the parts. Only the contact condition is set between the hanger and the main channel and between the main channel and the clip, and no other fixed conditions are set. The total number of nodes was 26,806, the number of BEAM elements was 828, and the number of SHELL elements was 21,999 elements.

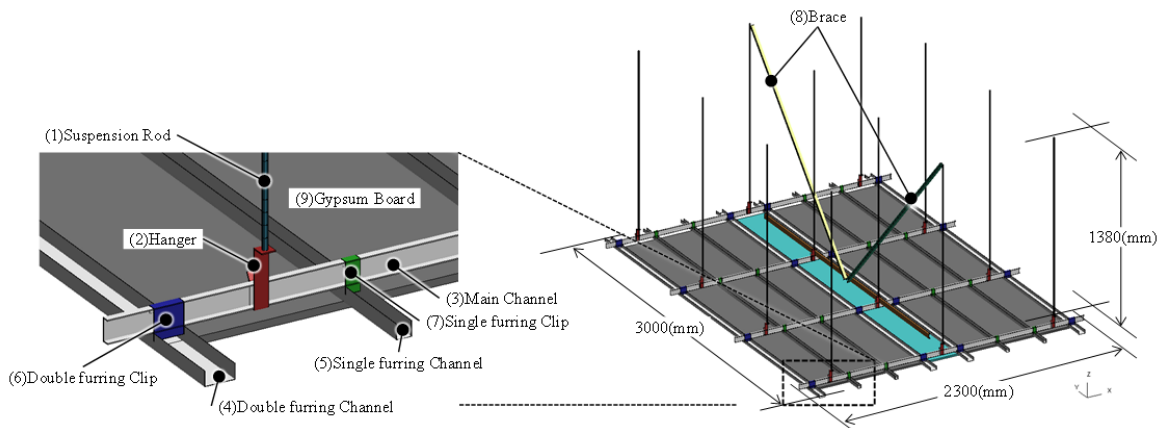


Fig.1 Suspended ceiling system

Table.1 material

	CODE	Material(JIS)	size	Density (ton/mm ³)	Young's modulus (MPa)	Poisson ratio	Yield Stress (MPa)
Suspension Rod	-	JIS G 3505	φ9	7.89E-09	206,000	0.3	215
Hanger	-	JIS G 3302	23x98x2.0				
Main Channel	CC-25	JIS G 3302	38x12x1.6				
Double Furring Channel	CW-25	JIS G 3302	50x25x0.5				
Single Furring Channel	CS-25	JIS G 3302	25x25x0.5				
Double Furring Clip	W-25	JIS G 3302	47.5x48.5x0.8				
Single Furring Clip	S-25	JIS G 3302	25x48.5x0.8				
Brace	AS-25	JIS G 3302	25x19x5x1.0	1.00E-09	28,900	0.2	
Gypsum board + Rock wool sound absorbing plate	GB-R	JIS A 6901 JIS A 6301	t=9.0mm				

3.2 Push over analysis (Static characteristic)

A forced displacement of 50 mm was applied to the end of the model, and displacement-load relationship was obtained. Fig.2 shows the deformation of the system in the final stage. The calculation time was 1 h 24 m (160 parallel).

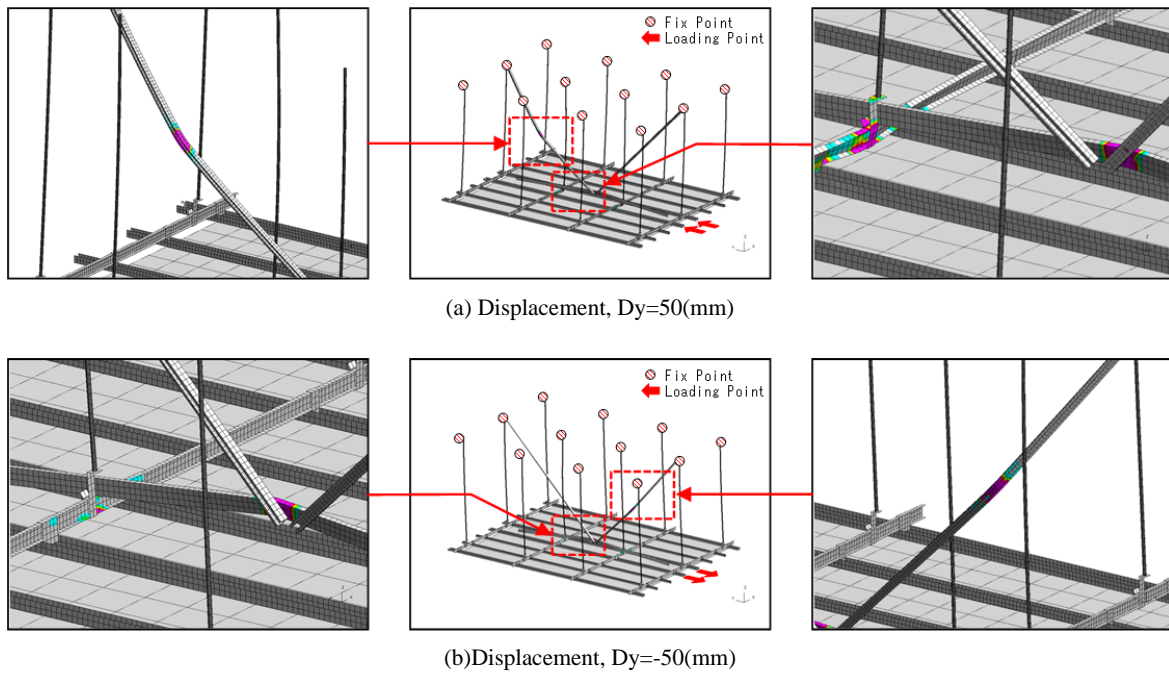


Fig.2 Plastic strain distribution

Forced displacement was loaded in the [+ y] and [- y] directions, and the load-displacement relationship were evaluated. The obtained load-displacement relationships of two loadings are shown in Fig.3

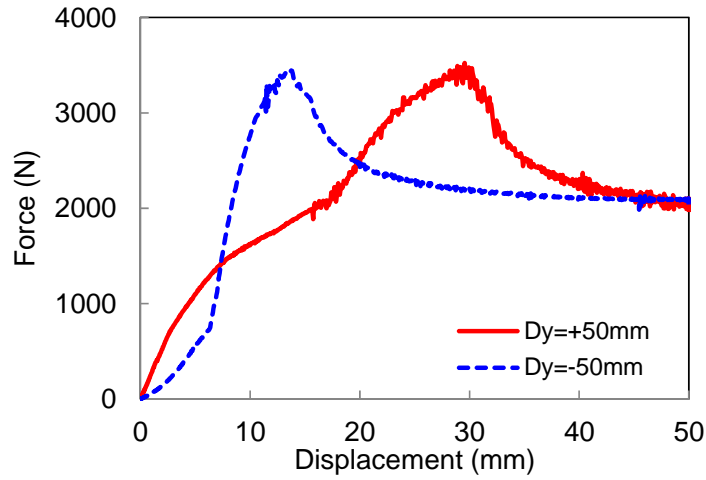


Fig.3 Force Displacement

3.3 Seismic response analysis (Dynamic characteristic)

By earthquake response acceleration wave was loaded to the upper end of the suspension rod, and earthquake response analysis was performed. As the seismic waves, "Takatori wave" observed JR Takatori station in Kobe in 1985 was used. The time history of the input seismic wave is shown in Fig.4.

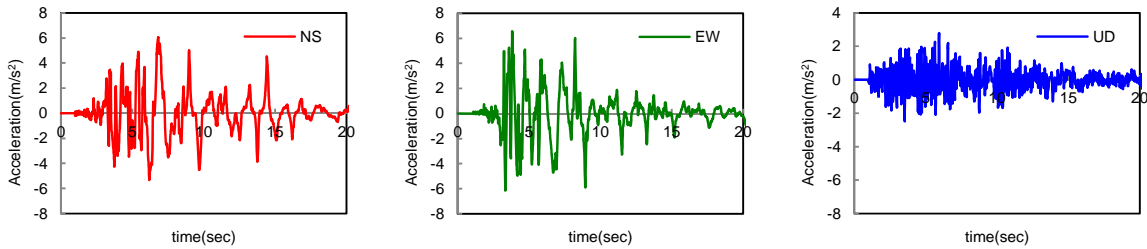


Fig.4 Input seismic acceleration

The calculation time is 5h36m (160 parallel). Fig.5 shows the response behavior.

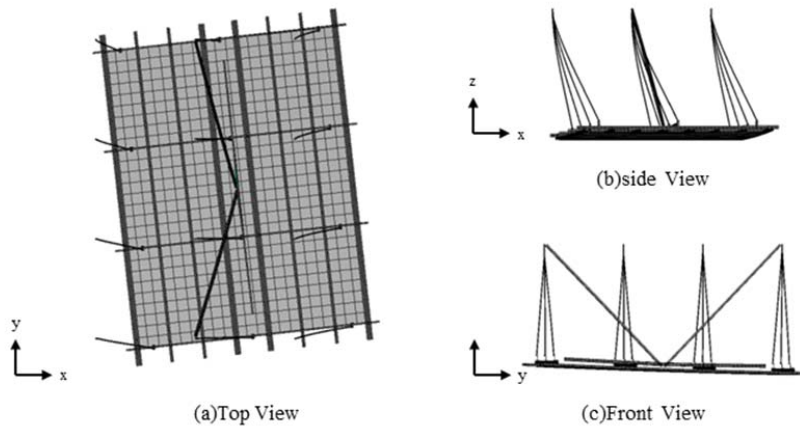


Fig.5 Displacement (t=8.0s)

Fig.6 shows the response displacement and the motion locus at the input (loading) points and the ceiling surface measurement points on the ceiling surface. From this, the ceiling surface responds greatly (swaying) in the X direction, but in the Y direction the brace for steady rest is effective and the response is small.

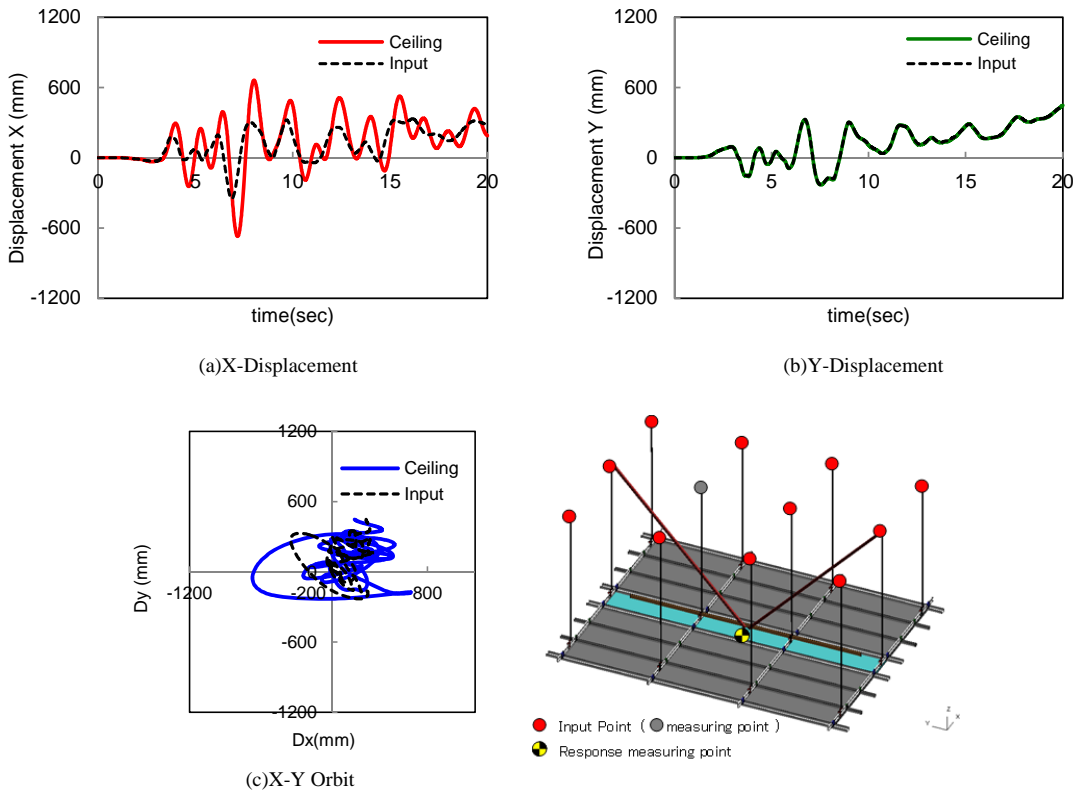


Fig.6 Time history of response displacement

4 BUILDING STRUCTURE MODELING

Since the input earthquake acceleration to the suspended ceiling is the earthquake response acceleration of the upper floor of the building, it is necessary to model the building, perform the earthquake response analysis, and input the result to the suspended ceiling. Detailed responses of the building should be obtained in general by detailed FEM analysis^[5,6], but, in this research, we tried to model the building into a simple frame model and incorporate the suspended ceiling model to the building frame model in order to reproduce the behavior of the suspended ceiling at the earthquake.

4.1 Model Overview

The plans and elevations of the building is shown in Fig. 7^[8], and the details of the structural members are shown in Table.2 and Table.3. The building is a 7-story steel frame structure including the penthouse, which has 5 spans in the X direction and 3 spans in the Y direction. The columns of the building were modeled into shell elements from the necessity of expressing the behavior of local buckling, and the beam was modeled into the BEAM element. The floor slab was modeled into a shell element. Both columns and beams were modeled as elastoplastic and all material models were installed in the software so that column models are in (*MAT_KINEMATIC_HARDENING_TRANSVERSELY_ANISOTROPIC) and beam model is in (*MAT_RESULTANT_PLASTICITY). For the floor slab, a reinforced concrete model is in (*MAT_CONCRETE_EC2). The total number of nodes was 242,812, the number of BEAM elements was 11,252, and the number of SHELL elements was 226,703.

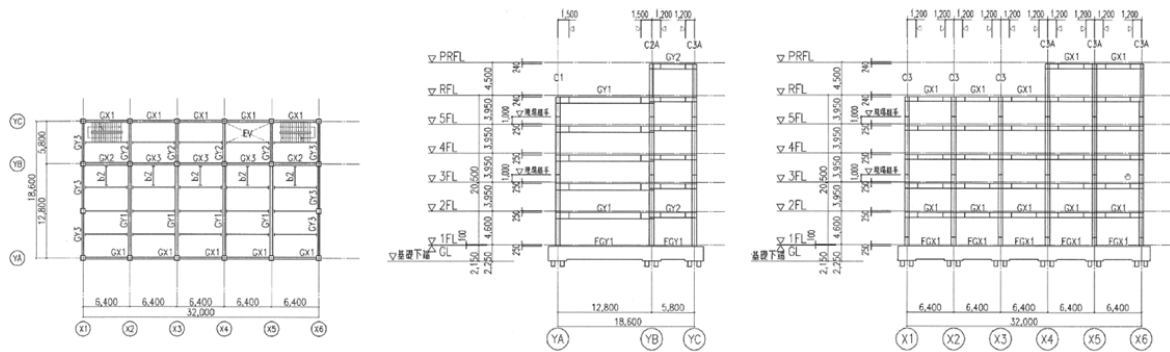


Fig.7 Framing plan

Table.2 Section list of columns

	C1	C2,C2A	C3,C3A	C4
RF	-	B-460x16	B-460x16	-
5F	B-500x22	B-500x22	B-500x22	B-500x22
4F				
3F				
2F				
1F				

Table.3 Section list of beams

	GX1		GX2		GX3	
	edge	center	edge	center	edge	center
PRF	H-600x250x12x19		H-600x250x12x22		H-600x200x12x22	
RF			H-600x200 x12x25	H-600x200 x12x22		
5F						
4F						
3F	H-600x250 x12x22	H-600x250 x12x19	H-600x200 x12x22	H-600x200 x12x19	H-600x250 x12x22	H-600x250 x12x19
2F						

	GY1		GY2		GY3	
	edge	center	edge	center	edge	center
PRF	H-800x350x16x25		H-600x200x12x19		-	
RF					H-600x200x12x22	
5F					H-600x200 x12x25	H-600x200 x12x22
4F						
3F			H-600x200 x12x22	H-600x200 x12x19	H-600x250 x12x22	H-600x250 x12x19

In order to evaluate the behavior of the ceiling of the 2nd floor of the building, a suspended ceiling model was placed under the 3rd floor. In the ceiling, three unit models explained in Chapter 3 of this paper were connected in the X direction and placed, and the upper end of the suspension rod was attached beneath the 3rd floor of the building. A schematic diagram of the analysis model is shown in Fig.8.

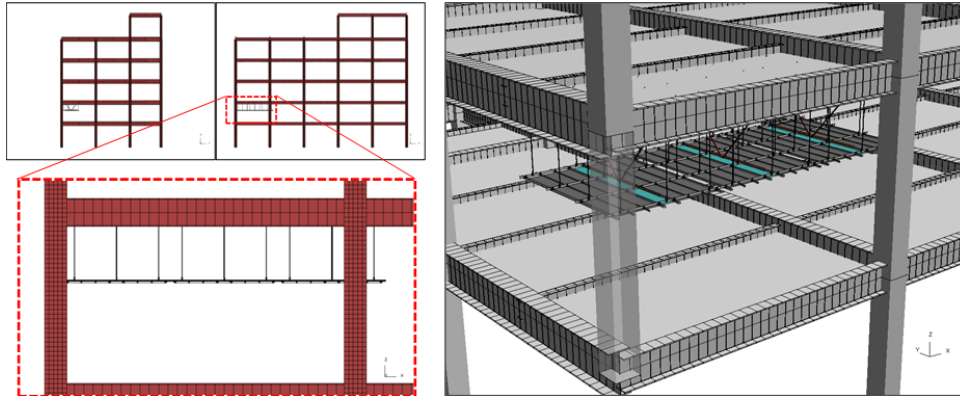


Fig.8 Building with ceiling system

4.2 Seismic response analysis

Earthquake response analysis was carried out by inputting the seismic wave (Takatori wave) shown in Fig. 4 to the column bases of the first floor of the building. The calculation time was 15 h 18 m (320 parallel). Fig. 9 shows the time history of displacement at the response measurement position of the column (X1 - YA) on the 3F, 6F floor and the ceiling surface.

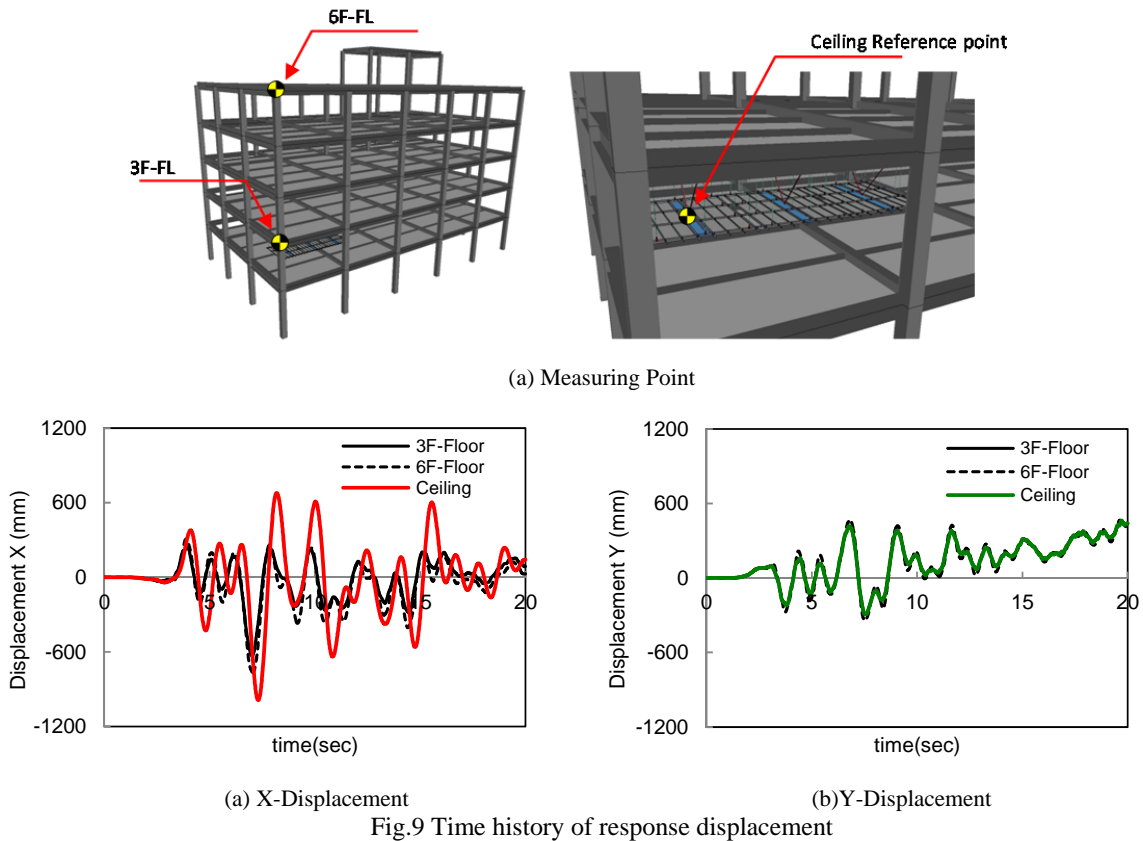


Fig.9 Time history of response displacement

It is understood that the response of the building in the X direction is large and the response displacement of the ceiling is larger than the building 3F - FL. In the Y direction the response of the building is small and the response to the ceiling is hardly seen due to the effect of the braces for steady rest.

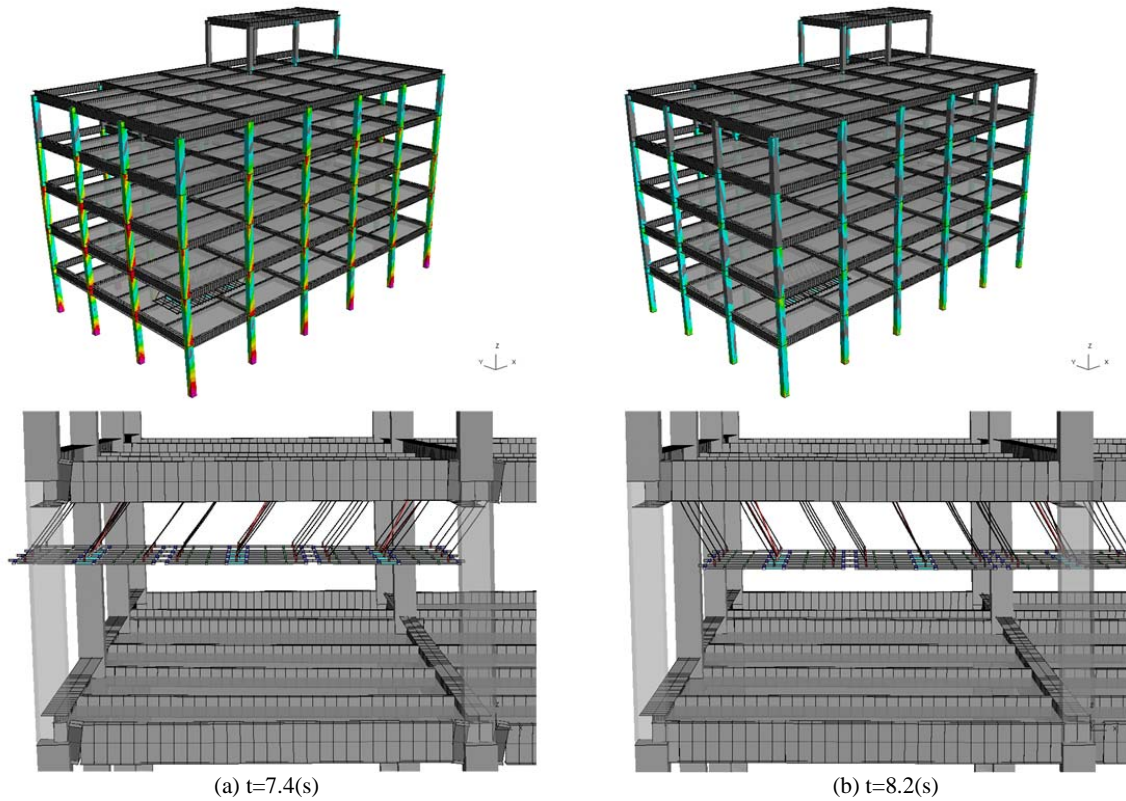


Fig.10 Building and ceiling behavior

The behavior during the earthquake response is shown in Fig10. The ceiling surface was greatly displaced, and the maximum displacement in the X direction was $+x = 678.9$ mm and $-x = 986.9$ mm. The behavior of the ceiling in the response is shown in Fig.11. The dynamic behavior of the ceiling surface causes the clip to deform and slip, and it can be seen that the load is divergent from the stress distribution state.

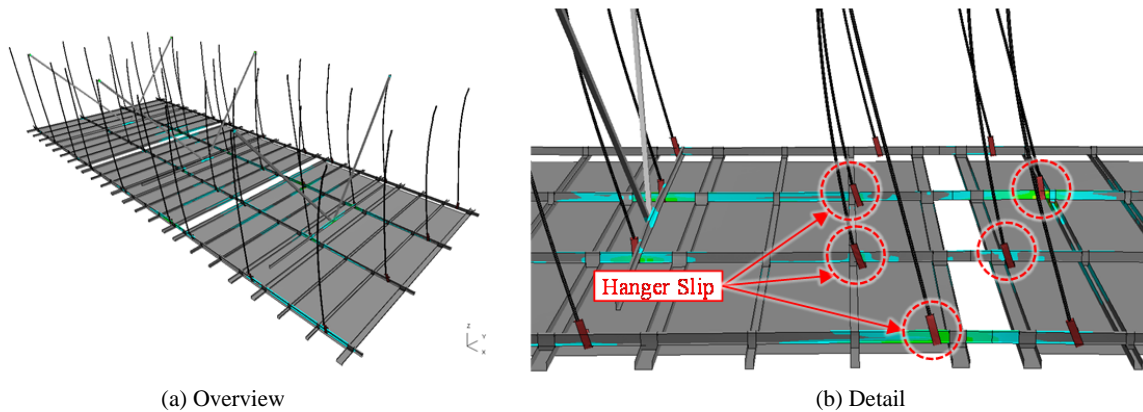


Fig.11 Detail around hanger (Von-Mises Stress)

5 CONCLUSIONS

- - By detailed modeling of suspended ceilings, the structural characteristics of the suspended ceiling system could be accurately reproduced.
- - Coupled analysis with buildings allowed us to explain in detail the dynamic behavior of the ceiling in the building at the time of the earthquake.
- - We were able to accurately grasp the changes in load transmission mechanism due to deformation and movement of parts.
- - It was suggested that the accurate grasp of the behavior of nonstructural members at the earthquake can contribute to improvement of safety of building and improvement of accuracy of evacuation plan.

ACKNOWLEDGMENTS

This work was supported by JSPS KAKENHI Grant Number JP16H03124.

REFERENCES

- [1] YAMAMOTO Takuya, TAGAWA Hiroyuki, YAMASHITA Takuzo and ISOBE Daigoro, Numerical Study on the Ceiling Collapse in Large-Space Building during Earthquakes –Part1 Basic Study, Summaries of technical papers of annual meeting Architectural Institute of Japan, 2014.9, 1107-1108. (in Japanese)
- [2] Shojiro MOTOYUI and Yasuaki SATO, EVALUATION METHOD FOR HORIZONTAL STIFFNESS OF CEILING WITH STEEL FURRING IN DIRECTION OF ‘NOBUCHI’, J. Struct. Constr. Eng., AIJ, Vol. 79 No. 703, 1395-1403, Sep., 2014 (in Japanese)
- [3] ARAI Tomokazu, Yuri Takayuki, and KOBAYASHI Toshio, Study on Aseismic

Tomoharu Saruwatari, Yasuyoshi Umezu, Yoshitaka Ushio, Lyu Zhilun, Yasuyuki Nagano

Ceiling Part 3 Lateral Loading Test of Ceiling with Steel Furrings, Summaries of technical papers of annual meeting Architectural Institute of Japan, 2006.9, 841-842. (in Japanese)

[4] Toshio KOBAYASHI, Takayuki YURI and Tomokazu ARAI, STUDY ON ASEISMIC SUSPENSION CEILING WITH STEEL FURRINGS, J. Struct. Constr. Eng., AIJ, Vol. 73 No. 630, 1295-1302, Aug., 2008 (in Japanese)

[5] Yasunori Mizushima, Yoichi Mukai, Hisashi Namba, Kenzo Taga and Tomoharu Saruwatari : Super-detailed FEM simulations for full-scale steel structure with fatal rupture at joints between members -Shaking-table test of full-scale steel frame structure to estimate influence of cumulative damage by multiple strong motion: Part 1, Japan Architectural Review, AIJ, Vol.1, Issue 1, pp.96-108, DOI : <https://doi.org/10.1002/2475-8876.10016>

[6] Yasunori Mizushima, Yasuyuki Nagano and Yoichi Mukai : Construction of damage observation system for both structural and non-structural members with overlaying, #2019117, proc. 13th WCCM(2018).

[7] Yasuyuki Nagano, Yoichi Mukai, Kensuke Yaufuku, Harunori Mizushima and Tomoharu Saruwatari : KEY ELEMENT BUILDINGS DESIGN METHOD WITH BIDIRECTIONAL EVALUATION BETWEEN STRUCTURAL ANALYSIS AND EVACUATION ANALYSIS, #2020193, proc. 13th WCCM(2018).

[8] The Japan building Disaster Prevention Association: Case Examples of Structural Design of Buildings and Their Members, (2007) (in Japanese)

[9] LS-DYNA KEYWORD USER'S MANUAL VOLUME (I) LS-DYNA R9.0 08/29/16 (r:7883), LIVERMORE SOFTWARE TECHNOLOGY CORPORATION (LSTC), 2016.

[10] LS-DYNA KEYWORD USER'S MANUAL VOLUME (II) LS-DYNA R9.0 08/29/16 (r:7883), LIVERMORE SOFTWARE TECHNOLOGY CORPORATION (LSTC), 2016.

Force-Driven Recruitment of Receptors into Cell Adhesion Sites

Alireza Sarvestani*

*Ohio University, Department of Mechanical Engineering, Athens OH 45701

ABSTRACT

The hallmarks of cell mechanotransduction shared by "focal adhesions" and intercellular "adherens junctions" include the enlargement and strengthening of these adhesion sites in response to actomyosin tension. We developed a thermodynamically admissible model for the mature adhesion sites subjected to time-dependent pulling tractions. The adhesion zone is presented by a bounded surface in which the ligands and receptors can interact and form physical bonds. Free receptors and/or ligands are mobile and can diffuse on cell membrane and cross the boundary of the adhesion site. Implementing the three fundamental laws, namely the conservation of receptors/ligands and first and second laws of thermodynamics along with the Hadamard jump condition at the boundary of the adhesion site, we found the fundamental equations that control the growth kinetics of the adhesion sites in response to an applied tension that changes with time. The coupled equations can be solved numerically, assuming a simple geometry for the adhesion site. We show that the pulling traction tilts the free energy landscape and mediates the flux of receptors into the adhesion zone and leads to its spontaneous growth, independent from any other sensory function.

Level Set-Based Topology Optimization of Fluid Flows Using the Moving Particle Semi-implicit Method

Yusuke Sasaki^{*}, Takayuki Yamada^{**}, Kazuhiro Izui^{***}, Shinji Nishiwaki^{****}

^{*}Kyoto University, ^{**}Kyoto University, ^{***}Kyoto University, ^{****}Kyoto University

ABSTRACT

Structural optimization has been successfully used in many industries. In particular, topology optimization [2] which has the most potential for exploring optimized structures, can be applied to a wide range of structural optimization problems such as stiffness maximization problems, thermal problems and fluid dynamics problems [3]. However, most existing topology optimization methods for fluid flows problems are based on the finite element method or finite volume method and have difficulty in handling problems which include free surface and two-phase flows, where the shape of the interface continuously changes depending on time. Moving particle semi-implicit (MPS) method is one of the particle methods, which can be used to analyze incompressible free surface flow without surface tracking. The motion of each particle is calculated through interactions with neighboring particles covered with the kernel function. This mesh-less numerical approach as a Lagrangian gridless particle method, proposed by Koshizuka, et al [1] has been proven to be useful in a wide range of engineering applications, such as numerical analysis of turbines and mixers. In this study, we propose a topology optimization method using the level set method and the MPS method for fluid dynamics problems, including free surface and two-phase flows. First, we explain briefly about topology optimization and the MPS method. Next, optimization problems are formulated based on the level set method and the MPS method. The design sensitivity analysis, performed using the adjoint variable method, is then explained. Finally, numerical examples are provided to confirm the validity and utility of the proposed method. [1] Koshizuka, Seiichi, and Yoshiaki Oka. "Moving-particle semi-implicit method for fragmentation of incompressible fluid." Nuclear Science and Engineering 123.3 (1996): 421-434. [2] Yamada, Takayuki, et al. "A topology optimization method based on the level set method incorporating a fictitious interface energy." Computer Methods in Applied Mechanics and Engineering 199.45 (2010): 2876-2891. [3] Deng, Yongbo, et al. "Optimization of unsteady incompressible Navier–Stokes flows using variational level set method." International Journal for Numerical Methods in Fluids 71.12 (2013): 1475-1493.

A Model Enhancement Approach for the Free Surface Simulations by the MRT-LBM Toward Three-dimensional Tsunami Analysis

Kenta Sato*, Shunich Koshimura**

*Graduate School of Engineering, Tohoku University, **International Research Institute of Disaster Science,
Tohoku University

ABSTRACT

Free surface flow problems occur in numerous in disaster simulations such as tsunami in urban area. This application requires three-dimensional, highly resolved and efficient simulations. Consequently, the demand for powerful simulation models is larger than ever before. It is, however, difficult to carry out three-dimensional large-scale tsunami simulations because of the pressure Poisson equation in the incompressible Navier-Stokes fluid modeling. In recent years, the lattice Boltzmann method (LBM) has attracted attention as an efficient computational fluid dynamics tool. By contrast with traditional flow solvers, which calculate the macroscopic Navier-Stokes equations, LBM solves such problems on a microscopic scale and represents the fluid as the virtual particles. The key features of LBM are as follows: (i) fully explicit method in time integration, which means LBM does not have to solve the pressure Poisson equation, (ii) easy implementation with high-performance computing using multiple core processors or GPU because of the algorithmic operations and data locality. In this regards, LBM is considered to have an advantage to execute a high-performance three-dimensional tsunami simulation as an alternative tool of the other simulation methods. In current study, we have developed a three-dimensional free surface fluid model by LBM with the piecewise Linear Interface Reconstruction, Volume of Fluid (PLIC-VOF) approach. This type of VOF methods determines the interface location and hence the flux terms more accurately and avoids non-physical oscillations near the interface. The free surface is represented as a linear function segment, which can be determined by the interface normal and distance from Cartesian origin. It is well known that the lattice BGK model, which is the simple collision term of LBM, becomes numerical instability in high Reynolds number flow easily. In our model, the more advanced Multiple-Relaxation-Time (MRT) model is used to enhance the model robustness and accuracy. Three-dimensional breaking wave in a rectangular tank was simulated to verify our model. Lubin et al.[1] has calculated the benchmark by the three-dimensional PLIC-VOF with the incompressible Navier-Stokes equations. We used their solutions to compare our results. From the benchmark problem, we found that our model calculates the breaking waves well and is robustness in such complex flow field. We can conclude that our model is extremely useful as a way to simulate tsunami in three-dimensional flow field. [1] Lubin P., Vincent S., Abadie S., Caltagirone. J., Three-dimensional Large Eddy Simulation of air entrainment under plunging breaking waves, *Coast. Eng.*, 53, pp.631-655. 2006.

Substitution Approach for De-coupled Two-scale Analysis of Composite Plates

Masami Sato^{*}, Mayu Muramatsu^{**}, Kenjiro Terada^{***}, Tatsuya Kawada^{****}

^{*}Tohoku University, ^{**}Tohoku University, ^{***}Tohoku University, ^{****}Tohoku University

ABSTRACT

We propose a new substitution approach to perform de-coupled nonlinear two-scale analysis for composite plates with an in-periodic meso-structure, which is referred to as in-plane unit structure (IPUS). In the suggested approach, the heterogeneity in the meso-structure is substituted or replaced by an equivalent laminated structure, which might not be unique, but must be proper in the sense that the macroscopic mechanical responses are uniquely determined. The macroscopic nonlinear mechanical characteristics of the plate are determined from the numerical plate testing for the IPUS that provides a set of relationships between macroscopic resultant stresses and generalized strains [1]. Since the obtained plate sectional properties cannot be represented by an equivalent homogeneous plate stiffness of a single material, we assume that an equivalent laminated structure (ELS) that exhibits the same macroscopic response can be substituted for the original composite plate. Then, the material parameters of each layer of an IPUS of this ELS, which is regarded as a mesoscopic substitution model (meso-SM), are identified by an optimization method so as to be equivalent to the original IPUS. After the parameter identification, the corresponding macroscopic substitution model (macro-SM) can be utilized with laminated plate elements to analyze the overall responses. We first validate the appropriateness of the proposed approach by comparing representative numerical examples with the results obtained by the original composite plate. Then, we apply the proposed approach to characterize the thermo-mechanical behavior of a plate-shaped device typified by solid oxide fuel cells (SOFC). Since the solid-shell type finite element modeling of the macro-SM is possible in the proposed method, we demonstrate the capability of analyzing a structure with stratified plate-shaped devices like a cell stack of SOFC. [1] K. Terada, N. Hirayama, K. Yamamoto, M. Muramatsu, S. Matsubara & S. Nishi Numerical plate testing for linear two-scale analyses of composite plates with in-plane periodicity, IJNME, 105, pp. 111–137, 2016.

Multiple-phase-field Simulation of Multiple Dendritic Growth with Motion

Ryotaro Sato*, Tomohiro Takaki**

*Kyoto Institute of Technology, **Kyoto Institute of Technology

ABSTRACT

Equiaxed structure formed during a solidification process of metals and alloys determines the mechanical property of those materials. Therefore, it is crucial to accurately predict and control the formation process of the equiaxed structure. Phase-field method has been widely used to predict the solidification microstructures as a powerful and accurate numerical model. Meanwhile, since the formation process of the equiaxed structure is very complex phenomenon including growth, motion and collision of multiple dendrites and subsequent grain growth after formation of grain boundary, there are no phase-field models expressing all physics in the formation process of equiaxed structure. In this study, we construct a new model which can express the growth, motion and collision of multiple dendrites and subsequent grain growth. In this model, the growth and motion of multiple dendrites are expressed by a multi-phase-field method and equations of motion, respectively, and the liquid flow is computed by lattice Boltzmann method. The collision and coalescence of multiple grains are also modeled in this model. The validity of the model is confirmed by performing simulations of a collision of two circular objects and a grain growth in three grains system. After that, the formation simulations of the equiaxed structure is demonstrated by employing the developed model.

Topology Optimization Incorporating Reliability Design under Geometrical Uncertainties

Yuki Sato^{*}, Kazuhiro Izui^{**}, Takayuki Yamada^{***}, Shinji Nishiwaki^{****}, Makoto Ito^{*****}, Nozomu Kogiso^{*****}

^{*}Kyoto University, ^{**}Kyoto University, ^{***}Kyoto University, ^{****}Kyoto University, ^{*****}Osaka Prefecture University, ^{*****}Osaka Prefecture University

ABSTRACT

Geometrical uncertainties caused by manufacturing errors and operational wear can affect the physical performance of various devices. In microfabrication processes, the effect of geometrical uncertainties can be particularly detrimental, due to the small dimensions at these scales. However, since the physical performance of a device usually depends on the details of its shape in implicit and radically non-linear ways, it is difficult for design engineers to predict the effects of geometrical variations and modify their designs accordingly. Therefore, consideration of geometrical uncertainties in the early design stage is of primary importance. For structural conceptual designs, topology optimization is a useful tool that can yield effective optimal configurations based on mathematical and physical principles. Since the pioneering study by Bendsoe and Kikuchi, topology optimization has successfully been applied to various physics problems, as widely reported in the literature. Some researchers have proposed robust topology optimization methods under geometrical uncertainties based on stochastic threshold Heaviside projection [1,2] or stochastic shifting of finite element nodes [3] under the assumption of sufficiently small perturbation. In the present study, we propose a reliability-based topology optimization under geometrical uncertainty. First, topology optimization is briefly discussed. Geometrical uncertainty is then modeled using an advection equation in which the advection velocity is treated as a stochastic field representing the magnitude and direction of variations, and the inverse reliability method is briefly discussed. Next, optimization problems are formulated based on the proposed geometrical uncertainty modeling, and the design sensitivity analysis, performed using the adjoint variable method, is explained. A two-level optimization algorithm is then constructed, where reliability analysis is conducted in the first level of the iterated procedure and the second level is used for updating design variables. Finally, the proposed method is applied in two numerical examples to demonstrate its validity and utility. References [1] M. Schevenels, B. S. Lazarov, O. Sigmund, Robust topology optimization accounting for spatially varying manufacturing errors, *Computer Methods in Applied Mechanics and Engineering*, Vol 200(49) 2011 pp. 3613–3627. [2] B. S. Lazarov, M. Schevenels, O. Sigmund, Topology optimization with geometric uncertainties by perturbation techniques, *International Journal for Numerical Methods in Engineering*, Vol 90(11) 2012, pp. 1321–1336. [3] M. Jansen, G. Lombaert, M. Schevenels, Robust topology optimization of structures with imperfect geometry based on geometric nonlinear analysis, *Computer Methods in Applied Mechanics and Engineering*, Vol 285 2015, pp. 452–467.

On the Isogeometric Modeling of Phase Transitions on Deforming Surfaces

Roger A. Sauer^{*}, Christopher Zimmermann^{**}, Deepesh Toshniwal^{***}, Chad M. Landis^{****},
Thomas J.R. Hughes^{*****}, Kranthi K. Mandadapu^{*****}

^{*}RWTH Aachen University, ^{**}RWTH Aachen University, ^{***}UT Austin, ^{****}UT Austin, ^{*****}UT Austin, ^{*****}UC
Berkeley

ABSTRACT

Many physical applications are governed by phase transitions. An example from biophysics are lipid membranes. They can separate into two distinct phases when quenched from high to low temperatures. Due to the coupling between in-plane phase transitions and out-of-plane bending, this can lead to severe shape changes of the membrane. This work presents a general theory and isogeometric finite element implementation for studying mass conserving phase transitions on deforming surfaces [1]. The mathematical problem is governed by two coupled fourth-order partial differential equations (PDEs) that live on an evolving two-dimensional manifold. For the phase transitions, the PDE is the Cahn-Hilliard equation for curved surfaces, which can be derived from surface mass balance in the framework of linear irreversible thermodynamics [2]. For the surface deformation, the PDE is the (vector-valued) Kirchhoff-Love thin shell equation. Both PDEs can be efficiently discretized using C1-continuous interpolations without derivative degrees-of-freedom (dofs). Structured NURBS and unstructured spline spaces with pointwise C1-continuity are utilized for this. The resulting finite element formulation is discretized in time by the generalized-alpha scheme with adaptive time-stepping, and it is fully linearized within a monolithic Newton-Raphson approach. A curvilinear surface parameterization is used throughout the formulation to admit general surface shapes and deformations [3]. The behavior of the coupled system is illustrated by several numerical examples exhibiting phase transitions on deforming spheres, tori and double-tori. [1] C. Zimmermann, D. Toshniwal, C.M. Landis, T.J.R. Hughes, K.K. Mandadapu and R.A. Sauer (2017), "An isogeometric finite element formulation for phase fields on deforming surfaces", arXiv:1710.02547 [2] A. Sahu, R.A. Sauer and K.K. Mandadapu (2017), "The irreversible thermodynamics of curved lipid membranes", Phys. Rev. E, 96:042409 [3] T.X. Duong, F. Roohbakhshan and R.A. Sauer (2017), "A new rotation-free isogeometric thin shell formulation and a corresponding continuity constraint for patch boundaries", Comput. Methods Appl. Mech. Engrg., 316:43-83

The Influence of Grain Size and Shape on the Mechanical Properties of AM Parts

Robert Saunders^{*}, Ajit Achuthan^{**}, Amit Bagchi^{***}

^{*}U.S. Naval Research Lab, ^{**}Clarkson University, ^{***}U.S. Naval Research Lab

ABSTRACT

Metal powder-based additive manufacturing (PAM) processes involve localized melting and solidification of a small amount of metallic powder, with large temperature gradients and cooling rates that influence the evolution of the local microstructure. Typically, the resulting microstructure has a texture and consists of columnar grains of different grain sizes, which affect the mechanical properties of the material. In a previous study, a microstructure-informed constitutive model was developed to describe the mechanical behavior of solidified material produced by PAM. This model was based on crystal plasticity and took into account the grain size and aspect ratio of the microstructure by considering a core and mantle configuration for the grain volume, with the mantle representing the grain boundary influence region. A representative volume element (RVE) using the developed constitutive model was used to validate the method and the overall mechanical properties were obtained. The results of the previous work showed that grain size and shape have a significant influence on individual grain strength and hardening modulus. In particular, smaller grains with larger aspect ratios exhibit the most dramatic effect. However, the influence of these size and shape effects on the overall mechanical behavior of the RVE is not known. In this work, a design of experiments (DoE) study is performed where the average grain aspect ratio, load direction, and grain size and shape influences of the RVE are varied. Preliminary results indicate that, as expected, the RVEs with their average aspect ratio larger have a higher predicted strength but little change in the hardening modulus. However, when the grains in the RVE are closer to equiaxial (i.e., microstructure of a conventionally cast metal part), the hardening modulus is greatly increased along with a lowered yield strength. This initial result indicates that there may be potential to tailor mechanical properties of a part by controlling the process parameters that determine the microstructure. The complete results of this DoE will help to determine the extent to which this tailoring can be done as well as shed light on the effect of grain size and shape on mechanical behavior of PAM parts.

Novel Kinetic Model and Kinetic Consistent Algorithm of Magneto Hydro Dynamics

Valeri Saveliev*, Boris Chetverushkin**, Andrey Saveliev***

*Institute of Applied Mathematics, Russian Academy of Sciences, **Institute of Applied Mathematics, Russian Academy of Sciences, ***Immanuel Kant Baltic Federal University

ABSTRACT

New kinetic model of dynamic of charged particles on base implementation of electromagnetic interactions inside Boltzmann like statistical distribution function and development of effective parallel algorithms for high performance computing systems will be presented. We propose a new approach to define of unified complex Boltzmann like distribution function, which includes the electromagnetic terms for the solution of the Boltzmann equation for charged particles in electromagnetic field. It was shown that electromagnetic fields do not destroy the validity of the Boltzmann equation which opened the way for the implementation of the electromagnetic term in the Boltzmann-like distribution function. Due to the vector nature of the electromagnetic interaction the distribution function should take into account the vector behavior and provide correct formulation for the evolution of the magnetic field, i. e. the magnetic field should be generally defined as a moment of the Boltzmann-like distribution function. In order to provide the validity of the proposed statistical complex distribution function, we show that the equilibrium state of Boltzmann equation for charged particles reproduced correctly the ideal magneto gas dynamics system of equations, including the evolution of the magnetic field. The computational algorithms are based on the kinetic consistent approach of the solution of the Boltzmann equation i.e. evolution of Boltzmann like statistical distribution function at discrete time and integration with the summational coefficients to getting the magneto gas dynamic system of equations. The numerical method is based on the explicit schemes. Due to logical simplicity and high efficiency, the algorithm is easily adopted to modern high performance parallel computing systems, including hybrid computing system with graphic processors. The weakness of explicit schemes is a strictly limited time step that ensures computational stability. This restriction becomes critical with the growing number of nodes and the reduction in the step of a spatial mesh. The advanced explicit kinetic finite difference schemes hyperbolic type have a soft stability condition giving the opportunity to enhance the stability and to use very fine meshes. The results of numerical calculations of test benches physical task of MHD in 3D space will be presented. It also can be mentioned the using of the proposed approach for the biomedical study in particular blood flow under strong magnetic field conditions.

Polytopal Stokes Weights Transport

Yann Savoye*

*Robert Gordon University

ABSTRACT

Deformation mechanism of non-rigid surfaces in motion is a long-standing problem in Computational Mechanics with numerous of applications in Engineering Sciences and Computer Graphics. In this work, we focus on estimating generalized coordinates on polyhedral meshes required for cage-based deformation. In particular; our approach relies on Computational Fluid Mechanism as a computational model of deformation mechanisms. Recent years have seen an increasing attention for physics-inspired rigging methods to enable visually-pleasant elastic shape animations. Cage-based deformation is a well-studied technique in Geometry Processing. Deformable Cages are purely shape-aware geometric subspaces, allowing non-isometric stretching strains. Also, shape coordinates are the key ingredients to rig an input coarse cage deformer to the enclosed surface, and then deform a shape with meaningful properties. Inspired by the mass-preserving vorticity in incompressible fluid transport, we reformulate the cage-based rigging as an incompressible Stokes problem to estimate weight functions suitable for cage-based deformation. Hence, we derive cage-based coordinates from Stokes equation by devising a vorticity-stream function formulation as the computational model for cage-based weighting functions. Our central contribution is a novel derivation of streamline-vorticity and its polyhedral discretization using finite difference method to obtain our compact-stenciled Stokes Coordinates. Our solver takes benefit from a linearization and biharmonic formulation. First, a linear formulation is derived from the Navier-Stokes equation. Then, starting from the linearized Stokes equations, we solve the Newtonian Stokes flow using the vorticity-velocity stream function. To speed up the computation, we approximate our Stokes-wise biharmonic operator using a compact second-order approximation with center-differencing. Finally, our cage-based Stokes Coordinates are the solution of the vorticity-stream equation for the Stokes flow at the steady state. We demonstrate the effectiveness of our Stokes Coordinates with several geometric applications such as shapes encoding, interactive cage-based shape editing as well as cartoon-style deformation of performance capture meshes. Overall, our technique does not modify the traditional cage-based metaphor for deforming objects such as point clouds, triangles soup, manifold or non-manifold surfaces. [1] - Stokes Coordinates, Yann Savoye, Proceedings of the 30th Spring Conference on Computer Graphics, 2017. [2] - Cage-based Performance Capture, Yann Savoye, SIGGRAPH ASIA 2016 Courses, 2016. [3] - Compact Stokes Coordinates for Cage-based Shapes, Yann Savoye, Proceedings of the 20th ACM SIGGRAPH Symposium on Interactive 3D Graphics and Games, 2016.

Application of the Harmony Search Algorithm to the Optimization of Laminated Composite Plates and Shells

Felipe Schaedler de Almeida*

*Federal University of Rio Grande do Sul

ABSTRACT

This work presents the application of an extended implementation of the harmony search algorithm (HSA) to the optimization of the stacking sequence of laminated composite plates and shells in order to maximize the buckling load of these structures. Due to usual manufacturing restraints, only few angles are allowed for the fiber direction of the plies, which are represented by discrete design variables in the optimization. Practical aspects such limitation to symmetric laminates and restraint on the number of plies with the same fiber orientation are also considered. The HSA used in this work extends the algorithm presented in de Almeida (2016) by the incorporation of additional strategies to dynamically change the parameters that control the generation of new design points. The modifications are introduced in order to adjust the exploration and exploitation efforts of the algorithm at different stages of the search. The first problem studied in this work deals with the optimization of a simply supported rectangular plate subjected to a biaxial uniform in-plane compressive load. The buckling load factor is given by an analytic expression, which make this a computationally inexpensive objective function. Many optimizations are performed for this problem in order to evaluate the reliability and efficiency of the method. The comparison of results obtained in this study to the result reported in other works shows that the modification proposed for the HSA can improve the performance of the algorithm. The last part of the paper shows the application of HSA to a more advanced structural optimization problem. The stacking sequence of a composite shallow shell is optimized to maximize the stiffness of the structure with respect to a pressure load. The objective function is formulated taking into account the critical load and the maximum displacement of the shell. These quantities are evaluated in a geometrically nonlinear analysis performed using a finite element solver presented by Almeida and Awruch (2009). The results obtained using HSA are compared to the optimizations performed by Almeida and Awruch (2009) using Genetic Algorithms. It is shown that the methodology used in this work reveals effective for the solution of optimization problems involving laminated composite structures with nonlinear behavior. de Almeida, F.S. Stacking sequence optimization for maximum buckling load of composite plates using harmony search algorithm. (2016) Composite Structures, 143. Almeida, F.S., Awruch, A.M. Design optimization of composite laminated structures using genetic algorithms and finite element analysis (2009) Composite Structures, 88 (3).

Runge-Kutta Based Generalised Convolution Quadrature Within an Elastodynamic BEM

Martin Schanz*

*Graz University of Technology

ABSTRACT

Boundary element formulations in time domain are well established in the engineering and the mathematical literature. In principle three types of formulations can be found: • Direct in time domain with analytical integration of the time convolution • Calculation in Laplace or Fourier domain with a subsequent numerical inverse transformation • Formulations based on the Convolution Quadrature Method (CQM) Common to all these approaches is the restriction to a constant time step size. The generalisation of the CQM to a non-uniform time mesh has been done by Lopez-Fernandez and Sauter [1], where the initial works use the implicit Euler as underlying time stepping method. To obtain higher order methods Runge-Kutta methods has been utilised within the generalised CQ [2]. These formulations have been presented for the single layer potential in acoustics or for acoustics with absorbing boundary conditions [3]. Here, the generalised CQ is applied to elastodynamics, where the single and double layer approach as well as a direct formulation for mixed boundary value problems will be presented. Essentially, the performance of the Runge-Kutta based generalized CQ is studied with respect to its convergence behaviour. As usual, the convergence order of the formulation is restricted by either the order of the Runge-Kutta method or by the spatial convergence order. In the presentation only a low order spatial discretisation is used. Numerical examples show the expected behavior. Further, first approaches to utilise fast methods within the generalised CQ will be presented. References [1] M. Lopez-Fernandez and S. Sauter, Generalized Convolution Quadrature with Variable Time Stepping. *IMA Journal of Numerical Analysis* 33 (2013), pp. 1156–1175. [2] M. Lopez-Fernandez and S. Sauter, Generalized Convolution Quadrature based on Runge-Kutta Methods. *Numerische Mathematik* 133 (2016), pp. 743–779. [3] M. Schanz and S. Sauter, Convolution Quadrature for the Wave Equation with Impedance Boundary Conditions. *Journal of Computational Physics* 334 (2017), pp. 442–459.

Effect of Occupant Size on Load and Displacement Response of the GHBMC Detailed Occupant Models in a Frontal Sled Environment

Jeremy Schap*, Bharath Koya**, F. Scott Gayzik***

*Wake Forest School of Medicine, Virginia Tech-Wake Forest Center for Injury Biomechanics, **Wake Forest School of Medicine, Virginia Tech-Wake Forest Center for Injury Biomechanics, ***Wake Forest School of Medicine, Virginia Tech-Wake Forest Center for Injury Biomechanics

ABSTRACT

Computational human body models (HBMs) are playing a more prominent role in the development of safety systems across a variety of vehicle platforms. To use these tools to mitigate injuries, it is vital to take into account the full spectrum of potential occupant sizes. Therefore, the Global Human Body Model Consortium (GHBMC) detailed occupant 5th percentile female (F05-O), 50th percentile male (M50-O) and 95th percentile male (M95-O) models were simulated in a frontal sled validation case. Comparisons were made between the three models to better understand effect of occupant size on load and displacement response. The previously published experimental sled decelerated from an initial velocity of 40 km/h with approximately 50th percentile male PMHS [1]. The sled minimized lower extremity movement via a rigid knee bolster and foot pan, each in contact with the PMHS throughout the event. No airbag or retractor was present. Three-dimensional kinematic response data were collected from the pelvis through head. Kinetic data were collected at each rigid part and seatbelt. By simulation, each HBM was first appropriately positioned and then gravity settled onto a published finite element sled model [2]. Then each HBM was belted in a three-point shoulder and lap belt. The experimental deceleration pulse was then applied to the rigid sled in the final simulation. Simulations ran with LS-Dyna R7.1.2 on a high-performance cluster. HBM biofidelity was first objectively verified by running CORA on M50-O load and displacement responses with respect to experimental corridors, created from five of the PMHS. The M50-O attained CORA scores of 0.84, 0.64, 0.77, 0.59, and 0.64 for seatbelt loads, reaction loads, head deflection, chest deflection, and spine deflection, respectively. The average score is 0.70, demonstrating reliable biofidelity. M95-O was morphed from M50-O. Additionally, CORA results for a morphed version of F05-O were previously published and were in line with the M50-O results. Higher load and displacement was generally observed as the size of the occupant increased. Compared with M50-O, peak forward head excursion is 11% greater and peak upper shoulder belt load is 7% greater in M95-O. M95-O experienced just over 60% higher chest compression on the left side of the chest where the shoulder belt passed compared to the M50-O. [1] Shaw et al., "Impact response of restrained PMHS in frontal sled", Stapp, 2009 [2] Poulard et al., "Contribution of pre-impact posture on restrained occupant", TIP, 2015

Interactions of Matrix and Interface Crack Growth in Composites

Johannes Scheel^{*}, Andreas Ricoeur^{**}

^{*}University of Kassel, ^{**}University of Kassel

ABSTRACT

Imperfect interfaces, e.g. occurring in composites, are having a crucial impact on propagating matrix cracks due to defect interaction [1]. The delamination, in return, is controlled not only by external loads but also by the matrix crack growth. In this numerical study, the interactions between the defects are investigated by examining the crack tip loadings, resulting crack paths and interface debonding, being crucial aspects of structural strength. The matrix crack tip loading is calculated by the J-integral. In order to incorporate the influence of imperfect interfaces, the J-integral needs to be reformulated. This influence depends on the appropriate modeling particularly of imperfect interfaces, where cohesive zones are an often used approach. The thermodynamical consistency of the implemented models is thus investigated. Above that, a consistent fracture mechanical frame work, involving both singular and cohesive cracks is presented, based on a thermodynamical approach. The matrix crack growth simulations require a continuous modification of the geometry due to incremental crack extensions. An intelligent re-meshing procedure is applied, where the loading history cannot be neglected due to the presence of dissipative processes at imperfect interfaces [2,3]. The distance between matrix crack tip and interface is essential for their interaction, going to extremes in the case of penetration, leaving several possibilities depending on the boundary value problem. The crack growth can stop, continue across the interface, in general with a kinking, or continue along the interface. In this regard, a criterion based on the J-integral is presented and applied to several test cases. [1] J. Scheel, A. Ricoeur; *Procedia Structural Integrity* 2017; 5: 255-262. [2] P. Judt, A. Ricoeur; *International Journal of Fracture* 2013; 182: 53-66. [3] P. Judt, A. Ricoeur, G. Linek; *Engineering Fracture Mechanics* 2015; 138: 33-48.

Nonlocal Modeling of Deformation and Damage Behavior of an Inhomogeneous Interphase in Nano-Particle Supercrystals

Ingo Scheider^{*}, Songyun Ma^{**}, Swantje Bargmann^{***}

^{*}Helmholtz-Zentrum Geesthacht, Institute of Materials Research, ^{**}RWTH Aachen, Institute of General Mechanics, ^{***}University of Wuppertal, Chair of Solid Mechanics

ABSTRACT

A novel nano-particle composite synthesized by bio-inspired design has been fabricated [1], which shows extraordinary mechanical characteristics due to the well-organized arrangement of soft and hard constituents in the microstructure. For this material, the inhomogeneous interphases surrounding the nano-particles play an important role in the mechanical performance of nano-composite. In order to describe this material on the nano-scale, particularly the interphase region, a nonlocal material model based on micropolar theory is proposed [2]. The new model is able to account for the scale of microstructure and describe the inelastic behavior, namely damage and plasticity, of interphases with gradient material properties. Micromechanical simulations are performed to investigate the relationship between nanostructures and mechanical properties of nanocomposites. The proposed damage model is validated by 3D micromechanical simulations for the nanoparticle super-crystals fabricated at different temperatures. The simulation results are in good agreement with the experimental data from micro-cantilever beams in terms of the stiffness, tensile strength and fracture energy absorption of the nanocomposites. [1] A. Dreyer, A. Feld, A. Kornowski, E. D. Yilmaz, H. Noei, A. Meyer, T. Krekeler, C. Jiao, A. Stierle, V. Abetz, H. Weller, G.A. Schneider, Organically linked iron oxide nanoparticle supercrystals with exceptional isotropic mechanical properties, *Nature Materials* 15(2016) 522{ 528. [2] S. Ma, I. Scheider, S. Bargmann; Ultrastrong nanocomposites with interphases: nonlocal deformation and damage behavior, submitted.

Robust Numerical Integration of Plasticity Models

William Scherzinger*, Brian Lester**

*Sandia National Laboratories, **Sandia National Laboratories

ABSTRACT

Recent work on the integration of plasticity models has enabled many high-fidelity models to be reliably implemented in production computing codes. A key aspect of this work is the adoption of line search methods for the return mapping algorithms. A Newton algorithm augmented with a line search method provides a very reliable technique for integrating plasticity models using a closest point projection algorithm. While the method is robust, little work has been done investigating the method to improve the convergence. Line search methods written for general minimization problems have a few parameters that govern the behavior of the method. Usually these parameters are set to some default value found in the optimization literature. However, for return mapping algorithms, improved convergence can be found by modifying these parameters. Furthermore, scaling, or conditioning, the residual can also improve the closest point projection algorithm. This work presents an overview of line search methods applied to closest point projection algorithms used with plasticity models, and looks to improve performance of the algorithms for complex plasticity models by choosing better line search parameters. The effect of scaling the residual is also examined with the goal of finding optimal scaling parameters for a given plasticity model. The anisotropic plasticity models of Barlat and co-workers are used to investigate the line search methods and scaling strategies. Results are presented that show significant improvement in the convergence of the return mapping algorithms.

In-Plane/Out-of-Plane Separated Representations of Navier-Stokes Solutions in Thin Geometries

Adrien Scheuer^{*}, Rubén Ibañez^{**}, Emmanuelle Abisset-Chavanne^{***}, Francisco Chinesta^{****},
Roland Keunings^{*****}

^{*}Université catholique de Louvain, Louvain-la-Neuve, Belgium; Ecole Centrale de Nantes, Nantes, France, ^{**}Ecole Centrale de Nantes, Nantes, France, ^{***}Ecole Centrale de Nantes, Nantes, France, ^{****}ENSAM ParisTech, Paris, France, ^{*****}Université catholique de Louvain, Louvain-la-Neuve, Belgium

ABSTRACT

Fluid flows in degenerated geometries, in which the characteristic length in one direction is much smaller than in the others, are a challenging task for standard mesh-based simulation techniques, that often require a tremendous number of discretization points or elements to provide accurate resolutions. Classically, ad-hoc simplifications or approximations (e.g. lubrication theory) are rather called for in order to conduct tractable simulations. In this work, we consider, within the Proper Generalized Decomposition (PGD) framework, an in-plane / out-of-plane separated representation of the solutions of the Navier-Stokes equations in thin geometries. The use of such separated representation let us decouple the meshes in the plane (coarse) and thickness (fine) directions, allowing a high-resolution representation of the solution evolution along the thickness coordinate while keeping the computational complexity characteristic of 2D simulations. This technique is particularly well suited to obtain efficiently fine and accurate solutions in boundary layers or in narrow geometries when approximations based on lubrication theory are not suitable.

A Small Strain Crystal Plasticity Formulation Based on the Primal Dual Interior Point Method

Lisa Scheunemann*, Paulo Salvador Britto Nigro**, Jörg Schröder***, Paulo Pimenta****

*Institute of Mechanics, University Duisburg-Essen, Germany, **Institute of Mechanics, University Duisburg-Essen, Germany, ***Institute of Mechanics, University Duisburg-Essen, Germany, ****Structural and Geotechnical Engineering, Polytechnic School at University of Sao Paulo Brazil Sao Paulo, Sao Paulo

ABSTRACT

Single crystal plasticity plays a major role in the analysis of material anisotropy. The polycrystalline material response is obtained upon considering a structure consisting of various individual, single grains, often also considering interface effects at the grain boundaries. On the individual grain level, single crystal plasticity can be treated in the mathematical framework of multisurface plasticity, leading to a constrained optimization problem wherein multiple constraints are defined as yield criteria on the different slip systems. Different approaches have been established in this field, see, e.g., [2], [3]. In rate-independent models, the set of active slip systems in the grain is possibly nonunique and is identified in, e.g., an active set search. Rate dependent approaches are based on power-type creep laws which do not differentiate into active or inactive slip systems. However, the constitutive equations of these formulations are often very stiff and require a small time increment. Here, a new algorithm for the solution of the constrained optimization problem based on the primal dual interior point method (PDIPM), [1], involving slack variables is presented for the framework of small strain single crystal plasticity. The use of slack variables therein stabilizes the conventional method and allows for a temporary violation of the constraint during the optimization. The optimization is solved using a Lagrange functional, wherein the nonlinear system of equations resulting from the derivation of the Lagrange functional is linearized using Taylor expansion and solved by a Newton Raphson scheme. All slip systems are considered simultaneously, omitting an iterative active set search. PDIPM has been found to lead to very efficient algorithms and better convergence rates than barrier or penalty methods. The stability of the algorithm would be especially beneficial in complex material models, such as a multiscale description of polycrystalline materials. Several numerical examples are presented, showing the performance of the developed algorithm based on academic slip system setups as well as face-centered-cubic crystals. References [1] El Bakry, A.S., Tapia, R.A., Tsuchiya, T. and Zhan, Y.: On the formulation and Theory of the Newton Interior Point Method for Nonlinear Programming. *Journal of Optimization Theory and Applications*, 89 (1996), 507-541. [2] Cuitino, A.M. and Ortiz, M.: Computational modelling of single crystals. *Modelling and Simulation in Materials Science and Engineering*, 1 (1992), 225-263. [3] Peirce, D., Asaro, R.J. and Needleman, A.: An analysis of nonlinear and localized deformation in ductile single crystals. *Acta Metallurgica*, 30 (1982), 1087-1119.

GENERIC-based numerical methods for the thermodynamically consistent simulation of coupled thermomechanical solids

Mark Schiebl*, Peter Betsch**

*Institute of Mechanics, Karlsruhe Institute of Technology (KIT), Germany, **Institute of Mechanics, Karlsruhe Institute of Technology (KIT), Germany

ABSTRACT

This work deals with the Energy-Momentum-Entropy (EME) consistent time integration of open thermoelastic systems. While energy-momentum preserving integrators are well-known for conservative mechanical systems, Romero introduced in (I. Romero, Thermodynamically consistent time-stepping algorithms for nonlinear thermomechanical systems, *IJNME*, 79(6): 706-732, 2009) the class of thermodynamically consistent integrators for coupled thermomechanical systems, which further respect symmetries of the underlying coupled system and are therefore capable of conserving associated momentum maps. As mathematical framework for the geometric structure of the non-equilibrium thermodynamics the GENERIC (General Equation for Non-Equilibrium Reversible-Irreversible Coupling) framework is used. The GENERIC framework, originally proposed by Grmela and Öttinger for complex fluids (M. Grmela and H.C. Öttinger, Dynamics and thermodynamics of complex fluids. i. development of a general formalism. *Physical Review E*, 56(6):6620, 1997), expresses the evolution equation as the sum of reversible and irreversible contribution via a Poisson and a dissipative bracket. Since the GENERIC framework does not depend of a specific choice of the thermodynamical state variables (A. Mielke. Formulation of thermoelastic dissipative material behavior using generic. *Continuum Mechanics and Thermodynamics*, 23(3):233–256, 2011), we explore the structure of GENERIC framework using the entropy density, see e.g. (M. Krüger, M. Groß and P. Betsch. An energy-entropy-consistent time stepping scheme for nonlinear thermo-viscoelastic continua. *ZAMM-Journal*, 96(2):141–178, 2016), the absolute temperature, see e.g. (M. Hütter and B. Svendsen. Thermodynamic model formulation for viscoplastic solids as general equations for non-equilibrium reversible–irreversible coupling. *Continuum Mechanics and Thermodynamics*, 24(3):211–227, 2012), and further the internal energy density as thermodynamical state variable from which the weak form of the initial boundary value problem can be gained. Applying the notion of a discrete gradient in the sense of Gonzalez (O. Gonzalez. Design and analysis of conserving integrators for nonlinear Hamiltonian systems with symmetry. PhD thesis, Stanford University, 1996) leads to an EME integrator. As boundary conditions rely on the specific choice of the thermodynamical state variable we extend the GENERIC framework to be suitable for open systems following the procedure in (H. C. Öttinger. Nonequilibrium thermodynamics for open systems. *Physical Review E*, 73(3):036126, 2006). The presentation will indicate key differences and similarities between the alternative choices of thermodynamical state variables and will include several simulations with different boundary conditions using an energy-based termination criterion.

Superelements in a Screw Theory based Floating Frame of Reference Formulation

Jurnan Schilder*, Marcel Ellenbroek**

*University of Twente, **University of Twente

ABSTRACT

The floating frame of reference formulation is a commonly applied method for the simulation of flexible multibody system dynamics in which the elastic behavior of each body is small relative to the body's local floating frame. Hence, the local elastic behavior of a body can be described by its linear finite element model. For this reason, the formulation naturally allows for use of substructuring methods, since modal order reduction techniques can be applied to describe the local elastic behavior with a limited number of generalized coordinates. The use of substructuring methods has led to the development of superelements for flexible multibody dynamics. In this, the absolute position and orientation of coordinate systems attached to a body's interface points are used as generalized coordinates. In terms of these coordinates, kinematic constraints between bodies can be enforced directly and do not require the use of Lagrange multipliers. In order to develop these superelements, a coordinate transformation is required that expresses the absolute floating frame coordinates and the local elastic displacement field in terms of the absolute interface coordinates. In literature, several methods for creating superelements have been proposed. In recent work [1], the authors presented a new method that enables a coordinate transformation to absolute interface coordinates in a way that the floating frame can be attached to a material point, not being an interface point. Here, Craig-Bampton interface modes are used as a reduction basis for the local mass and stiffness matrices. It is shown that by demanding zero elastic deformation at the location of the floating frame, the floating frame coordinates can be eliminated from the degrees of freedom. The method as described in [1] is formulated in terms of engineering coordinates, i.e. in terms of position vectors, rotation matrices, linear and angular velocities et cetera. In this work, this method is reformulated based on screw theory. In particular, a full and complete derivation of the inertia forces will be presented in terms of the twists of the interface points. In this way, the authors intend to make the method convenient to use for a broad range of fields and applications, independent of whether scientists and engineers use engineering coordinates or screw theory in that particular field. [1] Ellenbroek, M. & Schilder, J., "On the use of absolute interface coordinates in the floating frame of reference formulation for flexible multibody dynamics", *J. Multibody Syst Dyn* (2017). <https://doi.org/10.1007/s11044-017-9606-3>

Multiscale and Variational Modeling of Amorphous Silica Glass

William Schill*, Michael Ortiz**

*California Institute of Technology, **California Institute of Technology

ABSTRACT

We develop a critical-state model of fused silica plasticity on the basis of data mined from molecular dynamics (MD) calculations. The MD data is suggestive of an irreversible densification transition in volumetric compression resulting in permanent, or plastic, densification upon unloading. The MD data also reveals an evolution towards a critical state of constant volume under pressure-shear deformation. The trend towards constant volume is from above, when the glass is overconsolidated, or from below, when it is underconsolidated. We show that these characteristic behaviors are well-captured by a critical state model of plasticity, where the densification law for glass takes the place of the classical consolidation law of granular media and the locus of constant volume states denotes the critical-state line. A salient feature of the critical-state line of fused silica, as identified from the MD data, that renders its yield behavior anomalous is that it is strongly non-convex, owing to the existence of two well-differentiated phases at low and high pressures. We argue that this strong non-convexity of yield explains the patterning that is observed in molecular dynamics calculations of amorphous solids deforming in shear. We employ an explicit and exact rank-2 envelope construction to upscale the microscopic critical-state model to the macroscale. Remarkably, owing to the equilibrium constraint the resulting effective macroscopic behavior is still characterized by a non-convex critical-state line. Despite this lack of convexity, the effective macroscopic model is stable against microstructure formation and defines well-posed boundary-value problems [1]. We study continuum mechanics examples of silica glass involving ballistic impact. We then study connections between this anomalous shear yield behavior and strain rate effects in loading of the glass employing time scale bridging techniques with specific interest in the behavior of amorphous solids. 1. W. Schill, S. Heyden, S. Conti, M. Ortiz, The Anomalous Yield Behavior of Fused Silica Glass, submitted to the Journal of Mechanics and Physics of Solids, 2017

Discontinuous Galerkin Methods through the Lens of Variational Multiscale Analysis

Dominik Schillinger^{*}, Stein K.F. Stoter^{**}, Bernardo Cockburn^{***}

^{*}Department of Civil, Environmental, and Geo- Engineering, University of Minnesota, Twin Cities, USA,

^{**}Department of Civil, Environmental, and Geo- Engineering, University of Minnesota, Twin Cities, USA, ^{***}School of Mathematics, University of Minnesota, Twin Cities, USA

ABSTRACT

The variational multiscale method was introduced by Tom Hughes and his students in the mid-1990s and has been primarily used as a unifying framework for stabilized finite element methods and to design effective subgrid-scale models in computational fluid dynamics. In this talk, we employ the variational multiscale method to open up an alternative perspective on discontinuous Galerkin methods. We first establish a multiscale variational formulation, based on the decomposition of the true solution into a discontinuous coarse-scale solution and a discontinuous fine-scale solution in each element domain. We tie discontinuous elements together by fine-scale interface conditions that naturally arise from the strong-form transmission conditions. We argue that the resulting multiscale variational form represents a general unifying framework for discontinuous Galerkin methods. In support of this claim, we show that standard discontinuous Galerkin methods can be recovered from this multiscale framework by choosing appropriate fine-scale closure models that relate coarse- and fine-scale solutions. We explain specific closure models for the examples of the interior penalty (IP) method and the local discontinuous Galerkin (LDG) method. We then show that these closure models offer new insights into the inner workings of the IP and LDG methods, in particular with respect to the numerical behavior at element interfaces. We close our talk with a few personal recollections of the speaker (D. Schillinger) on his advisor, mentor and friend Tom Hughes.

A Computational Modeling Approach to Model Patterned Strain Localizations in Magnesium Alloys

Sara Schlenker^{*}, Konstantinos Baxevanakis^{**}, Brian Wisner^{***}, Antonios Kotsos^{****}

^{*}Drexel University, ^{**}Drexel University, Loughborough University, ^{***}Drexel University, ^{****}Drexel University

ABSTRACT

A number of non-local constitutive theories have been developed to account for the phenomena of size dependence in material behavior. In the case of metals, several of these theories incorporate the gradient of plastic strain, or of plastic slip, as an independent state variable in the free energy equation. This introduces a dimensionally required length scale into the constitutive law and allows a connection between microstructural information and macrostructural behavior. Implementation of this class of theory into a finite element code additionally has been shown to induce patterning or localization of strains that could inform understanding of the mechanics and causes of the instabilities related to the transition from homogenous to locally-dominated behavior. This could additionally lead to more reliable predictions of plastic deformation in metal alloys such as in the case of Magnesium which is characterized by pronounced plastic anisotropy as well as the appearance of strain localization bands that have been associated with spatially inhomogeneous deformation twinning. Several computational methods used to predict strain localizations in the form e.g. of shear bands rely on geometrical changes such as reduction of thickness or a priori imposed defects to initiate such localized effects. In others, the material properties of a region are modified to induce localizations. In this talk, a computational model is presented which is capable to induce strain localizations as a result of the defined constitutive law. To achieve this goal, the approach explores the effect of gradient-based constitutive laws on inducing strain localizations in models free of triggering flaws. To demonstrate this approach, Finite Element models incorporating custom higher gradient constitutive laws are employed. The obtained simulation results are compared against available multiscale experimental strain measurements obtained using advanced optical metrology methods. Furthermore, an approach to include this computational formulation in a crystal plasticity framework is presented.

Imperfect Interfaces in Magnetolectric Composites and Their Impact on Coupling Coefficients

Alexander Schlosser*, Andreas Ricoeur**

*University of Kassel, **University of Kassel

ABSTRACT

The efficiency in converting magnetic into electric energy and vice versa makes magnetolectric (ME) composites promising candidates for many technical applications. The ferroelectric matrix as well as the magnetostrictive inclusions of particle composites and the layers of laminates are mostly ceramics or other brittle materials, thus being prone to cracking. Independent from the kind of composite the transmission of stresses via the interfaces between the constituents plays the key role in the functionality of ME composites. Therefore, the investigation of delamination processes is of great interest for the prediction of durability and coupling factors. In order to investigate delamination processes in ME composites, cohesive elements are being developed and applied in combination with nonlinear ME finite elements described in [1] and [2]. The mechanical behavior of the cohesive zone is classically prescribed by a bilinear traction-separation-law. Magnetic and electric fluxes emanate from evolution laws of magnetic and electric permeabilities, respectively, accounting for micro crack damage in the process zone and electrostatic stresses at the interfaces. Electric and magnetic properties change during damaging processes, being controlled by damage variables, which in turn are determined by the separation between the boundaries. Based on these cohesive elements, possible influence factors on delamination like the geometry of the composites or the ME poling processes are investigated, finally with regard to coupling coefficients. References: [1] Avakian, A., Gellmann, R., and Ricoeur, A. (2015). Nonlinear modeling and finite element simulation of magnetolectric coupling and residual stress in multiferroic composites. *Acta Mechanica*, 226(8), 2789-2806. [2] Avakian, A., and Ricoeur, A. (2016). Constitutive modeling of nonlinear reversible and irreversible ferromagnetic behaviors and application to multiferroic composites. *Journal of Intelligent Material Systems and Structures*, 27(18), 2536-2554.

Relating the Horizontally Averaged Wind Profile to the Geometry of Idealized Urban Surfaces

Manuel F. Schmid^{*}, Marco G. Giometto^{**}, Marc B. Parlange^{***}

^{*}University of British Columbia, Vancouver, Canada, ^{**}Columbia University, New York, USA, ^{***}Monash University, Melbourne, Australia

ABSTRACT

The near-wall behavior of flow over rough surfaces depends on the geometry of the roughness. In urban areas, atmospheric models either have to resolve individual buildings or include a model for their effect on the flow. Large-scale models often employ one-dimensional urban canopy parameterizations to account for the unresolved surface elements. In this study, we attempt to model the wall-normal velocity profile in terms of statistical properties of the surface roughness. The Navier-Stokes equations are horizontally averaged to obtain an expression for the one-dimensional profile. The relationship between each term and the surface properties is assessed based on a series of large-eddy simulations of flow over idealized urban surfaces where roughness elements are resolved.

Stress and Driving Force Calculation within Multiphase-field Models: Applications to Martensitic Phase Transformation in Dual-phase Microstructures

Daniel Schneider^{*}, Ephraim Schoof^{**}, Felix Schwab^{***}, Christoph Herrmann^{****}, Michael Selzer^{*****}, Britta Nestler^{*****}

^{*}Institute of Applied Materials -- Computational Materials Science (IAM-CMS), Karlsruhe Institute of Technology (KIT) and Institute of Digital Materials Science (IDM), Karlsruhe University of Applied Sciences, ^{**}Institute of Applied Materials -- Computational Materials Science (IAM-CMS), Karlsruhe Institute of Technology (KIT), ^{***}Institute of Applied Materials -- Computational Materials Science (IAM-CMS), Karlsruhe Institute of Technology (KIT), ^{****}Institute of Digital Materials Science (IDM), Karlsruhe University of Applied Sciences, ^{*****}Institute of Applied Materials -- Computational Materials Science (IAM-CMS), Karlsruhe Institute of Technology (KIT) and Institute of Digital Materials Science (IDM), Karlsruhe University of Applied Sciences, ^{*****}Institute of Applied Materials -- Computational Materials Science (IAM-CMS), Karlsruhe Institute of Technology (KIT) and Institute of Digital Materials Science (IDM), Karlsruhe University of Applied Sciences

ABSTRACT

Numerical simulations based on phase-field methods are indispensable in order to investigate certain interesting and important phenomena in the evolution of microstructures. Microscopic solid state phase transitions are highly affected by mechanical driving forces and therefore the accurate calculation of the stresses in the transition region is essential. We present methods for stress calculations within the phase-field framework for finite deformations, which satisfy the mechanical jump conditions corresponding to sharp interfaces, although the sharp interface is represented as a volumetric region. The model allows to calculate phase inherent stresses and deformations even in regions where many phases coexist. Since the phase-inherent variables are known, appropriate methods can be used for the calculation of the internal variables in the bulk as well as in transition regions. We demonstrate that the models reflect the mechanical configurational forces for phase transitions and present applications to the martensitic phase transformation process in dual-phase microstructures. [1] D. Schneider, O. Tschukin, M. Selzer, T. Böhlke, B. Nestler, Phase-field elasticity model based on mechanical jump conditions. *Comp. Mech.* (2015) 5:887--901 [2] D. Schneider, F. Schwab, E. Schoof, A. Reiter, C. Herrmann, M. Selzer, T. Böhlke, B. Nestler, On the stress calculation within phase-field approaches: A model for finite deformations. *Comp. Mech.* (2017) 60:203--217 [3] D. Schneider, E. Schoof, O. Tschukin, A. Reiter, C. Herrmann, F. Schwab, M. Selzer, B. Nestler Small strain multiphase-field model accounting for configurational forces and mechanical jump conditions. *Comp. Mech.* (2017) in print [4] E. Schoof, D. Schneider, N. Streichhan, T. Mitnacht, M. Selzer, B. Nestler, Multiphase-field modeling of martensitic phase transformation in a dual-phase microstructure. *International Journal of Solids and Structures.* (2017) in print

GRAPH AND HEURISTIC BASED TOPOLOGY OPTIMIZATION OF CRASHWORTHINESS COMPOSITE PROFILE STRUCTURES MANUFACTURED BY VACUUM INFUSION AND GLUING

DOMINIK SCHNEIDER¹ SIMON LINK¹ ALEX SCHUMACHER¹ AND CHRISTOPHER ORTMANN²

¹ University of Wuppertal, Chair for Optimization of Mechanical Structures
Gaussstraße 20, 42119 Wuppertal, Germany
e-mail: dschneider@uni-wuppertal.de; simon.link@uni-wuppertal.de;
schumacher@uni-wuppertal.de website: <https://www.oms.uni-wuppertal.de/>

² Volkswagen Aktiengesellschaft
Letterbox 1777, 38436 Wolfsburg, Germany
e-mail: christopher.ortmann@volkswagen.de website: <http://www.volkswagen-ag.de/>

Key words: topology optimization, crashworthiness, heuristic, graph theory, composite profile, gluing.

Abstract. *Composite structures enable lightweight solutions, which are required by the transportation industry to fulfil their weight targets. Many of those structures have high requirements regarding passive safety and manufacturing. Yet finding suitable designs for crashworthiness applications proves to be difficult because of material nonlinearities, contact, large displacements and in case of composite materials anisotropy, brittle failure and crushing. The Graph and Heuristic Based Topology Optimization (GHT)^[1] has already been utilized for the optimization of metal extrusion profiles under lateral crash loads. In order to enable the use of composite materials, the graph syntax, which is used to represent the geometry, is modified, so that it can carry information regarding fiber orientations and thicknesses of the layers. During the optimization, heuristics based on expert knowledge regarding crash applications evaluate the simulation data and propose new competing layouts with modified topologies. These designs are then evaluated with a single or multiple crash simulations in inner optimization loops. During the whole optimization process various manufacturing constraints prevent the occurrence of non-manufacturable designs. This paper illustrates, how the GHT can be extended for the optimization of crashworthiness composite profile structures under lateral loads. An extension of the graph syntax allows splitted structures which are glued together at flanges. New heuristics detect element failure and try to sustain the structural integrity. An Optimization of a test specimen laterally impacted by a drop weight is carried out where the maximum contact force is minimized while restricting the maximum intrusion. Two improved designs and the initial design are manufactured and tested in a drop tower. The test results are presented and compared with the simulations.*

1 INTRODUCTION

Composite materials enable lightweight structures because of their low density and high specific strength. In addition they show very good energy absorption capabilities if failing through stable crushing. They offer a great variety of design freedoms, like the type of matrix and fiber, the orientation and volume fraction of the fibers or the manufacturing process.

The large number of design freedoms and manufacturing constraints complicate the component development for crash applications. Popular commercially available topology optimization methods for linear static problems^[2,3] cannot be utilized in the process because of material nonlinearities, contact, large displacements and the explicit finite element method. Other methods^[4] try to overcome these issues. The Graph and Heuristic Based Topology Optimization (GHT)^[1] can be utilized to optimize the topology of structures with a constant cross section like extrusion profiles or rib layouts^[5]. The cross-section is described by a mathematical graph which enables algorithmic manipulations of the geometry while allowing to check manufacturing constraints. Heuristics that are based on expert knowledge regarding crash applications are used in an outer optimization loop to suggest new designs. They insert or remove walls from designs of the previous iteration after analysing their simulation results like nodal displacements, velocities, energy densities and element deletion. Inner optimization loops evaluate all new topologies by calling the commercial optimizer LS-OPT that changes e.g. the thicknesses to reach the given optimization objective while meeting the constraints. If desired a shape and sizing optimization of the best design can be carried out at the end of the optimization to try to reach further improvements.

To extend the field of application towards composite structures with constant cross-section, some adjustments are necessary, that are described in this paper. An optimization of a test specimen is carried out to demonstrate the procedure. The structure is built up by several parts with flanges that are glued together. Two improved designs as well as the initial design are manufactured by vacuum infusion and gluing to test the structures in physical experiments. Splitting the structure in several parts avoids the need to use pultrusion as the manufacturing process, which would have led to expensive tool costs for these small quantities.

2 ADAPTIONS FOR COMPOSITE STRUCTURES WITH FLANGES

Before using composite structures in an optimization, some adaptations in the GHT process are necessary. At first new information regarding the composite layup and the flanges have to be saved in the graph and taken into account while creating the input decks for the finite element simulations. In addition the material failure has to be considered. Besides new heuristics that are needed to address the material failure, the existing heuristics have to be modified to stop analyzing the finite element results after failure occurs in the observed area, since torn apart pieces flying through the space would lead to false interpretations of the deformation behavior. Furthermore the existing manufacturing constraints like limiting the minimum distance between two walls are extended by a new constraint that forbids to attach a new wall to a location with an already existing flange.

2.1 Graph syntax

The graph contains all the relevant information to describe the geometry of a structure with a constant cross section. As shown in Figure 1 each wall consists of different vertices connected by edges. The LINK-Vertices define the location of the walls with Cartesian coordinates. The BEAMG-Vertices save the thickness of each wall as well as its curvature and, in case of prescribed flange connections on outer walls, additional parameters like the overlapping length and the flange position. The BEAM1- and BEAM2-Vertices define the layer angles and layer fractions of a symmetrical composite layup or stay empty in case of applications with metal. Finally the PARAM-Vertex stores global parameters that describe the whole structure like the extrusion length and the density of the material, to allow internal mass calculations. In case of other applications like finding rib layouts^[5] the vertices can contain additional information like rib heights.

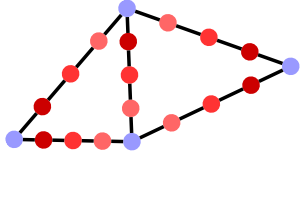
Graph Element	Contained information	
● BEAMG-Vertex	thickness, curvature, flange information	
● BEAM1-Vertex	composite layer angles	
● BEAM2-Vertex	composite layer fractions	
● LINK-Vertex	coordinates	
— EDGE	connected vertices	
○ PARAM-Vertex	e.g. extrusion length and density	

Figure 1: List of graph elements with their contained information, right: an exemplary graph

2.2 Flanges

There are two types of flanges currently implemented in the procedure. A custom flange connection can be defined on an outer wall by specifying the needed information in the BEAMG-Vertex. As displayed in Figure 2 the flange length, the flange position and the flange side can be stated. The overlapping length and the position are entered as a value between 0 and 1 with regard to the wall length. A position of 0 indicates that the flanges are located at the start of the wall and 1 respectively at the end, factoring in the edge direction. The side parameter controls on which side in edge direction the flange connection is established.

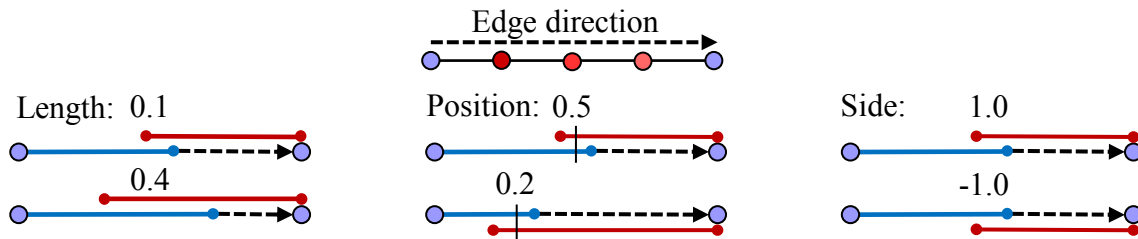


Figure 2: flange parameters, left: flange length, middle: flange position, right: side of the flange

Inner walls can automatically connect to the rest of the structure as new parts with flanges on both sides, so that each wall can be manufactured separately without undercuts. When inner walls share the same LINK-Vertex they connect to the other walls by creating a flange parallel to the next wall in clockwise direction, as displayed in Figure 3a. In case that two inner walls are connected nearly straight they are realised as a single part (Figure 3b).

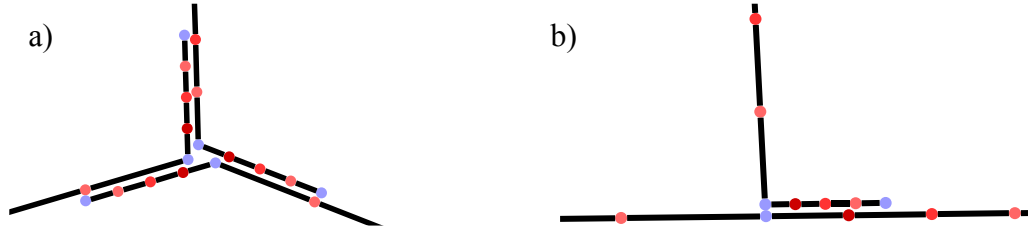


Figure 3: a) clockwise orientation of flanges of inner walls, b) no flanges created between straight connected inner walls

During the automatic creation of a finite element model, tied contacts are created between the flanges and the corresponding walls with a material defined by the user to represent the adhesive. Figure 4a shows an exemplary graph that is internally split into a converted graph (Figure 4b) with the presented rules to outline the flange connections. It is then extruded and meshed (Figure 4c) by GRAMB (Graph based Mechanics Builder), that was developed to create the input decks. As displayed, the composite layups are currently modeled with single layer elements, that contain the ply information in the material card (ESI VPS) or in the *PART_COMPOSITE definition (LS-DYNA), depending on the solver to be used. This approach saves computation time but is not capable of capturing delamination.

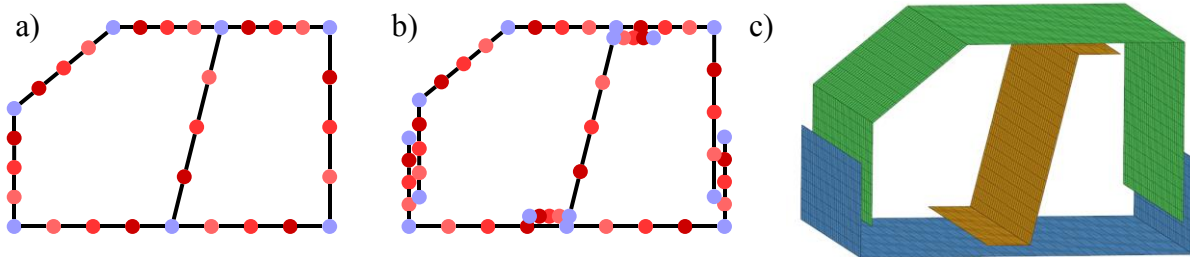


Figure 4: a) original graph, b) converted graph with flanges, c) extruded mesh

2.3 Heuristic Support Collapsin Walls

In addition to the existing heuristics^[1], the heuristic Support Collapsing Walls (SCW) is introduced to address a possible loss of the structural integrity through material failure. If detecting sudden and extensive failure, the wall with the highest failure index f is supported perpendicularly at the position of the most severe damage as displayed in Figure 5, where a cylinder impacts a structure that experiences material failure in the impact area. The failure index is calculated for each wall in each load case by formula (1).

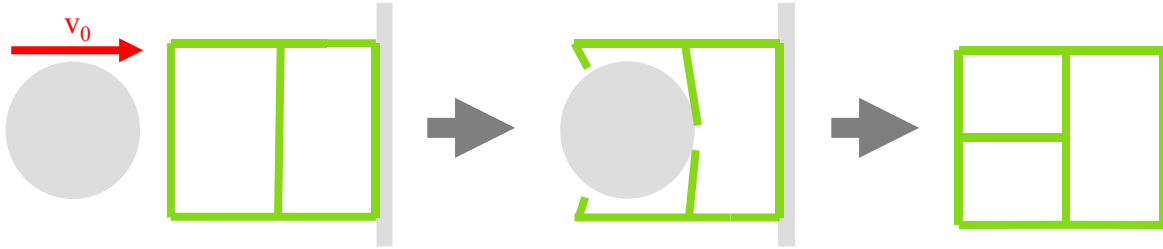


Figure : Principle of the heuristic Support Collapsing Walls

$$f = \max_{t_1, t_2} \left[\frac{n(t_1, t_2)}{0.9 \cdot \frac{(t_2 - t_1)}{\Delta t_{ref}} + 0.1} \right] \quad (1)$$

Here the number of elements deleted between the time t_1 and t_2 is divided by the fraction of this duration in relation to the period Δt_{ref} between the first and last occurrence of element deletion of the whole structure during the simulation. This allows to put more emphasis on strong failure in a short amount of time in contrast to less failure occurring during a longer period. To find the interval that delivers the highest failure index, t_1 and t_2 are varied in a heuristic approach to identify the maximum failure index for each wall. The heuristic then tries to support the wall with the highest failure index of all load cases perpendicular at the middle point of the deleted elements of the corresponding wall. If this fails the heuristic continues to support the wall with the next highest failure index.

2.4 Optimization variables

To evaluate the heuristic proposal, inner optimization loops can be carried out where the thicknesses of the structure are modified to improve the optimization goal. If working with composites an option is added to vary the global laminate direction that turns the complete layup of the composite. When running the final size and shape optimization, not only the thickness, the curvature and the shape can be optimized, but also the layer directions and/or the layer fractions of the layup of the whole structure. Changing the layer angles and fractions of each individual wall is not intended since it would lead to a large number of design variables that would increase the optimization time enormous and could not be handled efficiently by the optimization algorithms.

3 OPTIMIZATION OF A TEST SPECIMEN

With the new adaptations to the GHT, an optimization is carried out, that deals with a composite profile being laterally impacted by a semi-cylindrical weight in a drop tower. Since three different designs of the optimization will be manufactured and tested, the optimization problem and the simulation model are chosen to represent the test setup.

3.1 Simulation model and test setup

The simulation model is displayed on the left side of Figure 6. The rigid steel drop weight with a mass of 50 kg is guided along the Z-axis and moves with an initial velocity of 3 m/s against the Z-direction. The lower part of the drop weight has a semi-cylindrical shape with a diameter of 80 mm. The profile rests on a rigid steel plate, whose contact force with the profile is tracked during the simulation. For all contacts a friction of 0.2 is defined. The simulation is terminated by a sensor short after the drop weight starts to move back after the maximum intrusion. The model represents the test setup, visible on the right side of Figure 6. It only differs by the buffer elements on the sides that start to stop the drop weight roughly 27 mm before hitting the ground to avoid damaging the force sensor and the underlying structure in case the profile cannot stop the drop weight. Bidirectional $\pm 45^\circ$ -layers with 300 or 400 g/m² made of TENAX STS40 24K carbon fibers are used to create one of the following symmetric stacking sequences with the corresponding thicknesses assuming a fiber volume content of 48%:

- $[90^\circ, 0^\circ, 90^\circ, 0^\circ, 45^\circ, -45^\circ, 45^\circ, -45^\circ]_s \rightarrow 2.8 \text{ mm with } 300\text{g/m}^2$
- $[90^\circ, 0^\circ, 45^\circ, -45^\circ]_s \rightarrow 1.87 \text{ mm with } 400\text{g/m}^2$
- $[90^\circ, 0^\circ, 45^\circ, -45^\circ]_s \rightarrow 1.4 \text{ mm with } 300\text{g/m}^2$

The material cards for the tight contact and the composite are chosen from a set of existing cards of similar materials since no testing can be conducted to fit new material cards. Hence differences between the simulation model and the experiments are to be expected. The simulations are carried out with the commercial solver Pam-Crash.

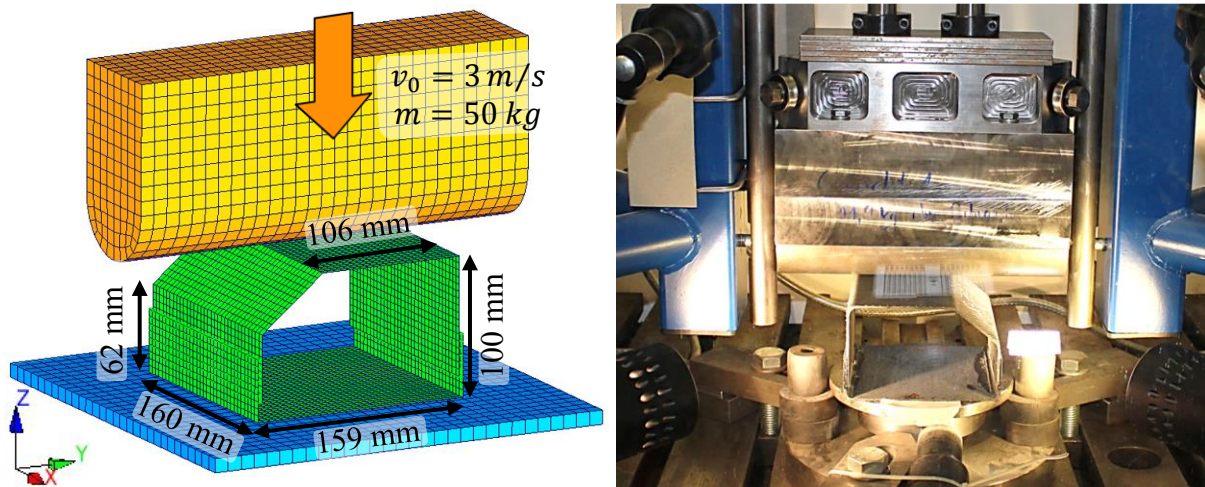


Figure 6: Simulation model (left) and corresponding test setup (right)

3.2 Optimization problem

As displayed in Table 1 the objective of the optimization is to minimize the maximum occurring force between the ground and the profile, filtered with a SAE-1000Hz-filter. The intrusion of the drop weight is restricted to 60 mm, to leave some deformation room in case the

drop weight is stopped later than predicted during the tests. During the heuristic evaluation the uniform thickness of the walls can be modified. In addition to that the shape can be varied in the final size and shape optimization. It should be mentioned that the restriction to forbid inner walls from ending at flanges of outer walls had not been implemented at the time of the optimization. All other manufacturing constraints are active and are listed in Table 1. The constraints are chosen quite restrictive to guarantee easy to manufacture structures, especially increasing the number of chambers would cause a much higher number of parts to be manufactured and glued together. During the inner optimization loops sequential domain reduction is applied combined with a genetic algorithm that is used for the optimization on the metamodel.

Table 1: Optimization problem

Objective	Minimize the maximum filtered contact force with the ground F_{max}
Constraints	Intrusion of drop weight (Z-direction) $d_z \leq 60$ mm
Design variables	Uniform thickness of the walls t Shape variables (only in final size and shape optimization)
Manufacturing constraints	Connection angle between two walls $> 60^\circ$ Wall distance > 20 mm Wall thickness > 1.4 mm and < 2.8 mm Size ratio between the largest and smallest chamber < 20 Number of chambers ≤ 3

3.3 Optimization results

The optimization starts with an empty profile without inner structures. During the Optimization in 3 Iterations 26 further designs are created and evaluated, causing about 1000 crash simulations for the heuristic evaluation and additional 1000 crash simulations for the final size and shape optimization of the so far best result. Three designs from that optimization, the initial design and the two best designs of the optimization, are chosen to be manufactured and tested. The graph and the results are displayed in Figure 7 and Table 2.

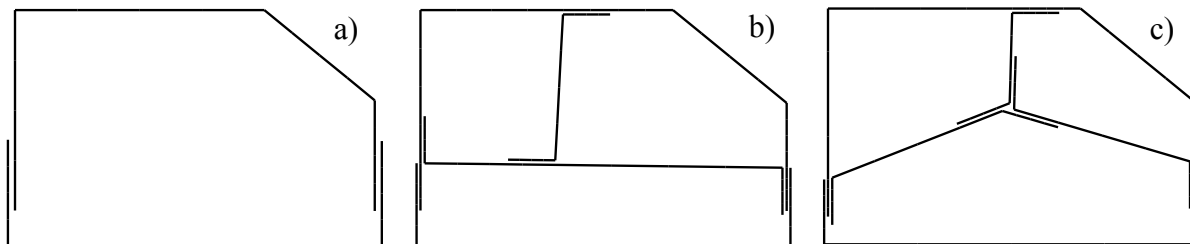


Figure 7: graphs (without vertices) of a) start design, b) option 1 and c) option 2

Table 2: Results of the selected designs from the optimization

Original Design	F_{max} [kN]	d_z [mm]	mass [kg]	t [mm]	Layup
Start	11.0	48.3	0.336	2.52	[90°,0°,90°,0°,45°,-45°,45°,-45°]s
Option 1	6.52	55.5	0.297	1.49	[90°,0°,90°,0°,45°,-45°,45°,-45°]s
Option 2	7.44	57.9	0.332	1.61	[90°,0°,90°,0°,45°,-45°,45°,-45°]s

The initial design only uses 80% of the allowed intrusion since a further reduction of the thickness would lead to a complete failure of the structure without stopping the mass. The new topologies meet the requirements to only consist of 3 chambers and are able to reduce the maximum force by 41% respectively 32%.

Since the optimization with continuous thicknesses delivers designs, that cannot be manufactured, the layups of the 3 designs are matched with the best fitting available stacking sequence for the inner and outer walls and new simulations are carried out (results in Table 3).

Table 3: Results of the adjusted designs

Adjusted Design	F_{max} [kN]	d_z [mm]	mass [kg]	t_{inner} [mm]	t_{outer} [mm]	Layup
Start S	15.3	26.0	0.372	-	2.8	[90°,0°,90°,0°,45°,-45°,45°,-45°]s
Option1 O1	7.72	55.3	0.313	1.87	1.4	[90°,0°,45°,-45°]s
Option2 O2	8.14	57.9	0.326	1.87	1.4	[90°,0°,45°,-45°]s

4 COMPARISON OF SIMULATION AND EXPERIMENT

For each adjusted design five test examples are manufactured by vacuum infusion and later glued together to create the structures displayed in Figure 8. Three of each structure are then tested in a drop tower and the results are compared with the simulations. The tests should deliver more knowledge about crash applications with composite profiles and point out necessary adjustments of the flange creation and new proposals for heuristics. Since not all structures are able to stop the drop weight before it hits the puffer elements, one of each structure is tested with a lower velocity of 2.45 m/s.

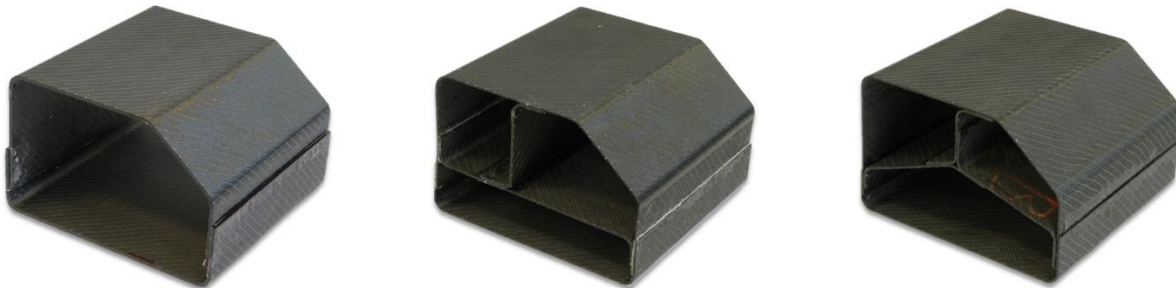


Figure 8: The manufactured profiles

4.1 Startin desig n S

As displayed in Figure 9 and Figure 10 all tests of the start design S as well as the simulation are able to stop the drop weight although the maximum intrusion varies between 20 mm for experiment S-3 with the lower velocity and 40 mm for S-1. The simulation S-Sim delivers the highest peak force of 15.3 kN whereas the tests show more smooth force curves that reach between 9.6 and 12.8 kN. The general deformation behavior from the tests matches the simulation quite well, although the simulation develops a crack in the upper left corner. All flange connections remain undamaged during the tests and the simulation.

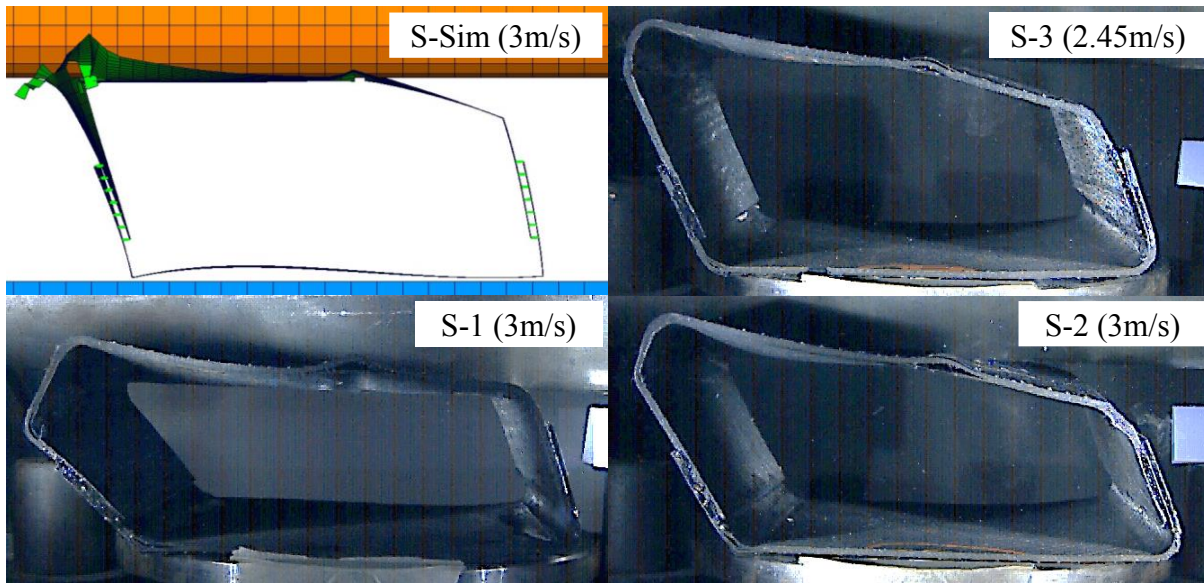


Figure 9: Deformations of the start designs S

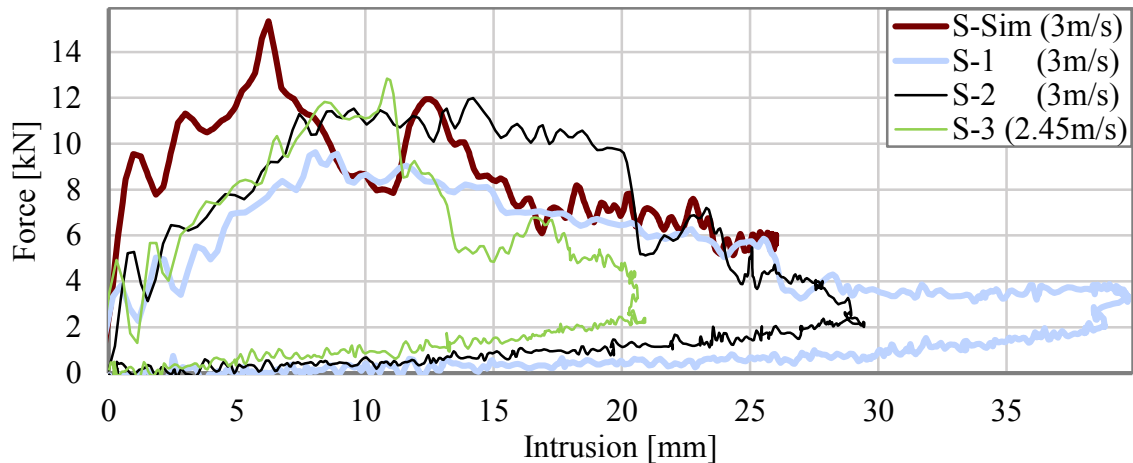


Figure 10: Force curves of the start designs S

4.2 Optimization result O1

Figure 11 reveals more differences between the deformation behavior of the simulation and the tests. While the upper wall is torn apart in the simulation and some more areas experience damage, the tests reveal failing flange connections that in case of O1-2 even lead to the drop weight crushing the structure and only getting stopped by the puffer elements. During the deformation of O1-1 and O1-3 the flange on the left side fails but the perpendicular middle wall gets in contact with the ground and stays stable so that it increases the resistance against the drop weight and stops it. The force curves in Figure 12 also reveal the differing deformation behaviors. The maximum forces range between 5.3 kN for O1-3 and 10.4 kN for O1-1, although O1-2 could have also experienced a peak at the end if the energy of the drop weight had not been absorbed by the puffers, that were placed next to the force measuring plate. The intrusions vary between 52.1 mm (O1-3) and more than 81.8 mm (O1-2).

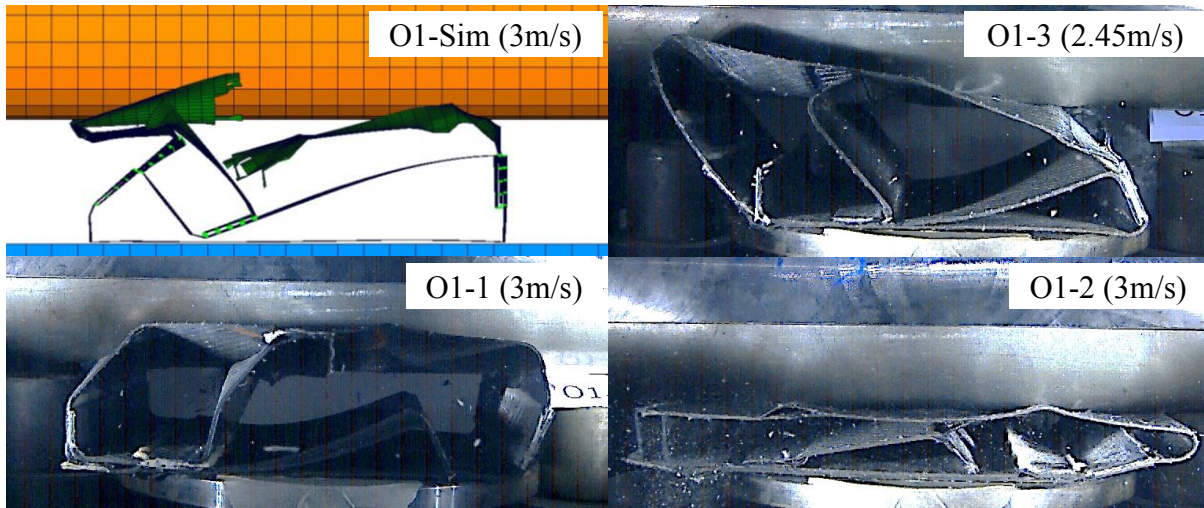


Figure 11: Deformations of the options 1 (O1)

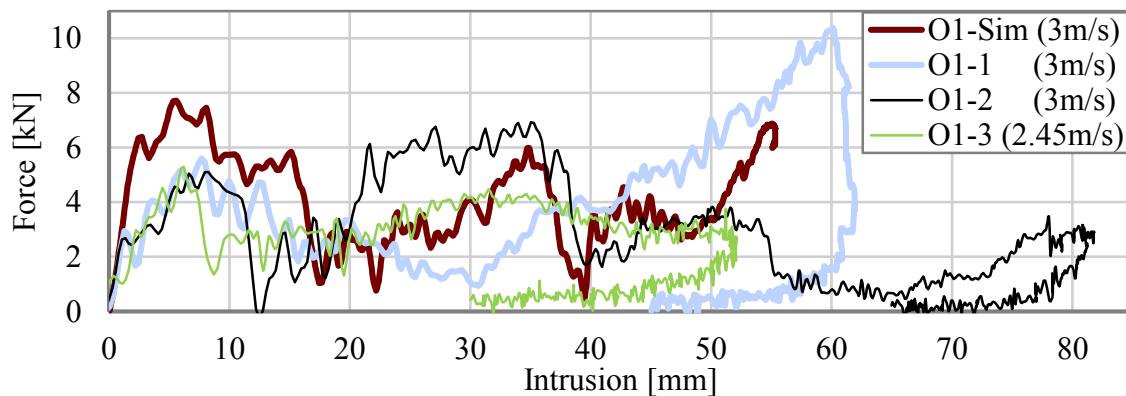


Figure 12: Force curves of the options 1 (O1)

4.3 Optimization result O2

The results for O2 are shown in Figure 13. The results of O2-1 do not exist since the recording failed. Nevertheless in comparison to O1 the same difference of tearing and failing walls in the simulation versus detached flanges in the tests occurs. During the tests the perpendicular walls get in contact with the ground and resist against the drop weight and cause a higher force level towards the end of the simulation (Figure 14). The forces vary between 5.9 kN for O2-3 and 8.1 kN for O2-Sim and the intrusions between 57.9 mm for O2-Sim and 75.4 mm for O2-2, which comes slightly in contact with the puffer elements. Both tests exceed the allowed intrusion of 60 mm.

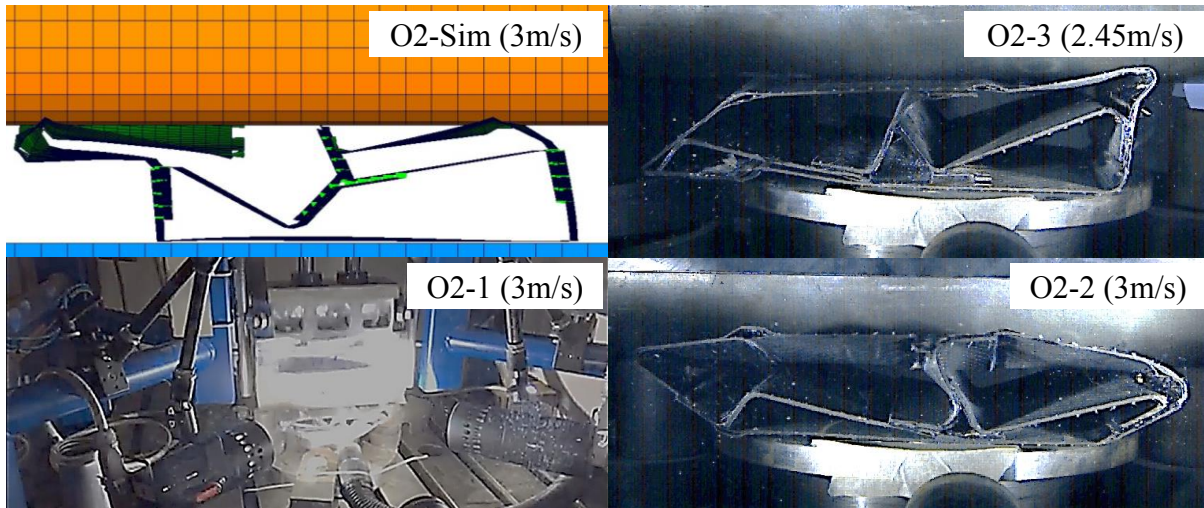


Figure 13: Deformations of the options 2 (O2)

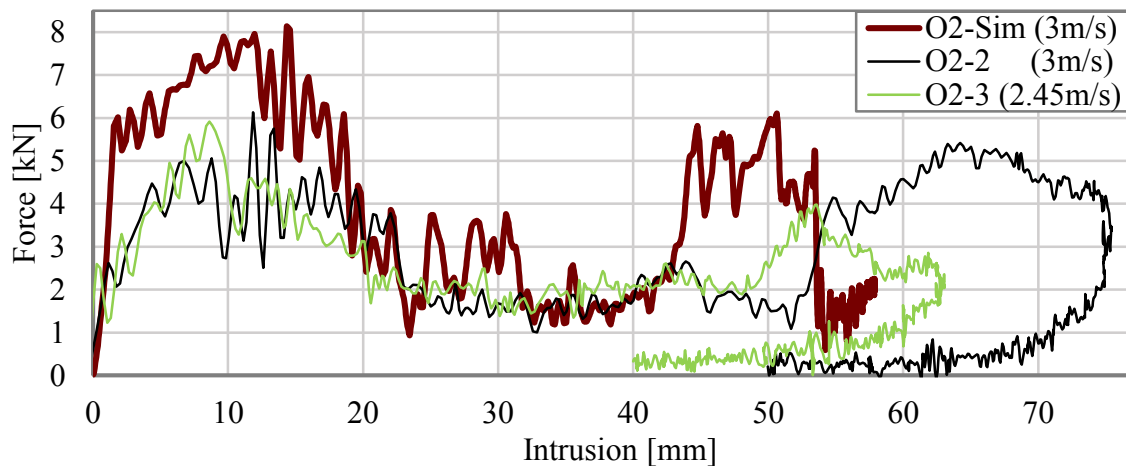


Figure 14: Force curves of the options 2 (O2)

CONCLUSIONS

This paper presents the adaptations that are necessary to consider composites during the optimization with the Graph and Heuristic Based Topology Optimization in a crashworthiness application. First, flange connections were introduced that allow to split the structure in several parts and enable to manufacture the structures by vacuum infusion without undercuts. Then a new heuristic was presented, that detects areas with sudden element failure and supports these locations with perpendicular walls. Also new options for composite specific design variables were presented. To demonstrate the process, the method was applied for a composite profile that is laterally impacted by a drop weight. During an optimization the maximum occurring force was minimized by up to 41% while not exceeding the maximum allowed intrusion. Since an optimization with discrete specified composite layups is not implemented yet, the layups of three chosen optimization designs were adjusted to fit the available composite stacks. The comparison between the drop tests and the simulations shows great deviations in the mechanical behavior. Especially the modeling of the adhesive does not depict the real behavior and underlines the importance of material testing. In addition the manufacturing by hand certainly favoured differing results. The start designs deformed more stable, but were not able to utilize the full potential of the allowed deformation space. In contrast the tests of the optimized designs exceed the intrusion restriction and show an undesired deformation behavior with risk of losing the structural integrity, which is caused by the more complex structures and the failing flanges. None of the structures experienced crushing during the tests, which is an important mechanism to increase the specific energy absorption of the composite. New heuristics could try to favour this mode of failure, although walls in lateral impacts rather tend to bending and breaking.

The method will be enhanced in further projects to fully capture the optimization of composite structures. Working with heuristics that analyze simulation data and suggest producible designs is a great opportunity for the optimization of crashworthiness applications in the future, where currently most structures are designed by empirical knowledge or trial and error without maxing out the potential of the structures.

REFERENCES

- [1] C. Ortmann and A. Schumacher, Graph and heuristic based topology optimization of crash loaded structures, *Structural and Multidisciplinary Optimization*, 47 (6), 839-854, 2013.
- [2] M. P. Bendsøe and O. Sigmund, *Topology Optimization*, Springer-Verlag, Berlin Heidelberg, 2004.
- [3] A. Schumacher, *Optimierung mechanischer Strukturen*, Springer-Verlag, Berlin Heidelberg, 2013.
- [4] J. Fang, G. Sun, N. Qiu et al., On design optimization for structural crashworthiness and its state of the art, *Structural and Multidisciplinary Optimization*, 55 (3), 1091-1119, 2017.
- [5] D. Schneider, A. Schumacher, Finding best layouts for rips on surfaces for crash loads using the Graph and Heuristic Based Topology Optimization, *Advances in Structural and Multidisciplinary Optimization, Proceedings of the 12th World Congress of Structural and Multidisciplinary Optimization (WCSMO12)* Springer Nature, 1615-1628, 2018

A Leray Regularized Ensemble-Proper Orthogonal Decomposition Method for Parameterized Convection-Dominated Flows

Michael Schneier^{*}, Traian Iliescu^{**}, Max Gunzburger^{***}

^{*}Florida State University, ^{**}Virginia Tech, ^{***}Florida State University

ABSTRACT

Partial differential equations (PDE) are often dependent on input quantities which are inherently uncertain. To quantify this uncertainty these PDEs must be solved over a large ensemble of parameters. Even for a single realization this can be a computationally intensive process. In the case of flows governed by the Navier-Stokes equation, a method has been devised for computing an ensemble of solutions. Recently a reduced order model derived from a proper orthogonal decomposition (POD) was incorporated into a newly developed ensemble algorithm. Although the ensemble-POD method was successful in the numerical simulation of laminar flows, it yields numerical inaccuracies for convection-dominated flows. In this work we put forth a regularized model, the Leray ensemble-POD model, for the numerical simulation of convection-dominated flows. The Leray ensemble-POD model employs spatial filtering to smooth (regularize) the convection term in the Navier-Stokes. For the new Leray ensemble-POD algorithm, we also propose a numerical discretization with better stability properties than those of the numerical scheme for the standard ensemble-POD method. For this new numerical discretization, we prove its stability and convergence. Furthermore, we show that the Leray ensemble-POD method is more accurate than the standard ensemble-POD method in the numerical simulation of a two-dimensional flow between two offset circles.

Mapped Tent Pitching Schemes for Hyperbolic Systems

Joachim Schoeberl^{*}, Jay Gopalakrishnan^{**}, Christoph Wintersteiger^{***}

^{*}TU Wien, ^{**}Portland State University, ^{***}TU Wien

ABSTRACT

A spacetime domain can be progressively meshed by tent shaped objects. Numerical methods for solving hyperbolic systems using such tent meshes to advance in time have been proposed previously. Such schemes have the ability to advance in time by different amounts at different spatial locations. This paper explores a technique by which standard discretizations, including explicit time stepping, can be used within tent-shaped spacetime domains. The technique transforms the equations within a spacetime tent to a domain where space and time are separable. After detailing techniques based on this mapping, several examples including the acoustic wave equation and the Euler system are considered. J. Gopalakrishnan, J. Schoeberl and C. Wintersteiger, "Mapped tent pitching schemes for hyperbolic systems", SIAM J. Sci. Comput. 39-6 (2017), pp. B1043-B1063

On the Fly Coarse-Graining in Molecular Dynamics Simulations: Adaptive Identification of the Dimensionality

Markus Schoeberl^{*}, Nicholas Zabaras^{**}, Phaedon-Stelios Koutsourelakis^{***}

^{*}Center for Informatics and Computational Science, University of Notre Dame, USA, ^{**}Center for Informatics and Computational Science, University of Notre Dame, USA, ^{***}Technical University of Munich, Germany

ABSTRACT

The efficient exploration of the configurational space of non-trivial molecular compounds retains a challenging problem and is subject to current and future research. We present a general framework for enhancing sampling of highly complex distributions e.g. occurring in peptide simulations having several local free-energy minima by biasing the dynamics and learning a probabilistic coarse-grained (CG) model simultaneously. Its main component represents a Bayesian CG model which is trained on the fly during the simulation of the target distribution. We in turn use insights, gathered from that CG model, to bias the fine-grained potential in order to enhance the exploration of the configurational space and overcome high energy barriers. Next to biasing dynamics, the CG model serves as probabilistic predictor while we quantify the epistemic uncertainty arising due to information loss. An important component of the presented methodology builds the coarse-to-fine mapping which implicitly extracts lower dimensional collective variables, the CG variables. Those potentially reveal physical insight from the data. We propose a mixture model serving as coarse-to-fine mapping while we sequentially add mixture components and increase the mapping's flexibility. Moreover, the complexity of the employed components is consecutively increased by adding features based on an information theoretic metric. A second critical question pertains to the dimensionality of the CG variables. The advocated information theoretic metric is crucial for the adaptive identification of the dimensionality of collective variables. We demonstrate the capabilities of the proposed methodology in the context of peptide simulations.

Utilizing Topology Optimization for the Design of Mechanical Test Fixtures to Optimize Dynamic Response

Tyler Schoenher^{*}, Peter Coffin^{**}

^{*}Sandia National Laboratories, ^{**}Sandia National Laboratories

ABSTRACT

Topology optimization is being used for many applications around the industrial world with objectives defined to reduce weight, minimize stress, and reduce costs through various means. Less common objective functions seek to match the dynamics (i.e. frequency response, mode shapes etc.) of a target model. One reason for optimizing on dynamic objectives would be to create shock and vibration test fixtures for laboratory tests. The goal of test fixture design is to replicate field hardware in a test laboratory. The dynamics of the test fixture affect how successful that effort is. This presentation will examine test fixture design utilizing topology optimization with dynamic objective functions to improve their performance.

Advances of a General Model for Tumor Growth and Drug Delivery

Bernhard A. Schrefler*, Raffaella Santagiuliana**, Johannes Kremheller***, Pietro Mascheroni****, Lena Yoshihara*****, Wolfgang A. Wall*****, Paolo Decuzzi*****

*Ias-Technical University of Munich, **Italian Institute of Technology, Genova, ***Technical University of Munich, ****University of Padua, *****Technical University of Munich, *****Italian Institute of Technology, Genova

ABSTRACT

We have developed a tumor growth model at macroscopic scale (tissue scale) based on first principles according to the concepts of transport onco-physics which state that physical properties of biological barriers control cell, particle, and molecule transport across tissues and this transport and its deregulation play an overarching role in cancer physics. The model allows not only for growth, hypoxia, necrosis and lysis of the tumor cells but also for invasion into the healthy tissue, transport of therapeutic agents and signalling molecules, mass exchange between the interstitial fluid and the cell populations, and angiogenesis. Further it includes deposition and remodelling of the extracellular matrix; the possibility of migration of the tumor cells through an existing ECM as is needed in case of ex-vivo experiments on decellularized extracellular matrix; the possibility of accounting for different interfacial tensions between the tumor cell, healthy cells, ECM, and interstitial fluid; mass exchange between the newly created and co-opted blood vessels and the interstitial fluid. All these features have been obtained with a growth model where the cell populations are treated as fluid phases, moving in a deformable ECM. Up to now the model was a four phases model consisting of tumor cells, healthy cells, interstitial fluid and extracellular matrix. Newly created vessels were modelled as a species of the IF. The model has now been extended to comprise the newly created vessels as a proper fifth phase which impacts the pores space. Further a diffusion advection equation has been added for the transport of therapeutic agents to the tumor. This model now allows to evaluate the efficacy of treatments which may either be based on chemotherapy or nanoparticle mediated drug delivery. Michor, F., J. Liphardt, M. Ferrari, and J. Widom, What does physics have to do with cancer? *Nat Rev Cancer*, (2011), 11(9): pp. 657-670. Santagiuliana, R., M. Ferrari, and B.A. Schrefler, Simulation of angiogenesis in a multiphase tumor growth model. *Computer Methods in Applied Mechanics and Engineering*, (2016), 304: pp. 197-216. Mascheroni, P., et al., Predicting the growth of glioblastoma multiforme spheroids using a multiphase porous media model. *Biomechanics and Modeling in Mechanobiology*, (2016), 15(5): pp. 1215-1228.

On Mixed Least-squares Finite Element Formulations for Finite J2 Plasticity

Jörg Schröder*, Maximilian Igelbüscher**, Alexander Schwarz***

*University of Duisburg-Essen, **University of Duisburg-Essen, ***University of Duisburg-Essen

ABSTRACT

The accurate approximation of the stress field is one important aspect in the field of elasto-plasticity, since the stresses are mainly responsible for the evolution of plastic deformations. Therefore, we discuss in this contribution an element formulation based on the least-squares finite element method (LSFEM) for finite J2 plasticity, see [3], where the stresses besides the displacements are used as an unknown field. A drawback within the consideration of elasto-plasticity using the LSFEM is that the variational approach given e.g. in [1], could lead to a discontinuity within the first variation of the functional initiated by the additional plastic constraint in the constitutive equation, see e.g. [2]. Thus, to avoid this drawback a modification of the method is performed to obtain a continuous first variation. Furthermore, an extended formulation is constructed by adding an additional redundant third residuum in order to enforce stress symmetry condition. For simplicity we restrict ourselves to a Neo-Hookean material model with a von Mises yield criterion regarding linear isotropic hardening. The numerical analysis is performed using a RTmPk finite element type, where m denotes the polynomial order of the stress approximation using vector-valued Raviart-Thomas functions and k is the interpolation order of the displacements considering standard Lagrange functions. Acknowledgment The authors acknowledge support by the Deutsche Forschungsgemeinschaft in the Priority Program 1748 “First-order system least squares finite elements for finite elasto-plasticity” (SCHR 570/24-1 and SCHW 1355/2-1). References [1] Z. Cai and G. Starke, Least-squares methods for linear elasticity. *SIAM Journal on Numerical Analysis*, 42, 826–842, 2004. [2] A. Schwarz and J. Schröder and G. Starke, Least-squares mixed finite elements for small strain elasto-viscoplasticity. *IJNME*, 77, 1351–1370, 2009. [3] J.C. Simo, Numerical analysis and simulation of plasticity. In P.G. Ciarlet and J.L. Lions, editors, *Handbook of numerical analysis*, No. 6. Elsevier Science, 1998.

The Logarithmic Finite Element Method: Approximation on a Manifold in the Configuration Space

Christian Schröppel*, Jens Wackerfuß**

*University of Kassel, **University of Kassel

ABSTRACT

The Logarithmic finite element method extends the Ritz-Galerkin method to approximations on a non-linear finite-dimensional manifold in the infinite-dimensional solution space. Formulating the interpolant on the logarithmic space allows for a novel treatment of the rotational component of the deformation, making this approach especially suitable for geometrically exact formulations involving large rotations. Using homogeneous coordinates, the logarithms of transformation matrices representing rotations and translations are given as elements of a linear subspace of the set of affine transformations, generating a Lie algebra. The degrees of freedom present in a finite element based on the LogFE method are associated with vector-valued shape functions which constitute the basis vectors of that subspace. Given an appropriate formulation of the finite elements, local degrees of freedom related to rotations and translations can be linked to global degrees of freedom and boundary conditions, and the interpolant is given by an immersion of the space of degrees of freedom into the configuration space. Thus, the LogFE method satisfies the general criteria for finite element models as given by Ciarlet [1]. A co-rotational formulation enables the model to exactly represent pure rigid body motions. This co-rotational formulation must also ensure that spurious high-order deformation components vanish with mesh refinement, in order to satisfy the interpolation theorem for finite elements [2]. Expanding on the work in [3], the authors will present co-rotational, geometrically exact formulations for both planar and spatial beam elements endowed with Bernoulli and Timoshenko kinematics. [1] Ciarlet, P.G. (1979) *The Finite Element Method for Elliptic Problems*. North-Holland, Amsterdam. [2] Oden, J.T. and Reddy, J.N. (2011) *An Introduction to the Mathematical Theory of Finite Elements*. Dover, Mineola. [3] Schröppel, C. and Wackerfuß, J. (2016) *Introducing the Logarithmic finite element method: a geometrically exact planar Bernoulli beam element*. *Advanced Modeling and Simulation in Engineering Sciences*, 3 (1).

A High-Order Method for Weakly Compressible Flows

Jochen Schuetz*, Klaus Kaiser**

*Universiteit Hasselt, **RWTH Aachen University

ABSTRACT

It is well-known that the Euler equations at low Mach number constitute a singularly perturbed system of equations as the speed of sound approaches infinity. Classical methods known from aerodynamics tend to fail because of the stiffness in the system. In particular, approaches based on purely explicit time integration suffer from a severe CFL restriction. On the other hand, purely implicit schemes introduce an excessive amount of numerical diffusion and, because the equations are nonlinear, are algebraically more difficult to solve. A remedy suggested in recent years is the use of mixed implicit/explicit (IMEX) time integration. IMEX schemes require a suitable identification of 'stiff' (to be treated implicitly) and 'non-stiff' (to be treated explicitly) terms. This is a highly nontrivial endeavor, because the splitting dictates such important features as stability, accuracy and efficiency. In this talk, we present a recently developed splitting [1-3] based on the incompressible limit solution of the Euler equations. Properties of the splitting are first discussed in a simplified, yet very instructive, ODE setting. The idea is then extended to the treatment of low Mach flows. We show that the combination of a discontinuous Galerkin scheme and IMEX time integration is asymptotically consistent, meaning that the discrete limit can be seen as an approximation to the incompressible limit. Numerical results demonstrate the behavior of the scheme. [1] Schütz, Kaiser, A new stable splitting for singularly perturbed ODEs, Applied Numerical Mathematics, Vol. 107, pp. 18-33, 2016 [2] Kaiser, Schütz, Schöbel, Noelle, A new stable splitting for the isentropic Euler equations, Journal of Scientific Computing, Vol. 70, pp. 1390-1407, 2017 [3] Kaiser, Schütz, A high-order method for weakly compressible flows, Communications in Computational Physics, Vol. 22, pp. 1150-1174, 2017

ON THE CURRENT NEED OF EXPERT RULES FOR THE TOPOLOGY OPTIMIZATION OF STRUCTURES WITH NON-LINEAR BEHAVIORS

AXEL SCHUMACHER

University of Wuppertal, Chair for Optimization of Mechanical Structures
Gaußstraße 20, 42119 Wuppertal, Germany
e-mail: schumacher@uni-wuppertal.de; website: <https://www.oms.uni-wuppertal.de/>

Key words: topology optimization, crash structures, non-linear material behavior, expert rules, heuristic.

Abstract. *In order to optimize the topology of structures with non-linear structural behavior like crash structures, pure mathematical optimization methods do not exist. This contribution shows the possibilities of the involving of expert rules and derived heuristics in the optimization process. It is a very interesting possibility to avoid time-consuming sensitivity calculations. Two methods are evaluated more precisely: The Hybrid Cellular Automaton (HCA), which works with one special rule and the Graph and Heuristic based Topology Optimization (GHT). The opportunities to find powerful design rules generated by experts or by analysis and clustering of many simulation data (big data) are shown. Supported by benchmarks examples, this contribution shows the limitation of optimization methods without expert rules and offers an overview of the possibilities to apply expert rules as an important part in an automatic topology optimization process.*

1 PROBLEM DESCRIPTION

Topology optimization for the layout finding of structures is commonly used for linear static mechanical problems within the industry. The most often used approach is the subdividing of the topology domain in small parts (pixel or voxel) and to distinguish whether there is material or not ^[1]. E.g. the well-known homogenization method minimizes the mean compliance considering a mass constraint. These methods work very fast, because they use existing analytical sensitivities of the most relevant objectives like mean compliance, stresses or mass.

Regarding to crash-loaded structures with highly non-linear behavior, there are a lot of more complex objectives and constraints:

- Consideration of special acceleration values like the head injury criterion (HIC-value)
- Energy absorption,

Axel Schumacher

- Special force levels,
- Smooth force-displacement curve,
- Smooth acceleration-time curve,
- Special force paths for special loadcases.
- High stiffness of special parts, e.g. parts in a main force paths in the passenger area
- Low stiffness of special parts, e.g. at positions of the head contact of a pedestrian,
- Special safety criteria, e.g. no leakage of the petrol system.

In addition to these optimization functions, the behavior of the crash-loaded structures is strongly non-linear, normally calculated by the explicit finite element approach:

- Material plasticity and material failure models
- Geometric nonlinearities
- Contact phenomena
- Numerical and physical bifurcation points
- Non-smooth structural responses
- Mesh dependent results
- No analytical determination of the sensitivities (explicit time integration)
- Huge number of local optima in the design space

There are two possibilities for the definition of the design variables. The first possibility is the density of the material in the already mentioned small parts. Therefore there are millions of design variables. The second possibility is the CAD description of the structural elements e.g. by support of graph theory.

There is an urgent need of topology optimization methods for crash-loaded structures. Especially the automotive industry needs support from the optimization society, e.g. for fulfilled legal requirements. There, it is necessary to find new ideas for efficient methods. The considering of mean compliance and stress constraints is not enough. It is necessary to involve all relevant objectives and constraint functions.

2 POSSIBILITY: TOPOLOGY DERIVATIVES FOR NON-LINEAR PROBLEMS

It is very costly and often not beneficial to generate sensitivities by using explicit finite element calculations. Research activities to find efficient methods of necessary Topological Derivatives (TD) exist ^[2,3]. The idea is to find analytical or semi-analytical descriptions of the Topological Derivatives for an arbitrary state of displacements and stresses. For a functional $J(\Omega)$, the Topological Derivative is described by

$$TJ(x) = \lim_{\rho \downarrow 0} \frac{J(\Omega \setminus \overline{B_\rho(x)}) - J(\Omega)}{|B_\rho(x)|}. \quad (1)$$

Here, $B_\rho(x)$ denotes a ball (in a 3D structure) or a hole (in a 2D structure) with the radius. As an example, Figure 1 shows the scheme for the calculation of the Topology Derivatives depending on the principal stresses.

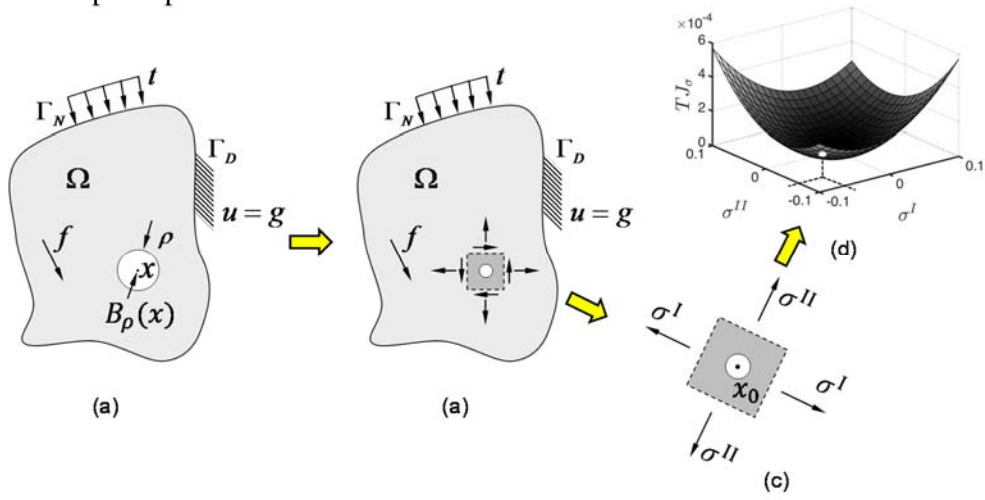


Figure 1: Calculation of Topological Derivatives depending on the principal stresses: a) mechanical Problem, b) Identification of the state in the area of the hole, c) Submodel for the numerical calculation of the Topology Derivatives, d) Meta-model of the Topological Derivatives depending on the principal stresses ^[2]

For creating the sample points for calculating the meta-model of the Topological Derivatives, the finite element model with a non-linear material behavior shown in Figure 2 is used as basic for the approximation in figure 3.

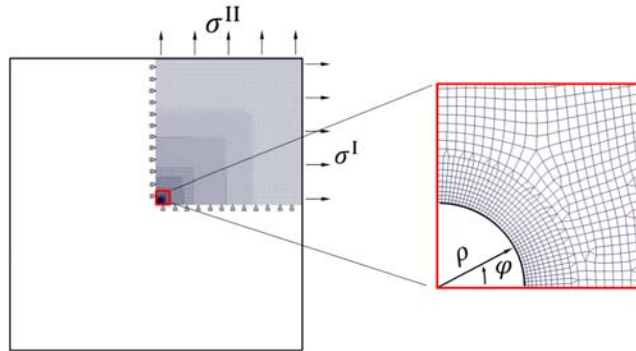


Figure 2: Finite element model with a non-linear material behavior ^[2]

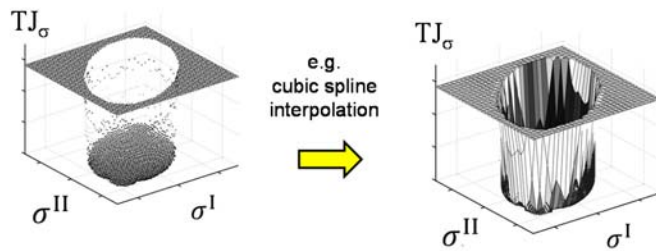


Figure 3: Approximation of the Topological Derivative depending on arbitrary principal stresses ^[2]

The research of finding Topology Derivatives is still at the beginning and it needs additional years to find a solution for structures with a highly non-linear behavior.

3 EXPERT RULES IN THE OPTIMIZATION PROCESS

Expert rules are a powerful possibility to avoid the need for the calculation of sensitivities. The idea is the addition of these automatic expert rules in the optimization process (Figure 4).

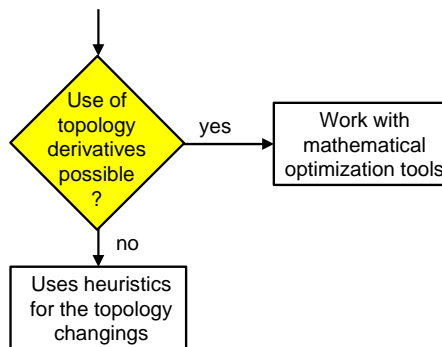


Figure 4: Practical approach for the topology optimization of structures with non-linear behavior

3.1 One-rule approaches - example: Hybrid Cellular Automaton (HCA)

The Hybrid Cellular Automaton (HCA) ^[4] is one example of an expert rule. The modification of the structure is carry out by finding a homogeneous distribution of the inner energy density. Neighboring elements in the Cellular Automaton lattice are considered. There is a direct connection of Cellular Automaton lattice and finite element mesh. The HCA is a density approach dealing with relative densities. A rule homogenizes the energy density in a way that no sensitivity calculation are necessary.

3.2 Competing rules approach - example: Graph and Heuristic based Topology Optimization (GHT)

For complex optimization tasks as mentioned in chapter 1, there is a need to consider different competing heuristics. The Graph and Heuristic based Topology Optimization (GHT) [5] combines topology, shape and sizing optimizations in one optimization process. It uses widely used finite element shell models for executing crash simulations. The optimization task is divided into an outer optimization loop, which performs the topology optimization with heuristics (derived from expert rules) and an inner optimization loop, which performs the mathematical shape optimization and sizing to evaluate the design. The heuristics use result data of finite element simulations like strains, stresses, displacement, velocities and accelerations. Based on this information the heuristics make proposals for modifications of the structure. Figure 5 shows the basic scheme of the GHT. For the flexible geometry description, mathematical graphs are used. The heuristics are used to perform structural modifications. The optimization problem is devised into two optimization loops, the outer loop for the structural modifications performed by heuristics (mainly topology changes) and the inner loop with a common shape and/or sizing optimization for a design layout, which is coming from the outer loop. The GHT has different strategies of the combination of the topology changing by heuristics and the shape optimization. E.g. the tracking of E competing designs in parallel (with $E \geq 1$) comes to a branching strategy to avoid local optima. A higher E leads to a higher probability to skip local optima, but leads to higher computer time.

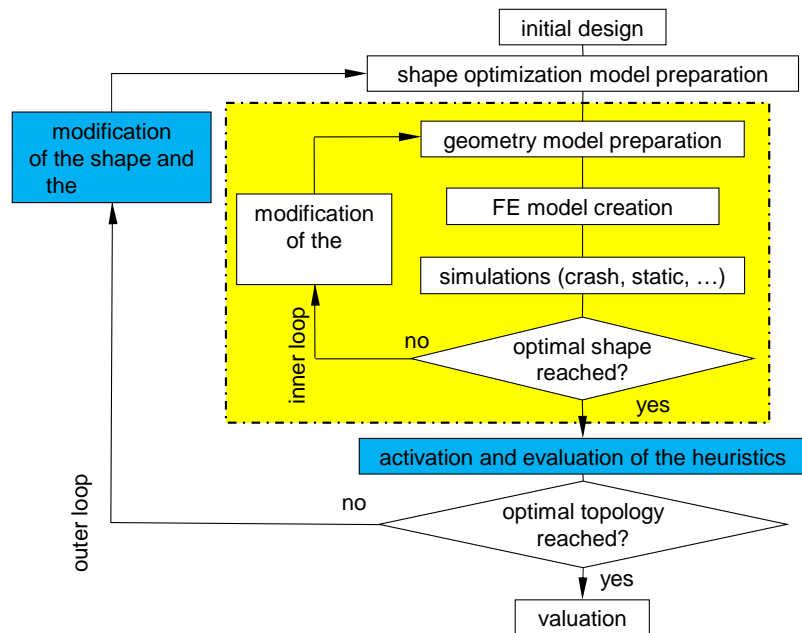


Figure 5: Basic scheme of the Graph and heuristic based topology optimization (GHT)

4 GENERATION OF RULES FROM EXPERT KNOWLEDGE

There are two possibilities for generating rules, first the organization of brainstorming meetings with experts and secondly the clustering of many simulation data (big data) ^[7]. This chapter has the focus on brainstorming meetings with crash development groups of several car producers ^[8]. Some results are sorted in the following list:

Increasing the stiffness in crash:

- Support components with buckling tendency
- Increasing of corner stiffness
- Inserting of Y-junctions
- Split high-loaded structures.
- No arch shaped components
- Use the full design domain:
- Filling of large cutouts
- If the torsion is to large, insert circular structures
- ...

Reducing the stiffness in crash:

- Including of crash elements
- Arching of straight components
- Inserting of triangle cutouts
- ...

Simplification:

- Delete unloaded components
- Use a small number of chambers
- ...

Balancing the energy density:

- Homogenize the buckling length
- Moderate changing of the wall thickness
- ...

Manufacturing constraints:

- Boundaries of the wall thicknesses,
- Boundary of the angle between two walls,
- Boundary of the distance between two walls
- ...

Based on the results of the brainstorming meetings the heuristics are implemented in the GHT software. Figure 6 shows the basic heuristics.

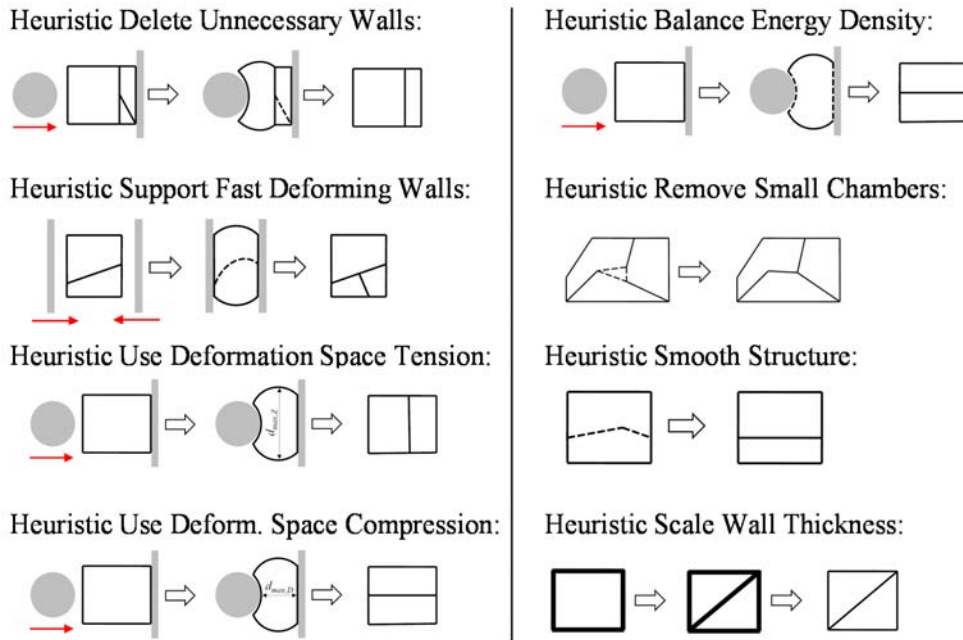


Figure 6: Examples of the implemented heuristics

5 BENCHMARK OPTIMIZATION RESULTS

Supported by benchmarks examples, this contribution shows the limitation of optimization methods without expert rules and offers an overview of the possibilities of using expert rules as an important part in an automatic topology optimization process.

5.1 Cantilever frame structure

The considered cantilever frame structure is shown in Figure 7. The optimizer has to find an optimal layout of walls in the structure. The optimization tasks are the following:

- Application 1: minimize maximum intrusion so that the frame mass ≤ 0.027 kg
- Application 2: minimize maximum acceleration so that the intrusion ≤ 49 m

The manufacturing constraints for both applications are:

- $0.5 \text{ mm} \leq \text{wall thickness} \leq 10 \text{ mm}$
- wall distance $\leq 10 \text{ mm}$
- wall connection angle $\leq 15^\circ$

The HCA can only optimize application 1 without the given manufacturing constraints. The results are shown in figure 7.

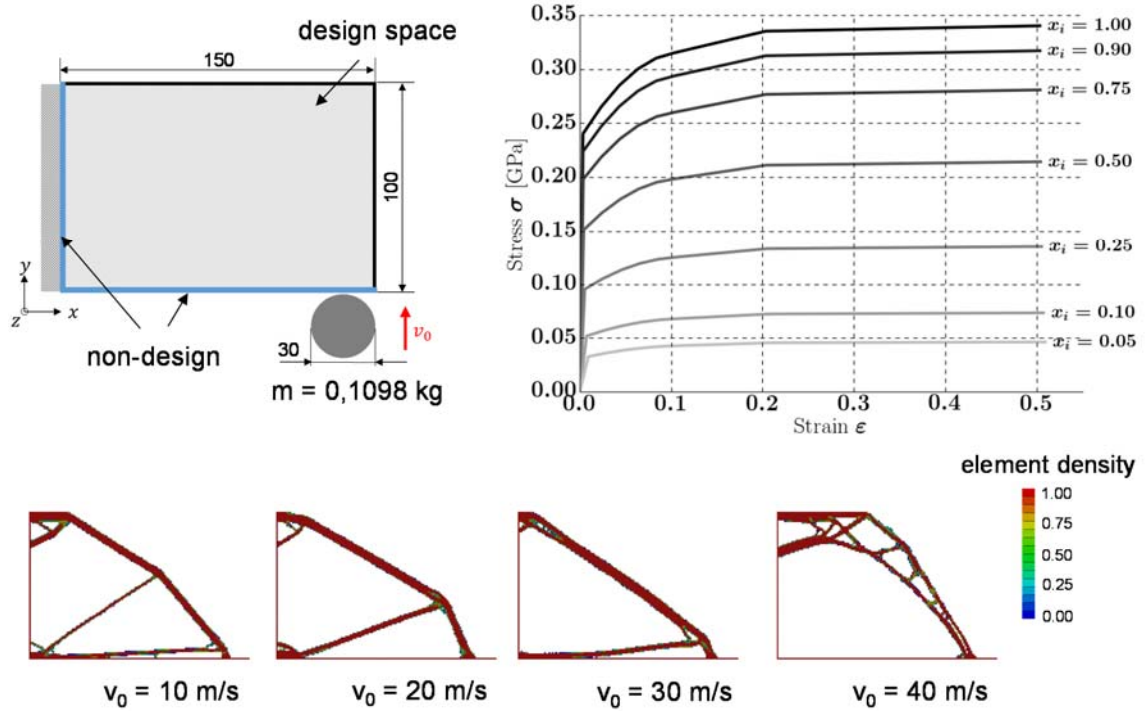


Figure 7: Maximum stiffness design with HCA for different initial velocities the mass m with the element density x_i [9]

Figure 8 shows the optimization results of the GHT.

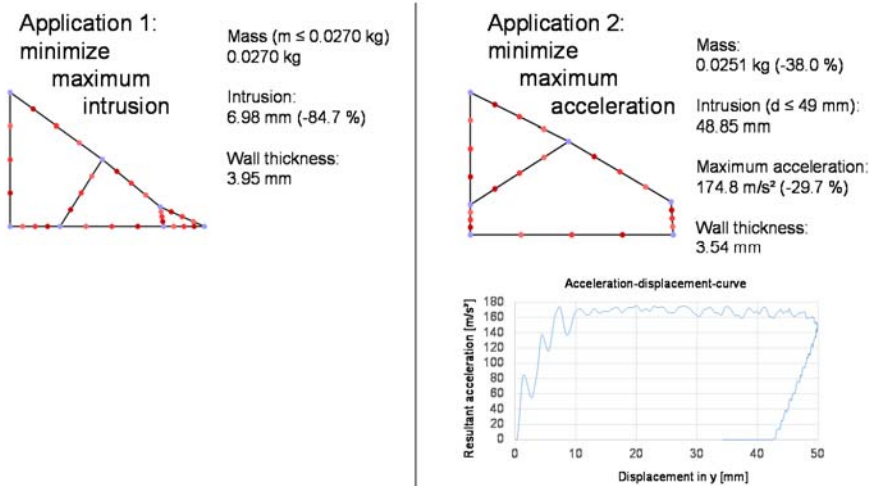


Figure 8: Maximum stiffness design with HCA for different initial velocities the mass m with the element density $v_0 = 25 \text{ m/s}$ x_i [5]

5.2 Rocker of a vehicle body-in-white structure

The optimization task is to find the optimal topology and shape of the cross section of the rocker profile shown in figure 9.

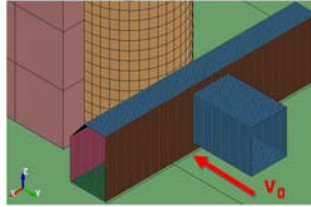


Figure 9: Mechanical problem of the rocker ^[6]

The objective is to minimize the maximal force at a moved rigid wall (velocity v_0), so that functional constraints

- mass ≤ 2.801 kg
- intrusion (pole crash) ≤ 70 mm
- stiffness(bending and torsion) ≥ 50 % stiffness initial design

and the manufacturing constraints

- $1.6 \text{ mm} \leq \text{wall thickness} \leq 3.5 \text{ mm}$
- distance of walls $\geq 10 \text{ mm}$
- connection angle of walls $\geq 15^\circ$
- maximum chamber size ration 1 : 20

are fulfilled. HCA is not able to optimize this problem, so figure 10 and 11 show only the GHT results.

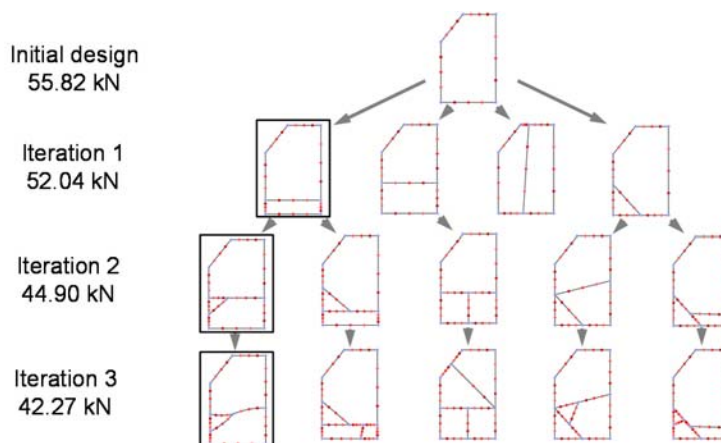


Figure 10: Optimization history (branching - competing designs) of the optimization of the rocker ^[6]

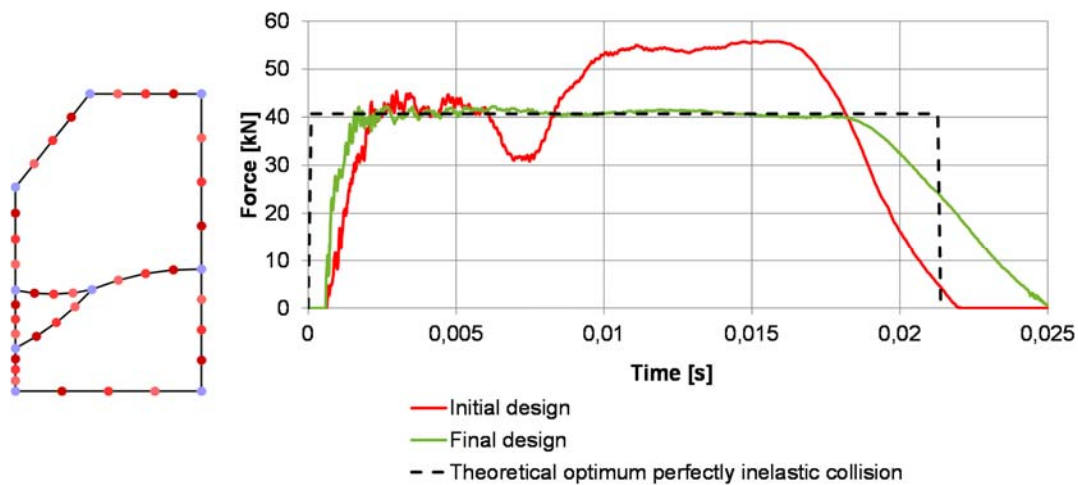


Figure 11: Optimization history (branching - competing designs) of the optimization of the rocker ^[6]

6 CONCLUSIONS

GHT and HCA as representatives of rule-based optimization methods provide interesting results, which cannot be achieved with purely mathematical methods. The expert knowledge based generation of powerful heuristics is time consuming. In the future, attention must be paid to a suitable interplay of mathematical methods and heuristics.

ACKNOWLEDGEMENT

The author thanks Katrin Weider for her contribution in the research project "Topological derivatives for layout generation of crash-loaded structures" funded by the German Research Foundation (DFG-No. Schu915/4-1, project number 350645830). He also thanks Christian Olschinka, Christopher Ortmann and Dominik Schneider for their works in the GHT method. He is also pleased about the numerous hints of the crash engineers of the German automotive industry in the scope of the research project "Methodological and technical realization of the topology optimization of crash loaded vehicle structures" funded by the German Federal Ministry for Education and Research within the scope of the research project ".

REFERENCES

- [1] M. P. Bendsøe and O. Sigmund, Topology Optimization, Springer-Verlag, Berlin Heidelberg, 2004.

Axel Schumacher

- [2] K. Weider and A. Schumacher, A., On the calculation of Topological Derivatives considering an exemplary nonlinear material model, *Proc. Appl. Math. Mech.* 16, 717-718, 2016.
- [3] K. Weider and A. Schumacher, A topology optimization scheme for crash loaded structures using Topological Derivatives, *Advances in Structural and Multidisciplinary Optimization, Proceedings of the 12th World Congress of Structural and Multidisciplinary Optimization (WCSMO12)* Springer Nature, 1601-1614, 2018
- [4] N.M. Patel, B.S. Kang, J.E. Renaud and A. Tovar, Crashworthiness design using topology optimization. *J Mech Des* 131:061013.1–061013.12, 2009
- [5] C. Ortmann and A. Schumacher, Graph and heuristic based topology optimization of crash loaded structures, *Structural and Multidisciplinary Optimization*, 47 (6), 839-854, 2013.
- [6] C. Ortmann, Development of a graph and heuristic based method for the topology optimization of crashworthiness profile structures, *PhD thesis, University of Wuppertal*, 2014.
- [7] C. Diez, P. Kunze, D. Toewe, C. Wieser, L. Harzheim and A. Schumacher, A., Big-Data based rule-finding for analysis of crash simulations, *Advances in Structural and Multidisciplinary Optimization, Proceedings of the 12th World Congress of Structural and Multidisciplinary Optimization (WCSMO12)* Springer Nature, 396-410, 2018
- [8] A. Schumacher and C. Ortmann, Rule generation for optimal topology changes of crash-loaded structures, *Proceedings of the 10th World Congress on Structural and Multidisciplinary Optimization*, May 19 -24, 2013.
- [9] K. Weider, A. Marschner and A. Schumacher, A Systematic Study on Topology Optimization of Crash Loaded Structures using LS-TaSC, *Proc. of the 11th European LS-DYNA Conference 2017*, 9. - 11. Mai 2017, Salzburg, Austria, 2017

Characterization and Modeling of Spot Welds for Double-Lap Joints

Lilia Schuster*, Silke Sommer**, Vitali Schilow***

*Fraunhofer Institute for Mechanics of Materials IWM, **Fraunhofer Institute for Mechanics of Materials IWM,
***Fraunhofer Institute for Mechanics of Materials IWM

ABSTRACT

Resistance spot welding is still the most commonly used process in the production of the body-in-white. Extensive research conducted on spot-welded single-lap joints has provided a good understanding of this type of spot weld joints. However, in order to adequately address material efficiency and construction limit aspects, automobile engineers are increasingly incorporating joints, which connect three layers of metal sheets with one single spot weld. These joints introduce an increasing complexity for possible combinations in sheet thickness, materials and load application points. Due to this large number of possible configurations it is not feasible to encompass the entirety of combinations by experimental testing. Therefore, the use of finite element simulations is necessary to investigate additional configurations to describe the load bearing capacity, fracture behavior and energy absorption in a comprehensive manner. Loading types such as tension, shear, torsion and bending lead to complex local stress states which require sophisticated damage and failure models. The GTN model is used to model the ductile failure under tensile loading and loadings with higher triaxialities and produces accurate predictions for various applications, but it is not capable to describe shear failure. Therefore the Gologanu damage model with additional fracture criteria was used by Sommer [1] and by Burget [2] to overcome this issue and simulate failure behavior of spot-welded single-lap joints under shear loading. It was able to provide reliable failure predictions for maximum load as well as fracture locations for single-lap joints of similar and dissimilar steel sheet metal joints. In this paper the arising challenges and modeling approaches in characterization of double-lap spot weld joints are outlined. Different loading cases like shear, tension and bending are investigated with variation of load points and their influences on load bearing capacities and fracture behavior are investigated. Also the sheet thicknesses, strength of sheet metals and layer positions in the spot-welded joints are varied. Experimental data will be presented for validation of the simulation results. [1] Silke Sommer, Modeling the fracture behavior of spot welds using advanced micro-mechanical damage models, IOP Conf. Ser.: Mater. Sci. Eng. 10 012057, 2010. [2] Sebastian Burget, Silke Sommer, Modeling of deformation and failure behavior of dissimilar resistance spot welded joints under shear, axial and combined loading conditions, 13th International Conference on Fracture, ICF 2013 pp.1589-1600.

Structural Metrics for the Collaboration of Design and Simulation Departments in Complex Product Development

Sebastian Schweigert*, Markus Zimmermann**

*Technical University of Munich, **Technical University of Munich

ABSTRACT

When managing product development including different sub-disciplines, communication at interfaces is crucial. Together with the increasing number and complexity of mechanical simulations, communication and collaboration of design and simulation departments becomes a system demanding for complexity management to handle it. Otherwise, wasted resources and demotivation especially in simulation departments occur. For instance, information generated by numerical simulations is not used, as redundant tests are performed even though numerical simulations were already conducted or design changes proposed by simulation experts never make it into the real product. Often this results from lacking trust between the two departments as emphasized by the following quote: "No one trusts in [numerical] simulation results, except those, who conducted the simulation. Everyone trusts in testing results, except those, who conducted the test." (Head of simulation, household appliances company) This contribution investigates barriers between design and simulation departments and recommendations to overcome them. Complexity management and network analysis are applied on collaboration graphs consisting of persons, artefacts, tasks, and tools. A toolset is proposed using structural metrics for engineering design processes of Kreimeyer and Lindemann (2011). Each metric is connected to barriers identified in an online survey and subsequent interview study. They include for instance lacking information transmission from design to simulation – especially in early design phases. Structural metrics like the number of unconnected nodes can identify those barriers from system graphs to find critical areas. Consequently, improvement measures like regular change notifications can be implemented. In an exemplary company with design and simulation departments consisting of dozens of experts the issue of lacking trust described above is met by integrating simulation experts earlier into product development processes. Using e-mails exchanged within and between departments and calendars of meetings, as well as product and simulation data management systems that track artifacts like CAD models or numerical simulation reports, system graphs of the collaboration and communication are generated. Within the graphs, nodes represent persons, tasks, artifacts, and tools, while edges represent communication channels, responsibilities, and links between datasets. Identifying people poorly integrated in the information flow by deleting edges of communication channels below a certain frequency and extracting the resulting unconnected nodes gives the possibility of systematically improving collaboration and communication and integrating these persons. The contribution of the approach lies in the systematic identification of barriers and suitable measures to improve the communication and collaboration of design and simulation departments in order to reduce avoidable epistemic uncertainty.

U-splines

Michael Scott^{*}, Derek Thomas^{**}, Kevin Tew^{***}, Stephen Schmidt^{****}

^{*}Brigham Young University, ^{**}Coreform, ^{***}Coreform, ^{****}Coreform

ABSTRACT

U-splines are a new spline technology which allows for local changes in mesh size, polynomial degree, and smoothness. There are no restrictions on proximity of T-junctions and it works for all degrees and smoothnesses. The resulting basis is positive, forms a partition of unity, and is complete. In this talk, U-splines will be described and applied as a basis for isogeometric analysis.

The Shifted Boundary Method: An Embedded Framework for Computational Mechanics

Guglielmo Scovazzi^{*}, Alex Main^{**}, Nabil Atallah^{***}, Ting Song^{****}

^{*}Duke University, ^{**}Duke University & ANSYS, ^{***}Duke University, ^{****}Duke University

ABSTRACT

Embedded boundary methods obviate the need for continual re-meshing in many applications involving rapid prototyping and design. Unfortunately, many finite element embedded boundary methods for incompressible flow are also difficult to implement due to the need to perform complex cell cutting operations at boundaries, and the consequences that these operations may have on the overall conditioning of the ensuing algebraic problems. We present a new, stable, and simple embedded boundary method, which we call “shifted boundary method” (SBM), that eliminates the need to perform cell cutting. Boundary conditions are imposed on a surrogate discrete boundary, lying on the interior of the true boundary interface. We then construct appropriate field extension operators, with the purpose of preserving accuracy when imposing the boundary conditions. We demonstrate the SBM on large-scale incompressible flow problems, multiphase flow problems, solid mechanics problems, and shallow water flow problems.

Stress Correlations in Discontinuously Thickening Suspensions

Omer Sedes^{*}, Abhinendra Singh^{**}, Jeffrey F Morris^{***}

^{*}CUNY City College of New York, Levich Institute, ^{**}CUNY City College of New York, Levich Institute, ^{***}CUNY City College of New York, Levich Institute

ABSTRACT

Very concentrated suspensions can shear thicken abruptly, and this is called discontinuous shear thickening. In the present work, the underlying statistical physical basis for this change in properties, which has the appearance of a nonequilibrium phase transition, are developed in terms of the spatial correlations of various measures of the contact network. We base our understanding on numerical simulations by a method which captures lubrication hydrodynamics, contact forces including friction, and stabilizing repulsive force or Brownian motion. At low stress, lubrication between particles maintains low viscosity, while at large stress, the stabilizing force is overwhelmed and a contact network develops. The stress correlations in these states will be described, as will be various measures of the contact network, to elucidate the role of the exchange of lubricated interactions for true contact in the abrupt change in properties. The behavior of similar measures in microrheology simulation, where a body is pulled through the suspension, will be briefly considered.

Towards a Scientific Understanding of Non-Schmid Behavior and Latent Hardening

Huseyin Sehitoglu*, Sertan Alkan**

*University of Illinois, **University of Illinois

ABSTRACT

In this presentation, we address two topics in crystal plasticity that need a better scientific understanding. The first topic is the modeling of CRSS (critical resolved shear stress) and the second topic is modeling of latent hardening. Firstly, we overview the dislocation-mediated slip in several alloys and then introduce a theory that addresses the strong non-Schmid behavior. By strong non-Schmid response, we refer to the strong orientation dependence and tension-compression asymmetry of the critical resolved shear stress for slip deformation. Unlike conventional fcc alloys, the critical resolved shear stress cannot be treated as a constant material parameter for BCC and B2 alloys. We show examples from transforming alloys such as shape memory alloys that exhibit strong tension-compression asymmetry and crystal orientation dependence. This deviation from the Schmid behavior has been overlooked in previous formulations and needs to be considered, and we illustrate its importance in this presentation. In the second part of the talk, we address the modeling of latent hardening and experiments to study the latent hardening phenomenon in metals. An empirical equation has been proposed in previous works in the literature and repeatedly used by the community. However, there are shortcomings with this empirical approach. The latent hardening behavior is rather complex especially in alloys that undergo simultaneous twinning and dislocation slip. It has been commonly accepted that latent hardening exceeds the hardening on the primary system which is a problematic assumption. We outline a new framework for determination of the latent hardening constants and show agreement with experimental trends in high entropy alloys.

Multiscale Modeling of Piezoresistivity and Damage Induced Sensing Of Nanocomposite Bonded Explosive Materials Under Dynamic Loading Using Electromechanical Peridynamics

Gary Seidel*, Naveen Prakash**, Krishna Talamadupula***, Engin Sengezer****

*Virginia Tech, **Virginia Tech, ***Virginia Tech, ****Virginia Tech

ABSTRACT

Polymer bonded explosives (PBXs) are composed of explosive grains at high volume fractions, for example RDX, HMX etc. surrounded by a polymer medium at low volume fractions such as epoxy, estane etc. They are susceptible to microstructural level damage due to impact events. This may degrade their operational reliability or even cause unwanted initiation leading to the detonation of the explosive. The prognostication of the life of PBX materials is therefore of significant interest. A nanocomposite piezoresistivity based sensing scheme is discussed as a solution to this problem. Carbon nanotube (CNT) based nanocomposite binders are used as the binder material in these explosive composites to give Nanocomposite Bonded Explosives (NCBXs). This leverages the ability of the CNTs to impart piezoresistive properties to the polymer and hence provide in situ sensing of strained and damaged states of NCBX materials. The effective piezoresistivity is derived from key multiscale aspects of the nanocomposite binder due to the presence of the CNTs such as electron hopping at the nanoscale, CNT bundle network formation and disruption at the microscale etc. The degree of piezoresistivity is informed in a hierarchical fashion from the lower scales to the microscale RVE being analyzed through a microscale gauge factor. A multifunctional coupled electromechanical peridynamics code is used to provide numerical analysis including the piezoresistive response of these composites under dynamic loading conditions. Peridynamics is a non-local theory of continuum mechanics that assumes material particles interact over a finite region. The strength of the peridynamic bonds are calibrated to their fracture energies in order to accurately reflect the energy dissipation during the fracture process. The model captures damage initiation and propagation mechanisms due to the progress of stress waves. In order to analyze the coupled piezoresistive and mechanical dynamic response, simulations are conducted on Charpy test specimens. This response is found to depend on many factors such as carbon nanotube content, electrical conductivity of the grain, impact velocity and fracture properties. The analysis of Charpy specimens enables comparisons with experimentally obtained preliminary piezoresistive and mechanical dynamic Charpy test data. This work aims to find qualitative agreement with the experimental data on the dynamic piezoresistive response of these nanocomposites to validate the sensing mechanism for explosive materials proposed here. It is expected that this study will improve the prognosis of life of NCBX materials.

Coupling Methods in Peridynamics for Effective Failure and Damage Simulation

Pablo Seleson*

*Oak Ridge National Laboratory

ABSTRACT

Predictive failure and damage simulation has been a topic of fundamental interest in materials science and engineering. A recently developed nonlocal theory called peridynamics has been a subject of increased interest in the computational mechanics community, due to its ability to naturally represent material discontinuities and handle complex dynamically evolving cracks. However, peridynamic simulations are significantly computationally more expensive than their classical (local) continuum mechanics analogues. Consequently, it is of interest to develop effective coupling methods with the capability to seamlessly combine nonlocal and local models. In this presentation, we will discuss methods to couple peridynamics and classical elasticity, and we will demonstrate the effectiveness of those methods through numerical simulations. References: [1] Seleson, Beneddine, Prudhomme, A force-based coupling scheme for peridynamics and classical elasticity, *Computational Materials Science* 66 (2013): 34–49. [2] Seleson, Ha, Beneddine, Concurrent coupling of bond-based peridynamics and the Navier equation of classical elasticity by blending, *International Journal for Multiscale Computational Engineering* 13(2) (2015): 91–113. [3] Silling, Littlewood, Seleson, Variable horizon in a peridynamic medium, *Journal of Mechanics of Materials and Structures* 10(5) (2015): 591–612.

Matrix Modulus and Ligand Density Effects on Cell Morphogenesis in Two-Dimensional and Three-Dimensional Cell Cultures

Dror Seliktar^{*}, Andrei Yosef^{**}, Olga Kossover^{***}, Iris Mironi-Harpaz^{****}, Arianna Mauretti^{*****},
Sonia Melino^{*****}, Joseph Mizrahi^{*****}

^{*}Technion, ^{**}Technion, ^{***}Technion, ^{****}Technion, ^{*****}University of Rome Tor Vergata, ^{*****}University of Rome Tor Vergata, ^{*****}Technion

ABSTRACT

There is a need to further explore the convergence of mechanobiology and dimensionality with systematic investigations of cellular response to matrix mechanics in 2D and 3D cultures. Here, we applied a semi-synthetic hydrogel capable of supporting both 2D and 3D cell culture to investigate cell response to matrix modulus and ligand density. The culture materials were fabricated from adducts of polyethylene glycol (PEG) or Pluronic®F127 and fibrinogen fragments, formed into hydrogels by free-radical polymerization, and characterized by shear rheology. Control over the modulus of the materials was accomplished by changing the concentration of synthetic PEG-diacrylate cross-linker, and by altering the molecular length of the PEG. Control over ligand density was accomplished by changing the fibrinogen concentration. Results indicate the modulus-dependent and ligand-dependent response from the cells in 2D culture was contradictory to the same measured responses in 3D culture. These differences arise from dimensionality constraints, most notably the encapsulation of cells in a non-porous hydrogel matrix. These insights underscore the importance of mechanical properties in regulating cell morphogenesis in a 3D culture milieu. The versatility of the hydrogel culture environment further highlights the significance of a modular approach when developing materials that aim to optimize the cell culture environment through static mechanical stimulation.

Modelling Ripple Morphodynamics Driven by Colloidal Deposition

Mathieu Sellier^{*}, James Hewett^{**}

^{*}University of Canterbury, ^{**}University of Canterbury

ABSTRACT

Fluid dynamics between a particle-laden flow and an evolving boundary are found in various contexts. We numerically simulated the morphodynamics of silica particle deposition from flowing water within geothermal heat exchangers using the arbitrary Lagrangian-Eulerian method. The silica particles were of colloidal size, with submicron diameters, which were primarily transported through the water via Brownian motion. First, we validated the Euler-Euler approach for modelling the transport and deposition of these colloidal particles within a fluid by comparing our simulation results with existing experiments of colloidal polystyrene deposition. Then we combined this multiphase model with a dynamic mesh model to track the gradually accumulated silica along the pipe walls of a heat exchanger. Surface roughness was modelled by prescribing sinusoidally-shaped protrusions on the wall boundary. The silica bed height grew quickest at the peaks of the ripples and the spacing between the protrusions remained relatively constant. The rough surface experienced a 20 % reduction in silica deposition when compared to a smooth surface. We also discuss the challenges of mesh deforming simulations with an emphasis on the mesh quality as the geometry changes over time.

Modeling and Quantification of Anisotropy and Heterogeneity in Geomaterials

Shabnam Semnani*, Ronaldo Borja**

*Stanford University, **Stanford University

ABSTRACT

Geomaterials are often anisotropic and heterogeneous, and consist of various phases that form complex structures persisting at multiple scales. Microstructural morphology of these materials has a great impact on their overall behavior such as deformation, failure and transport properties, and needs to be incorporated into the computational modeling efforts. In this work, we present recent advances in addressing two aspects of structural morphology of geomaterials, namely, anisotropy and heterogeneity. In the first part, we describe a recently developed anisotropic thermo-plasticity framework for modeling the thermo-mechanical response of transversely isotropic geomaterials, which is then used to predict the inception of shear band and strength of rocks. In the second part, we focus on quantification of heterogeneity of geomaterials across scales using high-resolution imaging techniques. A stochastic framework is presented which uses high-resolution images to enhance low-resolution images obtained over larger fields of view by incorporating features below the resolution limit. The application of this method is demonstrated using images of shale samples with two different resolutions and fields of view obtained using X-ray micro-tomography. The proposed multi-scale imaging approach has vast applications to computational modeling such as computational homogenization, mesh sensitivity studies and multi-scale modeling methods.

Optimal Actuator Layout for Adaptive Structures under Quasi-Static Loading

Gennaro Senatore*

*Swiss Federal Institute of Technology (EPFL), School of Architecture, Civil and Environmental Engineering
(ENAC), Applied Computing and Mechanics Laboratory (IMAC), Station 18, CH-1015 Lausanne

ABSTRACT

Adaptive structures are capable of counteracting the effect of external loads via controlled shape changes and redirection of the internal load path. These structures are integrated with sensors (e.g. strain, vision), control intelligence and actuators. Instead of using more material to cope with the effect of loads, controlled shape changes are employed to homogenise the stresses and to keep deflections within limits. Using a previously developed design methodology [1] it was shown that optimal material distribution in combination with strategic integration of the actuation system lead to significant whole-life energy savings when the design is governed by strong but rare loading events. The whole-life energy of the structure is made of an embodied part in the material and an operational part for structural adaptation. Experimental tests on a large scale physical prototype designed using this methodology [2], validated key assumptions confirming that for slender configurations adaptive structures can achieve up to 70% energy savings compared to passive structures. This presentation focuses on methods to derive optimal actuator layouts in reticular structures under quasi-static loading. A deformation vector akin to a lack of fit or eigenstrain is defined to assign the actuator length changes. A computationally efficient routine based on eigenstrain assignment via the Integrated Force Method is formulated to solve the actuator placement problem. The application of this method to planar and complex spatial structures is discussed to benchmark adaptive structures against optimised passive ones in terms of energy and monetary costs [3, 4]. References [1] G. Senatore, P. Duffour, S. Hanna, F. Labbe and P. Winslow, "Adaptive Structures for Whole Life Energy Savings," International Association for Shell and Spatial Structures (IASS), vol. 52, no. 4, pp. 233-240, 2011. [2] G. Senatore, P. Duffour, P. Winslow and C. Wise, "Shape Control and Whole-Life Energy Assessment of an "Infinitely Stiff" Prototype Adaptive Structure," Smart Materials and Structures, vol. 27, no. 1, p. 015022, 2018. [3] G. Senatore, P. Duffour and P. Winslow, "Exploring the Application Domain of Adaptive Structures," Engineering Structures, vol. 167, pp. 608-628, 2018. [4] G. Senatore, P. Duffour and P. Winslow, "Energy and Cost Analysis of Adaptive Structures - Case Studies," Journal of Structural Engineering (ASCE), 2018.

Uncertainty Quantification Methodologies and Linear Solvers in Cardiovascular Simulations in High-performance Computing

Jongmin Seo^{*}, Daniele Schiavazzi^{**}, Alison Marsden^{***}

^{*}Stanford University, ^{**}University of Notre Dame, ^{***}Stanford University

ABSTRACT

Cardiovascular simulations are widely used to aid in surgical planning and disease diagnostics. Cardiovascular blood flow simulations typically solve the incompressible Navier Stokes equations with physiologic boundary conditions in an anatomic model geometry constructed from image data. To account for variability of simulation predictions due to uncertainties in clinical data, material properties and the modeling process, we implement an uncertainty quantification (UQ) framework and report confidence intervals and output statistics on simulation prediction. We use non-intrusive UQ propagation strategies that requires multiple function evaluations. However, UQ propagation becomes numerically challenging when multiple function evaluations are required, each consisting of a solution of the Navier-Stokes equations in a complex 3-D patient specific geometry with deformable vessel walls. In this talk we compare a variety of numerical techniques aiming to accelerate forward uncertainty propagation for cardiovascular simulations. First, we assess the performance of several UQ propagation methodologies on an idealized coronary artery model coupled with a 0-D lumped parameter network (LPN) which consists of circuit elements to model the heart and coronary physiology. To obtain parameters for LPN network, we use parameter estimation methods to match clinical data for each patient. Performance of UQ methodologies including Markov-Chain Monte-Carlo, stochastic collocation, and a generalized multi-resolution expansion will be compared. The second part of this talk discusses the performance of iterative linear solver and preconditioning techniques in our flow solver on high performance clusters. We will show matrix characteristics from the linear system for example eigenvalues, bandwidth and condition number. Effect of boundary conditions and fluid-structure interaction on matrix characteristics and solver performance will be discussed. * Support from National Institute of Health (R01 EB018302) is greatly appreciated.

Towards Scalable Implicit FE Simulations of Continuum Plasma Physics Models

John Shadid^{*}, Sibu Mabuza^{**}, Roger Pawlowski^{***}, Sidafa Conde^{****}, Eric Cyr^{*****}, Edward Phillips^{*****}, Sean Miller^{*****}, Paul Lin^{*****}

^{*}Sandia National Laboratories, ^{**}Sandia National Laboratories, ^{***}Sandia National Laboratories, ^{****}Sandia National Laboratories, ^{*****}Sandia National Laboratories, ^{*****}Sandia National Laboratories, ^{*****}Sandia National Laboratories, ^{*****}Sandia National Laboratories

ABSTRACT

The mathematical basis for the continuum modeling of plasma physics systems is the solution of the governing partial differential equations (PDEs) describing conservation of mass, momentum, and energy, along with various forms of approximations to Maxwell's equations. The resulting systems are characterized by strong nonlinear and nonsymmetric coupling of fluid and electromagnetic phenomena, as well as the significant range of time- and length-scales that the interactions of these physical mechanisms produce. To enable accurate and stable approximation of these systems a range of spatial and temporal discretization methods are commonly employed. In the context of finite element spatial discretization methods these include mixed integration, stabilized and variational multiscale (VMS) methods [1], and structure-preserving (physics compatible) approaches [2]. For effective long-time-scale integration of these systems the implicit representation of at least a subset of the operators is required [1,2]. Two well-structured approaches, of recent interest, are fully-implicit and implicit-explicit (IMEX) type time-integration methods employing Newton-Krylov type nonlinear/linear iterative solvers. To enable robust, scalable and efficient solution of the large-scale sparse linear systems generated by a Newton linearization, fully-coupled multilevel preconditioners are developed. The multilevel preconditioners are based on two differing approaches. The first technique employs a graph-based aggregation method applied to the nonzero block structure of the Jacobian matrix [1,3]. The second approach utilizes approximate block factorization (ABF) methods and physics-based preconditioning approaches that reduce the coupled systems into a set of simplified systems to which multilevel methods are applied [2]. To demonstrate the flexibility of implicit/IMEX FE discretizations and the fully-coupled Newton-Krylov-AMG solution approaches various forms of resistive magnetohydrodynamic (MHD) and multifluid electromagnetic plasma models are considered. In this context we first briefly discuss the development of the VMS formulation for subset of these systems and then present results for representative plasma physics problems of current scientific interest. Additionally, the discussion considers the robustness, efficiency, and the parallel and algorithmic scaling of the preconditioning methods. Weak scaling results include studies on up to 1M cores. References [1] J. Shadid, R. Pawlowski, E. Cyr, R. Tuminaro, P. Weber and L. Chacon, "Scalable Implicit Incompressible Resistive MHD with Stabilized FE and Fully-coupled Newton-Krylov-AMG," Computer Methods in Applied Mechanics and Engineering, 2016, Vol. 304, pp. 1-25 [2] E. Phillips, J. N. Shadid, E. C. Cyr, and R. Pawlowski. Fast linear solvers for multifluid continuum plasma simulations. Extended abstract and presentation NECDC 2017 [3] P.T. Lin, J.N. Shadid, J.J. Hu, R.P. Pawlowski, E.C. Cyr, "Performance of Fully-coupled Algebraic Multigrid Preconditioners for Large-scale VMS Resistive MHD," Journal of Computational and Applied Mathematics, 2017, in press (<https://doi.org/10.1016/j.cam.2017.09.028>)

Probabilistic Calibration of Soil Parameters in Total Stress Models of Levees Using Bayes' Theorem

Abdollah Shafieezadeh^{*}, Mehrzad Rahimi^{**}, Dylan Wood^{***}, Ethan J. Kubatko^{****}

^{*}The Ohio State University, ^{**}The Ohio State University, ^{***}The Ohio State University, ^{****}The Ohio State University

ABSTRACT

Back analysis of parameters of geotechnical structures is an important yet challenging topic in geotechnical engineering. Deterministic approaches are the most commonly used techniques for back calculation of soil properties and model calibration. However, this group of techniques lack the ability to effectively utilize prior information on probabilistic properties of soil parameters and therefore may not yield realizations that have the highest likelihood. This paper proposes using post event investigations of the performance of levees to identify significant parameters, and Bayes' theorem to determine the posterior probability density function of identified significant parameters based on measured reliable responses of the system. The method is carried out on the total stress, plane strain numerical model of London Avenue South Canal in New Orleans, which is developed in FLAC3D finite difference platform. The horizontal displacement at the top of the floodwall is monitored under different water levels and compared with the measured response during a full-scale load test conducted on the same levee configuration. The calibration process involves evaluation of displacements of the levee model for a set of strategically selected training points. A response surface model is then fitted to these points in order to approximate the deviation of measured and simulated responses. Finally, posterior probability density functions of the significant variables are estimated according to Bayes' theorem [1] using Markov Chain Monte Carlo (MCMC) simulation strategy. Results of this study can help in proper and systematic calibration of soil properties of levee systems in a way that available information are effectively utilized and produced realizations of model parameters have the highest likelihood of occurrence. Produced calibrated models are essential for reliability analysis of levees and floodwalls, in particular, against extreme storm surge events. References: 1. Zhang, L. L., Zhang, J., Zhang, L. M., & Tang, W. H. (2010). Back analysis of slope failure with Markov chain Monte Carlo simulation. *Computers and Geotechnics*, 37(7), 905-912.

A Coupled Crystal Plasticity-Phase Field Framework for Modeling Ductile Failure in Polycrystals With Anisotropic Material Behavior

Ahmad Shahba^{*}, Jiahao Cheng^{**}, Xiaohui Tu^{***}, Somnath Ghosh^{****}

^{*}The Johns Hopkins University, ^{**}The Johns Hopkins University, ^{***}The Johns Hopkins University, ^{****}The Johns Hopkins University

ABSTRACT

Polycrystalline alloys with anisotropic material response, such as Al and Ti alloys, are widely used in the manufacturing of components for the aerospace and military applications. Failure of these components under service loads starts with the formation and propagation of short cracks at the microstructural level. Microstructural features, such as grain topology and crystallographic orientation, and dislocation-driven plasticity are known to affect the formation of microscale cracks. In this work, failure of polycrystalline alloys is modeled within a stabilized large-deformation crystal plasticity finite element framework coupled with a crack phase field model. The traditional phase field models require the elastic free energy density to be decoupled into dilatational and deviatoric parts; however, this decoupling is not generally achievable for anisotropic materials. Therefore, in this work a new model of crack phase field is proposed. Multiplicatively decomposing the elastic deformation gradient into fracture-sensitive and fracture-insensitive components and expressing the elastic free energy density in terms of the fracture-insensitive elastic deformation gradient, it is shown that one can simulate the fracture process in any anisotropic material. Furthermore, this methodology enables one to seamlessly accommodate the tension-compression asymmetry in the mechanical response of damaged materials. This feature is of paramount importance in modeling fatigue failure under partially (or fully) reversed cyclic loading conditions. Finite element modeling of degrading materials is numerically challenging since the traditional solvers fail to converge if instabilities, such as snap-back and snap-through, occur during the deformation. In this work, a simple remedy is proposed to overcome the numerical convergence issues in the event of instabilities as cracks propagate. To obtain plausible fracture patterns using crack phase field framework, fine discretization along the crack path is required in the computational domain. This requirement is crucial and can render the fracture simulations computationally intractable in problems where the crack path is not known a priori, such as failure in polycrystalline materials. An adaptive wavelet transformation-based projection technique is developed and mounted on a hierarchical finite element framework to model failure in polycrystalline materials. The hierarchical form allows one to increase the resolution on the fly in the critical region, i.e. the crack path, whereas the adaptive projection technique determines the necessary hierarchical degrees of freedom to keep and thus optimizes the computational cost. It is shown that this method can accurately predict the fracture patterns in polycrystals with nearly 25 times less number of nodes, compared to traditional finite element method.

A Multiscale Computational Homogenization Theory with Data-Driven Model Reduction for the Prediction of Ductile Damage

Modesar Shakoor*, Cheng Yu**, Orion L. Kafka***, Wing Kam Liu****

*Northwestern University, **Northwestern University, ***Northwestern University, ****Northwestern University

ABSTRACT

Metal forming processes such as extrusion or wire drawing induce large deformation and the nucleation, growth and coalescence of microscopic voids with complex distribution and morphology. The presence of these voids nucleated by either inclusion debonding or break-up can have disastrous effects and lead to ductile fracture both during processing and product life. There is hence an interest in modeling approaches that can relate microstructure to failure mechanisms in ductile materials. This presentation will introduce a multiscale computational homogenization theory with data-driven model reduction that can be applied at different stages of the life of metallic products. This theory is based on a FE-FFT method where the macroscale (product scale) problem is solved using a finite element approximation with a microscale problem solved at each integration point using a reduced version of the FFT-based numerical method [1]. The macroscale problem assumes a homogeneous material, while the microstructure's heterogeneity is modeled in microscale problems using model reduction. This model reduction is obtained by means of data clustering methods following the recently proposed Self-consistent Clustering Analysis (SCA) theory [2], herein extended to account for finite deformation and ductile damage. As opposed to its small strain version [2], the finite strain version of SCA requires a training data set for clustering that accounts for material nonlinearity, and micromechanical modeling of void nucleation, growth and coalescence. The latter is addressed in microscale problems using reduced versions of high-fidelity inclusion debonding and break-up models [3]. The potential of the new multiscale computational homogenization theory with reduced order modeling will be demonstrated through examples where heterogeneous deformation and stress states at the macroscale lead to heterogeneous microstructural evolution. For instance, the influence of macroscopic shear bands on the nucleation of voids and the evolution of their morphology will be investigated. [1] Moulinec, H., &&& Suquet, P. (1998). A numerical method for computing the overall response of nonlinear composites with complex microstructure. *Computer Methods in Applied Mechanics and Engineering*, 157(1–2), 69–94. [2] Liu, Z., Bessa, M. A., &&& Liu, W. K. (2016). Self-consistent clustering analysis: An efficient multi-scale scheme for inelastic heterogeneous materials. *Computer Methods in Applied Mechanics and Engineering*, 306, 319–341. [3] Shakoor, M., Bernacki, M., &&& Bouchard, P.-O. (2017). Ductile fracture of a metal matrix composite studied using 3D numerical modeling of void nucleation and coalescence. *Engineering Fracture Mechanics*. Article in Press.

Phase-field Modelling of Dislocation Interaction with Ordered Precipitates

Pratheek Shanthraj^{*}, Jaber Rezaei Mianroodi^{**}, Bob Svendsen^{***}

^{*}Max-Planck-Institut für Eisenforschung, ^{**}RWTH Aachen University, ^{***}RWTH Aachen University

ABSTRACT

Dislocation interaction with ordered precipitates is modeled here with the help of an extended atomistic phase-field micro-elasticity method taking into account elastic anisotropy and precipitate eigenstrain. In particular, the generalised stacking fault energy of the matrix and precipitate phases are incorporated into the free energy to capture dislocation dissociation and formation of planar faults. Ni-Al and Fe-Mn-Al-C alloys are considered as model systems and possible dislocation reactions and core structures in these alloys resulting in the formation of anti-phase boundaries and complex stacking faults inside the ordered precipitate are studied. Dislocations with different characteristics are placed in the matrix and driven toward the precipitate under external loading. The phase-field results thus obtained are also compared directly with the molecular dynamics simulation of the same system in order to validate the results.

Object Shape Feature Extraction from Motion Parallax Using Convolutional Neural Network

ChengJun Shao^{*}, Makoto Murakami^{**}

^{*}Toyo University, ^{**}Toyo University

ABSTRACT

We propose a neural network which can recognize objects from a sequence of RGB images captured with a single camera through two different convolutional neural networks. The learning process is divided into two steps: learning of CNN for spatial feature extraction and learning of CNN for spatiotemporal feature extraction. The spatial feature extraction CNN extracts spatial feature vectors with position invariance. And they are input to the following spatiotemporal feature extraction CNN, which convolutes them temporally to achieve depth information based on motion parallax. In the spatial feature extraction CNN, each frame of image sequence is convoluted with some spatial filters, the convoluted values are passed through an activation function, and some spatial features are extracted in the convolutional layer. The features are input to the local contrast normalization layer, and the following pooling layer for downsampling. With these three layers as a set, three sets of layers are concatenated to extract low, medium, and high level spatial features. Then, the high level features are converted to a one-dimensional vector, and weighted sums of elements of it are passed through an activation function in the fully connected layer. We may use dropout to reduce the degree of freedom of the network, and to prevent overfitting. In the spatiotemporal feature extraction CNN, a sequence of the low and medium spatial features extracted in the spatial feature extraction CNN with a frame length T is input to the convolutional layer. The sequence of the same spatial features is convoluted with some temporal filters, the convoluted values are passed through an activation function, and some temporal features including depth information from motion parallax can be extracted. The features are input to the local contrast normalization layer, the pooling layer, and the fully connected layer. And the high level spatial features extracted in the spatial feature extraction CNN are also input to the fully connected layer. And these different kinds of features are integrated in the output layer. To evaluate our proposed method we conducted an experiment using some objects with simple shapes, and extracted the shape information from motion parallax.

Global Sensitivity Analysis of Arlequin Method in Multiscale Models: Effect of Coupling Factors

Qian Shao^{*}, Qun Huang^{**}, Jian Liu^{***}, Shaobo Zhu^{****}, Heng Hu^{*****}

^{*}Wuhan University, ^{**}Wuhan University, ^{***}Wuhan University, ^{****}Wuhan University, ^{*****}Wuhan University

ABSTRACT

Being a kind of bridging techniques, the Arlequin method [1][3] uses Lagrange multipliers to couple mechanical or numerical models of different scales. Although this technique has been widely studied, the following key factors are still questionable: the definition of the weight functions, the choice of the characteristic length, the length of the coupling zone. The aim of this work is to investigate quantitatively and qualitatively the influences of these factors through the Global Sensitivity Analyses (GSA) [2]. The GSA uses Sparse Polynomial Chaos Expansion (SPCE) methodology that is based on the theory of Bayesian model averaging. In particular, Sobol' indices are calculated by variance decomposition to analyze the influence of each parameter on the accuracy of numerical model. Interaction effects among different parameters can also be captured. In this work, different multi-scale models (particle-continuum models and 2D-1D FE models) are analyzed by the proposed technique, and quantitative conclusions on the selection of the coupling factors are drawn. Keywords: Arlequin method; Global sensitivity analysis; Sparse polynomial chaos expansion; Bayesian model averaging; Multiscale models; References [1] H. Hu, N. Damil, M. Potier-Ferry. A bridging technique to analyze the influence of boundary conditions on instability patterns [J]. *Journal of Computational Physics*, 2011, 10: 3753–3764. [2] Q. Shao, A. Younes, M. Fahs, T. A. Mara. Bayesian sparse polynomial chaos expansion for global sensitivity analysis [J]. *Computer Methods in Applied Mechanics & Engineering*, 2017, 318: 474-496. [3] H. B. Dhia, G. Rateau. The Arlequin method as a flexible engineering design tool [J]. *International Journal for Numerical Methods in Engineering*, 2005, 62(11): 1442-1462.

Immersed Boundary Methods for Rigid and Deformable Particles in Viscoelastic Flows

Eric Shaqfeh^{*}, Will Murch^{**}, Chris Guido^{***}, mengfei yang^{****}

^{*}Stanford University, ^{**}Stanford University, ^{***}Stanford University, ^{****}Stanford University

ABSTRACT

The immersed boundary method will be used with a finite volume fluid solver to develop a unique tool to examine the properties of a viscoelastic suspension of particles. The tool will employ unstructured grids and is massively parallel, thus allowing very complex geometries to be simulated. Since the internal stress of the particles is handled using a finite element solver, nearly arbitrary stress-strain relationships for the particles can be handled and their shape can deform continuously. A number of interesting physical problems will be examined with the code including 1) Sedimentation of particles in orthogonal shear, 2) the rheology of particulate suspensions in a viscoelastic uid under shear and 3) the swimming of *C. Elegans* in an elastic fluid.

Hermite Polynomial Based Variational and Galerkin Integrators for Forced Lagrangian Systems

Harsh Sharma^{*}, Mayuresh Patil^{**}, Craig Woolsey^{***}

^{*}Virginia Polytechnic Institute and State University, ^{**}Virginia Polytechnic Institute and State University, ^{***}Virginia Polytechnic Institute and State University

ABSTRACT

Conventionally, symplectic methods have been applied to conservative dynamical systems which require accurate long-time simulation. Unlike the traditional numerical integrators with numerical dissipation, these symplectic methods exhibit long-time stable energy behavior. Variational integrators, a subclass of symplectic methods, are momentum-preserving in presence of symmetries and have been shown to have bounded energy error for conservative dynamical systems. Their numerical performance in presence of external forcing though still remains unsettled. Motivated by Hermite interpolation polynomials approach to discretization this work presents two novel approaches to derive structure-preserving numerical integrators for Lagrangian systems. The first one, a variational approach, obtains the discrete Lagrangian by adopting the Hermite interpolation polynomial approach which gives the discrete analogue of the action integral in terms of discrete configuration states and velocities. We set the discrete action stationary with respect to both discrete configuration states and velocities to derive novel variational integrators. We also extend this proposed method to systems with external forcing by considering the discrete analogue of the Lagrange-d'Alembert principle. The second one, a Galerkin approach, discretizes the trajectories using the Hermite interpolation polynomials and the numerical integrators are then obtained by setting the weighted average of the residual of the equations of motion over a time step to zero. Both of the resulting methods are compliant to control analysis since they naturally yield configuration states and velocities as the output, without the need to interpolate like in variational integrators. This paper presents a detailed comparison of the two proposed methods and existing variational integrators. The goal is to establish numerical results pertaining to the computational cost and energy accuracy. The superior energy performance of the proposed methods compared to existing variational integrators is demonstrated by means of two numerical examples which are representative model problems of nonlinear solid-mechanics and multi-body dynamics. This paper also investigates to which extent the advantages of symplectic structure preservation for long-time simulation of conservative dynamical systems carry over to Lagrangian systems with external forcing.

A Comparative Study of Nonlocal Interphase Models for Interface Failure

Luv Sharma^{*}, Ron Peerlings^{**}, Pratheek Shanthraj^{***}, Franz Roters^{****}, Marc Geers^{*****}

^{*}Department of Mechanical Engineering, Eindhoven University of Technology, PO Box 513, 5600 MB, Eindhoven, The Netherlands, ^{**}Department of Mechanical Engineering, Eindhoven University of Technology, PO Box 513, 5600 MB, Eindhoven, The Netherlands, ^{***}Microstructure Physics and Alloy Design, Max-Planck-Institut für Eisenforschung, Max-Planck-Str. 1, 40237 Düsseldorf, Germany, ^{****}Microstructure Physics and Alloy Design, Max-Planck-Institut für Eisenforschung, Max-Planck-Str. 1, 40237 Düsseldorf, Germany, ^{*****}Department of Mechanical Engineering, Eindhoven University of Technology, PO Box 513, 5600 MB, Eindhoven, The Netherlands

ABSTRACT

In this work, we discuss FFT based modelling of interface decohesion. The method is developed keeping in mind the application to multiphase polycrystalline materials. FFT methods are based on a regular and uniform (voxelised) grid of material points. Therefore, interface models, which collapse the multi-scale physical behaviour of the interfaces to a sub-dimensional space cannot be implemented in a straightforward fashion. This limitation is remedied by using the idea of an interfacial band—an interphase band is introduced along the physically sharp interfaces. This interphase band contains material points in the neighbourhood of the interface. The material points inherit the elastic-plastic properties of the grains they originally belong. The volumetric region of this interphase dissipates the fracture energy and also models the kinematics associated with the decohesion. To model the anisotropic kinematics of the cracking process, a damage eigen strain is introduced [1]. The eigen strain is decomposed into normal and tangential opening modes, the driving forces for which are the respective resolved tractions. The evolution equations for the openings have a softening character, which induces localisation. In order to avoid the localisation associated with softening, two nonlocal strategies—gradient based nonlocal damage [2] and integral based averaging [3]—are considered. These regularisation strategies smear the damage content outside the interphase domains where the interfacial damage has no physical meaning. To confine the damage content within the interphase band, the boundary conditions at the two edges of the band become important. This is also important from the point of view of possible interaction with the intragranular damage model. We discuss the implementation of such regularisation in integral averaging and gradient based approaches. Their effectiveness in giving proper scaling for the fracture energy is first discussed for a 1D case and then for a propagating crack. Both nonlocal approaches will also be compared from ease of implementation considerations. Finally, an application to cluster of grains is presented. References [1] P. Shanthraj, B. Svendsen, L. Sharma, F. Roters, and D. Raabe. Elasto-viscoplastic phase field modelling of anisotropic cleavage fracture. *Journal of the Mechanics and Physics of Solids*, 99:19–34, 2017. [2] R.H.J. Peerlings, R. de Borst, W.A.M. Brekelmans, and J.H.P. de Vree. Gradient enhanced damage for quasi-brittle materials. *International Journal for Numerical Methods in Engineering*, 39(19):3391–3403, 1996. [3] Z.P. Bažant and G. Pijaudier-Cabot. Nonlocal Continuum Damage, Localization Instability and Convergence. *Journal of Applied Mechanics*, 55(2):287, 1988.

Atomistic and Molecular Modeling of Amorphous Germanium as Negative Electrode for Sodium Ion Battery

Vidushi Sharma^{*}, Kamalika Ghatak^{**}, Siva Nadimpalli^{***}, Dibakar Datta^{****}

^{*}New Jersey Institute of Technology, Newark, ^{**}New Jersey Institute of Technology, Newark, ^{***}New Jersey Institute of Technology, Newark, ^{****}New Jersey Institute of Technology, Newark

ABSTRACT

In recent years, there have been significant concerns that available lithium (Li) resources buried in the earth would not be sufficient to meet the ever-increasing demands for the ubiquitous Lithium Ion Batteries (LIBs). The abundance and low-cost of sodium (Na) in the earth and low reduction potential provide a lucrative inexpensive, safe, and environmentally benign alternative to LIBs. The major challenges in advancing Sodium Ion Battery (NIB) technologies lies in finding the better electrode materials. Experimental investigations showed the potency of Germanium (Ge) as suitable electrode materials for NIBs. However, a systematic multiscale computational investigation is necessary to understand the fundamental of capacity-voltage correlation, microstructural changes of Ge, as well as diffusion characteristics. We, therefore, performed the atomistic simulation (Density Functional Theory (DFT) and Ab Initio Molecular Dynamics (AIMD)) and atomistic-informed molecular simulation (Molecular Dynamics (MD) and Monte Carlo (MD)) to investigate the sodiation-desodiation kinetics in Germanium-Sodium system (Na₆₄Ge₆₄). We find the Ge electrode yields high theoretical capacity of 369 mAhg⁻¹. We analyzed the intercalation potential and capacity correlation for intermediate equilibrium structures and our computational results are in excellent agreement with the existing experimental data. We further investigated the diffusivity of sodium in amorphous Ge (a-Ge), volume expansion, and possible microstructural changes taking place during charging and discharging. We find the energy barrier for diffusion of Na in a-Ge is much lower as compared to crystalline Ge (c-Ge). We computed the volume expansion of Na-Ge alloy electrode to be approximately 149.51% in the fully sodiated state (Na₆₄Ge₆₄). We further investigated Radial Distribution Function (RDF) to examine the possible phase changes from amorphous to crystalline for intermediate structures of sodiated Ge. Furthermore, with input from DFT, we performed MD and MC computation to model the charge-rate of sodiated Ge. Moreover, we analyzed microstructural changes for a sodiated-Ge system with larger time and length scale. Our computational results provide a fundamental insight at the atomic and molecular level and help experimentalists design the Ge based NIBs for real-life applications.

Extracting Atomic Energy Barriers from Dynamics at Grain Boundaries

Tristan Sharp^{*}, Spencer Thomas^{**}, David Srolovitz^{***}, Andrea Liu^{****}

^{*}University of Pennsylvania, ^{**}University of Pennsylvania, ^{***}University of Pennsylvania, ^{****}University of Pennsylvania

ABSTRACT

The tendency for atoms at grain boundaries to rearrange leads to enhanced diffusion and permits phenomena such as lattice defect absorption and emission and grain boundary migration. Most grain boundaries have complex atomic structure which encumbers efforts to connect the local region with its likelihood to rearrange under thermal fluctuations. Here we investigate the connection between structure and atomic dynamics with a technique that uses machine learning (a support vector machine) to analyze simulations of poly-crystalline metals. Having trained on a portion of the simulation, the method applied to the full system readily distinguishes grain boundary atoms that tend to rearrange from those that will not. A quantity calculated from the support vector machine for each atom, "softness," allows identification of structures that follow an approximately Arrhenius likelihood to rearrange, similar to previous findings in glasses. This indicates an energy barrier and generalized attempt frequency for rearrangements which may be determined for each atom. Correlations between softness and other microscopic quantities (e.g. local potential energy) led us to use a similar method with those quantities and find that consistent information could be extracted. Such considerations of the thermal atomic dynamics are a useful step towards machine-learning predictions of deformation of poly-crystalline materials.

Adaptive Reconnection-based Arbitrary Lagrangian Eulerian Method - A-ReALE

Mikhail Shashkov*

*XCP-4, Los Alamos National Laboratory

ABSTRACT

We present a new adaptive reconnection-based Arbitrary Lagrangian Eulerian method - A-ReALE. The main elements of an A-ReALE method are: An explicit Lagrangian phase on arbitrary polygonal mesh in which the solution and positions of grid nodes are updated; a rezoning phase in which a new grid is defined - both number of cells and their locations as well as connectivity (based on using Voronoi tessellation) of the mesh are allowed to change; and a remapping phase in which the Lagrangian solution is transferred onto the new grid. The design principles of A-ReALE method can be summarized as follows. First, it is using monitor (error indicator) function based on gradient or Hessian of some flow parameter(s), which is measure of interpolation error. Second, using equidistribution principle for monitor function for creating of adaptive mesh. Third, using weighted centroidal Voronoi tessellation as a tool for creating adaptive mesh. Fourth, we modify raw monitor function - we scale it to avoid very small and very big cells and smooth it to create smooth mesh and allow to use theoretical results related to weighted centroidal Voronoi tessellation. We present all details required for implementation of new adaptive ReALE methods and demonstrate their performance in comparison with standard ReALE method. on series of numerical examples.

Modeling Multi-Stage Hydraulic Fracturing from a Borehole within a GFEM Framework

Nathan Shauer^{*}, Carlos Armando Duarte^{**}, Alfredo Sanchez Rivadeneira^{***}, Piyush Gupta^{****}

^{*}University of Illinois at Urbana-Champaign, ^{**}University of Illinois at Urbana-Champaign, ^{***}University of Illinois at Urbana-Champaign, ^{****}University of Illinois at Urbana-Champaign

ABSTRACT

Hydraulic Fracturing is the process in which a fracture propagates through the injection of a pressurized fluid in its cavity. This process is widely used in the oil and gas industry to increase reservoir permeability which leads to high rates of both injection and production. Hydraulic fractures are normally created in a multi-stage process which leads to complex fracture geometries due to interactions and coalescence of fractures, and fracture realignment with preferential propagation direction. The fracture shape, and consequently pressure drop, varies significantly between fracture clusters. As a result, the majority of the gas and oil production, comes from only 20 to 30% of the clusters. Computational methods able to predict the near wellbore tortuosity and pressure drop can play a key role in improving the performance of multistage fracturing. This presentation reports on recent advances of an adaptive Generalized Finite Element Method (GFEM) for the simulation of multiple 3-D non-planar hydraulic fracture propagation near a wellbore. This method is particularly appealing for the discretization of the fractures since it does not require the fracture faces to fit finite element faces. Additionally, analytical asymptotic solutions are used to enrich the fracture fronts, which increases the accuracy of the approximation. Stress intensity factors (SIF) with fluid pressure on fracture faces are extracted using the displacement correlation method. The methodology is verified with analytical solutions and compared with experimental results from the literature. Various configurations and fracture geometries are investigated to demonstrate the non-intuitive propagation behavior in these near wellbore conditions and the robustness of the proposed GFEM methodology. P. Gupta and C.A. Duarte. Simulation of non-planar three-dimensional hydraulic fracture propagation. *International Journal for Numerical and Analytical Methods in Geomechanics*, 38:1397–1430, 2014. doi: 10.1002/nag.2305. P. Gupta and C.A. Duarte. Coupled formulation and algorithms for the simulation of non-planar three-dimensional hydraulic fractures using the generalized finite element method. *International Journal for Numerical and Analytical Methods in Geomechanics*, 40(10):1402–1437, June 2016. ISSN 1096-9853. doi: 10.1002/nag.2485. W. El Rabaa. 1987. 'Hydraulic Fracture Propagation in the Presence of Stress Variation'; in 62nd Annual Technical Conference and Exhibition of the Society of Petroleum Engineer, SPE, Dallas, TX, September 27-30.

On the Mechanical Response of Single Crystal Iron under Extreme Loading Conditions

Mu'asem Shehadeh*, Pascale El Ters**

*American University of Beirut, **American University of Beirut

ABSTRACT

Multiscale Discrete dislocation Dynamic Plasticity (MDDP) simulations are carried out to investigate the mechanical response and microstructure evolution of single crystal alpha-Fe subjected to high strain rate compression over wide range of temperature. The simulations are conducted at temperature ranging between 300K to 900K and strain rate ranging between 10^2 to 10^7 s⁻¹. Atomistically informed generalized mobility law was incorporated in MDDP to account for the effects of temperature and strain rate on dislocation mobility, Peierls stress and Elastic constants. MDDP based constitutive equation interrelating the temperature and strain rate with the flow stress at high strain rate monotonic and impact conditions are proposed. The simulation results of the yield strength, hardening rate and microstructure evolution are in good agreement with reported experimental results. Detailed investigations of the dislocation microstructure evolution show the formation of extended screw dislocation lines at temperatures below 340 K due large value of Peierls stress of the pure screw segments. Moreover, small sessile loops of radius in the order of few nanometers are formed; these sessile loops are facilitated by the easiness of multiple cross slip on available slip planes.

Statistical Reconstruction of Bone Microstructures to Study Osteoporosis

Azadeh Sheidaei^{*}, Fayyaz Nosouhi^{**}, Majid Baniassadi^{***}, Daniel George^{****}, Christine Chappard^{*****}

^{*}Iowa state university, ^{**}University of Tehran, ^{***}University of Tehran, ^{****}University of Strasbourg, ^{*****}University Paris Diderot

ABSTRACT

Osteoporosis is a major health problem for elderly people leading to weak bone stiffness and high risks of bone fracture under fall. The study and prediction of osteoporosis evolution is a difficult task. It involves both the development of multiphysics and multiscale models integrating bone physics and physiology through sophisticated theoretical numerical models (1-4) and it also requires to solve technical challenges about the integration of large scale numerical models to account for all the local physics through adequately homogenized theories (5). To address this problem, a 3D reconstruction of bone microstructures was extracted from high spatial resolution MR images. The real representation of the bone was converted into a finite element model based on small tetrahedral elements. To study potential microstructures distributions being patient dependent, an equivalent statistical representative volume element (RVE) has been created using a recently developed technique (6). Both real RVE and statistical RVE were studied and compare using FEM. The results showed good correlation between the two distributions. Several statistical RVEs were generated using the data obtained from MR images to study the effect of different parameters such as the influence of the geometrical distribution of the bone microstructure on its mechanical response. Study of the bone remodeling is currently our ongoing research project where the above bone microstructures are used to study and model the osteoporosis evolution. References 1. A. Madeo, D. George, T. Lekszycki, et al., A second gradient continuum model accounting for some effects of microstructure on reconstructed bone remodeling, *Compte Rendus Mécanique*, 2012, vol. 340 (8), pp. 575-589. 2. I. Scala, C. Spingarn, Y. Remond, et al., Mechanically-driven bone remodeling simulation : application to LIPUS treated rat calvarial defects, *Mathematics and Mechanics of Solids*, 2016, 22(10), 1976-1988. 3. D. George, C. Spingarn, C. Dissaux, et al., Examples of multiscale and multiphysics numerical modeling of biological tissues, *Bio-Medical Materials and Engineering*, 2017, 28(S1), S15-S27. 4. D. George, R. Allena, Y. Rémond, Mechanobiological stimuli for bone remodeling: mechanical energy, cell nutriments and mobility, *Computer Methods in Biomechanics and Biomedical Engineering*, 2017, 20(sup1), 91-92. 5. Y. Rémond, S. Ahzi, M. Baniassadi, et al., *Applied RVE Reconstruction and Homogenization of Heterogeneous Materials*, Ed. Wiley-ISTE, 2016; ISBN: 978-1-84821-901-4. 6. M. Tafazoli, M. Shakeri, M. Baniassadi, et al., Investigation of the geometric property hull for infiltrated solid oxide fuel cell electrodes, *International Journal of Energy Research*, 2017, 41(14), 2318-2331.

An Improved Formulation for Hybridizable Discontinuous Galerkin Fluid-Structure Interaction Modeling

Jason Sheldon^{*}, Jonathan Pitt^{**}, Scott Miller^{***}

^{*}Institute for Defense Analyses, ^{**}Applied Research Laboratory, The Pennsylvania State University, ^{***}Sandia National Laboratories

ABSTRACT

This work presents a novel application of the hybridizable discontinuous Galerkin (HDG) finite element method to the multi-physics simulation of coupled fluid–structure interaction (FSI) problems, along with formulation improvements that reduce the computational expense of the method. The FSI model utilizes monolithically coupled HDG formulations of nonlinear elastodynamics and incompressible arbitrary Lagrangian–Eulerian Navier–Stokes, with linear elastostatics for the motion of the fluid’s mesh. The elasticity formulations are written in a Lagrangian reference frame, with the nonlinear formulation restricted to hyperelastic materials. Two improvements over the HDG FSI formulation by Sheldon et al. [1] are presented: the elimination of a solid’s global displacement and the restriction of the mesh’s function spaces to only linear polynomials. These improvements significantly reduce the number of global degrees of freedom and reduce the method’s computational expense. The HDG FSI model formulations are compared to each other as well as to the FSI benchmark problem proposed by Turek and Hron [2]. [1] J. Sheldon, S. Miller, J. Pitt, A hybridizable discontinuous Galerkin method for modeling fluid–structure interaction, in: *Journal of Computational Physics*, 2016, pp. 91-114. [2] S. Turek, J. Hron, Proposal for numerical benchmarking of fluid–structure interaction between an elastic object and laminar incompressible flow, in: *Fluid–Structure Interaction*, 2006, pp. 371–385.

Damage and Failure Modeling of Heterogeneous Concrete Using Peridynamics

Feng Shen^{*}, Qing Zhang^{**}, Xiaozhou Xia^{***}, Dan Huang^{****}

^{*}School of Civil Engineering, Suzhou University of Science and Technology, Suzhou, China, ^{**}Department of Engineering Mechanics, Hohai University, Nanjing, China, ^{***}Department of Engineering Mechanics, Hohai University, Nanjing, China, ^{****}Department of Engineering Mechanics, Hohai University, Nanjing, China

ABSTRACT

The failure process and its mechanism of concrete structure is one of major concerns in the academic and engineering field for a long time. In the study of damage accumulation and progressive failure in concrete structures, nearly all traditional methods based on the classical theory of continuum mechanics attempt to solve the partial differential equations, but these methods are proved unsuitable since the limitations such as remeshing and mapping cannot be removed completely. To potentially solve this problem, a novel and promising non-local peridynamic theory is utilized in this paper. In contrast to these classical theories, the peridynamic equation of motion introduced by Silling is free of any spatial derivatives of displacement. After mathematical demonstration of the theory, peridynamics has been used in membranes, fibers, and so on. However, peridynamic theory has not been applied to model concrete very often. In this paper, a new constitutive model has been proposed, which was suitable for concrete based on the "bond-based" peridynamics, and some of its parameters have been discussed. Considering concrete as a heterogeneous material which is composed of aggregates, cement matrix and interfaces between them at the mesoscale, a mesoscale PD model was presented, which characterizing the microstructures of concrete, in order to reveal the failure mechanism of concrete and its whole process of damage. We have studied its deformation and characteristics under loading, and modeled the process of failure. Based on the result of peridynamics calculation, the whole process of microdefects growing, damage accumulation, crack initiation and propagation in concrete materials and structures were reappeared. The result of the example clarifies the unique advantage of modeling damage accumulation and progressive failure of concrete based on peridynamic theory. This study provides a new promising alternative for analyzing complicated discontinuity problems.

Acknowledgements This research is supported by the National Natural Science Foundation of China (Grants nos. 51709194, 11672101, 51679077). **References** [1] Silling S A. Reformulation of elasticity theory for discontinuities and long-range forces[J]. Journal of the Mechanics and Physics of Solids, 2000, 48(1): 175-209. [2] Silling S.A., Bobaru F. Peridynamic modeling of membranes and fibers. International Journal of Non-linear Mechanics, 2005, 40(2): 395-409. [3] Shen Feng, Zhang Qing, Huang Dan. Damage and Failure Process of Concrete Structure under Uni-axial Compression Based on Peridynamics Modeling [J]. Mathematical Problems in Engineering, 2013.

Discrete Modeling of Concrete Thermal Spalling

Lei Shen^{*}, Gianluca Cusatis^{**}, Qingwen Ren^{***}, Giovanni Di Luzio^{****}, Weixin Li^{*****}, Xinwei Zhou^{*****}, Jun Feng^{*****}

^{*}Hohai University, ^{**}Northwestern University, ^{***}Hohai University, ^{****}Politecnico di Milano, ^{*****}Northwestern University, ^{*****}ES3 Company, ^{*****}Northwestern University

ABSTRACT

When concrete is exposed to fire, the high temperature leads to the development of thermal stresses and elevated pore vapor pressure, which, in turn, cause spalling of a surface concrete layer (mostly the concrete cover). Such spalling exposes the steel reinforcement to high temperature resulting in a drastic reduction of the carrying capacity of the affected structural elements. Despite the catastrophic effect of thermal spalling, a clear explanation of the underlying mechanisms remains elusive. To gain a better understanding of the overall phenomenon, a discrete hydro-thermo-chemical model for the simulation of temperature and pore pressure evolutions in concrete at high temperature is proposed. Such model is then coupled with the so-called lattice discrete particle model (LDPM) that simulates cracking and damage in concrete. The multi-physical coupled model features the effect of pore vapor pressure and temperature on the mechanical response and the effect of cracking on mass and heat transport. The model is validated by comparison with experimental data. Results show that damage localization and fracture significantly reduce local pore pressure built-up due to the increase of pore volume. Hence the pore pressure increase causes crack initiation but it is not enough to explain spalling. Also, results demonstrate that thermal stresses alone cause only minor damage. However, thermal spalling is very well reproduced if both effects are included: pore pressure causes cracks to develop parallel to surface and, subsequently, thermal stresses induce the buckling of the concrete layer generated by the cracks.

A Phase Field Model for Viscoelastic Fracture Accelerated by Viscous Energy Dissipation

Rilin Shen^{*}, Haim Waisman^{**}, Licheng Guo^{***}

^{*}Harbin Institute of Technology; Columbia University, ^{**}Columbia University, ^{***}Harbin Institute of Technology

ABSTRACT

Fracture of viscoelastic materials plays an important role in many applications in science and engineering but is not well understood. In addition to the time and rate-dependent response of viscoelastic materials, fracture of these materials may be accelerated by a viscous energy dissipation mechanism. Moreover, environmental factors further accelerate damage growth but are not easily accounted for by traditional fracture or damage models. To this end, we propose a modified phase field method for modeling the fracture of such viscoelastic materials. Unlike most phase field methods that are driven by pure elastic energy effects, herein we introduce viscous energy dissipation as an additional mechanism that drives fracture. Hence, with a single additional parameter, complex environmental factors could be introduced in order to obtain accelerated damage growth. Viscoelastic material behavior is obtained through Prony-Series expansion and the phase-field viscoelastic formulation is shown to be thermodynamically consistent. We study the effect of fracture driven by viscous dissipation on three 3D benchmark problems. First, the behavior of a bar under creep, relaxation and strain rate loading cases is examined. Then, crack propagation in mode I and mixed mode conditions are studied on a typical 3-point asphalt bending problem and validated against available experiments. In all cases, it is shown that viscous dissipation accelerates the fracture growth rate but essentially in principle do not affect crack path.

A Numerical Method for Crack Problems of Nonhomogeneous Materials Based on Cohesive Damage Model

Rinlin Shen^{*}, Yanyan Zhang^{**}, Jianchao Pang^{***}, Mengxiao Zhang^{****}, LiCheng Guo^{*****}

^{*}School of Astronautics, Harbin Institute of Technology, Harbin 150001, China, ^{**}Institute of Metal Research, Chinese Academy of Sciences, Shenyang 110016, China, ^{***}Institute of Metal Research, Chinese Academy of Sciences, Shenyang 110016, China, ^{****}Institute of Metal Research, Chinese Academy of Sciences, Shenyang 110016, China, ^{*****}School of Astronautics, Harbin Institute of Technology, Harbin 150001, China

ABSTRACT

Abstract: Fractures phenomena can often be found in nonhomogeneous materials (NM). This paper aims to develop a set of a micro-scale damage cohesive finite element model (CFEM) method, combining the digital image-based technique (DIT) for analyzing the crack initiation and growth problems of NM. The agreement of stress-strain curve and fracture mechanism between in-situ tensile experimental test and simulation results shows that the developed method works effectively. Keywords: Nonhomogeneous materials; Cohesive finite element method; Crack initiation.

A Homogenization-based Phase Field Approach to Fracture

Yongxing Shen*, Cheng Cheng**

*University of Michigan-Shanghai Jiao Tong University Joint Institute, Shanghai Jiao Tong University, **University of Michigan-Shanghai Jiao Tong University Joint Institute, Shanghai Jiao Tong University

ABSTRACT

The regularized variational theory of fracture, or so called phase field approach to fracture, has gained popularity due to its ability to predict crack nucleation, propagation, and branching without extra criteria. This approach works by minimizing a total energy functional with the displacement field and phase field (0=intact material, 1=crack) as arguments, and eliminates the cumbersome geometric tracking compared with traditional discrete crack methods such as the extended finite element method. Since 2009, a few variants of this approach have been proposed to account for the unilateral constraint. In this presentation, I will detail our formulation for the unilateral constraint based on homogenization theory and micromechanics, followed by a comparison with major existing models.

Nonlinear Dynamic Performance of a Viscoelastic Dielectric Elastomer Actuator

Junjie Sheng^{*}, Bo Li^{**}, Hualing Chen^{***}, Yuqing Zhang^{****}, Junshi Zhang^{*****}

^{*}China Academy of Engineering Physics, ^{**}Xi'an Jiaotong University, ^{***}Xi'an Jiaotong University, ^{****}China Academy of Engineering Physics, ^{*****}Xi'an Jiaotong University

ABSTRACT

Dielectric elastomer (DE) is a new type soft smart material. Subjected to a voltage, a DE reduces its thickness and generates large expansion in its area of a maximum area strain of 1600% [1] and can be used in high performance applications as DE actuator (DEA). Because of its viscoelasticity of the elastomeric polymer matrix, DEA is able to produce a time dependent electromechanical deformation [2]. The time-dependency of a DEA can cause dissipation in the system and significantly affect its dynamic performance and coupling efficiency [3]. In the current study, by using the a thermodynamic free energy model, an analytical model is developed to characterize the dynamic performance of a homogeneously deformed viscoelastic DEA by taking into account of the inertial force and damping force, and also taking into account of the temperature dependent dielectric constant and shear moduli. The nonlinear dynamic behaviors of viscoelastic DEA subjected to combined loads of the electric field and mechanical press undergoing periodic electric loading were analyzed. The numerical results, such as displacement response, phase diagrams and amplitude-frequency response were analyzed. Poincaré maps were presented to show the influence of temperature, viscoelasticity, pre-stresses and frequencies on the nonlinear dynamic stability of viscoelastic DEA. Numerical results indicated that temperature, viscoelasticity, pre-stresses, frequencies and applied voltages could tune the natural frequency and modify the dynamic behavior of DEA. The results may guide the design of high-performance DEA and the control of its dynamic deformation. References: [1]C. Keplinger, T. Li, R. Baumgartner, Z. Suo, and S. Bauer, Harnessing snap-through instability in soft dielectrics to achieve giant voltage-triggered deformation, *Soft Matter*, 8 (2), 285-288 (2012). [2] Lei Liu, Wenjie Sun, Junjie Sheng, Longfei Chang, Dichen Li and Hualing Chen, Effect of temperature on the electromechanical actuation of viscoelastic dielectric elastomers, *EPL*, 112, 27006 (2015). [3] Junshi Zhang, Hualing Chen, Bo Li, David McCoul and Qibing Pei, Coupled nonlinear oscillation and stability evolution of viscoelastic dielectric elastomers, 11, 7483 (2015).

HULLFORM DESIGN DRIVEN BY GLOBAL FLOW OPTIMIZATION FOR A SWATH

SHENGZHONG LI, FENG ZHAO, QIJUN NI, AND PENG LIN

China Ship Scientific Research Center
Wuxi, China
shengzhonglee@126.com

Key words: Hullform Design Optimization, SWATH, SBD Techniques; MOPSO Algorithm; CFD; Total resistance.

Abstract. Hull geometry modification and reconstruction, optimization algorithms and CFD technique are combined together into what is known as Simulation-based Design (SBD) techniques, and its essence is the hydrodynamic configurations design driven by global flow optimization. The purpose of this paper is to show how the improvement of the hydrodynamics performance of a Small Water-Plane-Area Twin Hull (SWATH) can be obtained by solving a shape optimization design problem at different speeds using the SBD technique. In this paper, an example of the technique application for the SWATH hullform optimization at different speeds is demonstrated. In the procedure, the Free-form Deformation method is chosen to automatically modify the geometry of submerged pontoon, and the Multi-Objective Particle Swarm Optimization (MOPSO) algorithm is adopted for exploring the design space. The two objectives functions, the total resistance at two different speeds (11kn and 15kn), are assessed by RANS solvers. The optimization results show that the decrease of total resistance is significant for the optimization case at two different speeds (11kn and 15kn), with a reduction of about 5.1% and 6.3% respectively. Meanwhile, the displacement increases 3.7% and the transverse section of submerged pontoon becomes "flower vase" type from ellipse. Finally, dedicated experimental campaigns for optimized model have been carried out to validate the computations and establish the effects of the optimization processes. It shows that the computations of optimization scheme mainly fit the results of model test. The given, practical examples demonstrate the practicability and superiority of the proposed SBD technique for the SWATH multiple speeds integrated optimization problem

1 INTRODUCTION

Energy conservation has attracted more and more attention in ship industry, and hullform optimization which is one of the most significant approach to meet the requirements of energy conservation for shipbuilding industry, has been studied for years. Traditional optimization which is conducted usually aiming at one specific speed. However, cruise speed and design speed which are regardful design points to the respectable ships. It is hard to make the ship performance obtain significant optimization effects in different design aspects by optimizing

hullform of ship. In this paper, the SWATH (Small Water-Plane-Area Twin Hull) which has outstanding seakeeping performance, roomy deck and the appropriate platform for scientific investigate, acoustics research and other oceangoing missions, was selected as the subject of study. However, the excellent performance of high performance ship is not inherent, meaning that elaborate design is need to bring the advantages of hullform into play.

Compared with traditional ship, total resistance of SWATH is quite sensitive to the variation of speed. Along with the increase of speed, resistance may change greatly. The hullform optimization design aiming at only one design factor is hard to guarantee that the benefit of SWATH resistance meet the requirements at other speeds as well, which will make an adverse impact on the holistic economy of ship. Furthermore, the uniqueness of SWATH hullform and the sensibility to variation of weight and center of gravity, bringing about new difficulties to hullform optimization design. Therefore, the hullform optimization design of SWATH at different speeds is necessary to be conducted to guarantee its better resistance performance at all speeds.

With the development of CFD (Computational Fluid Dynamics), CAD and Optimization theory, a new ship design method/mode also known as SBD (Simulation Based Design) technique opens a new way for hull-form optimization design and configuration innovation^[1]. In this process, the objective functions (the hydrodynamic performance of a ship) will be evaluated with CFD codes, and the solutions space of the design problem will be explored with optimization theory, then the optimized hullform under the given constraints will be attained at last. In summary, SBD techniques can solve the complex multi-objective hullform design optimization problem, and its essence is the hydrodynamic configurations design driven by global flow optimization.

2 GENERAL SPECIFICATIONS REVIEW OF SBD TECHNIQUE AND SWATH

For years, numerous researches around SBD technique have been conducted at home and abroad. Among them, it gives first place to the research related to monohull. Han, etc.^[2] conducts the optimization design of container ship and LPG (liquefied petroleum gas) ship. Different hullforms are obtained by varying the curve of transverse section area and the hullform geometry reconstruction is conducted based on Lackenby hullform transformation idea. Kim^[3] amends three shape parameters, including curve of transverse section area, waterline and bulbous bow, to achieve hull geometry reconstruction and conduct the multi-objective overall optimization of KVLCC2 ship model. Kim, Yang, etc.^[4] adopts ship overall geometry reconstruction method based on Lackenby transformation, hull part geometry reconstruction method based on radial basis function interpolation and the combination of these two methods to conduct optimization design on series 60 hullform. LI Shengzhong, etc.^[5] regards the total resistance and flow field of propeller disk as object function, adopts multi-objective particle swarm optimization (MOPSO) and FFD geometry construction method to conduct automatic optimization design on stern hullform of 6600DWT bulk cargo ship, and the results are satisfactory. Among them, one of the optimization schemes improves the wake flow field quality and decreases 10% of the residuary resistance.

The hullform and hydrodynamic performance characteristic of SWATH are different from monohull. On the aspect of appearance, SWATH is similar to catamaran and they both have two slices. SWATH is special on the following aspects: the waterplane area in design waterline is small; most of the volume locates in the underwater far away from waterplane, forming the pontoon shape which is called submerged body and connected with upper platform by strut. The special appearance of SWATH causes a decrease in wave turbulence and motion in waves, owning excellent seakeeping performance, which is the reason why this kind of hullform is high-profile. The developed countries, mainly including America, Japan and German, have built a great amount of SWATH with different purposes.

America is typical in this respect. The "Victorious" (3384T) and "Impeccable" (5380T) are all high seakeeping performance underwater acoustic surveillance ship, which are built by American navy at the end of 20th century and the beginning of 21th century^[6]. Two "Sea Slice" high speeds SWATH passenger ships used for oil field traffic and one 1000t SWATH harbor ferry with ice breaking function are built in this century. Japan has conducted related research in earlier period and built the first civil SWATH passenger ferry "Seagull" in 1979 and 12 SWATH ships with different purposes in total. German imports the relevant techniques from America from 1990s. Until 2012 September, 25 SWATH ships have been built, including 6 series and 11 types according to length and function which covers harbor diversion, test research, customs anti-smuggling, oceanographic survey and so on^[7]. In addition, other countries like Finland, Russia, Norway, Canada etc. also built SWATH with different purposes in succession.

SBD technique has been adapted to the design of multihull ship like catamaran and SWATH in recent years. Peri, Tahara, Campana etc.^[8, 9, 10] adopts MOGA, PSO and DRAGO mix algorithm to conduct single object optimization design of high speed catamaran at given speed, single object optimization design and multiple object optimization design at multi speed. Model test result of one of the optimization schemes indicates that the total resistance of optimal design scheme decrease 9.3% compared with original scheme. Stefano Brizzolara etc.^[11] conducted the concept design and hydrodynamic performance optimization of SWATH USV, adopting a set of automatic process which based on geometry parameters definition, latest CFD solver and unique differential evolution global minimum algorithm to conduct a systematic optimization.

It shows that SBD technique has attracted more and more attention in ship hydrodynamic design domain. In this paper, SBD is adopted to conduct double speeds optimization of SWATH. The main contents of this paper include the following three respects. Firstly, the concept and the key modules of SBD are introduced. Secondly, a double speeds (cruise speed and design speed) hullform optimization design is conducted on SWATH. During the optimization process, FFD free-form deformation is adopted to modify hull geometry shapes automatically, MOPSO is used to explore solution space and RANS solver is adopted to evaluate the resistance of ship at different speeds. Finally, resistance towing test is conducted on optimization scheme model to verify the accuracy of numerical calculation and reliability of optimization method.

3 SBD TECHNIQUE ELEMENTS AND FEATURES

SBD hullform optimization design technique includes three main modules: 1) Optimizer. This technique can be used to search overall optimal solution in hullform design space accurately and fast under the given constraint conditions; 2) hull geometry and mesh manipulation. It is used to provide the connection between optimization algorithm (design parameter) and evaluation of ship performance (object function); 3) CFD solver. It is not only the foundation of establishment of numerical model of hullform optimization problem, but also the bond between hull geometric shape and optimization platform. The relationship between each main module is shown in Fig. 1.

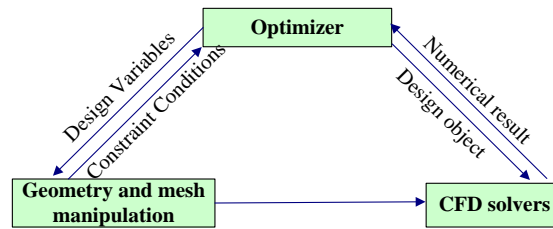


Figure 1 SBD-based hullform optimization design environment

3.1 Optimization method

Optimization is used to explore solution space and obtain the optimal solution of optimization problem. Therefore, to seek the optimal solution in design space quickly and accurately, the selection of optimization algorithm becomes one of the research emphasis in hullform optimization design. Random search algorithm does not rely on specific domain of problems and has high robustness and can find the overall solution easily. Among them, particle swarm optimization (PSO) has the following advantages compared with other random search algorithms. 1) It is simple and easy to implement; 2) It does not need a great amount of adjustments of parameters; 3) It has a stronger overall search ability in some particular areas; for instance, nonlinear problems. Therefore, overall optimization algorithm is recommended for solving practical engineer optimization problem. In this paper, MOPSO is adopted to solve the SWATH double speed design problems. The basic principle and its development are shown in Li [1].

3.2 Hullform geometry reconstruction

Hullform geometry reconstruction technique is the key link of SBD optimization technique and different reconstruction methods will make different influence on the degrees of freedom of optimization algorithm searching design space. Hullform geometry reconstruction should obey the following rules:

- 1) Taking a few control parameters to decrease the scale of problem;
- 2) Different hull shapes should be produced as more as possible to expand the scale of feasible solution;

3) When reconstructing part of hull, the reconstructed part hullform should connect the original hull smoothly;

4) The feasible scheme should be reserved, and the various constraint of geometric shape should be easy to realize in optimization process.

The free-form deformation (FFD) approach is proposed by Sederberg and Parry in 1986, which is a very flexible 3d geometry deformation approach, used for entire and part deformation. Nowadays, FFD approach is brought in the appearance optimization design domain such as ship, aviation and so on, used for the geometry reconstruction of design object. FFD approach is used for modifying hull geometry in this paper. The original approach and its development of FFD approach are shown in Sederberg [12] and Campana [13].

3.3 CFD solver

The CFD solver is adopted as the tools of analysis and forecast, the accuracy of which has a direct influence on the quality of optimization design. Generally, before the optimization design starts, the validity of CFD solver needs to be verified firstly. In addition, the improvement obtained by optimization design should exceed the numerical noise of CFD solver.

In order to redesign the existed appearance, accurate analysis tools are needed to be applied to lead the optimization platform to seek the optimal solution. To guarantee the success of optimization design, RANS method with high accuracy is adopted in this paper for numerical prediction of ship resistance. RANS method is the most widely applied numerical simulation method in practical engineer at present and it has low requirements for computer and high accuracy of prediction, and it is also capable of identifying the influence produced by the detailed variation of hullform geometry on ship performance in the optimization process and adaptable for hullform optimization design.

4 MULTIPLE SPEEDS INTEGRATED OPTIMIZATION OF A SWATH HULLFORM

The effect of ship shape on resistance performance is closely related to ship speed. It is not suitable for all ships to evaluate the resistance performance if only at the design speed. There are two main reasons. On the one hand, the optimal hull form obtained for a given speed may not have a consistent resistance reduction in the entire speed range. It may have a large resistance increase at other off-design speeds. On the other hand, for mid-high speed ship, the influence of hullform change on the resistance is closely linked with speed. In different speed range, the influence of the same hullform change is different, and even has very big difference. It is particularly obvious to the mid-high speed ships that utilize favorable wave interference by the bulb produced to reduce wave resistance. Thus, the present study is focused on the hydrodynamic optimization for a given speed range only, i.e., to develop optimal hull forms with minimum total resistance at the given design speeds.

In this paper, a SWATH is selected as the research object. Its main parameters are shown in table 1. The pontoon configuration is ellipsoid. The view is shown in Fig.2.

Table1 Principal Dimensions and Constraint Conditions

Principal dimensions and coefficients($\lambda =25$)			Constraint conditions		
<i>Parameter</i>	<i>Ship</i>	<i>Model</i>	<i>Type</i>	<i>Definition</i>	
$L_{pp}(m)$	86.7	3.468	<i>Main dimensions</i>	L_{pp}	<i>fixed</i>
$T(m)$	7.8	0.312		T	<i>fixed</i>
$B(m)$	32	1.280		B	<i>fixed</i>
$\nabla(t)$	5850	0.374	<i>Displacement</i>		<i>Maximum variation: 2%~5%</i>
$S(m^2)$	1756	2.810	<i>Wetted surface area</i>		<i>Maximum variation: 1%~4%</i>
$L_{CB}(m)$	44.3	1.772	<i>Buoyancy position</i>		<i>Maximum variation: $\pm 2.5\%$</i>

4.1 Definition of problems

1) Objective functions and its evaluation

In order to get obvious benefit in different speeds, the total resistance of ship at 11kn($F_n=0.186$) and 14kn ($F_n=0.254$) is regarded as object function as follows:

$$\begin{cases} F_1 = R_{r1}^1 / R_{r0}^1 & \text{at } F_n = 0.186 \\ F_2 = R_{r2}^2 / R_{r0}^2 & \text{at } F_n = 0.254 \end{cases} \quad (1)$$

Where R_{r0}^1 and R_{r0}^2 denote the total resistance evaluated for the original hull form and intermediate hull form obtained during the optimization process, respectively.

RANS flow solver is used to evaluate the value of object function. Cell-center finite volume method is applied to discretize the control equation of RANS. The convection item in RANS equation is discretized by second-order upwind scheme, and the viscous flow item is discretized by two-order center scheme. PISO algorithm is used for solving pressure-velocity coupling equation. Wall function is used to confirm the average speed and the wall boundary condition of vorticity transport equation. SST k- ω equation is selected as turbulence model. Level-set method is selected to numerically simulate the moving free surface. H-O multi-block structured grid is adopted as the mesh type (the background grid is Cartesian grid and the body-fitted grid is double-O grid). Hull mesh distributes more intensively near bow, stern, hull surface and free surface. The diagram of mesh generation is shown in Fig. 3.

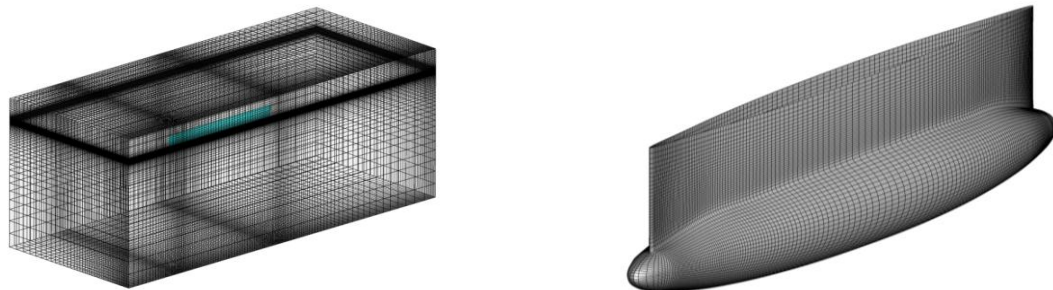


Figure 3 Computation region and hull surface mesh

In this paper, mesh amount and topology structure for the different hulls obtained in optimization process need to be coincident and the first level mesh of hull surface remain constant. Thus the numerical noise produced by the difference of mesh type is avoided.

2) Hull geometry reconstruction and constraint conditions

FFD approach is used for hull geometry reconstruction in the process of multi-objective optimization design for two different speeds. The whole hull area is normalized, and then it is put in a cube with 343 control points (see Fig.4). Twenty-four groups control points are chosen as Twenty-four design variables. Through the change of these design variables, the geometrical surface of the ship-hull at X, Y, Z directions can be reconstructed and deformed. The hull geometry FFD reconstruction diagram is shown in Figure 3. To introduce a realistic design problem, geometrical constraints about the submerged body length, buoyancy center, displacement and principal dimensions of the SWATH are imposed on the design variables. Complete definition of the problem, objective function and constraints, are given below in Tabell.

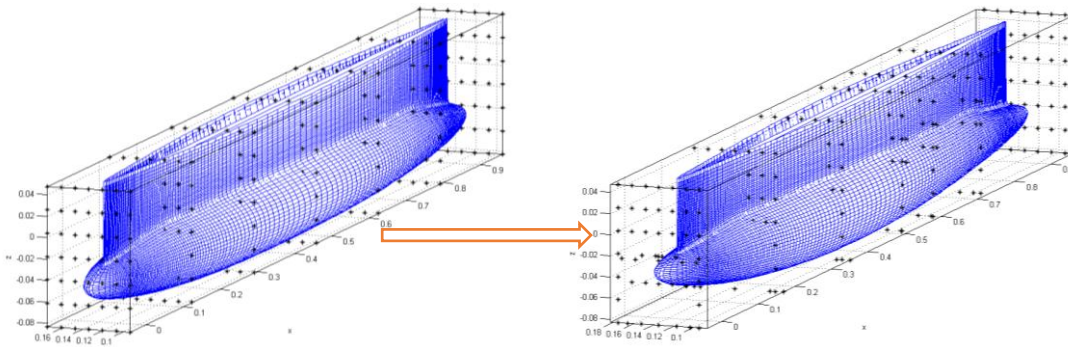


Figure 4 Hullform reconstruction using FFD approach

3) Multi-objective optimization algorithm

It is necessary to employ the multi-objective optimization algorithms to search for the hull forms that have possible resistance reduction at two design speeds. In this study, MOPSO algorithm has been extended to provide a set of optimal solutions using the Pareto front technique.

4.2 Design Optimization Results

In the SWATH optimization process, the particle population number is 36, generation number is 12. Only six points of the complete Pareto optimal sets of solutions are chosen to compare their resistance performances to the original ones. As shown in Table 2, the second and third columns report two objective functions, which are non-dimensionalized compared to its original value. The last three columns report the variation in wetted surface area, displacement and buoyancy position.

Table 2 The part optimal solution sets and constraint condition

Optimal Solutions	F_1	F_2	$(S'-S)/S$	$(\Delta'-\Delta)/\Delta$	$(L'_{CB} - L_{CB})/L$
<i>Opt1</i>	0.931	0.995	1.3%	1.7%	1.7%
<i>Opt2</i>	0.940	0.972	1.8%	2.3%	2.1%
<i>Opt3</i>	0.949	0.937	2.5%	3.7%	1.1%
<i>Opt4</i>	0.973	0.911	2.2%	3.2%	2.1%
<i>Opt5</i>	0.982	0.873	2.1%	2.6%	2.2%
<i>Opt6</i>	0.993	0.854	2.2%	3.4%	2.4%

According to the overall design requirement and resistance reduction effect, the optimized (Opt3) is more satisfactory in six optimized. Its model total resistance at $F_n=0.186$ and $F_n=0.254$ is reduced by 5.1% and 6.3%, respectively. In this paper, the resistances of the optimized at different speed are numerically simulated by RANS, and the results are shown in Table 3 and Fig.5. At the possible speed range, the total resistance coefficients is reduced by 4.5% ~ 19.5%, and the higher the speed, the greater the resistance reduction.

The comparison of hull shape between optimized (Opt3) and original case is shown in Fig. 6. It shows that the variation about transverse section hullform of the optimized has three main points compared with original. Firstly, the bottom of the transverse sections of pontoons becomes wider. Secondly, the vertical radius of transverse pontoon section decreases slightly except of the section near midship, while the transverse radius is nearly invariant. Thirdly, the strut breadth of different shape transverse sections increases. In general, the shape of section varies from ellipsoid to "vase shape".

Table 3 Comparison of resistance between the original and the optimized

F_n	R_{tm} (N)			C_{tm} (10^{-3})		
	<i>Design</i>	<i>Optimized</i>	<i>Reduction</i>	<i>Design</i>	<i>Optimized</i>	<i>Reduction</i>
0.169	12.2	11.9	-2.6%	4.101	3.915	-4.5%
0.186	15.1	14.3	-5.1%	4.190	3.898	-7.0%
0.203	17.7	16.9	-4.6%	4.141	3.873	-6.5%
0.220	22.5	20.4	-9.2%	4.468	3.975	-11.0%
0.237	25.1	23.0	-8.1%	4.301	3.872	-10.0%
0.254	30.5	28.6	-6.3%	4.565	4.191	-8.2%
0.271	44.3	37.8	-14.7%	5.816	4.861	-16.4%
0.300	52.3	43.0	-17.8%	6.087	4.901	-19.5%
0.318	49.4	44.9	-9.0%	5.124	4.568	-10.8%

The free surface wave profiles and the wave contours of the original model and the optimized models at two speeds are reported in Fig.7. The decrease of the bow wave amplitudes of the optimized is significant when compared to the original at $F_n=0.186$. When $F_n=0.254$, the wave amplitude of optimization is close to original nearbow and outboard of slice, while it increases slightly near the inboard of slice. However, the wave amplitude decreases obviously near the stern.

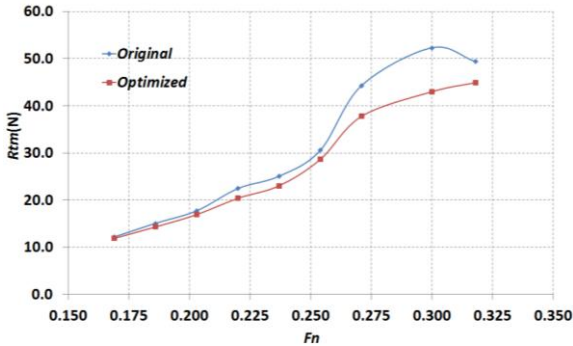


Figure 5 Comparison of the total resistance between the original and the optimized at different speeds

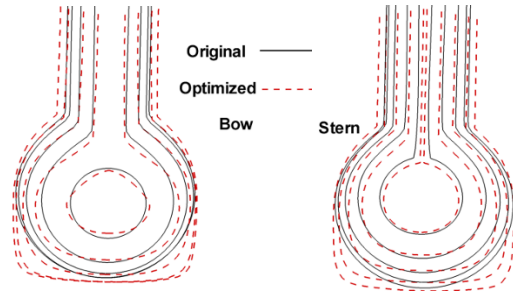


Figure 6 Comparison of transverse section between the original and the optimized

According to the design results mentioned above, through SBD technique, the design optimization problem in multiple speeds will be completed efficiently. The design results obtained decreases the resistance of SWATH in multiple speeds practically. It is hard to achieve only by traditional design method and experience of designer. At the same time, the optimized design results of the paper show the innovation capability of SBD technique, and the shape of the "vase" is obtained from the elliptic submarine line. Its essence is the hydrodynamic configurations design driven by global flow optimization.

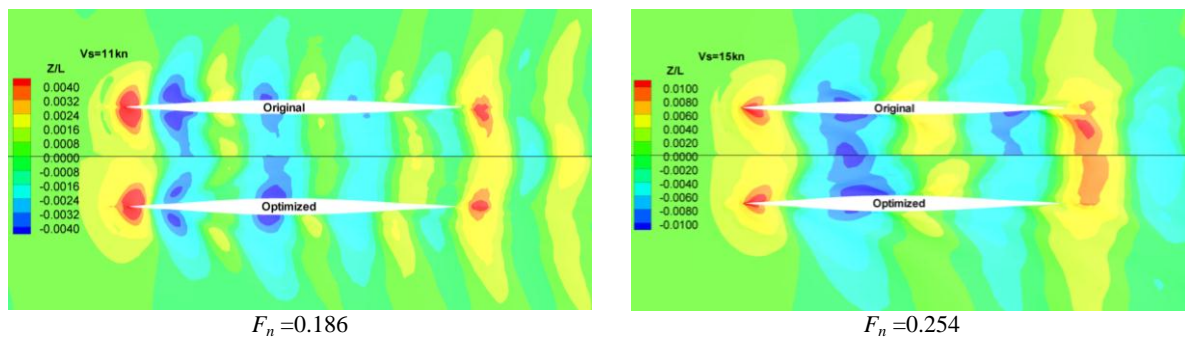


Figure 7 Comparison of wave contours between the original and the optimized

5 EXPERIMENTAL VALIDATION

In order to validate the reliability of optimization design results, the towing test of the optimized model is conducted in CSSRC towing tank. The photos are shown in Fig. 8 (Testing

condition: naked hull with rudders). The CFD (with rudders) and experiment results are shown in Table 4 and Fig.9 ~ Fig.11.

Table 4 The resistance results of experimental and CFD for the optimized with rudders

F_n	R_m (N)		C_m (10^{-3})			θ ($^\circ$)		δ_m (mm)	
	Exp.	CFD	Exp.	CFD	Reduction	Exp.	CFD	Exp.	CFD
0.169	11.908	12.338	3.865	4.005	3.6%	-0.08	-0.12	-69.1	-65.7
0.186	14.32	14.792	3.842	3.968	3.3%	-0.09	-0.15	-74.7	-78.0
0.203	17.174	17.645	3.871	3.978	2.8%	-0.12	-0.19	-93.7	-94.4
0.220	20.631	21.337	3.963	4.098	3.4%	-0.17	-0.25	-117.4	-114.3
0.237	23.325	23.964	3.863	3.969	2.7%	-0.21	-0.29	-143.6	-139.0
0.254	29.125	29.602	4.202	4.271	1.6%	-0.32	-0.44	-189.9	-160.9
0.271	40.284	39.333	5.108	4.987	-2.4%	-0.46	-0.55	-249.7	-203.1
0.300	44.501	44.594	4.998	5.009	0.2%	-0.49	-0.58	-279.2	-260.5

Through comparing the model experiment and CFD results, it is shown that the errors of total resistance, total resistance coefficient and heave value are relatively small. Although the pitch angle results contains some errors, the trend that pitch angle varies along with speed is similar. On the whole, the numerical calculation on the resistance of SWATH has relatively high accuracy and reliable result of prediction. Thus, according to the calculated results before, it is considered that the calculation of resistance benefit from optimization design is relatively credible. It also means the optimized has effect on resistance reduction to some extent at different speeds. When $F_n=0.186$ the total resistance decreases 5.1%, while when $F_n=0.254$ the total resistance decreases 6.3% accordingly.



Figure 8 Experimental models of the optimized

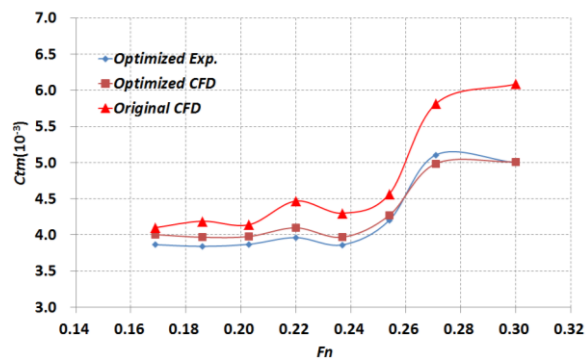


Figure 9 Comparison of the CFD and EFD results of the optimized total resistance coefficient

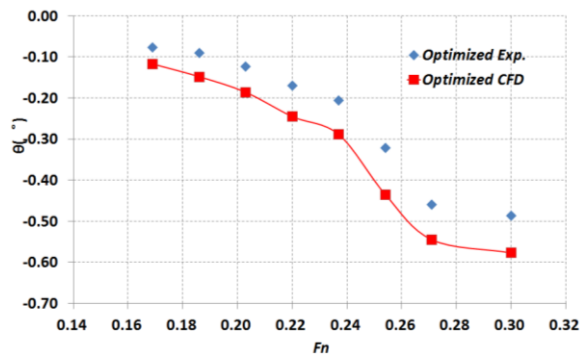


Figure 10 Comparison of CFD and EFD results of the optimized pitch angle

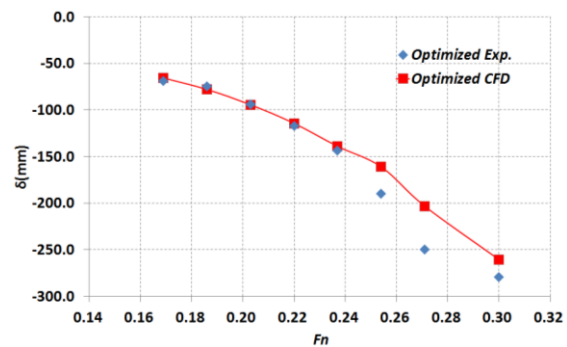


Figure 11 Comparison of CFD and EFD results of the optimized heave value

6 CONCLUSIONS

In this paper, SWATH is regarded as design object, of which the double speed integrated hullform optimization is performed by SBD technique. FFD approach is used to modify the hull geometry and MOPSO algorithm is applied to explore design space. The target response, i.e. total resistance is numerically calculated by high-precision solver based on RANS. Finally, dedicated experimental campaigns for the optimized model have been carried out to validate the accurate of the computations and the success of the optimization processes.

The optimization results show that the decrease of total resistance is significant for the optimization case at two different speeds (11kn and 15kn), with a reduction of about 5.1% and 6.3% respectively. The success of the optimization processes is nicely confirmed by the experimental measurements. The "vase" pontoon configuration is obtained from the ellipsoid, which fully demonstrates the innovation ability of SBD technique. In summary, the result of SWATH double speeds optimization given in this paper demonstrates that SBD technique is not only applicable for special appearance ship such as SWATH, but also quite practical and obviously effective. Its essence is the hydrodynamic configurations design driven by global flow optimization.

REFERENCES

- [1] Li Sheng-Zhong. Research on Hull Form Design Optimization Based on SBD Technique. Ph. D. Dissertation, China Ship Scientific Research Center, 2012.
- [2] Han S, Lee Y S, Choi Y B. Hydrodynamic hull form optimization using parametric models [J]. Journal Mar SciTechnol, 2012.
- [3] Kim H J, Chun H H. Optimizing using Parametric Modification Functions and Global Optimization Methods[C]//27th Symposium on Naval Hydrodynamics. Seoul, Korea, 2008.
- [4] Kim H, Yang C, Chun H H. A Combined Local and Global Hull Form Modificati on Approach for

Hydrodynamic Optimization. 28th Symposium on Naval Hydrodynamics, 2010[C].

- [5] LI Shengzhong, NI Qijun, ZHAO Feng, LIU Hui. Multi-Objective Design Optimization of Stern Lines for Full-Formed Ship[J]. Shipbuilding of China Vol. 54 No.3, 2013: 1-10
- [6] SHI Wen-qiang, YU Xian-zhao. The development and future trend of foreign SWATH ships [J]. Ship Science and technology Vol.34, Supplement 2, 2012: 4-19
- [7] ZHONG Kai, ZHANG Pei-yuan, ZHENG Ming. SWATH vessels development and future in Germany [J]. Ship Science and technology Vol.34, Supplement 2, 2012: 20-34, 51.
- [8] Peri D, Campana E F. Simulation Based Design of Fast Multihull Ship[C]. 26th Symposium on NavalHydrodynamics. Rome, Italy, 2006.
- [9] Campana E F, Peri D. Shape optimization in ship hydrodynamics using computational fluid dynamics[J]. Computer Methods in Applied. Mechanics and Engineering. 2006. 196: 634–651.
- [10] Tahara Y, Peri D, Campana E F, Stern F. Single and Multiobjective Design Optimization of a FastMultihull Ship: numerical and experimental results[C]. 27th Symposium on Naval Hydrodynamics.2008.
- [11] Stefano Brizzolara, Tom Curtin, Marco Bovio, Giuliano Vernengo. Concept design and hydrodynamic optimizationof an innovative SWATH USV by CFD methods [J]. Ocean Dynamics, 2012, 62:227–237
- [12] Sederberg T W, Parry S R. Free-Form Deformation of Solid Geometric Models [J]. Proc.SIGGRAPH'86, Computer Graphics, 20(4):151-159.
- [13] Campana E F, Peri D, Tahara Y, Kandasamy M, and Stern F. Numerical Optimization Methods for Ship Hydrodynamic Design[C], SNAME Annual Meeting 2009.

Geometry and Meshing for Automated High-Order Simulations

Mark Shephard*, Mark Beall**

*Rensselaer Polytechnic Institute, **Simmetrix, Inc.

ABSTRACT

The development of isogeometric finite element methods represent a major advance in effective high-order discretization methods both in terms how high-order discretizations can be constructed and controlled, as well as in increased understanding of the properties and advantages of these methods. The application of high-order finite element methods place additional requirements on the mesh generation processes, and their interaction with the geometric domain definition, due to the need for elements on curved domain boundaries to be properly curved to those boundaries and the desire to often generate coarse meshes such that only a small number of finite elements are used to represent entire geometric model features. This presentation will summarize a set of technologies that have been, and continue to be, developed to support the automatic generation and adaptation of curved high-order meshes with an emphasis on being able to interact with the geometric domain definitions ranging for those housed in CAD systems [1], to domains defined by image data [2], to evolving domains as defined by the simulation of physical processes of interest. Key capabilities to be discussed and demonstrated are tools supporting the construction of proper geometric domain topological models from the original geometry, procedures to automatically generate and anisotropically adapt meshes for those geometries that maintain the required levels of geometric approximation while allowing the mesh configurations to be defined by the needs to most effectively represent the physical behavior being simulated. [1] Beall, M.W., Walsh, J. and Shephard, M.S., 2004. A comparison of techniques for geometry access related to mesh generation. *Engineering with Computers*, 20(3), pp.210-221. [2] Klaas, O., Beall, M.W. and Shephard, M.S., 2013. Construction of models and meshes of heterogeneous material microstructures from image data. In *Image-Based Geometric Modeling and Mesh Generation* (pp. 171-193). Springer Netherlands.

Modeling of Ultra-High Performance Concrete Flyer Plate Experiments

Jesse Sherburn*, William Heard**

*U.S. Army Engineer Research and Development Center, **U.S. Army Engineer Research and Development Center

ABSTRACT

Ultra-high performance concrete (UHPC) has emerged as a viable material in protective structures of interest to the defense community. A significant amount of research has been completed on characterizing UHPC under quasi-static loading conditions [1] and more recently under dynamic loading conditions [2] such as Koslky bar experiments. One area that has little study is under extreme loading conditions such as high velocity flyer plate impacts that induce shock wave propagation. Recent research efforts by Neel et al. [3] produced a number of carefully controlled flyer plate impact experiments for a UHPC. This data provides an excellent testbed to evaluate some current computational solid mechanics codes and their respective constitutive models ability to model this extreme loading condition. The data from Neel et al. [3] can be used to calibrate and validate various computational methods subjected to this type of loading condition. This study investigates modeling the flyer plate experiments of Neel et al. [3] using a number of different methods such the Eulerian shock wave code CTH, and the meshfree method known as the reproducing kernel particle method (RKPM). Multiple constitutive models in CTH and RKPM will be evaluated in order to match the flyer plate experiments. A discussion of the different current strengths and weaknesses of the respective models will be discussed as well as some future recommended research areas. [1] Williams, E.M., Graham, S.S., Reed, P.A., and Rushing, T.S. 2009. Laboratory Characterization of Cor-Tuf Concrete With and Without Steel Fibers. ERDC/GSL TR-09-22, U.S. Army Engineer Research and Development Center, Vicksburg, MS. [2] Martin, B.E., Heard, W.F., Loeffler, C.M., and Nie, X. 2017. Specimen Size and Strain Rate Effects on the Compressive Behavior of Concrete. *Experimental Mechanics*, <https://doi.org/10.1007/s11340-017-0355-2>. [3] Neel, C., Martin, B.E., and Chhabildas, L. 2017. Shock and Spall of the Ultra-High Performance Concrete Mortar "Cortuf" without Steel Fibers. AFRL-RW-EG-TR-2017-082, Air Force Research Laboratory, Eglin Air Force Base, FL. * Permission to publish was granted by Director, Geotechnical and Structures Laboratory.

FREE VIBRATION ANALYSIS OF BEAMS AND PLATES WITH ELASTIC BOUNDARY CONDITIONS BY DIFFERENTIAL QUADRATURE FINITE ELEMENT METHOD

Dongyan Shi*, Xianlei Guan[†], Gai Liu[‡]

*College of Mechanical and Electrical Engineering, Harbin Engineering University
Harbin, China
Email: shidongyan@hrbeu.edu.cn

[†]College of Mechanical and Electrical Engineering, Central South University
Changsha, China
Email: guanxianlei@hrbeu.edu.cn

[‡]College of Mechanical and Electrical Engineering, Harbin Engineering University
Harbin, China
Email: liugai@hrbeu.edu.cn

Keywords: Free vibration; DQFEM; Elastic boundary conditions; virtual springs

Summary: *A virtual or artificial spring technique is used in the weak form differential quadrature finite element method (DQFEM) in order to simulate the effects of elastic restraints in the analysis of free vibrations of beams and plates. By introducing the virtual spring technique, the applicability of the DQFEM is expanded to deal with free vibration problems with general elastic boundary conditions. The elastic boundary conditions can be easily achieved by setting the stiffness of corresponding springs to be desired values. Firstly, the expressions of the potential and kinetic energy of a beam or plate element are given based on the Timoshenko beam theory and Mindlin's plate theory, respectively, and the differential operators in which are discretized by the differential quadrature (DQ) rules. Secondly, the stiffness and mass matrices of beam element and plate element are derived in form of weighting coefficient matrices. Next, the translational springs and rotational springs are used to restraint the translational and rotational degree of freedoms of a node, respectively. Therefore, the potential energy of the springs is taken into account as part of the stiffness matrix of the elements. Finally, global stiffness and mass matrices of the whole system is*

assembled according to the traditional finite element method (FEM). Several numerical examples are presented. The accuracy of the present method is validated by comparing the results with those from references and FEM.

1 INTRODUCTION

The finite element method (FEM) and finite difference method (FDM) have been widely used in many engineering problems. Another alternative algorithm also called as the differential quadrature method (DQM) is proposed by Bellman et al. [1,2]. The greatest advantage of this algorithm is merely using a little of grid points to achieve high accuracy. However, there are some drawbacks in determining the weighting coefficients [3] in the original DQM. Many researchers have concerned the application of the multiple boundary conditions in DQM [4-5]. Recently, a differential quadrature finite element method (DQFEM) has been proposed by Yufeng Xing [6]. The discretization is operated on the partial derivative in the strain energy and kinetic energy, which is different from the operation in most of the literatures, where the discretization is operated directly on the differential equations [7-9]. Also, in DQFEM the boundary conditions are imposed similarly as that in FEM while in other literatures the discretized expressions of classical boundary conditions are imposed to modify the coefficient weighting matrix, which makes it complicated to apply the multiple boundary conditions to the structures.

The DQFEM has been used to solve many vibration problems with irregular geometries [10]. However, few works on the vibration characteristic of structures with elastic restraints can be found. The elastic restraints are simulated by employing translational and rotational springs linking the structure and the ground [11]. By setting different spring stiffness to achieve desired boundary conditions including several ideal classical boundary conditions. Many works have been done on the influence of spring stiffness on the vibration characteristic of the structure [11-15]. The main purpose of the authors is to introduce the concept of elastic restraints into the DQFEM to expand the application of the method to the analysis of vibration problems with elastic restraints as well as irregular domains.

The main contents of this paper are shown as follows: Firstly, introduce the basic rules of DQ and elaborate the specific principles of DQFEM. Then, a beam structure with elastic restraints is given to illustrate how the virtual translational and rotational springs are applied into equations of motion. Next, an example of a rectangular plate with elastic restraints is given to illustrate the procedures of applying the elastic restraints to a two-dimensional problem. Finally, the vibration of a plate with curved side is presented. Some numerical results are presented and compared with the literatures available, which proves the accuracy of the present work.

2 THEORY AND FORMULATIONS

2.1 The DQ rules

The basic idea of the DQM is to express the differential operator by the summation of a set of weighting coefficients multiplied by the function values corresponding to specified nodes. For instance, the s th-order derivative of function $f(x)$ can be written as:

$$\left. \frac{d^s f(x)}{dx^s} \right|_i = \sum_{j=1}^N A_{ij}^{(s)} f_j \quad (1)$$

where $A_{ij}^{(s)}$ is the first-order weighting coefficient. The partial derivatives of two-dimensional function $f(x,y)$ at grid point (x_i, y_j) can be written as

$$\left. \frac{\partial^r f}{\partial x^r} \right|_{ij} = \sum_{m=1}^M A_{im}^{(r)} f_{mj}, \quad \left. \frac{\partial^s f}{\partial y^s} \right|_{ij} = \sum_{n=1}^N B_{jn}^{(s)} f_{in}, \quad \left. \frac{\partial^{r+s} f}{\partial x^r \partial y^s} \right|_{ij} = \sum_{m=1}^M A_{im}^{(r)} \sum_{n=1}^N B_{jn}^{(s)} f_{mn} \quad (2)$$

where, $A_{im}^{(r)}$ and $B_{jn}^{(s)}$ are the weighting coefficients along x and y directions, respectively. Refer to references [16] for detailed expressions of the weighting coefficient matrix.

2.2 Equations of motion of the beam element

An elastically restrained beam is shown in Fig. 1. The stiffness of the translational springs and the rotational springs on the grid point x_1 and x_M are denoted by k_{t1} , k_{tM} and k_{r1} , k_{rM} , respectively. Base on the Timoshenko beam theory and take the axial effect of the beam into account, the displacements of a point in the beam can be given as:

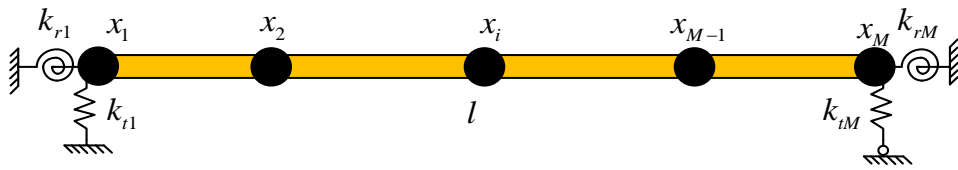


Fig. 1 The beam with elastic restraints on both ends.

$$u^e(x, z, t) = u_x^e(x, t) - z\varphi^e(x, t), \quad w^e(x, t) = w^e(x, t) \quad (3)$$

$$\{u_x^e(x), \varphi^e(x), w^e(x)\} = \sum_{i=1}^N l_i(x) \{u_{xi}^e, \varphi_i^e, w_i^e\}$$

where $l_i(x)$ is the i th Lagrange polynomial, $u_{xi}^e = u_x^e(x_i)$, $\varphi_i^e = \varphi^e(x_i)$ and $w_i^e = w^e(x_i)$ are the displacements at i th Gauss-Lobatto-Legendre (GLL) quadrature points [16]. According to the

Dongyan Shi, Xianlei Guan, Gai Liu

elastic theory of Timoshenko beam, the normal and shear strain are

$$\boldsymbol{\varepsilon} = [\varepsilon_t \quad \varepsilon_b \quad \gamma_{xz}]^T = \left[\frac{\partial u_x}{\partial x} \quad -z \frac{\partial \varphi}{\partial x} \quad \frac{\partial w}{\partial x} - \varphi \right]^T \quad (4)$$

where the normal strain contains the compression and extension strain ε_t and bending strain ε_b . By applying the DQ rules, the derivatives in Eq. (4) can be written in the matrix form as

$$\boldsymbol{\varepsilon}^e = \begin{bmatrix} \mathbf{A}^{(1)} & \mathbf{0} & \mathbf{0} \\ \mathbf{0} & \mathbf{0} & -z\mathbf{A}^{(1)} \\ \mathbf{0} & \mathbf{A}^{(1)} & -\mathbf{E} \end{bmatrix} \begin{bmatrix} \mathbf{u}^e \\ \mathbf{w}^e \\ \boldsymbol{\varphi}^e \end{bmatrix} = \mathbf{B}\boldsymbol{\delta}^e \quad (5)$$

where

$$\mathbf{u}_x^e = [u_x^e(x_1) \quad u_x^e(x_2) \quad \cdots \quad u_x^e(x_N)]^T, \quad \mathbf{w}^e = [w^e(x_1) \quad w^e(x_2) \quad \cdots \quad w^e(x_N)]^T \quad (6)$$

$$\boldsymbol{\varphi}^e = [\varphi^e(x_1) \quad \varphi^e(x_2) \quad \cdots \quad \varphi^e(x_N)]^T$$

The superscript e denotes that the corresponding displacement vectors is for element e , $\mathbf{A}^{(1)}$ is the first-order $N \times N$ weighting coefficient matrix for one-dimensional problem, \mathbf{E} is $N \times N$ unit diagonal matrix. Assuming the Young's modulus and the shear modulus are denoted by E and G , the normal and shear stresses of the beam can be obtained as

$$\boldsymbol{\sigma}^e = \begin{bmatrix} \mathbf{E}^* & \mathbf{0} & \mathbf{0} \\ \mathbf{0} & \mathbf{E}^* & \mathbf{0} \\ \mathbf{0} & \mathbf{0} & \kappa\mathbf{G} \end{bmatrix} \boldsymbol{\varepsilon}^e = \mathbf{D}\boldsymbol{\varepsilon}^e \quad (7)$$

where \mathbf{E}^* and \mathbf{G} are $N \times N$ diagonal matrices where the diagonal elements are Young's modulus and shear modulus, respectively. κ the shear correction factor of the beam.

The strain potential energy V is given as

$$V^e = \frac{1}{2} \iiint \boldsymbol{\sigma}^T \boldsymbol{\varepsilon} dx dy dz = \frac{1}{2} \iiint (\boldsymbol{\delta}^e)^T \mathbf{B}^T \mathbf{D} \mathbf{B} \boldsymbol{\delta}^e dx dy dz \quad (8)$$

The potential energy V_t stored in the translational springs and the potential energy V_r of the rotational springs are given as

$$V_t = \frac{1}{2} k_{t1} (w_1^e)^2 + \frac{1}{2} k_{tM} (w_M^e)^2, \quad V_r = \frac{1}{2} k_{r1} (\varphi_1^e)^2 + \frac{1}{2} k_{rM} (\varphi_M^e)^2 \quad (9)$$

The kinetic energy T of the beam is given as

$$T^e = \frac{1}{2} \iiint \rho \left[(\dot{u}_x^e)^2 + (-z\dot{\phi}^e)^2 + (\dot{w}^e)^2 \right] dx dy dz = \frac{1}{2} \int_0^l \rho (S\dot{u}^2 + S\dot{w}^2 + I\dot{\phi}^2) dx \quad (10)$$

The Lagrange function (L) of the beam can be expressed in terms of the total strain energy U and kinetic energy T as

$$L = T - U, \quad U = U_b + V_t + V_r \quad (11)$$

By applying the Hamilton's principle and extracting the time dependent function, one can get the stiffness matrix, mass matrix and the eigenvalue equations easily.

2.3. Equations of motion of the rectangular plate element

Next consider a plate meshed into M grid points along the x direction and N grid points along the y direction with translational and rotational springs supported at the grid points. In the two-dimensional problem, two types of rotational springs are introduced which are denoted by k_{rxi} and k_{ryi} . k_{rxi} restrains the rotation of the plate in x direction while k_{ryi} restrains the rotation in y direction. The displacement of point in the plate can be given as

$$u^e(x, y) = u_x^e(x, y) - z\phi_x^e(x, y), \quad v^e(x, y) = v_y^e(x, y) - z\phi_y^e(x, y); \quad w^e(x, y) = w^e(x, y) \\ \left\{ \begin{array}{l} u_x^e(x, y), v_y^e(x, y), \\ \phi_x^e(x, y), \phi_y^e(x, y), w^e(x, y) \end{array} \right\} = \sum_{i=1}^M l_i(x) \sum_{j=1}^N l_j(y) \left\{ \begin{array}{l} u_{xij}^e, v_{yij}^e, \\ \phi_{xij}^e, \phi_{yij}^e, w_{ij}^e \end{array} \right\} \quad (12)$$

where $l_j(x)$ is j th Lagrange polynomial in x direction, $u_{xij}^e = u_x^e(x_i, y_j)$, $v_{yij}^e = v_y^e(x_i, y_j)$, $\phi_{xij}^e = \phi_x^e(x_i, y_j)$, $\phi_{yij}^e = \phi_y^e(x_i, y_j)$ and $w_{ij}^e = w^e(x_i, y_j)$ are the displacements at the GLL quadrature points (x_i, y_j) . According to the Mindlin's plate theory, the shear deformation effect is taken into account. The normal and shear strain of a moderately thick plate are

$$\varepsilon_{xx}^e = \frac{\partial u^e(x, y)}{\partial x}, \quad \varepsilon_{yy}^e = \frac{\partial v^e(x, y)}{\partial y}, \quad \gamma_{xy}^e = \frac{\partial v^e(x, y)}{\partial x} + \frac{\partial u^e(x, y)}{\partial y} \\ \gamma_{xz}^e = \frac{\partial w^e(x)}{\partial x} + \frac{\partial u^e(x)}{\partial z}, \quad \gamma_{yz}^e = \frac{\partial w^e(x)}{\partial x} + \frac{\partial v^e(x)}{\partial z} \quad (13)$$

By applying the DQ rules, the derivatives in Eq. (13) can be written in the matrix form as the Eq. (14), in which $\mathbf{0}$ is $N \times N$ zero matrix, \mathbf{E} is $N \times N$ unit diagonal matrix, \mathbf{L}_t and \mathbf{L}_b are weighting coefficient matrix of tension or compression differential operators and bending differential operators, respectively.

Dongyan Shi, Xianlei Guan, Gai Liu

$$\boldsymbol{\varepsilon}_t^e = \begin{bmatrix} \varepsilon_{xxt}^e \\ \varepsilon_{yyt}^e \\ \gamma_{xyt}^e \end{bmatrix} = \begin{bmatrix} \mathbf{A}_{02}^{(1)} & \mathbf{0} \\ \mathbf{0} & \mathbf{B}_{02}^{(1)} \\ \mathbf{B}_{02}^{(1)} & \mathbf{A}_{02}^{(1)} \end{bmatrix} \begin{bmatrix} \mathbf{u}_x^e \\ \mathbf{v}_y^e \end{bmatrix} = \mathbf{L}_t \boldsymbol{\delta}_1^e; \quad \boldsymbol{\varepsilon}_b^e = \begin{bmatrix} \varepsilon_{xxb}^e \\ \varepsilon_{yyb}^e \\ \gamma_{xyb}^e \\ \gamma_{xz}^e \\ \gamma_{yz}^e \end{bmatrix} = \begin{bmatrix} -z\mathbf{A}_{02}^{(1)} & \mathbf{0} & \mathbf{0} \\ \mathbf{0} & -z\mathbf{B}_{02}^{(1)} & \mathbf{0} \\ -z\mathbf{B}_{02}^{(1)} & -z\mathbf{A}_{02}^{(1)} & \mathbf{0} \\ -\mathbf{E} & \mathbf{0} & \mathbf{A}_{02}^{(1)} \\ \mathbf{0} & -\mathbf{E} & \mathbf{B}_{02}^{(1)} \end{bmatrix} \begin{bmatrix} \varphi_x^e \\ \varphi_y^e \\ \mathbf{w}^e \end{bmatrix} = \mathbf{L}_b \boldsymbol{\delta}_2^e \quad (14)$$

Then, the normal and shear stresses are

$$\boldsymbol{\sigma}_t^e = \mathbf{D}_1 \boldsymbol{\varepsilon}_t^e, \quad \boldsymbol{\sigma}_b^e = \mathbf{D}_2 \boldsymbol{\varepsilon}_b^e$$

$$\mathbf{D}_1 = \frac{E}{1-\mu^2} \begin{bmatrix} \mathbf{E}^* & \mu\mathbf{E}^* & 0 \\ \mu\mathbf{E}^* & \mathbf{E}^* & 0 \\ 0 & 0 & \frac{1-\mu}{2}\mathbf{E}^* \end{bmatrix}; \quad \mathbf{D}_2 = \frac{E}{1-\mu^2} \begin{bmatrix} \mathbf{E}^* & \mu\mathbf{E}^* & \mathbf{0} & \mathbf{0} & \mathbf{0} \\ \mu\mathbf{E}^* & \mathbf{E}^* & \mathbf{0} & \mathbf{0} & \mathbf{0} \\ \mathbf{0} & \mathbf{0} & \frac{1-\mu}{2}\mathbf{E}^* & \mathbf{0} & \mathbf{0} \\ \mathbf{0} & \mathbf{0} & \mathbf{0} & \frac{1-\mu}{2}\kappa\mathbf{E}^* & \mathbf{0} \\ \mathbf{0} & \mathbf{0} & \mathbf{0} & \mathbf{0} & \frac{1-\mu}{2}\kappa\mathbf{E}^* \end{bmatrix} \quad (15)$$

where \mathbf{E}^* is $N \times N$ diagonal matrices where the diagonal elements are Young's modulus, κ is shear factor, usually $\kappa = \pi^2/12$.

The strain energy U_p and kinetic energy T for the plate are given as

$$V_p^e = \frac{1}{2} \iiint (\boldsymbol{\sigma}_t^{eT} \boldsymbol{\varepsilon}_t^e + \boldsymbol{\sigma}_b^{eT} \boldsymbol{\varepsilon}_b^e) dx dy dz \quad (16)$$

$$T^e = \frac{1}{2} \iiint \rho \left[(\dot{u}_x^e)^2 + (\dot{v}_y^e)^2 + (-z\dot{\varphi}_x^e)^2 + (-z\dot{\varphi}_y^e)^2 + (\dot{w}^e)^2 \right] dx dy dz$$

The potential energy V_{tx} , V_{ty} and V_{tw} stored in the three types of translational springs and the potential energy V_{rx} and V_{ry} of the two types of rotational springs are given as

$$V_{tx} = \frac{1}{2} \sum_{i=1}^2 \int_0^{l_i} k_{txi} (u_{xi}^e)^2 dl_i, \quad V_{ty} = \frac{1}{2} \sum_{i=1}^2 \int_0^{l_i} k_{tyi} (v_{yi}^e)^2 dl_i, \quad V_{tw} = \frac{1}{2} \sum_{i=1}^4 \int_0^{l_i} k_{twi} (w_i^e)^2 dl_i \quad (17)$$

$$V_{r1} = \frac{1}{2} \sum_{i=1}^2 \int_0^{l_i} k_{rxi} (\varphi_x^e)^2 dl_i, \quad V_{r2} = \frac{1}{2} \sum_{i=1}^2 \int_0^{l_i} k_{ryi} (\varphi_y^e)^2 dl_i$$

The Lagrange function (L) of the plate can be expressed in terms of the total strain energy U and kinetic energy T as

$$L = T - U, \quad U = U_p + V_{tx} + V_{ty} + V_{tw} + V_{rx} + V_{ry} \quad (18)$$

Similarly, by applying the Hamilton's principle and extracting the time dependent function, the stiffness matrix, mass matrix and the eigenvalue equations can be obtained.

2.4. Curvilinear quadrilateral plate element

The mass and stiffness matrices derived in the section 2.3 are limited to rectangular plates. It is necessary to extend the plate element to be applicable for irregular plate structures. Curvilinear quadrilateral plate defined in the Cartesian coordinate system can be mapped into a square parent domain defined in $-1 \leq \xi \leq 1$, $-1 \leq \eta \leq 1$, namely the natural coordinate system as shown in Fig. 3, through a mapping technique with serendipity element [16]:

$$x = \sum_{k=1}^{N_k} S_k(\xi, \eta) x_k, \quad y = \sum_{k=1}^{N_k} S_k(\xi, \eta) y_k \quad (19)$$

where x_k, y_k are the coordinates of nodes in the Cartesian coordinate system, S_k is the shape function with respect to node (x_k, y_k) . There are no limitations on the locations and the total numbers of the nodes except that the nodes are arranged anti-clockwise. Assuming the nodes distributions on the edges of a curvilinear quadrilateral plate are given as

$$\begin{aligned} \text{On side 1: } & (\alpha_1, -1), (\alpha_2, -1), \dots, (\alpha_{m-1}, -1), (\alpha_m, -1); \quad \text{On side 2: } (1, \beta_1), (1, \beta_2), \dots, (1, \beta_{n-1}), (1, \beta_n) \\ \text{On side 3: } & (\gamma_1, 1), (\gamma_2, 1), \dots, (\gamma_{p-1}, 1), (\gamma_p, 1); \quad \text{On side 4: } (-1, \lambda_1), (-1, \lambda_2), \dots, (-1, \lambda_{q-1}), (-1, \lambda_q) \end{aligned} \quad (20)$$

The general expressions of shape functions with respect to the i th node on each side except the corner nodes are given as

$$\begin{aligned} S_{1,i} &= \frac{1}{2}(1-\eta)(1-\xi^2) \frac{1}{1-\alpha_i^2} \prod_{\substack{j=2 \\ j \neq i}}^{m-1} \frac{\xi - \alpha_j}{\alpha_i - \alpha_j}, \quad S_{2,i} = \frac{1}{2}(1+\xi)(1-\eta^2) \frac{1}{1-\beta_i^2} \prod_{\substack{j=2 \\ j \neq i}}^{n-1} \frac{\eta - \beta_j}{\beta_i - \beta_j} \\ S_{3,i} &= \frac{1}{2}(1+\eta)(1-\xi^2) \frac{1}{1-\gamma_i^2} \prod_{\substack{j=2 \\ j \neq i}}^{p-1} \frac{\xi - \gamma_j}{\gamma_i - \gamma_j}, \quad S_{4,i} = \frac{1}{2}(1-\xi)(1-\eta^2) \frac{1}{1-\lambda_i^2} \prod_{\substack{j=2 \\ j \neq i}}^{q-1} \frac{\eta - \lambda_j}{\lambda_i - \lambda_j} \end{aligned} \quad (21)$$

The shape functions corresponding to the four corner nodes are given as

$$\begin{aligned} S_{p1} &= \frac{1}{4}(1-\eta)(1-\xi) \left[\prod_{j=2}^{m-1} \frac{\xi - \alpha_j}{-1 - \alpha_j} + \prod_{j=2}^{q-1} \frac{\eta - \lambda_j}{-1 - \lambda_j} - 1 \right]; \quad S_{p2} = \frac{1}{4}(1-\eta)(1+\xi) \left[\prod_{j=2}^{m-1} \frac{\xi - \alpha_j}{1 - \alpha_j} + \prod_{j=2}^{n-1} \frac{\eta - \beta_j}{-1 - \beta_j} - 1 \right] \\ S_{p3} &= \frac{1}{4}(1+\eta)(1+\xi) \left[\prod_{j=2}^{p-1} \frac{\xi - \gamma_j}{1 - \gamma_j} + \prod_{j=2}^{n-1} \frac{\eta - \beta_j}{1 - \beta_j} - 1 \right]; \quad S_{p4} = \frac{1}{4}(1+\eta)(1-\xi) \left[\prod_{j=2}^{p-1} \frac{\xi - \gamma_j}{-1 - \gamma_j} + \prod_{j=2}^{q-1} \frac{\eta - \lambda_j}{1 - \lambda_j} - 1 \right] \end{aligned} \quad (22)$$

The function $f(x, y)$ defined in the Cartesian coordinate system now can be expressed in terms of ξ and η in the natural coordinate system as $f=f[x(\xi, \eta), y(\xi, \eta)]$. Using the rule of differentiation, one can obtain the derivatives with respect to the ξ and η , namely the

expressions of $\partial f/\partial \xi$ and $\partial f/\partial \eta$ [16]. Then the modified weighting coefficient matrices derived for irregular plate can be obtained. By substituting the modified weighting coefficient matrices into the strain and stress expressions to replace the original matrices, the mass matrix and stiffness matrix for curvilinear quadrilateral plate can be obtained.

3 NUMERICAL EXAMPLES

In this section, several numerical examples will be presented to validate the accuracy of the present method. The discussions on the influence of the allocation of the nodes in the mapping procedures on the accuracy of the vibration results of curvilinear quadrilateral plate are also presented.

The convergence results of the first six frequency parameters $\lambda=l/\pi(\omega(\rho h/D)^{1/2})^{1/2}$ of a free beam are presented in Fig. 2(a), which shows that the results converge quickly to the accurate results as the number of nodes increases. Next example is a two-dimensional problem of a rectangular plate with length a and width b . The results of rectangular plate converge even faster than those of the beam from Fig. 2(b).

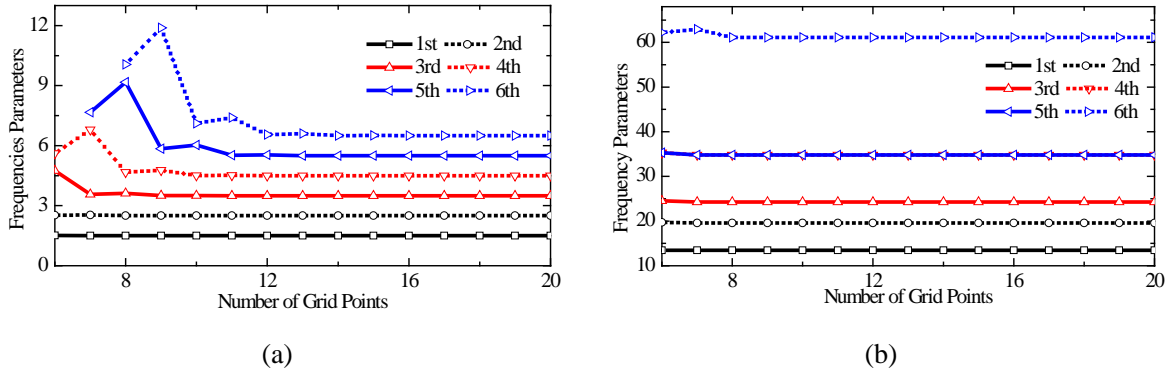


Fig. 2 Convergence studies of the first six frequency parameters of (a) free beam and (b) square plate.

Next, the virtual springs are introduced to simulate the practical boundary conditions and the effect on the natural frequencies and mode shapes are presented. Fig. 3 and Fig. 4 shows the variations of the frequency parameters with different stiffness of springs.

From Fig. 3, one can conclude that the frequency parameters increase as the stiffness of the translational springs increases firstly and then remain almost constant when the stiffness exceeds a certain value (for example $k_t/D=1e6$). For comparison, the results with classical boundary conditions: simply supported (SS) and clamped-clamped (CC) are also presented in Fig. 3(a) and Fig. 3(b), respectively. The same rules which can be observed as those for the beam from Fig. 4 are that the frequency parameters vary obviously in a certain interval of stiffness and remain almost constant when the stiffness is relatively small or large. Therefore, the simply supported boundary conditions can be achieved when the stiffness translational

springs is rather larger than the bending rigidity of the beam. The clamped boundary conditions can also be obtained by setting the stiffness of both the translational and rotational springs to be very large.

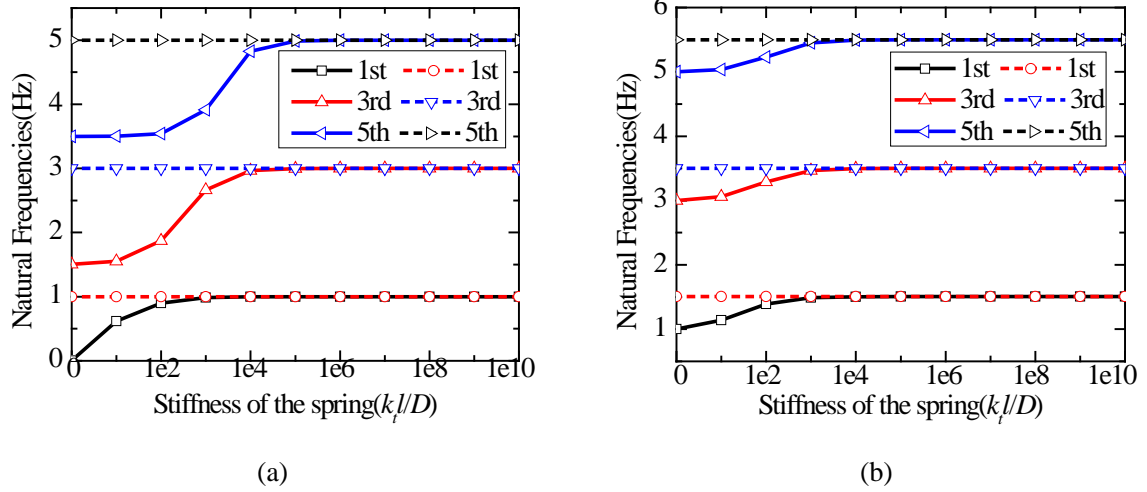


Fig. 3 Variations of the frequency parameters of a beam versus different stiffness of (a) translational springs and (b) rotational springs, —, elastic restraints, ---, classical boundary conditions.

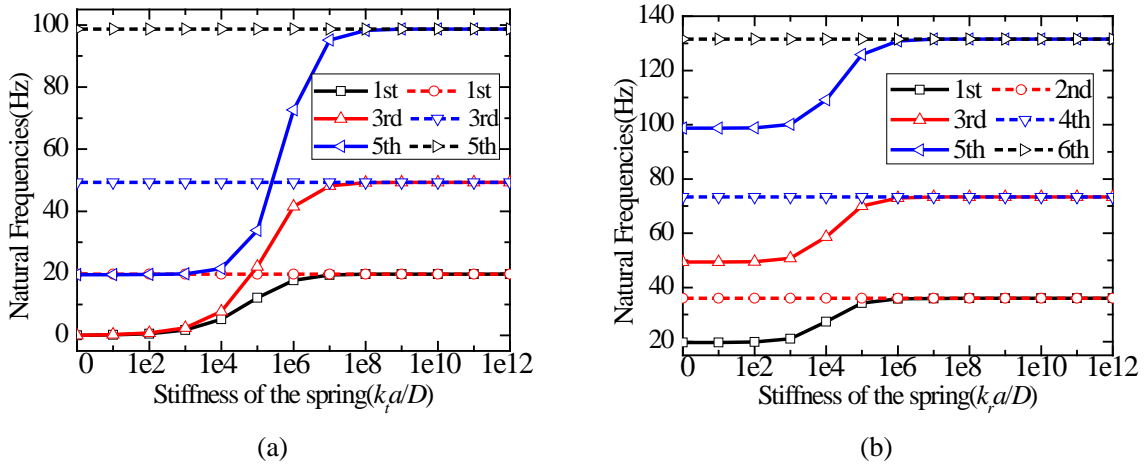


Fig. 4 Variations of the first six frequency parameters versus different stiffness of (a) translational springs and (b) rotational springs for $a/b=1$, —, elastic restraints, ---, classical boundary conditions.

The virtual springs introduced simplify the imposing procedures of boundary conditions. A certain boundary conditions can be easily achieved by setting the desired stiffness with respect to each spring. Table 1 lists some results obtained with different stiffness, which match well with the results in literature. The good agreement between the results

demonstrates the accuracy of the present method. The ^aresults come from the Ref[11].

Table 1 The first four frequency parameters $\lambda=l/\pi(\omega(\rho h/D)^{1/2})^{1/2}$ for various stiffness of the rotational springs.

$k_{rN}l$	Mode number			
	1	2	3	4
1	1.28657	2.27077	3.26479	4.26145
	1.28656 ^a	2.27081	3.26491	4.26175
10	1.41020	2.37137	3.34920	4.33353
	1.41020 ^a	2.37138	3.34927	4.33370
100	1.49137	2.47681	3.46883	4.46107
	1.49137 ^a	2.47681	3.46884	4.46108
10 ¹⁰	1.50561	2.49975	3.50001	4.50000
	1.50562 ^a	2.49975	3.50001	4.50000

Table 2 The frequency parameters $\lambda=\omega a^2(\rho h/D)^{1/2}$ obtained with the 3rd type of nodes collocation methods of a free curvilinear quadrilateral plate under classical boundary conditions.

BC	Mode number					
	1	2	3	4	5	6
CCCC	96.01167	144.50359	190.18585	220.10220	258.74942	312.49447
	96.01943 ^a	144.28894	190.11589	220.48642	258.88697	311.99135
SSSS	49.85197	86.89633	132.00638	147.02897	197.77649	225.75121
	49.95280 ^a	87.00176	132.04367	147.41741	197.90891	225.37268
FFFF	20.96940	26.32154	55.37219	58.81766	74.03596	99.88516
	20.97836 ^a	26.31016	55.43785	58.77528	74.09149	99.83140
CCFC	29.00088	65.78078	95.81549	120.13331	158.34002	188.40518
	29.02093 ^a	65.78392	95.85332	120.11561	158.19744	188.25917
CFFF	12.51200	23.16806	39.38176	64.63335	83.98056	110.89167
	12.52553 ^a	23.13964	39.39007	64.69837	83.93515	110.76724

^aResults from FEM.

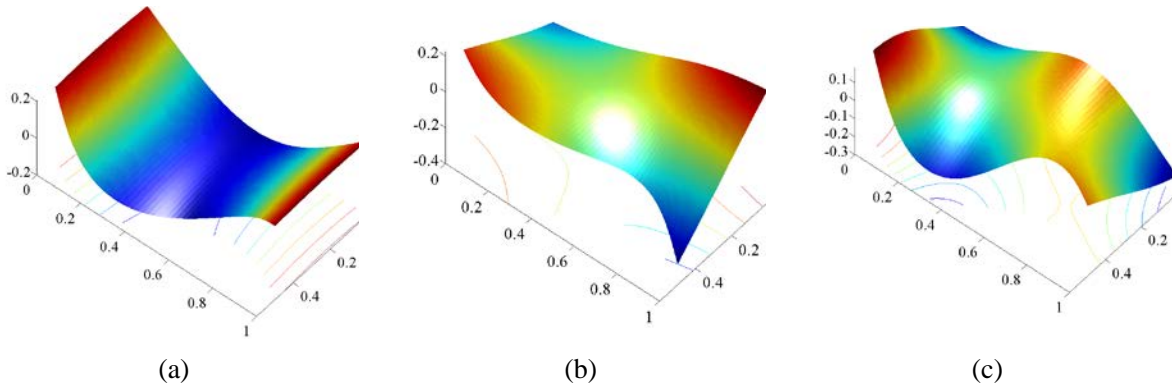


Fig. 5 The mode shapes except the rigid modes of the FFFF plate. (a) the 1st, (b) the 2nd, (c) the 3rd.

4 CONCLUSION

In this paper, the virtual springs are introduced into DQFEM to simulate the practical elastic restraints. The translational springs and rotational springs respectively restrain the translational movement and rotation of the point on the sides of the structures. Owing to the springs introduced, the imposing procedures of the boundary conditions are simplified so that a certain kind of boundary conditions can be achieved just by setting different stiffness of the springs. The frequency parameters and the mode shapes of the structures vary as the stiffness changes. The variations are obvious in a certain interval of stiffness of springs, beyond which the frequency parameters remain almost the same. Consequently, classical boundary conditions can be regarded as typical situations when stiffness is relatively small or large.

ACKNOWLEDGMENTS

This paper is funded by the International Exchange Program of Harbin Engineering University for Innovation-oriented Talents Cultivation. The works also supported by the National Natural Science Foundation of China (No. 51679056), and Natural Science Foundation of Heilongjiang Province of China (E2016024).

REFERENCES

- [1] Bellman, R., & Casti, J. Differential quadrature and long-term integration. *Journal of Mathematical Analysis and Applications*. (1971) 34:235-238.
- [2] Bellman, R., Kashef, B. G., & Casti, J. Differential quadrature: a technique for the rapid solution of nonlinear partial differential equations. *Journal of computational physics*. (1972) 10:40-52.
- [3] Du, H., Lim, M. K., & Lin, R. Application of generalized differential quadrature method to structural problems. *International Journal for Numerical Methods in Engineering*. (1994) 37:1881-1896.
- [4] Karami, G., & Malekzadeh, P. A new differential quadrature methodology for beam analysis and the associated differential quadrature element method. *Computer Methods in Applied Mechanics and Engineering*. (2002) 191:3509-3526.
- [5] Fung, T. C. Imposition of boundary conditions by modifying the weighting coefficient matrices in the differential quadrature method. *International Journal for Numerical Methods in Engineering*. (2003) 56:405-432.
- [6] Xing, Y., Liu, B., & Liu, G. A differential quadrature finite element method. *International Journal of Applied Mechanics*. (2010) 2:207-227.
- [7] Wang, X., & Wang, Y. Free vibration analyses of thin sector plates by the new version of

differential quadrature method. *Computer Methods in Applied Mechanics and Engineering*. (2004) 193:3957-3971.

[8] Wu, L., & Liu, J. Free vibration analysis of arbitrary shaped thick plates by differential cubature method. *International journal of mechanical sciences*. (2005) 47:63-81.

[9] Viola, E., Tornabene, F., & Fantuzzi, N. Generalized differential quadrature finite element method for cracked composite structures of arbitrary shape. *Composite Structures*. (2013) 106:815-834.

[10] Bert, C. W., & Malik, M. The differential quadrature method for irregular domains and application to plate vibration. *International Journal of Mechanical Sciences*. (1996) 38:589-606.

[11] Li, W. L. (2000). Free vibrations of beams with general boundary conditions. *Journal of Sound and Vibration*, 237(4), 709-725.

[12] Wang, Q., Shi, D., Liang, Q., & Shi, X. A unified solution for vibration analysis of functionally graded circular, annular and sector plates with general boundary conditions. *Composites Part B: Engineering*. (2016) 88:264-294.

[13] Wang, Q., Qin, B., Shi, D., & Liang, Q. A semi-analytical method for vibration analysis of functionally graded carbon nanotube reinforced composite doubly-curved panels and shells of revolution. *Composite Structures*. (2017) 174:87-109.

[14] Wang, Q., Shi, D., Liang, Q., & Pang, F. Free vibrations of composite laminated doubly-curved shells and panels of revolution with general elastic restraints. *Applied Mathematical Modelling*. (2017) 46:227-262.

[15] Wang, Q., Shao, D., & Qin, B. A simple first-order shear deformation shell theory for vibration analysis of composite laminated open cylindrical shells with general boundary conditions. *Composite Structures*. (2018) 184:211-232.

[16] Guan, X., Tang, J., & Wang, Q. Application of the differential quadrature finite element method to free vibration of elastically restrained plate with irregular geometries. *Engineering Analysis with Boundary Elements*. (2018) 90:1-16.

Effect of Rehabilitation Exercise Durations on the Dynamic Bone-repair Process by Coupling Polymer Scaffold Degradation and Bone Formation

Quan Shi^{*}, Qiang Chen^{**}, Zhiyong Li^{***}

^{*}School of Biological Science & Medical Engineering, Southeast University, 210096 Nanjing, PR China, ^{**}School of Biological Science & Medical Engineering, Southeast University, 210096 Nanjing, PR China, ^{***}School of Biological Science & Medical Engineering, Southeast University, 210096 Nanjing, PR China

ABSTRACT

Bone disorders are common, and the implantation of biodegradable scaffold is considered as a promising method to treat the disorders, but the knowledge of the dynamic mechanical process of the scaffold-bone system is extremely limited. In this study, based on the representative volume cell (RVC) of a periodic scaffold, the influence of rehabilitation exercise duration per day on the bone repair was investigated by a computational framework. The framework coupled the polymer scaffold degradation and the bone remodeling. The scaffold degradation was described by a function of stochastic hydrolysis independent of the mechanical stimulation, and the bone formation was remodeled by a function of the mechanical stimulation, i.e., strain energy density (SED). Then, numerical simulations were performed to study the dynamic bone repair process. The results showed that the scaffold degradation and bone formation in the process were competitive. The greater exercise duration per day could not improve the bone stiffness, and 0.3 is the optimal case. All exercise durations promoted the bone maturation with a final Young's modulus around 1.9 ± 0.3 GPa. The present study is helpful to understand and monitor the bone repair process, and useful for the bone scaffold design in bone tissue engineering.

Simulating Shrinkage Cracking in ECC Overlay Using an Efficient Discrete Model

Tiansheng Shi*, Christopher K. Y. Leung**

*Hong Kong University of Science and Technology, **Hong Kong University of Science and Technology

ABSTRACT

Concrete structures always experience deterioration during their service time and a common practice of repairing is to replace the damaged part with an overlay system (usually made of mortar). However, the early age failures of the repair system are usually observed due to differential shrinkage between the old concrete substrate and the new overlay. With high ductility and good control of crack width, ECC is found to show an excellent performance in repairing the deteriorated concrete structure, and many numerical and experimental studies are carried out in this area to understand its behavior. Here a novel discrete model, which can efficiently simulate the realistic multiple cracking process in ECC, is adopted to assess the performance of ECC overlay system subjected to shrinkage. The proposed discrete model is first used to simulate a tensile test (for the purpose of model verification), and then the ECC overlay subjected to shrinkage. It is found that the failure modes of the overlay system, i.e., interface delamination and ECC multiple cracking, can be captured by the proposed model. The important parameters in the process are further discussed, which would provide insight in optimizing the overlay system.

A Numerical Simulation Model of Cleavage Crack Propagation in Steel Based on the Extended Finite Element Method

Kazuki Shibamura^{*}, Yuta Suzuki^{**}, Kazuya Kiriyama^{***}, Takuhiro Hemmi^{****}, Hiroyuki Shirahata^{*****}, Shuji Aihara^{*****}, Katsuyuki Suzuki^{*****}

^{*}The University of Tokyo, ^{**}The University of Tokyo, ^{***}The University of Tokyo, ^{****}The University of Tokyo, ^{*****}Nippon Steel & Sumitomo Metal Corporation, ^{*****}The University of Tokyo, ^{*****}The University of Tokyo

ABSTRACT

Preventing crack propagation is extremely important in ensuring the integrity of steel structures such as hulls and cryogenic tanks. However, any theories and models to evaluate quantitative and universal relationship between microstructure and crack arrest toughness based on physical model of cleavage crack propagation has not been established. In the present study, we propose a model for cleavage crack propagation in steel based on the extended finite element method (XFEM) [1]. Although the cleavage crack propagation is a phenomenon without large plastic deformation, it is a geometrically complicated phenomenon, where the fracture surface is composed of cleavage plane facets formed in the respective grains. These features indicate that the linear fracture mechanics modeling using XFEM is suitable to simulate the cleavage crack propagation in steel. In the proposed model, geometries and spatial distribution of grains are defined independently from finite element mesh, as well as the crack. For simplification, only one cleavage facet is assumed to be formed in each grain. A criterion proposed by Aihara and Tanaka [2] is employed as fracture condition of crack propagation across a grain boundary. In the criterion, one of the three $\{1\ 0\ 0\}$ cleavage planes in a grain located in front of a crack front is selected so that normal stress acting on the plane is maximum and the grain is cleaved if the maximum normal stress exceeds the cleavage fracture stress. The normal stress on each $\{1\ 0\ 0\}$ plane is calculated from mixed mode local stress intensity factors which are evaluated by the fast interaction integral method. As validation of the proposed model, the numerical simulation results of fracture surface morphology are compared with experimental result obtained by the crack arrest test using double cantilever beam (DCB) specimen of low-alloy steel. The result shows that the proposed model can successfully simulate complicated cleavage crack propagation behaviors, such as micro-branching and wraparound of cracks on the fracture surface. In addition, the numerical and experimental results of distribution of the nominal directions of cleavage facets showed good agreement with each other. References [1] 2002 N. Moës, A. Gravouil, T. Belytschko, Non-planar 3D crack growth by the extended finite element and level sets - Part I Mechanical model, Int. J. Numer. Meth. Engng. 53 (2002) 2549-2568. [2] S. Aihara, Y. Tanaka, A simulation model for cleavage crack propagation in bcc polycrystalline solids, Acta Materialia 59 (2011) 4641-4652.

Multi-resolution Simulation by the Overlapping Particle Technique and the Ellipsoidal Particle Model for Particle Methods

Kazuya Shibata^{*}, Daisuke Yamada^{**}, Seiichi Koshizuka^{***}, Issei Masaie^{****}, Takuya Matsunaga^{*****}

^{*}Department of Systems Innovation, School of Engineering, The University of Tokyo, ^{**}Department of Systems Innovation, School of Engineering, The University of Tokyo, ^{***}Department of Systems Innovation, School of Engineering, The University of Tokyo, ^{****}Prometech Software Inc., ^{*****}Department of Systems Innovation, School of Engineering, The University of Tokyo

ABSTRACT

This presentation explains the overlapping particle technique [1] and the ellipsoidal particle model [2], which are multi-resolution techniques developed for fluid simulation of particle methods. The overlapping particle technique divides a whole simulation domain into sub-domains. Each sub-domain has an individual constant spatial resolution. The sub-domains partially overlap to give boundary condition about pressure and velocity. The ellipsoidal particle model allows us to use non-spherical particles. An extended Laplacian model for ellipsoidal particles was used to discretize the viscous term and the pressure Poisson equation. Compared to the traditional spherical particles, the ellipsoidal particles can reduce the required number of particles and the computation time. We applied the developed technique and model to the MPS method and SPH. Dam breaking and water waves were simulated by the multi-resolution techniques. The improved pressure calculation method [3] was applied to the MPS simulations. As a result, it was confirmed that the developed multi-resolution techniques can reduce the required number of particles and shorten the computation time of particle simulations. [1] K. Shibata, S. Koshizuka, T. Matsunaga, I. Masaie, The overlapping particle technique for multi-resolution simulation of particle methods, *Computer Methods in Applied Mechanics and Engineering*, Vol. 325, pp.434-462 (2017) [2] K. Shibata, S. Koshizuka, I. Masaie, Cost reduction of particle simulations by an ellipsoidal particle model. *Computer Methods in Applied Mechanics and Engineering*, Vol.307, pp.411-450 (2016) [3]K. Shibata, I. Masaie, M. Kondo, K. Murotani, S. Koshizuka, Improved pressure calculation for the moving particle semi-implicit method, *Computational Particle Mechanics*, Vol. 2, Issue 1, pp. 91-108 (2015)

Modeling Non-Gaussianity in Non-linear Stochastic Dynamic Systems

Michael Shields^{*}, Lohit Vandanapu^{**}, Hwanpyo Kim^{***}

^{*}Johns Hopkins University, ^{**}Johns Hopkins University, ^{***}Johns Hopkins University

ABSTRACT

It is well-known that nonlinear stochastic systems often exhibit non-Gaussian features. Examples of such phenomena are abundant in nature from fluid-structure interactions in turbulent flow to shoaling ocean waves. When modeling these non-Gaussian phenomena, it is common to develop an expansion for the stochastic process using methods such as the Karhunen-Loeve (K-L) expansion or spectral representation method (SRM). Under classical assumptions, the K-L expansion and SRM are used to model Gaussian processes and some non-linear transformation is then applied to induce the desired non-Gaussianity using e.g. translation process theory or orthogonal polynomials. However, in the more general case, the non-Gaussianity can be modeled by understanding the dependence structure of the random variables in the stochastic expansion. In this work, we derive analytical relationships relating phase difference distributions to higher-order spectra (bispectrum, trispectrum, etc.) in the spectral representation method that enable direct modeling of non-Gaussian stochastic processes derived from nonlinear dynamical systems. A brief comparison of the resulting models with classical non-linear transformation based approaches is provided along with some discussion of the advantages and disadvantages of each approach.

The Prediction of Bone-Remodeling Morphology and Peri-implant Osseointegration for Dental Implants

Chien Shih-Shun*, Nien Ti-Tsou**, Li Ming-Jun***

*National Chiao Tung University, **National Chiao Tung University, ***Industrial Technology Research Institute

ABSTRACT

In recent years, a number of algorithms have been proposed to predict the adaptive bone-remodeling, primary stability, and osseointegration around the dental implants under load, such as Strain energy density (SED) and cell differentiation based theory. The SED model can provide a balanced nonhomogeneous distribution state of the bone density/elastic modulus; the cell differentiation model can predict the osseointegration level between the considered implants and bones after surgical treatment. However, bone density and elastic modulus are typically assumed as constant in the most of the models. Thus, in order to improve the accuracy of the model, the current study firstly adopts SED model to determine the distribution of anisotropic bone density/elastic modulus around the natural teeth and set that distribution as the initial condition for the cell differentiation model. The SED and cell differentiation algorithms are incorporated by using finite element package ANSYS. The model consists with a 3-D segment of the mandible in premolar region, and the effect of the periodontal ligament is also considered. The current model is verified by the animal experiment. The results show that the current model has a more accurate prediction of osseointegration performance, compared with the model without considering the nature bone density and elastic distribution.

Multiscale Parametric Analysis of Strain Amplification in Cartilage under Different Loading and Tissue Conditions

Vickie Shim^{*}, Sophia Leung^{**}, David Musson^{***}, Sue McGlashan^{****}, Iain Anderson^{*****}, Jill Cornish^{*****}

^{*}University of Auckland, ^{**}University of Auckland, ^{***}University of Auckland, ^{****}University of Auckland, ^{*****}University of Auckland, ^{*****}University of Auckland

ABSTRACT

Articular cartilage lines the surfaces of diarthroidal joints and supports the joint motion by providing a load bearing and low friction material. Due to its large deformation under normal daily activities, the cells in the cartilage (chondrocytes) are exposed to a complex mechanical environment. The cartilage tissue also exhibits complex material properties that are both location and rate dependent. Yet, the avascular nature of the tissue means that any damage to the tissue is irreversible and as a result, osteoarthritis is one of the most widespread causes of morbidity and impaired quality of life in the western world. However, the pathogenesis of cartilage degeneration is largely unknown and the disease is untreatable. We have developed a unique system that combines multiscale computational models with a cell mechanical device. Our multiscale knee joint model is composed of three levels – joint, tissue and cell levels for predicting strains at multiple spatial scales [1]. Our cell device is a novel mechanical device that is capable of applying tension, compression and shear strains to cell seeded 3D cultures [2]. We have performed mechanical experiment that measured cell deformation patterns under these three mechanical loading conditions with confocal microscope imaging. Our results showed that chondrocytes experience significant strain amplification (up to 50 %) under mechanical loading and shear strains caused the highest strain amplifications. This result was then used in our multiscale computational model to predict how different loading conditions and tissue mechanical properties affect the degree of strain amplification. A parametric study was performed to quantitatively analyse the role of tissue stiffness and different loading conditions on cellular strains. Our results indicate that a change in tissue stiffness due to degeneration is one of the leading causes of abnormal strain amplification in chondrocytes. This result will be used in designing functional tissue engineering constructs for replacing damaged cartilage.

1. SHIM, V; MITHRARATNE, K., LLOYD, D., BESIER, T., FERNANDEZ, J. 'The influence and biomechanical role of cartilage split-line pattern on tibiofemoral cartilage stress distribution during the stance phase of gait' Biomechanics and Modeling in Mechanobiology 2016 15 (1), 195-204

2. LEUNG, S.; MCGLASHAN, S., MUSSON, D., ANDERSON, I.A.; CORNISH, J.; MCGLASHAN, S., SHIM, V; Investigation of strain fields in 3D hydrogels under dynamic confined loading, Journal of Medical and Biological Engineering (Accepted for publication)

Petascale Computing to Accelerate High-Temperature Alloy Design

Dongwon Shin^{*}, Patrick Shower^{**}, James Morris^{***}, Amit Shyam^{****}, James Haynes^{*****}

^{*}Oak Ridge National Laboratory, ^{**}The University of Tennessee, ^{***}Oak Ridge National Laboratory, ^{****}Oak Ridge National Laboratory, ^{*****}Oak Ridge National Laboratory

ABSTRACT

Recent progress in high-performance computing and data informatics has opened up numerous opportunities to aid and accelerate the design of advanced materials. Herein, we demonstrate a computational workflow that includes rapid population of high-fidelity materials datasets via petascale computing, utilization of those datasets for multi-scale modeling, and subsequent analyses with modern data science techniques. We use a first-principles approach based on density functional theory to derive the segregation energies of 34 microalloying elements at the coherent and semi-coherent interfaces between the aluminum matrix and the θ -Al₂Cu precipitate, which requires several hundred supercell calculations. We also perform extensive correlation analyses to identify materials descriptors that affect the segregation behavior of solutes at the interfaces. These atomic-scale data are integrated into a micro-scale model using phase field theory to investigate the effect of solute segregation on the high-temperature microstructural stability, and the temperature-dependent effects of both thermodynamic driving forces and kinetics. Finally, we show an example of leveraging machine learning techniques to predict segregation energies without performing computationally expensive physics-based simulations. The approach demonstrated in the present work can be applied to any high-temperature alloy systems for which key materials data can be obtained using high-performance computing. The research was sponsored by the Laboratory Directed Research and Development Program of Oak Ridge National Laboratory, managed by UT-Battelle, LLC, for the U. S. Department of Energy.

Convex Splitting Runge-Kutta Methods to Solve the Phase Field Equations

Jaemin Shin^{*}, Hyun Geun Lee^{**}, June-Yub Lee^{***}

^{*}Ewha Womans University, ^{**}Kwangwoon University, ^{***}Ewha Womans University

ABSTRACT

We introduce Convex Splitting Runge-Kutta (CSRK) methods to solve the gradient flow considering the energy stability, which provide a simple unified framework. The gradient systems have been fundamental in the development of many important concepts in dynamical systems. In particular, it is important in many phenomenological models of phase transition like as the phase field model. The core idea of CSRK method is the combination of convex splitting methods and multi-stage implicit-explicit Runge-Kutta methods. The proposed methods are high-order accurate in time. In addition, the energy stability is completely proved when we consider the special design of implicit-explicit Runge-Kutta tables, called a resemble condition. We present numerical experiments with the phase field equations to show the numerical accuracy and stability of the proposed methods. [1] Eyre, D. J., "An unconditionally stable one-step scheme for gradient systems", Unpublished article, 1998. [2] Shin, J., Lee, H. G. and Lee, J.-Y., "Convex Splitting Runge-Kutta methods for phase-field models", Computers & Mathematics with Applications, Vol. 73, 2017, pp. 2388-2403. [3] Shin, J., Lee, H. G. and Lee, J.-Y., "Unconditionally stable methods for gradient flow using Convex Splitting Runge-Kutta scheme", Journal of Computational Physics, Vol. 347, 2017, pp. 367-381.

CYBER-INFRASTRUCTURAL COMPUTE/DATA FRAMEWORK FOR THE AERODYNAMIC RESEARCH OF INDUSTRIAL AIRFOILS

JUNGHUN SHIN*, JEONGHWAN SA[†], JIN MA[†],
SIK LEE[†], AND KUMWON CHO[†]

*Supercomputing Division, Korea Institute of Science and Technology Information (KISTI)
245 Daehak-ro, Yuseong-gu
Daejeon, Republic of Korea
shandy77@kisti.re.kr

[†]Supercomputing Division, Korea Institute of Science and Technology Information (KISTI)
245 Daehak-ro, Yuseong-gu
Daejeon, Republic of Korea
sa_c@kisti.re.kr, majin@kisti.re.kr, siklee@kisti.re.kr, ckw@kisti.re.kr

Key words: Instructions, Multiphysics Problems, Applications, Computing Methods Abstract.

Abstract. This document provides information and instructions for preparing an extended abstract to be made available for downloading from the WCCM2018 website.

1 INTRODUCTION

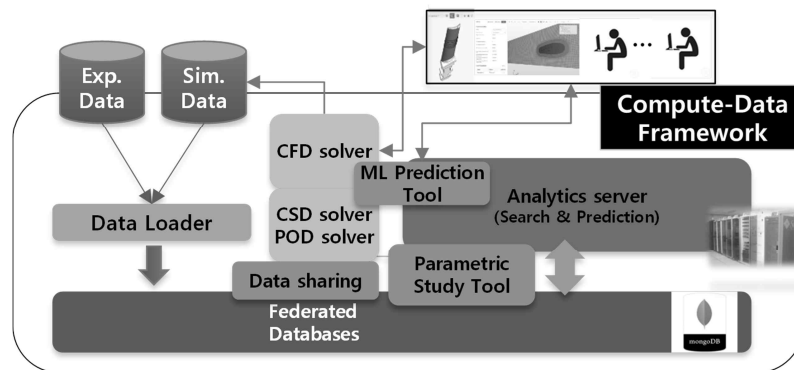
Computation has traditionally played a powerful role in a wide range of research and development areas, from the beginning of the computer to scientific research, product development, and knowledge services¹. The engineering analysis for industrial wings or blades has been performed in various disciplines such as aerodynamics analysis. This study was motivated by a blade manufacturer who was interested in the shape error effects in the earlier stage of the manufacturing.

From the manufacturers' viewpoint, the airfoil aerodynamics is a fundamental that must go through. In this study, a cyber-infrastructure framework which could conduct both compute and data techniques was developed to research airfoil aerodynamic performances, targeted for quickly predicting the aerodynamic performances and discussing them to make decision soon. Although the aerodynamic parameters differ from industries, in this study, the aerodynamic coefficients were employed following the wing airfoil ways².

In addition to the studies on the theoretical models and computer simulation techniques that have been actively carried out in industry and academia, there are not many ones about the environments in which this simulation studies can be performed. Currently, it became common for commercial software companies and many hardware system companies to construct the environment for running computer simulations, but it is difficult to maintain it costly unless it is

a large organization. In this situation, it would be helpful especially for small and medium companies to have high accessibility to large computing resources, to be able to perform analysis easily, to share information such as simulation results, and to produce additional information using some data analytics tools. Now it is believed that this kind of a compute-data framework for communicational or educational purposes can help apply the digital technology appropriately to the advanced manufacturing process³. Recently, new service types that can perform computation in the emerging cloud environment of internet technology have appeared, and there have been various kinds of technology prototypes in which the computation and the network are merged⁴. For example, an emerging software team company originated from the ‘Solidworks’ which is a representative CAD tool provided a cloud service called Onshape⁵ to perform CAD work and access to the data on web browsers or mobile devices without installing additional software. ANSYS, a software manufacturer of engineering analysis software, and many engineering consulting service companies, are developing a cloud-based analysis environment, which unlike the CAD cloud displays only the screen on the user's desktop or terminal. It is based on the Virtual Desktop Infrastructure (VDI), which is a method performed at the backend. Engineering consulting service companies in Europe, such as Simscale⁶ and CONSELF⁷, are administering novel cloud computing simulation environments which are different from VDI method to provide engineering consulting and community services. In the case of professional cloud computing companies such as Rescale⁸, there is a tendency to acquire a large number of users by providing cloud services including both of them. Besides there have been similar developments to the current cloud services based on high-performance computers^{9,10}.

This paper aims to efficiently utilize gas turbine blade aerodynamics computer simulation and data-driven analysis with cyber-infrastructure resource at the product development site. Fig. 1 shows the concept of the framework. As for the data-driven analysis, recently accepted techniques of machine learning were tried for airfoil aerodynamics and the feasibility was evaluated preliminarily. Therefore, it introduces and develops contents and features of computerized research environment (user-specific authority and resource allocation, CAD and grid processing, analysis execution, sharing various information) using web browser based cloud computing system service model similarly to Onshape and Simscale described above. Finally the use scenario using the analytical system was presented. The development of airfoil aerodynamics solvers was briefly described, and the details will be discussed in separate documents.



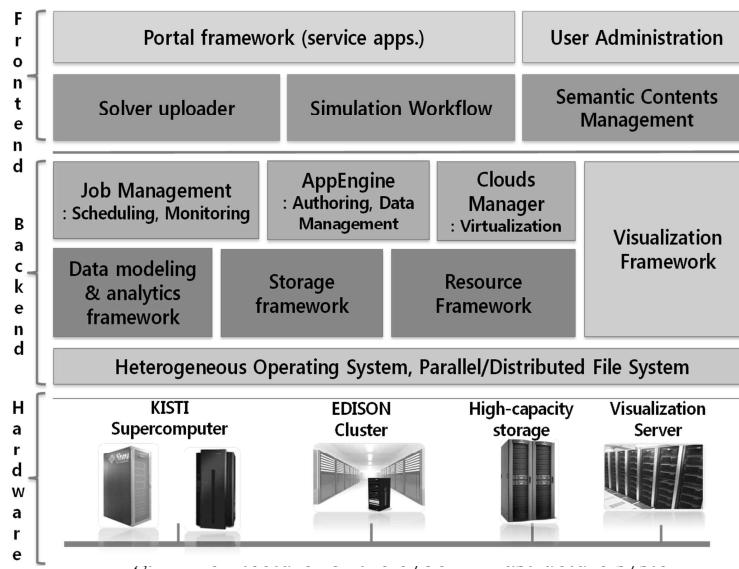
2 REQUIRMENT AND FUNCTION DESIGN

In manufacturing sites, engineers always conduct quality assessment by measuring shape error and etc. The aerodynamic performance is considered to be most affected by the shape deviation, which is the main concern of this paper. For example, it is known in the field that there is a case where a free vibration characteristic is changed due to some manufacturing error and is discarded. Two-dimensional airfoil analysis provides information that they can understand aerodynamic performance variations most intuitively.

The aerodynamic solver can hold two-dimensional airfoil and three-dimensional blade RANS analysis. It could not be only a single airfoil or blade, but also multi-staged. In addition, flows experienced by gas turbine blades are very complex, but especially in large gas turbines, complex turbulent flows occur in the full speed range of subsonic, transonic, and supersonic speeds. Therefore, the aerodynamic solver must be able to simulate the full speed range and also simulate moving rotor, vane stator interface treatment, centrifugal flow, and etc. They are originated from the fact that the blades in gas turbine show multi-staged arrangement. Finally, a flow model for turbulent transitions should be included since there is a transitional heat transfer in which the heat transfer characteristics vary greatly at the surface due to the shape of the blade with a large curvature. The aerodynamic solver using structured grid system has already been verified for the simulation efficiency and accuracy of various wings¹¹, so appropriate tuning of the base flow solver was performed to suit the turbine blade analysis, reflecting the above requirements.

Considering data-driven techniques using the dataset generated from the above full-order model (FOM) analysis could improve the efficiency of computation by applying a reduced-order modeling (ROM) such as proportional orthogonality decomposition (POD) method¹² and recently emerging machine-learning (ML) techniques. In this study, we handle with ML based simulation results reusing techniques.

The detailed description of the above solvers will be provided in other papers.



3 SYSTEM ARCHITECTURE AND COMPUTATIONAL MODULES

Fig. 2 shows the base architecture of the engineering system. This architecture was developed by modifying an existing system of so-called EDISON compute platform⁹ into compute-data platform which data modeling and analytics modules were added. The computational science and engineering platform host various compute software like flow solvers and share the input/output data. The computational procedures can be performed via the web-portal.

3.1 Computational modules

Fig. 3(a) depicts primary user interface of the web-portal. The web-based pages are quite friendly so that community could be build-up using project-sharing module, social network service module and etc. Fig. 3(b) shows the flow solver running tool which can throw

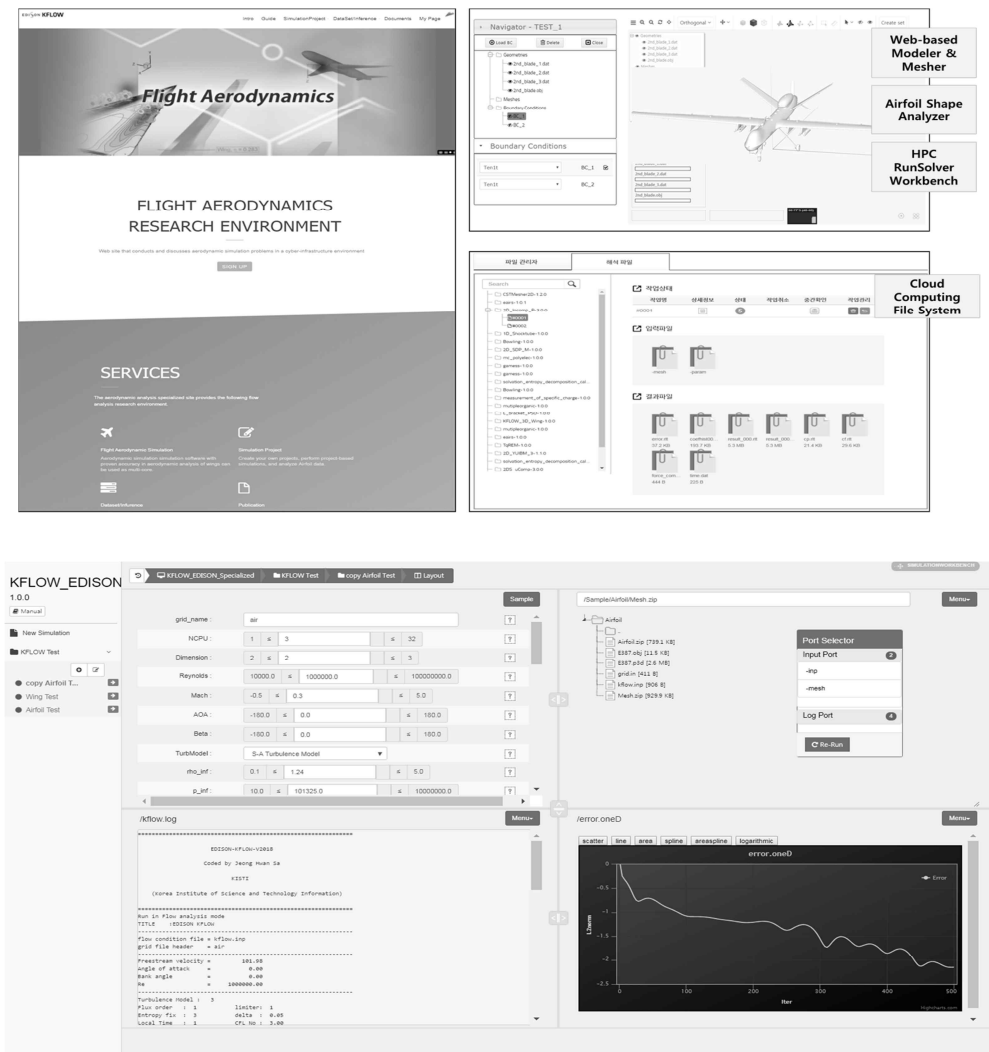


Fig. 3 Web-portal for cloud computing and data

parallelized jobs into the backend high performance computing system

The simulation data were arranged in accordance with shape parameter schema since the shape parameters are used to distinguish the airfoil shape. The airfoil might abruptly changes aerodynamic characteristics even if the shape is slightly different, so it is necessary to use numerically expressed parameters so that it can be accurately classified. It should be able to accurately express the airfoil shape using as few parameters as possible. As the number of parameters increases, the process of classifying shapes becomes complicated. In this study, the airfoil shape was defined using the Bezier-Parsec parameter¹³. The Bezier-Parsec parameter used the thickness profile and camber profile to represent the airfoil shape. Thickness and Camber curves were obtained by combining two cubic Bezier curves, respectively. One cubic Bezier curve requires eight control points in total using four control points in the horizontal and vertical directions respectively. Because there are the leading edge and trailing edge coordinates and overlapping control points, the thickness curve uses 8 control points and the camber curves uses 9 control points respectively. In order to extract the 17 control points constituting the Bezier-Parsec parameter from the airfoil shape, the Newton Raphson method was used until the error between the shape realized by the parameter and the airfoil shape became 10^{-4} or less. Because the number of control points and the number of coordinates to compare shapes are not same, the Least Squares Method has been used. The generated 17 parameters are used to define and compare the shape, and the parameters of the shape used are databased and updated continuously to the data-driven system. Fig. 4(b) shows the meshing tool which can automatically handle the small deviations of airfoils.

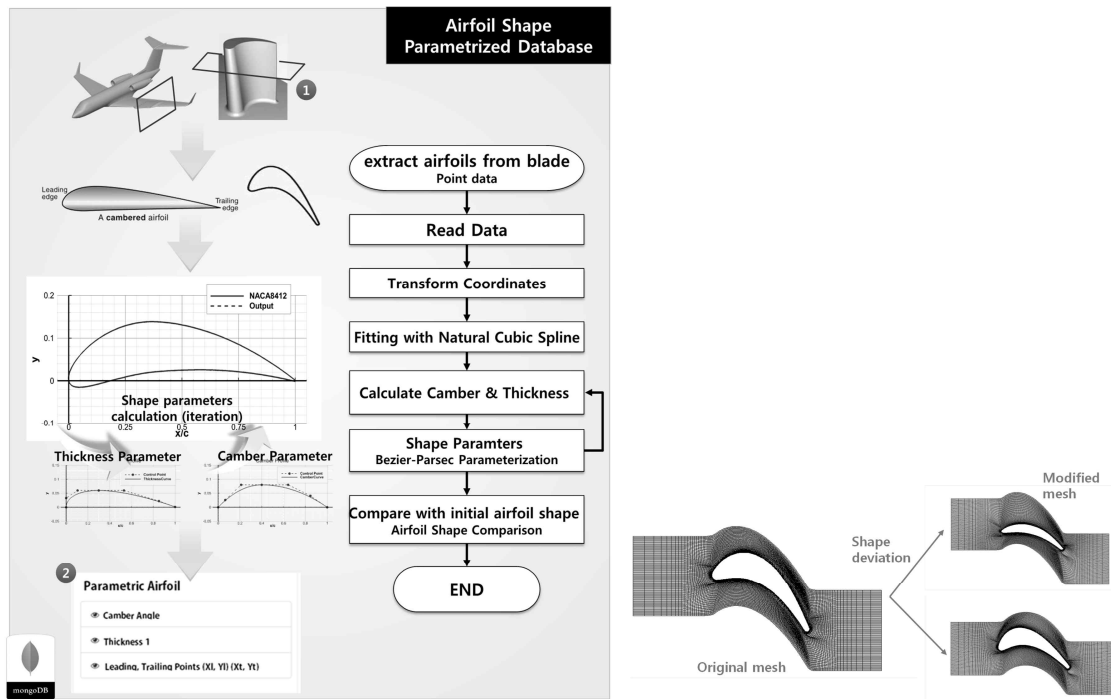


Fig. 4 Airfoil shape parametrization and meshing process

3.2 Data-driven inference module

The Navier-Stokes equations, which are mainly used in modern computational fluid dynamics, cannot be obtained exact Solutions, so approximate numerical solutions must be obtained through discretization of space and time and numerical analytical techniques. To do this, it is necessary to obtain the converged solution while reducing the error of the numerical solution through iterative calculation. Even if the computation time is reduced by the development of hardware or numerical algorithms, there is a limit in reducing the time required for such iterative calculations. In this study, data-driven technology was used to increase the efficiency of flow analysis.

The main function of currently developed data-driven system for the airfoil is three.

- a. Loading simulation results
- b. Re-using simulation results
- c. Predicting simulation results

Fig. 5 shows the overall system of operation process. When the user submits the airfoil shape and flow conditions, shape parameters are extracted through the data system. Then, multidimensional data mining using R is performed, and when the same or similar shape is found in the analysis database stored in Mongo DB, the result is transmitted to the user. However, if there is no identical shape, the prediction is performed through machine learning, the result is displayed to the user, and the information is stored in the analysis database.

Machine Learning analytics framework used Mongo DB to store simulation results and metadata in JSON documents. We used R to develop the prediction function, and we used JAVA as the development language to call the commands of the R script.

We used Node.js to retrieve the results of the simulation requested by the user through the web interface.

The main functions provided by machine learning analytics framework¹⁴ are as follows:

- A. Simulation Result Load
 - a. Loading the execution result of simulation program into Mongo DB as JSON document.
 - b. Bulk loading function.
 - c. Implemented language: Java
- B. Simulation Query Interface
 - a. Retrieves the execution result of the simulation requested by the user through the web interface and returns the result.
 - i. If the result is in the database, return it immediately without re-executing.
 - ii. If the result is not in the database, give the user a prediction option.
 - b. Implemented language: Node.js
- C. Simulation Result Reuse
 - a. If the simulation results you have requested are already in the database, return results directly without performing a simulation
- D. Simulation Result Predict
 - a. If the simulation result requested by the user is not in the database, analyze and predict results
 - b. Implemented language: JAVA (internally calls R script execution command)

- c. Then, use of several statistical machine learning techniques
 - i. Multiple Linear Regression (MLR)
 - ii. General Addictive Model (GAM)
 - iii. Support Vector Machine (SVM)
 - iv. Classification and Regression Trees (CART)
 - v. Random Forests (RF)
 - vi. Generalized Boosted Models (GBM)
 - vii. Multivariate adaptive regression splines (MARS)
 - viii. Local Regression (LR)
 - ix. K-Nearest Neighbor Regression (KNN)
 - x. Multi-Layer Neural Network (MLNN)

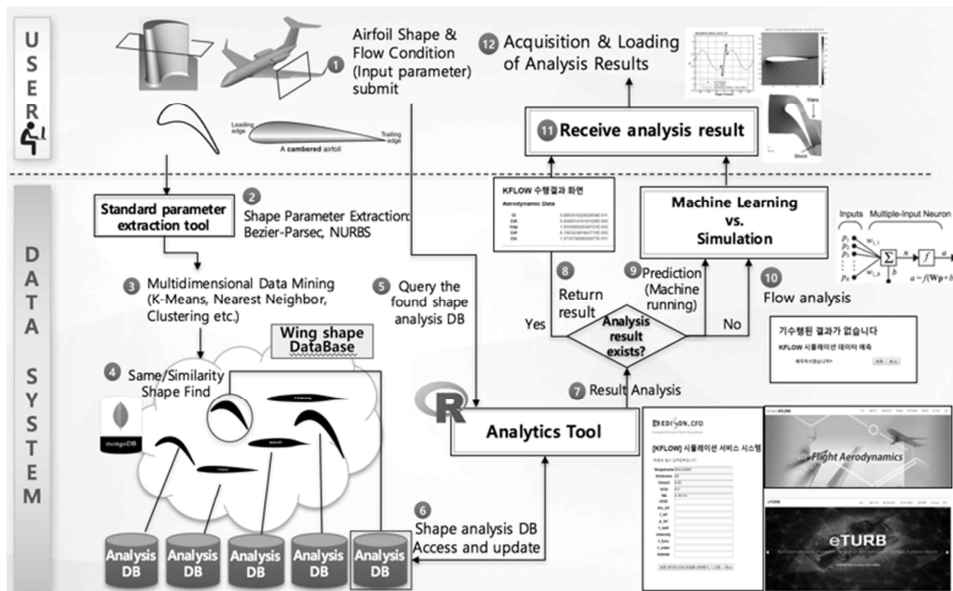
3.3 Verification study using the compute-data framework

Table 1 describes how the dataset was generated from FOM-calculated result data. The four input parameters were selected as the data indexes. Therefore high-fidelity flow solver was run with these indexes, and resulted in a dataset with the number of 7,679 simulation data.

Table 1. Configuration of airfoil aerodynamics dataset

Airfoil thickness	NACA 0009, 0010, 0011, 0012
Mach number	0.05, 0.10, 0.15, ..., 0.6
Angle of attack	0, 1, 2, ..., 10
Reynolds number	1x10 ⁵ , 2x10 ⁵ , ..., 10 ⁶

Now learning with various ML methods were conducted in 70% of the simulation data, then prediction tools was developed. We could test the results of 30% of the simulation data, which



means the comparisons of the ML-inferred and FOM-simulated values. Table 2 shows the comparison errors between ML-inferred and FOM-simulated values which include five features of the aerodynamic coefficients: lift, total/pressure/friction drag, and moment coefficients.

Table 2. Inference errors in accordance with ML techniques

	CL	CDt	CDp	CDf	CM	Avg.	Rank.
MLR	12.6	46.3	153	10.9	59.3	56.4	10
GAM	10.6	41.1	130	8.70	65.1	51.1	9
SVM	3.70	6.90	19.6	2.50	21.4	10.8	6
CART	5.80	7.20	15.2	3.50	17.4	9.82	5
RF	0.9	1.60	2.60	1.20	7.50	2.76	1
GBM	23.7	3.40	7.80	2.20	18.3	11.1	7
MARS	3.90	9.30	20.7	3.70	30.9	13.7	8
LR	1.30	1.70	2.70	1.10	7.40	2.84	2
KNN	3.00	3.70	6.50	2.00	10.3	5.10	3
MLNN	2.10	2.80	13.8	3.00	10.6	6.46	4

The comparison results indicate that Local Regression and famous decision-tree based method called Random Forest showed better accuracy performance.

It was worth being noted that the computation time of the ML-inference was immediate while the FOM simulation time was about 50 min.

4 CONCLUSIONS

A new web-based compute/data engineering system for the aerodynamics analysis of industrial airfoils has been explained in this paper. Some conclusions can be summarized as follows:

- Cyber-infrastructure engineering system can run a high-fidelity aerodynamic simulation and also machine learning based inference tool using the pre-run simulation results. The web-based running environment is expected to work particularly for quick airfoil aerodynamics prediction and compute-data correlation researches.
- Machine learning based framework of inferring aerodynamic coefficients was developed. The full-order flow simulation results in a platform-like computation system are consistently loaded into a database. The framework learned and tested the pre-run dataset using ten primary machine learning methods. The results showed that Local Regression and Random Forest Regression ranked the highest.

More indexes like more detailed airfoil shape and more features like other output parameters will be considered in the future

ACKNOWLEDGEMENTS

This research was supported by the EDISON Program through the National Research Foundation of Korea (NRF) funded by the Ministry of Science & ICT (No. NRF-2011-0020576). This research was supported by Korea Institute of Science and Technology Information (KISTI- 2018)

REFERENCES

- [1] Glotzer, S. C. et al, 2009, International Assessment of Research and Development in Simulation-Based Engineering and Science, WTEC Report, Maryland.
- [2] Petrilli, Justin, Paul, Ryan, and Gopalarathnam, Ashok, 2014, A CFD Database for Airfoils and Wings at Post-Stall Angles of Attack, *31st AIAA Applied Aerodynamics Conference* (AIAA 2013-2916).
- [3] Andreadis, G., Fourtounis, G., Bouzakis, K. D., 2015, Collaborative design in the era of cloud computing, *Advances in Engineering*, 81, pp. 66-72.
- [4] Sakellari, G., Loukas, G., 2013, A survey of mathematical models, simulation approaches and testbeds used for research in cloud computing, *Simulation Modelling Practice and Theory*, 39, pp. 92-103.
- [5] Onshape, <https://www.onshape.com/>.
- [6] SIMSCALE GmbH, <https://www.simscale.com/>.
- [7] CONSELF Url, <https://consself.com/>.
- [8] Rescale Url, <https://www.rescale.com/>.
- [9] Yu, J. L., Ryu, H., Byun, H. J., Lee, J. R., K. W. Cho, and Jin, D. S., 2013, EDISON Platform: A Software Infrastructure for Application-Domain Neutral Computational Science Simulations, *Lecture Note in Electrical Engineering*, 235, pp. 283~291.
- [10] Seo, D. W., Lee, J. Y., Lee, S. M., Kim, J. S., and Park, H. W., 2013, Multi-View Supporting VR/AR Visualization System for Supercomputing-based Engineering Analysis Services, *Korean Journal of Computational Design and Engineering*, 18(6), pp. 428-438.
- [11] Sa, J.H., Park, S.H., Kim, C.J., and Park, J.K., 2015, Low-Reynolds number flow computation for Eppler 387 wing using hybrid DES/transition model, *Journal of Mechanical Science and Technology*, 29(5), pp.1837-1847.
- [12] Taira, K. et al, 2017, Modal Analysis of Fluid Flows: An Overview, *AIAA Journal*, 55(12), pp. 4013-4041.
- [13] Derksen, R.W. and Rogalsky, T., 2010, Bezier-PARSEC: An optimized aerofoil parameterization for design, *Advances in Engineering Software*, 41, pp. 923-930
- [14] Lee, K. Y., Suh, Y. K., and Cho, K. W., 2017, Development of a simulation result management and prediction system using machine learning techniques, *Int. J. Data Mining and Bioinformatics*, 19(1), pp.75-96.

A method for seamless transition from degradation of material stiffness to formation of strong discontinuity

Yuichi Shintaku^{*}, Seiichiro Tsutsumi^{**}, Kenjiro Terada^{***}

^{*}University of Tsukuba, ^{**}Osaka University, ^{***}Tohoku University

ABSTRACT

The objective of this contribution is to develop a method for seamless transition from degradation of material stiffness to formation of a strong discontinuity of displacement with theoretical consistency of cohesive zone models (CZMs) for fracture. In existing CZMs, a fracture process is divided into two stages to realize the crack nucleation and propagation. At the first stage of the fracture process, the material stiffness reduces at a macro-scale due to the evolution of defects at a micro-scale, which is supposed to form a crack tip of the cohesive fracture. At the final stage, which corresponds to the crack propagation process after the stress reaches the maximum value in the material response, the displacement field develops an explicit crack opening due to the coalescence of the microscopic defects. In this study, the macroscopic stiffness reduction at the first stage is represented by the cohesive-traction embedded constitutive law, which is a damage-like constitutive law capable of embedding an appropriate CZM. Then, the proposed method bridges a transition from continuous to discontinuous displacements by the combination of the same CZM, employed to represent the first stage of the fracture process, and the finite cover method (FCM)[1]. In other words, a finite element in which the cohesive traction attains the maximum value is adaptively divided into two domains to represent the strong discontinuity by the FCM endowed with the CZM at their interface. Moreover, these two stages of the cohesive fracture process are seamlessly connected thanks to the unique feature of the cohesive-traction embedded damage-like constitutive law, in which deformation under tensile loading is consistent with the conventional CZMs. Several numerical examples are presented to verify the equivalence between the fracture processes represented by the cohesive-traction embedded damage-like constitutive law and the FCM combined with the CZM. After validating the performance of the proposed constitutive law, we demonstrate the capability of the proposed method of crack propagation equipped with the suggested seamless transition algorithm from the degradation of the material stiffness to the formation of an actual crack propagating within finite elements. . [1] T. Ishii, K. Terada and T. Kyoya, Int. J. Num. Meth. Engng, 67, 960-988 (2006).

Space - Time Trefftz-DG Approach for Elasto-Acoustic Wave Propagation Problem

Elvira Shishenina^{*}, H el ene Barucq^{**}, Henri Calandra^{***}, Julien Diaz^{****}

^{*}Team-project Magique-3D, Inria, LMAP-CNRS, France; Total S.A., USA, ^{**}Team-project Magique-3D, Inria, LMAP-CNRS, France, ^{***}Total S.A., USA, ^{****}Team-project Magique-3D, Inria, LMAP-CNRS, France

ABSTRACT

Discontinuous Finite Element Methods (DG FEM) have proven their numerical accuracy and flexibility. However, numerically speaking, the high number of degrees of freedom required for computation makes them more expensive, compared to the standard techniques with continuous approximation. Among the different variational approaches to solve boundary value problems there exists a distinct family of methods, based on the use of trial functions in the form of exact solutions of the governing equations. The idea was first proposed by Trefftz in 1926 [1], and since then it has been largely developed and generalized. By its definition, Trefftz-DG methods reduce numerical cost, since the variational formulation contains the surface integrals only. Thus, it makes it possible exploration of the meshes with different geometry, in order to create more realistic application. Trefftz-type approaches have been widely used for time-harmonic problems, while their implementation is still limited in time domain. The particularity of Trefftz-DG methods applied to the time-dependent formulations is in the use of space-time meshes. Even though it creates another computational difficulty, due to a dense form of the matrix, which represents the global linear system, the inversion of the full "space-time" matrix can be reduced to the inversion of one block-diagonal matrix, which corresponds to the interactions in time. In the present work, we develop a theory for solving the coupled elasto-acoustic wave propagation system. We study well-posedness of the problem, based on the error estimates in mesh-dependent norms. We consider a space-time polynomial basis for numerical discretization. The obtained numerical results are validated with analytical solutions [2]. Regarding the advantages of the method, the following properties have been proven by the numerical tests: high flexibility in the choice of basis functions, better order of convergence, low dispersion. References [1] E. Trefftz. Ein Gegenstuck zum Ritzschen Verfahren. Proc 2nd Int Cong Appl Mech Zurich (1926), 131–137. [2] H. Barucq, H. Calandra, J. Diaz, and E. Shishenina. Space-Time Trefftz - Discontinuous Galerkin Approximation for Elasto-Acoustics. Research Report, Inria RR-9104 (hal-01614126), (2017).

A Heterogeneous Multiscale Method Connecting Kinetic Theory and Molecular Dynamics

Gil Shohet^{*}, Jake Price^{**}, Jeff Haack^{***}, Mathieu Marciante^{****}, Michael S. Murillo^{*****}

^{*}Stanford U, ^{**}University of Washington, ^{***}Los Alamos National Laboratory, ^{****}Los Alamos National Laboratory,
^{*****}Michigan State University

ABSTRACT

Multimethod multiscale modeling, in which two or more separate models are used simultaneously to describe disparate scales in the same problem, provides an avenue for increasing the accuracy of macroscale models used in isolation. We have developed a concurrent multiscale using the traditional heterogeneous multiscale method (HMM) framework where molecular dynamics (MD) provides the missing microscale closure information for a macroscale kinetic model. The kinetic model is constructed such that only collision times are needed from the MD, greatly decreasing the memory and computation times needed. Computational cost is further reduced by a simple machine learning model that predicts future collision time information based on previous MD data. We illustrate the new model for the simple problems of temperature and momentum relaxation in a plasma composed of both weakly and strongly coupled species; we chose these zero dimensional problems to allow for a complete molecular dynamics solution, which allows us to examine choices made in the coupling between the two methods. HMM variants of this kind should be very useful for modeling a wide range of high energy-density environments.

High-precision Control Method for Large Space Structure Subject to Thermal Deformation

Kaori Shoji*, Motofumi Usui**, Daigoro Isobe***

*University of Tsukuba, Japan, **Japan Aerospace Exploration Agency, ***University of Tsukuba, Japan

ABSTRACT

As the sizes of space antenna reflectors increase, the radio wave transmissions will become more susceptible to small structural deformations that occur in the reflectors. When the Engineering Test Satellite -VIII (ETS-VIII) communications satellite entered the Earth's shadow, radio wave transmissions from the large deployable reflector (LDR) to the Earth were observed to change [1]. Moreover, the temperature of the LDR was observed to decrease for about 200 °C. Therefore, it is conceivable that radio wave transmissions were significantly affected by temperature transition on the LDR. This phenomenon may become critical for the satellites because highly accurate beams are expected to be required for large space structures in the near future. Therefore, not only the means by using materials in which thermal deformation is hardly generated but also the means of active shape changing in orbit have been required to deal with various issues. In this study, the LDR model mounted on the ETS-VIII is constructed for investigation. As a result of numerical simulation of the deformation behavior under the actual thermal history detected on the ETS-VIII, the midpoint of the LDR was confirmed to deform by approximately 5 mm as the temperature decreased [2]. 5 mm deformation is equivalent to 65 km transition of the footprint of communication beam on the surface of the Earth, which explains the phenomena actually observed in the ETS-VIII. Based on these results, we developed an effective method for mechanically compensating the thermal deformation by adjusting the combined coefficient of thermal expansion of structural members which is calculated from the constituent ratio of CFRP and titanium alloy components, and by focusing on springs used to deploy a modular space structure. As a consequence, the thermal deformations at every apex that support the antenna reflector were all suppressed at a high correction rate. It is shown that the combination of these means is best for large space structure to actively suppress the thermal deformation in orbit. References [1] M. Usui, K. Wakita, L. T. T. Thanh, Y. Matsui, and D. Isobe: Suppression of thermal deformation of the large deployable reflector, Transactions of the Japan Society of Mechanical Engineers, Series C, Vol.77, No.777, 2011, pp.2107–2119 (in Japanese). [2] K. Shoji, D. Isobe and M. Usui: Numerical Investigations to Suppress Thermal Deformation of the Large Deployable Reflector during Earth Eclipse in Space, The Aeronautical Journal, Vol. 121, No. 1241, (2017), pp. 970-982, (<https://doi.org/10.1017/aer.2017.33>).

Unified Programming Framework for Parallel FEM Multi-physics Analysis

Tatsuhiro Shono^{*}, Gaku Hashimoto^{**}, Hiroshi Okuda^{***}

^{*}The University of Tokyo, ^{**}The University of Tokyo, ^{***}The University of Tokyo

ABSTRACT

For innovative manufacturing and design, multi-physics problem is important. Fluid-structure interaction analysis for blow molding and thermal fluid analysis for welding are good examples. Generally speaking, Multi-physics problems need longer computation time than mono-physics problems, and degrees of freedom becomes larger than conventional analysis when complex shape of products should be considered. Parallel computation is therefore effective in analysis of these problems. There are many programs for multi-physics analysis. On the other hand, there are more applicable programs to parallel computation, which is specialized in a particular analysis. FrontISTR[1], which is an open-source large-scale parallel FEM program for nonlinear structural analysis, is good example. It achieves high parallel efficiency based on overlapping domain decomposition, then has high applicability large-scale structural problems. Programming framework which extends parallel FEM program like FrontISTR for multi-physics problem is consequently beneficial for innovative manufacturing and design. In this presentation, we will show you a unified programming framework for parallel FEM multi-physics analysis. We will show you a unified programming framework for parallel FEM multi-physics analysis. In this presentation, we will deal with fluid-structure interaction problems and two-phase fluid flow problems. This framework is implemented on nonlinear structural analysis software without breaking a framework of original structural analysis. Additional loop is achieved two-way coupling scheme. Displacement of structures is replaced with flow velocity and pressure when element stiffness matrices at fluid element are calculated in the code. Elements in structures and elements in fluid share nodes at their interfaces, then boundary conditions for interaction between different physical fields are satisfied. This framework is implemented into FrontISTR to achieve high parallel efficiency. Some numerical results (flow over a thin elastic beam attached to a fixed square block[2], for example) solved by FrontISTR will also be shown as verification. [1] FrontISTR Forum, http://www.multi.k.u-tokyo.ac.jp/FrontISTR/index_en.php, 2018/01/10 accessed. [2] Wall, W. A., Fluid-Struktur-Interaktion mit stabilisierten Finiten Elementen, Ph. D. thesis, Institut für Baustatik, Universität Stuttgart.

Simulating the Tensile Response of a Composite Lap-Joint Using a Combined Discrete and Continuum Damage Modeling Approach

Ofir Shor*

*Rafael Advanced Defense Systems LTD

ABSTRACT

Designing structural components using composite materials often requires the use of connectors and joints, which are expected to withstand various structural loads. The talk will focus on the numerical simulation of a bi-material composite lap-joint under a tensile load, using a combination of discrete and continuum damage mechanics modeling approaches. An overall introduction of the modeling strategy will be given, followed by the description of the finite element model and the material models used in the analysis. The model was able to capture the ultimate tensile strength of the joint, as well as the joint's failure mode, which was initiated by delamination between the laminate plies, followed by the growth of intralaminar damage.

Calibration of a Conductive Thermal Model for SS 316L and 17-4 PH in Selective Laser Melting

Yi Shu^{*}, Adrian Lew^{**}, Daniel Galles^{***}

^{*}Stanford University, ^{**}Stanford University, ^{***}U.S. Army Research Laboratory

ABSTRACT

Precise thermal models for Additive Manufacturing are an important prerequisite for developing thermal control strategies as well as for predicting residual stresses for printed parts. We present a three dimensional finite element model for heat transfer in Selective Laser Melting (SLM) processes in which the laser beam parameters (power and its distribution) are calibrated by fitting the meltpool area section outlines in simulations with those in experiments. The experimental data are obtained by shining stainless steel 316L and 17-4 blocks with static and moving laser sources for different time periods periods, and samples are sectioned to extract the meltpool area profiles. The parametric spaces of possible meltpool profiles are constructed with various simulations with real, temperature-dependent material properties, in terms of appropriate non-dimensional parameters. We iterated the parameters and found those that produce least error between experimental meltpool outlines and simulated ones . With the optimal parameter values, we have achieved a good match of the meltpool outlines.

Trabecular-bone Adaptation to High-impact Exercise in Postmenopausal Women: A Combined Computational and Experimental Study

Vadim V Silberschmidt*, Juan Du**, Chris Hartley***, Katherine Brooke-Wavell****, Margaret A Paggiosi*****, Simin Li*****

*Loughborough University, UK, **Loughborough University, UK, ***Loughborough University, UK, ****Loughborough University, UK, *****University of Sheffield, UK, *****Loughborough University, UK

ABSTRACT

Osteoporosis is a common condition, with a bone loss and structural deterioration increasing risk of fracture [1]. Exercise can stimulate localised structural adaptation and increase bone density [2] that may reduce fracture risk. Different mathematical models were suggested to predict a bone-remodelling process improve understanding of this mechano-biological process, by which bone adapts to mechanical forces. To observe these changes, a few in-vivo mice models were develop; however, there is still no in-vivo assessment based on human models for investigation of the trabecular-bone adaptation in response to mechanical loading. In this study, a combined experimental and computational approach was used to predict this adaptation in postmenopausal women. caused by high-impact exercise A randomized controlled trial of a six-month unilateral exercise intervention was conducted with healthy postmenopausal women, with changes in an exercise leg compared to those in a control leg of the same participant. Microstructural changes in trabecular bone were assessed using high-resolution peripheral quantitative computed tomography (HR-pQCT; Scanco) at the distal tibia. 3D rigid registration was used to obtain resorption and formation areas between pre- and post-intervention scans. Finite-element (FE) models based on the obtained HR-pQCT data were used to determine a structural response of trabecular bone to loading – a high-impact hopping test; strain and strain gradients were used as two different mechanical stimuli. FE models were coupled with an algorithm for remodelling, a modification of a generic trilinear-curve relationship between the mechanical stimulus and adaptation for an equilibrium zone and two additional stages – over-loading and micro-damage. This is the first longitudinal study using HR-pQCT to investigate the effect of exercise on trabecular-bone adaptation across distal tibia. It demonstrated that this novel computational model is able to predict mechanoadaptation of trabecular bone to exercise of postmenopausal women. Such an approach could be used to design, investigate and optimise exercise strategies that target relevant physiological mechanisms. References 1. J. Kanis et al. (2002) Lancet 359(9321), 1929–1936. 2. S.J. Allison et al. (2015) J Bone Miner Res 30(9), 1709–16.

A Computational Investigation of Composites Augmented by Interfacially Bonded Mechanophores

Meredith Silberstein*, Meenakshi Manivannan**

*Cornell University, **Cornell University

ABSTRACT

Interfacial debonding is an important failure mode for polymer composites. A novel approach to manage this damage mechanism is to develop self-healing and self-reporting capabilities through the interfacial augmentation of chemicals termed mechanophores that have useful reactions in response to mechanical work (e.g. color change, chemiluminescence, small molecule release). We refer to such a composite system as an Interfacial Mechanophore Augmented Composite (IMAC). In this talk we will first present our study on activation of mechanophores at interfaces and then application of the key results to predict mechanophore activation in a particulate-filled composite. In the first study, we investigate the critical parameters for mechanophore-functionalized interfaces by building two computational models: a kinematic model with rigid non-interacting walls forming the interface and a molecular dynamics model with metallic substrates. In both the models the mechanophore is idealized as a coarse grained two-bead system governed by a double-well potential that emulates a force directed chemical reaction. Under substrate shear mechanophores progressively activate as interfacial displacement increases as long as detachment from the substrate requires more force than transitioning to the active mechanophore state. Further this activation progression is well approximated by a kinematic interpretation where change in the mechanophore attachment point separation is the dominant factor for determining mechanophore state. In the particulate composite analysis framework, this extensible link mechanophore concept is then used in conjunction with classical elasticity displacement field solutions for far field loading to determine the relative progression of damage and activation. Equibiaxial plain strain loading is used to explore the critical parameters governing mechanophore response within the composite. The results are summarized in terms of a design plot for selecting the appropriate critical mechanophore length change needed for a given composite. We will then also present results for uniaxial plain strain and full 3D uniaxial loading.

Peridynamic Models for Complex Materials

Stewart Silling*

*Sandia National Laboratories

ABSTRACT

Recent advances in the technology of metamaterials and nanoscale composites suggest the need to systematically derive a continuum mechanics material model from a given detailed small-scale description. Since long-range forces may be involved at the nanoscale, an appropriate continuum description would take these forces into account. Peridynamics may provide a suitable continuum mechanics theory for this purpose. In this talk, I will describe a new method for deriving a peridynamic micromodulus function, which is the fundamental peridynamic material property, from a small-scale model of a material. In this method, the material is discretized into cells that individually may contain many atoms or molecules. The mean displacement of the material within each cell is constrained to equal zero except for a single cell. Within this single cell, the mean displacement is a prescribed small nonzero vector. By solving the small-scale equilibrium equation subject to these constraints, we compute the position of every atom or molecule. The resulting net force between the perturbed cell and all of its neighboring cells provides the micromodulus function. This micromodulus function is suitable for peridynamic computations at the length scale of the cell spacing. The horizon emerges naturally from the method, since the micromodulus decays to nearly zero for cells separated by large distances. By constraining the time-averaged displacements of atoms and molecules, rather than their equilibrium displacements, a temperature-dependent micromodulus function can be derived similarly that allows for thermal oscillations.

Analysis of Extremely Flexible Structures Through a Geometrically Exact Bernoulli-Euler Rod Model

Cátia Silva^{*}, Sascha Maassen^{**}, Paulo Pimenta^{***}, Jörg Schröder^{****}

^{*}Polytechnic School at University of São Paulo, Brazil, ^{**}Universität Duisburg-Essen, Germany, ^{***}Polytechnic School at University of São Paulo, Brazil, ^{****}Universität Duisburg-Essen, Germany

ABSTRACT

This work presents a geometrically exact Bernoulli-Euler rod formulation that is an extension of [1,2] and based in [3]. Displacements and rotations can be unlimited large. Linear elastic constitutive equations for small strains are considered in the numerical examples. Energetically conjugated cross-sectional stresses and strains are defined. A straight reference configuration is assumed for the rod, but initially curved rods can be accomplished, if one regards the initial configuration as a stress-free deformed state from the plane position. The parameterization of the rotation field is done by the rotation tensor with the Rodrigues formula that makes the updating of the rotational variables very simple. A family of interpolation for the displacements for the torsion degree of freedom were applied in order to verify the most efficient combination. These were employed with the usual Finite Element Method, leading to adequate C1 continuity within the element. The connection between elements is enforced by Rodrigues parameter being equal on both connecting ends, this can be achieved by adding a penalty or Lagrangian term to the potential energy. The finite element method is used to discretize the potentials on a computational domain in terms of the nodal degrees of freedom. Bearing in mind that the potential is nonlinear a Newton-Raphson iteration scheme is chosen to solve this problem. A set of numerical benchmark examples illustrates the usefulness of the formulation and numerical implementation. These problems were performed, and presented satisfying results. Hence, it can be concluded that this formulation shows great promises to be extensively used for general 3D problems with flexible rods with a smooth connection scheme. 1. Pimenta P. M. and Yojo T., "Geometrically-exact analysis of spatial frames", Applied Mechanics Reviews, ASME, New York, v.46, 11, 118-128, 1993. 2. Viebahn, N., Pimenta, P.M. &&& Schroeder, J., "A simple triangular finite element for nonlinear thin shells - Statics, Dynamics and anisotropy", Computational Mechanics, online, 2016. 3. Silva, C.C., Maassen, S., Pimenta, P.M. &&& Schröder, J. "Geometrically exact analysis of Bernoulli-Euler rods" in preparation for Computer Methods In Applied Mechanics and Engineering, 2017.

Topology Optimization Applied to the Design of a Tesla Pump

Emílio Silva^{*}, Diego Alonso^{**}, Luís Sá^{***}, Juan Romero^{****}

^{*}Polytechnic School of the University of São Paulo, ^{**}Polytechnic School of the University of São Paulo,
^{***}Polytechnic School of the University of São Paulo, ^{****}Federal University of Espírito Santo

ABSTRACT

Tesla devices consist of rotating disks (without blades) and their operation principle is based on the boundary layer effect (i.e., viscous friction forces and Coandă effect). The Tesla pump may be used in various applications, however, its operation efficiency is quite low, which makes room for the optimization of its design. Therefore, in this work, a Topology Optimization formulation is proposed to optimize the Tesla pump rotor by using a 2D swirl flow model. The 2D swirl laminar fluid flow modelling is solved by using the finite element method. A traditional material model is adopted while considering nodal design variables, and is extended to take into account the optimization being performed in a rotating reference frame and the relative tangential velocity being smaller than the other velocity components. A multi-objective function is defined in order to minimize energy dissipation and vorticity. In order to reduce the generation of grayscale results, as it has been observed in previous works, an extra term is proposed in the vorticity function. An interior point optimization algorithm (IPOPT) is applied to solve the optimization problem. Numerical results taking into account some of the different aspects of the design of the rotor of a Tesla pump are presented.

Quasi-static and Dynamic FEM Simulation of Trabecular Bone with Bone Marrow Using a Constitutive Material Model Subject to Strain Rate and Anatomic Location

Juan Diego Silva Henao^{*}, Juan Pablo Casas Rodríguez^{**}, Alejandro Marañón Leon^{***}, Roberto Javier Rueda Esteban^{****}

^{*}Universidad de Los Andes, ^{**}Universidad de Los Andes, ^{***}Universidad de Los Andes, ^{****}Universidad de Los Andes

ABSTRACT

Previous studies have shown that mechanical properties of trabecular bone samples such as yield strength, modulus of elasticity and plateau stress are highly dependent on the anatomic location within the bone itself as well as strain rate. Several tests were conducted on specimens taken from different anatomical sites and orientations within the distal metaphysis of the femur in order to identify the dependency of mechanical properties with the anatomic location as well as their anisotropic behaviour. Samples were tested with and without bone marrow using three different tests devices: a conventional constant strain rate apparatus, a drop weight impact tests (DWIT) device and a split Hopkinson pressure bar system (SHPB) covering strain rates between 10^{-1} /s and 10^3 /s. A constitutive material model that predicts the behaviour of cancellous bone from several anatomic locations was derived from the experimental data gathered. FEM simulation were performed to validate the model estimation at several strain rates and its proximity to experimental data.

Optimized Phase Change Material Distribution for Adsorption Systems Using Topology Optimization Method in Axisymmetric Model

Diego Silva Prado*, Emílio Carlos Nelli Silva**

*Escola Politécnica da Universidade de São Paulo, **Escola Politécnica da Universidade de São Paulo

ABSTRACT

Gas transport and storage are two key factors to be considered when analysing potential solutions involving gas employment. The system efficiency and capacity often determine how attractive the gas solution is. One known solution for gas transport and storage is the adsorbed natural gas (ANG). It consists in the adhesion of gas in a porous matrix by the adsorption phenomena. Adsorption is an exothermic phenomenon, when gas is adsorbed, heat is liberated, heating up the system. One of the issues regarding ANG technology is the fact that increasing temperature causes adsorption capacity to decrease. To solve this problem, methods for controlling the temperature inside the vessel can be found in literature. One temperature control method consists in placing phase change material (PCM) bodies inside the vessel. In literature, it can be verified that placing PCM inside an adsorption tank can increase its adsorption and desorption capacity by reducing the system thermal amplitude. Results vary by changing the amount and position of PCM bodies at the tank interior. Employing a systematic tool for optimized material distribution, such as Topology Optimization Method (TOM) is an attractive solution for this material distribution problem. Several studies have been conducted regarding TOM capacities and implementations and it is considered a versatile tool for material distribution inside a domain. The study presented in this paper consists in the employment of a PCM model for porous media to create a topology optimization formulation capable of improving ANG tanks by optimizing PCM distribution at the vessel interior. The modelled tank consists in a cylindrical vessel with adsorbed material in its interior which is exposed to a pressure increase at the inlet. The FEniCS library is used to handle the differential equations problem and the routine is implemented in python. Sensitivities calculation are aided by dolfin-adjoint libraries. For TOM, the Project variable is set as the PCM distribution inside the vessel. For handling the non-linearity inherent of phase change problems, an analytical solution for phase change is linearized and applied in the numerical system. The portion of PCM at each phase is, then, determined by a variable presented in the mentioned model. This implementation benefits TOM once it avoids the necessity of adaptive mesh solutions, often needed when tackling phase change problems. Finally, PCM distribution inside a 2D axis symmetric ANG vessel is optimized by employing TOM. Optimization results are presented and the benefits the optimization brings are discussed.

AN ACCURATE APPROACH TO THE FINITE-ELEMENT SIMULATION OF FLUID-STRUCTURE INTERACTION WITH CURVILINEAR INTERFACES

VITORIANO RUAS* AND MARCO ANTONIO SILVA RAMOS[†]

* *∂*Alembert, Sorbonne Université - Campus de Jussieu
Couloir 55-65, 4^{ème} étage. 4 place Jussieu. 75005 Paris, France
and CNPq research grant holder, PUC-Rio, Brazil
ruas.vitoriano@gmail.com

[†] Department of Computer Science, Institute for Computing
Universidade Federal Fluminense, Niterói, Rio de Janeiro state, Brazil
marco@dcc.ic.uff.br

Key words: Curvilinear interface, Finite element, Hermite, High order, Simplex, Straight-edged.

Abstract. In many technical or scientific applications involving fluid-structure interaction, such as cardiovascular flow modeling, the solid walls are curved and therefore so is the flow domain. As long as velocity and displacement finite-element representations of order higher than one are employed, the interface degrees of freedom must be properly interpolated, otherwise method's theoretical accuracy will be eroded. We present a simple approach to avoid such a loss, based on a variational formulation that allows achieving this with straight-edged elements of the simplex type and polynomial algebra only. Examples with quadratic Lagrange and Hermite finite elements to represent displacements and classical mixed methods to approximate the primitive variables of viscous incompressible flow, illustrate the efficiency of the proposed approach.

1 WORK'S OVERVIEW

Among a few known techniques the isoparametric version of the finite element method (cf. [1]) for meshes consisting of curved triangles or tetrahedrons is the one most widely employed to solve partial differential equations with essential conditions prescribed on curved boundaries. It allows recovering optimal approximation properties that hold for elements of order greater than one in the energy norm for polytopic domains. However, besides a greater geometric complexity, this method requires the manipulation of rational functions and the use of numerical integration. We consider a simple alternative to deal with essential (i.e. Dirichlet) boundary conditions that bypasses these drawbacks, without eroding qualitative approximation properties.

Moreover, in contrast to other methods such as the isoparametric version of the finite element method, our technique is universal, for it applies to different types of degrees of freedom, such as normal components of vector or tensor fields. Actually the idea behind it was first disclosed during the talk given by the authors on a Hermite method with normal-derivative degrees of freedom, at ICNAAM - the International Conference of Numerical Analysis and Applied Mathematics -, which was held in Rhodes, Greece, in September 2016. Later on this work was published in the form of article [2]. In the present work we first recall the main principle the new technique is based upon, by taking as a model the solution of the Poisson equation with quadratic Lagrange finite elements. A detailed description thereof in both the two- and the three-dimensional case can be found in the open access article [3] and references therein. Then we show that the new method extends very naturally to both classical elasticity systems and viscous incompressible flow equations. This forms a basis for technique's application to fluid-structure finite-element modeling. In the particular case of the Stokes system, we show that the new method can be combined with any velocity-pressure pairing of global order greater than one. As an illustration we consider the classical Taylor-Hood (cf. [4]) and the Crouzeix-Raviart method, for which examples are given in two-dimension space. Some simulations of deformations of solid bodies of curved shape using our technique in connection with quadratic Lagrange finite elements are also supplied (see also [5]).

2 TECHNIQUE'S SHORT DESCRIPTION

First of all it is important to recall that the technique under consideration is aimed at interpolating Dirichlet conditions prescribed on curvilinear boundaries of bi- or tridimensional computational domains. It can provide a significant cost reduction of finite-element simulations in pure CFD or in fluid-structure modeling, as long as the method in use is of order greater than one. In this respect we can take as an example the popular Taylor-Hood method to solve the incompressible Navier-Stokes equations in a region delimited by two deformable excentric cylinders, both rotating with given angular velocities. The precision of this second order method to simulate the flow of an incompressible viscous fluid in such a domain will be considerably eroded, in case it is simply approximated by the polygon formed by the union of the straight-edged triangles, when a standard mesh is used. This effect will be amplified in case the deformation of the solid walls has to be taken into account, and a method of order greater than one is used to compute it, such as quadratic finite elements. A classical solution to overcome such an accuracy loss is to employ the isoparametric version of the finite element method to represent both the velocity of the fluid and the displacement of the solid walls, which requires the use of interface elements with parabolic edges. However, besides obvious geometric complications, this technique transforms the original local polynomial shape-functions into rational functions. Handling such functions can become a delicate issue. This is because the use of numerical integration is inevitable to compute the matrices inherent to the simulation, and the right choice of a quadrature rule is not always so clear. For those reasons our method provides an

efficient alternative, since it avoids the use of curved elements and handles only polynomial shape- and test-functions, thereby allowing for exact integration without any qualitative loss, as compared to the isoparametric technique.

Our method's guiding principle can be well understood in the framework of the finite-element solution of the following model-problem. Let us consider the Laplace equation $\Delta u = 0$ in a smooth curved plane domain Ω , with Dirichlet conditions $u=g$ on its boundary Γ , where g is assumed to be sufficiently smooth as well. Suppose that classical Lagrange finite elements are used to solve this problem, based on a straight-edged triangular mesh, in association with continuous functions which are a polynomial of degree less than or equal to k in each triangle.

Suppose again that Ω is approximated by the polygon Ω_h with boundary Γ_h , formed by the union of the triangles of a mesh with maximum edge-length equal to h . If the values of g at the nodes on Γ_h different from vertexes are taken from points on Γ close to them, it is well-known that, whatever $k > 1$, the error of the approximation of u in the energy norm will be an $O(h^{1.5})$ (see e.g. [6]), instead of the $O(h^k)$ one could hope for with this kind of interpolation. With the new technique it suffices to substitute the Lagrangian nodes in the interior of the edges contained in Γ_h , by nodes on Γ located nearby. The choice of the latter nodes is very wide, since anyway integration remains restricted to the triangles that form the polygon Ω_h . We further observe that the test-functions are not defined in this manner, but rather in the usual way for Lagrange finite elements. This is one of the main advantages of our method. In short this procedure allows generating approximations of optimal order k in the energy norm. A rigorous analysis of this property in both 2D and 3D can be found in two *arXiv* papers cited in [3].

A possible construction of the nodes located on Γ pertaining to the new method, generically denoted by P , is illustrated in Figure 1 for $k=3$.

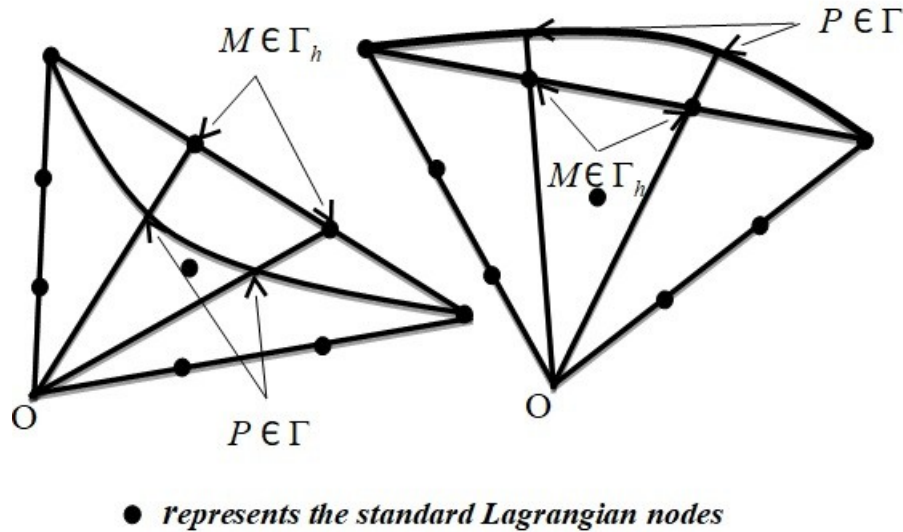


Figure 1- Lagrangian nodes $M \in \Gamma_h$ for $k=3$ and corresponding nodes $P \in \Gamma$ for typical boundary triangles

3 AN EXAMPLE WITH NORMAL-DERIVATIVE DEGREES OF FREEDOM

In this section we apply the principles described in Section 2 to a finite element method based on Hermite interpolation incorporating degrees of freedom of the normal-derivative type. The aim is to show that, in contrast to classical methods to handle Dirichlet conditions for second order boundary-value problems posed in curved domains, the technique studied in this work is as universal as can be. For this purpose we solve a model-problem using a variant of the classical Raviart-Thomas mixed finite element of the lowest order [7], commonly known as RT_0 . This variant studied in first author's work [8] among other papers of his, is to be employed in the framework of variational formulations mimicking corresponding mixed formulations. A Hermite interpolation with discontinuous piecewise quadratic functions allows for better accuracy of an approximate unknown field in the mean-square sense, as compared to the RT_0 finite element, though at equivalent cost. Solution's gradients in turn, are identically represented.

Suppose that we wish to determine the deflection u of an elastic membrane occupying a smooth plane domain Ω with edge Γ , under the action of a force density f perpendicular to its plane. It is well-known that this problem is governed by the Poisson equation $-c \Delta u = f$ in Ω , supplemented with appropriate boundary conditions, where c is a constant accounting for the mechanical properties of the material the membrane is made of. We consider that a portion Γ_0 of membrane's edge is kept fixed, that is, the essential boundary condition $u = 0$ holds on Γ_0 . On the other hand we assume zero traction on the complementary portion Γ_1 of Γ , which corresponds to the natural boundary condition $\partial u / \partial n = 0$ on Γ_1 , where $\partial u(\cdot) / \partial n$ denotes the outer normal derivative along Γ .

In order to solve this problem with our method, we first recast it in mixed form, by introducing the auxiliary field $\mathbf{p} = \text{grad } u$, which satisfies $\text{div } \mathbf{p} = -c^{-1}f$. The underlying mixed variational form writes: Find (\mathbf{p}, u) in $\mathbf{Q} \times W$ such that

$$\int_{\Omega} (v \text{div } \mathbf{p} + \mathbf{p} \cdot \mathbf{q} + u \text{div } \mathbf{q}) d\mathbf{x} = -c^{-1} \int_{\Omega} f v d\mathbf{x} \text{ for all } (\mathbf{q}, v) \text{ in } \mathbf{Q} \times W, \quad (1)$$

where W is the space of integrable functions in Ω (i.e. $W = L^2(\Omega)$), and \mathbf{Q} is a subspace of the space of vector fields which are square integrable in Ω , and whose divergence is also square-integrable in Ω , that is, the space $\mathbf{H}(\text{div}, \Omega)$ (cf. [7]). More precisely \mathbf{Q} is the subspace of $\mathbf{H}(\text{div}, \Omega)$ consisting of fields \mathbf{q} whose component $\mathbf{q} \cdot \mathbf{n}$ vanishes on Γ_1 , where \mathbf{n} is the outer normal vector to Γ .

It is important to recall that in the framework of formulation (1) the condition $\mathbf{p} \cdot \mathbf{n} = 0$ on Γ_1 is to be treated as an essential (Dirichlet) boundary condition, while the prescribed deflection $u = 0$ on Γ_0 is regarded as a natural (Neumann) boundary condition.

We actually solved a toy-problem with an empty Γ_0 . This requires taking an f satisfying the condition $\int_{\Omega} f d\mathbf{x} = 0$, and in this case u is defined up to an additive constant.

Now let \mathbf{T}_h be a mesh consisting of triangles with maximum edge length equal to h , satisfying the usual compatibility conditions (cf. [1]). Here again we denote by Ω_h the union of the triangles in \mathbf{T}_h and by Γ_h the boundary of this polygon. We define two subspaces \mathbf{Q}_h and W_h associated with \mathbf{T}_h , which are discrete counterparts of \mathbf{Q} and W . We recall that the Raviart-Thomas mixed method RT_0 consists of choosing W_h to be the space of functions which are constant in each triangle of the mesh. \mathbf{Q}_h in turn is the subspace of \mathbf{Q} consisting of fields of the form $a\mathbf{x} + \mathbf{b}$ in each triangle, where a is a real coefficient and \mathbf{b} is a vector of \mathbf{R}^2 , whose normal component is continuous on the edges of the elements in \mathbf{T}_h .

As for the Hermite variant of RT_0 , an approximation u_h of u is searched for in a space V_h defined as follows: In each triangle T of \mathbf{T}_h a function v in V_h is of the form $a\mathbf{x}^2/2 + \mathbf{b} \cdot \mathbf{x} + e$ where a and e are real coefficients and \mathbf{b} is a vector of \mathbf{R}^2 . Then, like the flux variable \mathbf{p} in the RT_0 method, the gradient of v is of the form $a\mathbf{x} + \mathbf{b}$ and its normal component along an edge is constant according to [7]. We require that this normal component of every v in V_h along a mesh edge be single valued if the edge is common to two triangles in the mesh, or to vanish if the edge is contained in Γ , in order to prescribe the zero traction condition on the edge of the membrane. Then following [8], we recast the finite-element counterpart of the mixed formulation (1) in the following variational form: Find u_h in V_h such that,

$$\sum_{T \in \mathbf{T}_h} \left[\int_T (v \Delta u_h + \text{grad } u_h \cdot \text{grad } v + u_h \Delta v) d\mathbf{x} \right] = -c^{-1} \int_{\Omega_h} f v d\mathbf{x} \quad \text{for all } v \text{ in } V_h. \quad (2)$$

Owing to these continuity requirements the local construction of functions in V_h must rely upon Hermite interpolation. Actually the degrees of freedom of V_h are precisely the (constant) normal derivatives along the edges, besides the function mean values in the elements of the mesh (cf. [8]). Since this method represents the gradient of the unknown field in the same way as the RT_0 mixed method, both methods differ only in the (discontinuous) representation of the deflection itself. Indeed in each triangle it is a linear function enriched with a quadratic term in the case of the Hermite method, whereas it is just constant for the mixed method. As long as Ω is a polygon, the Hermite variant of RT_0 described above is a second order method in the mean-square sense (cf. [8]), in contrast to the mixed method, which is just of the first order in the same sense.

Here we endeavor to show that, unless u_h is searched for in a suitable space U_h different from V_h such a property no longer holds, and moreover a substantial accuracy loss occurs in case Ω is a curved domain

Our choice of U_h is a space defined in the same way as V_h , except for elements in the subset of \mathbf{S}_h of \mathbf{T}_h consisting of triangles having an edge in Γ_h upon which a zero normal derivative condition must be enforced. However instead of enforcing this condition along such an edge, we require that the first order derivative of a function in U_h in the direction normal to it vanish along the tangent to the boundary at the intersection with it of the line joining the mid-point of this edge to the opposite vertex. This means that for each triangle in \mathbf{S}_h we pick up

the normal derivative where it is prescribed, that is, on the neighboring portion of the true boundary. This is precisely the counterpart of the Hermite finite element under study, for the technique designed to treat Dirichlet boundary conditions with Lagrange finite elements described in Section 2.

We next proceed to the numerical solution of our model-problem, taking $c = 1$ and Ω to be the ellipse with semi-axes equal to 0.5 and 1.0. We consider a manufactured exact solution given by $u(x,y) = (x^2/8+y^2/32-x^4/4-y^4/64-x^2y^2/8)$, f being defined accordingly. For symmetry reasons the computational domain is a quarter ellipse. We assess the convergence rates to the exact solution for three different approaches, namely, the classical RT_0 method, its Hermite variant taking $U_h=V_h$ and the latter combined with our method to approximate Dirichlet boundary conditions on curved boundaries. The meshes employed in these computations, indexed by an integer M with $h=1/M$, are the transformation of a uniform mesh of the unit square into the mesh of the quarter ellipse, by letting polar coordinates play the role of cartesian coordinates.

From the error evolution measured in the mean-square norm, it turned out that the power of h in the corresponding **OACR** is roughly 1, 1.8 and 2, respectively, where the acronym **OACR** stands for observed asymptotic convergence rate. We refer to Table 1 for such data. Moreover we checked the evolution as the mesh is refined of numerical solution's maximum absolute value at the centroids of the elements in the mesh. The **OACR** in this sense is roughly an $O(h^2)$ for the three methods. Nevertheless it is noteworthy that the accuracy of the boundary-modified Hermite variant of RT_0 in this respect is considerably improved, even for the coarser meshes, taking into account that the maximum absolute value of the exact solution is 1.56250, up to the fifth decimal. This comparison is illustrated in Figure 2.

All these results indicate that the modification in order to enforce on the true boundary the normal derivative boundary condition, with the Hermite variant of RT_0 , is indeed necessary whenever Ω is a curved domain. Indeed in doing so one takes the same advantage thereof in terms of accuracy enhancement, as in the case of polygonal domains (cf. [8]).

$M \rightarrow$	8	16	32	64	128	OACR
$h \rightarrow$	0.01250000	0.00625000	0.00312500	0.00156250	0.00078125	\downarrow
Raviart-Thomas mixed method RT_0	0.53435×10^{-3}	0.20712×10^{-3}	0.90368×10^{-4}	0.42781×10^{-4}	0.21005×10^{-4}	$O(h^{-1.0})$
Hermite variant of RT_0 ($U_h=V_h$)	0.32559×10^{-3}	0.99666×10^{-4}	0.29191×10^{-4}	0.83411×10^{-5}	0.24152×10^{-5}	$O(h^{-1.8})$
Modified Hermite variant of RT_0	0.18500×10^{-3}	0.48191×10^{-4}	0.12493×10^{-4}	0.32565×10^{-5}	0.82059×10^{-6}	$O(h^{-2.0})$

Table 1 - Absolute errors of the solution to a toy-problem in an ellipse in the mean-square norm

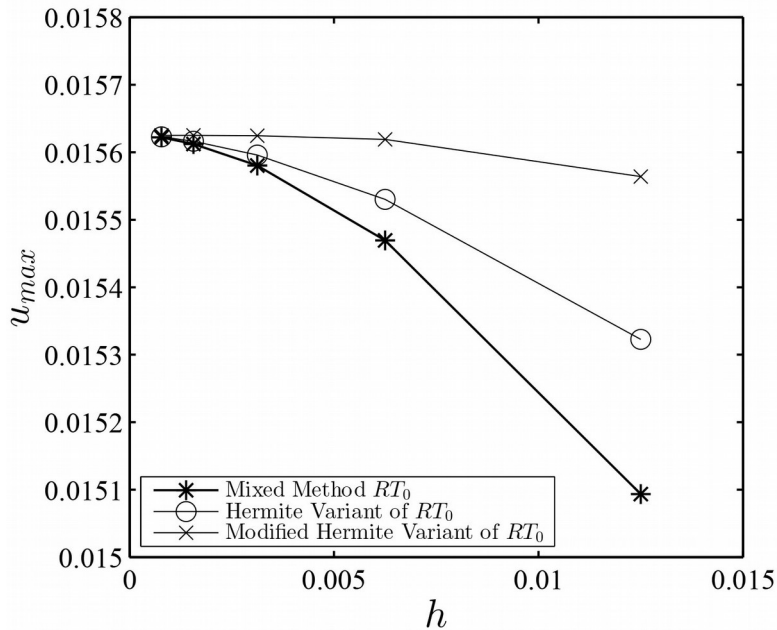


Figure 2 - Approximate solution's maximum absolute value u_{max} at the centroids of the elements

CONCLUSION

From the numerous experiments carried out so far with the new method to take into account Dirichlet boundary conditions prescribed on curved boundaries, it is possible to assert that it is a simple, reliable and accurate tool to handle interface conditions in fluid-structure or fluid-fluid higher order finite-element modeling. Moreover, as shown in this work, it is a universal technique, for it applies to different types of interpolations and degrees of freedom, and not only to those based only on function values, such as Lagrange finite elements.

ACKNOWLEDGEMENT

The first author gratefully acknowledges the financial support provided by CNPq through grant number 307996/2008-5.

REFERENCES

- [1] Zienkiewicz, O.C. and Taylor, R.L. The Finite Element Method. McGraw Hill, Vol. I., (1989), Vol. II., (1991).
- [2] Ruas, V. and Silva Ramos, M.A. A Hermite finite element method for Maxwell's equations. *Applied Mathematics and Information Sciences*, (2018) 12-2 : 271–283.
- [3] Ruas, V. Variational formulations yielding high-order finite-element solutions in smooth domains without curved elements. *Journal of Applied Mathematics and Physics*, (2017) 5-11: DOI:10.4236/jamp.2017.511174.
- [4] -, -. Accuracy enhancement for non-isoparametric finite-element simulations in curved domains; application to fluid flow. *Computer and Mathematics with Applications*, to appear.
- [5] -, -. Optimal Calculation of Solid-Body Deformations with Prescribed Degrees of Freedom over Smooth Boundaries. In: *Advanced Structured Materials*, H. Altenbach et al. Eds., Magdeburg, Springer International Publishing, Vol.1 (2018), 695–704.
- [6] Ciarlet, P.G., *The Finite Element Method for Elliptic Problems*, North-Holland, 1978.
- [7] Raviart, P.A. and Thomas, J.M. *Mixed Finite Element Methods for Second Order Elliptic Problems*, *Lecture Notes in Mathematics*, Springer Verlag, (1977) 292-315.
- [8] Ruas, V. Hermite finite elements for second order boundary value problems with sharp gradient discontinuities, *Journal of Computational and Applied Mathematics*, (2013) 246 : 234-242.

Numerical Evaluation of the Out-of-plane Response of Fiber Networks Using a Representative Volume Element

Jaan-Willem Simon^{*}, Yujun Li^{**}, Zengzhi Yu^{***}

^{*}Institute of Applied Mechanics, RWTH Aachen University, ^{**}Department of Advanced Manufacturing Engineering, Northwestern Polytechnical University, ^{***}Institute of Applied Mechanics, RWTH Aachen University

ABSTRACT

Many natural and synthetic materials have fibrous microstructures, such as nonwoven fabrics, paper, and fiberboard. It is usually difficult to experimentally evaluate their out-of-plane mechanical behavior due to the small thickness compared to the in-plane dimension. Hence, to properly predict such properties, network-scale models are required to obtain homogenized material mechanics by considering fiber-scale mechanism. The current study demonstrates a three-dimensional representative volume element (RVE) for fiber networks using the finite element method. First the classical deposition procedure has been adopted to generate fiber networks with random or preferential fiber orientations. Thereafter, an artificial compression step has been performed to achieve the practical fiber volume fraction. The hollow fibers, described with elastic-plastic brick elements, have been joined by interface-based cohesive zone elements introduced in all fiber-fiber contact areas. Then, the fiber networks have been subjected to displacement boundary conditions, and their apparent mechanical responses have been evaluated by means of homogenization of resulting stresses. Further, an RVE size convergence study has been conducted in order to determine the appropriate RVE dimension. In particular, the out-of-plane responses in compression and in tension have been investigated by varying specimen length while keeping the specimen thickness constant. Finally, the apparent out-of-plane responses of the obtained RVE have been evaluated for several loading cases including out-of-plane compression, tension, simple shear, and pure shear. The results show a quite different mechanical behavior of fiber networks between all these out-of-plane loading cases, particularly between tension and compression. In addition, the study showed that the smallest RVE which represented a reasonable response has required at least 160 fibers. The framework established in this work can be used to model numerous kinds of fiber networks at the individual fiber level and pass the information up to the macro scale for further analysis. This model is suitable to analyze the out-of-plane deformation, where a model with beam elements shows difficulty.

Topological Optimization of Patient Specific Maxillofacial Implants

Janos Simonovics*, Peter Bujtar**

*Budapest University of Technology and Economics, Budapest, Hungary, **Monkland University Hospital,
Lanarkshire, Scotland

ABSTRACT

Head and neck tumors affecting the facial bones are a challenging area of reconstruction. Combined biological and mechanical understanding has already rewritten the scenario from scratch multiple occasions. Resection of the so called load-bearing buttress system alters the skeleto-musculo-neurological equilibrium. Segmental mandible defects, for this reason, benefit from engineering input to provide restitution of the original physiological estate. The current load-bearing workhorse, reconstruction plates or implants are manufactured in mass production. A mixture of locking and non-locking screws are used to anchor these into the residual skeleton. The implant currently in used were redesigned in the past on many occasion, still could not fulfill the multi-faceted demand requiring mechanical, aesthetical, radiological, restorative and functional aspects. Additive manufacturing offer the most recent option to rethink patient specific implants. In the current study, the data of a 57-year-old edentulous female, imaged with a Cone Beam Computer Tomography (CBCT - iCat), was selected to build a detailed Computer Aided Design (CAD) mandible model using reverse engineering techniques. The most frequently occurring segmental defects were modelled including some worst case defect scenarios. The cover surface was inserted as the design space for the reconstruction plate topology optimization. Topology, shape optimization and Finite Element Analysis (FEA) were used to reach desired development goals with literature based anatomical boundaries and loads during chewing. The stress values within the plate were recorded. We found the redesigned implants would provide more physiological load transfer, more likely to preserve and support the regeneration of bone. Eventually dental implant restoration would become more a viable option. The final implant weight was reduced with 60% compared to the original geometry while keeping the von Mises stress within the structural limits. It would be a unique novel feature of personalized implants to divert the micro strains ranges which would promote bone growing in resected areas. The availability of optimized implants can change the indication of resection. The current model can increase our understanding of the biomechanics and may help to translate additive manufacturing principles into the implant design practice.

A Micromorphic Approach Modelling the Anisotropic Material Behaviour of the Human Heart

Sebastian Skatulla^{*}, Markus von Hoegen^{**}, Joerg Schroeder^{***}, Ntobeko Ntusi^{****}

^{*}University of Cape Town, ^{**}Universität Duisburg-Essen, ^{***}Universität Duisburg-Essen, ^{****}University of Cape Town

ABSTRACT

Computational cardiac mechanics models need to take into account the complex underlying micro-structure of the cardiac tissue in a sufficiently accurate manner, address biological effects such as residual stresses, remodelling or rearrangement of micro-structural components and are numerically robust and efficient. It has been discovered that the initially crimped and coiled collagen fibres straighten during diastolic filling, the interconnected fibre sheets are able to slide over one another and fiber rearrangement and spatial reorientation is taking place. This work proposes a generalized continuum approach which features extra degrees of freedom and corresponding strain and stress measures. The approach can therefore account for the hierarchical fibrous characteristics of the myocardium which are associated with micro-structural deformation of muscle-fibre bundles as well as their motion relative to the bulk material representing the constraining cytoskeleton. The micromorphic generalised cardiac mechanics model is applied to finite element modelling of patient-specific hearts making use of cardiac magnetic resonance (CMR) scans provided for this investigation by the Cape Universities Body Imaging Centre (CUBIC). With the anatomical heart models calibrated, the fibre strain, fibre stress and active tension distributions are computed. The comparison with simulated results using a classical myocardial tissue model indicates clear differences due to elastic non-affine fibre reorientation which renders the tissue more compliant.

Numerical Investigations of the Out-of-plane Stiffness Behavior of Hybrid Core Sandwich Panels

Isabella C. Skrna-Jakl*, Dieter H. Pahr**

*TU Wien, Institute of Lightweight Design and Structural Biomechanics, **TU Wien, Institute of Lightweight Design and Structural Biomechanics; Karl Landsteiner Private University of Health and Science

ABSTRACT

Hybrid core sandwich structures, consisting of a foam core reinforced with thin composite beams, are among the most efficient lightweight design concepts. Besides aerospace applications, they are employed in industrial fields such as wind energy, transportation systems, ship building and roof constructions. The advantage of the hybrid core is that, due to the specific orientation of the anisotropic 1D reinforcements, a low weight sandwich design with an improved out-of-plane stiffness can be obtained. Aim of the present study is to numerically investigate the influence of specific core reinforcement design parameters on the out-of-plane stiffness behavior. Sandwich configurations with reinforcements oriented at $\pm 45^\circ$ are studied and Finite Element unit cell analyses are performed with boundary conditions corresponding to the standardized sandwich shear and compression tests. The effective out-of-plane engineering constants are computed, employing the homogenization software MEDTOOL [www.dr-pahr.at]. At first 3D-solid FE-models are analyzed and variations of the effective out-of-plane engineering constants due to • changes of the reinforcement material, • the presence of matrix joints in the crossing region of adjacent stiffeners, • stiffeners that penetrate each other at the crossing point, and • removal of the foam core are examined taking into account the weight of the investigated configurations. The results show that the specific values of the out-of-plane pressure and shear moduli can be increased up to 16-fold and 60-fold, respectively, in comparison to the data obtained from unit cell analyses of the unstiffened foam core sandwich. In a second step an FE-unit cell model was developed with the aim of reducing computational requirements for subsequent analyses. Therefore, the face sheets and the foam were modeled employing a coarse 3D-solid element mesh and beam elements were used for the reinforcements. The results show that particular modeling techniques are required to correctly model the transversally, isotropic material behavior of the beams as well as the connection of the beams to the face layers. Finally, FE-analyses of standardized sandwich shear and compression tests are performed. As the size of the standardized test samples and the size of the unit cell are of the same order of magnitude, "structural" rather than periodicity boundary conditions must be used. The comparison of the effective out-of-plane engineering constants obtained by the numerical test and unit cell analyses, can be used to evaluate the experimental results.

Mesh Dependent Properties to Produce Mesh Independent Results in Fracture Mechanic Simulations

Damián Smilovich*, Raúl Radovitzky**, Eduardo Dvorkin***

*Sim&Tec;, Buenos Aires, Argentina, **MIT, Cambridge, MA, USA, ***Sim&Tec;, Buenos Aires, Argentina

ABSTRACT

The fundamental criteria that govern the fracture mechanics behavior of materials are (i) the fracture initiation criterion that controls the onset of fractures and (ii) the propagation criterion that controls the release of fracture energy when the already initiated fractures increment their opening. The Discontinuous Galerkin (DG) technique in conjunction with cohesive interface elements has been successfully used for many years in the modeling of fracture mechanic problems [1] [2] [3]. When simulating fracture propagation using the DG technique, a fracture opened at an interface element will propagate to a neighbor one when the initiation criterion is also fulfilled at it. The initiation criterion is usually stated as a function that combines the stress state at a point with the material ultimate stress; hence, it is a mesh independent criterion. However, it must be considered that the numerical model approximates the stress singularity at the crack tip using non-singular interpolation functions; therefore, the fulfillment of the initiation criterion depends on the mesh density at the crack tip; therefore, larger elements may numerically arrest the fracture propagation. To circumvent this problem and get results that are independent of the mesh it is possible to introduce in the initiation function a measure of the elements size. Numerical experiments are presented to back-up the proposed methodology illustrating that a mesh dependent initiation function decreases the dependence of the fracture mechanic results on the elements size. References [1] G. Camacho and M. Ortiz, "Computational modelling of impact damage in brittle materials," Int. J. of Solids and Structures, vol. 33, no. 20, pp. 2899-2938, 1996. [2] L. Noels and R. Radovitzky, "A general discontinuous Galerkin method for finite hyperelasticity. Formulation and numerical applications," Int. J. Numerical Methods Engrg., vol. 68, pp. 64-97, 2006. [3] R. Radovitzky, A. Seagraves, M. Tupek y L. Noels, «A scalable 3D fracture and fragmentation algorithm based on hybrid, discontinuous Galerkin, cohesive element method,» Computer Methods Appl. Mech. and Engrg., vol. 200, p. 326.344, 2011.

Topology Optimization of Primitives with Material Anisotropy

Hollis Smith^{*}, Julian Norato^{**}

^{*}University of Connecticut, ^{**}University of Connecticut

ABSTRACT

Anisotropic materials, such as fiber-reinforced bars or composite laminates, are widely used in industry to achieve lightweight structures with greater performance than is possible using homogeneous isotropic materials. In this presentation, we introduce a topology optimization method for the design of structures made of bars or plates that exhibit specified material anisotropy (e.g. fiber-reinforced bars or composite-laminate plates) within a 3-dimensional design region. The geometry and the elasticity tensor associated with each primitive are analytically and explicitly expressed in terms of their relevant geometric design parameters: position, orientation, and dimensions. In addition to these geometric variables, an auxiliary size variable is ascribed to each primitive and penalized in the spirit of solid isotropic material with penalization (SIMP) enabling the optimizer to entirely remove a primitive from the design if its size variable attains a near-zero value. To perform the primal and sensitivity analyses, we employ the geometry projection method to smoothly map the analytical geometry of the primitives onto a continuous density field defined over a fixed uniform finite element grid. Following the projection of the geometry, we use an ersatz material whereby the effective elasticity tensor at each finite element, and consequently its stiffness matrix, is modified by a suitable function of the projected density. The distinct advantage of this method is to enable topology optimization using readily-manufacturable anisotropic materials. Moreover, our method retains two significant advantages that existing free-form topology (i.e. density-based and level set-based) optimization techniques exhibit: 1) we circumvent re-meshing upon design changes because the projected ersatz material defined over the fixed finite element grid simplifies the primal and sensitivity analyses; and 2) the differentiability of the projection and the chain rule enable the implementation of efficient gradient-based optimization methods. We demonstrate the applicability of our proposed method by presenting several numerical examples.

Tendon Cell and Tissue Activation by Matrix Damage

Jess Snedeker^{*}, Fabian Passini^{**}, Stefania Wunderli^{***}

^{*}University and ETH Zurich, ^{**}University and ETH Zurich, ^{***}University and ETH Zurich

ABSTRACT

Introduction: Efforts to elucidate degenerative tendon disease mechanisms have been hindered by a lack of valid experimental models, a limitation that is at least partly attributable to large challenges in maintaining in vitro tissue homeostasis after explanting. Tendon tissue equilibrium very heavily depends on appropriate mechanical loading within a narrow, and still poorly defined, physiological range. We will present an overview of our recent work on the tendon cell-matrix interactions that drive tissue homeostasis, matrix remodeling and eventual tissue degeneration, and discuss a roadmap for unravelling these mechanically regulated signaling pathways for the development of effective treatment strategies. Results and Discussion: First results using a mouse tail tendon explant model to investigate the role of mechanical loads on tissue homeostasis and degeneration suggest that tissue damage accumulates in the tendon until “intrinsic repair mechanisms” are overwhelmed. At this point, the metabolic cost of extracellular matrix remodeling exceeds the locally available nutrient supply. We hypothesize that upon reaching this “Metabolic Tipping Point”, the vascular system is recruited along with accompanying nerve supply (and pain) and the tissue enters into a chronic disease state characterized by high matrix turnover and increasingly poor tissue quality. In this paradigm, a delicate mechanically regulated balance exists between recruitment and suppression of the extrinsic vascular system by the resident tendon core cells. Upon injury or damage, this regulation pin turn steers the tissue towards either functional remodeling or chronic tendon disease. We believe that future research should focus on exploring the possibility of gaining control of the involvement of the intrinsic and extrinsic tendon compartment in the disease/repair process. Studying such synergetic involvement is experimentally challenging, but deserves our efforts when striving for resolving tendon disorders.

Integrated Computational Framework for Simulating the Failure Response of Materials with Complex Microstructures

Soheil Soghrati^{*}, Anand Nagarajan^{**}, Bowen Liang^{***}, Hossein Ahmadian^{****}, Ming Yang^{*****}

^{*}The Ohio State University, ^{**}The Ohio State University, ^{***}The Ohio State University, ^{****}The Ohio State University, ^{*****}The Ohio State University

ABSTRACT

We present an integrated computational framework relying on a new microstructure reconstruction algorithm and a non-iterative mesh generation technique, named Conforming to Interface Structured Adaptive Mesh Refinement (CISAMR), for creating high fidelity FE models of composite materials. A NURBS-based reconstruction algorithm is implemented to synthesize the material microstructure by packing arbitrary shaped particles, morphologies of which are extracted from digital data such as micro-computed tomography images. A genetic algorithm (GA) based optimization framework is also employed to simulate the target statistical microstructural descriptors such as the size distribution, volume fraction, and spatial arrangement of particles. CISAMR is then employed to create a FE model of the material by transforming a structured mesh into a high quality conforming mesh with low element aspect ratios and a negligible discretization error. This non-iterative transformation is carried out by combining customized versions of four algorithms: h-adaptivity, r-adaptivity, face-swap, and sub-tetrahedralization. Compared to enriched methods such as extended FEM, CISAMR obviates the additional computational burden associated with evaluating enrichment functions and provides a higher accuracy for recovering the gradient field. Further, unlike conventional mesh generation algorithms such as the Delaunay triangulation, CISAMR can easily handle problems with highly complex geometries without the use of iterative smoothing or relaxation algorithms to improve the elements quality. In this work, we show the application of this integrated reconstruction-meshing framework for simulating the failure response a variety of heterogeneous materials, including particulate and fiber-reinforced composites, as well as non-woven entangled materials such as fiberglass insulation packs. Multiple sources of material and geometrical nonlinearity, including the damage, contact, and cohesive debonding are considered in each simulation.

Numerical Experiments for Improvement of Material Deposition during OLED Manufacturing Process Using Direct Simulation Monte Carlo

Ilyoup Sohn^{*}, Insoo Seo^{**}, Sanghyun Lee^{***}, Sean Jeong^{****}

^{*}Korea Institute of Science and Technology Information, ^{**}Metariver Technology Co., Ltd., ^{***}Metariver Technology Co., Ltd., ^{****}Metariver Technology Co., Ltd.

ABSTRACT

OLED (Organic Light Emitting Diode) has a high degree of brightness, high speed response, low power and high resolution in the current display industry, increasing the scope of applications from computers and mobile devices. In 2012, a small size panel, such as smartphones, has been applied to tablet PCs and laptops, and has been applied to conventional TV screens with existing LCD screens to become an important part of the display panel. To obtain high demand and price competitiveness of the recent OLED panels, the effective mass production is required and the deposition process of a key material on a large panel with high degree of uniformity is required to produce a large amount of sub-panels. The most important technique in the face-qualification process is to increase the uniformity of the thin film thickness during the deposition process. However, it is a time-consuming process to predict and monitor the behavior of the evaporation, motion and deposition on panel of organic material under low pressure, rarefied condition experimentally. Also, since the organic materials are generally expensive, there is clearly a limit to perform experiments repeatedly. Therefore, a novel numerical analysis is essential so that it can effectively explain the behavior of deposition material under low pressure environment. Most studies of OLEDs have been conducted primarily about the studies of thermo-chemical behavior of materials, and the numerical analysis of the entire transport behavior of deposited materials within the low-pressure chamber was not actively studied. Therefore, Direct Simulation Monte Carlo (DSMC) method, which effectively simulates the behavior of the low pressure gas dynamics, is performed to simulate the actual model of the deposition of the evaporated organic material, and it is evaluated how the numerical solution obtained from DSMC calculations works for prediction of the actual OLED deposition process and improvement of uniformity of deposited materials on the display panel. This work primarily deals with two parts, one is a validation of a novel DSMC simulation operating on GPU architecture by comparing with measurements and another is an improvement of material uniformity with respect to the change of nozzle diameter where organic material is evaporated. REFERENCES 1. E. K. Lee, J. of the Semiconductor &&& Display Equipment Technology 8, 37-42 (2009). 2. M. S. Ivanov and S. F. Gimelshein, Annu. Rev. Fluid Mech 30, 469-505 (1998). 3. I. Sohn, J. Kim, J. Bae and J. Lee, IEEE Trans. Plasma Phys. 44 1823-1833 (2016).

Homogenization of Hyperelastic Composites with Stochastic Interface Defects

Damian Sokolowski*, Marcin Kamiński**

*Chair of Structural Reliability, Faculty of Civil Engineering, Architecture and Environmental Engineering, Lodz University of Technology, **Chair of Structural Reliability, Faculty of Civil Engineering, Architecture and Environmental Engineering, Lodz University of Technology

ABSTRACT

The main objective of this study is determination of degradation of the homogenized hyperelastic particulate composites stiffness resulting from the random interface defects between its components – the reinforcement and the matrix. These are introduced by means of an interphase coming from an artificial smearing of the stochastic defects of spherical shape, whose volume is the input Gaussian random variable. Both, the interphase and the matrix are hyper-elastic materials, while the reinforcement remains in the linear elastic regime. Homogenization is done with the use of unitary cubic Representative Volume Element (RVE) and the computations of probabilistic stiffness properties are performed within the framework of the Iterative Stochastic Finite Element Method (ISFEM). The ISFEM is implemented using the generalized stochastic perturbation method, whereas Monte-Carlo simulation as well as the semi-analytical approach serve as reference solutions. The non-linear Finite Element Method serves here as a basis for the ISFEM; the uniform uniaxial and biaxial deformations of this RVE are modeled in the system ABAQUS. Computational experiments include the deterministic results, basic probabilistic moments and coefficients (expectations, coefficients of variations, skewness and kurtosis) of the strain energy density potential. Principal novelty in this study is stochastic approach to probabilistic interface defects in composite made of hyperelastic and linear elastic constituents exhibiting a very high contrast of the stiffness. [1] A. Clément, C. Soize, J. Yvonnet, Computational nonlinear stochastic homogenization using a nonconcurrent multiscale approach for hyperelastic heterogeneous microstructures analysis. *Int. J. Numer. Meth. Eng.* 91: 799–824, 2012. [2] M. Kamiński, *The Stochastic Perturbation Technique for Computational Mechanics*, Wiley, Chichester, 2013. [3] D. Sokolowski, M. Kamiński, Computational homogenization of carbon/polymer composites with stochastic interface defects. *Compos. Struct.* 183: 434-449, 2018. Acknowledgements: The first Author would like to acknowledge financial support of the grant 2016/21/N/ST8/01224 from the National Science Center in Cracow, Poland.

Residual Limb Deformation and Mechanical Properties using Digital Image Correlation and Finite Element Analysis

Dana Solav^{*}, Hugh Herr^{**}, Kevin Moerman^{***}

^{*}Massachusetts Institute of Technology, ^{**}Massachusetts Institute of Technology, ^{***}Massachusetts Institute of Technology

ABSTRACT

Local changes in the volume, shape, and mechanical properties of the residual limb can be caused by adjacent joint motion, muscle activation, hydration, atrophy, and more. These changes affect socket fit quality and might cause inefficient load distribution, discomfort, and dermatological problems. Analyzing these effects is an important step in considering their influence on socket fit, and in accounting for their contribution within the socket design process. In this study, a 360° 3D digital image correlation (3D-DIC) system was developed for the full-field shape and deformation measurements of the residuum. A multi-camera rig was designed for capturing synchronized image sets as well as 6DOF force and torque measurements from a hand-held indentation device. Custom camera calibration and data-processing procedures were specifically designed to transform image data into 3D point clouds, and automatically merge data obtained from multiple views into continuous surfaces. Moreover, a specially developed data-analysis procedure was applied for correlating pairs of largely deformed images of speckled surfaces, from which displacements, deformation gradients, and strains were calculated. The entire procedure was validated by analyzing the strains of synthetically deformed 3D objects. First, a reference finite element (FE) model of a speckled cylinder was created. Then, different cases of prescribed deformation were simulated (e.g. homogeneous uniaxial tension, radial inflation, axial torsion). The simulated deformed objects contain the deformed state of reference speckle pattern. The reference and deformed models were then manufactured using a multi-color 3D printer, and were analyzed using the imaging system in order to evaluate its accuracy. Furthermore, the residuum skin of five transtibial amputees were speckled using a custom speckling stamp, and imaged in different configurations, e.g. in various knee angles and muscle contraction levels, different times after doffing of the prosthetic socket, and at different times of the day. The images were processed to obtain the associated full-field displacements and strains. Characterization of the full-field deformations provided essential insights into the patterns and sources of the phenomena. Furthermore, local and subject-specific soft tissue mechanical properties were obtained by analyzing simultaneous surface deformation and force measurements during indentation. The experiment were simulated using a Finite Element model, and the hyperelastic and viscoelastic material parameters were determined by minimizing the error between the experimental and FE data. These results can be used to accurately describe the residuum's biomechanical behavior and interaction with the prosthetic socket. Consequently, prosthetic socket designs which take into account these effects can be considered.

Partitioned Coupling for Simulations of Flow-Induced Vibration Using Quasi-Newton and Fictitious-Mass Approaches

Jerome Solberg*

*Lawrence Livermore National Laboratory

ABSTRACT

Flow-induced vibration is a significant engineering challenge, especially in the design of heat exchangers. The desire for increased efficiency and decreased plant footprint and cost necessitate thinner walled tubes, longer spans, greater packing density, and higher flow velocities. All these features lead to greater fluid-structure interaction, with the concomitant need for improved analytical tools. One approach common within the industry is one-way-coupled analysis, where the flow pressure loads, varying in time, are applied to the structure. The response of the fluid to structural motions is approximated via “added mass” and “added damping” terms included in the structural equations. These terms are generally a function of the fluid and the geometry, and can be difficult to calculate even for simple geometries [1]. Forward coupled analyses have great utility within the design cycle, but at high enough velocities a fully-coupled approach is necessary. A staggered approach is desirable because it allows disparate fluid and structural solvers to be coupled together whilst treating each solver as a “black box” in relation to the other. Such schemes can be slow to converge (or even not converge at all), because at low stiffness values of the structural components correct accounting for the “added mass” term is critical, as the well-known analysis of Causin and his coworkers has demonstrated. Recently, a related concept, that of “fictitious mass/damping” has been used in the context of a fully-coupled analysis where the fluid and structure solvers are solved in a staggered scheme incorporating relaxation [2]. In this work, we examine approaches based initially on [2] where the added mass/damping terms are monitored based on the progress of the solution. Solution strategies based on Quasi-Newton methods [3] are also explored, and the results from both approaches used to calibrate one-way-coupled analyses. The advantages of each of these methodologies is compared, with a special focus on their ability to inform one-way-coupled analyses. This presentation is a follow-on to work presented at the 2017 USNCCM conference. [1] Wambsganss, M. W., Chen, S.S., and Jendrzejczyk, J.A., 1974, "Added mass and damping of a vibrating rod in confined viscous fluid" ANL-CT-75-08, Report, Argonne National Laboratory, Argonne, Illinois. [2] Baek, H. and Karniadakis, G. E., "A convergence study of a new partitioned fluid-structure interaction algorithm based on fictitious mass and damping," *Journal of Computational Physics*, 231 (2012), 629-652. [3] Bogaers, A. E. J., Kok, S., Reddy, B. D. and Franz, T. "Quasi-Newton methods for implicit black-box FSI coupling" *Comp. Meth. in Appl. Mech. and Eng.*, 279 (2014), 113-132.

Simulation of Selective Beam Melting Processes Using Multi-Time-Stepping

Dominic Soldner^{*}, Julia Mergheim^{**}, Paul Steinmann^{***}

^{*}Institute of Applied Mechanics - Friedrich-Alexander-Universität Erlangen-Nürnberg, ^{**}Institute of Applied Mechanics - Friedrich-Alexander-Universität Erlangen-Nürnberg, ^{***}Institute of Applied Mechanics - Friedrich-Alexander-Universität Erlangen-Nürnberg

ABSTRACT

Additive manufacturing (AM) processes usually allow for more complex part geometries. In the context of powder bed based AM they are realised via the fusion of powdered material in locally defined regions by means of e.g. a laser or electron beam. Parts are then build in a layer-by-layer fashion. Simulating these manufacturing processes from a macroscopic point of view usually leads to computational demanding models, due to different scales in space and time, highly non-linear material behaviour, and the modelling of the layer-wise building process, i.e. dynamic growth of the computational domain. Therefore, multiple numerical methods are combined, aiming towards a reduction of the computational cost. Besides adaptive mesh refinement and coarsening, line heat input models, where the scan path is integrated in time, are often employed to reduce computational expenses. Yet the time step size of the model is constrained by the chosen resolution of the beam path, which clearly limits the size of the problem under investigation. Within the present contribution we decompose the computational domain and carry out the computations on the rendered sub-domains with distinct time step sizes in order to account for the different requirements of the temporal resolution of the model. This allows to employ smaller time step sizes in areas that are exposed to the beam, while other regions are discretised with a coarser temporal resolution.

Simulation of Red Blood Cells in Stenosed Vessels Using a Coupled Shell-fluid Analysis Purely Based on the Smoothed Particle Hydrodynamics (SPH) Method

Meisam Soleimani^{*}, Michele Marino^{**}, Peter Wriggers^{***}

^{*}Institute of Continuum Mechanics, Leibniz Universität Hannover, Germany, ^{**}Institute of Continuum Mechanics, Leibniz Universität Hannover, Germany, ^{***}Institute of Continuum Mechanics, Leibniz Universität Hannover, Germany

ABSTRACT

In this work, a novel 3D numerical method has been developed to simulate the mechanical response of Red Blood Cells (RBC) in the stenosed vessels. If the rheological behavior of the RBC changes, for example due to some infections, it is reflected in its deformability when it passes through the microvessels. It can severely affect its proper function which is providing the oxygen and nutrient to the living cells. By virtue of the numerical modeling, one can examine and predict the possibility of microvessel blockage due to less deformability of an infected RBC. If the RBC is healthy, it can easily squeeze while passing a capillary although the dimension of the capillaries is less than the RBC dimensions, see [1]. But in case of being infected by a disease such as Malaria, the RBC may stiffen as much as ten times and this can seriously hamper its passage through the microvessels. In extreme cases where vessel occlusion happens, it may result in death or coma. From the computational point of view, RBC is assumed to be a thin shell-like structure filled with an interior fluid (cytoplasm) and being submerged in an exterior fluid (plasma). The model is entirely based on the smoothed particle hydrodynamics (SPH) method for both fluid and the shell structure. Since the problem technically falls into the category of Fluid-Solid-Interaction (FSI), the presence of a moving interface (moving boundary condition) poses serious challenges in establishing coupling between the well-known fluid solvers (which are mainly Eulerian and grid-based) and solid solvers (which are generally Lagrangian and mesh-based). Utilizing the SPH method for both fluid and solid phases, one can significantly benefit from the Lagrangian and mesh-less features of this method. For example, no re-meshing is needed and the mesh movement is inherently and automatically handled. Adopting a Total Lagrangian (TL) formulation for the shell in the realm of finite deflection, the presented computational tool is capable of handling relatively large displacements and rotations appearing in RBC mechanical response. This work is actually a new application and extension to an in-house numerical code developed by the authors, see [2]. [1] Tenghu Wu, James J. Feng, Simulation of malaria-infected red blood cells in microfluidic channels: Passage and blockage, *Biomicrofluidics* (2013). [2] Meisam Soleimani, Peter Wriggers, Numerical simulation and experimental validation of biofilm in a multi-physics framework using an SPH based method, *Computational Mechanics* (2016).

Boundary Element Frame Fields for Hexahedral Meshing

Justin Solomon*, Amir Vaxman**

*MIT, **Utrecht University

ABSTRACT

A key geometric task in numerical partial differential equations (PDE) is hexahedral meshing, which involves dividing a volumetric domain into cube-shaped cells on which a physical quantity is approximated. Desiderata for the quality of a hexahedral mesh include uniformity of the shapes of the cubic cells as well as conformation to the geometry of the outer boundary; the latter constraint invalidates trivial grid-based techniques and implies complex topological structures for the set of elements. A promising approach for hexahedral meshing under exploration in the computer graphics community involves the design of frame fields. These fields assign six orthogonal directions to each point in a volumetric domain, used to guide the orientations of the cube elements; a subsequent discrete pass extracts individual elements aligned to the computed field. While the field-guided approach has many commonalities with popular two-dimensional quadrilateral meshing techniques, however, subtle challenges preclude direct extension of these algorithms to 3D, most prominently the non-commutative structure of rotations in 3D space. Instead, alternative structure emerges in the volumetric case. Whereas two-dimensional surfaces are curved, the volume bounded by the outer surface of the domain is homogeneous, inheriting the flat Euclidean metric from surrounding space. This allows the application of boundary element methods (BEM), which are effective for solving differential equations based on only boundary integrals. In this talk, we will discuss recent applications of boundary element techniques to frame-guided hexahedral meshing. This approach alleviates dependence of hexahedral meshing on an input tetrahedral mesh of the domain, suggesting the possibility of hexahedral meshing directly from a boundary representation and removing a key source of instability in existing techniques. Empirically, these algorithms also appear to generate smooth singular structures desirable for meshing in practice. In addition to describing details of two BEM-based hexahedral meshing pipelines, we will identify several open problems in this space in need of expertise in the BEM community.

Image Based Computational and Experimental Study on HIFU Ablation Close to Major Blood Vessels

Maxim Solovchuk*, Tony Sheu**

*National Health Research Institutes, **National Taiwan University

ABSTRACT

High intensity focused ultrasound is a rapidly developing technology for many therapeutic applications, including treatment of cancer. In comparison with the conventional treatment modalities, such as open surgery, radio- and chemotherapy, HIFU has the advantages of non-invasion, non-ionization and fewer complications after treatment. Despite the methods' clinical potential, it still remains challenging to treat several organs: including liver, breast, brain tumors. Accurate computer simulations are necessary in order to expand the application range of focused ultrasound and to predict and prevent unwanted secondary effects. It is still remain quite challenging to ablate the tumor close to blood vessel. The mathematical model has been developed to predict the treatment outcome which couples nonlinear acoustic equations with relaxation effects being taken into account, bioheat equations in tissue and blood domains, and hydrodynamic equations with acoustic streaming effect taken into account. In order to validate the model in vivo experiments have been performed in minipig. Temperature elevation during focused ultrasound therapy has been measured. The predicted results have been compared with experimental data and good agreement has been obtained. Numerical simulations have been performed in a patient specific geometry. Numerical modeling of thermal and acoustic fields plays a key role in the treatment planning of focused ultrasound ablation. It was shown that numerical simulations can help to reduce the treatment time.

Fracture Simulation Using a Damage Model Considering Contact and Frictional Sliding

Yuto Soma*, Mao Kurumatani**

*Department of Urban and Civil Engineering, Ibaraki University, **Department of Urban and Civil Engineering, Ibaraki University

ABSTRACT

We present a method for simulating behavior of crack propagation including contact and frictional sliding of fracture surface. The crack propagation is analyzed using a damage model based on fracture mechanics for quasi-brittle material considering fracture energy as fracture property of material. The contact and the frictional sliding are modeled on the local coordinate system in which a first coordinate axis corresponds the contact direction. The contact is determined using the strain of the contact direction. The contact behavior is represented by maintaining the stiffness of damaged element of contact direction. The sliding is determined using the Coulomb friction and the shear strain on the local coordinate system. The frictional sliding is represented using the shear stress which consider the frictional force. First, we explain the modeling of crack propagation including contact and frictional sliding of fracture surface, and show the formulation of the damage model considering the contact and the frictional sliding. Next, several numerical examples are presented to demonstrate the performance of the proposed method. Finally, we compare the numerical results with the experimental results of direct shear tests to demonstrate the validity of the proposed method.

Computational Modeling of 3D Printed Parts for Analysis of Constitutive Behavior of Material

Madhukar Somireddy*, Aleksander Czekanski**

*York University, **York University

ABSTRACT

Abstract: Additive manufacturing techniques are gaining popularity in recent times and have been used for printing parts in industries such as aerospace, mechanical, electronics and biomedical [1]. These techniques fabricate a three-dimensional (3D) part by layer upon layer deposition of the material. In addition, fabrication of a complex geometry part is not a limitation unlike the subtractive machining methods. However, one of the main challenges with these latest fabrication methods is the anisotropy in the material properties of the printed parts [2]. Although isotropic material is used for printing the part, the final material properties are not same as initial. This change in the material properties is due to change in the mesostructure that is happening during the layer upon layer deposition of the material while printing the part. Printed parts from one of the AM techniques, fused deposition modeling, are considered here for the study. The present work addresses estimation of the final material properties of the printed parts using computational homogenization [3] and their constitutive material behavior. Then the failure analysis of printed parts based on fracture mechanics is studied. The investigation revealed that mechanical behavior of the printed parts is same as that of laminated composite structures and further, the behavior is influenced by their build orientation and thickness. Tensile and bending experimental investigation on printed parts revealed that the crack is initiated at interface of the fibers and then propagated across layer. The propagation of the crack occurs along the voids which exist at interface of the layers. The failure is then followed in the load carrying fibers of layers of the part. Potential damage modes such as debonding, fiber breaking in the 3D printed parts subject to tension and bending loads are identified for computational failure analysis. Then the procedure for computational modeling of printed parts for failure analysis using Abaqus is discussed. 1. Guo, N. and Leu, M.C., 2013. Additive manufacturing: technology, applications and research needs. *Frontiers of Mechanical Engineering*, 8(3), pp.215-243. 2. Parandoush, P. and Lin, D., 2017. A review on additive manufacturing of polymer-fiber composites. *Composite Structures*, 182, pp.36-53. 3. Hollister, S.J. and Kikuchi, N., 1992. A comparison of homogenization and standard mechanics analyses for periodic porous composites. *Computational Mechanics*, 10(2), pp.73-95.

Discrete Element Modeling and Simulation of Atomized and Spray Dried Granules of Metal Powder

Kwon Joong Son*

*Hongik University

ABSTRACT

This work presents the modeling and simulation of the dynamics of atomized and spray dried granules of metal powder using the discrete element method. The use of granules of metal powder in a powder metallurgy process improves the mechanical properties such as the density and tensile strength of sintered products compared to those from the conventional powder metallurgy or metal injection molding processes. Such an improvement can be achieved mainly due to the granule's better flowability during die filling and compactibility during die pressing than non-granulated fine powder. Despite many advantages from manufacturing aspects such as a high sintered density and a low sintering temperature, the granulated powders have not yet been widely used in powder metallurgy industries because of their relatively low material productivity and high cost. To increase the yield rate of the metal powder granules, further process optimizations are required in the rotary disc atomization and spray drying processes. The discrete element method (DEM) can be used as a computational tool to improve the granulation and drying of fine metal powders. DEM can compute particle-to-structure and particle-to-particle interactions with consideration of contact, impact, friction, bonding, and cohesion. Therefore, it can numerically investigate the effect of granule size, inter-particular cohesion and bonding, inter-granular adhesion, and spraying rate on the dynamics of granulated powders. This work particularly focuses on three types of discrete element simulations: (1) spraying of granules from the rotary disc atomizer (2) collision of a single granule with the drying chamber wall, and (3) discharging or clogging of granules at the spray dryer outlet. This computational work may contribute to the process optimizations in the metal powder granulation for powder metallurgy purposes.

DangShin: Intelligent Path Recommendation System for 3-Cusion Billiard Game

Kyuho Son*, Dongsoo Han**

*Korea Advanced Institute of Science and Technology, **Korea Advanced Institute of Science and Technology

ABSTRACT

With the advances of computer vision techniques, many intelligent services continue to come out in various application domains utilizing the vision techniques. 3-Cusion billiard game is one of such applications. This paper proposes an intelligent path recommendation system for 3-cusion billiard game. The system is named DangShin. The system recommends successful play scenes in the real world billiard game for a given topology, which is the positions of three balls on a billiard table. To recommend the scenes, a topology is recognized with a picture of the table captured by a camera installed on the ceiling above the table. Then video scenes of successful hit with a similar topology are searched in a scene context database. Scene context is a bundle of scene data needed for the service. Initial topology and count of bounds to cushions are the examples. The system consists of a ball localizer, a position refiner, a context analyzer and a scene search engine. The ball localizer recognizes the positions of balls in each frame of a scene. The position refiner corrects time-series records of positions generated by the ball localizer based on background knowledge such as physics and billiard play rules. The context analyzer extracts scene contexts from the time-series ball positions refined by the position refiner. The scene search engine searches video scenes appropriate for recommendation in the scene context database. The system achieved an acceptable accuracy in the analysis of scene contexts for a practical service.

On the Equivalence between the S-method, XFEM and Ply-by-Ply Discretization for Delamination Analyses of Laminated Composites Using Shell Elements

Timothy Sonderman^{*}, Yang Jiao^{**}, Jacob Fish^{***}

^{*}Columbia University, ^{**}Columbia University, ^{***}Columbia University

ABSTRACT

Two hierarchical approaches, the s-method and the extended finite element method (XFEM), are compared to the classical ply-by-ply discretization approach in terms of their effectiveness in modeling delamination in laminated composites using shell elements. In the two hierarchical approaches, a smooth approximation field based on the mesh made of laminated shell elements is first introduced to resolve a delamination-free response of the composite structure. The initiation and propagation of delamination is modeled by either superposition of element patches (s-method) or by enrichment functions (XFEM). A cohesive zone model is employed to model decohesion at the inter-ply interfaces. In terms of representing strong discontinuities, the two hierarchical methods have been shown to represent an identical approximation space as the classical ply-by-ply discretization approach, even though the s-method gives rise to sparser matrix structure. In terms of representing weak discontinuities, the s-method has been shown to be equivalent to the ply-by-ply discretization approach and provides a seamless transition from weak to strong discontinuity.

Elastoplastic Analysis Using Scaled Boundary Finite Element Method

Chongmin Song^{*}, Lei Liu^{**}

^{*}University of New South Wales, ^{**}University of New South Wales

ABSTRACT

The scaled boundary finite element method has been employed to formulate polygon and polyhedral elements (Ooi, et al. 2014; Talebi, et al. 2016). In complementary with this type of polygon and polyhedral elements, a quadtree/octree algorithm has been developed. Using these two developments, fully automatic stress analyses are performed on geometric models provided in CAD, digital image and STL formats (Talebi, et al. 2016; Saputra, et al. 2017; Liu et al. 2017). This study extends the technique for 2D elastoplastic analysis in Ooi, et al. (2014) to 3D. A novel, simple and efficient scaled boundary elastoplastic formulation with stabilisation is developed. In this formulation, the return-mapping calculation is only required to be performed at a single point in a polygon/polyhedral element, which improves the computational efficiency of the elastoplastic analysis and facilitates the implementation. Numerical examples are presented to validate the proposed technique and to demonstrate its applications. References Liu, Y., Saputra, A. and Song, Ch. (2017) "Automatic polyhedral mesh generation and scaled boundary finite element analysis of STL models", *Computer Methods in Applied Mechanics and Engineering*, Vol. 313, 106–132. Ooi, E. T., Song, Ch. and Tin-Loi, F. (2014) "A scaled boundary polygon formulation for elasto-plastic analyses", *Computer Methods in Applied Mechanics and Engineering*, Vol. 268, 905–937. Saputra, A., Talebi, H., Tran, D., Birk, C. and Song, Ch. (2017) "Automatic image-based stress analysis by the scaled boundary finite element method", *International Journal for Numerical Methods in Engineering*, Vol. 109, 697–738. Talebi, H., Saputra, A. and Song, Ch. (2016) "Stress analysis of 3D complex geometries using the scaled boundary polyhedral finite elements", *Computational Mechanics*, Vol. 58, 697–715.

Molecular Dynamics Study on Temperature-dependent Screw Dislocation Behavior in BCC Metal Nanopillars

Gyuho Song*, Seok-Woo Lee**

*University of Connecticut, **University of Connecticut

ABSTRACT

Recent studies on body-centered-cubic (bcc) metal nanopillars revealed that dislocation are more easily multiplied in bcc structure than face-centered-cubic (fcc) structure. Computational studies in both bcc and fcc nanopillars suggested that cross-slip, which occurs at the free surface, plays an important role in dislocation multiplication at small length scales. Particularly for bcc structure, the relative difference in mobility between screw and edge dislocation is critical to induce the surface-controlled dislocation multiplication. The dislocation mobility of bcc metal is strongly dependent of intrinsic lattice resistance, which is a function of temperature, and the surface controlled multiplication behavior should also be dependent of temperature. In this study, therefore, we investigated how a single pure screw dislocation is multiplied through surface-controlled multiplication in a bcc nanopillars at a different stress, temperature (10~650 K), and nanopillars size by using constant stress molecular dynamics simulation. We chose [0 0 1]-oriented niobium and molybdenum nanopillars due to their different intrinsic lattice resistances. We created a single pure screw dislocation in a nanopillar, and applied the constant uni-axial compressive stress to drive the dislocation to move. We characterized the critical stress of dislocation multiplication as a function temperature and nanopillars size. Our results revealed the conservative decrease and increase in critical stress of multiplication with temperature, implying that surface-controlled multiplication is dependent of an absolute value of dislocation mobility as well as the relative difference in mobility between screw and edge dislocation. Also, we found that multiplication behavior has a distinct dependence on materials while being affected by the nanopillars size and the temperature. Our simulation results will be carefully analyzed to provide rationale for experimental results in literature. dislocation-free bcc nanopillars and dislocation-containing nanopillars at cryogenic temperatures. We will discuss how surface-controlled multiplication affects general dislocation multiplication behavior and strain burst size of bcc nanopillar. Our study will be able to bridge between experiment and computation on dislocation multiplication behavior in bcc structure at the nanometer scale.

Computational Design of Complex Ceramic Oxides from First-principles Calculations

Jun Song^{*}, Guoqiang Lan^{**}

^{*}McGill University, ^{**}McGill University

ABSTRACT

Complex ceramic oxides have found great use in aerospace applications, particularly on thermal insulation to enhance energy efficiency of turbine engines. However, the design and exploration of such materials is a daunting task given their complex structures and composition variation. In this talk, I will show that first-principles density functional theory (DFT) calculations, augmented by the Hubbard U correction, can serve as an effective computational route to accelerate the design and exploration of complex ceramic oxides. Focusing on rare-earth (RE) pyrochlores for thermal barrier coatings (TBCs), we performed a comprehensive set of DFT+U calculations, where the Hubbard U values were determined using the linear response approach. We show that the essential material properties, such as thermal conductivity and coefficient of thermal expansion, can be accurately predicted by first-principles calculations. With the first-principles based computational framework established, a design example of enhancing the performance of RE pyrochlores through alloying is then demonstrated.

The Shifted Boundary Method: A New Approach to Embedded Domain Computations of Waves and Shallow Water Flows

Ting Song^{*}, Alex Main^{**}, Guglielmo Scovazzi^{***}, Mario Ricchiuto^{****}

^{*}Duke University, ^{**}Duke University, ^{***}Duke University, ^{****}INRIA Bordeaux--Sud-Ouest

ABSTRACT

We present a new embedded boundary method for wave equation problems in time domain. Embedded boundary methods obviate the need for continual re-meshing in many applications involving rapid prototyping and design. Unfortunately, many finite element embedded boundary methods for incompressible flow are also difficult to implement due to the need to perform complex cell cutting operations at boundaries, and the consequences that these operations may have on the overall conditioning of the ensuing algebraic problems. We present a new, stable, and simple embedded boundary method, which we call “shifted boundary method” (SBM), that eliminates the need to perform cell cutting. Boundary conditions are imposed on a surrogate discrete boundary, lying on the interior of the true boundary interface. We then construct appropriate field extension operators, with the purpose of preserving accuracy when imposing the boundary conditions. We demonstrate the performance of the proposed method in simulations of problems in acoustics and shallow water flows.

A Material Point Method for Cavitating-fluid Flows

Yan Song*, Xiong Zhang**

*School of Aerospace Engineering, Tsinghua University, **School of Aerospace Engineering, Tsinghua University

ABSTRACT

The material point method (MPM) is an effective way to simulate the fluid-structure coupling problem with large deformations, which combines the advantages of both Lagrangian method and Eulerian method. In the MPM, the history-dependent properties are carried by particles and the equations of motion are solved on background grid which is remeshed every time step. However, one of the major challenges of the MPM is the low rate of convergence and accuracy. A great improvement has been made by Sulsky and Gong in 2016, who improved the MPM (IMPM) based on the moving least squares (MLS) and Gaussian integration. This scheme eliminates the crossing errors and reaches second-order accuracy. The simulation of cavitating-fluid flows is an important aspect of marine-vehicle simulations. Because of the physical feature that the density changes severely across the fluid-vapor interfaces, the volume of a particle in the MPM may grows over than that of a grid cell, which causes the numerical fracture. On the other hand, the IMPM replaces material point integration in MPM by Gaussian integration, thus the particles only serve as the points where the physical properties such as the density, the pressure and the volume ratio of vapor in cavitating-fluid flows are indicated. In this paper, we propose a particle-reassignment algorithm which regenerates particles in a grid cell where the original particles are overcrowded or undercrowded based on the IMPM. This method can deal with the problem caused by the high density gradient in the cavitation region. Moreover, a simply and efficient method to impose the inflow and outflow boundary condition is proposed in the same way. We also formulate a MPM scheme to simulation cavitating-fluid flows. Numerical examples are also given to validate the proposed method.

A Localized Interface Scheme for Connecting Dissimilarly Partitioned Systems

Yeo-UI Song^{*}, K. C. Park^{**}, Sung-Kie Youn^{***}

^{*}Korea Hydro & Nuclear Power, ^{**}University of Colorado at Boulder, ^{***}KAIST

ABSTRACT

A new interface method for dissimilar interfaces is presented. Interface schemes in computational mechanics are widely used to handle large scaled systems effectively. Large scaled systems are partitioned into several subsystems which have independent meshes for individual target accuracy. When subsystems have flat interfaces, it is easy to control the interface constraint. However, the subsystems usually contain curved interfaces. These curved interfaces make gaps at the shared boundaries due to different mesh sizes. Various studies exist for the treatment of curved interfaces but they employ complicated projection procedures for the dissimilar meshes. Especially in arbitrary three-dimensional curved interfaces, complicated numerical integration is required. Present method introduces a gap element having zero strain condition. Localized Lagrange multiplier method is used to enforce the displacement compatibility. Several numerical examples are presented for the verification of the proposed method.

Modeling of Ice Fragmentations by Impact Based on Nonordinary State-Based Peridynamics

Ying Song^{*}, Shaofan Li^{**}, Zhuang Kang^{***}, Aman Zhang^{****}, Shaofei Ren^{*****}

^{*}College of Shipbuilding Engineering, Harbin Engineering University, Harbin 150001, China, ^{**}Department of Civil and Environmental Engineering, University of California, Berkeley, CA 94720, USA, ^{***}College of Shipbuilding Engineering, Harbin Engineering University, Harbin 150001, China, ^{****}College of Shipbuilding Engineering, Harbin Engineering University, Harbin 150001, China, ^{*****}College of Shipbuilding Engineering, Harbin Engineering University, Harbin 150001, China

ABSTRACT

Ice-structure interaction is currently one of the hot topic in engineering fields and has not yet been addressed. Traditional numerical methods derived from classical continuum mechanics have difficulties in resolving discontinuous problems of ice fragmentations. In the present paper, a non-ordinary state-based peridynamics formulation has been developed to simulate the behavior of the ice under impact loads applied by a rigid ball. Ice is assumed as an elastic-brittle materials and simulated by the modified Drucker-Prager plasticity model, the failure criterion of ice is defined based on fracture toughness. Furthermore, a continuous contact algorithm has been developed to detect the contact area between the rigid ball and ice particles. It is shown that numerical results are in good agreement with experimental data from open literatures, the behavior of ice under the impact loads can be assigned to four fragmentation classes, cratering, erosion, disruption, and total fragmentation, and the proposed peridynamics model can capture the detail fragmentation features of ice under low velocity impact loads.

MULTI-LINK VISCOELASTIC CONTACT MODEL FOR NUMERICAL SIMULATION OF SEISMIC POUNDING BETWEEN ADJACENT STRUCTURES

STEFANO SORACE* and GLORIA TEREZI†

* Polytechnic Department of Engineering and Architecture, University of Udine
Via delle Scienze 206, 33100
Udine, Italy
e-mail: stefano.sorace@uniud.it

† Department of Civil and Environmental Engineering, University of Florence
Via S. Marta 3, 50139
Florence, Italy
e-mail: gloria.terenzi@unifi.it

Key words: Seismic Pounding, Viscoelastic Analytical Model, Finite Element Contact Model.

Abstract. A special multi-link viscoelastic (MLV) finite element contact model is devised and calibrated in this study to reproduce Jankowski's non-linear viscoelastic analytical model in time-history analyses including the effects of seismic pounding. The MLV model is constituted by an in-series assemblage of n linear dampers and n associated in-parallel linear springs. Its response is based on the sequential activation and disconnection of the dampers, following the variation of the time-variable interpenetration depth $\delta(t)$ between the colliding structures. This way, the resulting equivalent damping coefficient $c(t)$ of the assemblage becomes a function of $\delta(t)$, and thus the relation between $c(t)$ and $\delta(t)$ can be easily reproduced in piece-wise linear form in the finite element computation. Detailed information on the practical implementation of the MLV model in time-history seismic analyses, as well as on the calibration of relevant geometrical and mechanical parameters, are offered in the paper, based on the results of a simple case study, represented by a couple of one-storey colliding reinforced concrete frames.

1 INTRODUCTION

Earthquake-induced pounding between closely spaced buildings is one of the highest sources of seismic vulnerability, as it can cause severe damage to non-structural and structural members, and even contribute to structural collapse. Pounding impacts derive from the out-of-phase vibrational response of the colliding structures induced by their different dynamic characteristics, when their separation joints at rest are not wide enough to accommodate the maximum relative displacements.

In order to assess the effects of pounding, a special multi-link viscoelastic (MLV) finite element contact model is devised and calibrated in this study to reproduce the classical Jankowski's non-linear viscoelastic analytical model [1]. Indeed, the damping coefficient of the latter is defined as a non-linear function of time, and thus it cannot be directly implemented in commercial structural calculus programs, because the damping coefficient of the damper elements included in their basic libraries is assumed to be a constant. A detailed description of the MLV model and information on its practical implementation in time-history seismic analyses, as well as on the calibration of relevant geometrical and mechanical parameters, are offered in the next Sections.

2 FINITE ELEMENT IMPACT MODEL FOR POUNDING ANALYSIS

Jankowski's model [1] (lower image in Figure 1) represents a substantial enhancement of the traditional Kelvin-Voigt rheological scheme[2] (upper image in Figure 1), given by in-parallel combination of an elastic spring with k_1 stiffness, which is capable of transmitting impact forces, and a linear viscous damper with damping coefficient c_1 , simulating the impact-related energy dissipation. The contact element becomes activated when the width of the separation gap at rest (gap_r in Figure 1) between the impacting structures—idealized as rigid masses, indicated with symbols m_1 and m_2 in Figure 1—shrinks. In Jankowski's model, a second gap element (gap_c in Figure 1) with initial width equal to zero is incorporated in series with the damper, so that the latter is activated at the approaching stage of the colliding structures only, rather than in the rebound phase too (i.e. when the relative velocity between m_1 and m_2 becomes negative). Moreover, an additional elastic spring with stiffness k_d is placed in parallel with the damper, so as to drive it to its pre-impact position before a new contact occurs.

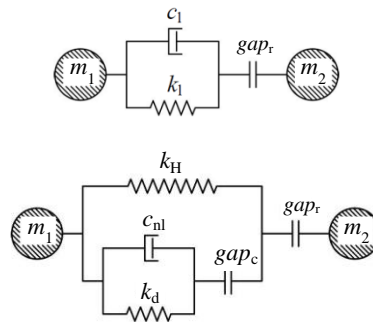


Figure 1. Rheological scheme of Kelvin-Voigt linear viscoelastic and Jankowski non-linear viscoelastic impact models

Further improvements of Jankowski's model as opposed to Kelvin-Voigt basic scheme consist in assuming non-linear behavioural characteristics both for the force-transmitting spring and the damper, consistently with the results of experimental studies carried out on

several different material and geometrical configurations of the impacting masses [3]. The response of the force-transmitting spring is governed by Hertz analytical law, which expresses the spring contact force, F_s , as a n -power law of the time-varying interpenetration depth $\delta(t)$ between the colliding members, with

$$\delta(t) = u_1(t) - u_2(t) - w_r \quad (1)$$

where $u_1(t)$, $u_2(t)$ are the displacements of the first and second mass, respectively, both functions of time, t , and w_r is the gap_r width. For pounding analyses, the n exponent in the Hertz-type expression of F_s is fixed at $3/2$ [1,4], that is

$$F_s(t) = \beta \cdot \delta(t)^{3/2} \quad (2)$$

where β is the impact stiffness parameter of the spring, which has the dimensions of a force divided by a $3/2$ -power law of displacement. Based on this assumption, k_H stiffness of the force-transmitting spring is regarded as an “effective impact stiffness”, given by the following function of $\delta(t)$ [1]:

$$k_H(t) = \beta \cdot \sqrt{\delta(t)} \quad (3)$$

For impacting R/C frame structures β is normally set as equal to $2.75 \cdot 10^6 \text{ kN/m}^{3/2}$ [1]. The damping coefficient of the non-linear damper, c_{nl} , is defined as a non-linear function of $\delta(t)$ too, according to the following relation [1]:

$$c_{nl}(t) = 2\zeta \sqrt{\beta \sqrt{\delta(t)} \frac{m_1 m_2}{m_1 + m_2}} \quad (4)$$

where ζ is the impact damping ratio, expressed as [1]:

$$\zeta = \frac{9\sqrt{5}}{2} \frac{1 - e^2}{e[9\pi - 16] + 16} \quad (5)$$

In relation (5) e is the coefficient of restitution, which accounts for the energy dissipation related to the damage effects occurring during collision, defined as follows [3]:

$$e = \frac{v_1'(t) - v_2'(t)}{v_1(t) - v_2(t)} \quad (6)$$

being $v_1(t)$, $v_2(t)$ the approaching velocities of the two structures, and $v_1'(t)$, $v_2'(t)$ the post-impact (restitution) velocities. For concrete-to-concrete impact, a value of 0.65 is basically adopted for e [1,4]. Consequently, the impact ratio ζ given by (5) is equal to 0.373. Based on relations (1) through (5), the total viscoelastic non-linear contact force, F_t , results to be:

$$F_t = \beta \cdot \delta(t)^{\frac{3}{2}} + c_{nl}(t) \cdot \dot{\delta}(t) \quad (7a)$$

for $\delta(t) > 0$ and $\dot{\delta}(t) > 0$ (contact-approach phase)

$$F_t(t) = \beta \cdot \delta(t)^{3/2} \quad (7b)$$

for $\delta(t) > 0$ and $\dot{\delta}(t) \leq 0$ (contact-restitution phase)

$$F_t(t) = 0 \quad (7b)$$

for $\delta(t) \leq 0$ (no contact) with $\dot{\delta}(t)$ = interpenetration velocity.

As observed in the Introduction, the damper elements currently incorporated in the libraries of commercial finite element programs, like SAP2000NL software [6] used herein, are characterized by constant damping coefficients. Therefore, time-dependent expressions like (4) can only be reproduced by “equivalent” finite element modelling strategies, such as the above-mentioned MLV model, constituted by an in-series assemblage of m linear dampers and m associated in-parallel linear springs. The sequential activation (approaching stage) and disconnection (restitution stage) of dampers allows reproducing the time-history evolution of c_{nl} .

A numerical performance evaluation study of the MLV model carried out at previous stages of this research [7,8] highlighted that the 5-link version in Figure 2 offers the best balance between simulation capacities, very similar for m values greater than 5 (slightly poorer for $m=3$ and $m=4$), and computational effort, processing times being approximately an exponential function of the number of damper+gap+spring elements.

Dampers are denoted by relevant damping coefficients c_i (with $i=1, \dots, 5$ in this case, and $i=1, \dots, m$ in general) in the model scheme drawn in Figure 2. The activation of each damper is governed by a gap (named gap_{ci} in Figure 2), to which a prefixed opening, w_i , is assigned. As the gap closes, the damper starts to react, adding its response to the already activated dampers. Similarly to the non-linear damper of the rheological scheme in Jankowski’s model in Figure 1, each element is combined in-parallel with a linear spring, with stiffness k_{di} , which drives it to its pre-impact position. The remaining components of the assembly (non-linear Hertzian spring, whose stiffness is denoted by symbol k_{HFE} in the finite element assembly, and the separation gap at rest gap_r in Figure 2) are the same as in Jankowski’s rheological scheme. For the practical implementation of the MLV model, the damping coefficients c_i of the dampers, the openings w_i of relevant gap elements gap_{ci} and the stiffness k_{di} of the linear springs must be specified. To this aim, the first step consists in tentatively predicting the maximum interpenetration depth, δ_{max} , expected from the time-history analysis. Then, the tentatively fixed value of δ_{max} , $\delta_{max,t}$, is discretized in m equal intervals with width $\Delta = \delta_{max,t}/m$, at the end of each one of which a new damper is activated. Therefore, the gap openings are obtained by the following rule: $w_i = (i-1) \cdot \Delta$. This holds $w_1 = 0$, consistently with the fact that the

first damper must be immediately activated when impact begins. Moreover, $w_m=(m-1)\cdot\Delta$, i.e. the m -th damper of the assembly is activated at the last step of the closing sequence of the gap elements.

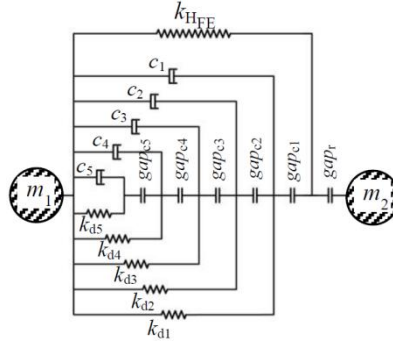


Figure 2. 5-link version of the MLV finite element model

Concerning the damping coefficients c_i , in the approaching phase the contribution of each damper is numerically added to the contribution of the already activated dampers, following the progressive increase in $\delta(t)$. As a result, each c_i value is assigned in such a way that the resulting “summed” damping coefficient of all the elements activated for a given interpenetration depth $\bar{\delta}$, $c_s(\bar{\delta})$, satisfactorily matches the corresponding analytical value

$c_{nl}(\bar{\delta})$ calculated by (4). Then, the fitting process of c_s to c_{nl} is carried out by fixing the value of the “summed” damping coefficient reached at the activation of the i -th damper, c_{si} , as equal to the c_{nl} coefficient calculated by (4) for the δ value situated in the middle of the interval of activation of the same damper, $\bar{\delta}_i$, i.e. $c_{si} = c_{nl}(\bar{\delta}_i)$, with $\bar{\delta}_i = w_i + \frac{\Delta}{2}$. Finally, c_i is obtained as

follows: $c_i = c_{si} - \sum_{j=1}^{i-1} c_j$, i.e. by subtracting from c_{si} the sum of the damping coefficients of the

dampers activated before the i -th damper. This criterion for the selection of w_i and c_i parameters is iterative, as it starts from a reasonable $\delta_{max,t}$ estimate—as suggested in Section 3—and terminates when the δ_{max} value resulting from the time-history analysis converges to a constant.

The k_{di} stiffness values of the linear springs are calibrated, according to a trial-and-error process too, so as to help the springs disconnect the dampers completely (i.e. reopen the relevant gaps) in the restitution phase, before a new contact occurs. The analyses carried out on several R/C frames with different geometrical dimensions and number of stories suggest adopting for the k_{di} values the same mutual proportions as among the c_i coefficients calculated according to the criterion formulated above. This way, the tentative choice of the spring stiffness values is reduced only to k_{d1} . For several numerical test multi-storey R/C structures

examined in this study, k_{d1} resulted to vary from about 1000 kN/m to about 5000 kN/m. Thus, to properly start the iterative search of a set of k_{di} values, it is recommended to select k_{d1} within this range, and then to impose the relations: $k_{d2}=(c_2/c_1)\cdot k_{d1}$; $k_{d3}=(c_3/c_2)\cdot k_{d2}$; ...; $k_{dm}=(c_m/c_{m-1})\cdot k_{dm-1}$, for k_{d2} through k_{dm} .

In addition to the mechanical parameters of the model discussed above, an internal elastic spring is assigned by default to the gaps and dampers constituting the MLV assembly, with the aim of preventing local unstable conditions in the solution of the equations governing the computational problem. Therefore, although such a spring has no direct physical meaning, the influence of relevant stiffness on the numerical performance of the model is evaluated in the next Section, along with the c_i , w_i and k_i parameters selected by the proposed criteria, for a simple numerical test pounding case study.

3 NUMERICAL TEST CASE STUDY FOR CALIBRATION OF MLV MODEL PARAMETERS

The two one-storey/one-span R/C frames sketched in Figure 3 are considered in this Section as pounding-prone numerical test structures. Both frames are square-shaped, with height and span of 5000 mm, and are situated at a 20 mm distance. Columns and beams were designed for gravitational loads only, so as to simulate a typical condition of most pre-normative pounding-prone R/C structures.

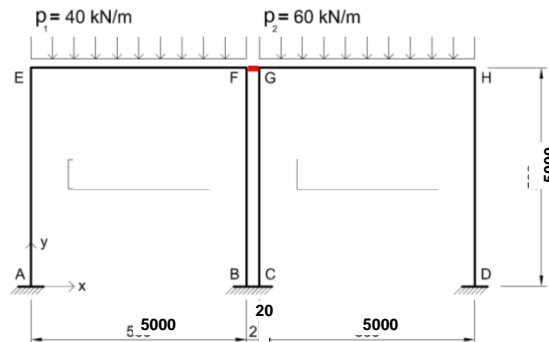


Figure 3. Geometrical (dimension in millimeters) and gravitational load scheme of the numerical test frames

The four columns and two beams have (350×350) mm×mm mutual cross sections, reinforced with 3 Φ 16 bars per side, and are made of concrete with cylindrical compressive strength equal to 25 MPa. The p_1 and p_2 uniformly distributed gravitational loads assigned to the beams, corresponding to the dead and live loads transferred by relevant floors (with greater tributary area for frame 2), are equal to 40 kN/m and 60 kN/m, respectively. The impacting masses, given by the contributions of p_1 and p_2 plus the weight of the beams, are: $m_1=21,9$ t and $m_2=32,1$ t. Time-history analyses were carried out by assuming a set of seven artificial ground motions as inputs, generated from the normative pseudo-acceleration elastic response

spectrum at 5% equivalent linear viscous damping ratio displayed in Figure 4, for two different earthquake levels (BDE and MCE, with peak ground accelerations of 0.234 g and 0.295 g, respectively, with g =acceleration of gravity). The response spectra of the two sets of ground motions are superimposed to relevant normative spectra in the two graphs of Figure 4.

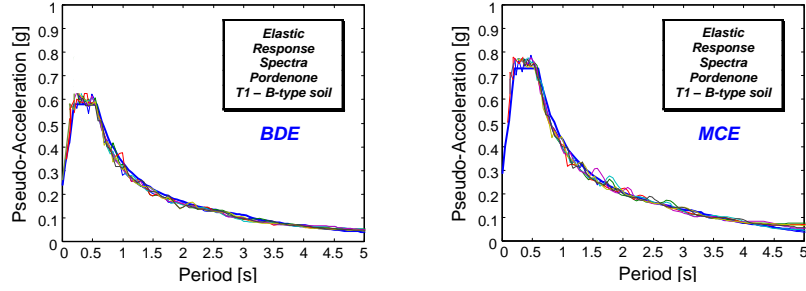


Figure 4. Reference normative pseudo-acceleration elastic response spectra, and superimposed spectra of the generated artificial ground motions

Beams and columns were modelled as elastic “frame”-type elements. The solution of the equations of motion was carried out with the Fast Non-linear Analysis method [9], implemented in SAP2000NL software for dynamic problems with a limited number of non-linear degrees-of-freedom.

The 5-link version of the MLV contact model was adopted, according with the observations in Section 2. The first step in the implementation of the model consists in fixing the gap openings w_i . These values are related to the tentatively predicted value of the maximum interpenetration depth δ_{max} that will be achieved in the time-history analysis of the colliding structures. A numerical enquiry carried out on low-to-medium rise R/C frame structures with total heights up to 25 m showed δ_{max} values always ranging between 2.5×10^{-4} and 5×10^{-4} times the height of the top contacting spots of the structures, h_{tcs} , for medium-to-severe input earthquake levels (i.e. for peak ground acceleration values of 0.2–0.3 g) [7,8]. Then, the tentative value of δ_{max} , $\delta_{max,t}$, can be selected within this range, e.g. as the mean value of it. For the considered numerical test case study, the peak ground acceleration for the BDE-scaled seismic action, equal to 0.234 g, is included in the reference PGA range above. Consistently, by considering that the height of the contact joints is equal to 5000 mm, $\delta_{max,t}$ can be located in the range $[2.5 \times 10^{-4} \times 5000 = 1.25 \text{ mm} - 5 \times 10^{-4} \times 5000 = 2.5 \text{ mm}]$. The mean value is equal to 1.88 mm, which can be rounded to $\delta_{max,t} = 2 \text{ mm}$ for this preliminary estimation. Therefore, for $m=5$, $\Delta = \delta_{max,t}/m = 0.4 \text{ mm}$, which holds: $w_1=0$, $w_2=0.4 \text{ mm}$, $w_3=0.8 \text{ mm}$, $w_4=1.2 \text{ mm}$ and $w_5=1.6 \text{ mm}$. Based on these w_i estimates, the following $\delta_i = w_i + \frac{\Delta}{2}$ mean interpenetration depths are obtained for the five intervals: $\delta_1=0.2 \text{ mm}$; $\delta_2=0.6 \text{ mm}$; $\delta_3=1 \text{ mm}$; $\delta_4=1.4 \text{ mm}$; and $\delta_5=1.8 \text{ mm}$. The “summed” damping coefficients $c_{si} = c_{ni}(\delta_i)$ calculated by substituting in (4)

the standard ξ and β values discussed in Section 2 ($\xi=0.373$ and $\beta=2.75 \cdot 10^6 \text{ kN/m}^{3/2}$) and the $m_1, m_2,$ and δ_1 through δ_5 values computed for this case study amount to: $c_{s1}=531 \text{ kN}\cdot\text{s/m}$; $c_{s2}=699 \text{ kN}\cdot\text{s/m}$; $c_{s3}=794 \text{ kN}\cdot\text{s/m}$; $c_{s4}=864 \text{ kN}\cdot\text{s/m}$; and $c_{s5}=920 \text{ kN}\cdot\text{s/m}$. Hence, the following

$$c_i = c_{si} - \sum_{j=1}^{i-1} c_j \text{ damping coefficients of the five dampers are obtained: } c_1=c_{s1}=531 \text{ kN}\cdot\text{s/m};$$

$$c_2=c_{s2}-c_1=168 \text{ kN}\cdot\text{s/m}; c_3=c_{s3}-c_1-c_2=95 \text{ kN}\cdot\text{s/m}; c_4=c_{s4}-c_1-c_2-c_3=70 \text{ kN}\cdot\text{s/m}; \text{ and } c_5=c_{s5}-c_1-c_2-c_3-c_4=56 \text{ kN}\cdot\text{s/m}.$$

The mean value of the [1000–5000] kN/m range indicated in Section 2 was adopted as tentative choice of the stiffness of the first damper-disconnecting spring, i.e. $k_{d1}=3000 \text{ kN/m}$.

By applying the relations reported in the same Section, the following tentative stiffness rounded values of the remaining springs are derived: $k_{d2}=(c_2/c_1) \cdot k_{d1}=950 \text{ kN/m}$;

$$k_{d3}=(c_3/c_2) \cdot k_{d2}= 540 \text{ kN/m}; k_{d4}=(c_4/c_3) \cdot k_{d3}=400 \text{ kN/m}; k_{d5}=(c_5/c_4) \cdot k_{d4}=320 \text{ kN/m}.$$

Concerning the internal elastic spring of gaps and dampers of the MLV model, the users' manuals of several commercial structural analysis programs, including SAP2000NL, suggest to adopt stiffness values—named $k_{ies,gap}$ and $k_{ies,damp}$, respectively—significantly greater than the maximum axial stiffness of the elements connected to them (in this case represented by k_{HFE}), so as to avoid any spurious influence on the response of the latter. In particular, said α_{gap} and α_{damp} the multiplying coefficients to be applied to k_{HFE} to obtain $k_{ies,gap}$ and $k_{ies,damp}$, it is suggested to select α_{gap} and α_{damp} values no lower than 100. The maximum value of k_{HFE} ,

$k_{HFE,max}$, is computed by substituting $\delta_{max,t}=2 \text{ mm}$ in the corresponding k_H analytical expression (3). For $\beta=2.75 \cdot 10^6 \text{ kN/m}^{3/2}$, $k_{HFE,max}$ results to be equal to around 120,000 kN/m.

Based on the users' manual indication above, both α_{gap} and α_{damp} were preliminarily fixed at 100. Therefore, the following initial values of $k_{ies,gap}$ and $k_{ies,damp}$ were assumed in the time-history analyses: $k_{ies,gap}=\alpha_{gap} \cdot k_{HFE,max}=12,000,000 \text{ kN/m}$, and $k_{ies,damp}=\alpha_{damp} \cdot$

$k_{HFE,max}=12,000,000 \text{ kN/m}$. The $F_t-\delta$ response cycles of the MLV model obtained from the time-history analysis carried out with the most demanding of the seven input ground motions scaled at the BDE amplitude level are plotted in Figure 5, for the set of mechanical and numerical parameters assumed above.

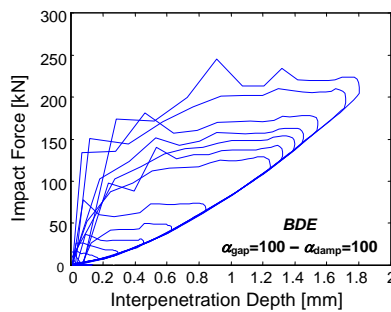


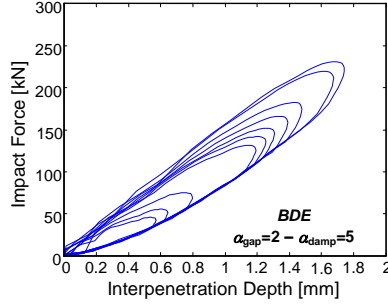
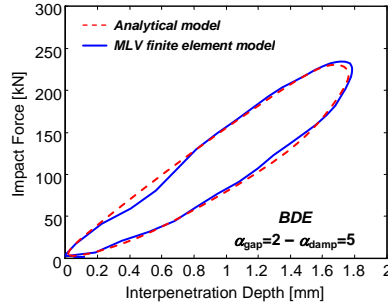
Figure 5. Response cycles of MLV model obtained for $\alpha_{gap}=100$ and $\alpha_{damp}=100$

Remarkable imperfections are noted in the approaching phase of all cycles, with saw-tooth shaped curves highlighting a too stiff response of gaps and dampers, due to the high $k_{ies,gap}$ and $k_{ies,damp}$ values initially adopted. As a consequence, the energy dissipated by the model, E_d , quantified by the area subtended by the cycles, is overestimated. On the other hand, the restitution branch of the cycles, ruled by the non-linear Hertzian spring, exactly follows equation (2). This demonstrates the effectiveness of the five damper-disconnecting springs, which allow the dampers disconnecting completely (i.e. reopening relevant gaps) in the restitution response phase. The δ_{max} value computed from the analysis is equal to 1.8 mm, close to the $\delta_{max,t}$ value of 1.88 mm, rounded to 2 mm, approximately estimated by the criterion presented above.

In order to improve the quality of MLV model response in the approaching pounding stage, the influence of $k_{ies,gap}$ and $k_{ies,damp}$ was analyzed by varying the α_{gap} and α_{damp} coefficients within the range [1–100]. The results of this analysis showed a negligible influence of α_{gap} and α_{damp} on δ_{max} , except for the case where they are both set as equal to 1. The number of contacts is rather insensitive too, since it is equal to 12 for α_{gap} and α_{damp} greater than 10, and 11 in the remaining cases. More appreciable differences come out for F_{max} , reaching around 15% between the highest and the smallest force values for α_{gap} and α_{damp} ranging from 100 and 2, and 25% for $\alpha_{gap}=\alpha_{damp}=1$. Differences are strong, instead, for E_d , which is a decreasing function of the internal stiffness of gaps and dampers, as a consequence of the progressive smoothing of the segmental saw-tooth shape of the approaching branch of response cycles. The processing time is a decreasing function of α_{gap} and α_{damp} too.

Based on the results of the numerical enquiry, the criterion followed to select the most appropriate α_{gap} and α_{damp} coefficient pair consisted in targeting the best correlation between the response cycles of the MLV numerical model and the corresponding cycles produced by Jankowski's analytical model. The latter were obtained by imposing the $\delta(t)$ time-history deduced from the response of the finite element model to the analytical model implemented via Excel software, and by computing relevant total contact force $F_t(t)$. The highest correlations were obtained for $\alpha_{gap}=2$ and α_{damp} ranging from 10 to 2, with the best superimposition reached for $\alpha_{damp}=5$. The cycles derived from the time-history analysis carried out with the same input accelerogram as in Figure 5, for the MLV model calibrated with $\alpha_{gap}=2$ and $\alpha_{damp}=5$, are displayed in Figure 6.

The maximum cycle extrapolated from the graph in Figure 6 is compared to the corresponding analytical cycle in Figure 7, highlighting a satisfactory superimposition, with nearly identical contained areas, and thus, coinciding amounts of dissipated energy. Therefore, it can be concluded that, whereas the basic users' manual suggestion concerning the adoption of α_{gap} and α_{damp} values no lower than 100 is well-suited for single non-linear link elements, it must be critically evaluated for assemblies of multiple elements, since it can negatively affect their hysteretic response, as ascertained for the MLV model examined here.

Figure 6. Response cycles of MLV model obtained for $\alpha_{\text{gap}}=2$ and $\alpha_{\text{damp}}=5$ Figure 7. Maximum response cycle of MLV model, for $\alpha_{\text{gap}}=2$ and $\alpha_{\text{damp}}=5$, and Jankowski's analytical model

Once the coefficient pair $\alpha_{\text{gap}}=2$, $\alpha_{\text{damp}}=5$ was fixed as the best performing choice for the calibration of the internal stiffness of gaps and dampers, the numerical enquiry was completed by evaluating the influence of the initial choices of the k_{di} stiffness values of the damper-disconnecting springs, and the openings w_i of the gaps. Concerning disconnecting springs, in addition to the basic value of 3000 kN/m, k_{d1} was varied over the entire [1000-5000] kN/m range suggested in Section 2, and k_{d2} through k_{d5} according to the mutual proportions expressed therein. The influence on the peak response quantities proved to be negligible, with F_{max} ranging from 236 kN ($k_{d1}=1000$ kN/m) to 230 kN ($k_{d1}=5000$ kN/m), and δ_{max} from 1.78 mm to 1.76 mm. The values of F_{max} and δ_{max} for $k_{d1}=3000$ kN/m coincide with the ones found for the upper limit of 5000 kN/m. More appreciable variations are found for E_d , as it ranges from 386 J ($k_{d1}=1000$ kN/m) to 491 J ($k_{d1}=5000$ kN/m), but with very small differences in the sub-range 3000–5000 kN/m, with E_d equal to 473 J for $k_{d1}=3000$ kN/m. Furthermore, for k_{d1} values below 3000 kN/m, a complete re-opening of the damper elements is not obtained, which causes small imperfections in the cycle contours at the restitution phase. These data show a stable response for the sub-range 3000–5000 kN/m, within which the basic choice of 3000 kN/m provides the most conservative results, as it determines the lowest E_d value (i.e. the lowest attenuation of pounding effects induced by the energy dissipation of contact elements).

The influence of the initial set of gap openings w_i was finally examined by varying their tentative choice based on the $\delta_{\max,t}=2$ mm value by which the calibration procedure was initialized. In particular, attention was focused on the consequences of $\delta_{\max,t}$ on the time-history analysis computation of the actual maximum interpenetration depth δ_{\max} . Relevant results show that, for $\delta_{\max,t}$ ranging from $\frac{1}{2}$ to 2 times the assumed basic value of 2 mm (i.e. ranging from 1 mm to 4 mm, with a step of 0.25 mm), δ_{\max} is nearly constant, as it varies from 1.79 mm to 1.77 mm, with a minimum of 1.76 mm for $\delta_{\max,t}$ equal to 1.25 mm through 2.5 mm. This underlines a substantial insensitivity of δ_{\max} with respect to $\delta_{\max,t}$, and thus the possibility of reaching a nearly “exact” calculation of δ_{\max} at the first round of the time-history analysis, for a reasonably wide range of $\delta_{\max,t}$ values around the basic choice suggested for the initial calibration of the MLV model. After the first round of the analysis, the w_i values are re-calculated for the computed δ_{\max} value, requiring a one step-only final calibration process of gap openings.

The parametric enquiry discussed here for the pair of one storey-one bay numerical R/C frames was carried out also for several other numerical test structures, by varying the number of storeys and bays from two to five, highlighting similar results. The choice ranges and criteria suggested above for the computational parameters involved in the analysis can thus be reasonably extended to the assessment of real case study pounding R/C structures.

6 CONCLUSIONS

The possibility of following the time-history evolution of impacts and related effects by non-linear force-transmitting springs and contact-energy dampers, offered by Jankowski’s analytical model for lumped colliding masses, can be duplicated in the computational analysis of complex structural systems by means of properly designed finite element assemblages, like the multi-link viscoelastic contact model devised and implemented in this research. Specific remarks deriving from the results of the calibration analyses presented in this paper are summarized below.

- A remarkable influence of the stiffness of the internal elastic springs of gaps and dampers on the response cycles of the MLV model emerged from the analyses carried out on the two single-storey test frames. In particular, noticeable imperfections came out in the approaching phase, with saw-tooth shaped curves highlighting a too stiff response of both types of elements, when $k_{ies,gap}$ and $k_{ies,damp}$ were assumed—as basically suggested by SAP2000NL users’ manual—100 times greater than the axial stiffness of the connected element, represented in this case by the force-transmitting Hertzian spring.
- The parametric analysis developed on the stiffness multiplying coefficients α_{gap} and α_{damp} showed the highest correlation between the response cycles of MLV and Jankowski’s models for $\alpha_{gap}=2$ and α_{damp} ranging from 10 to 2, with the best superimposition reached for $\alpha_{damp}=5$. For these coefficient values, satisfactorily smooth curves were observed for the MLV model

cycles also in the approaching stage. Furthermore, nearly identical contained areas, and thus coinciding amounts of dissipated energy, were obtained, as compared to analytical cycles. These results highlight that the users' manual suggestion of adopting α_{gap} and α_{damp} values no lower than 100, well-suited for single non-linear link elements, is not effective for the MLV model, and should always be critically evaluated when multi-link assembled models are implemented in time-history analyses.

– The influence of the mechanical parameters of the MLV model, i.e. the openings w_i of gap_{ci} elements, the c_i damping coefficients of dampers and the k_{di} stiffness values of damper-disconnecting springs, was relatively low on all response quantities, for parameter values selected within the tentative choice ranges determined according to the mathematical relations and empirical criteria presented in Section 2.

ACKNOWLEDGEMENTS

The study reported in this paper was sponsored by the Italian Department of Civil Protection within the ReLUIIS-DPC Project 2016/2018, research Line 6: Isolation and Dissipation. The authors gratefully acknowledge this financial support.

REFERENCES

- [1] Jankowski, R. Non-linear viscoelastic modelling of earthquake-induced structural pounding. *Earthquake Engineering and Structural Dynamics* (2005) 34: 595–611.
- [2] Anagnostopoulos, S.A. Pounding of buildings in series during earthquakes. *Earthquake Engineering and Structural Dynamics* (1988) 16: 443–456.
- [3] Jankowski, R. Experimental study on earthquake-induced pounding between structural elements made of different building materials. *Earthquake Engineering and Structural Dynamics* (2010) 39: 343–354.
- [4] Davis, R. O. Pounding of buildings modelled by an impact oscillator. *Earthquake Engineering and Structural Dynamics* (1992) 21: 253–274.
- [5] Goldsmith, W. *Impact: the theory and physical behaviour of colliding solids*, Edward Arnold, London, UK (1960).
- [6] SAP2000NL. Theoretical and users' manual. Release 19.06. Berkeley (USA): Computers & Structures Inc. (2018).
- [7] Pratesi, F., Sorace, S. and Terenzi, G. Analysis and mitigation of seismic pounding of a slender R/C bell tower. *Engineering Structures* (2014) 71: 23–34.
- [8] Licari, M., Sorace, S. and Terenzi, G. Nonlinear modeling and mitigation of seismic pounding between R/C frame buildings. *Journal of Earthquake Engineering* (2015) 19: 431–460.
- [9] Wilson, E.L. *Three dimensional static and dynamic analysis of structures*, Computers and Structures Inc., Berkeley, California (2002).

Hydrodynamic Modeling by Macroscopic Balance Equations at Simultaneous Different Length Scales and for Different Time Durations

Shaul Sorek*

*Ben-Gurion University of the Negev

ABSTRACT

Averaging over a Representative Elementary Volume (REV), yield concurrent primary and secondary macroscopic balance equations that respectively consider the REV and a significantly smaller length scale (Sorek and Ohana, 2015). Two sets of assumptions address their corresponding primary and secondary macroscopic balance equations. One accounts for the advective flux of the extensive quantity as dominant over the dispersive flux; the other refers to the intensive quantity as dominant over the one deviating from it. At the REV scale, we obtain extended forms of the macroscopic Navier-Stokes (NS) equation. These can vary from inertia fluxes in the form of a nonlinear wave equation, Forchheimer's law expressing the microscopic fluid inertia transmitted to the solid matrix through their interface, or conform to Darcy's law when friction at that interface is dominant. The secondary balance equations are in the form of hyperbolic balance PDEs'. Field observations of colloidal motion at pores scale comply with these hyperbolic PDEs' being pure advection mass balance associated with the deviation from the average concentration and a wave driven migration propagating the deviation from the average intensive momentum quantity. Controlled experiments supplemented by numerical predication assessing the interaction between the primary and secondary macroscopic balance PDEs are needed to study the hydrodynamic interrelation between these two adjacent spatial scales. Further, we address the primary macroscopic balance PDE's concerning a fluid mass and momentum and a component mass, following an onset of pressure impulse. We obtain different forms of dominant PDE's at evolving temporal scales (Sorek, 1996). Numerical simulations were found to be consistent in excellent agreement with experimental observations. During the second time increment we address theoretically the efficiency of expansion wave for extracting solute from a saturated matrix. Simulations comparing between pumping using an approximate analytical form based on Darcy's equation and numerical prediction addressing the emitting of an expansion wave, suggest (Sorek and Ohana, 2015) that the latter extracts by far more solute mass for a spectrum of different porous media. References Sorek S. and Ohana Y., Macroscopic Balance Equations for Spatial or Temporal Scales of Porous Media Hydrodynamic Modeling, Austin J Hydrol., 2(1): 1-9, 2015. Sorek S. A model for solute transport following an abrupt pressure impact in saturated porous media, Transport in Porous Media. 22: 271-285, 1996.

Coupled CFD/CSD Simulations of Dust Production by Fragmenting Charges Using Stabilized Linear Tetrahedral Elements

Orlando Soto^{*}, Joseph Baum^{**}, Rainald Lohner^{***}, Robert Frank^{****}

^{*}Applied Simulations Inc., ^{**}Applied Simulations Inc., ^{***}George Mason University, ^{****}Applied Research Associates

ABSTRACT

This paper presents coupled Computational Fluid-Dynamics/Structural-Dynamics simulations of internal detonations of cased munitions against reinforced-concrete walls. These simulations are part of a test, analysis, and modeling effort studying air blast propagation through breached walls. The coupled simulations are providing additional insight and details not measured in the tests, as well as developing a synthetic database to supplement the test matrix. The simulations are performed to calibrate the CFD/CSD model and to determine the physics impacting the internal environments, wall breach, and blast propagation through the breach. Here we modeled the response of reinforced-concrete walls to loads from a cased charge, placed in close proximity to the center of wall-1. In the test, the detonation room (composed of two culverts) incurred a large amount of plastic damage due to the fragments and blast load, and both culverts failed. Test wall-1 initially breached over the middle third, with the wing walls removed by the later time blast loads. Debris from test wall 1 impacted test wall 2, which failed under the combined blast and debris. Initial coupled CFD/CSD simulations modeled the culverts as rigid, non-responding surfaces. These simulations reproduced the damage to the test walls, but the pressure histories matched the experimental data only out to 10 ms. Subsequent air blast reflections were significantly reduced, as if a large amount of energy has been evacuated from the facility. Post-test damage analysis showed significant fragment damage to the culverts, with the concrete stripped to the first layer of rebars. We estimate that the fragment impacts produced several hundred kilograms of dust that was ejected into the room. Repeat simulations, where the culvert response was modeled and the dust was allowed to absorb both kinetic and thermal energy, matched the experimental data significantly better. Furthermore, recent developments of stabilized linear-tetrahedral elements for non-linear CSD applications (see [1-2]) have shown a great improvement on capturing plastic localization zones and, therefore, fracture prediction in benchmark problems. Hence, this work addresses how the implementation of such techniques improves the accuracy and the computer time savings for real life applications. [1] Cervera, M., Chiumenti, M., Benedetti, L., Codina, R. "Mixed stabilized finite element methods in nonlinear solid mechanics. Part III: Compressible and incompressible plasticity". *Computer Methods in Applied Mechanics and Engineering*, 285, 752-775 (2015). [2] Soto, O.A., Baum, J.D., Löhner, R. "An efficient fluid-solid coupled finite element scheme for weapon fragmentation simulations". *Eng. Fracture Mech.*, 77, 549-564 (2010).

A Higher Resolution MOOD Framework Using a Flow Oriented Gradient Reconstruction Applied to Water-Oil Displacements in Anisotropic and Heterogeneous Petroleum Reservoirs

Márcio Souza^{*}, Fernando Contreras^{**}, Paulo Lyra^{***}, Darlan Carvalho^{****}

^{*}Federal University of Paraíba, ^{**}Federal University of Pernambuco, ^{***}Federal University of Pernambuco, ^{****}Federal University of Pernambuco

ABSTRACT

First-order upwind method is routinely used to discretize the advective terms of general transport problems due to its robustness and reliability. Nevertheless, in the presence of steep gradients, its excessive numerical diffusion spuriously spreads out the shock representation. To remedy this, numerous higher-resolution strategies, based on the limited gradient reconstruction, have been proposed in literature [1]. In the finite volume approach, second-order of accuracy in space can be achieved by means of the suitable limited linear reconstruction with a MUSCL-type strategy [2]. This procedure, in general, captures discontinuities in the solution without producing spurious oscillations. However, due to its intrinsic 1-D nature, it is difficult to obtain monotone and accurate solutions for multidimensional flows. In this paper, a segregated mathematical model composed by a pressure equation and a saturation equation is approximated by a full finite volume formulation [1]. The saturation equation is explicitly approximated by a higher-resolution formulation using the Multidimensional Optimal Order Detection (MOOD) framework. This strategy, originally proposed in [2] and adapted to reservoir simulation in [1], produces monotone solutions by detecting, a-posteriori, the optimal order of each control volume (CV) in a multidimensional way. In our proposal, an alternative properly biased reconstruction strategy is adopted. In the gradient reconstruction step, we consider the local orientation of the flow to choose, only those neighbors CV classified as upwind regarding to the one evaluated. Thus, we achieve a flow oriented-based reconstruction instead of using that traditional non-biased used in [1] or even the conventional least-squares technique [2], which consider either full or face-based vicinity for building the reconstruction support. The pressure equation is implicitly solved by a robust Multi-Point Flux Approximation Method with a Diamond support (MPFA-D). This formulation used in [1] in reservoir simulation context is capable to produce convergent solutions, even for problems with non-diagonal permeability tensors and distorted meshes. The solution of some relevant benchmark problems with our formulation shows the enhancement of the accuracy and some reduction of grid orientation effects in the numerical solutions. References [1]. Contreras, F.; Souza, M.; Lyra, P.; Carvalho, D. K. A MPFA Method Using Harmonic Points Coupled to a Multidimensional Optimal Order Detection Method (MOOD) for the Simulation of Oil-Water Displacements in Petroleum Reservoirs. In XXXVII CILAMCE. 2016. Brasília. Brasil. [2]. Clain, S.; Diot, S.; Loubere, R. A. High-Order Finite Volume Method for Systems of Conservation Laws. Multi-Dimensional Optimal Order Detection (MOOD). Journal Comput. Physics. 2011; 230: 4028-4050.

3D Stochastic Bicontinuous Composites: Determination of Effective Elastic Properties through Computational Homogenization

Celal Soyarslan^{*}, Swantje Bargmann^{**}, Marc Pradas^{***}

^{*}Chair of Solid Mechanics, School of Mechanical Engineering and Safety Engineering, University of Wuppertal, Germany, ^{**}Chair of Solid Mechanics, School of Mechanical Engineering and Safety Engineering, University of Wuppertal, Germany, ^{***}School of Mathematics and Statistics, The Open University, Milton Keynes, United Kingdom

ABSTRACT

Considering linear and infinitesimal elasticity and using computational homogenization along with finite element method, we study effective elastic properties of 3D bicontinuous random composites. In generation of the microstructures, a leveled-wave model based on the work of J. W. Cahn [1] is used. The influence of box size, phase contrast, relative volume fraction of phases and applied boundary conditions on computed apparent elastic moduli is investigated. Only with periodic boundary conditions the effective properties can be determined at reasonable box sizes and up to a numerical error. For this minimum box size allowing the effective property determination, also referred to as the representative volume element (RVE) size, we scrutinize macroscopic response of gold-epoxy nanocomposites of various phase volume fractions. For all computations, kinematically uniform boundary conditions are found to be overestimating. This is especially the case for increasing phase contrast and volume fraction bias towards the weaker phase. Still, for the observed phase volume fraction interval, the apparent moduli computed using kinematically uniform boundary conditions fall much below the upper bounds of Hashin-Strikhman, three-point Beran-Molyneux and Milton-Phan-Tien analytical bounds. Thus, computational homogenization devising periodic boundary conditions is justified to be the only tool in efficient and accurate determination of the effective properties of 3D bicontinuous random composites with high contrast and volume fraction bias towards the weaker phase. References 1. J.W. Cahn. Phase separation by spinodal decomposition in isotropic systems. *The Journal of Chemical Physics*, 42(1):93-99, 1965. 2. C. Soyarslan, S. Bargmann, M. Pradas, and J. Weissmüller. 3D stochastic bicontinuous microstructures: generation, topology and elasticity. Submitted, 2017. 3. C. Soyarslan, M. Pradas, and S. Bargmann. Determination of Effective Elastic Properties of 3-D Bicontinuous Random Composites through Computational Homogenization: Influence of Phase Contrast and Applied Boundary Conditions. Submitted, 2017.

Canonical Generalization of Lyapunov's Second Method and General Procedure of Utilization of Lyapunov Functions

Myroslav Sparavalo*

*NYC Transit Authority

ABSTRACT

The objective of the research is to develop a general method of constructing Lyapunov functions for non-linear non-autonomous differential inclusions described by ordinary differential equations with parameters. The goal has been attained through the following ideas and tools. First, three-point Poincaré strategy of the investigation of differential equations and manifolds has been used. Second, the geometric-topological structure of the non-linear non-autonomous parametric differential inclusions has been presented and analyzed in the framework of hierarchical fiber bundles. Third, a special canonizing transformation of the differential inclusions that allows to present them in special canonical form, for which certain standard forms of Lyapunov functions exist, has been found. The conditions establishing the relation between the local asymptotical stability of two corresponding particular integral curves of a given differential inclusion in its initial and canonical forms are ascertained. The global asymptotical stability of the entire free dynamical systems as some restrictions of a given parametric differential inclusion and the whole latter one per se has been investigated in terms of the classificational stability of the typical fiber of the meta-bundle. The general procedure of the utilization of Lyapunov functions is applied to the problem of the wide-sense robust control design for van der Pol nonlinear dynamics. References 1. Sparavalo, M. K. The Lyapunov Concept of Stability from the Standpoint of Poincaré Approach: General Procedure of Utilization of Lyapunov Functions for Nonlinear Non-Autonomous Parametric Differential Inclusions, 2014, arXiv:1403.5761, [cs.SY]. 2. Sparavalo, M. K. Lyapunov Functions in Nonlinear Unsteady Dynamics and Control: Poincaré's Approach from Metaphysical Theory to Down-to-Earth Practice, 1st Edition, NY, 2016, ISBN 9780692694244. 3. Sparavalo, M. K. Wide-Sense Robust and Stable in the Large Terminal Control for Van Der Pol Dynamics: Poincaré's-Approach-Based Backstepping Method, Procedia Engineering, Vol. 199, 2017, pp. 850-856.

A Comparison of NMAP and CTH for Modeling Projectile Impact on Steel Plates

Paul Sparks*, Jesse Sherburn**, William Heard***, David Roman-Castro****

*U.S. Army ERDC, **U.S. Army ERDC, ***U.S. Army ERDC, ****U.S. Army ERDC

ABSTRACT

Ballistic impact modeling of steel plates is of extreme importance to the military community. Research efforts have been devoted to developing analytical and numerical models to analyze and predict the outcome of ballistic impact problems [1, 2]. Dey et al. [1] carefully characterized the effect of different projectiles impacting steel targets and studying residual projectile velocity and the ballistic limit. The experimental test conducted in [1] provided the material constants necessary to model the failure criterion of Johnson and Cook [3]. The data from Dey can be used to calibrate and validate the numerical models. In this study, in-house experimental data produced from different projectiles impacting steel plates with velocities in the ordnance regime will be compared to two different numerical methods. Nonlinear Meshfree Analysis Program (NMAP) is a meshless based code which employs reproducing kernel particle methods (RKPM) in a semi-Lagrangian framework and CTH is an Eulerian shock physics based wave code. Both numerical codes are advantageous for modeling impact and penetration/perforation problems that predict deformation and material fragmentation. The effectiveness of each numerical codes is demonstrated by modeling and validating analogous impact experiments of steel plates to demonstrate the physical mechanisms in the perforation process. A discussion of the inherent strengths and weakness of each of the models will be discussed. [1] Dey, S., Børvik, T., Hopperstad, O., Leinum, J., Langseth, M. 2004. The effect of target strength on the perforation of steel plates using three different projectile nose shapes. *International Journal of Impact Engineering*. 30(8–9):1005–1038. Eighth International Symposium on Plasticity and Impact Mechanics (IMPLAST 2003). [2] Yreux, E., and Chen, J. S. 2016. A quasi-linear reproducing kernel particle method. *Int. J. Numer. Methods Eng.*, 109(7), 1045–1064. [3] Johnson, G. R., Cook, W.H. 1983. A constitutive model and data for metals subjected to large strains, high strain rates and high temperatures. *Proceedings of the Seventh International Symposium on Ballistics*, Hague. p. 541–7.

The Relaxation Properties of Poroelastic Scaffolds for Stem Cell Differentiation

Alexander Spector^{*}, Rahul Yerrabelli^{**}, Daniel Yuan^{***}

^{*}Johns Hopkins University, ^{**}Johns Hopkins University, ^{***}Johns Hopkins University

ABSTRACT

The mechanical properties of the extracellular matrix are significant to its interaction with the stem cells inside, affecting the processes of stem cell differentiation. Scaffolds mimic the structure and mechanical properties of the extracellular matrix and provide differentiation of the seeded stem cells similar to that in the native tissue. Stem cell differentiation is a dynamic process occurring on many time scales, a reflection of different biological events and signaling pathways involved. Thus, the time-dependent properties of the extracellular matrix (and scaffolds) must have a significant effect on stem cell differentiation, and it was recently confirmed by the experiments with stem cells in scaffolds with tunable stress relaxation [1] and strain creep parameters [2]. The question of the mechanism behind the relaxation/creep properties of the scaffolds and its relation to the scaffold structure is of key importance. Typically, the scaffolds are biphasic, including solid and fluid components. We consider porous-fibrous scaffolds and develop their poroelastic model that relates the relaxation properties to the diffusion of the fluid component through the scaffold. The problem reduces to the Bessel equation in terms of the Laplace transform of the displacement of the scaffold solid component. The model parameters are the Young's moduli in the fiber direction and perpendicular plane, corresponding Poisson's ratios, and the gel diffusion time that characterizes the scaffold fluid component. These parameters are estimated by fitting the theoretical time course of the applied force relaxing after the ramp loading to the experimental data on the relaxation of cylindrical specimens [3]. Using the estimated parameters, we compute the local mechanical factors sensed by the stem cell inside, including the stresses, pressure, and fluid velocity. The scaffold relaxation has a spectrum of times proportional to the gel diffusion time and satisfying a characteristic equation. The developed approach can be used for the effective design of scaffolds applied in stem cell therapies. [1] Chaudhuri et al. Hydrogels with tunable stress relaxation regulate stem cell fate and activity. *Nature Mats.*, 2015, 15, 326-334. [2] Cameron A.R. et al. The influence of substrate creep on mesenchymal stem cell behavior and phenotype. *Biomaterials*, 2011, 32, 5979-5993. [3] Cook, C. A. et al. Characterization of a novel bioreactor system for 3D cellular mechanobiology studies. *Botech&Bioeng.* 2016, 13, 1825–1837.

Isogeometric Analysis on Meshes with Polar Singularities: B-Spline Construction

Hendrik Speleers^{*}, Deepesh Toshniwal^{**}, Rene Hiemstra^{***}, Thomas Hughes^{****}

^{*}University of Rome "Tor Vergata", ^{**}University of Texas at Austin, ^{***}University of Texas at Austin, ^{****}University of Texas at Austin

ABSTRACT

One of the needs of CAD representations of arbitrary genus surfaces with finite number of polynomial patches is the introduction of holes surrounded by periodic configurations. Such holes can then be filled by means of polar spline surfaces, where the basic idea is to use periodic spline patches with one collapsed boundary invoking a polar singularity. Applications of this approach include subdivision surfaces, free-shape modeling, and, as we demonstrate here, isogeometric analysis. In order to obtain polar spline surfaces with specified continuity, the admissible set of control point configurations shrinks. In particular, imposition of C^k continuity constrains the inner k -rings of control points surrounding the singular point to a limited number of configurations. In hole-filling applications, the outer k -rings of control points are used to match the cross-derivative information at the hole boundary. In this talk, keeping in mind applications to design as well as analysis, we focus on C^k polar spline parametric patches with arbitrary degree and arbitrary number of elements at the hole boundary. We present a simple, geometric construction of B-spline basis functions over such polar parametric domains possessing interesting properties as non-negativity and partition of unity. In addition, the constructed spline spaces show optimal approximation behavior, even at the polar singular point [1]. [1] D. Toshniwal, H. Speleers, R.R. Hiemstra, and T.J.R. Hughes. "Multi-degree smooth polar splines: A framework for geometric modeling and isogeometric analysis", Comput. Methods Appl. Mech. Engrg. 316, 1005-1061, 2017.

Predicting Mechanical Properties of Epoxy from Molecular Models

Simcha Srebnik^{*}, Irena Yungerman^{**}

^{*}Technion - Israel Institute of Technology, ^{**}Technion - Israel Institute of Technology

ABSTRACT

Epoxy resins are the most commonly used adhesives in industry due to their versatility, low cost, low toxicity, low shrinkage, high strength, resistance to moisture, and effective electrical resistance. Diverse mechanical properties can be obtained depending on the chemical structure of the curing agent and the conditions of the curing process. An outstanding goal is the ability to predict material properties and failure under stress based on the underlying chemistry of its constituents. In principle, all-atom simulations can be used to predict material properties without the need for empirical parameters. In practice, however, such simulations of epoxy resins that can be used to cheaply and systematically investigate chemistry-property relationship are only beginning to be realized due to the complexity of the system and the presence of unknown variables. Computational experiments are further complicated as the cross-linked system is nonergodic and sample dimensions are generally small, and therefore different realizations of the crosslinking reaction must be modeled to obtain sufficient statistical measurements. The small samples tend to show a wide scatter of properties, that also depend on the rate of deformation, whether thermal or mechanical. Moreover, the differences in spatial and temporal scales between mechanical experiments and molecular computations are vast and make it difficult to directly compare between the two. Coarse-grained simulations serve to bridge the gap between the length and temporal scales of the atomistic simulations with those of experiments, while retaining a non-constitutive model. Using bottom-up approach, we develop coarse-grained models parametrized against all-atom simulations for model epoxy and hardener, and analyze the behavior of the cross linked epoxy matrix under deformation. Failure at the interface of single walled carbon nanotube is examined for different nanotube diameters in an effort to understand the effect of curvature on adhesion at the interface.

VMS-based Error Estimation and Adaptivity in the Joint Physical and Stochastic Space

Vignesh Srinivasaragavan^{*}, Jason Li^{**}, Assad Oberai^{***}, Eric Phipps^{****}, Eric Cyr^{*****}, Onkar Sahni^{*****}

^{*}Rensselaer Polytechnic Institute, ^{**}Rensselaer Polytechnic Institute, ^{***}University of Southern California, ^{****}Sandia National Laboratories, ^{*****}Sandia National Laboratories, ^{*****}Rensselaer Polytechnic Institute

ABSTRACT

This presentation will focus on the formulation and application of an adaptive approach for stochastic PDEs with uncertain input data based on the variational multiscale (VMS) method. In this approach, we employ finite elements in the physical domain and spectral approximation (based on generalized polynomial chaos) in the stochastic domain. The VMS method allows in computing an accurate solution in a coarse space while accounting for the missing/fine scales through a model term. This model term is algebraically approximated within each element using the strong-form residual and a stochastic stabilization parameter, which is used in the variational statement for computing the numerical solution. Similarly, a model term is derived to estimate the error in the numerical solution in a local/element-wise fashion, where the model term for the local error is approximated using the same stabilization parameter used in computing the numerical solution, making error estimation computationally inexpensive. The procedure is designed to provide local and global error estimates and to drive adaptivity in the joint physical and stochastic space. By adaptivity in the joint space, we imply resolution control in the spatial approximation or the mesh (e.g., a graded or non-uniform unstructured mesh) together with the spectral approximation (e.g., a spatially varying spectral order over the mesh). We demonstrate the effectiveness of our approach on multiple example cases including transport problems spanning both advective and diffusive regimes in the stochastic domain as well as non-trivial geometries or physical domains.

Ductile Fracture of Multiphase Steel Sheets under Bending

Ankit Srivastava*, Yu Liu**

*Texas A & M University, College Station, TX 77843, **Texas A & M University, College Station, TX 77843

ABSTRACT

The fracture characteristics of steel sheets under bending mode are governed, at least in part, by the microstructural features such as the size, shape, distribution and properties of inclusions. Experiments suggest that the bend fracture of steel sheets of interest are determined by the size and location of large inclusions or clustered small inclusions (stringer of inclusions). The properties of inclusions have also been found to affect the damage nucleation process. Hence our aim is to analyze the collaborative effects of microstructural features on ductile fracture of steel sheets under bending. Here, finite element, finite deformation calculations are carried out using a constitutive framework for progressively cavitating ductile solids. In the finite element calculations, the individual phases of the multiphase steel together with the inclusions are discretely modeled. The extent to which the microstructural length scale originating from the multiphase microstructure and the length scale originating from the distribution of inclusions affect the ductile fracture of sheets under bending will be discussed.

An Implicit, Conservative, Hybrid Particle-kinetic-ion Fluid-electron Algorithm

Adam Stanier^{*}, Luis Chacon^{**}, Guangye Chen^{***}

^{*}Los Alamos National Laboratory, ^{**}Los Alamos National Laboratory, ^{***}Los Alamos National Laboratory

ABSTRACT

Bridging the inherent multi-scale nature of many important problems in plasma physics requires a combination of model reduction and algorithmic innovation. The hybrid model with full-orbit kinetic ions and fluid electrons is a promising approach to describe a wide range of space and laboratory plasmas. In particular, it has been recently demonstrated that the hybrid model is the minimum sufficient model to correctly capture the rate and global evolution of a reconnecting system for arbitrary guide magnetic field [1,2,3], with important consequences for space weather modeling. Here we focus on the quasi-neutral hybrid model using macro-particles to model the kinetic ion species, which avoids the need to solve for the distribution function in 6D (3D-3V) phase space, but is subject to discrete particle noise that scales as \sqrt{N} for the number of macro-particles N . The majority of existing algorithms employ explicit time-stepping, and much of the development has focused on the accuracy and stability of the time integration schemes. Key unresolved issues with these approaches involve the numerical instability of cold ion beams moving through the spatial grid due to aliasing errors [4], and the quadratic CFL condition ($dt \sim dx^2$) associated with fast dispersive Whistler waves. Recent work [5,6] has explored the use of fully implicit methods to step over such timescales in a stable manner, but have not addressed the topic of momentum or energy conservation. Here we present a novel fully implicit hybrid algorithm that features discrete mass, momentum and energy conservation, as well as discrete preservation of the solenoidal condition. The algorithm features sub-cycling and orbit averaging of the ions, with cell-centred finite differences and implicit midpoint time advance. To reduce numerical noise, the algorithm allows arbitrary-order shape functions and conservative smoothing on the gather and scatter operations. We discuss the implementation of the algorithm into a Jacobian-Free Newton Krylov solver framework, and then verify it for a number of test problems. These demonstrate the correctness of our implementation, the unique conservation properties, and its favorable stability properties. References: [1] A. Stanier et al., Phys. Plasmas 24, 022124 (2017). [2] J. Ng et al., Phys. Plasmas 22, 112104 (2015). [3] A. Stanier et al., Phys. Rev. Lett. 115, 175004 (2015). [4] P. W. Rambo, Journal of Computational Physics, 118, 152-158 (1995). [5] B. Sturdevant et al., Journal of Computational Physics, 316, 519 (2016). [6] J. Cheng et al., Journal of Computational Physics, 245, 364 (2013).

Parallel and Dirty CAD Tolerant Tetrahedral Mesh Generation with Feature Capture

Matt Staten^{*}, David Noble^{**}, Corey McBride^{***}, C. Riley Wilson^{****}, Manoj Bhardwaj^{*****}

^{*}Sandia National Laboratories, ^{**}Sandia National Laboratories, ^{***}ELEMENTAL TECHNOLOGIES INC, ^{****}Sandia National Laboratories, ^{*****}Sandia National Laboratories

ABSTRACT

With well documented and robust Delaunay and advancing-front algorithms, tetrahedral mesh generation is often considered a solved problem. However, automatic tetrahedral mesh generation on complex and dirty CAD assemblies on HPC systems remains an open problem due to the presence of small geometric features and imperfect geometry. We present the latest status on an effort to implement a massively parallel tet mesher for CAD assemblies using an overlay grid technique. Our approach extends to 3D CAD the 2D CISAMR [1] used successfully for material interface construction. We start by overlaying the CAD assembly with a cartesian hexahedral grid. Intersection points are computed where CAD vertices, curves, and surfaces intersect the overlay grid. Nodes in the overlay grid are snapped to closest intersection points, morphing the cartesian overlay. No cells are cut by geometry intersections. Finally, the hexahedral overlay grid cells are converted into tetrahedral elements following a Body Centered Cubic (BCC) structure [2]. By postponing the conversion of the overlay grid to tetrahedrons until after the grid is morphed, tetrahedral topology is chosen to maximize tetrahedral quality by considering the snapped node locations, eliminating need for post-processing smoothing and swapping. This approach to tetrahedral mesh generation implicitly captures CAD curves and vertices at the resolution of the overlay grid, while ignoring features smaller than the overlay grid resolution. The cell center node in the BCC pattern doubles the degrees of freedom for a given cell size. However, we choose the BCC pattern for the following reasons: First, it offers better quality tetrahedron than conversion of each cell into six tetrahedron; second, it allows for embarrassingly parallel conversion of the cells into tetrahedron; and third, it allows for better CAD approximation to non-planar CAD features by projecting the center node to the CAD. Future plans include replacing the hexahedral overlay grid with a balanced octree allowing for adaptive resolution of geometric features. [1] Soheil Soghrati, Anand Nagarajan, and Bowen Liang, Conforming to Interface Structured Adaptive Mesh Refinement: New Technique for the Automated Modeling of Materials With Complex Microstructures, Finite Elements in Analysis and Design, 125 (2017) 24-40. [2] Jun Wang, Zeyun Yu, Adaptive and Quality Tetrahedral Mesh Generation, Proceedings 19th International Meshing Roundtable, 2010. ^{*}Sandia National Laboratories is a multi-program laboratory managed and operated by Sandia Corporation, a wholly owned subsidiary of Lockheed Martin Corporation, for the U.S. Department of Energy's National Nuclear Security Administration under contract DE-AC04-94AL85000. SAND2018-0293 A

Computational Homogenization for Embossing of Thin Fibrous Structures based on FEM-FFT Coupling

Sarah Staub^{*}, Julia Orlik^{**}, Heiko Andrä^{***}

^{*}Fraunhofer Institute for Industrial Mathematics, ^{**}Fraunhofer Institute for Industrial Mathematics, ^{***}Fraunhofer Institute for Industrial Mathematics

ABSTRACT

Structured fiber networks play an important role in many different applications in the field of filter and hygiene media. Examples are different types of wipes as e.g. baby wipes or structured wipes for the trapping of dust. Another important class of embossed fiber networks are pleated filters. The current work focuses on the simulation of the structuring process of thin porous media. As the stamps applied for the embossing are large compared to the fibers of the network, a two-scale framework is elaborated. The structure mechanical equations on both scales are solved concurrently within a suitable homogenization framework similar to FE². The macroscopic scale is treated as heterogeneous thin plate, similar to [1], within a finite element method (FEM). In each integration point the membrane deformation and the deflection is computed and applied to formulate the microscopic boundary condition on a representative volume element (RVE). Within the nested solution scheme, the homogenized microscopic quantities yield the macroscopic effective properties and thus substitute the macroscopic constitutive behavior. At the microscale, the fibers and the bonds (melt points or resin) are captured in highly resolved voxelized RVEs, see [2] for examples. Due to the high porosity and the complexity of these structures a FEM formulation is not suitable at the microscale. Instead, a Fast-Fourier transform (FFT) based approach for the solution of the Lippmann-Schwinger (LS) integral equations in elasticity is applied. This approach allows the fast and effective solution of large and complex microstructures for an infinite material contrast. In contrast to LS-FFT methods in elasticity, which are based on second order elasticity operators with constant coefficients, here a fourth order bi-harmonic operator is considered instead. The novelty of the presented approach is the the scale coupling via the Green's function to this bi-harmonic operator. This allows the computation of the effective bending and torsion coefficients of the macroscopic plate, see [3]. References [1] E.W.C. Coenen, V.G. Kouznetsova and M.G.D. Geers "Computational homogenization for heterogeneous thin sheets", Int. J. Num. Meth. Eng. 83, 1180-1205, 2010. [2] S. Staub, H. Andrä and M. Kabel "Fast FFT based solver for rate-dependent deformations of composites and nonwovens", Int. J. Solids Struct., in press. [3] M. Hauck, A. Klar and J. Orlik "Design optimization in periodic structural plates under the constraint of anisotropy", Z. Angew. Math. Mech. 97, 1120-1235, 2017.

Bone Loss in Space Travellers: Systematic Review and Meta-analysis

Mariya Stavnichuk^{*}, Corlett Tatsuya^{**}, Svetlana Komarova^{***}, Nicholas Mikolajewicz^{Shriners Hospital for Children; Faculty of Dentistry, McGill University}^{****}, Martin Morris^{*****}

^{*}Shriners Hospital for Children, ^{**}Shriners Hospital for Children, ^{***}Shriners Hospital for Children; Faculty of Dentistry, McGill University, ^{****}Shriners Hospital for Children; Faculty of Dentistry, McGill University, ^{*****}Schulich Library of Science and Engineering, McGill University

ABSTRACT

Bone loss in astronauts is identified as a major challenge for long-duration space exploration. Understanding underlying mechanisms responsible for bone density changes observed in astronauts is imperative for a design of successful countermeasures. With the goal to examine the spatial and temporal aspects of microgravity-induced bone loss, the electronic databases were searched for studies presenting numerical values for measurements of bone health in astronauts. We identified 30 studies containing bone density estimates for 138 of 553 astronauts, obtained using X-ray radiography, single-energy photon and dual-energy X-ray absorptiometry or quantitative computed tomography before and immediately after the space flights that lasted from 4 to 252 days. Sample size-weighted changes in bone density compared to pre-flight in the region of head, shoulders and cervical vertebrae were +2.2% (95% confidence interval: 1.1, 3.3; n = 32 astronauts); in the region of forearms, thoracic vertebrae and ribs: -2.0% (-3.0, -0.9; n = 72); in the region of lumbar vertebrae and pelvic bones: -5.8% (-7.2, -4.5; n = 66); and in the region of lower extremities: -3.9% (-5.7, -2.2; n = 110). Bone density decreased with an increase in flight duration, at the rate of $-0.84 \pm 0.37\%$ per month. Changes in serum or urine biochemical markers of bone resorption and formation during space flight were available for 33 astronauts. Bone resorption markers consistently increased within the first 40 days and thereafter stabilized at 100-140% above baseline. Bone formation markers were more variable than bone resorption markers, however in general they remained unchanged or decreased during the first 30 days of the flight, and slowly increased thereafter. Comparison of the difference between bone formation and resorption markers to the changes in bone density demonstrated a notable disconnect in the time-dependent bone changes predicted by the markers, and the observed changes in bone density. This disconnect can be potentially explained by i) microgravity-specific effects uncoupling bone formation markers from bone gain; ii) temporal delay between bone formation markers and actual bone deposition, or iii) anatomical site differences in the effect of microgravity, with bone markers collecting information from the whole skeleton, while bone loss is observed only in lower half of the body.

SHAPE OPTIMIZATION OF UNIT CELLS FOR VIBRATION ISOLATION USING AUXETIC MATERIALS

Panayiotis I. Koutsianitis Georgios A. Drosopoulos Georgios K. Tairidis and
Georgios E. Stavroulakis

* Technical University of Crete
School of Production Engineering and Management
Institute of Computational Mechanics and Optimization
Chania, Crete, Greece
panoskout@gmail.com, Tairidis@gmail.com, gestavr@dpem.tuc.gr ;
<http://www.comeco.tuc.gr>

+ University of KwaZulu-Natal
Discipline of Civil Engineering
Structural Engineering & Computational Mechanics Group
Durban, South Africa
DrosopoulosG@ukzn.ac.za ; <http://secm.ukzn.ac.za>

Key words: Auxetic material, Band gaps, Vibration

Abstract. *In the present investigation, a band-gap region, i.e. the isolation of certain frequencies, through the optimization of the shape of the unit cells of a lattice is considered. In general, a lattice is considered as an assembly of classical structural elements, such as beams, plates, etc. Each cell of the lattice is discretized using the finite element method, and more specifically with plane stress elements. The homogenized behavior of the system is extracted from the detailed investigation of the representative volume cell. In the present investigation, a lattice with a microstructure is considered. The shape of the unit cells can be triangular, quadratic, hexagonal, etc. The shape and the microstructure of the lattice can be optimized in order to achieve isolation of the desired frequencies. This can be done using either the trial-and-error method or global optimization methods, such as genetic algorithms. Auxetic materials can be useful in this direction.*

1 INTRODUCTION

Isolation of structures against vibrations which are caused by external loadings is a typical problem in engineering. There are a lot of techniques which are proposed in literature for this purpose. The design of a microstructure which consist of a lattice as an assembly of classical elements, such as beams and plates, is quite common. The overall mechanical behavior is determined from a representative unit cell and suitable loadings, using homogenization techniques. For dynamic loadings various directions of wave propagation and all frequencies of interest must be taken into account. The unit cells can be of several different shapes, e.g. square, triangular, hexagonal honeycomb etc. One can say that the mechanical behavior of a unit cell is determined by its shape, i.e. by its topology as described in [1]. In fact, the design parameters of the unit cell can

be tuned in order to find the band-gap regions, if any. As for the loading, a wave vector is applied at a particular cell, at the two directions x and y , thus it is a two-dimensional problem. This vector takes into account the periodic boundary conditions, which in turn are defined using the Floquet theorem [2].

The propagation of the waves can be considered according to the work of Brillouin and Kittel [3,4], where the motion can present pass and stop band gaps, that is specific frequencies where the wave is able or unable to propagate through the lattice. The wave propagation in two-dimensional periodic lattices is described in detail in [1,5]. More specifically, the Floquet-Bloch principles are considered in order to design lattices within a desired band. The objective is the study of wave propagation, i.e. bandgaps and wave directionality, in three regular honeycombs; hexagonal, square and triangular and in the semiregular Kagomé lattice. The results provide the dispersion curves for the different 2-D topologies of the studied unit cells.

Auxetics are mechanical metamaterials with negative Poisson ratio. Among their interesting properties is the enhanced vibration suppression [6]. An auxetic cell with star-shaped form is used here. A band gap analysis of star-shaped honeycombs with varied Poisson's ratio is studied in [7]. More specifically, star-shaped honeycombs with auxetic properties are analyzed in terms of their band gap properties, along with their equivalent mechanical behavior. The purpose of the selection of a material with auxetic behavior lies to its ability to provide enhanced Young's modulus of star-shaped structures. Moreover, it is known that band gap properties are observed not only in classical materials, but in ones with negative Poisson's ratio as well. In fact, negative values of this ratio can be an important factor in the design. Thus, the work presented in [7] can be used as a guide for the optimal design of such structures, with respect to band gap regions.

2 BLOCH THEOR

In general, the whole lattice can be obtained from the correlation of the unit cell with the basis vectors ε_i . However, the first step of the study should be the suitable definition of a unit cell. The lattice points r_j of a unit cell are in fact a small subset of the nodes of its finite element model. The displacement $q(r_j)$ of the lattice points of the unit cell for the case of plane waves is given as:

$$q(r_j) = q_j e^{(i\omega t - kr_j)} \quad (1)$$

where q_j is the amplitude, ω is frequency and k is the wave vector. The parameters n_1 and n_2 can identify any other cell which can be obtained by n translations across the e directions with respect to the unit cell of reference.

According to the Bloch's theorem, the displacement at the j^{th} point in any cell can be identified by a unique pair of integers n_1 and n_2 as:

$$q = q(r_j) e^{k(r-r_j)} = q(r_j) e^{(k_1 n_1 + k_2 n_2)} \quad (2)$$

where:

$$k_1 = k e_1 = \delta_1 + i\varepsilon_1 \quad (3)$$

$$k_2 = k e_2 = \delta_2 + i\varepsilon_2 \quad (4)$$

In the above equation, k_1 and k_2 denote the components of wave vector k which is propagated and at the same time dissipated along the vectors e_1 and e_2 . The real part δ denotes the attenuation constant, i.e. it is a measurement of the propagation of the wave among cells, while the imaginary part ε represents the change of the phase across the unit cell and it is called phase constant. Practically, this means that if a wave is propagating without any attenuation, then the real part δ is zero and thus, the wave vector can be given by:

$$k_1 = i\varepsilon_1 \quad (5)$$

$$k_2 = i\varepsilon_2 \quad (6)$$

The possible extraction of band gaps is based on the assumption of wave vectors which are following the Brillouin zone, i.e. vectors with edges restricted to the irreducible part of this zone^[2] as seen in Figure 1 below.

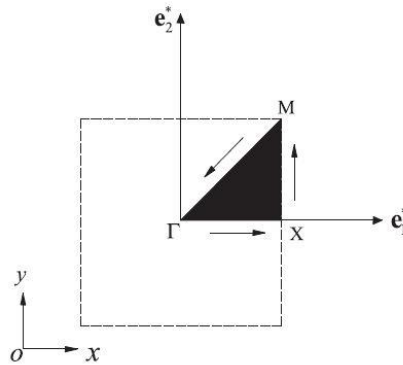


Figure 1: The first Brillouin zone and the irreducible Brillouin zone ($\Gamma - X - M$)

In general, periodic structures are systems with identical segments, coupled to their neighboring. More specifically, uniform 2-D structures can be considered as a special case of periodic structures which are homogeneous in x and y directions. These structures are, in fact, an assembly of rectangular segments with length to the x and y directions which equals to L_x and L_y respectively.

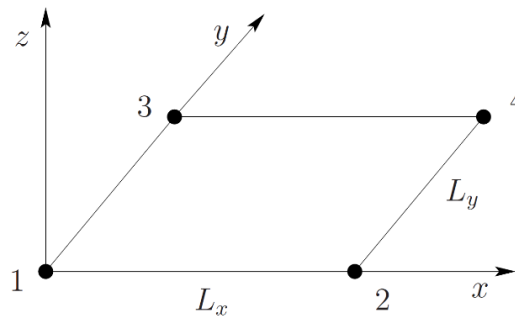


Figure 2: A rectangular segment with a 4-noded rectangular finite element

As seen in Figure 2, the degrees of freedom q of the segment of reference can be considered with respect to the nodal degrees of freedom as:

$$q = [q_1^T \ q_2^T \ q_3^T \ q_4^T] \quad (7)$$

where q_j are the nodal degrees of freedom of the nodes of the j^{th} corner of the segment and T denotes the transpose.

The equation of motion of the element of reference is given as:

$$(-\omega^2 M + i\omega C + K)q = f \quad (8)$$

where M, C and K are the mass, damping and stiffness matrices respectively, ω is the natural frequency, f is the loading vector and i the imaginary number. Note that nodal forces dissipate the wave motion between the neighboring elements, thus the external loading vector is not zero, even though free wave motion is considered. The 2-D free wave propagates along the structure and thus it can be considered to be a Bloch wave [8]. Bloch's theorem is also called Floquet's theorem since it represents a generalisation of the Floquet's theorem for 1-D problems [9].

The propagation of the wave can then be obtained from the so-called propagation constants $\mu_x = \kappa_x L_x$ and $\mu_y = \kappa_y L_y$, which in turn, provide the relation among the periodic displacements q on the sides of the periodic element as:

$$q_2 = \lambda_x q_1, \quad q_3 = \lambda_y q_1, \quad q_4 = \lambda_x \lambda_y q_1 \quad (9)$$

where:

$$\lambda_x = e^{-i\mu_x}, \quad \lambda_y = e^{-i\mu_y} \quad (10)$$

As a result, the nodal degrees of freedom can be rewritten as:

$$q = \Lambda_R q_1 \quad (11)$$

where:

$$\Lambda_R = [I \ \lambda_x I \ \lambda_y I \ \lambda_x \lambda_y I] \quad (12)$$

In the free response case, i.e. when no external loading is considered, a possible equilibrium at node 1 leads to the restriction that the nodal forces of every element which is connected to node 1 is equal to zero. Thus, we have:

$$\Lambda_L f = 0 \quad (13)$$

where:

$$\Lambda_L = [I \ \lambda_x^{-1} I \ \lambda_y^{-1} I \ (\lambda_x \lambda_y)^{-1} I] \quad (14)$$

By substituting the equation (11) in the equation (8) and multiplying by Λ_L , the equation of the free wave motion takes the form:

$$\left(-\omega^2 \bar{M}(\mu_x, \mu_y) + i\omega \bar{C}(\mu_x, \mu_y) + \bar{K}(\mu_x, \mu_y) \right) q = f \quad (15)$$

4 NUMERICAL RESULTS

In the present investigation, a square shaped unit cell was considered in order to study the possible appearance of band gaps. For this purpose, several cases were designed and studied. First, a simple unit cell without core was considered, corresponding to a simple homogeneous and isotropic material. A set of designs with an internal core, either with or without auxetic behavior, were studied in order to investigate whether the choice of the material influences the behavior of the unit cell in the dispersion curve, i.e. to detect possible appearance of band gaps. In the case of the auxetic material a further investigation was carried out, and more specifically, the thickness of the sides which connect the auxetic materials with their neighboring ones were changed, in order to test their behavior. The properties of the material which were considered are given in the following table:

	Material 1	Material 2
Young modulus (Pa)	$1 \cdot 10^9$	$100 \cdot 10^9$
Density (kg/m^3)	2000	7000
Poisson ratio	0.3	0.4

Table 1: Material properties

4.1 Study of unit cells with traditional materials

In the first investigation, a square lattice without core was considered. The dispersion curve for this case is shown in Figure 4 below. It is clearly observed that no band gap appears considering only a simple square-shaped unit cell.

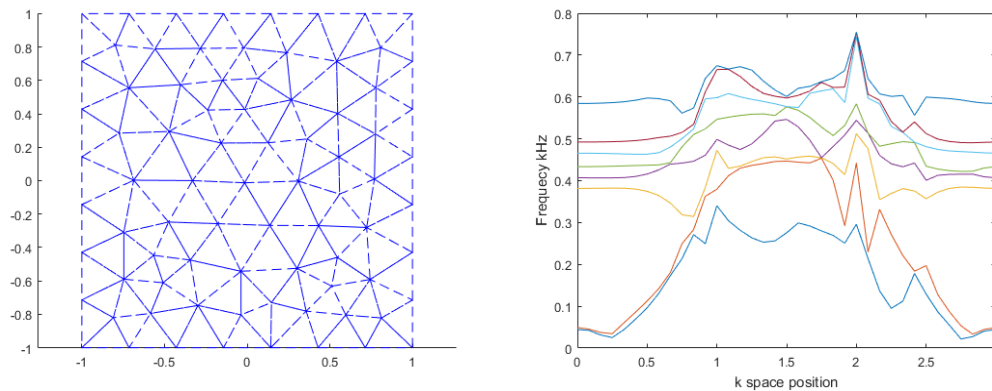


Figure 4: Square shape without core and its dispersion curve

Consequently, the case of a unit cell with an embedded stiff core was considered. This core is denoted with red color in Figure 5. In this case one can see that band gaps appear at some frequency areas, that is between the 2nd and the 3rd eigen frequencies.

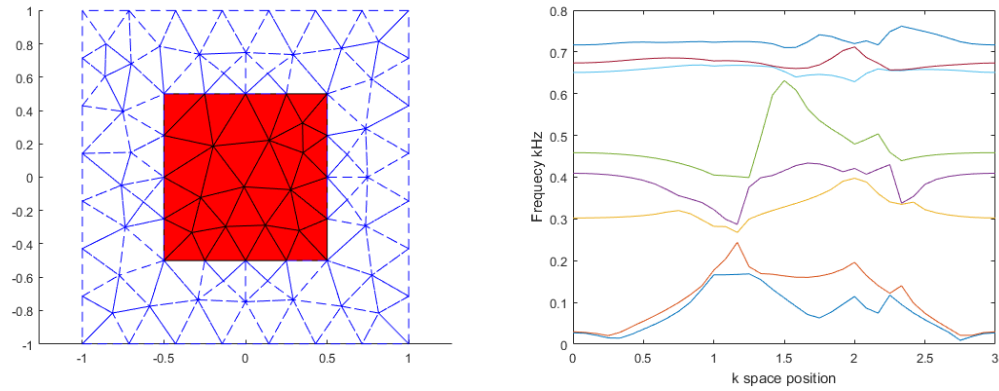


Figure 5: Square shape with core and its dispersion curve

4.2 Study of unit cells with auxetic materials

The following cases concern the design of an auxetic structure of a stiff material, with variable thickness as mentioned above. In this case we study not only the appearance of band gaps, but also the influence of the thickness of the auxetic material to the dispersion curve, as well as to the behavior of the band gap. In other words, we check if the change of the band gap is proportional to this thickness or not.

First, an auxetic star-shaped unit cell with thickness equals 0.1m is considered. In this case one can observe that some band gaps appear in a lot of regions, like between second and third eigenvalues, as seen in the following Figure 6.

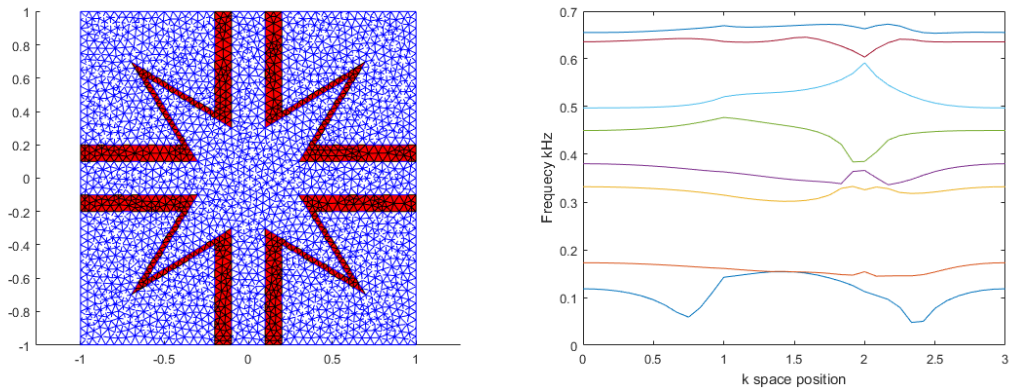


Figure 6: Square unit cell with auxetic core with thickness=0.1m and its dispersion curve

The second case is referred to an auxetic star unit cell with thickness of 0.2m. In this case we observe that no band gaps are created (see Figure 7).

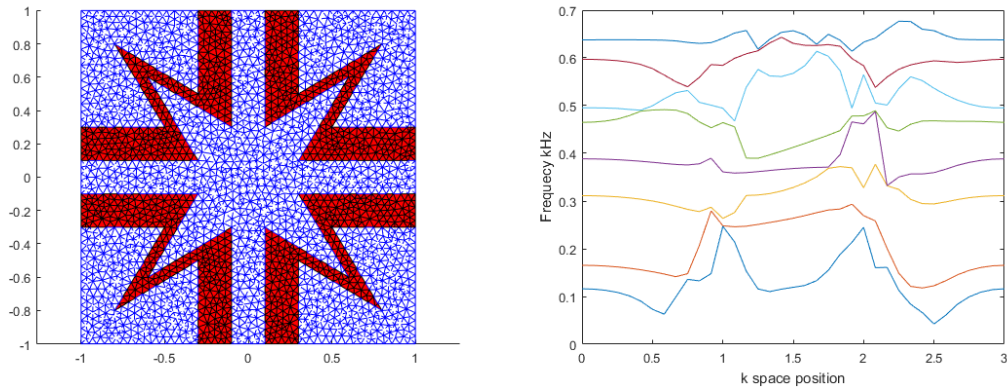


Figure 7: Square unit cell with auxetic core with thickness=0.2m and its dispersion curve

In the final case which is considered here, the auxetic star-shaped lattice has a thickness of 0.3m. It is clearly observed by Figure 8 that band gaps appear, however they are narrower compared to the case of thickness which equals to 0.1m.

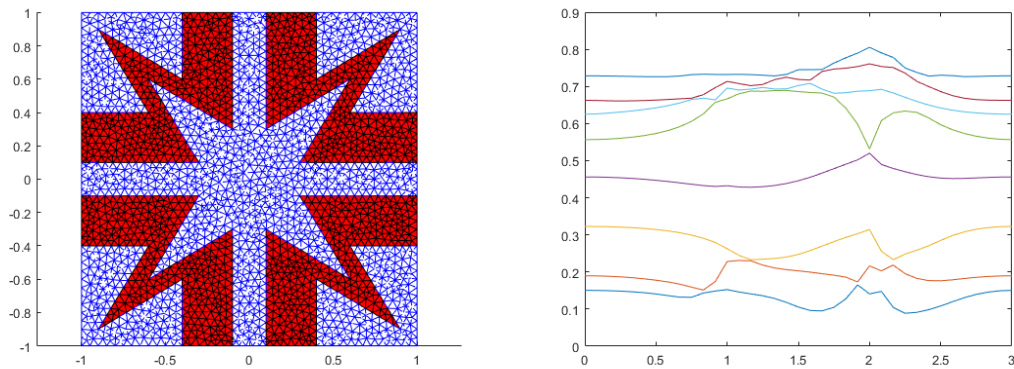


Figure 8: Square unit cell with auxetic core with thickness=0.3m and its dispersion curve

. CONCLUSIONS

The main goal of this investigation was the proper design and the analysis of a unit cell of a lattice in order to study wave propagation effects, the appearance of band gaps and eventually design with the purpose of blocking wave propagation through the structure. As a first step, several topologies of a square unit cell have been studied in order to understand the behavior of the dispersion curve, i.e. to investigate if a simple band gap was presented at the area of the first eight eigenvalues.

According to the present study, one can observe that with a simple square unit cell, no band gap occurs. Instead, with a core with enhanced mechanical properties, located in the middle of the square lattice, the first band gaps appeared. In addition, a star shape, part of the square cell, with auxetic behavior was selected in order to study the wave propagation through this hybrid unit cell. The star shape has the same mechanical properties with the previous core. Three cases with variable thickness of the star were considered. In two of the tree cases, a band gap area has achieved. However, the change

Panagiotis I. Koutsianitis, Georgios A. Drosopoulos, Georgios K. Tairidis and Georgios E. Stavroulakis

of the thickness does not affect proportionally the behavior of the dispersion curve and the band gaps.

In conclusion, the method proposed here is a systematic investigation for the dynamic behavior of the considered microstructure in the whole interval of frequencies. Based on this, optimization of band gaps is possible, according to the specific application. Extension to topology optimization in the future will allow the investigation of further, innovative auxetic microstructures.

ACKNOWLEDGEMENTS

The work of Panagiotis Koutsianitis has been supported by a doctoral grant of The Hellenic Foundation for Research and Innovation (H.F.R.I.) through the “First call for the financial support of doctoral candidates who already implement or wish to implement their doctoral theses in Greek Universities”.

REFERENCES

- [1] Spadoni, A., Ruzzene, M., Gonella, S. and Scarpa, F. Phononic properties of hexagonal chiral lattices. *Wave Motion* (2009) 46(7):435-450
- [2] Phani, A.S., Woodhouse, J. and Fleck, N.A. Wave propagation in two-dimensional periodic lattices. *J. Acoust. Soc. Am.* (2006) 119(4):1995-2005
- [3] Brillouin, L. *Wave Propagation in periodic structures*. 2nd ed. Dover, (1953)
- [4] Kittel, C. *Elementary solid state physics: A Short Course*. 1st ed. Wiley, New York, (1962)
- [5] Mace, B. R. and Manconi, E. Modelling wave propagation in two-dimensional structures using finite element analysis. *Journal of Sound and Vibration* (2008) 318:884–902
- [6] Ma, Y., Scarpa, F., Zhang, D., Zhu, B., Chen, L. and Hong, J. A nonlinear auxetic structural vibration damper with metal rubber particles. *Smart Materials and Structures*, (2013) 084012
- [7] Meng, J., Deng, Z., Zhang, K., Xu, X. and Wen, F. Band gap analysis of star-shaped honeycombs with varied Poisson’s ratio. *Smart Materials and Structures*. (2015) Vol. 24, No9
- [8] Bloch, F. *Über die quantenmechanik der elektronen in kristallgittern*. *Z. Physik.* (1928) 52:555–600
- [9] Floquet, G. *Sur les equations differentielles lineaires a coefficients periodiques*. *Annales scientifiques de l’Ecole Normale Superieure*. (1883) 12:47-88

Panagiotis I. Koutsianitis, Georgios A. Drosopoulos, Georgios K. Tairidis and Georgios E. Stavroulakis

[10] Theocaris, P.S., Stavroulakis, G.E., Panagiotopoulos, P.D. Negative Poisson's ratios in composites with star-shaped inclusions: a numerical homogenization approach. *Arch. Appl. Mech.* (1997) 274–286

[11] Kaminakis, N.T., Stavroulakis, G.E. Topology optimization for compliant mechanisms, using evolutionary-hybrid algorithms and application to the design of auxetic materials. *Composites Part B: Engineering* (2012) 43(6), 2655-2668

[12] Kaminakis, N.T., Drosopoulos, G.A., Stavroulakis, G.E. Design and verification of auxetic microstructures using topology optimization and homogenization. *Arch. Appl. Mech.* (2015), 85(9-10), 1289-1306

An Efficient Computational Procedure for the Determination of the Stochastic Mechanical Properties of Defective Graphene Sheets

George Stefanou*, Dimitrios Savvas**

*Aristotle University of Thessaloniki, Greece, **National Technical University of Athens, Greece

ABSTRACT

In this paper, an efficient computational procedure is developed for the determination of the stochastic mechanical properties of graphene with different types and density of defects. The lattice of graphene is modeled using the molecular structural mechanics (MSM) approach, where the C-C covalent bonds are replaced by energetically equivalent beam elements [1]. Random fields describing the spatial variation of the anisotropic elasticity tensor of defective graphene sheets are determined using the moving window technique and Monte Carlo simulation [2, 3]. Three types of randomly dispersed defects are examined, namely Stone-Wales (SW), single vacancy (SV) and double vacancy (DV). The effect of window size, defect type and density on the random elastic properties of graphene sheets of area $100 \times 100 \text{ nm}^2$ is investigated. The results reveal that vacancy defects can reduce the axial stiffness of graphene up to 60% with respect to that of pristine graphene, whereas the effect of SW defects is less significant. Moreover, vacancy defects (especially DV defects) lead to substantial variability of the material properties. The computed random elasticity tensors can be used as input in the framework of stochastic finite element modeling of graphene structures. [1] C. Li, T.-W. Chou, A structural mechanics approach for the analysis of carbon nanotubes, *International Journal of Solids and Structures* 40 (10) (2003) 2487-2499. [2] S. Baxter, L. Graham, Characterization of random composites using moving-window technique, *Journal of Engineering Mechanics* 126 (4) (2000) 389-397. [3] D. Savvas, G. Stefanou, M. Papadrakakis, Determination of RVE size for random composites with local volume fraction variation, *Computer Methods in Applied Mechanics and Engineering* 305 (2016) 340-358.

Adaptive Systems in Lightweight Structures

Michael Stein*

*schlaich bergemann partner

ABSTRACT

The implementation of active control systems in the construction industry come with challenges due to safety requirements for any building in the public realm and the unpredictability of the performance of real world applications during a 50 or 100 year lifespan. Most of the times active systems are used to improve the performance of the structure or material, without being an essential part of the safety concept assuring the integrity of the structure. Two of these concepts, focused on applications in lightweight structures are shown in this presentation. The dynamic performance of pedestrian bridges is a great concern for owners and users with respect to safety and comfort. The most common solution to the problem is nowadays to install passive dampers at strategic locations and which are adjusted to basic dynamic performance parameters of the bridge. These parameters are strongly related to the active mass on the bridge itself. Light structures typically have low damping properties and experience high vibration sensitivity. The change in mass due to pedestrians on the bridge is relatively high and as passive dampers cannot react to this they lose their efficiency. For a stress ribbon bridge an active control system has been developed, which consists of sensor, controllers and actuators. The effectiveness of this measure in establishing a comfortable system for the pedestrian will be described in this presentation. The new BC Place Stadium Roof in Vancouver was designed to rest on an existing bowl structure, resulting in a lightweight cable fabric structure. However, large snow loads of 42psf plus snow drift had to be considered in the design. For the primary structure the prestress level in the cable system was chosen to avoid excessive deformations. The center part of the roof, which consists of deployable and inflatable fabric cushions was designed such, that only under these large snow loads the inside pressure of the cushions would have to be increased to keep their structural integrity. Thus, the detrimental growth of material creep under high long term stresses of the fabric cushions was reduced to acceptable levels. The technical challenge to implement this active control system will be described in this presentation.

Natural Boundary Conditions for Smoothing in Geometry Processing

Oded Stein^{*}, Eitan Grinspun^{**}, Max Wardetzky^{***}, Alec Jacobsen^{****}

^{*}Columbia University, ^{**}Columbia University, ^{***}Columbia University, ^{****}Columbia University

ABSTRACT

In geometry processing, smoothness energies are commonly used to model scattered data interpolation, dense data denoising, and regularization during shape optimization. The squared Laplacian energy is a popular choice of energy and has a corresponding standard implementation: squaring the discrete Laplacian matrix. For compact domains, when values along the boundary are not known in advance, this construction bakes in low-order boundary conditions. This causes the geometric shape of the boundary to strongly bias the solution. For many applications, this is undesirable. Instead, we propose using the squared Frobenius norm of the Hessian as a smoothness energy. Unlike the squared Laplacian energy, this energy's natural boundary conditions (those that best minimize the energy) correspond to meaningful high-order boundary conditions. These boundary conditions model free boundaries where the shape of the boundary should not bias the solution locally. Our analysis begins in the smooth setting and concludes with discretizations using finite-differences on 2D grids or mixed finite elements for triangle meshes. We demonstrate the core behavior of the squared Hessian as a smoothness energy for various tasks.

Grain Structures of Additive Manufactured Ni-base Superalloys Simulated by a Mesoscopic Phase-field Model

Ingo Steinbach^{*}, Mahesh Prasad^{**}, Oleg Shcayglo^{***}, Alexander Hartmaier^{****}

^{*}Ruhr-University Bochum, ICAMS, ^{**}Ruhr-University Bochum, ICAMS, ^{***}Ruhr-University Bochum, ICAMS,
^{****}Ruhr-University Bochum, ICAMS

ABSTRACT

Additive manufacturing is characterized by extreme thermal gradients which also change their orientation rapidly during the process depending on the track, speed and power of the incident beam. Correspondingly, the grain structure can vary from equiaxed to columnar with varying orientations. Also large single crystalline regions can be realized with epitaxial growth of successive layers. Numerical simulation of the competitive nucleation and growth in additive manufacturing of Ni-base superalloy samples using a mesoscopic phase field model are presented. The modelling approach takes orientation, speed and power of the incident beam as an input parameter and simulates the grain structure evolution in a mesoscopic region of the generated structure. Aspects of concurrent integration into a macroscopic simulation are discussed.

Experimental Observation of Three-Dimensional Hydraulic Fracture Dynamics in Heterogeneous Hydrogel

William Steinhardt*, Shmuel Rubinstein**

*Harvard University, **Harvard University

ABSTRACT

Hydraulic fractures occur miles underground, below complex, layered, heterogeneous rocks, making direct measurements of their dynamics or structure extremely challenging. As such, these fractures are typically studied in the lab within blocks of classically brittle materials like glass, PMMA, or rocks that are hydraulically broken with air or fluid (Bunger (2008), Alpern (2012)). Developments in polymer science have shown that heavily cross-linked hydrogels behave nearly identically both qualitatively and quantitatively to these same brittle materials and thus are another good material in which one can study hydraulic fractures (Livne et al (2004)). We have developed a system to study hydraulic fractures within these hydrogels, which have the benefits of highly tunable material properties, being optically clear, and fracture speeds and breakdown pressures 2-3 orders of magnitude lower than PMMA. Using a combination of fast camera photography and laser sheet microscopy, we can study the three dimensional morphology and dynamics of hydraulic fractures at extremely high spatiotemporal fidelity. While the fractures in the gels show excellent agreement with the tip asymptotics outlined in Rice (1968) and Spence and Sharp (1985). However, we also observe instabilities in the propagating fracture front that generate small steps, which leave behind "step lines" that segment an otherwise smooth fracture surface. We show that the density of these lines are the result of increasing mechanical heterogeneity, which we can control in our system, and that at high density, the lines interact resulting in a very rough and uneven fracture surface. This has important practical applications as roughness can be a dominant effect in hydraulic fracture propagation, as well as acting as a nucleation point for the clogging of proppants.

New Results for Stabilized Finite Element Methods for Reissner-Mindlin Plates

Rolf Stenberg*

*Department of Mathematics, Aalto University, Finland

ABSTRACT

We consider stabilized finite element methods for Reissner-Mindlin plates [1,2]. The advantages of these methods are: - They circumvent the “inf-sup” stability conditions needed for traditional mixed methods, i.e. the formulations are stable for all finite element spaces. - The conditioning of the stiffness matrix is optimal, which implies that iterative solution methods can be used [3]. A theoretical drawback of the method has been that the error analysis required the solution to be smooth, and due to this, the methods have often been questioned. We now present a new error analysis, which do not require additional smoothness. Numerical results supporting the analysis are presented. [1] T.J.R. Hughes, L.P. Franca. A mixed finite element formulation for Reissner-mindlin plate theory: Uniform convergence of all higher-order spaces. *CMAME* 67 (1988) 223--240 [2] R. Stenberg. A new finite element formulation for the plate bending problem. *Asymptotic Methods for Elastic Structures. Proceedings of the International Conference, held in Lisbon, Portugal, October 4-8, 1993.* P.G. Ciarlet, L. Trabucho and J.M. Viaño, Eds. Walter de Gruyter & Co. 1995, pp. 209–221 [3] J. Schöberl, R. Stenberg. Multigrid methods for a stabilized Reissner-Mindlin plate formulation. *SIAM Journal of Numerical Analysis* 47 (2009) 2735–2751

Process Modeling of LENS Manufacturing; Effects of Laser Scan Path on Residual Stress

Michael Stender^{*}, Lauren Beghini^{**}, Michael Veilleux^{***}, Joshua Sugar^{****}, Samuel Subia^{*****}

^{*}Sandia National Laboratories, Livermore, CA, USA, ^{**}Sandia National Laboratories, Livermore, CA, USA,
^{***}Sandia National Laboratories, Livermore, CA, USA, ^{****}Sandia National Laboratories, Livermore, CA, USA,
^{*****}Sandia National Laboratories, Albuquerque, NM, USA

ABSTRACT

This presentation will outline the application of a multi-physics process model of metal additive manufacturing (AM) to elucidate the effect of laser scan pattern on residual stress distribution following manufacturing. The AM process considered herein is referred to as Laser Engineered Net Shaping (LENS®); a subclass of directed energy deposition (DED) technologies. In the LENS process, a stream of metal powder is sprayed into the focal point of a laser heat source aimed at a moving stage. As the stage moves and the melt pool progressively cools, material is built up to create a final part geometry. In this work, a Lagrangian finite element analysis workflow is implemented to model the associated physical phenomena including: laser-induced heating; material deposition; heat transport through radiation, convection, and conduction; liquid-to-solid phase transition; re-melting; temperature and deformation-dependent evolution of material properties and, thermally driven deformation and residual stress accumulation. Through the application of this finite element process model, it is possible to simulate in situ LENS processing conditions as well as the resulting residual stresses, and distortions following manufacturing. A simple cylindrical part is considered and simulations are compared to experimental builds of similar laser scan patterns. Through modification of the simulated laser scan pattern, thermal conditions during manufacturing and the resulting residual stresses and distortions following manufacturing are shown to change. This work is useful in understanding the resulting properties and performance of LENS built parts and demonstrates the potential to engineer a desired residual stress state into a structure through control of LENS manufacturing strategy. *Sandia National Laboratories is a multimission laboratory managed and operated by National Technology and Engineering Solutions of Sandia, LLC., a wholly owned subsidiary of Honeywell International, Inc., for the U.S. Department of Energy's National Nuclear Security Administration under contract DE-NA0003525.

Structure-preserving Numerical Integrators for Relaxation Oscillators, with Application to Neuronal Dynamics

Ari Stern*

*Washington University in St. Louis

ABSTRACT

Relaxation oscillators pose a challenge for numerical integration, due to the presence of fast and slow time scales. Conventional exponential integrators (such as exponential Euler) allow for numerical stability at large time steps, but do a poor job at capturing the limit cycles governing oscillatory behavior unless the time step size is taken very small. In practice, this results in numerical solutions with the wrong amplitude and/or frequency of oscillation. We present a new family of methods that can maintain stability and preserve limit cycles for much larger time step sizes, with no increase in computational effort over exponential Euler. This is illustrated for the Van der Pol oscillator, as well as for the Hodgkin-Huxley model of neuronal dynamics (whose oscillations correspond to neuronal spiking). In particular, these methods allow for accurate simulation of neuronal dynamics at much lower computational cost than the methods currently used in computational neuroscience.

Ductile Fracture Representation Using the Phase-Field Model in SIERRA

Andrew Stershic^{*}, Brandon Talamini^{**}, Jakob Ostien^{***}, Michael Tupek^{****}

^{*}Sandia National Laboratories, California, ^{**}Sandia National Laboratories, California, ^{***}Sandia National Laboratories, California, ^{****}Sandia National Laboratories, New Mexico

ABSTRACT

The ability to computationally model the ductile fracture and failure of metals remains a compelling problem in the aerospace industry. This failure mechanism is preceded by significant plastic deformation and is characterized by a significant plastic zone at the blunted crack tip, rendering the typical brittle linear-elastic fracture models inadequate. In this work, we develop a phase-field model to represent the degradation of material condition in the vicinity of the strain localization. The introduction of a length-scale to limit the damage gradient acts to prevent spurious damage localization in the softening regime. This approach is implemented in SIERRA, a scalable multi-physics finite element code, and is applied to fundamental problems of interest to demonstrate its effectiveness. The specific choice of thermodynamic energy quantity used to drive the fracture process is discussed. Sandia National Laboratories is a multi-mission laboratory managed and operated by National Technology & Engineering Solutions of Sandia, LLC., a wholly owned subsidiary of Honeywell International, Inc., for the U.S. Department of Energy's National Nuclear Security Administration under contract DE-NA0003525.

The NRL Additive Manufacturing Multiphysics Discrete Element Method (NAMMDEM) Framework

John Steuben^{*}, Athanasios Iliopoulos^{**}, John Michopoulos^{***}

^{*}U.S. Naval Research Laboratory, ^{**}U.S. Naval Research Laboratory, ^{***}U.S. Naval Research Laboratory

ABSTRACT

Additive Manufacturing (AM) has become a topic of great interest over a broad spectrum of research communities. These processes operate by successive depositions of mass and energy in a spatially resolved and highly non-uniform fashion. Feedstock materials are typically noncontinuum (i.e. large ensembles of powder particles), which are melted or sintered into a continuous object. Because of the irregular and highly localized time history of heat and mass deposition associated with these processes, a wide range of quality issues arise, including unusual microstructure morphologies, porosity, high residual stresses and strains, and generally reduced or indeterminate macro-scale mechanical properties. In powder-bed applications interaction of the recoater with both loose and sintered/melted particles, as well as atmospheric flow interaction with powder particles, have been observed to have major effects. This suggests that a simulation method that accounts for all these interactions must be implemented in order to enable the adoption of AM technologies for the production of performance-critical components. This work focuses on the development of a modeling and simulation framework for AM, based on the Discrete Element Method (DEM) [1]. Discussion of thermoplastic particle contact modeling and bond formation to capture the relevant multiphysics of the AM process will be presented. Other effects, such as gas pressure driven particle denudation are also included. Modeling of phase transformation using physics-informed level set methods will be introduced, as will appropriate boundary conditions to model relevant AM processes. This work also discusses the computational implementation of the NRL Additive Manufacturing Multiphysics Discrete Element Method (NAMMDEM) framework [2]. Particular focus will be paid to the necessity of high performance contact detection, which is required due to the highly polydisperse nature of AM feedstock powders. We will discuss improvements and optimizations to the contact detection algorithms of NAMMDEM, which have generated an order of magnitude performance improvement over its initial implementation. We will conclude with remarks regarding the integration of the NAMMDEM tool with continuum mechanics tools, such as point collocation or finite element methods. [1] Steuben, J. C., Iliopoulos, A. P., & Michopoulos, J. G. (2016). Discrete element modeling of particle-based additive manufacturing processes. *Computer Methods in Applied Mechanics and Engineering*, 305, 537-561. [2] Steuben, J. C., Iliopoulos, A. P., & Michopoulos, J. G. (2017, August). Recent Developments of the Multiphysics Discrete Element Method for Additive Manufacturing Modeling and Simulation. In *ASME 2017 IDETC/CIE* pp. V001T02A025-V001T02A025.

Computational Sciences and Math at Sandia – Algorithms, Software, and Applications

James Stewart*

*Sandia National Laboratories

ABSTRACT

The Computational Sciences and Math Group at Sandia National Laboratories fills a broad spectrum of R&D. Areas of focus include optimization, uncertainty quantification, multiphysics numerical methods, scalable numerical linear algebra, high-energy density physics, materials science spanning atomistic to continuum scales, and large-scale multiphysics application analysis. The group also develops widely-used, open-source software products including Dakota, many Trilinos packages, Albany, and LAMMPS. This talk will provide an overview of the group's research and present highlights of work across these areas of interest to the computational mechanics community.

Towards a Four-chamber Heart Model for Whole Heart Cardiac Motion Simulation

Marina Strocchi^{*}, Caroline Roney^{**}, Anton Prassl^{***}, Gernot Plank^{****}, Edward Vigmond^{*****},
Christopher Rinaldi^{*****}, Martin Bishop^{*****}, Justin Gould^{*****}, Steven Niederer^{*****}

^{*}King's College London, ^{**}King's College London, ^{***}Medical University of Graz, ^{****}Medical University of Graz,
^{*****}Fondation Bordeaux Université, ^{*****}King's College London - Guy's and St Thomas' NHS Foundation Trust,
^{*****}King's College London, ^{*****}King's College London - Guy's and St Thomas' NHS Foundation Trust,
^{*****}King's College London

ABSTRACT

Computational models of cardiac electromechanics are increasingly used for clinical applications simulating normal physiology, pathologies and treatments. Previous models have focused on the ventricles, which limit the capacity to simulate the effects of the atria, aorta and pulmonary artery on cardiac physiology. Developing models that explicitly present these surrounding structures will greatly improve simulations of changes in pre-load and afterload and move models closer to representing the clinical setting. In this work we present our four chamber cardiac modelling framework in a clinical case study. A four chamber heart model was generated from CT images with in and out-plane resolution of 0.36mm and 0.5mm, acquired from a 78-year-old female heart failure patient indicated for cardiac resynchronization therapy. Blood pools of the left ventricle, the right ventricle and the atria were automatically segmented and dilated of 6mm, 3.5mm and 2mm to obtain labels for the myocardium. The multi-label segmentation was then smoothed and upsampled to an isotropic resolution of 0.15mm, and finally meshed with an element target size of 0.8mm. The resulting tetrahedral mesh had 391551 nodes and 1875186 elements. Ventricular and atrial fibers were generated using two different rule-based mapping methods based on histological and DT-MRI measurements. Electrical excitation of the whole heart was simulated with a reaction-eikonal model. Atria and ventricles were stimulated at one right atrial and four ventricular endocardial sites. Cardiac tissue was modelled as a transversely isotropic conducting medium, with conduction velocities in the fiber and in the transverse direction tuned to achieve full atrial and ventricular activation within 90ms and 80ms, respectively. Mechanical deformations of the heart were modelled with the finite elasticity equations. Cardiac tissue was modelled as hyperelastic, incompressible, non-linear material. For the ventricles, we used a transversely isotropic constitutive law and a phenomenological active contraction model, while atria were modelled as isotropic and passive. Homogeneous Dirichlet boundary conditions were applied at the inflow tracts of the pulmonary veins, the left atrial appendage, the superior vena cava and the inferior vena cava. The model simulates the activation wave spreading across the heart. Apex-to-base shortening results in an ejection fraction of 27%. We have demonstrated in a single case the capacity to simulate both electrics and active mechanics in a four chamber heart and this provides the foundation framework for developing patient-specific four chamber heart models for studying the electrical and mechanical interaction between the atria and ventricles, in healthy and in diseased states.

Stochastic SFBEM Based on Erdogan's Solutions for Static Analysis of Crack Problems with Structural Uncertainties

Cheng Su^{*}, Zhi Xu^{**}, Zhongwei Guan^{***}, Xueming Fan^{****}

^{*}South China University of Technology, ^{**}South China University of Technology, ^{***}University of Liverpool,
^{****}South China University of Technology

ABSTRACT

Mathematical formulation and computational implementation of the stochastic spline fictitious boundary element method (SFBEM) are presented for static analysis of crack problems with structural parameters modeled as random fields. The stochastic governing differential equations of crack problems are decomposed into two sets of governing differential equations with respect to the means and the deviations of cracked plate responses by including the first order terms of deviations. These equations are in similar forms to those of deterministic crack problems, and they can be solved using deterministic fundamental solutions of cracked plates, namely the Erdogan's solutions, resulting in the means and covariances of the stress intensity factors and structural responses. The stress boundary conditions on the crack surface are automatically satisfied and the singular behaviour at the crack tip can be naturally reflected without setting boundary elements on the crack surfaces due to the use of the Erdogan's fundamental solutions. The proposed method is validated by comparing the solutions with those obtained by Monte Carlo simulation for a number of example problems.

A Phase-Field Study of the Grain-Size and Frequency Dependent Ferroelectric Characteristics of BaTiO₃ nanoceramics

Yu Su*

*Beijing Institute of Technology

ABSTRACT

In this work, we address a couple of fundamental issues in one of the most widely studied functional materials - ferroelectric ceramics, but with nano-sized grains. As the grain size decreases to the nanometer range, the characteristics of the ferroelectric nanoceramic can be ultimately determined by the competition between two effects: the intrinsic effect that is associated with the local properties of the grain boundary and the extrinsic effect that arises from the dynamics of domain structure which is highly influenced by the depolarization field caused by the grain boundary. In this work we investigate such a competition with a phase-field simulation based on the time-dependent Ginzburg-Landau (TDGL) kinetic equation. The study is performed on poled/unpoled nanoceramics under high- and low-amplitude bipolar alternating electric field with selected grain size and loading frequency. Our calculations for poled BaTiO₃ at 100 Hz show that, for the grain size from 170 to 50 nm, its properties are dominated by the extrinsic effect, and from 50 to 10 nm, they are dominated by the intrinsic one. As the grain size decreases, the dielectric and piezoelectric constants at the remnant state continuously rise in the extrinsic-dominated region and then drop sharply in the intrinsic-dominated region. Our frequency calculations from 10 to 2,500 Hz at the grain size of 100 nm indicate that the high-frequency behavior is very similar to that of the small grain-size, intrinsic-dominated one, whereas the low-frequency behavior is closely related to that of the large grain-size, extrinsic-dominated part, with the demarcation line occurring around 400 Hz. For the un-poled ceramics under small signal loading, the intrinsic effect is dominant over the entire range of grain size and frequency.

A Computational and Experimental Co-designed Framework for Confined Impact Test of Powder Materials

Waad Subber^{*}, Sangmin Lee^{**}, Karel Matous^{***}

^{*}University of Notre Dame, ^{**}University of Notre Dame, ^{***}University of Notre Dame

ABSTRACT

The confined impact test is a common experiment to investigate the dynamical response of powder materials at high strain rates. The goal of the experiment is to generate the high internal pressure and temperature that can lead to synthesis of a new material, when reactive powder materials are used. The numerical simulations of such an experiment are challenging due to the high strain rates, large deformations, complex material behavior, and the high computational cost. To better understand the physical phenomena and to optimize the conditions under which a new material can be synthesized, a co-designed computational and experimental framework is investigated. The simulations of the experiment are performed using in-house massively parallel finite strain Lagrangian code PGFem3D equipped with a newly developed poro-viscoplastic constitutive model for powder material. Based on a sensitivity analysis we noticed that the dimensions governing the shape of the sample have equally important roles in achieving the maximum pressure inside the sample. To optimize the shape of the sample, we construct a probabilistic response surface based on Gaussian process (GP). A training dataset is used to build the response surface and an independent testing dataset is used to verify the prediction of the GP. The mean of the GP is exploited to obtain the optimal dimensions required to achieve the maximum pressure inside the sample. For validation under uncertainty, quantities of interest (QOIs) within subregions of the computational domain are introduced. The QOIs are the reaction force at the bottom face of the sample and the deformed shape represented by the displacement trajectory at the center point of the sample. To provide a confidence bound on the numerical predictions of the QOIs, the impact velocity is represented by a suitable stochastic expansion and propagated forward through the computational model. The numerical predictions of the QOIs with the associated confidence intervals are compared with the co-designed experimental results.

A Transformed Path Integral Approach for Linear-Quadratic Control

Gnana Subramaniam*, Prakash Vedula**

*University of Oklahoma, **University of Oklahoma

ABSTRACT

We present an adaptive path integral based method for optimal, linear-quadratic (LQ) control of a nonlinear stochastic dynamical system. In our proposed approach, termed the transformed path integral control (TPIC), we utilize a short-time propagator formulation that allows the governing partial differential equation for LQ control to be solved in a transformed computational domain where the stochastic optimal controls are obtained, while preserving short-time properties of the underlying system dynamics. The formulation ensures non-negativity of the underlying probability density functions (PDFs) and realizability of the associated cost-functions, while better accommodating nonlinearities in drift and non-Gaussian behavior in PDFs. The choice of transformation considered, which maps a fixed grid in transformed space to a dynamically adaptive grid in the original state space, enables us to explore controls in desired domains of importance (or regions of high probability). The proposed method also allows for estimation of error bounds on the probability in the computational domain using Chebyshev's inequality. In addition, the method can accurately represent the underlying PDFs and better address challenges in processes with large diffusion, large drift and large concentration of the PDFs similar to the TPI method [1]. These features enable the TPIC approach to have better computational performance and efficiency, in comparison to conventional Monte Carlo and fixed grid based approaches. Additionally, we also present formulations to further enhance the computational efficiency of TPIC through application of Fast Gauss Transform techniques and bandlimiting approaches on the propagator matrices. We evaluate the performance of the TPIC method over conventional methods for LQ control of linear and nonlinear stochastic dynamical systems via consideration of canonical problems in one-dimensional and multi-dimensional state spaces. Generalization of the proposed framework to non-LQ context will also be discussed. [1] Gnana M Subramaniam and Prakash Vedula. "A transformed path integral approach for solution of the Fokker–Planck equation". In: *Journal of Computational Physics* 346 (2017), pp. 49– 70.

A Meshfree Generalized Finite Difference Method for Surface PDEs

Pratik Suchde^{*}, Joerg Kuhnert^{**}

^{*}Fraunhofer ITWM, Germany, ^{**}Fraunhofer ITWM, Germany

ABSTRACT

We propose a novel meshfree Generalized Finite Difference Method (GFDM) approach to discretize PDEs defined on manifolds. Derivative approximations for the same are done directly on the tangential plane at each point. As a result, the proposed method not only does not require a mesh, it also does not require an explicit reconstruction of the manifold. In contrast to existing methods for surface PDEs, it avoids the complexities of dealing with a manifold metric, while also avoiding the need to solve a PDE in the embedding space. As a result, a further advantage is that developments in usual (volume/bulk based) GFDM operators can be easily carried over, in this framework, to surface-based GFDM differential operators. We propose discretizations of the surface gradient operator, the surface Laplacian and surface Diffusion operators. Possibilities to deal with anisotropic and discontinuous surface properties (with large jumps in the diffusion coefficient, up to several orders of magnitude) are also introduced. The scope of using a moving Lagrangian framework for surface PDEs discretized using a meshfree GFDM will also be brought to light.

Computational Methods for Supporting Patient-Specific Treatment on Orthodontics

Kazuhiro Suga*

*Kogakuin University

ABSTRACT

It is an essential need for both patients and medical doctors to realize safe and effective treatments on orthodontics. Numerical prediction through computational mechanics has the potential to achieve it. However, a few trials have been carried out and there is no trial in clinical practice. We are developing a supporting system on orthodontics with the orthodontists in TMDU (Tokyo Medical and Dental University) in Japan. This report gives the goal of our support system and its current status in (1) a tooth-PDL modeling in order to predict the initial tooth movement for patient-specific clinical use, and (2) evaluation of orthodontic force and moment by a super elastic wire during tooth movement for designing treatment plan.

Ultimate State Simulations by Finite Cover Method with Damage Model

Hirofumi Sugiyama^{*}, Koji Saito^{**}, Kazumi Matsui^{***}, Shigenobu Okazawa^{****}

^{*}University of Yamanashi, ^{**}University of Yamanashi, ^{***}Yokohama National University, ^{****}University of Yamanashi

ABSTRACT

This paper examined the ultimate state of the metal, which called ductile fracture, by using finite cover method with damage model. Estimating the ultimate state is interests in many fields of engineering. In these days, high tensile strength steel and so on has used, finite element simulations play important roles to predict the complex material behavior. Especially, the ductile properties of metals are important to control the ultimate state of the metals. The continuum damage mechanics has been developed for that purpose, and relates the microscopic voids and the macroscopic damage parameters. The damage parameter is defined as between zero to one, which means the propagation of the ductile fracture. However, the propagation of the ductile fracture is described as the merely increase of the value. Therefore, this model is not able to represent the discontinuous deformation clearly. The conventional finite element simulation(FEM) is not good at handling the discontinuities, especially in crack propagation analysis because the FEM describes the discontinuities by elements boundaries. Some special techniques are necessary in order to describe the discontinuous deformation. Moreover, generalized finite element method have been developed mainly in fracture mechanics. extended finite element method(X-FEM) is well-known method. This method can easily simulate the nucleation and growth of discontinuities (cracks) by the character of enhanced approximation function. The X-FEM is mainly used for elastic body, thus the elasto-plastic analysis is less frequently. By contrast, finite cover method(FCM)is also proposed as one of the generalized finite element method. The FCM is able to describe the discontinuities obviously by multiple covers, which based on the basic concept of this method. In this paper, we examine the material behavior up to ultimate state by using FCM with damage model. Here firstly focuses on the force displacement curve at post peak and compare with some load condition by some shape of test pieces. Moreover, considering the crack initiation condition and some representative simulations are demonstrated. Consequently, we confirm proposed method using simple techniques is able to represent the ultimate state of material.

Spectral Finite Elements and Enriched Partition-of-unity Methods for Band Structure Calculations in Phononic Crystals

N. Sukumar^{*}, Ankit Srivastava^{**}

^{*}UC Davis, ^{**}IIT Chicago

ABSTRACT

Phononic crystals are periodic composites in 1-, 2- and 3-dimensions, which can be used to control vibration and waves (acoustic and/or elastodynamic) in these dimensions [1]. They differ from homogeneous materials most strikingly in the presence of the frequency bandgaps, which indicates regions of frequencies where such waves are prohibited from propagating in the crystal. Applications of phononic crystals range from noise and vibration control and collimation and refraction to determining their thermal properties (heat conductivity and heat capacity) and in topology design. The fundamental Bloch-periodic problem that is solved in the unit cell is: for a given wavevector (k-point) in the irreducible Brillouin zone, the solution of the elastodynamic eigenproblem provides the eigenpairs (eigenfrequencies and eigenmodes) that are used to construct the band structure. The most common approaches to solve the phononic eigenproblem are those based on planewaves (Fourier basis), variational methods such as the displacement-based finite element method, and multiple scattering, with recent advances including multiscale finite elements and Bloch-mode synthesis techniques. In this talk, we will first show the benefits of using spectral finite elements to compute the band structure of a two-phase 1-dimensional phononic crystal that has an exact solution. We will compare spectral finite elements to planewave expansion with displacement and mixed Rayleigh quotients [2], and show that spectral finite elements is particularly accurate and efficient when the two phases have sharp contrasts in material properties. For modeling a domain containing holes in two dimensions, we adopt a new numerical integration scheme [3] that permits use of a fixed Cartesian mesh with higher-order finite elements. Band structure calculations on perforated phononic materials will be presented to demonstrate the accuracy of the method. REFERENCES 1. M. I. Hussein, M. J. Leamy and M. Ruzzene, Dynamics of phononic materials and structures: Historical origins, recent progress and future outlook, *Applied Mechanics Reviews*, 66(4), 040802, 2014. 2. Y. Lu and A. Srivastava, Variational methods for phononic crystals, *Wave Motion*, 60, pp. 46-61, 2016. 3. E. B. Chin, J. B. Lasserre and N. Sukumar, Numerical integration of homogeneous functions on convex and nonconvex polygons and polyhedra, *Computational Mechanics*, 56(6), pp. 967-981, 2015.

THE STABILITY AND DYNAMIC BEHAVIOUR OF ELASTIC NON-LINEAR FLUID-LOADED STRUCTURES

R. SULIMAN^{*†}, O.F. OXTOBY[†], AND N. PEAKE^{*}

^{*}Department of Applied Mathematics and Theoretical Physics

University of Cambridge

Cambridge, Cambridgeshire, United Kingdom

R.Suliman@damtp.cam.ac.uk, N.Peake@damtp.cam.ac.uk

[†]Aeronautics System

Council for Scientific and Industrial Research

Pretoria, Gauteng, South Africa

ooxtoby@csir.co.za

Key words: Modal Analysis, Fluid-structure Interaction, Multiphysics Problems, Stability Analysis, Strong-coupling.

Abstract. The deformation of slender elastic structures due to the motion of fluid around it is a common multi-physics problem encountered in many applications. This work details the development and implementation of a numerical model capable of solving such strongly-coupled fluid-structure interaction problems.

In most fluid-structure interaction problems the deformation of the slender elastic bodies is significant and cannot be described by a purely linear analysis. We present a new formulation to model these larger displacements. By extending the standard modal analysis technique for linear structural analysis, the governing equations and boundary conditions are updated to account for the leading-order non-linear terms and a new modal formulation with quadratic modes is derived. The quadratic modal approach is tested on standard benchmark problems of increasing complexity and compared with analytical and full non-linear numerical solutions.

Two computational fluid-structure interaction approaches are then implemented in a partitioned manner: a finite volume method for discretisation of both the fluid and solid domains and the quadratic modal formulation for the structure coupled with a finite volume fluid solver. Strong-coupling is achieved by means of a fixed-point solver with dynamic relaxation. The fluid-structure interaction approaches are validated and compared on benchmark problems of increasing complexity and strength of coupling between the fluid and solid domains.

Fluid-structure interaction systems may become unstable due to the interaction between the fluid-induced pressure and structural rigidity. A thorough stability analysis of finite elastic plates in uniform flow is conducted by varying the structural length and flow velocity showing that these are critical parameters. Validation of the results with those from analytical methods is done. An analysis of the dynamic interactions between multiple finite plates in various configurations is also conducted.

1 INTRODUCTION

Computational mechanics is a growing discipline which uses computational methods to obtain approximate solutions to problems governed by the principles of mechanics. Fluid-structure interaction (FSI) constitutes a branch of computational mechanics in which there exists an intimate coupling between fluid and structural or solid domains; the behaviour of the system is influenced by the interaction of a moving fluid and a flexible solid structure. Examples of such FSI systems include wing flutter on aircraft, aeroelasticity of turbomachinery blades, flows in elastic pipes and blood vessels, heart valve dynamics, swimming of fish and in the processing of paper. In this work, we make use of a blend of mathematical and computational approaches to study strongly-coupled fluid-structure interaction problems involving long thin structures.

2 STRONGLY-COUPLED FLUID STRUCTURE INTERACTION APPROACHES

Two computational fluid structure interaction (FSI) approaches are implemented in a partitioned manner to model FSI problems. In the first approach a finite volume method is developed and implemented in *OpenFOAM* by coupling fluid and structural solvers. The finite element method has primarily been used for modelling the mechanics of solids¹. The finite volume method² has traditionally been more dominant in the field of fluid mechanics but has received increased attention for use in solid mechanics over the last two decades. Both schemes can be considered as methods of weighted residuals where they differ in the choice of weighting function³. In terms of computational FSI approaches, many recent studies have made use of a single discretisation scheme, either finite element^{4,5,6} or finite volume^{7,8,9}, to solve the entire domain. This simplifies the treatment at the interface of the fluid and solid domains. The fluid is assumed to be viscous, incompressible and isothermal with the governing equations given by the continuity and Navier-Stokes equations in an arbitrary-Lagrangian-Eulerian (ALE) reference frame. The solid is assumed to be a homogeneous isotropic elastic solid undergoing large, non-linear deformation with the motion governed by Cauchy's first equation of motion. We make use of the finite

volume method for discretisation of the entire domain. In the second approach a reduced-order modal approach for solving the structural equations is implemented and coupled with an incompressible finite volume fluid solver in *OpenFOAM*. Strong-coupling of the fluid and solid domains is achieved by means of a fixed-point solver using a dynamic relaxation parameter based on Aitken's method. It is a simple yet highly robust and efficient approach.

2.1 Governing Equations

The equations governing viscous incompressible isothermal fluid flow in an arbitrary-Lagrangian-Eulerian (ALE) reference frame¹⁰ are given by the continuity and Navier-Stokes equations. To close the governing equations, a constitutive relation for stress is required. We assume a Newtonian fluid to relate the stress to strain.

The partial differential equations that describe a homogeneous isotropic elastic solid undergoing large, non-linear deformation are given by Cauchy's first equation of motion¹¹. Assuming an isotropic hyperelastic St. Venant--Kirchhoff material model, the stress-strain relationship is given in terms of the second Piola--Kirchhoff stress. The first Piola--Kirchhoff stress is related to the second Piola--Kirchhoff stress by the deformation gradient, which relates quantities in the undeformed configuration to their counterparts in the deformed configuration. The constitutive stress-strain relationship is given in terms of the Green--Lagrange strain, which is related to the displacement field through the gradients of displacement.

The finite volume method of discretisation is used for the spatial discretisation of the equations above. This is done by placing them into weak form or integrating over an arbitrary control volume and applying the divergence theorem of Gauss.

2.2 Modal FSI Analysis

Tangential to the full finite volume FSI approach, a reduced-order modal approach to solving the structural equations has been used and coupled with an incompressible finite volume fluid solver in *OpenFOAM*.

For a modal structural analysis, Lagrange's equations of motion in the general case are used, which provides an expression for the eigenvalues or natural frequencies and eigenvectors or mode shapes.

2.3 Fluid-Solid Coupling

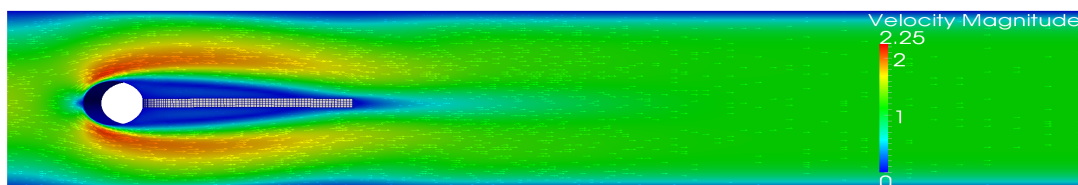
In this work we limit our analyses to incompressible flows and have made use of the incompressible *pimpleDyMFoam* flow solver. The coupling between the fluid and solid is done once at the beginning of every time-step when movement of the mesh occurs. The fluid flow provides a traction onto the structure. This results in a deformation of the structure which in turn affects the fluid flow. Coupling conditions for the traction, displacement and velocity are applied to ensure momentum conservation or force equilibrium at the interface, as well as to enforce the kinematic or geometric continuity and no-slip conditions respectively. The above conditions require an iterative procedure such that a strongly-coupled solution is obtained.

FSI systems can be solved using a single or monolithic solution method, which is inherently strongly-coupled, or a partitioned solution method, which can be strongly- or weakly-coupled. Monolithic methods ensure stability and convergence of the solution, since all equations are discretised and solved simultaneously. However, this approach may suffer from ill conditioning and convergence is generally slow. Conversely, partitioned approaches allow for the use of two independent solution techniques for solid and fluid equations in isolation. Weakly-coupled partitioned methods may diverge or result in inaccurate solutions when applied to problems where there are strong interactions between solid and fluid domains. The FSI implementation described above is a weakly-coupled one: the modal equations are solved as a boundary condition only once at the beginning of each time-step. If applied to strongly-coupled problems, the solver results in inaccurate solutions or diverges.

A separate coupling algorithm or additional outer iterations between the fluid and solid is therefore required to achieve strong-coupling. The most popular strongly-coupled FSI algorithms either use fixed point iteration or interface Newton--Krylov methods. Both approaches have their own shortcomings: fixed point methods are generally slow to converge as they make use of Gauss--Seidel iterations and methods to speed up convergence are needed, whilst Newton--Raphson methods require the computation of Jacobians that may be difficult to calculate exactly. A strongly-coupled fixed-point solver with dynamic relaxation, has been implemented in this work. It is the most basic of the above approaches yet is highly robust and efficient. The fixed point solver uses a relaxation parameter based on Aitken's method. The solver was modified to call the mesh movement algorithm after every iteration, thus allowing a re-calculation of interface forces, displacements and velocities with every iteration hence resulting in a fully-coupled scheme upon convergence.

2.4 Two-dimensional Flapping Beam

Both FSI approaches have been successfully validated and compared on benchmark cases and the results for a common FSI benchmark problem, proposed by Turek and Hron¹², of an elastic beam in the wake of a cylinder undergoing vortex-induced vibration are included here. The properties of the fluid and solid are as described in¹². A uniform constant fluid velocity, Reynolds number, $Re = 100$, was applied at the inlet while at the exit pressure was set to zero. Flow is assumed to be laminar. Snapshots of the beam deflection and velocity contours at various times are shown in Figure 1, showing large oscillations of the beam in its second mode of vibration as vortices are shed periodically from either side of it.



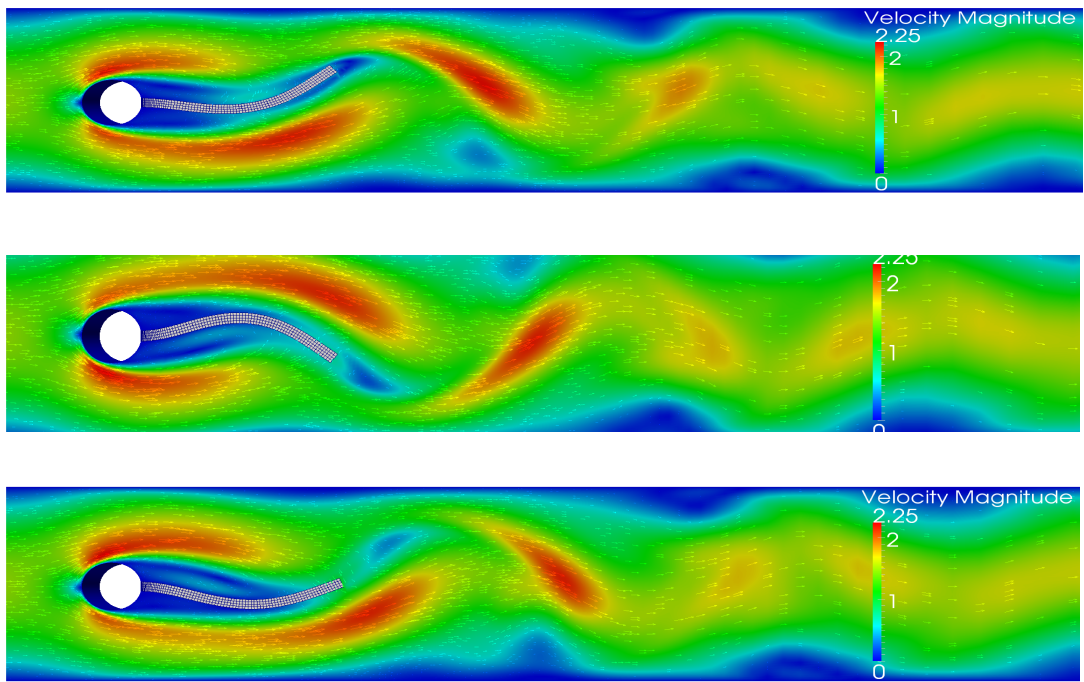


Figure 1: Velocity contours for a 2D beam oscillating in its second mode of vibration.

The vertical tip displacements of the beam using the modal FSI solver and the finite volume FSI method are compared with the results of Turek and Hron¹² in Figure 2. There is a good correlation between these results.

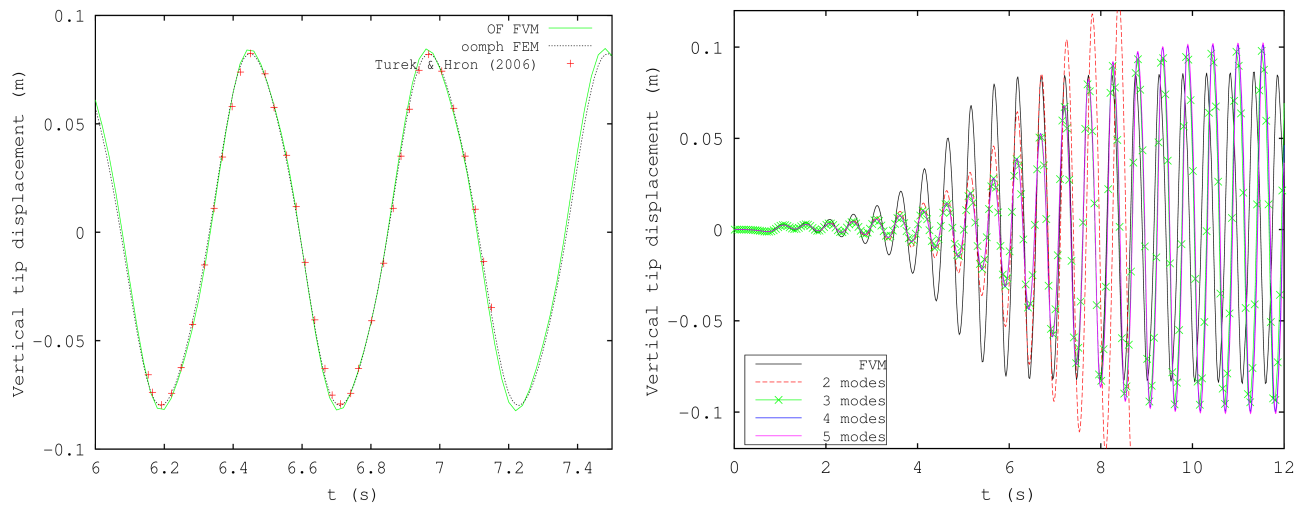


Figure 2: Vertical tip displacement for the Turek & Hron case using the finite volume method (left) and modal approach (right).

The finite volume FSI results, however, required a very fine mesh for the solid domain and consequently a long run-time. Upon further investigation of just a cantilever beam under a tip load it was found that the finite volume method for structural mechanics suffered from a phenomenon of shear locking. When the aspect ratio of the elements (ratio of element width to height) is large, a numerical shear strain component is produced in addition to a bending strain. This absorbs strain energy and results in a decrease in displacement or stiffening, as shown by the results in Figure 3 (left). In addition, an evaluation of the accuracy of the finite volume scheme shows that the scheme is only first-order accurate, see Figure 3 (right), which also explains the slow convergence in the result.

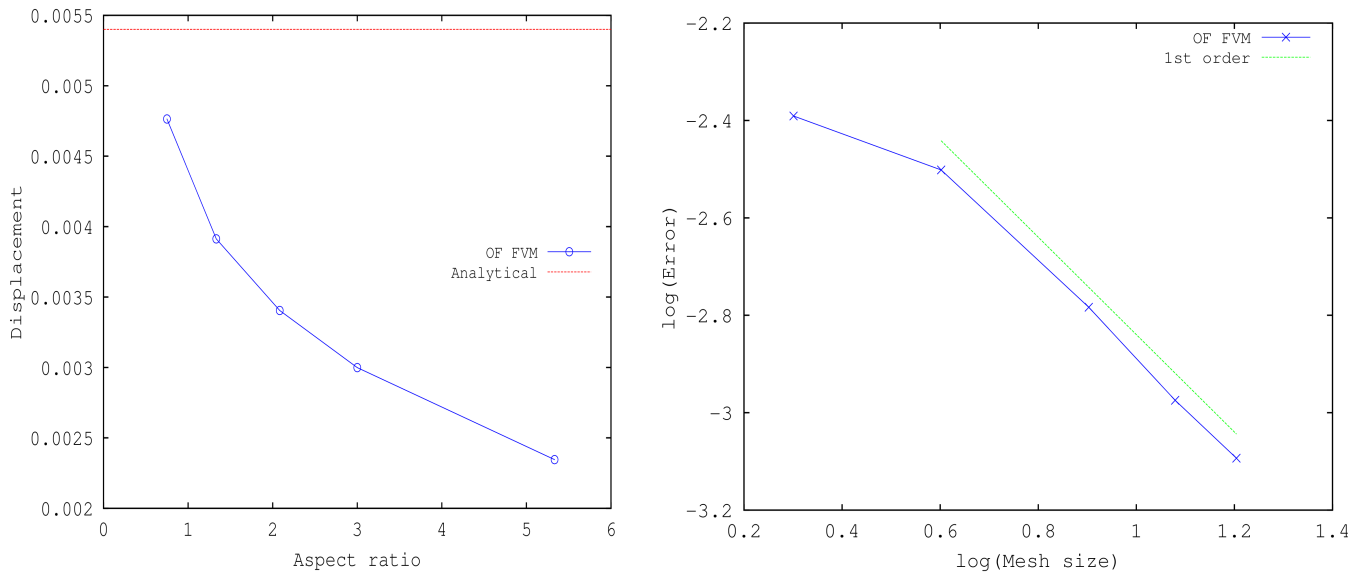


Figure 3: Analysis of a cantilever beam using the finite volume method: shear locking (left) and order of accuracy (right).

3 STABILITY ANALYSIS

The FSI system may become unstable due to the interaction between the fluid-induced pressure and structural rigidity, with flow velocity and structural length being critical parameters that influence the stability of the system. Three distinct theoretical approaches have traditionally been used to study the flapping stability of slender elastic structures immersed in axial flow. These include the traditional hydrodynamic stability theory, which can be viewed as a fluid-centric approach, the structural acoustic or wave-based approach and the aeroelastic theory or structure-centered approach. A number of detailed experimental studies have also been conducted including soap-film, water-tunnel and wind-tunnel experiments. If the flow velocity is below a certain critical value, the structure remains unmoved or in a so-called stretched-straight state. Above the critical flow velocity, the structure undergoes self-sustaining and regular flapping, while at a much greater velocity irregular and chaotic flapping results. In terms of structural length, it has been shown that below a critical length the structure always remains in the stretched-straight state. Most theoretical studies have been restricted to linear analyses and two

dimensions, whilst only a few studies have looked at the effect of multiple slender bodies. The use of computational methods may help to overcome these limitations.

The modal FSI approach was validated by application to a two-dimensional two degree-of-freedom airfoil. Theoretical methods predict a critical velocity of 51.5 m/s. The results from the transient analysis with an inlet velocity of 51.5m/s show constant amplitude flapping, Figure 4, which corresponds well with theoretical predictions.

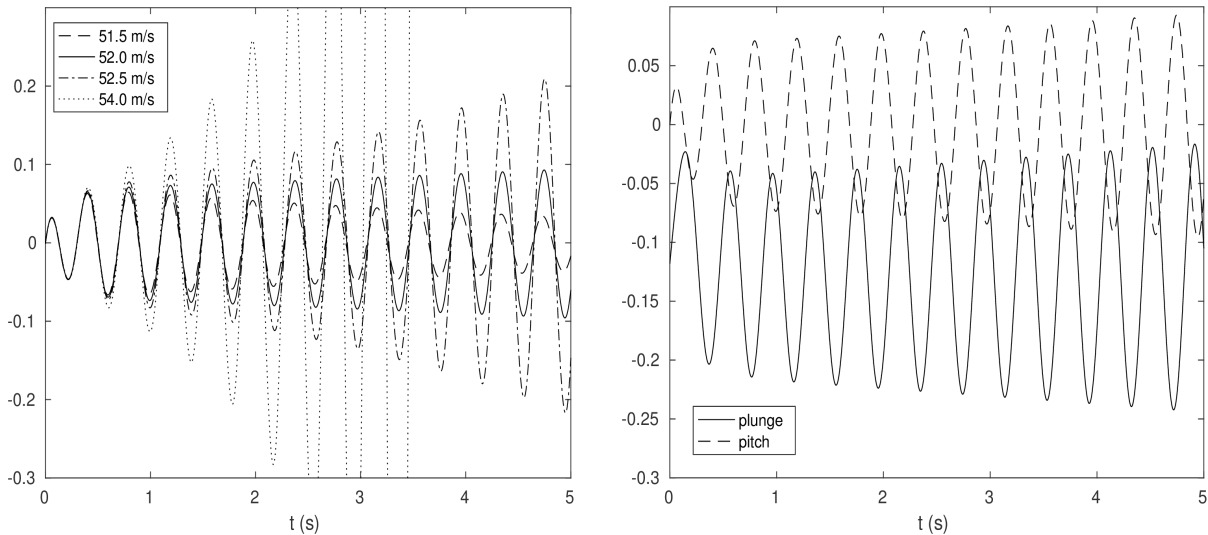


Figure 4: Flutter analysis of a two-degree-of-freedom airfoil.

A rigorous stability analysis of a two-dimensional finite plate under axial flow is conducted. The plate, which is initially at rest, is clamped at the leading edge and free at the trailing edge. A small initial perturbation is applied and the long-term transient behaviour of the plate is analysed. The bending rigidity of the structure stabilises the system, whilst an increase in aerodynamic pressure due to an increase in flow velocity destabilises the system and results in flutter. Following previous work^{13,14,15}, the critical stability curves can be defined in terms of the non-dimensional flag density and non-dimensional velocity. The critical stability curves are shown in Figure 5. Also shown on this figure are various points that were studied in this analysis. For comparison the flow is assumed to be inviscid in this case.

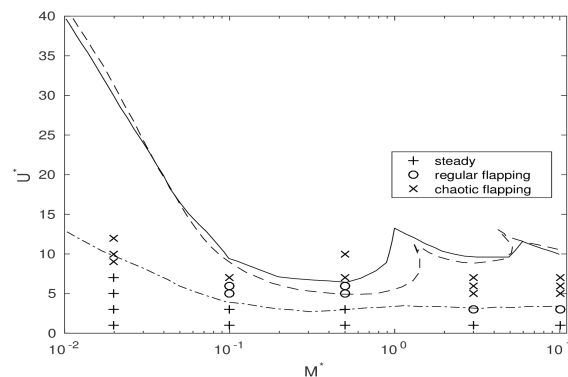


Figure 5: Critical stability curves for a finite flag under axial flow together with data points in this study.

The critical stability curves shown in Figure 5 contain branches that correspond to a different mode structure, as also observed experimentally by Eloy et al.¹⁴. The first branch for $M^* < 1$ corresponds with a flapping of the plate in its second mode of vibration, while the branch for $1 < M^* < 8$ corresponds with flapping in the third mode and $M^* > 8$ corresponds with the fourth mode. An analysis of the flapping behaviour shows good agreement with the results of Eloy et al.¹⁴ and Michelin et al.¹³. Snapshots of the flapping behaviour of the plate at $M^* = 0.002$ and $U^* = 9$ are shown in Figure 6. The second mode of vibration dominates this flapping behaviour and can be observed by the single node, or position of zero displacement, along the plate.

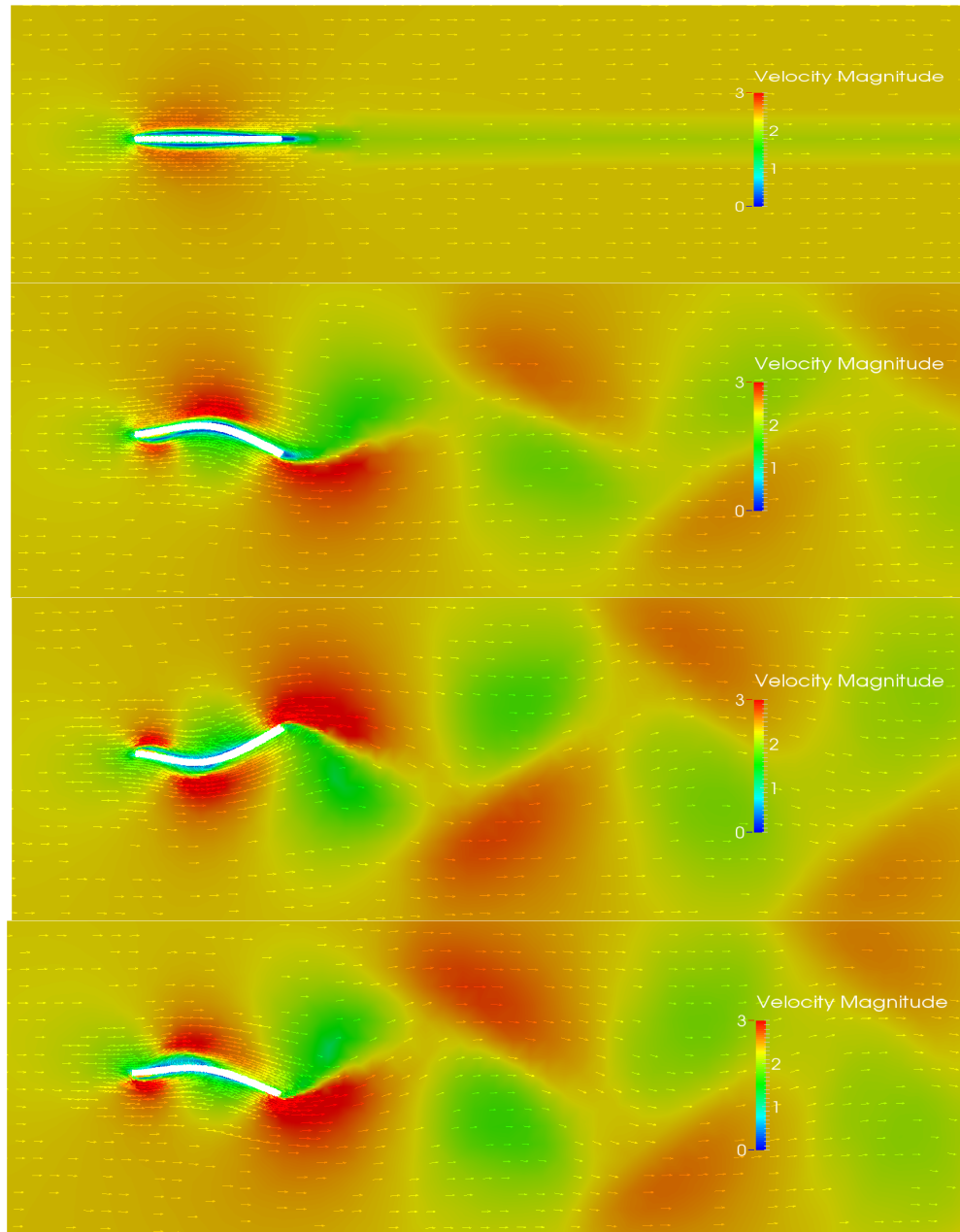


Figure 6: Snapshots of the flapping behaviour of the plate at $M^* = 0.002$ and $U^* = 9$.

12 REFERENCES

- [1] Zienkiewicz, O. C., and Taylor, R. L., 2000. *The Finite Element Method: Volume 2 - Solid Mechanics*, fifth ed. Butterworth-Heinemann, Oxford.
- [2] Patankar, S. V., 1980. *Numerical Heat Transfer and Fluid Flow*. McGraw-Hill, New York.
- [3] Suliman, R., Oxtoby, O., Malan, A., and Kok, S., 2014. “An enhanced finite volume method to model 2D linear elastic structures”. *Applied Mathematical Modelling*, 38(7-8), pp. 2265–2279.
- [4] Hubner, B., Walhorn, E., and Dinkler, D., 2004. “A monolithic approach to fluid–structure interaction using spacetime finite elements”. *Comput. Methods Appl. Mech. Engrg.*, 193, pp. 2087–2104.
- [5] Dettmer, W., and Peric, J., 2006. “A computational framework for fluid-structure interaction: Finite element formulation and application”. *Computer Methods in Applied Mechanics and Engineering*, 195, pp. 5754–5779.
- [6] Teixeira, P., and Awruch, A., 2005. “Numerical simulation of fluid-structure interaction using the finite element method”. *Computers and Fluids*, 34, pp. 249–273.
- [7] Slone, A., Pericleous, K., Bailey, C., and Cross, M., 2002. “Dynamic fluid-structure interaction using finite volume unstructured mesh procedures”. *Computers and Structures*, 80, pp. 371–390.
- [8] Weller, C. G. H., 2005. “A unified formulation for continuum mechanics applied to fluid-structure interaction in flexible tubes”. *International Journal for Numerical Methods in Engineering*, 64, pp. 1575–1593.
- [9] Suliman, R., Oxtoby, O., Malan, A., and Kok, S., 2015. “A matrix free, partitioned solution of fluid-structure interaction problems using finite volume and finite element methods”. *European Journal of Mechanics - B/Fluids*, 49A, pp. 272–286.
- [10] Hirt, C., Amsden, A., and Cook, J., 1974. “An arbitrary Lagrangian-Eulerian computing method for all flow speeds”. *Journal of Computational Physics*, 14, pp. 227–253.
- [11] Holzapfel, G., 2001. *Nonlinear Solid Mechanics: A continuum Approach for Engineering*. John Wiley & Sons Ltd., West Sussex, England.
- [12] Turek, S., and Hron, J., 2006. “Proposal for numerical benchmarking of fluid-structure interaction between an elastic object and laminar incompressible flow”. *Lecture Notes in Computational Science and Engineering*, 53(371).
- [13] Michelin, S., Stefan, G., Smith, L., and Glover, B. J., 2008. “Vortex shedding model of a flapping flag”. *Journal of Fluid Mechanics*, 617, Nov., p. 1.

[14] Eloy, C., Lagrange, R., Souilliez, C., and Schouveiler, L., 2008. “Aeroelastic instability of cantilevered flexible plates in uniform flow”. *Journal of Fluid Mechanics*, 611, Aug., pp. 97–106.

[15] Alben, S., and Shelley, M. J., 2008 “Flapping States of a Flag in an Inviscid Fluid: Bistability and the Transition to Chaos”. *Physical Review Letters*, 100(100), Jan., pp. 074301–1–074301–4.

Comparison between 1-D Versus 2-D Modelling Approach of Concrete Shell Design and Optimization

Concetta Sulpizio^{*}, Bruno Briseghella^{**}, Ivo Vanzi^{***}, Giuseppe Carlo Marano^{****}, Alessandra Fiore^{*****}

^{*}University of Chieti-Pescara "G. d'Annunzio", Pescara, Italy, ^{**}College of Civil Engineering, Fuzhou University, Fuzhou, Fujian, China, ^{***}University of Chieti-Pescara "G. d'Annunzio", Pescara, Italy, ^{****}Technical University of Bari, Bari, Italy, ^{*****}Technical University of Bari, Bari, Italy

ABSTRACT

During last years architecture is searching for new shapes inspired by natures. On the other hand, engineering is searching for lightweight structures and efficient application of materials. These are challenging goals for designers who want to combine these aspects. In this paper, different approach and related results have been compared. The first method is 1-D approach and it models the structure as a network of beams and nodes: this is the simplest one and it neglects some aspects. The second method is 2-D approach and it models the structure as a shell assembly: this is the finest one and can be useless for simplest cases. The aim of this work is to give to avantgarde designers an aid to optimal shape finding. He should use the right way in each case, avoiding serious mistakes choosing the simplest way when it is not applicable or the finest way when it is not necessary. The analyses involved two different types of surfaces: synclastic and anticlastic one. The optimization of shaping design could be conducted with different approaches. In this paper density methods has been used: Force Density Method FDM for 1-D and Surface Density Method SDM for 2-D. keywords: shell optimization, comparison approach, Force Density Method, Surface Density Method

Scaling laws in engineering science

Bohua Sun*

*Cape Peninsula University of Technology

ABSTRACT

The most powerful use of dimensional analysis (Bridgman [1]; Sedov [2]; Barenblatt [3]; Cantwell [4]; Sun [5, 6]) is to predict the outcome of an numerical experiment, depending on the variables, whilst providing theoretical insight [7]. Dimensional analysis may come across as simply trying to fit pieces of a puzzle together by trial and error. However, identifying the quantities that are relevant for a given problem is a demanding task, which requires deep physical insight [7]. The success or failure of using dimensional analysis depends on how to select the basic parameters of the problem. This may be done as follows: make a list of all quantities on which the answer must depend, then write down the dimensions of these quantities, and finally demand that these quantities should be combined into a functional form that provides the right dimension. This scheme was cast into a formal framework by Buckingham in 1921 and is often referred to as the Buckingham π -theorem [8]. Recently, the author has successfully applied the dimensional analysis to following complicated engineering problems [9–13]. In this paper, we will present our formulations for the problems of compressible turbulence, aquatic locomotion, capillary wrinkling of a thin film, as well as Kepler's third law of n-body periodic orbits in a Newtonian gravitation field. References [1] Bridgman, P.W. Dimensional Analysis. Yale University Press (1922) [2] Sedov, L.I. Similarity and Dimensional Analysis in Mechanics. Academic Press (1959) [3] Barenblatt, G.I. Similarity, Self-similarity and Intermediate Asymptotics. Cambridge University Press (1996) [4] Cantwell, B.J. Introduction to Symmetry Analysis. Cambridge University Press (2002) [5] Bohua Sun. Dimensional Analysis and Lie Group. China High Education Press (2016) [6] Bohua Sun. Dimensional analysis and applications. Phys. and Eng. (in Chinese) 26, 6(2016). [7] Hecksher, T. Insights through dimensions, Nature Physics, 13, 2017. [8] Buckingham, E. Phil. Mag. 42, 696–719 (1921). [9] Bohua Sun, The temporal scaling laws of compressible turbulence. Modern Physics Letters B, 30, 1650297 (2016) [10] Bohua Sun, Scaling laws of compressible turbulence, Applied Math Mech. 38(6):765–778 (2017) DOI 10.1007/s10483-017-2204-8 (the only Hot paper in the issue) [11] Bohua Sun, Scaling laws of aquatic locomotion, Sci. China-Phys. Mech. Astron. 60, 104711 (2017), doi: 10.1007/s11433-017-9073-1 [12] Bohua Sun, Capillary wrinkling scaling laws of floating elastic thin film with a liquid drop, Sci. China-Phys. Mech. Astron.61, 024721 (2018), <https://doi.org/10.1007/s11433-017-9116-5>

Dynamic Free Surface of Thermocapillary-Buoyancy Convection in Liquid Column

Chengtong Sun*, Ruquan Liang**

*School of Mechanical and Vehicle Engineering, Linyi University, Shangdong, China, **School of Mechanical and Vehicle Engineering, Linyi University, Shangdong, China; Northeastern University, Shenyang, China

ABSTRACT

The coupling of buoyancy convection and thermocapillary convection can be observed in the residual gravity, and its corresponding phenomenon is universal and important for industrial processes, particularly the space technology (such as heat exchangers in space station, life support system, and growth of crystal. In this paper, we investigate numerically the thermocapillary-buoyancy convection for large Pr number fluid under the residual gravity based on the improved mass conserving level set approach and a new algorithm which is used to capture any micro-scale migrations of dynamic free surface. Against former studies, the coupling influence of thermocapillary-buoyancy convection on the change of flow pattern and the free surface movement has been investigated simultaneously for the first time. Present results show that the flow modes can be divided into four stages: the inchoate thermocapillary convection, the dominated buoyancy convection, the balanced thermocapillary-buoyancy convection ($Bod=1.005$), and the dominated thermocapillary convection. The free surface shape of liquid column changes from the “?”-shape to the twisted “M”-shape, the standard “M”-shape corresponding balanced stage of thermocapillary-buoyancy convection (at $t=975$, $Bod=1.005$), and finally becomes “S”-shape corresponding the fourth stage ($Bod=0.98$). Meanwhile, there is a weak response disturbance on the dynamic free surface during the transformation process of each stage. In this paper, some peculiar phenomena are found, which are not limited only to the research on thermocapillary convection but also can provide the necessary theoretical basis for the nonlinear dynamical system control and the study on complex behavior in chemical and biological systems. The present work is supported financially by the National Natural Science Foundation of China under the grants of 51676031 and 51376040. References [1] Liang R Q, Yang S, Li J Z. Thermocapillary convection in floating zone with axial magnetic fields. *Microgravity Sci. Technol.*, 25:285-293, (2014) [2] Kawaji M, Liang R Q, M. Nasr-Esfahany, Simic-Stefani S, Yoda S. The effect of small vibrations on Marangoni convection and the free surface of a liquid bridge. *Acta Astronautica*. 58 622-632, (2006)

Slope Stability Assessment by Mixed Cover Meshless Method

Pan Sun^{*}, Yudan Gou^{**}, Yongchang Cai^{***}, Hehua Zhu^{****}

^{*}Tongji Univeristy, ^{**}Tongji Univeristy, ^{***}Tongji Univeristy, ^{****}Tongji Univeristy

ABSTRACT

In slope stability analyses, the traditional finite element method (FEM) encounters the mesh alignment problem mainly due to the complex slope geometry, layered and staged excavation sequences, multiple material interfaces and joints/faults/bedding planes. In this work, a recently proposed meshless method, i.e., the mixed cover meshless method (MCMM), is utilized combined with the strength reduction method (SRM) to obtain the potential sliding surface and the safety factor in slope stability assessment. In MCMM, an arbitrary computational geometry is discretized using regular square cells and local h-refinement in key regions is readily implemented using the quadtree data structure. The MCMM alleviates the necessity of generating conforming meshes in FEM and has advantages of a simple formulation, convenient computer implementation and low computational cost compared to classic meshless methods such as the element-free Galerkin method (EFGM) and the meshless method based on Shepard function and partition of unity (MSPU). The developed technique was applied to some benchmark examples and the accuracy, efficiency and robustness were verified by the agreement between modelling results and reference solutions.

Deep-learning Enhanced Computational Failure Mechanics across Multiple Scales

WaiChing Sun*

*Columbia University

ABSTRACT

We introduce a new hybridized deep-learning/material modeling framework to capture localized failures, in particular, shear bands and fracture across multiple length scales. This modeling framework introduces deep learning as a mean to connect simulations and data across different scales through recursive homogenization. Directed graph, a concept to analyze the hierarchy of information will be used to generate optimal configurations of hybrid deep-learning/material models for a given set of data across length scale such that the effects of evolving microstructures due to micro-cracks, plastic slip and wear can be propagated to the macroscopic scales. To ensure efficiency, an ensemble of theoretical and deep-learning-based material models of different sophistication will be used to predict constitutive responses within a phase field framework. Each phase field represents the weights of a model of a particular scale in the ensembled constitutive predictions. By evolving the phase fields, the ensemble predictions will always capture the domain of interests, such as the moving crack tips during crack growth or shear bands forming in the softening regime, with the most sophisticated predictions, while the far field predictions will be adaptively simplified for efficiency. These evolutions of the phase fields in the space-time continuum is controlled by the driving force. This driving force is a scalar function that depends on the results of validations. Meanwhile, unconventional information from the microstructures, such as coordination number, fabric tensors, void size distribution, grain size distribution, will be analyzed and put into the directed graph that represents the hybridized constitutive laws without hand-crafting new phenomenological models as surrogates.

Adaptive Peridynamics-FEM Superposition

Wei Sun^{*}, Jacob Fish^{**}

^{*}State Key Laboratory of Hydrosience and Engineering, Tsinghua Univ., ^{**}Civil Engineering and Engineering Mechanics, Columbia Univ.

ABSTRACT

An Adaptive Peridynamics-FEM superposition scheme based on the enrichment theory is proposed. It features a superposition of a nonlocal peridynamics and the underlying FEM mesh, and the appropriate using of the principle of virtual work that enforce equilibrium. Furthermore, the adaptive scheme is also designed to take advantage of the superposition based method without any need of remeshing the underlying mesh. Numerical studies are conducted for one-, two- dimensional problems. It is shown that the proposed method is patch test consistency and no spurious force founded.

Nonlinear Dynamic Buckling of Viscoelastic Plate Considering Higher Order Modes

Yuanxiang Sun*, Cheng Wang**

*Beijing Institute of Technology, **Beijing Institute of Technology

ABSTRACT

The nonlinear dynamic buckling of viscoelastic plates with large deflection is investigated in this paper by using chaotic and fractal theory. The problem of the simply-supported viscoelastic plate subjected to an in-plane periodic load is considered. The von Karman nonlinear geometry equations are introduced and standard linear solid model is employed. The nonlinear and dynamic governing equations of viscoelastic plates are the combination of the equilibrium equations and the deformation compatibility equation, which are nonlinear high-order integral partial differential dynamic equations. In order to obtain an accurate solution, the deflection function is expressed as a sinusoidal series with four terms rather than only one term in the computation (in the most of previous studies [1,2], the deflection function were expressed as a sinusoidal series with only one term). The Lyapunov exponent spectrum, the fractal dimension of strange attractors and the time evolution of deflection are obtained. The effect of high order modes on dynamic buckling of viscoelastic plate is obtained. References [1] Y.X.Sun, S.Y.Zhang. Chaotic dynamic analysis of viscoelastic plates. *International Journal of Mechanical Sciences*, 2001, 43: 1195-1208. [2] D.Touati, G..Cederbaum. Influence of large deflections on the dynamic stability of nonlinear viscoelastic plates. *Acta Mechanica*, 1995, 113, 215-231.

Effects of Geometric Parameters on the Fracture Mechanism of Bionic Suture Joint

Yupei Sun^{*}, Wenzhi Wang^{**}, Chao Zhang^{***}

^{*}Northwestern Polytechnical University, ^{**}Northwestern Polytechnical University, ^{***}Northwestern Polytechnical University

ABSTRACT

Fiber reinforced polymer composites have been widely used in the manufacture of high strength lightweight structures because of their superior mechanical properties. However, due to the brittle characteristic of the materials, the structure made of such materials has the defect of low fracture toughness. Moreover, this defect is magnified at the composite joint due to the stress concentration caused by the presence of drilling, adhesive and material stiffness mismatch, which eventually lead to structural premature failure. In the biological world, the long-term evolution process has created the rigid characteristics of bone structure. However, the connection between bone structures has taken a very special form - the suture joint. The suture joint can be described as a mixed connection composed of two rigid elements, which are connected by a thin, relatively compliant interface layer. With the deepening of the research, the advantages of this kind of joint on the mechanical properties have been discovered: on the one hand, the suture joint ensures the connecting stiffness, mechanical strength and impact energy absorption characteristics of bone connection in the growing process; on the other hand, the change the suture joint makes the mechanical properties of the interface area change constantly, and keeps higher adaptability when the environment changes. Inspired by the above biological suture joint, the bionic composite suture joint was developed. In this study, we transform the typical triangular tooth connection interface into a parameterized model of the suture joint structure based on the fractal algorithm. According to the parameters of the baseline shape, tooth angle and arc baseline amplitude of the connection structure interface, the mechanical properties of this structure were studied by combining experimental and numerical simulation. In experimental, based on the parameterization construction method of the suture joint, these structure models with different parameters were made by 3D printing technology, and the structural bearing properties with different geometric parameters were obtained under tensile load. In numerical simulation, the parameterized numerical models of the suture joint were built and calculated based on the finite element method, and the correctness of the numerical model was validated by comparing with experimental. The experimental and numerical results displayed excellent performance of this kind of structure in controlling the fracture toughness, and the influences of geometric parameters on the fracture toughness were summarized.

The Mechanical Properties of the Boron Nitride Hexagonal Nanosheets

Yuzhou Sun*

*Zhongyuan University of Technology

ABSTRACT

This paper presents a multiscale method to study the mechanical properties of the hexagonal nanosheets of boron-nitride. A nanosheet is viewed as a higher-order gradient continuum planar sheet, in which the strain energy density depends not only on the first-order deformation gradient but also on the second-order deformation gradient. A representative cell is imaged on at a point where the constitutive response needs to be evaluated. The higher-order Cauchy-Born rule is used to approximate the bond vectors in the representative cell, and the minimizing of the strain energy density results with the constitutive relationships. The elastic constants, including Young's modulus, shear modulus, Poisson's ration and bending rigidity, are calculated by analyzing the physical meaning of the first- and second-order strain gradients. The developed model can also be used to study the nonlinear behavior of nanosheets under some simple loading situations, such as the uniform tension, torsion and bending. The stress-strain relationship of nanosheets is presented in the environment of uniform tension.

Optimization of Truss-Type Fiber Reinforced Plastic Composite Structures Based on Moving Morphable Components Method

Zhi Sun^{*}, Weisheng Zhang^{**}, Junfu Song^{***}, Xu Guo^{****}

^{*}Dalian University of Technology, ^{**}Dalian University of Technology, ^{***}Dalian University of Technology, ^{****}Dalian University of Technology

ABSTRACT

Fiber reinforced plastic (FRP) composite structures, which possess advanced specific stiffness and strength, have been widely used in various fields, for instance, transporting vehicles, wind turbine, and other light weight structures. For decades, extensive studies have been made, especially in the designing and analyzing of FRP composite structures, which further triggers the development of stacking sequence method and topology optimization method. However, typical FRP composite shell structures, including aircraft radar domes, composite overwrapped pressure vessel, and wind turbine blade, are designed into the geometry with changing curvature radius to meet aerodynamic or gas-tightness requirements. By using common plying or overwrapping process, the fiber angle and thickness of the aforementioned FRP composite structures would change along with the curvature radius of structure. However, the exist stacking sequence method and topology optimization method fail to consider the manufacture-driven change of fiber angle and thickness, and therefore left a gap to fill in. In this study, Moving Morphable Components (MMC) method, which is able to explicitly describe the geometry of structures, is used to perform topology optimization for FRP composite structures with beam-type or truss-type geometry. The FRP composite structures are considered to be manufactured based on geodesic winding, with fiber plying angle and thickness calculated according to the curvature radius of each beam. The stiffness and deformation of FRP composite structures are then analyzed by Finite Element Method. Composite frame of bicycle and vertical plate of aircraft wing are selected as numerical examples. The numerical results indicate the validity of the proposed optimization method.

Uncertainty in Cardiac Myofiber Orientation and Stiffnesses Dominate the Variability of Left Ventricle Deformation Response

Joakim Sundnes^{*}, Rocio Rodriguez-Cantano^{**}, Marie Rognes^{***}

^{*}Simula Research Laboratory, ^{**}Simula Research Laboratory, ^{***}Simula Research Laboratory

ABSTRACT

Computational cardiac modelling is a mature area of biomedical computing, and is currently evolving from a pure research tool to aiding in clinical decision making. Assessing the reliability of computational model predictions is a key factor for clinical use, and uncertainty quantification (UQ) and sensitivity analysis are important parts of such an assessment. In this study, we apply new methods for UQ in computational heart mechanics to study uncertainty both in material parameters characterizing global myocardial stiffness and in the local muscle fiber orientation that governs tissue anisotropy. The uncertainty analysis is performed using the polynomial chaos expansion (PCE) method, which is a non-intrusive meta-modeling technique that surrogates the original computational model with a series of orthonormal polynomials over the random input parameter space. In addition, in order to study variability in the muscle fiber architecture, we model the uncertainty in orientation of the fiber field as an approximated random field using a truncated Karhunen-Loeve expansion. The former is used as a basis to build a reduced-dimensionality representation of the random field, essential to manage UQ analysis in extremely high-dimensional problems. Although the fiber arrangement exhibit a typical gross architecture, there are local and individual variations through the ventricular wall, as well as uncertainty derived from noisy measurements that may affect the global mechanical properties of the model. The results give insight into the applicability of the truncated KLE method for representing noisy fiber architecture fields, and demonstrate a substantial impact of fiber angle variations on the selected outputs, highlighting the need for accurate assignment of fiber orientation in computational heart mechanics models. Furthermore, the uncertainty and sensitivity analysis of global material parameters identify clear differences in their impact global output quantities. An interesting finding is that the impact of local uncertainty, or noise, in the fiber field appears to be significantly larger than the impact of uncertainty in the global parameters determining the fiber direction. This result indicates that as long as the organized, helical structure of fiber orientation is maintained, the actual helix angle has a moderate impact on the mechanical properties of the ventricle. However, as noise is introduced so that the helical structure is lost, the mechanical properties are severely affected.

Ductile Fracture Initiation Analyses with Consideration of Stress Triaxiality ahead of Axial Crack Fronts in Pressure Tubes of Hydrided Irradiated Zr-2.5Nb Materials without and with Split Circumferential Hydrides

Shin-Jang Sung^{*}, Jwo Pan^{**}, Poh-Sang Lam^{***}, Douglas A. Scarth^{****}

^{*}University of Michigan, ^{**}University of Michigan, ^{***}Savannah River National Laboratory, ^{****}Kinectrics Inc.

ABSTRACT

Ductile fracture initiation with consideration of stress triaxiality ahead of the fronts of axial cracks in pressure tube (PT) specimens of hydrided irradiated Zr-2.5Nb materials without and with split circumferential hydrides at room temperature is examined by conducting three-dimensional finite element analyses with submodeling. First, a strain-based failure criterion with consideration of stress triaxiality is developed from the Gurson yield model with use of the experimental/computational results of transverse tensile tests and the effective plastic strain of the critical material element in CT specimens without hydride at fracture initiation. Next, three-dimensional finite element analyses of PT specimens of irradiated Zr-2.5Nb materials without and with three pairs of split circumferential hydrides are conducted with the similar mesh design, the same material definition, and the same applied stress intensity factor as those for CT specimens. The results of the three-dimensional finite element analysis of a PT specimen of irradiated Zr-2.5Nb materials without split circumferential hydrides suggest that circumferential hydrides ahead of the crack front in the middle of a PT specimen should fracture for the given internal pressure corresponding to the fracture toughness of the irradiated Zr-2.5Nb materials without circumferential hydrides. Based on the strain-based failure criterion with consideration of stress triaxiality, the applied stress intensity factor to reach the failure criterion at a critical distance ahead of the axial crack front in the middle of the thickness of an unhydrided irradiated PT specimen is 3% higher than that obtained from the computational results of unhydrided irradiated CT specimens. For a PT specimen with three pairs of split circumferential hydrides with various heights and ligament thicknesses along the crack front, three types of strain concentration are shown in the middle of the ligaments ahead of the crack front. The strain concentration is higher when the ratio of the ligament thickness to the hydride height is less than 3. The computational results suggest that with the strain-based failure criterion with consideration of stress triaxiality, only 60% to 70% of the internal pressure for fracture initiation of an unhydrided irradiated PT specimen is needed to fracture a hydrided irradiated PT specimen with many randomly distributed split circumferential hydrides along the crack front. The computational results can be used to explain the near 35% reduction of the fracture toughness at room temperature obtained from hydrided irradiated PT specimens when compared with that from unhydrided irradiated ones.

Non-Equilibrium Molecular Dynamics Simulations of Interfacial Wetting Behavior between Single Walled Carbon Nanotubes and Liquid Copper

Bryan Susi*, Jay Tu**

*Applied Research Associates, Inc., **North Carolina State University

ABSTRACT

Multi-scale simulations with molecular resolution are more tractable now than ever and these simulations can have an overwhelmingly positive impact in many scientific disciplines if the practitioner fully understands the methods and models. These lessons are even more applicable for Non-Equilibrium Molecular Dynamics (NEMD) simulations. In this work, nano-scale NEMD simulations of a Single Walled carbon Nanotube (SWNT) intrusion into liquid copper in a Wilhelmy Balance configuration are performed to determine the propensity for incorporation of a SWNT in liquid copper. The objective of this research is ultimately to contribute to the understanding of how to fabricate Carbon Nanotube-Metal Matrix (CNT-MM) composites when the nanotubes are not wetted by the metal. This is a challenging problem with many underlying phenomena to investigate, but specific to this presentation will be results pertinent to selection of the appropriate MD pair-potential models, a new parameter set for the Morse potential model between carbon and copper which adequately describes their interfacial behavior, and an evaluation of the rate of carbon nanotube intrusion from the Wilhelmy-Balance simulations with emphasis on SWNT accommodation in the liquid medium. The primary contributions to the field are the new pair-potential coefficients to model the correct static contact angle between liquid copper and sp² hybridized carbon surfaces, a framework for accurate NEMD simulations of a nanoscale Wilhelmy-Balance experiment, and deviations between the molecular scale results and continuum fluid mechanics relationships as a function of nanotube intrusion rate.

Electrospinning Process Simulation for the Application in Predictive Cardiovascular Disease

Tijana Sustersic*, Liliana Liverani**, Aldo R. Boccaccini***, Nenad Filipovic****

*Faculty of Engineering, University of Kragujevac, 34000 Kragujevac, Serbia; Bioengineering Research and Development Center (BioIRC), 34000 Kragujevac, Serbia, **Institute of Biomaterials, University of Erlangen-Nuremberg, 91058 Erlangen, Germany, ***Institute of Biomaterials, University of Erlangen-Nuremberg, 91058 Erlangen, Germany, ****Faculty of Engineering, University of Kragujevac, 34000 Kragujevac, Serbia; Bioengineering Research and Development Center (BioIRC), 34000 Kragujevac, Serbia

ABSTRACT

The aim of this research was to simulate two-phase electrospinning jet from the syringe nozzle to the collector by using computational methods. Previous numerical studies have dealt only with one-phase flows or had too many simplifications when it comes to electrospinning process [1]. Since the application of electrospinning lies in manufacturing of cardiovascular implants (to allow and promote cell infiltration within the scaffolds), as well as in fiber modification methods for improving myocardial regeneration (various biodegradable polymers can be used for fiber fabrication) [2], these kind of simulations can offer a full insight into coupled physical laws that govern the process. This will be useful for optimization of the electrospinning parameters reducing the trial-and-error approach, decreasing the amount of chemicals, reducing waste management and equipment maintenance costs. Data obtained during experiments with 10wt% PVA solution were used as input for computational simulation. Three voltage pairs (15kV applied on the nozzle, 0kV on the collector; 13kV applied on the nozzle, -2kV on the collector; 20kV applied on the nozzle, 0kV on the collector) were investigated in order to examine their effect on jet shape and implicitly fiber structure. A two-phase flow model is simulated using turbulent k- ϵ model, volume of fluids (VOF) for the interphase region between the polymer and air and Magnetohydrodynamics(MHD) model for the behavior of the polymer in strong electric field. The simulation results show good agreement with experiments in terms of outcome - no fiber differences in experiments were present when proposed voltage pairs were used as boundary conditions, and similar jet shapes were obtained during simulations. These jet shapes for electrospinning are also visually very different from jet shapes when non-optimal parameters are used. This confirms the hypothesis that the jet shape during electrospinning can be a factor of indication whether the chosen electrospinning parameters would result in fibers with good quality. Differences that may occur between experiments and simulation can be a result of simplifications in simulations; influence of uniform and non-uniform electric field, as well as adopted parameters that were used based on literature values and could not be determined experimentally at this point. [1] Spivak, A. F., Dzenis, Y. A., &&& Reeker, D. H. (2000). A model of steady state jet in the electrospinning process. *Mechanics research communications*, 27(1), 37-42. [2] Kim, P. H., &&& Cho, J. Y. (2016). Myocardial tissue engineering using electrospun nanofiber composites. *BMB reports*, 49(1), 26.

Tunable Architected Metamaterials for Bone Implants

Alok Sutradhar*, Jaejong Park**

*The Ohio State University, **The Ohio State University

ABSTRACT

The design of medical bone implants involves multiscale consideration. The structure in macro level needs to satisfy the space, functional, aesthetic and load-transfer requirements. Additional considerations of stress-shielding and localized stress-concentrations to improve the effectiveness and functionality can be increased using architected metamaterials. For example, the mechanical properties of the bone implants and their adjacent bone need to be similar to reduce these effects. Topology optimization is a numerical tool that is suitable for obtaining optimized geometries under several constraints. Earlier efforts used inverse homogenization technique to attain the microstructures of scaffold geometries. These equivalent material model would be valid when there is a significant dimensional difference between the large and the small scales. With recent advances, 3D printing of multiscale multi-material structures is realizable. We present an approach to design tunable architected metamaterials for implants which may alleviate localized stress-concentration and stress-shielding. We develop a topology optimization framework to design the architecture materials in different scales which varies smoothly within the design domain. The preliminary study shows easy control in connectivity and provides more topological variability. The metamaterial implant models designed using the methodology in this work are 3D printed, and their performance is studied using mechanical testing.

Model Parameter Identification of Keloid-Skin Undergoing Large Deformations

Danas Sutula^{*}, Emmanuelle Jacquet^{**}, Jerome Chambert^{***}, Arnaud Lejeune^{****}, Franz Chouly^{*****}, Stéphane Bordas^{*****}

^{*}Université Bourgogne Franche-Comté, ^{**}Université Bourgogne Franche-Comté, ^{***}Université Bourgogne Franche-Comté, ^{****}Université Bourgogne Franche-Comté, ^{*****}Université Bourgogne Franche-Comté, ^{*****}Université du Luxembourg

ABSTRACT

The aim of this paper is to characterize the mechanical behavior of cutaneous tissues with the long-term goal to prevent keloid development in patients. Keloids are non cancerous tumors that grow continuously on the skin for several reasons. These specific tumors affect 11 million patients of all ages and are particularly common in Asian and African populations. The evolution of keloids is related to genetic, biological, biophysical, and biomechanical factors. Here we focus on the biomechanical influence, such as the state of stress inside a keloid and in the surrounding skin, which is known to play an important role. To predict the stresses in the keloid-skin, the patient-specific mechanical behavior of the keloid-skin needs to be determined. To this end, we present a patient-specific methodology for the identification of the hyper-elastic keloid-skin model parameters. In our approach, a keloid is observed on a patient using ultrasound and optical microscopy. The 3D image of the surface is used to develop the keloid-skin geometrical model. The hyper-elastic material model parameters for the healthy skin and the keloid are determined using an inverse analysis approach; essentially, the parameters are obtained by minimizing the mismatch between the numerical and the experimentally obtained displacements on the surface of the keloid-skin. The experimental measurements are obtained in-vivo using a custom-made extensometer and a digital image correlation technique. The inverse analysis is carried out incrementally over a series of loading steps. The motivation is to observe any variability in the model parameters during the different levels of loading. Significant variability in the model parameters would suggest a limitation of a particular hyper-elastic model to characterise the keloid-skin effectively due to the parameter dependence on the applied load. In the end, we are able to select a hyper-elastic model and determine the model parameters that adequately characterize the keloid-skin for the range of loading conditions of practical interest. We then investigate the nature of the stress field at the interface between the healthy skin and the keloid. The knowledge of the stress field has the potential to help design a specific device able to contain the growth of the keloid; this, however, is the topic of further investigation. Our next steps will focus on quantifying the sensitivity of the model parameters to the uncertainty in the experimental measurement data.

Generalized Fractional-Order Visco-Elasto-Plasticity with Damage for Anomalous Materials

Jorge Suzuki^{*}, Mohsen Zayernouri^{**}

^{*}Department of Computational Mathematics, Science, and Engineering (CMSE), Michigan State University,

^{**}Department of Computational Mathematics, Science and Engineering (CMSE); Department of Mechanical Engineering, Michigan State University

ABSTRACT

In this work we introduce an efficient framework that uses a generalized, fractional-order visco-elastic model, coupled to a fractional-visco-plastic component [1] and a modified Lemaitre damage model to introduce material degradation. The visco-plastic/damage coupling is thermodynamically consistent, with the constitutive laws derived using appropriate fractional-order Helmholtz free-energy potentials [2]. The dissipation potential for visco-plasticity is defined by the use of a time-fractional yield function. The damage potential has the same form as the classical Lemaitre approach, but the damage energy density release rate is described by a fractional-order potential. We perform a time-fractional integration of the resulting system of FODEs using a fractional return-mapping algorithm, with fast convolution scheme with computational complexity $O(n \log(n))$. The model is then implemented in a Finite Element framework for the analysis of geometrically nonlinear trusses. To the authors knowledge, this is the first contribution that couples a fractional visco-elasto-plastic model with damage in a thermodynamically consistent way. References: [1] J.L. Suzuki, M. Zayernouri, M.L. Bittencourt, and G.E. Karniadakis. Fractional-order uniaxial visco-elasto-plastic models for structural analysis. *Computer Methods and Applied Mechanics and Engineering*, 308:443 – 467, 2016. [2] A. Lion. On the thermodynamics of fractional damping elements. *Continuum Mech. Thermodyn.*, 9:83 – 96, 1997.

Three-stage Failure Simulation with Dynamic Frictional Contact Based on Co-rotational Technique

Shun Suzuki^{*}, Kenjiro Terada^{**}, Shuji Moriguchi^{***}, Norio Takeuchi^{****}

^{*}Tohoku University, ^{**}Tohoku University, ^{***}Tohoku University, ^{****}Hosei University

ABSTRACT

Based on the co-rotational formulation to deal with large displacements and rotations of a solid, we propose a method of three-stage failure simulation of brittle materials and structures involving dynamic contact behavior. On the premise of the standard three-dimensional finite element method with tetrahedral and hexahedral elements, a finite element model is composed of multiple blocks, each of which is constructed with several sets of elements. Here, the interface between adjacent blocks are assumed to be potential discontinuities equipped with the cohesive-zone model and the penalty method is employed to connect these sets of blocks, each of which is supposed to move and deform independently after complete separation without cohesive forces. Then, one of them possibly hits other blocks and divides some of them into several sub-blocks. The so-called node-to-segment approach is employed for non-matching meshes of blocks contacting with each other. In addition, the augmented Lagrangian method is applied to the constrained optimization problem associated with the bilateral contact with friction. In order to obtain stable solutions even after the complete failure, we adopt the energy-momentum conservation method for time-integration. To this end, the energy dissipation due to the stick/slip frictional behavior is also considered based on the Coulomb friction law. The three stages we are concerned with in our numerical simulations are the following: • At the first stage: a structure deforms in response to dynamic or static excitations and displays cracks along prescribed discontinuities so that it would be separated into several blocks. • At the second stage: several sets of blocks lose static equilibria and start to move dynamically. • At the third stage: moving blocks collide each other with friction and some of them further break up due to the shock generated by the collision. The proposed method has been designed to enable us to simulate all of these deformation and failure stages continuously. The implementation of the formulation is verified by conducting some numerical tests with a simple structure containing a potential discontinuity. Also, several numerical examples are presented to demonstrate the capability and performance of the proposed method to simulate three-stage failure processes involving large deformation and rotations with dynamic frictional-contact behavior.

Hysteretic Modeling Method by Recurrent Neural Network

Takuya Suzuki*, Yasutomo Matsuoka**

*Takenaka Corporation, **Takenaka Corporation

ABSTRACT

In nonlinear structural analyses, it is important to use an accurate hysteretic model. However, there are some materials and structural members that have too complex hysteresis to make hysteretic model for analysis for human. For such situations, we propose to use a recurrent neural network (RNN) system. A recurrent neural network is one of neural network. It can be changed by a system based on previous hysteresis inputs and outputs. The aim of this study was to confirm the applicability of RNN modeling method to the normal bilinear model of nonlinear hysteresis that is most popular model in structural analysis. First, we identified RNN model with long short-term memory (LSTM) using training data comprising bilinear historical displacement as input and force as output data. Then, it was confirmed that the identified RNN model could be applied to the system, and that it was equivalent to a theoretical bilinear model. As a result, following findings are obtained: (1) A RNN model with LSTM units is required for a bilinear system. This was determined using training data comprising theoretical bilinear input-output data. Comparison of the output of the identified RNN model with that of a theoretical model revealed good agreement. The changeability of an RNN by a system based on previous hysteresis inputs and outputs was confirmed in the case of basic hysteretic bilinear model, which is often used for structural seismic design. (2) The sparsity of the weight matrix of the identified RNN model was investigated. The weight matrix does not have sparsity when its layer contained "drop out". This indicated that the RNN model was very large and had many weight coefficients, which would make its analysis very difficult. The findings of this study show the applicability of RNN modeling to structural hysteresis. However, there is the need for further improvement of the procedure.

The Influence of Elastic Heterogeneity on the Strength of Dislocation-Obstacle Interactions

Benjamin Szajewski^{*}, Joshua Crone^{**}, Jarek Knap^{***}

^{*}Army Research Laboratory, ^{**}Army Research Laboratory, ^{***}Army Research Laboratory

ABSTRACT

The Influence of Elastic Heterogeneity on the Strength of Dislocation-Obstacle Interactions. B. A. Szajewski, 1, J. C. Crone, J. Knap Army Research Laboratory Abstract The interaction between glissile dislocations and spherical obstacles (e.g., voids and precipitates) within a continuum is responsible for marked increases in material strength. Due to their desirable engineering features, dislocation-obstacle interactions have been the subject of theoretical study for many decades [1,2]. Despite ongoing efforts, these studies have often been limited to crude approximations whose validity is difficult to assess. Towards enhancing our understanding of these complex interactions, we employ a three dimensional coupled dislocation dynamics and finite element method computational scheme [3] to directly compute the strength (i.e. Orowan stress) of a variety of dislocation-obstacle interactions. The coupled framework accounts for elastic mismatch between the host matrix and obstacles via the inclusion of elastic image stresses and stress concentrations computed through the finite elements. Our simulations span a range of elastic mismatch, linear obstacle densities, and sizes. Additionally, the influence of the surface formation energy on both the obstacle strength and critical dislocation nucleus size is explored via the introduction of a tunable parameter, γ_{surf} . Through our simulations, we demonstrate the influence of these four parameters on both the final stable configuration, and the dislocation-obstacle strength. We devise a simple mechanical model which yields insight into the results of both our numerical simulations as well as others found within the literature. 1. D. J. Bacon, U. F. Kocks and R. O. Scattergood, Philosophical Magazine 28:1241 (1973), DOI: 10.1080/14786437308227997 2. R. O. Scattergood and D. J. Bacon, Acta Metallurgica 30:1665 (1982), DOI: 10.10116/0001-6160(82)90188-2 3. J. C. Crone, P. W. Chung, K. W. Leiter, J. Knap, S. Aubry, G. Hommes, A. Arsenlis, Modelling and Simulation in Materials Science and Engineering 22:035014 (2014), DOI: 10.1088/0965-0393/22/3/035014

Altered Collagen Organization in Fatigue-Loaded Tendon Initiates Changes in Cell Mechanotransduction

Spencer Szczesny^{*}, Tristan Driscoll^{**}, Pen-Hsiu Chao^{***}, Robert Mauck^{****}

^{*}Pennsylvania State University, ^{**}University of Pennsylvania, ^{***}National Taiwan University, ^{****}University of Pennsylvania

ABSTRACT

A primary cause of tendon degeneration is overuse (i.e., fatigue loading), which produces microscale damage of collagen fibrils and the accumulation of atypical tissue components (e.g., cartilaginous, fat, and calcium deposits) [1]. Why resident tenocytes produce these atypical matrix deposits rather than repair the native tissue structure is unknown. We hypothesized that fatigue damage induces changes in the tissue mechanical microenvironment (e.g., stiffness, topography), which alters the biophysical stimuli presented to tenocytes and leads to their adoption of abnormal (i.e., non-tenogenic) phenotypes. To test this hypothesis, we investigated the effects of fatigue loading on tendon microscale structure and mechanics using multiphoton microscopy and atomic force spectroscopy. Surprisingly, we found no change in the local tissue modulus after fatigue loading, despite widespread collagen fiber kinking and molecular denaturation. These data suggest that changes in tissue structure (i.e., altered collagen fiber crimping) may be responsible for early changes in tendon cell phenotype as a consequence of fatigue loading. To investigate this further, we used crimped electrospun nanofibrous scaffolds [2] to investigate the role of altered fiber crimping on cellular mechanobiology. Specifically, we used a fiber-reinforced structural constitutive model [2] to characterize the mechanics of these scaffolds as a function of fiber crimp and investigated the effect of crimping on mesenchymal stem cell (MSC) mechanotransduction. We found that MSCs seeded on crimped scaffolds (compared to straight fiber controls) had increased ERK activation in response to static stretch. Interestingly, nuclear aspect ratios were increased with stretch to similar amounts on both scaffold types, suggesting that the effect of the crimped scaffolds was not due to increased strain transmission from the scaffold to the cells. Instead, based on the results of our structural constitutive model, we found a significant stress response from fiber-fiber interactions/reorientations within the crimped scaffolds that are absent in the straight fiber controls. These results suggest that cell mechanotransduction is sensitive to the local fiber topography and that increased fiber reorientation associated with collagen disorganization in fatigue-loaded tendons may initiate the tissue remodeling responsible for tendon degeneration. Future work will investigate and model the effects of fatigue loading on the microscale mechanics and endogenous cellular mechanotransduction in live tendon explants. Such information will determine the role of mechanical loading in tendon degeneration and identify mechanotransduction signaling pathways as potential therapeutic targets. [1] Kannus & Jozsa 1991 JBJs 73:1507-25; [2] Szczesny et al. 2017 ACS Biomater Sci Eng 3: 2869-2876.

Discrete Methods in Ice Accretion Modelling

Krzysztof Szilder*, Edward Lozowski**

*National Research Council Canada, **University of Alberta

ABSTRACT

Atmospheric icing due to freezing rain and freezing drizzle occurs when large, airborne supercooled water drops freeze on objects they encounter. The resulting ice can accumulate to a thickness of several centimetres during severe freezing rain events called ice storms. This ice can be hazardous for ground-based engineering structures such as overhead transmission lines, wind turbines, telecommunication masts and bridge cables. And it is especially hazardous to aircraft, where the build-up of ice due to impinging supercooled cloud droplets changes the stability and control characteristics of aerodynamic surfaces. Most current icing models are constrained in their verisimilitude by their reliance on solving continuous partial differential equations and their boundary conditions. By definition, continuous PDE's and their boundary conditions require that the simulated ice accretions have continuous properties, unless the discontinuities are known ahead of time. But typically they are not. We have circumvented these limitations by developing an original icing modelling capability, which we call "morphogenetic". It is based on a discrete formulation and simulation of ice formation physics. The original 2D development of this unique approach for the prediction of ice accretion shapes in the aerospace industry is given in [1]. Recent 3D modelling advances are described in [2-3]. The morphogenetic approach considers the behaviour of discrete ensembles of cloud drops, which impinge, move along the icing surface and freeze according to physically-based, stochastic rules. In essence, the method simulates ice accretion in the way it occurs naturally – drop by impinging drop. Because of this, it improves on existing ice accretion models. For example, it is capable of predicting complex ice accretions, such as simultaneous rime and glaze, ice accretions with variable density and discontinuous ice accretions such as rime feathers, lobster tails and icicles. It is also capable of predicting ice accretions on substrates with complex geometry, ranging from aircraft instrumentation and engines to power line insulators. [1] K. Szilder and E.P. Lozowski, "Novel Two-Dimensional Modeling Approach for Aircraft Icing", *Journal of Aircraft*, 41, 4, 854-861 (2004). [2] K. Szilder and E.P. Lozowski, "Three-Dimensional Numerical Simulation of Ice Accretion using a Discrete Morphogenetic Approach", *AIAA AVIATION Forum*, AIAA 2017-3418 (2017). [3] K. Szilder, "Theoretical and Experimental Study of Ice Accretion due to Freezing Rain on an Inclined Cylinder", *8th Int. Conference on Snow Engineering*, 183-192 (2016).

Fluid Structure Interaction Simulation for the Prediction of Car Water Crossing and Aquaplaning Using ESI Virtual Exterior Solution

Alain TRAMECON*, Matthias Schäfer**, Matia Oriani***

*ESI Group, **ESI Group, ***ESI Group

ABSTRACT

To develop cars and in particular electrical and autonomous cars, it is important to virtually test the car in real driving circumstances, including on wet road or under heavy rain conditions. ESI Group has introduced Virtual Exterior Solution which includes the Finite Point Method (FPM) technology as a CFD mesh free module to simulate the interaction of water with the car structure. It is used as a standard product in the industry for getting predictive airbag deployment simulation, tank sloshing and water drain applications and is now extended to other application fields like water crossing simulation and tire hydroplaning prediction. The objective is to enable a holistic prediction of the car behavior under realistic driving conditions, using a virtual car prototype. Detailed water behavior is accounted for, along with the deformation of structural part (tire, suspension, car body), in order to:

- Predict car drivability for water crossing for deep as well as shallow water crossing scenarios.
- Help tire design accounting for detailed thread geometry, tire pressure, and road conditions.
- Prevent accidental failures of structural parts due to water splash and brutal thermal effects by predicting the structural deformations in a fully coupled mode.

A technical introduction of the FPM mesh free technology, part of Virtual Exterior Solution will be shown. Validation cases vs. experimental results will be documented regarding fluid structure interaction. In a second part, current application examples will be presented covering deep car water crossing simulations and aquaplaning cases, focusing on fluid interaction with deformable structures.

A Fractional-order PID Controller Design Based on Fractional Calculus for Enhanced Performance of Dead-time Processes

LUAN VU TRUONG NGUYEN*, HOAI SON NGUYEN**, TAN HAI PHAN***, MAI VAN TRAN****

*FIRST AUTHOR AND CORRESPONDING AUTHOR, **CO-AUTHOR, ***CO-AUTHOR, ****CO-AUTHOR

ABSTRACT

A design method for the fractional-order proportional-integral-derivative controller based on fractional calculus is proposed in this paper. The analytical tuning rules are derived for achieving the performance improvement for both disturbance rejection and set-point tracking problems. Many illustrative examples are considered to confirm the effectiveness of the proposed algorithm for both integer and fractional order processes with time delays. In addition, the robust stability of fractional-order system is also carried out in order to demonstrate that the proposed fractional-order PID controller can hold well the robustness against perturbation uncertainty in the process models.

A Coupled Peridynamics/Finite Element Method for Modeling Dynamic Fracture

Alireza Tabarraei*, Shank Kulkarni**, Xiaonan Wang***

*University of North Carolina at Charlotte, **University of North Carolina at Charlotte, ***Ansys Software Company

ABSTRACT

Peridynamics is a nonlocal continuum model which, in contrast to other continuum models, uses integration instead of spatial derivations in its governing equations. Utilizing integration instead of derivatives is advantageous in modeling fracture since the governing equations remain valid even after the initiation or growth of discontinuities. Although peridynamics can model material behavior and fracture with a higher accuracy than classical continuum mechanics, however, nonlocal formulation makes peridynamics computationally expensive. To reduce the computational costs, we propose to couple peridynamics with local continuum domain (discretized by finite elements) using peridynamics only in small zones where higher accuracy is needed, e.g. vicinity of crack tips, and finite elements elsewhere where the solution is smooth. In the proposed multiscale model, peridynamics captures all the fine-scale behavior which finite element model is not able to capture. The main challenge in developing such a concurrent multiscale method is to eliminate the artifacts introduced by the interface of the two subdomains. One of the main issues that arises in dynamic coupling is spurious wave reflections; the high frequency (short wavelength) waves traveling from peridynamic cannot enter the finite element zone. The interface acts as a rigid boundary to the high-frequency waves, making them reflect back into the peridynamic zone. Hence, if the two subdomains are not appropriately linked to each other, the high-frequency waves get trapped in the peridynamic zone. This will lead to an increase in the energy of the peridynamic zone and will drastically reduce the computational accuracy. We propose a coupling technique which can effectively eliminate the spurious wave reflections at the interface of the two zones. The elimination of the spurious reflections is achieved by introducing an overlapping zone between the finite element and peridynamic zones. The consistency of the mechanical deformation in the overlapping zone is imposed using Lagrange multipliers while the high-frequency waves are damped by introducing a damping parameter in the equation of motion of the peridynamic nodes located in the overlapping zone. Using this approach we show that high-frequency waves are effectively damped before they reach the finite element zone.

A Study on Permeability Coefficient of Porous Media Using Immersed Boundary Method

Ikkoh Tachibana^{*}, Shuji Moriguchi^{**}, Kenjiro Terada^{***}, Takayuki Aoki^{****}

^{*}Tohoku University, ^{**}Tohoku University, ^{***}Tohoku University, ^{****}Tokyo Institute of Technology

ABSTRACT

This study aims to analyze the permeability behavior of porous media with the help of a numerical simulation which can represent microscopic flow behaviors. 3D Navier-Stokes equation is employed for the governing equation of fluid movement in the simulation, while the immersed boundary method [1] is utilized to embed spherical boundary on the grains' surface [2] in the finite difference formulation with the staggered grid system. In present study, a series of numerical permeability tests were carried out on the representing volume unit (RVE) of granular material, expressed as a cuboid region where solid spheres were randomly packed. Unidirectional flow was considered and static pressure gradient is applied as the boundary condition, while the other perpendicular directions were treated as periodic. The profile of each RVE as a granular material was controlled with its void ratio and distribution of inner particle diameter. Also, in order to compare results from different simulation conditions and inner structures, the Reynolds number for the porous media is taken into account. The results were compared to the former simulations with grid-wise uniformed inner structures conducted by the corresponding author [3] and several popular empirical formulae for an estimation of macroscopic permeability coefficient. The discussion is aimed at clarifying the relationship between present results and existing empirical formulae of permeability coefficient for soils within wide range of material profile index. References [1] C. Peskin, Flow patterns around heart valves: A numerical method, *Journal of Computational Physics*, 10-2, pp. 252-271, 1972 [2] M. Uhlmann, An immersed boundary method with direct forcing for the simulation of particulate flows, *Journal of Computational Physics*, 209-2, pp. 448-476, 2005 [3] I. Tachibana, S. Moriguchi, S. Takase, K. Terada, T. Aoki, K. Kamiya, and T. Kodaka, Characterization of transition from Darcy to non-Darcy flow with 3D pore-level simulations, *Soils and Foundations*, 57 pp. 707-719, 2017

Multiscale Modeling of 2D Heterostructures

Ellad Tadmor^{*}, Kuan Zhang^{**}, Mingjian Wen^{***}

^{*}University of Minnesota, ^{**}University of Minnesota, ^{***}University of Minnesota

ABSTRACT

The synthesis of graphene, a one-atom thick 2D graphitic sheet, was a revolution in materials physics. Since then a host of other 2D materials have been discovered that can be stacked to create layered heterostructures with remarkable properties. Due to the weak van der Waals interaction between layers, the resulting structures can be incommensurate and therefore challenging to model. We describe recent work on developing a hybrid continuum-atomistic computational method for simulating the mechanical response of 2D heterostructures. This multiscale framework includes a stack of finite element plate models interacting via a newly developed interlayer potential. In agreement with electron diffraction experiments, simulations of twisted bilayer graphene show a transformation from an initially incommensurate structure to commensurate structures separated by localized solitons [1]. This behavior is explained using a simple mechanics model. [1] "Structural and electron diffraction scaling of twisted graphene bilayers", K. Zhang and E. B. Tadmor, Journal of the Mechanics and Physics of Solids, 112, 225–238 (2018).

NUMERICAL SIMULATION OF PROGRESSIVE COLLAPSE OF PERIMETER FRAME IN SUPER-HIGH-RISE FRAMED-TUBE STRUCTURE USING SIMPLE STRUCTURAL MODEL

Hiroyuki TAGAWA*, Misaki OKADA*, Noritoshi SUGIURA*

*Mukogawa Women's University
1-13 Tozaki-cho
Nishinomiya-shi, Hyogo, Japan
tagawa@mukogawa-u.ac.jp; <http://arch.mukogawa-u.ac.jp/>

Key words: Super-high-rise Framed-tube Structure, Progressive Collapse, Dynamic Stability, Perimeter Frame, Lateral-support, Minimum Eigenvalue.

Summary. Typical super-high-rise framed-tube structures have stiff beams and columns around the perimeter of the building and have no or few seismic beams inside the building. The rigid moment frames in the perimeters and floor system provide lateral-supports to prevent perimeter column buckling. However, when perimeter columns deform towards the outside of the structure simple connections between perimeter columns and floor system with small strength may break in tension. The lack of strong, stiff connections between perimeter frames and the floor system may result in minimum resistance to out-of-plane motion by the perimeter frames and may lead to unstable behavior when perimeter frames are separated from the floor systems as a result of accidental or earthquake loading. To investigate this behavior, simulations of the progressive collapse of these framed-tube systems were carried out using simple structural model, referred to as the coupled shear-flexural-beam model with links, consisting of lumped mass, spring and beam element. The hysteresis loop of link element connecting a shear-beam and a flexural-beam can simulate the behavior, including the tension break, of the frame-floor connections and tensile strength of link element is varied from 3% to 4% and 5% of the axial yield strength of the perimeter columns. Structural stability was evaluated by conducting eigenvalue analysis for mass and instantaneous stiffness matrices at each time-step of the nonlinear time-history analysis and a minimum eigenvalue was computed to assess the stability of the global structure. The results of this simulation shows that 1) when frame-floor connections do not break, continuous column effect resulting from elastic columns in perimeter frames is observed and drift concentration is mitigated, 2) when frame-floor connections have insufficient tensile strength and break in tension, progressive collapse of perimeter frames may occur due to out-of-plane motion of the frames, and 3) on-set of progressive collapse may be predicted by a negative instantaneous eigenvalue.

1 INTRODUCTION

Super-high-rise framed-tube structures such as the World Trade Center Building in New York typically have stiff beams and columns around the perimeter of the building and have no or few

seismic beams inside the building, as shown in Figure 1. This framing system is attractive to designers because they provide flexibility for floor layout. However, with this system, progressive collapse of the perimeter frames, due to instability resulting from failure of the floor-frame connections is a concern. The connections between the perimeter frame and floor system prevent buckling of the perimeter columns by limiting the column buckling length to the story height. If a perimeter column deforms towards the inside of the structure as shown in Figure 2(a), the floor system resists this motion and prevents buckling. However, if a perimeter column deforms towards the outside of the structure, as shown in Figure 2(b), large tensile forces may develop in the connection between the perimeter frame and floor-system. Since simple connections between the floor system and perimeter frame typically have relatively small strength, tensile failure may occur at these connections. Tensile failure of the frame-floor connection results in a longer column buckling length and, possibly, progressive collapse, as shown in Figure 3. Relatively low tensile capacity of the simple connections between the perimeter frames and floor-system is considered to be one of many factors that contributed to the progressive collapse of the World Trade Center Building in New York [1]. Previous study [2] investigated the progressive collapse of the high-rise U.S. type steel moment frame structure, which consists of the seismic frames located at the perimeters and the gravity frames inside the structure. In this study, the progressive collapse of perimeter frames in super-high-rise framed-tube structure is simulated numerically. Eigenvalue analysis is carried out at each time-step of the nonlinear time-history analysis to evaluate how the structure loses its stability and exhibits large deformations is evaluated as tensile failure of frame-floor connections progresses under earthquake loading.

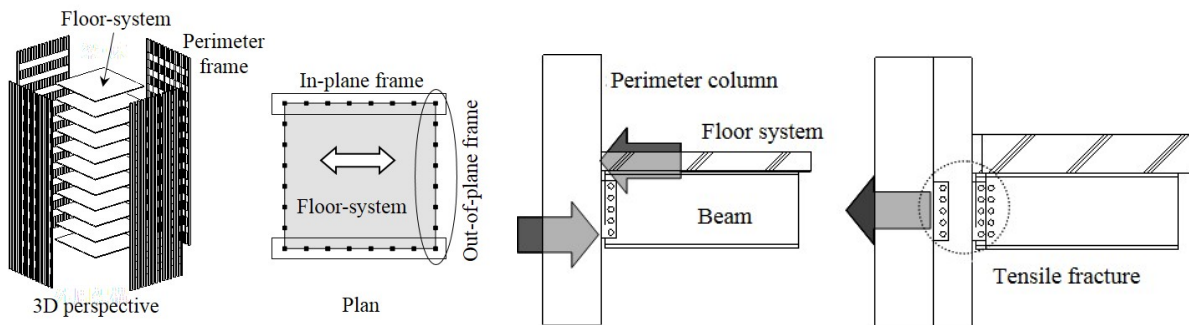
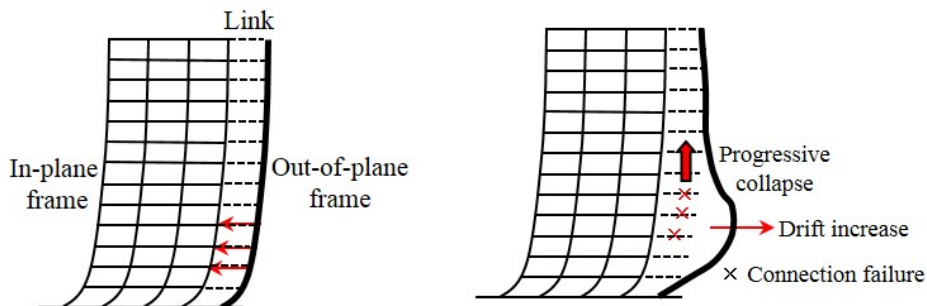


Figure 1. Framed-tube structure

(a) Deform towards the inside (b) Deform towards the outside
Figure 2. Connection between perimeter column and floor system



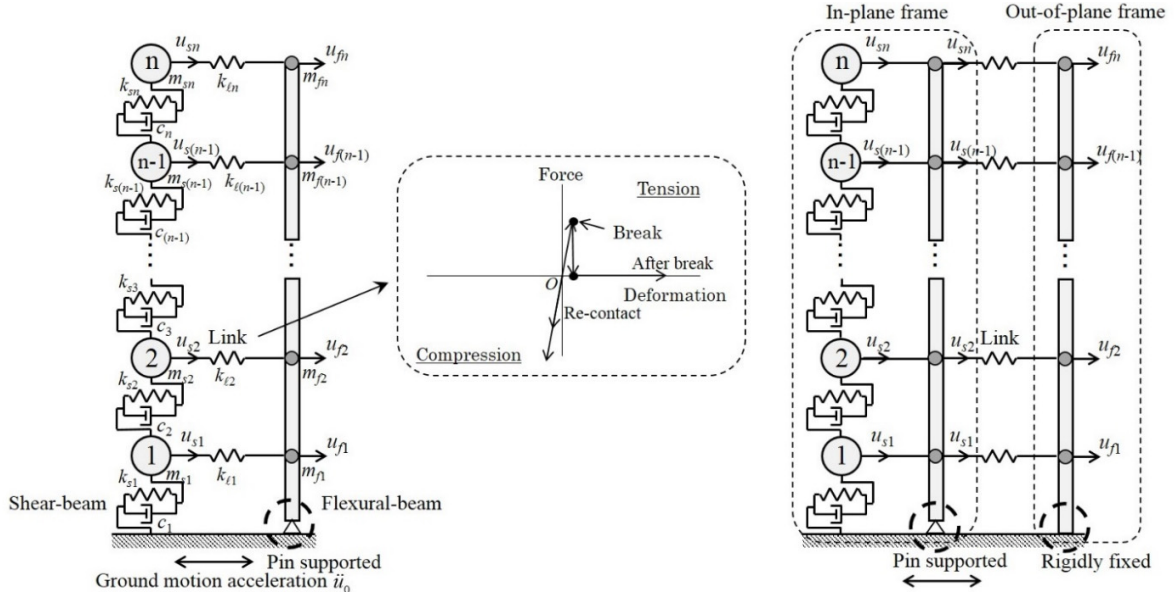
(a) Before connection failure

(b) After connection failure

Figure 3. Progressive collapse of perimeter frames due to connection failure in tensile direction

2 COUPLED SHEAR-FLEXURAL-BEAM MODEL WITH LINKS

The coupled shear-flexural-beam model with links is shown in Figure 4(a). This model consists of a shear-beam and a flexural-beam, which are connected with links. The model used in this study is shown in Figure 4(b), consisting of the shear-flexural-beam model representing the in-plane frame, the flexural-beam representing the out-of-plane frame, and connecting links.



(a) Coupled shear-flexural-beam model with links

(b) Model used for this study

Figure 4. Simple structural models

The formulation of the coupled shear-flexural-beam model with links is explained as bellow. The incremental form of equation of motion is given by Equation (1). Here, $[M]$ is mass matrix, $[C]$ is damping matrix, $[K(t)]$ is tangent stiffness matrix, $\{\Delta u_s\}$ and $\{\Delta u_f\}$ are the vectors of incremental displacements at each floor level for a shear-beam and flexural-beam, respectively, $\{\ell\}$ is a unit vector, and \ddot{u}_0 is the ground motion acceleration.

$$[M] \begin{Bmatrix} \{\Delta \ddot{u}_s\} \\ \{\Delta \ddot{u}_f\} \end{Bmatrix} + [C] \begin{Bmatrix} \{\Delta \dot{u}_s\} \\ \{\Delta \dot{u}_f\} \end{Bmatrix} + [K(t)] \begin{Bmatrix} \{\Delta u_s\} \\ \{\Delta u_f\} \end{Bmatrix} = -[M] \{\ell\} \Delta \ddot{u}_0 \quad (1)$$

Mass matrix is given by Equation (2). Here, $[M_s]$ and $[M_f]$ are the lumped mass matrices of the shear-beam and the flexural-beam, given by Equations (3) and (4), respectively.

$$[M] = \begin{bmatrix} [M_s] & [0] \\ [0] & [M_f] \end{bmatrix} \quad (2)$$

$$[M_s] = \begin{bmatrix} m_{s1} & 0 & 0 \\ 0 & \ddots & 0 \\ 0 & 0 & m_{sn} \end{bmatrix} \quad (3)$$

$$[M_f] = \begin{bmatrix} m_{f1} & 0 & 0 \\ 0 & \ddots & 0 \\ 0 & 0 & m_{fn} \end{bmatrix} \quad (4)$$

Tangent stiffness matrix is given by Equation (5).

$$[K(t)] = \begin{bmatrix} [K_S] + [K_I] & -[K_I] \\ -[K_I] & [K_F] + [K_I] \end{bmatrix} \quad (5)$$

Here, $[K_S]$ is the tangent stiffness matrix of the shear-beam given by Equation (6). Here, k_{si} is the tangent stiffness of the i^{th} -story spring in the shear-beam. If the geometrical nonlinearity, so called P - Δ effect in structural engineering, is considered, the tangent stiffness is reduced by $\theta_i^{P\Delta} = P_i/H_i$, where P_i is the weight of upper stories and H_i is the story height.

$$[K_S] = \begin{bmatrix} k_{s1} + k_{s2} & -k_{s2} & 0 & \cdots & 0 \\ -k_{s2} & k_{s2} + k_{s3} & \ddots & \ddots & \vdots \\ 0 & \ddots & \ddots & \ddots & 0 \\ \vdots & \ddots & \ddots & k_{s(n-1)} + k_{sn} & -k_{sn} \\ 0 & \cdots & 0 & -k_{sn} & k_{sn} \end{bmatrix} \quad (6)$$

$[K_f]$ is the stiffness matrix of the flexural-beam and the flexural-beam is assumed to be elastic in this study. The stiffness matrix of one beam element shown in Figure 5 is given by Equation (7). The stiffness matrix of the flexural-beam shown in Figure 6 is obtained by combining Equation (7) and rearranging the terms associated with displacement and rotation as given by Equation (8). By static condensation using the equilibrium condition, $\{M_i\} = \{0\}$, the stiffness matrix of the flexural-beam in terms of the force and the displacement is given by Equation (9). Finally, using the boundary condition, $u_0 = 0$, the stiffness matrix of the flexural-beam is given by Equation (10).

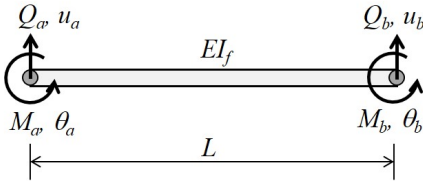


Figure 5. One beam element

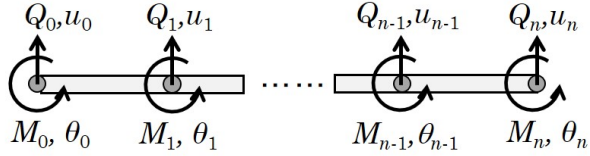


Figure 6. Flexural-beam

$$\begin{Bmatrix} Q_a \\ M_a \\ Q_b \\ M_b \end{Bmatrix} = \frac{EI_f}{L^3} \begin{bmatrix} 12 & 6L & -12 & 6L \\ & 4L^2 & -6L & 2L^2 \\ & & 12 & -6L \\ \text{sym.} & & & 4L^2 \end{bmatrix} \begin{Bmatrix} u_a \\ \theta_a \\ u_b \\ \theta_b \end{Bmatrix} \quad (7)$$

$$\begin{Bmatrix} \{Q_0, \dots, Q_n\}^T \\ \{M_0, \dots, M_n\}^T \end{Bmatrix} = \begin{bmatrix} [K_{11}]_{(n+1) \times (n+1)} & [K_{12}]_{(n+1) \times (n+1)} \\ [K_{21}]_{(n+1) \times (n+1)} & [K_{22}]_{(n+1) \times (n+1)} \end{bmatrix} \begin{Bmatrix} \{u_0, \dots, u_n\}^T \\ \{\theta_0, \dots, \theta_n\}^T \end{Bmatrix} \quad (8)$$

$$[\overline{K}_F]_{(n+1) \times (n+1)} = \frac{\{Q_0, \dots, Q_n\}^T}{\{u_0, \dots, u_n\}^T} = [K_{11}] - [K_{12}][K_{22}]^{-1}[K_{21}] \quad (9)$$

$$[K_F]_{n \times n} = [\overline{K}_f(2:n, 2:n)] \quad (10)$$

If geometrical nonlinearity is considered in beam element, the geometrical stiffness matrix given by Equation (11) is added to Equation (7), where P_i is the weight of upper stories and H_i is the story height. This geometrical stiffness matrix assumes small deformation.

$$[K_g] = \frac{-P_i}{H_i} \begin{bmatrix} \frac{6}{5} & \frac{H_i}{10} & -\frac{6}{5} & \frac{H_i}{10} \\ & \frac{2H_i^2}{15} & -\frac{H_i}{10} & -\frac{H_i^2}{30} \\ & & \frac{6}{5} & \frac{H_i}{10} \\ & & & \frac{2H_i^2}{15} \end{bmatrix} \quad (11)$$

sym.

$[K_L]$ is the stiffness matrix of the link element and given by Equation (12).

$$[K_L] = \begin{bmatrix} [K_\ell] & -[K_\ell] \\ -[K_\ell] & [K_\ell] \end{bmatrix} \quad (12)$$

$$[K_\ell] = \begin{bmatrix} k_{\ell 1} & 0 & 0 & 0 & 0 \\ 0 & k_{\ell 2} & 0 & 0 & 0 \\ \vdots & 0 & \ddots & 0 & \vdots \\ 0 & 0 & 0 & k_{\ell(n-1)} & 0 \\ 0 & 0 & 0 & 0 & k_{\ell n} \end{bmatrix} \quad (13)$$

Rayleigh damping is used for $[C]$ as given by Equation (14). The values of a_0 and a_1 are determined so that the structure has 2% viscous damping ratio at the 1st natural period of the system and at $T=0.2$ [sec].

$$[C] = a_0[M] + a_1[K] \quad (14)$$

The Newmark- β method ($\alpha=1/2$, $\beta=1/4$) is used to solve the incremental equation of motion given by Equation (1). The modified Newton-Raphson iteration scheme is used to compute nonlinear incremental displacements corresponding to incremental external forces.

3 SIMULATION

3.1 Model parameters

Dynamic time-history analysis is carried out for the 15-story coupled shear-flexural-beam model with links shown in Figure 4(b) subjected to the NF 17 ground motions^[3]. The 1st fundamental natural period of the entire structure is 1.81 [sec]. Every story has the same mass and the mass of the out-of-plane frame is assumed to be one fourth of the entire structure. The initial elastic stiffness of a horizontal spring in each story of the shear-beam is determined so that the shear-beam has the 1st fundamental natural of about 1.8 [sec] and the uniform story drift angle (SDA) under the horizontal design forces. This procedure is explained as follows. According to the UBC 1997 code^[4], the 1st fundamental natural period of the structure can be estimated by Equation (15).

Here, f_i is the horizontal design force acting on the i^{th} story, δ_i is the elastic horizontal displacement on the i^{th} story for f_i , g is the gravitational acceleration and w_i is the weight of the i^{th} story.

$$T = 2\pi \sqrt{\frac{\sum_{i=1}^n w_i \delta_i^2}{g \sum_{i=1}^n f_i \delta_i}} \quad (15)$$

If the story drift angle of every story is uniform, which is defined as θ_{SDA} , and the height of the i^{th} story is h_i , δ_i is given by $h_i \cdot \theta_{SDA}$. Then, Equation (15) becomes Equation (16). Therefore, Equation (17) is obtained and the initial elastic stiffness of a horizontal spring in the i^{th} story, k_{si} , is given by Equation (18).

$$T = 2\pi \sqrt{\frac{\sum_{i=1}^n w_i (h_i \theta_{SDA})^2}{g \sum_{i=1}^n f_i (h_i \theta_{SDA})}} = 2\pi \sqrt{\frac{\sum_{i=1}^n m_{si} h_i^2}{\sum_{i=1}^n f_i h_i}} \theta_{SDA} \quad (16) \quad \therefore \theta_{SDA} = \frac{T^2}{4\pi^2} \frac{\sum_{i=1}^n f_i h_i}{\sum_{i=1}^n m_{si} h_i^2} \quad (17)$$

$$k_{si} = \frac{Q_i}{\theta_{SDA} (h_{i+1} - h_i)} = \frac{4\pi^2}{T^2} \frac{\sum_{i=1}^n m_{si} h_i^2}{\sum_{i=1}^n f_i h_i} \frac{\sum_{j=i}^n f_j}{(h_{i+1} - h_i)} \quad (18)$$

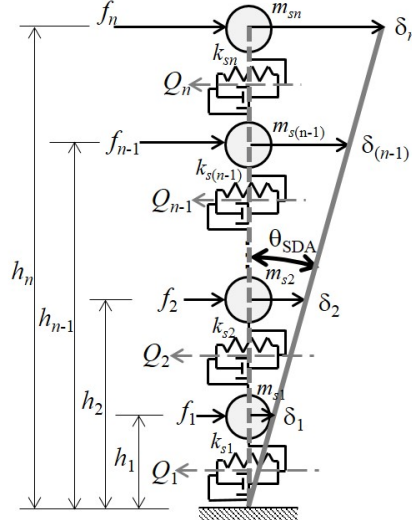


Figure 7. Uniform drift distribution of the shear-beam

Hysteresis loop of the horizontal spring of the shear-beam is set to be bilinear with kinematic hardening. The post-yield tangent stiffness ratio is set to be 3% and $P-\Delta$ effect is considered. The flexural-beam stiffness ratios, α_{cc} , of the in-plane frame and out-of-plane frame are 0.4 and 0.071, respectively. The axial force acting on the 1st-story perimeter column is assumed to be 30% of the axial yield strength of that column. The link element has the hysteresis loop shown in Figure 4(a) and the lateral-support strength is set to be from 3% to 4% and 5% of the axial yield strength of the 1st-story perimeter columns. The AIJ Recommendation for Limit State Design for Steel Structure ^[5] specifies lateral-support strength as 3% of the axial yield strength of columns.

3.2 Simulation results

Simulation results for the lateral-support strength ratio of 3%, 4% and 5% are presented below.

(a) 3% lateral-support strength ratio

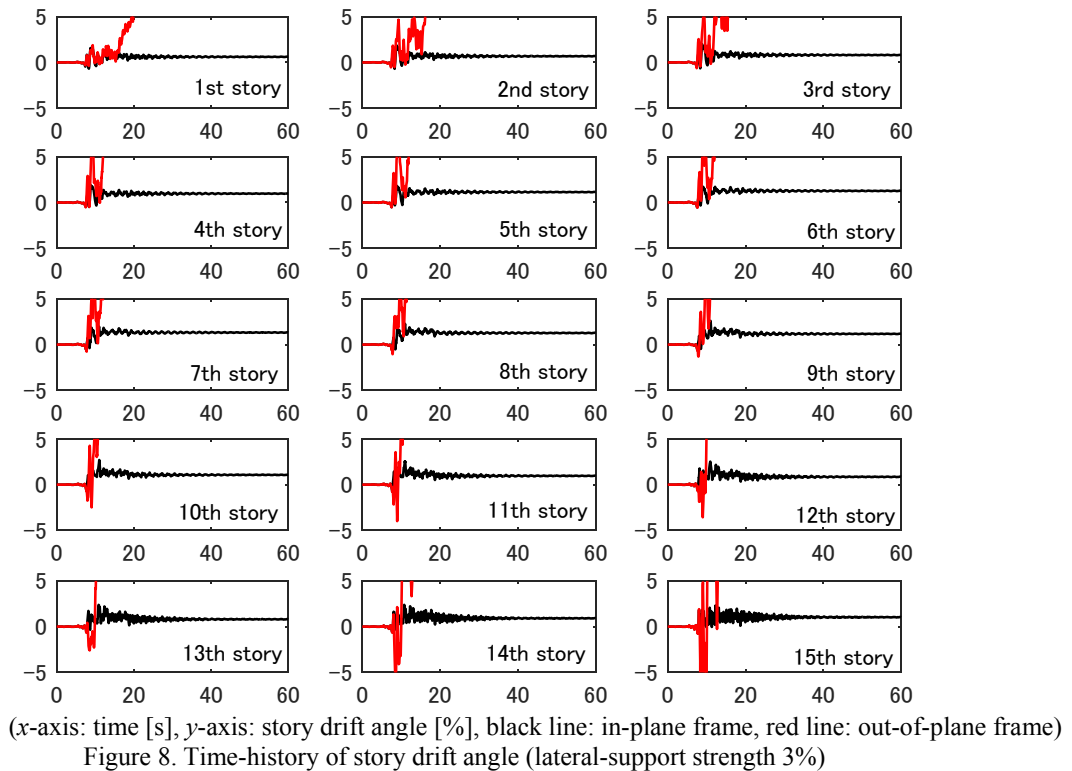
The time-history of the SDAs of the in-plane and out-of-plane frames for every story is shown in Figure 8. The in-plane and out-of-plane frames behave differently after about 10 [sec]. This is due to the tension breaks of the links. The relations of the axial force and axial deformation are shown in Figure 9. Distributions of the drifts of the in-plane and out-of-plane frames at connection failure are shown in Figure 10. The time-history of the minimum eigenvalue is shown in Figure 11. The minimum eigenvalue becomes negative after about 9 [sec], which results in unstable response and further, progressive collapse.

(b) 4% lateral-support strength ratio

The time-history of the SDAs is shown in Figure 12. Distributions of the drifts of the in-plane and out-of-plane frames at connection failure are shown in Figure 13. The minimum instantaneous eigenvalue continues to be negative as shown in Figure 14, which results in progressive collapse.

(c) 5% lateral-support strength ratio

The time-history of the SDAs of the in-plane and out-of-plane frames is shown in Figure 15. The in-plane and out-of-plane frames behaves in slightly different manner since connection failure occurs at two links, at the 1st and 2nd floors, as shown in Figure 16. Distributions of the drifts of the in-plane and out-of-plane frames at connection failure are shown in Figure 17. The time-history of the minimum instantaneous eigenvalue is shown in Figure 18. The minimum eigenvalue is 0.437 and the instantaneous eigenvalue maintains positive value, which results in stable response.



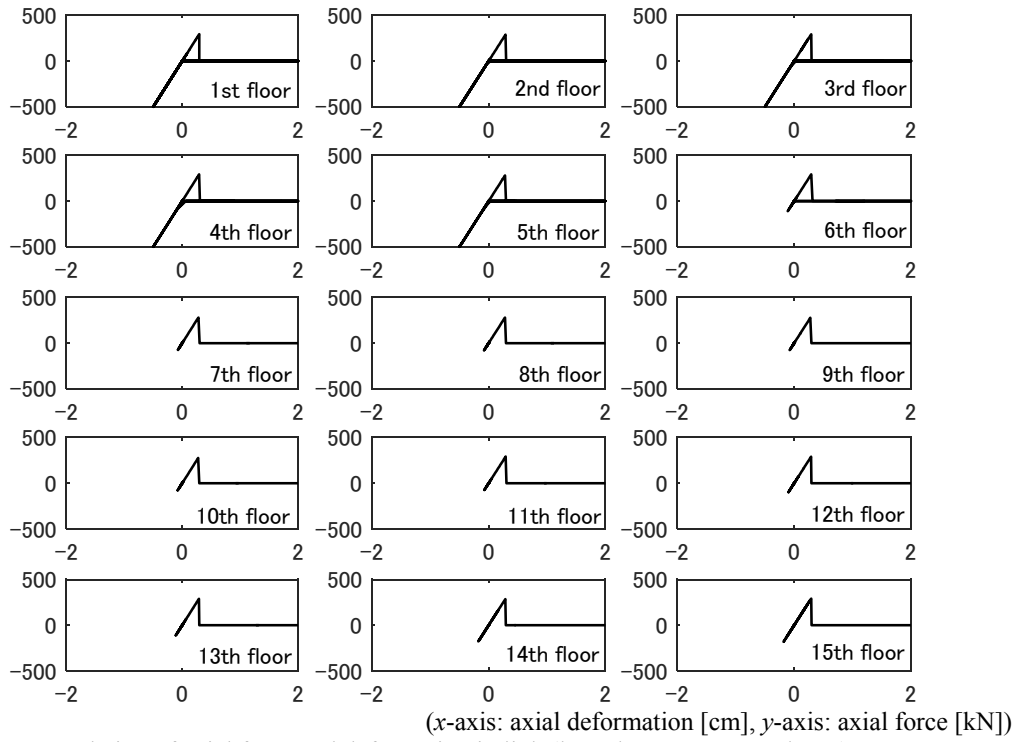


Figure 9. Relation of axial force and deformation in link (lateral-support strength 3%)

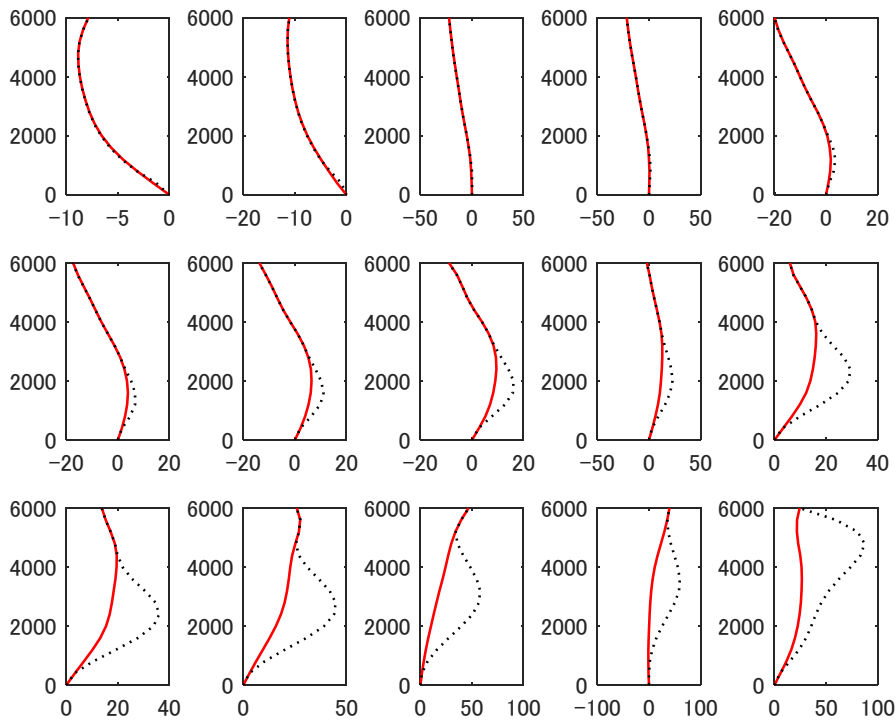


Figure 10. Displacement distribution at breaks (lateral-support strength 3%)

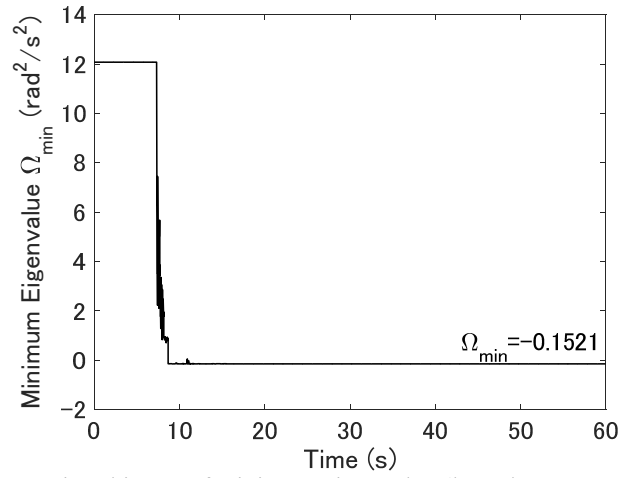


Figure 11. Time-history of minimum eigenvalue (lateral-support strength 3%)

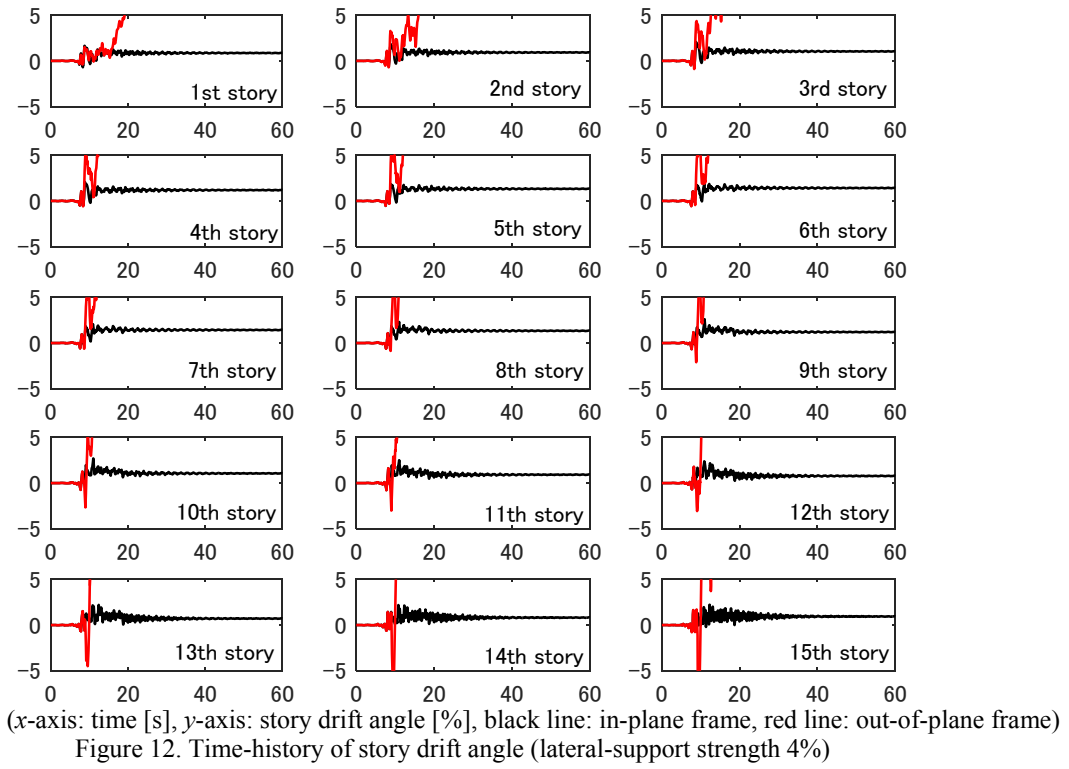
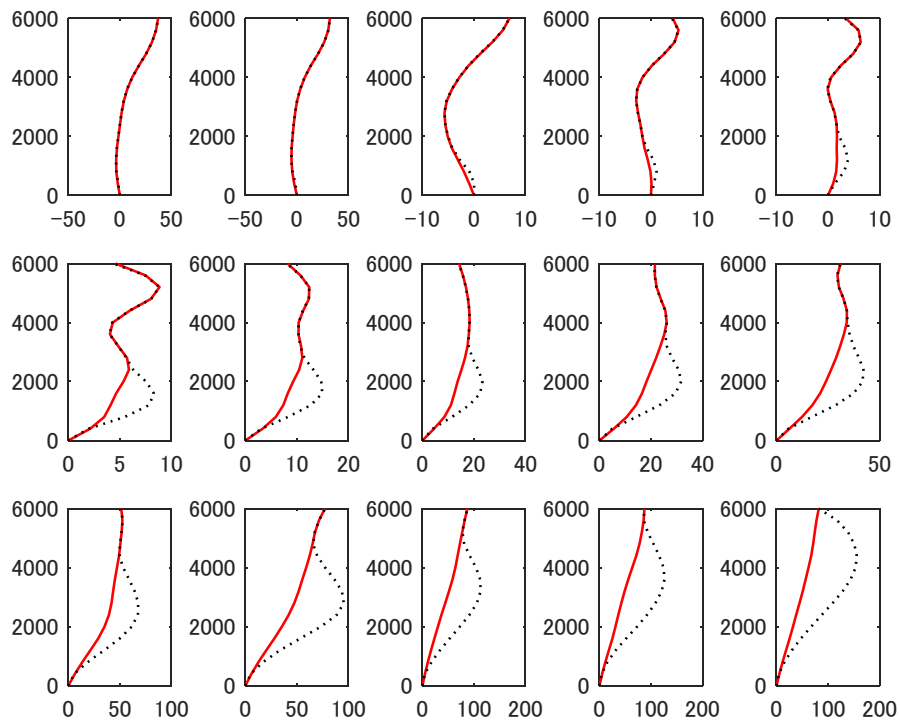


Figure 12. Time-history of story drift angle (lateral-support strength 4%)



(x-axis: Displacement [cm], y-axis: height [cm], solid line: in-plane frame, dotted line: out-of-plane frame)
 Figure 13. Displacement distribution at breaks (lateral-support strength 4%)

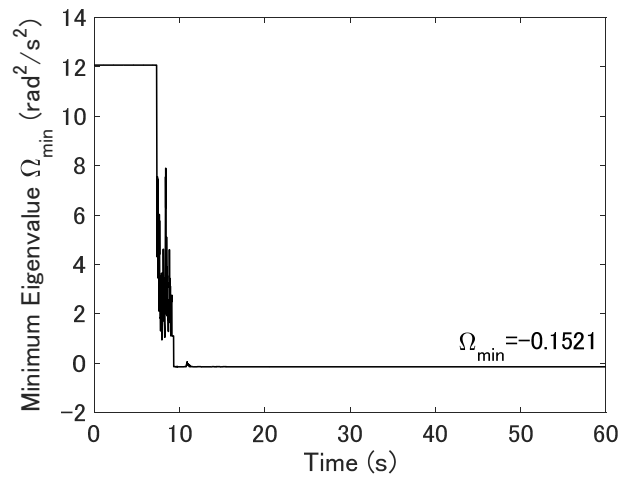
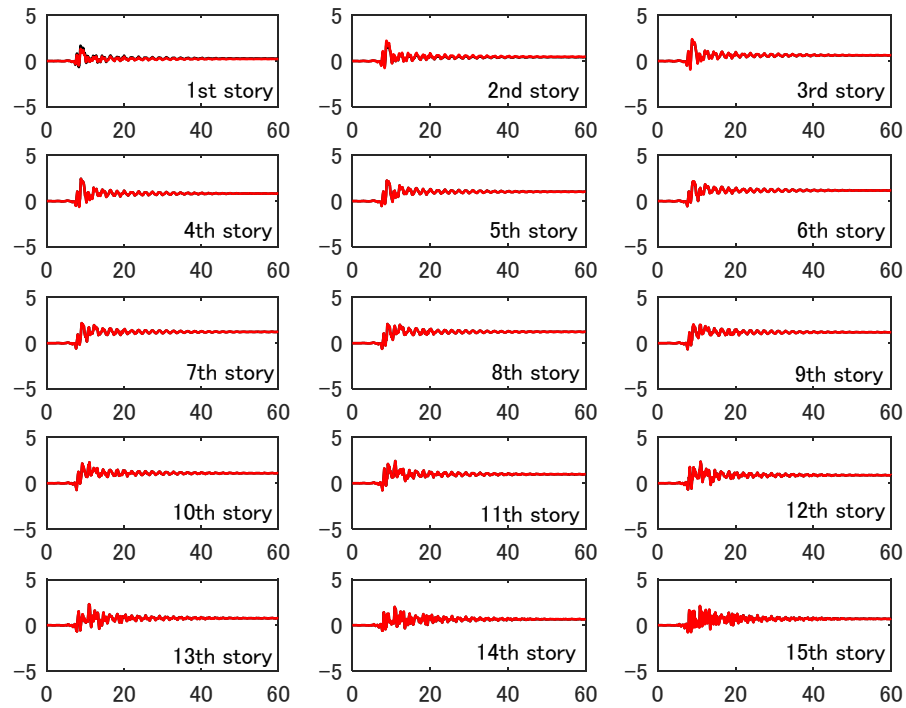
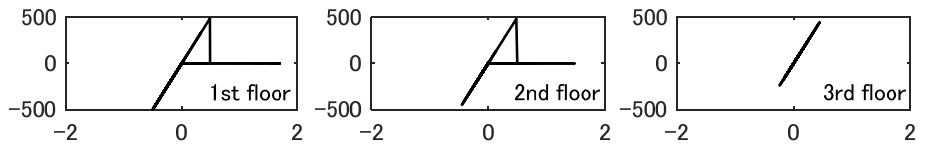


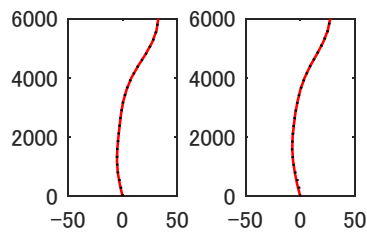
Figure 14. Time-history of minimum eigenvalue (lateral-support strength 4%)



(x-axis: time [s], y-axis: story drift angle [%], black line: in-plane frame, red line: out-of-plane frame)
 Figure 15. Time-history of story drift angle (lateral-support strength 5%)



(x-axis: axial deformation [cm], y-axis: axial force [kN])
 Figure 16. Relation of axial force and deformation in link (lateral-support strength 5%)



(x-axis: Displacement [cm], y-axis: height [cm], solid line: in-plane frame, dotted line: out-of-plane frame)
 Figure 17. Displacement distribution at breaks (lateral-support strength 5%)

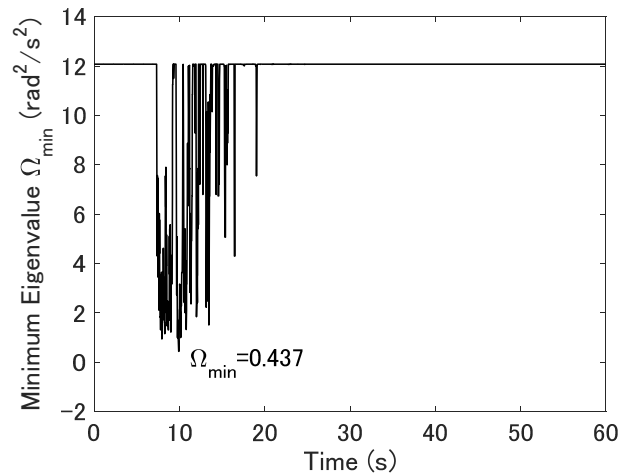


Figure 18. Time-history of minimum eigenvalue (lateral-support strength 5%)

4 CONCLUSIONS

In this study, the progressive collapse of super-high-rise framed-tube structure is simulated using simple shear-flexural-beam model with links. The link element simulates the restoring force of the simple connection between the perimeter, seismic frame and the floor-system. This link is modeled as possessing large stiffness and strength in compression and relatively small strength in tension. It was found that, when the tensile strength of the connection is 3% and 4%, the out-of-plane frame is separated from the in-plane frame and collapses as a result of severe earthquake loading. As the tensile strength of the links increases, the number of connection failures decreases and the in-plane and out-of-plane frames behaves as a single unit and in more stable manner.

REFERENCES

- [1] FEMA403, World Trade Center Building Performance Study, Data Collection, Preliminary Observations, and Recommendations, Appendix B, Structural Steel and Steel Connections, FEMA, Washington, DC. (2002).
- [2] Tagawa, H., MacRae, G., Lowes, L. and Wada, A. Analytical simulation of progressive collapse of perimeter frames due to out-of-plane behavior. The 14th World Conference on Earthquake Engineering, Beijing, China, October 12-17, (2008).
- [3] Somerville, P. et al. Development of Ground Motion Time Histories for Phase 2 of the FEMA/SAC Steel Project, Rep. No. SAC/BD97/04, SAC Joint Venture, Sacramento, California, (1997).
- [4] Uniform Building Code 1997 (UBC1997), International Conference of Building Officials, (1997)
- [5] Architectural Institute of Japan. Recommendations for Limit State Design of Steel Structures, (1998).

Coarse Graining DEM for a Non-spherical Particle System

Kazuya Takabatake*, Mikio Sakai**

*The University of Tokyo, **The University of Tokyo

ABSTRACT

Non-spherical particles are often encountered in chemical engineering. The behavior of non-spherical particles are too complicated to predict the translational and rotational motion. In designing a device for a powder process, introduction of numerical simulation technique is desired. The Discrete Element Method (DEM) is one of the most practical and efficient methods for the granular flow simulation. Although the adequacy and applicability of DEM have been proven in the numerous previous studies, there is a critical problem in the existing DEM regarding the calculation cost. In the DEM, the calculation cost depends on the number of calculation particles. In order to solve this problem, the coarse grain model was developed in our group, where the coarse particle whose diameter was larger than that of the original particle was used to simulate group of the original particles. Since the number of calculation particles can be drastically reduced by the coarse grain model, the large scale problem can be simulated by using a single computer in a reasonable time. When shape of the non-spherical particle is modeled, calculation costs would become expensive in the existing DEM. In order to solve this problem, the rolling friction model was proposed in the DEM. In the rolling friction model, the rolling resistance torque is calculated in order to reflect the non-spherical particle behavior. Since the rolling resistance torque works reversely against the angular velocity of the solid particle, the numerical oscillation occurs when the angular velocity is close to 0. In order to solve this issue, we develop a new rolling friction model in this study, which is more stable than the existing model. Besides, the rolling friction model is introduced into the coarse grain model for the first time to show the applicability to the large scale system. The adequacy of the model is proven through some verification tests. Consequently, the feasibility of a large-scale non-spherical particle system by using a single computer is shown in this study.

A Phase-field Lattice Boltzmann Method for Simulation of Microscopic Multiphase Flows

Naoki Takada*

*National Institute of Advanced Industrial Science and Technology (AIST)

ABSTRACT

Microscopic multiphase flows are widely encountered in various science and engineering fields. It is often difficult to experimentally observe the flows and measure the velocity, the pressure and the volume fraction simultaneously or to theoretically analyze them using the classical continuum dynamics approach based on a sharp-interface model. Computational fluid dynamics (CFD) simulations facilitate the understanding and prediction of the flows for flexible and accurate fluid-motion control, which result in the optimal design and efficient evaluation of micro-fluidic devices and processes. The phase-field model (PFM) has recently been attracting much attention from many researchers as one of the mesoscopic models that efficiently simulate the behavior of multi-phase systems based on the free-energy theory. The PFM describes an interface as a finite volumetric zone between different phases, across which physical properties vary steeply but continuously. Multiphase coexistence is allowed through minimizing a free-energy functional of the system without imposing topological constraints on the interface as phase boundary. The contact angle is set through a simple boundary condition on the solid surface with a wetting potential. As a result, PFM-CFD methods do not necessarily require conventional elaborate algorithms for the advection and reconstruction of interfaces. They therefore have an advantage over others, namely the efficient simulation of motions of multiple fluid-fluid interfaces attached to solid surfaces. This study aims to construct a PFM-CFD method for multiphase flow based on the previous two-phase and multiphase PFM-CFD methods [1,2]. For calculations of diffuse-interface advection and formation in the flow, the proposed method adopts the conservation-modified Allen-Cahn (AC) equation instead of the Cahn-Hilliard (CH) equation. The AC form is advantageous over the CH form in terms of volume conservation, interfacial tension effect, and computational efficiency, because the former is free from the interfacial-curvature effect on diffuse-interface dynamics and also has a second-order differential diffusion term instead of the fourth-order term in the latter. For solving the fluid-dynamics equations, the lattice-Boltzmann method (LBM) is employed in semi-Lagrangian form. The LBM is useful for high-performance computing because of the explicit and simple particle-kinematic operation with discrete conservation on an isotropic spatial grid. Through simple test simulations of three-phase rotational advection in two dimensions, it is confirmed that the PFM-CFD method has the potential to simulate multiphase flows accurately and efficiently. References: [1] N. Takada, et al., J. Comput. Sci. 17 (2016) 315-324. [2] H.G. Lee and J. Kim, Physica A 423 (2015) 33-50.

Dislocation Dynamics Simulation of Dislocation Shielding Effect at Crack Tip

Akiyuki Takahashi*, Hayato Sugawara**

*Tokyo University of Science, **Tokyo University of Science

ABSTRACT

Ductile-brittle transition (DBT) in ferric steels is a critical issue to ensure the structural integrity of nuclear power plants. The main mechanism of the DBT is believed to be the shielding effect of dislocations at the crack tip. Therefore, in order to make a deep understanding of the DBT mechanisms, it is necessary to develop a computational method that can account for the dislocation nucleation, behavior and stress around the crack tip, and can derive the fracture toughness as a result of dislocation-crack interactions. This paper presents a dislocation dynamics (DD) simulation technique for the fracture toughness calculation with the consideration of dislocation shielding effect. In this study, the crack is represented with discrete dislocations, and the crack problem is solved using the DD method. The dislocation nucleation from the crack tip is simply modeled with a critical shear stress in the immediate vicinity of the crack tip. The nucleated dislocations move in the material, and produce the stress at the crack tip. The complex system of dislocation-crack interactions can be solved only with the DD method. In the DD method, the stress intensity factor at the crack tip can be easily computed by calculating the Peach-Koehler force, which is normally calculated in the DD simulations, acting at the crack tip dislocation. When the stress intensity factor reaches a critical value, the fracture toughness is determined using the analytical solution of stress intensity factor and the applied stress. To demonstrate the potential of the developed DD method, we performed a simulation of dislocation shielding effect with various dislocation mobility, which imitates the temperature dependence of dislocation behavior and fracture toughness. The numerical result clearly shows that the higher dislocation mobility gives higher fracture toughness, which is qualitatively in agreement with experimental results.

Tsunami Debris Simulation Considering Impact Loading Based on Finite Cover Method

Shinsuke Takase^{*}, Ryosuke Ogasawara^{**}, Kentaro Mori^{***}, Kenji Kaneko^{****}, Seizo Tanaka^{*****}, Kazuya Nojima^{*****}, Masaaki Sakuraba^{*****}

^{*}Hachinohe Institute of Technology, ^{**}Hachinohe Institute of Technology, ^{***}Hachinohe Institute of Technology, ^{****}Hachinohe Institute of Technology, ^{*****}University of Tsukuba, ^{*****}Nippon Koei Co., Ltd., ^{*****}Nippon Koei Co., Ltd.

ABSTRACT

We proposed a new fluid-structure interaction (FSI) analysis method, in which the finite cover method (FCM) is employed for interface capturing to properly evaluate the impact loading caused by tsunami debris. The stabilized finite element method is applied to solve the Navier-Stokes equations with a spatially fixed FE mesh, over which the Lagrangian meshes of structures are placed independently. In this study, the structures are assumed to be rigid bodies, and their motions and mutual contact are simulated with the discrete element method (DEM). Then, the key ingredient of the proposed method to accurately evaluate the impact loading caused by tsunami is the FCM, which enables us to realize appropriate discretization around the interfaces defined as intersections of the Eulerian mesh for fluids and the Lagrangian meshes for the rigid bodies. The continuity conditions of velocity and stress vectors at each interface are imposed with the penalty method. Also, we carry out the free surface flow simulations, for which the SUPG method is employed to discretize the Navier-Stokes equation. To capture the complex free surface motion such as breaking waves in case of tsunami impact, we apply the phase-field modeling with the conservation-modified Allen-Cahn equation. After verification analyses are carried out in comparison with experimental data, several representative numerical examples are presented to demonstrate the promise and performance of the proposed FSI analysis method. K.Terada, M. Asai, and Yamagishi : Finite Cover method for linear and nonlinear analyses of heterogeneous solids, Int. J. Numer. Meth. Engrg., 58, 1321-1346, 2003. N. Tanaka, J. Matsumoto and S. Matsumoto: Phase-field model-based simulation of motions of a two-phase fluid on solid surface, J. Comput. Sci. Technol, Vol.7 No.2, pp.322-337, 2013.

Multiscale Modeling of Piezoresistivity and Damage Induced Sensing Of Nanocomposite Bonded Explosive Materials Using Non-Local Damage Formulation

Krishna Talamadupula*, Gary Seidel**

*Virginia Tech, **Virginia Tech

ABSTRACT

Polymer bonded explosives (PBXs) are highly sensitive explosive composites that are susceptible to accidental detonation. They are composed of explosive grains at high volume fractions, for example RDX, HMX etc. surrounded by a polymer medium at low volume fractions such as epoxy, estane etc. The prognostication of life of PBX materials is of interest primarily due to its unstable nature. This work models the usage of CNT infused polymer binder in these explosive composites to give Nanocomposite Bonded Explosives (NCBXs). This leverages the ability of the CNTs to impart piezoresistive properties to the polymer and hence provide insitu sensing of strained and damaged states of NCBX materials. The effective piezoresistivity is derived from key multiscale aspects of the nanocomposite binder due to the presence of the CNTs such as electron hopping at the nanoscale, CNT bundle network formation and disruption at the microscale etc. The degree of piezoresistivity is informed in a hierarchical fashion from the lower scales to the microscale RVE being analyzed through a microscale gauge factor. Correlating the piezoresistive response of NCBXs to the model governing the mechanical behavior including damage will require a detailed understanding of the strain and damage sensing regimes. To this end, the use of local strain-softening damage laws has been found to lead to numerical instabilities and ill-posedness of boundary value problems or element size sensitivities. To move away from these limitations, this work adapts a non-local damage formulation in a continuum damage mechanics framework developed from previous research efforts and implements it in conjunction with a 2D finite element code with element deletion techniques. Interfacial damage between explosive grains and the surrounding nanocomposite binder is modeled with electromechanical cohesive zones. Quasi static tensile/compressive tests are conducted on selected RVEs of NCBXs. The non-local damage model and interfacial cohesive law should correctly reflect energy dissipation during the fracture process. Damage parameters are adjusted according to the material's fracture energy. Various damage modes within the RVE, final failure of the RVE and damage detection of individual damage modes through piezoresistive analysis are studied. The usage of the non-local damage formulations limits the spurious spreading of the damage band and leads to better crack convergence. The study of the damage mechanisms interlinked with the piezoresistive sensing response enhances the model's capabilities to track and describe various damage related phenomena. It is anticipated that this work will improve the prognosis of life of NCBX materials.

Advances in 10-node Composite Tetrahedral Elements for Solid Mechanics

Brandon Talamini^{*}, Jakob Ostien^{**}, Alejandro Mota^{***}, James Foulk^{****}, Kendall Pierson^{*****},
Nathan Crane^{*****}, Michael Veilleux^{*****}

^{*}Sandia National Laboratories, ^{**}Sandia National Laboratories, ^{***}Sandia National Laboratories, ^{****}Sandia National Laboratories, ^{*****}Sandia National Laboratories, ^{*****}Sandia National Laboratories, ^{*****}Sandia National Laboratories

ABSTRACT

In this work, we exhibit new developments to 10-node composite tetrahedral elements towards their use in demanding solid mechanics applications. First, we investigate the case of nearly incompressible material behavior, and find that use of the standard assumed gradient operator leads to volumetric locking. We reformulate the composite element through a generalized Hu-Washizu variational principle that allows independent approximations not just of the Piola stress and deformation gradient fields, but also the pressure and Jacobian. This allows the definition of lower order projections of the volumetric response in a variationally consistent way, thus preserving symmetry of the stiffness matrix. The element behavior is shown to be locking-free, without resorting to reduced integration, and without introducing spurious zero-energy modes. Second, we examine use of the composite tetrahedral elements in explicit dynamics analysis. We study the spectral properties of the time integration operator with various mass lumping schemes, and propose methods to estimate the largest stable time step size. Sandia National Laboratories is a multi-mission laboratory managed and operated by National Technology &&&&&&& Engineering Solutions of Sandia, LLC., a wholly owned subsidiary of Honeywell International, Inc., for the U.S. Department of Energy&&&&&&'s National Nuclear Security Administration under contract DE-NA0003525.

KEYNOTE: Multiscale Analysis of Progressive Damage in Composite Materials: Transverse Matrix Cracking as Example

Ramesh Talreja*

*Texas A&M; Univeristy

ABSTRACT

Damage in composite materials is necessarily progressive, i.e., it usually starts with a failure event that leads to a sequence of subsequent failure events, culminating in final failure. Depending on the fiber architecture and constituent material properties, and the imposed loading, the sequence of failure events occurs at multiple characteristic scales. The local stress fields change as the failure events rearrange the load sharing balance amongst the participating elements. The challenge of progressive damage analysis (PDA) is exacerbated by the multiple modes in which failure events collect themselves, e.g. as kink bands in axial compression versus random fiber breakage clusters in axial tension in unidirectional composites. In laminated configurations, the damage modes occur as multiple ply cracking and delamination, for example. While it is unrealistic to expect a single modeling approach to be able to address all damage modes, one can hope to find a strategy based on fundamental principles to lead to a common coherent approach. One such strategy will be put forth in this presentation. It will be guided by the laws of thermodynamics that govern all irreversible (energy dissipative) phenomena. The formation of a matrix crack in unidirectional polymer based composites under transverse tension will be taken as an example to illustrate the features of failure analysis at multiple scales, ranging from the molecular scale to the typical crack length of a few fiber diameters.

Second Gradient Poromechanics: Constitutive Modeling and Numerical Implementation in IGA-FEM

Claudio Tamagnini^{*}, Carlos Plua^{**}, Pierre Besuelle^{***}

^{*}University of Perugia, ^{**}Université Grenoble Alpes, ^{***}CNRS

ABSTRACT

In this work, a fully coupled hydromechanical formulation for unsaturated 2nd gradient elastoplastic porous media is presented and applied to the numerical modeling of some geomechanics IBVP characterized by strain localization into shear bands. The introduction of internal length scales associated to the weakly non-local character of the constitutive equations effectively regularizes the numerical solutions. The 2nd gradient elastoplastic model adopted is based on two independent plastic mechanisms. The first one is provided by a three-invariant isotropic-hardening elastoplastic model similar to the one presented by Nova et al. (2003), extended to unsaturated soils. In lack of sufficient experimental evidence, the second-gradient mechanism is based on a simple elastic-perfectly plastic formulation. For the numerical solution of the governing system of non-linear PDEs, the Isogeometric (IGA) Finite Element Method (Hughes et al., 2005) has been adopted. When applied to constrained micromorphic media such as second-gradient materials, IGA offers the advantage of providing higher-order continuity of the approximating functions across element boundaries, which allows a more efficient and straightforward implementation of the discrete equilibrium problem, as compared to existing mixed FE formulations based on conventional polynomial shape functions, see Collin et al. (2006). This feature is also very important in coupled hydromechanical problems. In fact, the smoothness of the approximated displacements and pore pressure fields can mitigate significantly the requirements for minimum time steps. The simulation of some relevant consolidation problems demonstrates the good performance of the IGA implementation, and shows its effectiveness in regularizing the FE solutions when localization patterns occur in the strain field. References Collin, F., Chambon, R., & Charlier, R. (2006). A finite element method for poro mechanical modelling of geotechnical problems using local second gradient models. *International journal for numerical methods in engineering*, 65(11), 1749-1772. Hughes, T. J., Cottrell, J. A., & Bazilevs, Y. (2005). Isogeometric analysis: CAD, finite elements, NURBS, exact geometry and mesh refinement. *Computer methods in applied mechanics and engineering*, 194(39), 4135-4195. Nova, R., Castellanza, R., & Tamagnini, C. (2003). A constitutive model for bonded geomaterials subject to mechanical and/or chemical degradation. *International Journal for Numerical and Analytical Methods in Geomechanics*, 27(9), 705-732.

A Reformulation of Pressure Poisson Equation for the Least Squares Moving Particle Semi-implicit Methods

Tasuku Tamai*, Seiichi Koshizuka**

*Graduate School of Engineering, The University of Toyko, **Graduate School of Engineering, The University of Toyko

ABSTRACT

Least Squares Moving Particle Semi-implicit (LSMPS) method[1] is one of the particle methods for analyses of incompressible free-surface flow. In this study, in order to improve the satisfaction of incompressible constraint, a reformulation pressure Poisson equation for the LSMPS Method is presented. [1] T. Tamai and S. Koshizuka, Computational Particle Mechanics, Vol.1, 2014.

Space/Time Staggered Computational Framework and Reduced Order Modeling for Optimal Space-Time Discretizations

Kumar Tamma*, Rohit Deokar**

*University of Minnesota, **University of Minnesota

ABSTRACT

Novel developments in "Space/Time staggered computational framework and reduced order modeling for optimal Space-Time discretizations" in computational mechanics are presented and highlighted. The focus is on developments in the field of model order reduction framework in space and time for the Generalized single step single solve (GSSSS*) family of algorithms. It encompasses the following: a) The GSSSS framework has been developed in the past two decades as a unified theory encompassing all the computationally competitive time integration schemes for first and second order systems over the past 50 years or so. Using the underlying versatility of the GSSSS framework, a novel model order reduction procedure in space is proposed to eliminate spurious high frequency participation in dynamical systems. Numerically dissipative schemes which were originally proposed to deal with these high frequency participation lose energy over time and damp out the physics in the system. The proposed method for elimination of high frequency participation deals with this very problem by combining the advantages of the energy conserving and numerically dissipative algorithms through projection techniques. b) In addition, the so called "Finite element in time" framework for the GSSSS algorithms is developed using the weighted residual methodology. Based on the finite element in time methodology, a novel general purpose a posteriori error estimator for first and second order systems under the umbrella of GSSSS family of algorithms is proposed to foster adaptive time stepping. The applicability of the proposed estimator to several existing time integration algorithms including the well known schemes like the Newmark method, HHT- , Classical midpoint rule, Crank Nicolson and in addition, new algorithms and designs as well is demonstrated with single and multi-degree of freedom, linear and nonlinear dynamical problems. c) Lastly, model reduction in space and time through the so called staggered space-time MOR procedure is proposed which aims at refining the discretizations in space while employing a reduced dimension in time. Conversely, a reduced dimension in space is used to improve the discretization in time and the process is performed in an iterative fashion. Reference: * J. Har and K.K. Tamma, Advances in Computational Dynamics of Particles, Materials and Structures, John Wiley, 2012,

Numerical Framework for the Direct Micro-Macro Simulation of Micro-Heterogeneous Materials under Impact Loading

Erik Tamsen^{*}, Wolfgang Weber^{**}, Daniel Balzani^{***}

^{*}Technische Universität Dresden, ^{**}Helmut-Schmidt-Universität – Universität der Bundeswehr Hamburg,
^{***}Ruhr-Universität Bochum

ABSTRACT

Heterogeneities at the microscale give rise to sophisticated wave propagations and thus, a complex macroscopic material behavior under dynamic loading. For instance in strain-hardening cement-based composites, where the favorable energy absorbing behavior under impact loading results from breaking of the concrete matrix and fiber pullout, microscopic dynamic effects may be significant. To establish a valid model for the effective macroscopic material properties, the finite element method can be used. A suitable RVE can then be considered and based on its discretization a microscopic boundary value problem including dynamics can be solved to compute the homogenized mechanical fields at the macroscale. A direct micro-macro formulation based on kinematic admissibility and the principle of multiscale virtual power [1,2] is presented, which allows for an energetically consistent scale-bridging. The focus of the presentation lies on the derivation of consistent tangent moduli for large strains, which take into account effects resulting from inertia forces. These are required for a consistent direct micro-macro approach. Implementation aspects for the numerical simulation of reinforced concrete under impact loading will be discussed and selected numerical examples will be presented showing the resulting convergence behavior. [1] E.A. de Souza Neto, P.J. Blanco, P.J. Sánchez, R.A. Feijóo. An RVE-based multiscale theory of solids with micro-scale inertia and body force affects, *Mechanics of Materials*, 80:136-144, 2015. [2] C. Liu and C. Reina. Variational coars-graining procedure for dynamic homogenization. *Journal of the Mechanics and Physics of Solids*, 104:187-206, 2017

Neural Network Based Surrogate Models for Effective Mechanical Properties of Microstructures

RenKai Tan^{*}, Wenjing Ye^{**}

^{*}Hong Kong University of Science and Technology, ^{**}Hong Kong University of Science and Technology

ABSTRACT

Effective mechanical properties of microstructures are required in a number of applications. One example is in the design of metamaterials using topological optimization. A key step in the design procedure is the repetitive evaluation of effective properties of the microstructure, which evolves constantly during the process. For microstructures with complex shapes, this calculation using traditional numerical methods such as the FEM could be quite computational intensive and lead to a long design cycle. Recent advancement in the field of machine learning has attracted great attention of researchers in various fields to start utilizing the technology and integrating within their researches. The success of machine learning methods in taking up the role of a universal function approximator [1] could be very advantageous in replacing the computationally intensive finite element calculation. In this talk, we present neural network based surrogate models constructed to rapidly predict effective mechanical properties of a given microstructure. We utilize Convolutional Neural Network (CNN) to automatically extract features from microstructures which were represented as images [2] and use network to link the features with mechanical properties of microstructures. The network was trained using 20000 sets of data and tested with 2000 sets of data. The average accuracy of the CNN in the prediction of 9 dimensional material stiffness matrix from a 20 by 20 pixel topology image is around 0.5%, and the evaluation time for the property prediction is on the order of milliseconds. These preliminary results have demonstrated the potential of the developed approach, which is believed to be able to greatly reduce the total computational time for the topology optimization process. References: [1] Hornik, K., Stinchcombe, M., & White, H. Multilayer feedforward networks are universal approximators. *Neural networks*, 2(5), 359-366, 1989. [2] Russakovsky, O., Deng, J., Su, H. et al. ImageNet Large Scale Visual Recognition Challenge. *IJCV*, 2015.

3D Printing Employed for the Design and Manufacture of Metal Based Diamond Tools

Songcheng Tan^{*}, Zhan Yang^{**}, Longchen Duan^{***}, Xiaohong Fang^{****}

^{*}China University of Geosciences, Wuhan, ^{**}China University of Geosciences, Wuhan, ^{***}China University of Geosciences, Wuhan, ^{****}China University of Geosciences, Wuhan

ABSTRACT

Diamond tools are widely used in cutting, grinding and drilling areas. According to their raw materials and manufacture technology, diamond tools can be divided into metal based, ceramic based and resin based. Among them, the most common metal based diamond tools are all kinds of diamond bits and saws. However, the development of metal based diamond tools is restricted by the new manufacture technologies and material systems. Recently, 3D printing has been one of the hottest topics in manufacture area, and Selective Laser Melting (SLM) is rapidly developed at the same time. Thus, the SLM technology could provide a new opportunity to the metal based diamond tools manufacture industry. Nevertheless, when apply the SLM technology to the diamond composite material's manufacture, there are some special issues need to overcome, such as metal powder components and performance, diamond size and shape, etc. To verify the practicability of SLM employed for metal based diamond tools manufacture, some tests and analyses were conducted. In primary study, we manufactured 9 rectangular column composite samples by SLM, with dimensional of 8.5mm × 8.5mm × 15mm. The raw metal materials are FAM-201 pre-alloy powder and FJT-06 brazing pre-alloy powder. The sizes of the pre-alloy powder are 200 meshes, and their main components are copper, tin, iron, cobalt and nickel. Test results indicate that, it is feasible to produce a metal composite by the SLM, even though the raw metal powder are much coarser than the conventional size for the SLM. Based on the primary study, we manufactured 8 rectangular column diamond composite samples, with dimensional of 20mm × 20mm × 6mm. The raw metal powders are the same with the primary study. The volume ratio of diamond within composite is 5%, and the diamond size is 70 meshes to 80 meshes. The optimized SLM process parameters are: Laser power, 180W to 200W; Scanning speed, 700mm/s to 900mm/s; Scanning line interval, 0.07mm; Powder-bed depth, 0.15mm. Test results indicate that, strength of the diamond composite samples is stronger than the previous metal composite samples. Possible reasons may include the SLM process parameters are selected and optimized, and the diamond composite samples are much thinner than the previous. However, SEM tests indicate that, there are many pores and some cracks within the diamond composite matrix. Also, the SEM tests show that the SLM process would cause serious damage to the diamond grits.

Computational Modeling of Blast Wave Induced Traumatic Brain Injury and Model Validations

X. Gary Tan^{*}, Robert N. Saunders^{**}, Amit Bagchi^{***}

^{*}U.S. Naval Research Laboratory, Washington DC, USA, ^{**}U.S. Naval Research Laboratory, Washington DC, USA, ^{***}U.S. Naval Research Laboratory, Washington DC, USA

ABSTRACT

Modeling of human biomechanics and traumatic brain injury (TBI) resulting from blast exposure is very challenging because of the complex geometry and the substantial material heterogeneity in the human body. We developed a detailed finite element (FE) model of human body which represents both the geometry and the material realistically [1]. The high-fidelity computational models were developed based on high-resolution computed tomography (CT) and magnetic resonance imaging (MRI) scans. Hyper-viscoelastic models were used for soft tissues to capture the rate dependent behavior and large strain material nonlinearity. The shock wave interaction with the human due to a C4 explosion was simulated using the computational fluid dynamics (CFD) method, via an efficient combination of 1-D and 3-D numerical techniques. The shock wave loads were applied to the exterior of the FE models to simulate the pressure wave transmission through the body and capture the biomechanical response. The resulting large-scale CFD and FE problems were solved using the coupled Eulerian and Lagrangian solvers, respectively, in the highly scalable DoD Open Source code CoBi. The predicted brain tissue stress-strain fields were used to determine the areas susceptible to the injury by using published mechanical injury thresholds. The computational approaches were validated by comparing simulation results of head surrogate and full-scale animal models with recently collected data from shock/blast tube tests at specific instrumented locations [2]. The validated animal model and human model were also used to examine potential brain injury similarities and differences under identical loads. These results form the basis for correspondence rules that are able to relate insult-injury outcomes in an animal to those in the human. A key contribution of this work is to develop a multi-scale modeling approach to couple blast physics, whole body biodynamics and injury biomechanics for the blast event, as well as the multi-physics solver suitable for high-performance computing. The implications of these results suggest that computational models could be used to predict the biomechanical response in the blast TBI event, understand blast induced TBI mechanisms, develop animal-human injury correspondence rules, and help assess and improve the protection against the blast TBI. Reference: 1. Tan X.G., Przekwas A.J., & Gupta R.K., Computational Modeling of Blast Wave Interaction with a Human Body and Assessment of Traumatic Brain Injury, Shock Waves 2017. 2. Tan X.G., Saunders R.N., Bagchi A., Validation of a Full Porcine Finite Element Model for Blast Induced TBI using a Coupled Eulerian-Lagrangian Approach, ASME-IMECE 2017-70611.

MULTI-RESOLUTION TECHNIQUES FOR LEAST SQUARE MPS METHOD

MASAYUKI TANAKA*†, RUI CARDOSO*, AND HAMID BAHAI*

*Brunel University London
Kingston Lane, Uxbridge
London, United Kingdom
masayuki.tanaka@brunel.ac.uk

†Toshiba Co., Ltd
33, Shinisogo-cho, Isogo-ku, Yokohama-shi
Kanagawa, Japan
masayuki11.tanaka@toshiba.co.jp

Key words: Least Square MPS Method, Multi-Resolution, Incompressible Fluid.

Abstract. The Moving Particle Semi-implicit (MPS) method is enhanced for multi-resolution simulations in this work. The spatial resolution is changed adaptively by the particle splitting and merging algorithms. The Least Square MPS (LSMPS) method is applied to obtain accurate results even if particles have different diameters. A new wall boundary scheme, which is represented by polygons, is also improved for a multi-resolution simulation. By conducting simulations for the Taylor Green vortex and for a dam break, the accuracy of the Multi-Resolution MPS method was verified. Also, it was shown that this method was able to reduce computational costs significantly.

1 INTRODUCTION

Full-Lagrangian particle methods have great advantages when compared with Eulerian methods due to the fact that the particle can move dynamically and there is no need to calculate the advection terms as in Eulerian methods. Originally, the Smoothed Particle Hydrodynamics (SPH) method, which is one of the most popular full-Lagrangian methods, was developed to simulate compressible fluid flows [10, 4]. On the other hand, the Moving Particle Semi-implicit (MPS) method was developed to simulate incompressible fluid flow strictly within a full-Lagrangian context [6].

However, the particle methods have some drawbacks such as longer computational time and inaccuracy. Generally, a particle method requires more computational resources when compared with an Eulerian method because of the extra computational effort required to handle particle interactions. Moreover, particle methods have been suffering from changing the resolution while Eulerian methods can easily change the sizes of meshes for different parts of the domain to reduce computational costs. In a Lagrangian description, however, the spatial resolution, i.e. diameters of

particles, is generally limited and non-uniform size diameters cannot be used. There have been several attempts to change the spatial resolution in the SPH methods: Kitsionas and Whitworth [5] proposed the particle splitting method to increase the spatial resolution locally. In this method a particle is split into thirteen particles to obtain a spherically symmetric kernel function; Lastiwka et al. [7] proposed changing resolution by adding or removing particles. They applied a first-order differentiation scheme and showed that it was accurate even if particles had non-uniform spacing; Liu et al. [9] proposed the Adaptive SPH method, in which a support domain was extended to non-spherical regions such as an ellipsoidal shape region for example; Adams et al. [1] proposed a method to change the spatial resolution adaptively. There have also been some noteworthy developments for multi-resolution techniques for the MPS method such as the works of Shibata et al. [12] on the overlapping technique and Tang et al. [17] for the extension of Shibata's work to three dimensions. Notwithstanding the great contributions of Shibata and Tang for multi-resolution methods for the MPS method, there is still a major drawback which is the inability of the technique to allow for two-way interactions between low-resolution and high-resolution domains. Tanaka et al. [15] developed further a multi-resolution technique for the MPS method in two dimensions, however, the formulation was derived for the classical MPS method and thus it suffers from inaccuracy and stability issues. Tang et al. [16] extended this method for three dimensions, however, no splitting or merging algorithms were adopted and therefore the spatial resolution cannot be changed dynamically.

In spite of a number of improvements, the particle methods have a key fundamental inaccuracy problem that can even lead to a total failure of simulations. The particle methods are usually formulated by assuming that particles are distributed uniformly. The source of inaccuracy starts to be more evident when consistency is lost due to the non-uniform arrangement of particles as the simulation goes on. The incompressible condition of the MPS method, which enforces the particle number density to be constant, is also one of the major sources for the loss of accuracy on the MPS method. Tamai and Koshizuka [13] have proposed the Least Square MPS (LSMPS) method to overcome the inaccuracies caused by the non-uniform particle distribution and other similar methods were proposed for the SPH method [2, 3].

In this work, the Multi-Resolution MPS method [14], which can change spatial resolution dynamically in incompressible fluid flow simulations is presented. A new boundary condition for a wall for multi-resolution simulations are also proposed.

2 MULTI-RESOLUTION MPS METHOD

2.1 Least Square Formulation

The LSMPS method [13], which recreates differential operators based on neighbouring particle positions for every time step, is applied in this work, because it can provide more accurate approximation even if diameters of particles differ. The formulation of the LSMPS for an arbitrary function f is shown next.

$$\mathbf{D}_x f(\mathbf{x}) = \mathbf{H}_i \mathbf{M}_i^{-1} \mathbf{b}_i \quad (1)$$

where \mathbf{x} is a coordinate, \mathbf{D}_x is a differential operator, \mathbf{H} is a matrix of coefficients, \mathbf{M} is a moment

matrix and \mathbf{b} is a moment vector. The second order formulation for two dimensions, for example, is represented as below:

$$\mathbf{D}_x = \left[\frac{\partial}{\partial x} \quad \frac{\partial}{\partial y} \quad \frac{\partial^2}{\partial x^2} \quad \frac{\partial^2}{\partial x \partial y} \quad \frac{\partial^2}{\partial y^2} \right]^T \quad (2)$$

$$\mathbf{H}_i = \text{diag}[L_i^{-1} \quad L_i^{-1} \quad 2L_i^{-1} \quad L_i^{-1} \quad 2L_i^{-1}] \quad (3)$$

$$\mathbf{M}_i = \sum_{j \neq i} w_{ij} \mathbf{p} \left(\frac{x_j - x_i}{L_i} \right) \otimes \mathbf{p} \left(\frac{x_j - x_i}{L_i} \right) \quad (4)$$

$$\mathbf{b}_i = \sum_{j \neq i} w_{ij} (f_j - f_i) \mathbf{p} \left(\frac{x_j - x_i}{L_i} \right) \quad (5)$$

$$\mathbf{p}(\mathbf{x}) = [x \quad y \quad x^2 \quad xy \quad y^2]^T \quad (6)$$

where L is a diameter of a particle and w is a weight function. By using this formulation, every derivative can then be calculated.

2.2 Incompressible Condition

In the Multi-Resolution MPS method [14], a higher order incompressible condition proposed by Nair and Tomar [11] is applied. The incompressible condition is given as:

$$\det \frac{\partial \mathbf{x}^{k+1}}{\partial \mathbf{x}^k} = 1 \quad (6)$$

If the time integration is calculated by using the Euler explicit scheme, the equation for pressure in 2D is denoted by

$$\mathbf{A}^k = \mathbf{I} + \Delta t \nabla^k \mathbf{u}^{k'} = \begin{pmatrix} a_{11} & a_{12} \\ a_{21} & a_{22} \end{pmatrix} \quad (8)$$

This incompressible condition is applied in the Multi-Resolution MPS method.

3 Multi-Resolution Techniques

In the Multi-Resolution MPS method, the size of the particles changes dynamically. A particle should be able to be split into smaller particles whenever a more refined resolution is required. Conversely, particles should be able to be merged into a larger particle whenever a coarser particle distribution is required. Splitting and merging are triggered by both the current diameter and a target diameter of each particle. The target diameter L^* can depend on many different parameters such as the position, the distance from a wall, the distance from a free surface, pressure, etc. The easiest way to define the target diameter is to make it to be a function of the coordinates, i.e., $L_i^* = L^*(\mathbf{x}_i)$. After evaluating the target diameter for each particle at every time step, then the particle can be judged to be split or merged according to the procedures described in the following sections.

2.3.1 Particle Splittin

A particle is split into two particles in this work. The particle volume, which is defined as $V = L^d$ by using the number of dimensions d , should be conserved during this particle splitting process, and then the diameter after splitting $L_{i'}$ is given as $L_{i'} = (1/2)^{1/d}L_i$. When the target diameter of a particle is much smaller than the current diameter, i.e. $L_i^* < \beta_s L_i$, the particle will be split. The threshold of the diameter to trigger the particle splitting should be in the middle of the current diameter L_i and the diameter after splitting $L_{i'}$, and then the splitting threshold β_s is defined as $\beta_s = 1/2\{(1/2)^{1/d} + 1\}$. The velocity for the new particles after splitting is obtained after the following interpolation:

$$\mathbf{u}_{i'} = \mathbf{u}_i + \langle \nabla \mathbf{u} \rangle_i (\mathbf{x}_{i'} - \mathbf{x}_i) \quad (10)$$

2.3.2 Particle Mer in

In this work, two particles are merged into a large particle. When the target diameter is much larger than the current diameter, i.e., $L_i^* > \beta_m L_i$, the particle i is merged with a neighbouring particle j . β_m is a merging threshold defined as $\beta_m = 2^{1/d}$. Particle j should be of the same kind of fluid as particle i and the distance between particles i and j should be smaller than a predefined threshold, i.e., $r_{ij} < \alpha \frac{L_i + L_j}{2}$. If there is no neighbouring particle which satisfies the above mentioned condition, then the merging process is terminated. Note that a particle which is going to be split should be ruled out from the merging judgement.

The position and velocity of the newly generated particles after merging are calculated so that the angular momentum and the linear momentum are conserved respectively:

$$\mathbf{x}_{i'} = \frac{V_i \mathbf{x}_i + V_j \mathbf{x}_j}{V_i + V_j} \quad (11)$$

$$\mathbf{u}_{i'} = \frac{V_i \mathbf{u}_i + V_j \mathbf{u}_j}{V_i + V_j} \quad (12)$$

The diameter of the new particle after merging is evaluated by considering volume conservation, i.e., $L_{i'} = (L_i^d + L_j^d)^{1/d}$.

2.4 Boundary Conditions for a Wall

In this work, wall geometries are represented by polygons and imaginary wall particles are generated on the boundaries at every time step, as shown in Figure 1. Note that the key difference from other conventional methods is that the imaginary wall particles are generated not beyond the boundary but right on the boundary. It would be much easier to impose boundary conditions for the viscosity and pressure terms if the imaginary particles were located right on the boundary because no interpolation technique would then be required for these particles. Note that this arrangement of the wall particles is only possible by the least square particle methods.

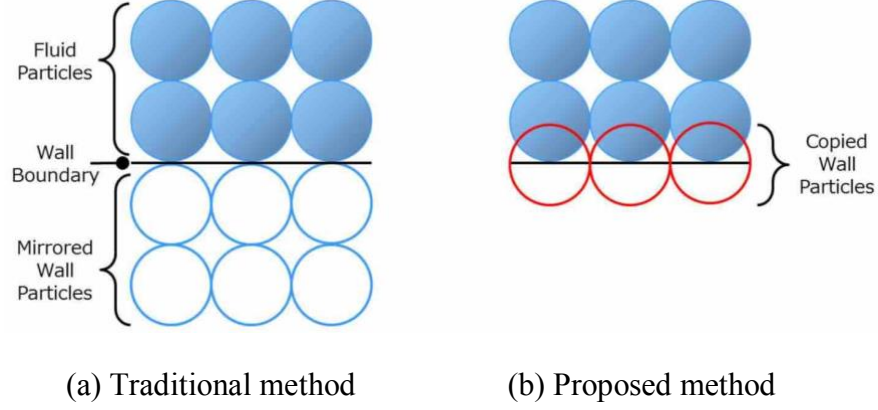


Figure 1: Imaginary wall particles

The boundary condition on the wall particles is defined as $\mathbf{u}^{k+1} \cdot \mathbf{n} = 0$. There are various ways to express the pressure boundary condition on wall particles. In this work, a semi-analytical wall boundary condition proposed Leroy et al. [8] is utilised:

$$\frac{1}{\rho} \nabla P \cdot \mathbf{n} = \frac{1}{\Delta t} \mathbf{u}^{k'} \cdot \mathbf{n} \quad (13)$$

The velocity of the wall is evaluated by using the velocities of the neighbouring particles.

3 RESULTS AND DISCUSSIONS

3.1 Taylor Green Vortex Simulation with Variable Resolution

The Taylor Green vortex example is simulated with the Multi-Resolution MPS method for the assessment of the conservation of energy and momentum. The Taylor Green vortex is a classical flow example with known analytical solution. The velocity $\mathbf{u}(x, y, t) = (u(x, y, t), v(x, y, t))$ and pressure $P(x, y, t)$ are expressed by using the coefficient $F(t) = U \exp(-2vt)$ as follows:

$$u(x, y, t) = F(t) \cos\left(2\pi \frac{x}{W}\right) \sin\left(2\pi \frac{y}{W}\right) \quad (14)$$

$$v(x, y, t) = -F(t) \sin\left(2\pi \frac{x}{W}\right) \cos\left(2\pi \frac{y}{W}\right) \quad (15)$$

$$P(x, y, t) = -\frac{\rho F(t)^2}{4} \left\{ \cos\left(4\pi \frac{x}{W}\right) + \cos\left(4\pi \frac{y}{W}\right) \right\} \quad (16)$$

where W is the size of the domain so that the coordinates are limited to $0 \leq x \leq W$ and $0 \leq y \leq W$, and U is the reference velocity.

The domain size used in the simulations was $W = 1$ m and the reference velocity was $U = 1$ m/s. The fluid density was 1000 kg/m^3 and the kinematic viscosity was $0 \text{ m}^2/\text{s}$. Because the viscosity term is neglected, the velocity and pressure distribution should remain still and the energy should be conserved. The particles whose diameters are 5 mm are located on the 200×200 grids in the

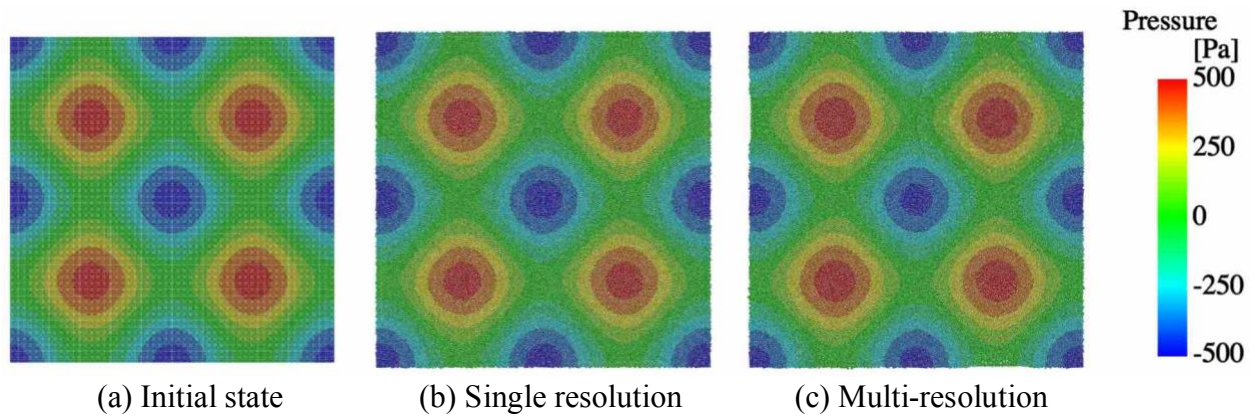


Figure 2: Pressure distribution of the Taylor Green vortex simulations

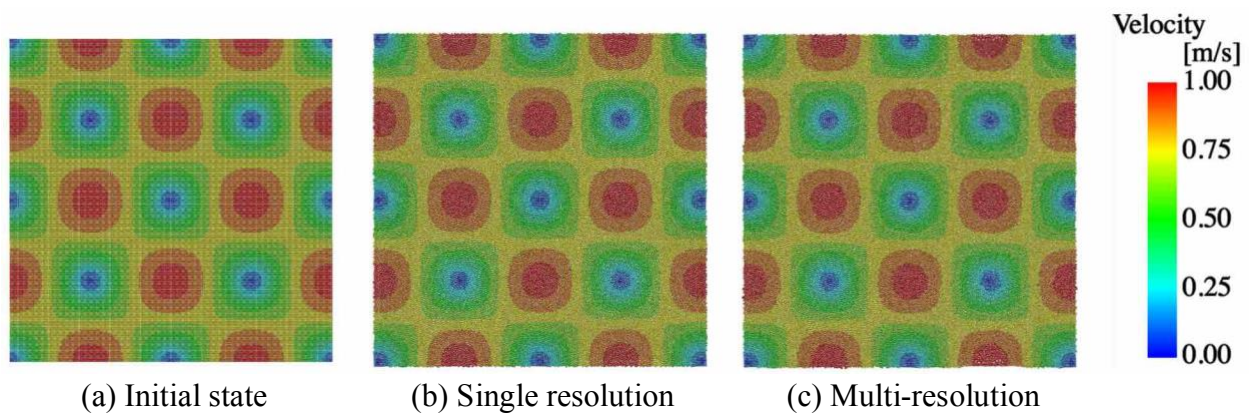


Figure 3: Velocity distribution of the Taylor Green vortex simulations

initial state for both single and multi-resolution simulations. In the multi-resolution simulation, the region within 0.25 m distance to the point (0.75 m, 0.75 m) is defined as the high resolution region, and the target diameter of the particles inside this region is 0.35 m. The simulations were conducted for a total time of 1.0 sec, which corresponds to one cycle for the vortex. The periodic boundary conditions are applied for X and Y directions by copying particles around edges of the simulation domain to the corresponding positions of the periodic boundary condition.

The pressure distribution and the velocity distribution before and after simulations are shown in Figure 2 and Figure 3 respectively. The distributions of the pressure and the velocity after both single and multi-resolution simulations are similar to the initial state although particles have moved for the time corresponding to one cycle of the vortex, and then it can be stated that the simulation was conducted accurately. The closeups of the regions where the resolution was changed are shown in Figure 4. In the left closeup, particles are moving from left to right direction and they are split when they enter the high resolution region. In the right closeup particles are moving from up to down direction and are merged whenever they get out of the high resolution region. In both the splitting and merging process, the velocity field was smooth and no strange particle arrangement was observed.

The pressure and velocity were measured on the evaluation points, shown in Figure 4, along the vertical line corresponding to $X = 0.75$ m and they were plotted together with the analytical

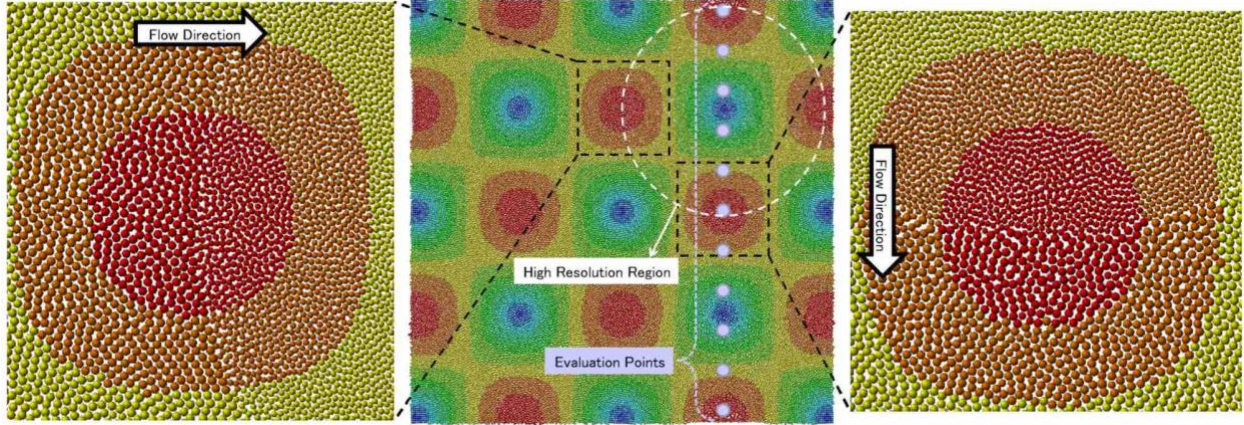


Figure 4: Closeups of resolution changing regions

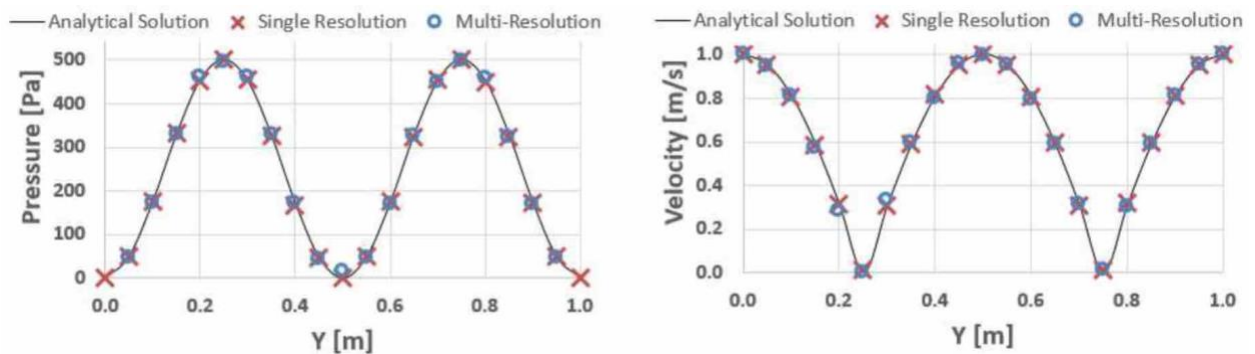


Figure 5: Comparison between the analytical solution and the simulation results

solutions in Figure 5. The results of both of the single and multi-resolution simulation were in good agreement with the analytical solutions although there was a slight difference for the pressure of the multi-resolution simulation around $Y = 0.5$ m. This point is near the interfacial region of the different size of particles and the error was supposed to be caused by changing the resolution. However the difference was small enough and did not affect the accuracy of the whole simulation. The linear and angular momentum and the total energy through the simulations were monitored in Figure 6. The errors for the momentum from the multi-resolution simulation was larger than those from the single resolution simulation although they are not significant. The error for the energy was as small as 0.1 % and thus it can be said that the accuracy of the Multi-Resolution MPS method is good enough so that the method can be successfully applied in the simulation of complex problems.

3.2 Multi-Resolution Dam Brea Simulation with Free Surface

Dam break simulations are conducted by using the multi-resolution techniques. The initial size of the fluid is $100 \text{ mm} \times 250 \text{ mm}$. The vessel has the width of 400 mm with a small obstacle in the middle of the vessel, located at the bottom of the vessel. The obstacle is as small as $10 \text{ mm} \times 10 \text{ mm}$ and therefore particles as small as 1 mm for the diameter are required around the obstacle. The single resolution simulation with the diameter of 1 mm for the particles and the multi-resolution simulation with the diameter for the particles ranging from 1 mm to 5 mm are conducted. The

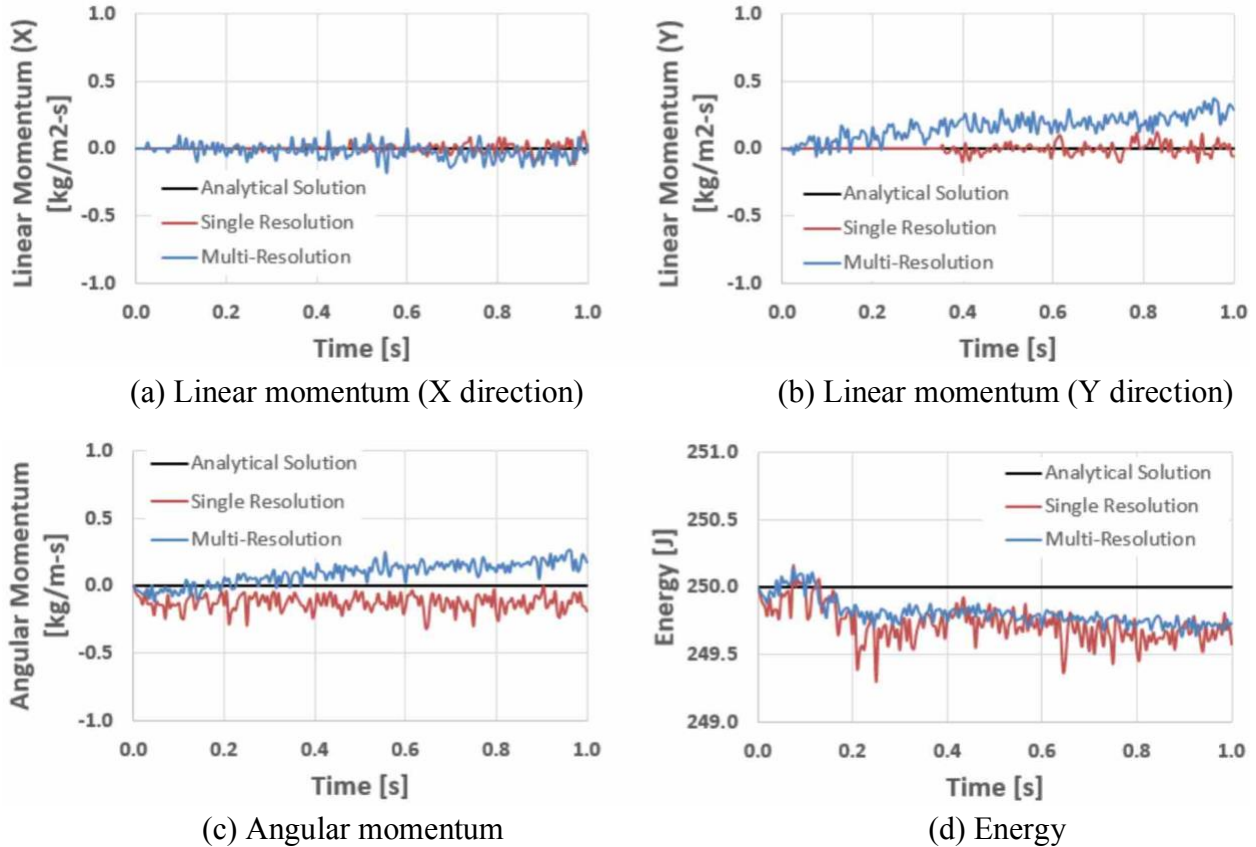


Figure 6: Profile of momentum and energy in the Taylor Green vortex simulation

target diameter in the multi-resolution simulation depends on the distance from the origin point, so that a finer resolution around the small obstacle can be obtained. The physical values and other simulation conditions are the same as for the first dam break example. The pressure and velocity values are monitored at the evaluation point which is 5 mm above the small obstacle.

Comparison of the pressure distribution between the single and multi-resolution simulations before colliding the small obstacle is shown in Figure 7. The fluid motion and the pressure distribution obtained by the multi-resolution simulation were similar in general to those by the single resolution simulation. Although some differences in the pressure distribution were observed around the small obstacle at 0.11 sec, this is due to the way the pressure value are computed as stated above. Such differences in pressure distribution did not influence the fluid motion crucially and then are considered to be acceptable.

The fluid motion and the velocity distribution after the collision with the small obstacle is illustrated in Figure 8. Both the fluid motion and the velocity field matched well up to 0.65 sec, however, the fluid shapes at 1.0 sec are different. This is because the characteristic part of the fluid is mainly in the region where the resolution is lower and so the simulation is not accurate anymore. Therefore the pre-selection for the configuration of the resolution should be done carefully.

The number of the fluid particles used in the multi-resolution simulation was 4,291 in average while it was 24,969 throughout the single resolution simulation. In other words, the number of

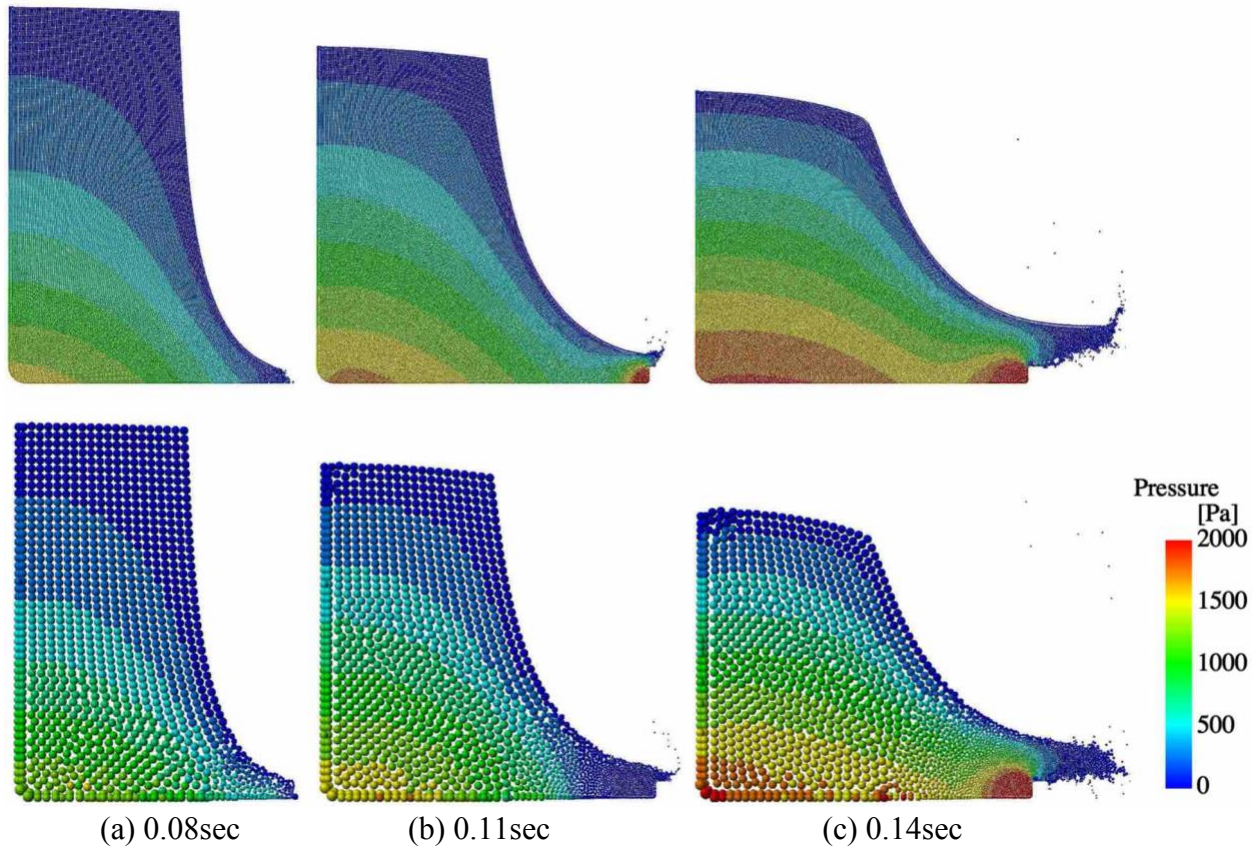


Figure 7: Comparison of the pressure distribution between the single and multi-resolution simulation (above: single resolution, bottom: multi-resolution)

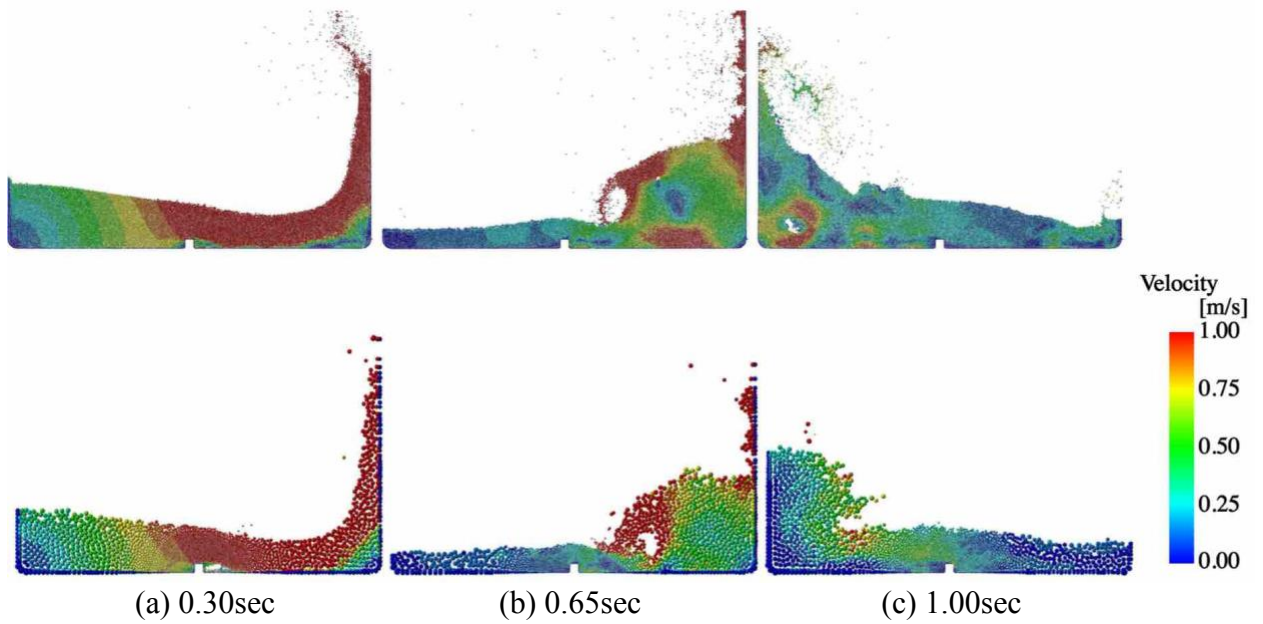


Figure 8: Velocity distribution of the dam break simulation with an obstacle (above: single resolution, bottom: multi-resolution)

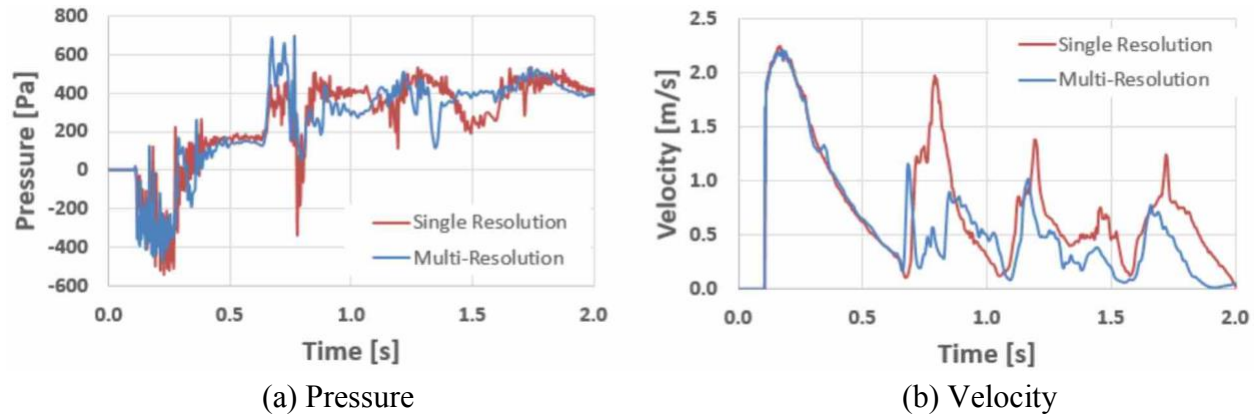


Figure 9: Pressure and velocity profile in the dam break simulation with an obstacle

fluid particles was reduced by 82.8 % by using the multi-resolution techniques, and as a result, the computational time was reduced by 93.4 %. In this case, the main reason why the reduction rate of the computational time is higher than that of the number of the fluid particles is because the size of the time step was able to be larger for the multi-resolution simulation. The particles which had the highest velocity were the splash particles after the fluid collided with the wall and the size of the splash particles in the multi-resolution simulation were larger than that in the single resolution simulation. Then, the time step could be larger in the multi-resolution simulation.

The pressure and velocity at the evaluation point located just above the obstacle were monitored for every 100 time steps as plotted in Figure 9. The results for the multi-resolution simulation provided similar pressure and velocity profiles with those of the single resolution simulation until 0.6 sec, but there were some differences observed as the simulation went on after that. This is mainly because a particle which had been in a lower resolution region came back to the higher resolution region carrying a bad level of accuracy with it as mentioned above. However, most importantly, the peak velocity at the first fluid impact around at 0.14 sec was almost the same. The multi-resolution technique is beneficial to reduce computational costs, but a proper resolution configuration for a proper problem to be simulated is required. This is a common issue not only for particle methods but also for many other numerical methods.

4 CONCLUSIONS

The Multi-Resolution MPS method is presented in this work. The spatial resolution is changed adaptively by the particle splitting and merging algorithms. The LSMPS method is applied to obtain accurate results even if particles have different diameters. A new wall boundary scheme, which is represented by polygons, is also improved for a multi-resolution simulation by copying fluid particles around walls and generating imaginary wall particles right on the boundaries. By conducting simulations for the Taylor Green vortex and for the dam break, the accuracy of the Multi-Resolution MPS method could be verified. Also, it was shown that this method was able to reduce computational costs significantly. Although only two dimensional simulations were conducted in this work, extension to three dimensions is straightforward.

REFERENCES

- [1] B. Adams, M. Pauly, R. Keiser, and L. J. Guibas. Adaptively sampled particle fluids. *ACM Transactions on Graphics - Proceedings of ACM SIGGRAPH 2007*, 26(3):Article No.48, 2007.
- [2] G. A. Dilts. Moving-least-squares-particle hydrodynamics-i. consistency and stability. *International Journal for Numerical Methods in Engineering*, 44(8):1115–1155, 1999.
- [3] G. A. Dilts. Moving least-squares particle hydrodynamics ii: conservation and bound-aries. *International Journal for Numerical Methods in Engineering*, 48(10):1503–1524, 2000.
- [4] R. A. Gingold and J.J. Monaghan. Smoothed particle hydrodynamics - theory and application to non-spherical stars. *Monthly Notices of the Royal Astronomical Society*, 181:375–389, 1977.
- [5] S. Kitsionas and A. P. Whitworth. Smoothed particle hydrodynamics with particle splitting, applied to self-gravitating collapse. *Monthly Notices of the Royal Astronomical Society*, 330(1):129–136, 2002.
- [6] S. Koshizuka, H. Tamako, and Y. Oka. A particle method for incompressible viscous flow with fluid fragmentation. *Computational Fluid Dynamics Journal*, 4:29–46, 1995.
- [7] M. Lastiwka, N. Quinlan, and M. Basa. Adaptive particle distribution for smoothed particle hydrodynamics. *International Journal for Numerical Methods in Fluids*, 47(10-11):1403–1409, 2005.
- [8] A. Leroy, D. Violeau, M. Ferrand, and C. Kassiotis. Unified semi-analytical wall boundary conditions applied to 2-d incompressible sph. *Journal of Computational Physics*, 261:106–129, 2014.
- [9] M. B. Liu, G. R. Liu, and K. Y. Lam. Adaptive smoothed particle hydrodynamics for high strain hydrodynamics with material strength. *Shock Waves*, 15(1):21–29, 2006.
- [10] L. B. Lucy. A numerical approach to the testing of the fission hypothesis. *Astronomical Journal*, 82:1013–1024, 1977.
- [11] P. Nair and G. Tomar. Volume conservation issues in incompressible smoothed particle hydrodynamics. *Journal of Computational Physics*, 297(15):689–699, 2015.

- [12] K. Shibata, S. Koshizuka, and T. Tamai. Overlapping particle technique and application to green water on deck. International Conference on Violent Flows, Nantes, France, September, 2012. 106-111.
- [13] T. Tamai and S. Koshizuka. Least squares moving particle semi-implicit method. *Computational Particle Mechanics*, 1(2):277–305, 2014.
- [14] M. Tanaka, R. Cardoso, and H. Bahai. Multi-resolution mps method. *Journal of Computational Physics*, 359:106–136, 2018.
- [15] M. Tanaka, T. Masunaga, and Y. Nakagawa. Multi-resolution mps method. *Transactions of Japan Society for Computational Engineering and Science*, pages Paper No.20090001, in Japanese, 2009.
- [16] Z. Tang, D. Wan, G. Chen, and Q. Xiao. Numerical simulation of 3d violent free-surface flows by multi-resolution mps method. *Journal of Ocean Engineering and Marine Energy*, 2(3):355–364, 2016.
- [17] Z. Tang, Y. Zhang, and D. Wan. Numerical simulation of 3-d free surface flows by overlapping mps. *Journal of Hydrodynamics, Ser. B*, 28(2):306–312, 2016.

Discontinuous Galerkin Method for Advection Equation of Interface Capturing Method

Seizo Tanaka*

*University of Tsukuba

ABSTRACT

The protection system against water hazards, such as tsunami and flood have to have enough performance to save the residents. The design of protection system against the disaster should consider a dynamic impact force of water. Also the flood area should be estimated accurately. The numerical simulation is a useful tool estimate the forces and flood inundation area. In such a simulation, the high accurate solution requires not only stability and robustness but also mass conservation. We develop the free surface flow analysis method for tsunami wave propagation based on interface capturing approach. For treatment of free surface motion, interface capturing approach based on Volume of Fluid (VOF) method [1] is useful to apply dramatic free surface motion such as hydraulic jump, breaking waves. The accuracy of interface location expressed by interface function depends on the solution of advection equation in interface capturing method. The discontinuous Galerkin method [2] is applied to the advection equation as the governing equation of interface motion. And stabilized finite element method based on SUPG and PSPG method with continuous Galerkin method [3] is applied to the governing equation of incompressible viscous flow. As for the numerical example to verify the present method, broken-dam problem is carried out. [1] C. W. Hirt, B.D. Nicols: Volume of Fluid (VOF) method for dynamics of free boundaries, Journal of Computational Physics, Vol.39, pp.201-225, 1981. [2] B. Cockburn, G.E. Karniadakis, C.-W. Shu: Discontinuous Galerkin Methods, Theory, Computation and Applications, Springer, 2000. [3] S. Aliabadi, T.E. Tezduyar: Stabilized-finite element/Interface-capturing technique for parallel computing, Compute Methods Applied Mechanics and Engineering, Vol.190, pp.243-261, 2000.

Aero Acoustic Investigation of Backward-Facing Step Controlled by Suction and Blowing with Large Eddy Simulation

Kamil Furkan Taner*, Furkan Cosgun**, Baha zafer***

*Istanbul University, **Istanbul Technical University, ***Istanbul University

ABSTRACT

Kamil Furkan Taner*1 Furkan Cosgun2 Baha Zafer3 Istanbul University Istanbul Technical University Istanbul University *Corresponding Author Aero Acoustic investigation of Backward-Facing Step controlled by Suction and Blowing with Large Eddy Simulation Although Backward-Facing Step (BFS) studies have a simple geometry but exhibits a highly complex flow structure. Main problem retains their interests due to that this geometry is suitable to try new control methods such as active suction and blowing. Additionally, Backward-Facing Step geometry is frequently encountered in both military and industrial applications. In this study, Low Mach number transient incompressible flow field and aerodynamically generated noise of BFS flows will be investigated. BFS flow with steady Suction and Blowing control mechanisms will be numerically studied using Large Eddy Simulation (LES) and Subgrid-Scale Model of Kinetic-Energy Transport Equation. All unsteady flow field results are used to compute a BFS noise using Ffowcs William-Hawking (FW-H) Equation. Governing equations will be solved using segregated solver and non-iteratively which provides us to solve problem spending less time compared to iterative solvers using commercial FLUENT 16.0 with finite-volume method. All numerical solutions are compared with experimental data for unsteady flow field. References 1.C.-R. Zheng,Y.-C. Zhang and W.-Y. Zhang," Large eddy simulation of separation control over a backward-facing step flow by suction", International Journal of Computational Fluid Dynamics,25:2,59-74,2011. 2.B.Zafer,F. Cosgun,"Aeroacoustics investigation of unsteady incompressible cavity flow", Journal of the Faculty of Engineering and Architecture of Gazi University,31:3,665-675,2016. 3. Özsoy, E., Rambaud, R., Stitou, A. and Riethmuller, M.L., "Vortex characteristics in laminar cavity flow at very low Mach number", Experiments in Fluids, Tome 38, 133-145, 2005.

Mechanical Properties Regulate the Wrapping of Nanoparticles by the Cell Membrane

Huayuan Tang^{*}, Hongwu Zhang^{**}, Hongfei Ye^{***}, Yonggang Zheng^{****}

^{*}Dalian University of Technology, P. R. China, ^{**}Dalian University of Technology, P. R. China, ^{***}Dalian University of Technology, P. R. China, ^{****}Dalian University of Technology, P. R. China

ABSTRACT

Understanding how the cell membrane wraps nanoparticles (NPs), which are promising for many biomedical applications, is essential to improve the performance of the NP-based drug delivery carriers. Mechanical properties of the NP-membrane system, such as the shape and deformability of NPs, the flexibility and tension of the membrane, have complex influences on the wrapping behaviors of NPs by the cell membrane. Though extensive studies have been conducted in recent years, there is still a lack of a thorough understanding on these behaviors and the underlying mechanisms. In our recent work, we investigate how the shape and deformability of NPs regulate the cellular wrapping behaviors based on continuum models. The simulation results show that, accompanied with the rotation of the NP induced by the competition between the bending and membrane tension, the endocytosis of NP with irregular shape proceeds through the symmetric-asymmetric or asymmetric-symmetric-asymmetric wrapping pathway. For the wrapping of deformable NP, higher NP-membrane adhesion strength is required for the softer NP to be fully wrapped and the NP is easier to be fully wrapped but harder to be shallowly wrapped when the NP locates outside than inside the vesicle. For the wrapping of multiple NPs, the competition between the NP-NP adhesion and the membrane-mediated repulsion leads the NPs to be wrapped cooperatively or independently. For the system with elongated elliptic cross-sectional NPs, the NPs are more likely to be wrapped independently as the shapes become more anisotropic, while the soft NPs tend to be wrapped cooperatively compared with the stiff NPs. These results may provide guidelines to control the internalization pathway of NPs and for the design of NP-based drug delivery systems. References [1] Zheng, Y.; Tang, H.; Ye, H.; Zhang, H. Adhesion and Bending Rigidity-Mediated Wrapping of Carbon Nanotubes by a Substrate-Supported Cell Membrane. *RSC Adv.* 2015, 5, 43772. [2] Tang, H.; Ye, H.; Zhang, H.; Zheng, Y. Wrapping of Nanoparticles by the Cell Membrane: The Role of Interactions between the Nanoparticles. *Soft Matter* 2015, 11, 8674. [3] Tang, H.; Zhang, H.; Ye, H.; Zheng, Y. Wrapping of a Deformable Nanoparticle by the Cell Membrane: Insights into the Flexibility-Regulated Nanoparticle-Membrane Interaction. *J. Appl. Phys.* 2016, 120, 114701.

New Derivative-based Importance Criteria and Their Applications to a Plasma-Combustion Coupling Mechanism

Kunkun Tang^{*}, Jonathan Freund^{**}

^{*}University of Illinois at Urbana-Champaign, ^{**}University of Illinois at Urbana-Champaign

ABSTRACT

Sobol' and Kucherenko [1, 2] introduced two derivative-based sensitivity indices (DSI) and have shown a link between global sensitivity indices (GSI) and DSI. Even though GSI are considered superior to DSI as an importance ranking tool since they contain more model information, they can be impractical for many applications due to their high cost [2]. Monte Carlo algorithms for computing DSI and GSI have been developed and compared and the advantageous properties of the algorithm for DSI have been shown. DSI are particularly attractive since their computation can be much faster than GSI in applications with relatively low derivative variation. The approach proposed by Sudret and Mai [3] can compute the DSI [1] analytically from a polynomial chaos expansion. However, the extension of this for computing the improved DSI [2] seems difficult because of additional terms in the integrand. In the paper, we will introduce two new derivative-based measures that can be efficiently computed using an adaptive ANOVA approach, and use them to target multi-physics applications with hundreds of uncertain parameters. We will compare our variation of DSI to the standard approaches [1, 2], both theoretically and numerically. The cost advantage of our DSI will be shown. A simple extension of DSI for correlated inputs will also be presented. The overall methodology will be demonstrated for a plasma-combustion system in a dielectric-barrier discharge (DBD) actuated fuel jet. Experimental data of ignition burn boundary will be compared to predictions. We will consider challenging multi-physical uncertain parameters from submodels of chemical kinetics, laser ignition, and the DBD actuator. The total number of uncertain parameters in this application is 73. References [1] I.M. Sobol' and S. Kucherenko. Derivative based global sensitivity measures and their link with global sensitivity indices. *Mathematics and Computers in Simulation*, 79(10):3009–3017, 2009. [2] I.M. Sobol' and S. Kucherenko. A new derivative based importance criterion for groups of variables and its link with the global sensitivity indices. *Computer Physics Communications*, 181(7):1212–1217, 2010. [3] B. Sudret and C.V. Mai. Computing derivative-based global sensitivity measures using polynomial chaos expansions. *Reliability Engineering & System Safety*, 134:241–250, 2015.

Multiscale Molecular Simulation of Morphology Evolution of Active Layer of Small Molecule Organic Solar Cell during Vacuumed Deposition Process

Ping-Han Tang^{*}, Chun-Wei Pao^{**}

^{*}Research Center for Applied Sciences, Academia Sinica, Taiwan, ^{**}Research Center for Applied Sciences, Academia Sinica, Taiwan

ABSTRACT

Recently, vacuum deposition of organic small molecule has been applied to the fabrication of many flexible optoelectronic device such as small molecule solar cells and organic light emitting diodes. In this study, we investigated the morphology evolution of DPDCPB:C70 small molecule solar cells during vacuum co-deposition processes by carrying out a series of GPU-accelerated, multiscale, coarse-grained molecular dynamics (CGMD) simulations. By coarsing DPDCPB and C70 molecules into ellipsoid beads, we were able to simulate morphology evolution of system with system length scale compatible with those with experiments (c.a. 50 nm). The Gay-Berne force field was parametrized using genetic algorithm to reproduce potential energy surfaces from respective all-atom molecular simulations. We systematically investigated morphology evolution of the active layer with different donor:acceptor ratio, as well as effects of substrate strains on resultant film morphologies. The present study demonstrates that, by using the ellipsoid-based coarse-grained model, it is possible to study morphology evolution of small molecule organic thin film during vacuum deposition processes with unprecedented details, which can provide valuable insights for experimental teams to further optimize device fabrication protocols for the next generation organic optoelectronic devices.

Fracture of Water-containing Soft Solids: Experiment and Phase Field Modeling

Shan Tang*

*Dalian University of Technology

ABSTRACT

A typical water-containing soft solid, hydrogel, is fabricated. Compression and three-point bending experiments on hydrogel blocks are carried out under plane strain conditions. To reveal the underlying physics behind the fracture behaviors at the large deformation regime observed in experiments, we reformulate a hyperelastic model for hydrogels with initial swelling that takes into account the initial volume fraction of water. In this model, the free energy is constructed based on decomposition of the deformation gradient into isochoric and volumetric parts. The model parameters are calibrated by curve fitting of the experimental results obtained under uniform compression. To simulate the fracture of hydrogels, a phase field modeling approach is adopted and incorporated into the hydrogel model. In the phase field formulation, the crack phase field only degrades the isochoric and positive volumetric parts of the deformation, which is a key for numerically stable fracture modeling. The present model is able to predict the crack initiation, fracture path and the force vs. displacement in good agreement with those in experiments. [1] Borden, M.J., Verhoosel, C.V., Scott, M.A., Hughes, T.J.R., Landis, C.M., 2012. A phase field description of dynamic brittle fracture. *Computer Methods in Applied Mechanics and Engineering* 217-220, 77-95. [2] Bourdin, B., Francfort, G.A., Marigo, J.J., 2000. Numerical experiments in revisited brittle fracture. *Journal of the Mechanics and Physics of Solids* 48, 797-826. [3] Tang, S., Kopacz, A.M., Chan, S., Olson, G.B., Liu, W.K., et al., 2013. Three dimensional ductile fracture analysis with a hybrid multiresolution approach and microtomography. *Journal of the Mechanics and Physics of Solids* 61, 2108-2124.

Multi-Level Hybridized Optimization Methods Coupling Local Search Deterministic and Global Search Evolutionary Algorithms

Zhili Tang^{*}, Lianhe Zhang^{**}, Jacques Periaux^{***}, Xiao Hu^{****}

^{*}NUAA, ^{**}ARI, ^{***}CIMNE, ^{****}NUAA

ABSTRACT

Efficient optimization methods coupling a stochastic evolutionary algorithm with a gradient based deterministic method are presented in this paper. Two kinds of hybridization are compared: one is a stochastic/deterministic alternate algorithm, the other is a stochastic/deterministic embedded algorithm. In the alternating hybridized algorithm, stochastic and deterministic optimizers are performed alternately, some individuals are selected from the previous population, and then to be sent to the deterministic algorithms for further optimization, the improved individuals were inserted into the above population to form a new population for stochastic algorithm. In the embedded hybridized algorithm, stochastic and deterministic optimization softwares run in parallel and independently, the connection between them is that deterministic optimizer works on a random selected individual (or the best individual) from the unevaluated population of stochastic algorithm, then its outcome (new individual) is re-injected into the evaluated population. Moreover, multi-level approximation (e.g. variable fidelity modeling and analysis, hierarchical approximate parameterization) is used in the algorithm, i.e. low fidelity modeling and rough parameterization are used to perform search on large population at lower level, and high fidelity modeling and detailed parameterization are used at higher level. After a validation of the methods on mathematical test cases, the methods are successfully applied to aerodynamic shape optimization of the fore-body of a hypersonic air breathing vehicle and provide significant acceleration in terms of CPU time.

Research on Thermo-hygro Coupling Problems of Early-age Concrete Based on Generalized Finite Difference Method

Zhuochao Tang^{*}, Zhuojia Fu^{**}, Rui Yang^{***}, Haitao Zhao^{****}

^{*}Center for Numerical Simulation Software in Engineering and Sciences, College of Mechanics and Materials, Hohai University, ^{**}Center for Numerical Simulation Software in Engineering and Sciences, College of Mechanics and Materials, Hohai University, ^{***}College of Civil and Transportation Engineering, Hohai University, ^{****}College of Civil and Transportation Engineering, Hohai University

ABSTRACT

Abstract: The microstructure of early-age concrete is constantly evolving due to hydration. Temperature and humidity of early-age concrete interact with each other and vary drastically, which has great influence on the formation and development of concrete. Thus, research on the quantitative relationship among temperature and humidity of early-age concrete has great significance to prevent deformation and cracking of concrete in early age. This paper applies a new-developed domain-type meshless method, the generalized finite difference method (GFDM), to solve thermo-hygro coupling problems of early-age concrete. The GFDM is free from mesh generation and numerical integration compared with the traditional finite difference method. And it is more flexible when the shape of the computational domain is irregular. Besides, the GFDM remains the merits of the simplicity and wide applicability in the classical finite difference method. For solving the coupling problems, the moving least squares theory and second-order Taylor series expansion have been used to construct the GFDM approximation formulation. And the second-order explicit Runge-Kutta method is used for time discretization. It is found that the generalized finite difference method combined with second-order explicit Runge-Kutta method provides the accurate numerical results in several numerical examples. Key words: early-age concrete; thermo-hygro coupling; the generalized finite difference method; second-order explicit Runge-Kutta method

Waves Scattering and Dissipation in Amorphous Materials

Anne Tanguy^{*}, Yaroslav Beltukov^{**}, Haoming Luo^{***}, Dmitry Parshin^{****}

^{*}INSA Lyon, France, ^{**}Ioffe Physical Technical Institute, St Petersburg, Russia, ^{***}INSA Lyon, France, ^{****}Saint Petersburg State Polytechnical University, Russia

ABSTRACT

In amorphous samples, acoustic waves scattering takes place at all scales. We show numerical results with evidence of simple scattering at long wave-lengths, multiple scattering at smaller wave-lengths, and mixed regimes in between. The transition from simple to multiple scattering, as well as possible localization regime, depends on the specificities of short range order.

Experimental and Modeling Strategies to Assess Micro and Nano-voids Growth and Coalescence in Irradiated Metallic Materials

Benoit Tanguy^{*}, Jérémy Hure^{**}, Pierre-Olivier Barrioz^{***}, Chao Ling^{****}, Jean-Michel Scherrer^{*****}, Jacques Besson^{*****}, Samuel Forest^{*****}

^{*}CEA Saclay, Université Paris–Saclay, ^{**}CEA Saclay, Université Paris–Saclay, ^{***}CEA Saclay, Université Paris–Saclay, ^{****}CEA Saclay, Université Paris–Saclay, ^{*****}MINES ParisTech, PSL Research University, MAT – Centre des matériaux, ^{*****}MINES ParisTech, PSL Research University, MAT – Centre des matériaux

ABSTRACT

Microporous and nanoporous metallic materials are observed in many industrial applications such as structural alloys used in nuclear power plants under irradiation. These alloys show a marked decrease of fracture toughness with increasing level of fluence. Void growth to coalescence is the classical mechanism involved in ductile fracture of structural alloys, thus are the key features to better understand fracture toughness of these materials. Growth regime is characterized by a diffuse plastic flow around voids, while coalescence corresponds to localized plastic flow between adjacent voids. Analytical models, numerical simulations and experimental data have clearly shown that both regimes strongly depend on the mechanical behavior of the material around the voids, where yield stress, strain-hardening modulus and anisotropy are key parameters. Besides the growth and coalescence of micro-voids in an irradiated matrix, fracture toughness properties may be affected by the presence of nanovoids resulting of vacancies clustering under irradiation so that assessing the structural integrity of these components may require using homogenized models relevant for nanoporous materials. However, as voids size decreases to the nanoscale, size effects are expected in the fracture of ductile solids. The present paper details the strategies developed in order to assess the micro and nano-voids growth and coalescence in irradiated metallic materials. In the first part of the paper, few examples of experimental studies carried out on CFC materials will be given. These studies are based on the use of heavy ions irradiations to mimic both matrix hardening and softening resulting from irradiation and the creation of intragranular nanovoids population. In the second part of the paper, the modeling strategies will be detailed. Assessment of hardening, size and orientation effects is based on crystal plasticity framework. Finite element simulations of voided unit cells are performed with a single crystal plasticity model accounting for strain hardening and loss of strain hardening capability associated with irradiation induced defects. A first assessment of voids size effects is performed based on a single crystal strain gradient plasticity model derived at finite strains [1]. Finally, a recently implemented model taking into account the presence of an interface associated with an interfacial energy [2] and its comparison with finite element calculations on porous unit cells will be discussed. [1] C. Ling, S. Forest, J. Besson, B. Tanguy, F. Latourte, Int. Journal of Solids and Structures (2017) in-press [2] L. Dormieux, D. Kondo, Int. Journal of Eng. Science 48 (2010) 575–581

Matrix-free Isogeometric Analysis: The Computationally Efficient k -refinement method

Mattia Tani*, Giancarlo Sangalli**

*Università di Pavia, **Università di Pavia

ABSTRACT

One of the distinguishing features of Isogeometric Analysis (IGA) is the possibility of using high-degree high-regularity splines (the so-called k -refinement) as they deliver higher accuracy per degree-of-freedom in comparison to C^0 finite elements. Unfortunately, if the implementation is done following the approaches that are standard in the context of C^0 finite elements, the computational cost increases dramatically with the spline degree. This is true both for the formation of the linear system and for its numerical solution. As a consequence, the k -refinement is unfeasible for practical problems, where quadratic or cubic splines are typically preferred. Several improvements have been achieved recently. In [SIAM J. Sci. Comput., 38 (2016), pp. A3644--A3671], we discuss a preconditioner for scalar elliptic problems, based on an old idea, which is robust with respect to both the mesh size h and the spline degree p . Moreover, in [Comput. Methods Appl. Mech. Engrg., 316 (2017), pp. 606--622] a novel method is developed that allows the formation of the stiffness matrix with almost optimal complexity. In the work [arXiv:1712.08565, (2017), pp. 1--21], these two approaches are combined with a third ingredient: a matrix-free implementation. In this talk we discuss the overall strategy, which is very beneficial in terms of both memory and computational cost. In particular, we show that memory required is practically independent of p and that the cost depends on p only mildly. The numerical experiments show that, with the new implementation, the k -refinement becomes appealing from the computational point of view. Indeed, increasing the degree and continuity leads to orders of magnitude higher computational efficiency with respect to standard approaches.

Numerical Simulation of Liquid Drop Motions at the Edge

Hiroki Tanuma^{*}, Junya Onishi^{**}, Naoki Shikazono^{***}

^{*}The University of Tokyo, ^{**}The University of Tokyo, ^{***}The University of Tokyo

ABSTRACT

Contact line motion plays an important role in many industrial applications. For example, in the heat exchanger of an air conditioning system, the draining process of condensate water strongly influences the heat exchanger characteristics, such as pressure loss and heat transfer rate. Thus, accurate prediction of the contact line motion is highly demanded for designing optimal heat exchanger fins. It is well known that the contact line is pinned at the edge of a solid object. When the contact line is pinned at the edge with an edge angle ϕ an apparent contact angle increases from its equilibrium value θ_y (Young's angle) to a critical maximum value, θ_c , i.e., $\theta_c = \theta_y + (180 - \phi)$, which is also known as the Gibbs inequality condition (Gibbs, J. W. Scientific Papers 1906, 326.). Fang and Amirfazli (Fang, G.; Amirfazli, A. Langmuir 2012, 28, 9421–9430.) developed a free energy model of a droplet on a single pillar and illustrated four wetting cases at the edge. However, their model can only be applied to micro order droplets since they neglected the effect of gravity. Furthermore, when considering engineering application, an extension of their theory to more complex geometries is essential. To the best of our knowledge, there has been no attempts to study the edge effects of more complex objects. In this research, numerical simulations of the motion of a liquid drop at the right angle edge was conducted. In the present simulation, the continuity equation and the Navier-Stokes equation for incompressible viscous fluids are solved for both liquid and gas phases. To capture the motion of the interface between the liquid and gas phases, the level-set method is used. The boundary conditions at the liquid-gas interface are treated in a sharp manner with the use of the Ghost-fluid method. A numerical method based on the Cox theory is used for modeling the dynamics of the contact angle. Finally, the numerical results were validated with the experimental data.

Systematic Risk Analysis of Dam Groups Using Fussy Bayesian Network

Liang Tao*, Yating Hu**

*Hohai University, **Hohai University

ABSTRACT

Nowadays, cascade development is the main trend in river development. The majority of risk analysis methods for dam groups are focused on the weighted superposition of risks of each dams in the river basin. However, the risk of individual dams in the whole river basin will be transmitted to each other. Once a certain dam is broken, it may lead to the collapse of downstream dams. Simply adding the risk of each dams in a basin does not objectively explain the systematic risk in the river basin. Here, based on the analysis of the mechanism of risk transmission in dam group, a fuzzy Bayesian network is used to establish the information fusion model for the risk of dam system in river basins. By example, we show the application of this model in the risk analysis of dam groups. The model has a good performance in the risk analysis of dam system in the basin, and can reasonably consider upstream and downstream risk transmission.

Computational-Experimental Approach to Evaluation of the Mechanical State of Laminate Composite Structures Using Embedded Fiber-Optic Strain Sensors

Mikhail Tashkinov^{*}, Valeriy Matveenkov^{**}, Igor Shardakov^{***}, Natalia Kosheleva^{****}, Grigoriy Serovaev^{*****}

^{*}Perm National Research Polytechnic University, ^{**}Institute of Continuous Media Mechanics of RAS; Perm National Research Polytechnic University, ^{***}Institute of Continuous Media Mechanics of RAS; Perm National Research Polytechnic University, ^{****}Perm National Research Polytechnic University, ^{*****}Institute of Continuous Media Mechanics of RAS; Perm National Research Polytechnic University

ABSTRACT

In the recent years, research in smart materials and their fields of applications had been developing very actively. The idea of creating materials that along with prescribed basic functional tasks provide real-time information about their internal state is highly relevant for polymer composite materials and structures. The concept of smart composite materials with self-diagnostic functions had found its implementation with involvement of fiber-optic sensors, which, in particular, are able to measure various physical and mechanical quantities. Embedded into composites fiber-optic sensors have a wide range of advantages over other methods of strain measuring. They are able to withstand strains equal to strains of composite laminate, are affordable and easy to manufacture, are immune to electrical interference. Thus, under severe loading conditions fiber-optic sensors have advantages, including sensitivity, in comparison with other types of sensors. The proposed technique for predicting strength and mechanical behavior of composite structures is to compare the set of measurements from fiber-optic sensors with the results of numerical modelling with consideration of the features of the microstructure, including occurrence and development of defects. The computational component of the technique provides finite element simulations of mechanical behavior and failure of composite structure. The experimental part is based on strains measurements obtained by fiber-optical strain sensors on Bragg gratings embedded between the layers of composite. The mathematical models based on strains, measured by the optical fiber, are used for identifying stress concentration zones as well as for assessment of the possibility of application of fiber sensors to recording of internal defects appearance and propagation. The models were found to be applicable in case of introduction of the calibration coefficients for the sensors or when the strains along the fiber are much higher than the strains in the plane perpendicular to the fiber. The stress and strain fields were calculated taking into account microstructure in the vicinity of embedded fiber and the accompanying technological defect in the form of a resin pocket. The results of the approach illustrate a possibility of application of suggested non-destructive monitoring tools for correcting the parameters of the mechanical models. The latter allows to increase precision of numerical prediction of behavior and failure of composite materials and structures.

An Accurate, Fast, and Scalable Solver for High-frequency Wave Propagation

Matthias Taus^{*}, Leonardo Zepeda-Núñez^{**}, Russell Hewett^{***}, Laurent Demanet^{****}

^{*}MIT, ^{**}Lawrence Berkeley National Laboratory, ^{***}Total E&P, ^{****}MIT

ABSTRACT

In many science and engineering applications, solving time-harmonic high-frequency wave propagation problems quickly and accurately is of paramount importance. For example, in geophysics, particularly in oil exploration, such problems can be the forward problem in an iterative process for solving the inverse problem of subsurface inversion. It is important to solve these wave propagation problems accurately in order to efficiently obtain meaningful solutions of the inverse problems: low order forward modeling can hinder convergence. Additionally, due to the volume of data and the iterative nature of most optimization algorithms, the forward problem must be solved many times. Therefore, a fast solver is necessary to make solving the inverse problem feasible. For time-harmonic high-frequency wave propagation, obtaining both speed and accuracy is historically challenging. Recently, there have been many advances in the development of fast solvers for such problems, including methods which have linear complexity with respect to the number of degrees of freedom. While most methods scale optimally only in the context of low-order discretizations and smooth wave speed distributions, the method of polarized traces has been shown to retain optimal scaling for high-order discretizations, such as hybridizable discontinuous Galerkin methods and for highly heterogeneous (and even discontinuous) wave speeds. The resulting fast and accurate solver is consequently highly attractive for geophysical applications. To date, this method relies on a layered domain decomposition together with a preconditioner applied in a sweeping fashion, which has limited straight-forward parallelization. In this work, we introduce a new version of the method of polarized traces which reveals more parallel structure than previous versions while preserving all of its other advantages. We achieve this by further decomposing each layer and applying the preconditioner to these new components separately and in parallel. We demonstrate that this produces an even more effective and parallelizable preconditioner for a single right-hand side. As before, additional speed can be gained by pipelining several right-hand-sides.

Recent Advances in the Interventional Planning Stage of the Transseptal Puncture

Joao Tavares*, Pedro Morais**, Jan D'hooge***, João Vilaça****

*Instituto de Ciência e Inovação em Engenharia Mecânica e Engenharia Industrial, Faculdade de Engenharia, Universidade do Porto, Portugal, **Instituto de Ciência e Inovação em Engenharia Mecânica e Engenharia Industrial, Faculdade de Engenharia, Universidade do Porto, Portugal, ***Lab on Cardiovascular Imaging & Dynamics, Department of Cardiovascular Sciences, KULeuven - University of Leuven, Leuven, Belgium, ****DIGARC – Polytechnic Institute of Cávado and Ave, Barcelos, Portugal

ABSTRACT

Abstract Access to the left atrium (LA) is required for several minimally invasive cardiac interventions. Hereto, the atrial septum is punctured using a catheter inserted via the venous system using a technique termed transseptal puncture (TSP). Although the TSP has been commonly used, complications are still common. Besides, the exact puncture location is defined based on experience, being sub-optimal in specific situations. In this project, multiple contributions have been made to improve the state-of-the-art of the TSP. We initiated with a review [1] concerning the technique in terms of guidance technologies, pre-procedural planning and used surgical tools. Although multiple advances can be found regarding the medical tools and guidance technologies, few studies focused on the planning exist. Then, we proposed strategies to automate the planning of the TSP, namely: 1) an atrial region segmentation methodology [2]; 2) a strategy to identify the optimal puncture region, which is usually known as fossa ovalis (FO), and 3) a personalized atrial phantom model [3]. Both segmentation methods were validated on 41 computed tomographic images. The automated segmentations were compared against manual delineations, and an error lower than 1.7 mm was found as to the atrial region [1]. Regarding the identification of the FO, a performance comparable to the inter-observer variability was achieved. Moreover, both methods proved to be much faster than the traditional practice. Regarding the phantom model, it led to a highly accurate production and a highly realistic model in terms of intra-procedural imaging [3]. The developed strategies have shown high feasibility and accuracy, corroborating their potential for the automated planning of TSP. Acknowledgement: The authors acknowledge FCT, in Portugal, and the European Social Found, European Union, for funding support through the "Programa Operacional Capital Humano" in the scope of the PhD grant SFRH/BD/95438/2013, and also the funding of Projects NORTE-01-0145-FEDER-000013 and NORTE-01-0145-FEDER-000022, cofinanced by FEDER. References: [1] - P. Morais, J.L. Vilaça, J. Ector, J. D'hooge, and J.M.R.S. Tavares, "Novel solutions applied in transseptal puncture: a systematic review," *Journal of Medical Devices*, 2017. [2] - P. Morais, J.L. Vilaça, S. Queirós, F. Bourier, I. Deisenhofer, J.M.R.S. Tavares, and J. D'hooge, "A competitive strategy for atrial and aortic tract segmentation based on deformable models," *Medical Image Analysis*, 2017. [3] - P. Morais, J.M.R.S. Tavares, S. Queirós, F. Veloso, J. D'hooge, J.L. Vilaça, "Development of a patient-specific atrial phantom model for planning and training of inter-atrial interventions". *Medical Physics*, 2017.

Dynamic Spring Element Model for the Effective Simulation of the Longitudinal Tensile Failure of Polymer Composite

Rodrigo Tavares*, Fermin Otero**, Albert Turon***, Pedro Camanho****

*DEMec, Faculdade de Engenharia, Universidade do Porto; AMADE, Polytechnic School, University of Girona; INEGI, Porto, **INEGI, Porto, ***AMADE, Polytechnic School, University of Girona, ****DEMec, Faculdade de Engenharia, Universidade do Porto; INEGI, Porto

ABSTRACT

The need to understand the failure mechanisms in composite materials at the micro level has gained additional importance due to the pressing need to develop high performance materials for more demanding applications. This understanding makes it possible to develop a new generation of polymer composite materials in-silico. To understand fibre dominated failure it is necessary to have accurate models that are able to capture the main failure mechanisms in this type of failure. Although complex micromechanical models that capture these mechanisms exist, they are computationally expensive and can only be used for a limited representative volume element size. Simplified models are, therefore, necessary to allow faster predictions, although at the cost of some accuracy. The faster computation times of simplified models allow also the study of more material variations and can be used for optimization purposes. In this work, an extension of the Spring Element Model to a random fibre packing and hybrid composites is presented. Additionally, this model extends the Spring Element Model to consider the dynamic effects of fibre failure. The dynamic stress waves that propagates within the in the intact fibres increases that surround the broken one increase the stress concentrations and, therefore, increase the failure probability of these fibres. This dynamic effect will change the formation process of clusters of broken fibres, which will influence the predicted behaviour of the material. A study on the influence of the dynamic effects on the local stress fields surrounding a broken fibre and on the behaviour of the material is done for both non-hybrid and hybrid composites.

Novel NIST Databases to Aid Material Discovery

Francesca Tavazza^{*}, Kamal Choudhary^{**}, Gabriel Joshua^{***}, Richard Hennig^{****}

^{*}National Institute of Standard and Technology, ^{**}National Institute of Standard and Technology, ^{***}University of Florida, ^{****}University of Florida

ABSTRACT

Technological advances heavily rely on discovery and characterization of materials. Computational investigations, both at the classical and quantum level, have been proven to be extremely effective tools in characterizing material-properties starting from crystal structure information. As part of the Materials Genome Initiative, National Institute of Standards and Technology (NIST) has developed the Joint Automated Repository for Various Integrated Simulations (JARVIS) available at <https://jarvis.nist.gov/>. Jarvis contains repositories designed to automate materials discovery using classical force-field (JARVIS-FF)¹, density functional theory (JARVIS-DFT)², and machine learning (JARVIS-ML) calculations. The JARVIS-FF database currently consists of 20000 entries including energetics, elastic property, surface energy and vacancy formation energy calculations, and it is still increasing. It also includes computational tools for convex-hull plots and force-field comparisons. The data covers 1471 materials and 116 force-fields. Both the complete database and the software coding used in the process have been released for public use online. The JARVIS-DFT database consists of more than 25000 DFT calculations for three-dimensional (3D) bulk and single layer 2D materials of structural, electronic and elastic properties. A novel lattice-constant criterion is used to identify potentially new 2D, 1D, and 0D materials. We predicted at least 1485 2D materials based on such criterion. For bulk structures, the database also contains optoelectronic properties (bandgap and frequency dependent dielectric function) computed using two different exchange-correlation functionals, vdW-DF-optb88 and the Tran-Blaha modified Becke-Johnson functional. Lastly, while DFT presents an in-principle exact theory, various approximations are required to perform practical simulations. To this day, a systematic evaluation of the uncertainties related to such approximations is still lacking, and NIST is developing the DFT benchmarking database to estimate the uncertainty due to various choices of key controlled approximations. 1. Kamal Choudhary, Faical Yannick P. Congo, Tao Liang, Chandler Becker, Richard G. Hennig &&& Francesca Tavazza, "Evaluation and comparison of classical interatomic potentials through a user-friendly interactive web-interface", Scientific Data 4, Article number: 160125 (2017), doi:10.1038/sdata.2016.125 2. Kamal Choudhary, Irina Kalish, Ryan Beams &&& Francesca Tavazza, "High-throughput Identification and Characterization of Two-dimensional Materials using Density functional theory", Scientific Reports 7, Article number: 5179 (2017), doi:10.1038/s41598-017-05402-0

Patient-specific Modeling of Blood Flow

Charles Taylor*

*HeartFlow, Inc.

ABSTRACT

Patient-specific models of blood flow constructed from coronary CT angiography (cCTA) images and using computational fluid dynamics are transforming the diagnosis of heart disease by providing a safer, cheaper and more efficient procedure as compared to the standard of care that often involves nuclear imaging and invasive diagnostic cardiac catheterizations [1]. Such image-based computations require an accurate segmentation of the coronary artery lumen from cCTA images and leverage biologic principles relating form (anatomy) to function (physiology). Leveraging research originally performed at Stanford University, HeartFlow has developed a non-invasive test, FFRCT, based on computing flow and pressure in the coronary arteries [2]. FFRCT has been validated against invasive pressure measurements in more than 800 patients and demonstrated to improve care in numerous clinical studies to date [3]. At present, FFRCT has been used for more than 15,000 patients in routine practice for clinical decision making in the United States, Canada, Europe, and Japan. In the United States, the Centers for Medicare and Medicaid Services and the majority of private insurance companies reimburse physicians for using FFRCT. Patient data is uploaded to the HeartFlow application running on Amazon Web Services (AWS). Image analysis methods leveraging deep learning are used to create an initial patient-specific geometric model, and then a trained analyst inspects and corrects the model. Fully-automated mesh generation techniques are used to discretize the model and computational fluid dynamic analysis is performed on AWS to compute the blood flow solution. Results are returned to the physicians through a web interface or mobile application. New developments including treatment planning and evaluating rupture risk of coronary plaques will be discussed. The impact of computational methods developed by Professor Thomas J.R. Hughes on the field of patient-specific modeling of blood flow will be described. References [1] Taylor CA., Hughes TJR., Zarins CK, (1998) Finite Element Modeling of Blood Flow in Arteries. *Computer Methods in Applied Mechanics and Engineering*. Vol. 158, Nos. 1-2, pp. 155-196. [2] Taylor CA, Fonte TA, Min JK., *Computational Fluid Dynamics Applied to Cardiac Computed Tomography for Noninvasive Quantification of Fractional Flow Reserve*, *J Am Coll Cardiol*. 2013;61(22):2233-2241. [3] Douglas PS, De Bruyne B, Pontone G, Patel MR, Norgaard BL, Byrne RA, et al. 1-Year Outcomes of FFRCT-Guided Care in Patients With Suspected Coronary Disease: The PLATFORM Study. *J Am Coll Cardiol* 2016;68:435-445.

Physical Experimentation and Analytics of Near-Surface Cohesionless Soil Dynamics

Oliver-Denzil Taylor^{*}, Robert Walker^{**}, Amy Cunningham^{***}, Katheryn Martin^{****}, Mihan McKenna^{*****}

^{*}US Army Engineer Research & Development Center, ^{**}US Army Engineer Research & Development Center, ^{***}US Army Engineer Research & Development Center, ^{****}US Army Engineer Research & Development Center, ^{*****}US Army Engineer Research & Development Center

ABSTRACT

For analytical modeling of low-confinement soil models, the soil is considered both as an elastic media, and also as an inelastic media with a skeleton matrix of soil with pores filled with air and water. The inelastic model is implemented within a Terzaghi effective stress model, using the HONDO computational platform, in an attempt to replicate observed in situ wave propagation phenomenology and laboratory behavior. In this paper, we investigate the applicability of such models to describe the behavior of sand within the upper meter of the subsurface. Typically, the analytical model assumes that the input frequency is not an artifact of location on the wetting-drying time curve in order for the analytical outputs to be considered valid. However, as presented herein, experiments into tip-to-tip oriented bender elements indicate that this assumption is invalid. Furthermore, laboratory experiments on unconfined sand illustrates the significant shortcomings of trying to model cohesionless soil within the near surface, down to approximately 1 meter in depth with a free surface upper boundary.

Tom Hughes at 75: From FEA to IgA

Robert Taylor*

*University of California, Berkeley

ABSTRACT

This presentation honors Tom Hughes on the occasion of his 75th birthday and summarizes the influence he has had on my activities in computational mechanics during the last 45 years. Our early interactions in studies on plate bending, contact/impact problems, time integration methods and fluid dynamics took place while he was at Berkeley in the 1970's. Later we interacted on solution of viscoplastic problems, discontinuous Galerkin methods and Isogeometric analysis. Accordingly I summarize these and dedicate my presentation to Tom as he celebrates another important milestone in his life.

Analyses of Fatigue Crack Propagation with Smoothed Particle Hydrodynamics Method

Koki Tazoe^{*}, Hiroto Tanaka^{**}, Masanori Oka^{***}, Genki Yagawa^{****}

^{*}YANMAR CO., LTD., ^{**}YANMAR CO., LTD., ^{***}YANMAR CO., LTD., ^{****}The university of Tokyo and Toyo university

ABSTRACT

Fatigue fracture is one of the most serious problems in mechanical structures under cyclic loadings. Particularly, the fatigue crack propagation is one of the typical phenomena in fatigue damage. To assess the damage, accurate simulation of crack growth history is considered to be important [1]. Accordingly, some numerical analyses for the crack propagation problem with meshes, for example X-FEM, have been investigated [2]. Meshing analysis method, however, has problems when dealing with complex situations such as single crack separation, merging of multiple cracks, high kink angled initial crack and so on [2]. This means that, especially from the view point of engineering, it is not easy to handle such complex problems by using meshing analysis methods. On the other hand, particle methods, such as the SPH [3], are thought to be useful to solve above mentioned problems. However, as far as the present authors know, little studies have been published about fatigue crack propagation analyses by employing particle methods. In this study, the fatigue crack propagation is studied by using the SPH method. The developed computer program is based on linear fracture mechanics, where crack is assumed to propagate within particles located around crack front line, which is represented as a chain of particles including crack tips. We have solved planar fatigue crack propagation crossing a hole by this method, showing that a single initial crack is separated into two cracks at the edge of the hole and the two cracks merge at the other side in a smooth manner. After the merging, the kinked crack front shape [2] is disappeared automatically without any problems. It is concluded that the SPH method is a useful tool for simulation of the complex crack propagation history. References [1] Toyosada M, Gotoh K, Niwa T (2004) Fatigue life assessment for welded structures without initial defects: an algorithm for predicting fatigue crack growth from a sound site. *Int J Fatigue*. 26-9:993-1002 [2] Colombo D (2012) An implicit geometrical approach to level sets update for 3D non-planar X-FEM crack propagation. *Comp Meth Appl Mech Engng*. 237-240:39-50 [3] Lucy L B (1977) A numerical approach to the testing of the fission hypothesis. *Astronom. J* 8:1013-1024

Scale-resolving Simulations of Turbulent Boundary Layers: Effect of Inflow Unsteadiness

Pedram Tazraei*, Sharath Girimaji**

*Texas A&M; University, **Texas A&M; University

ABSTRACT

Scale-resolving simulations (SRS) offer a computationally viable alternative to direct numerical simulations (DNS) or large eddy simulations (LES) for many flows of engineering interest. In wall-bounded SRS simulations, it is desirable to perform RANS (Reynolds-averaged Navier-Stokes) in the close proximity of the wall and gradually introduce fluctuations through the log-layer and approach a reasonably resolved simulation as the free-stream is approached. Such a SRS computation can, in principle, be computationally reasonable and yet yield accurate results. In the current work, the near-wall modeling of SRS is addressed. The SRS approach considered in this study is the partially-averaged Navier-Stokes (PANS). The PANS provides a formal framework for adapting two-equation RANS models to model different degrees of scale resolution. The implicit filtering is carried out by imposing a cut-off in the energy spectrum, and the cut-off is specified by defining the ratios of the unresolved-to-total kinetic energy and unresolved-to-total dissipation rate. In this work, we will examine a key aspect of near-wall PANS modeling - the effect of inflow unsteadiness on the development of a SRS boundary layer. OpenFOAM software is used to perform the simulations. The multi-layered nature of the turbulent boundary layer (TBL) dictates clustering of grid points near the wall. For the boundary conditions, no-slip condition is prescribed at the wall. Zero pressure is defined at the upper boundary and outlet. And in the spanwise direction, cyclic condition is applied. In order to generate the turbulent inflow, the so-called "recycling/rescaling" method is invoked at the inlet. Implementation of the recycling/rescaling condition includes running two independent, precursor and main, simulations. The inflow data is recycled from a downstream enough perpendicular plane, and rescaled such that the momentum thickness of the precursor case matches the momentum thickness at the inlet of TBL. Several test cases are considered for discrete momentum thickness Reynolds number in the range of 830 to 2400. The accuracy of the simulations is examined by inspecting the first and second order turbulence statistics. Further, the organization of coherent structures in the near-wall region of a spatially developing boundary layer is examined. Multi-point physics based on the λ_2 criterion is examined by visualizing hairpin vortices and their organization in a packet form in a fully-developed turbulent boundary layer.

Asymmetric Capping of Biconvex Tablets: A FEM Study

Pierre Tchoreloff^{*}, Harona Diarra^{**}, Vincent Mazel^{***}

^{*}Université de Bordeaux, ^{**}Université de Bordeaux, ^{***}Université de Bordeaux

ABSTRACT

Capping is a classical problem during the manufacturing of pharmaceutical tablets. It corresponds to the separation of the top layer of the tablet and can be observed just at the ejection from the die or some days after. It is well known that biconvex tablets are more prone to capping than flat-faced ones. The reason is the mechanism that makes the tablet break [1]. During relaxation, the material in the cup can expand radially whereas the main body of the tablet cannot. This promotes the development of large shear stresses that can lead to capping. Considering this mechanism, if the compaction is applied symmetrically, capping should appear on both side of the tablet. Nevertheless it is well known that, sometimes, capping can be asymmetric, i.e. failure occurs only on one side of the tablet. When this phenomenon happens, capping always occurs on the side that is ejected first (i.e. the “upper side” on most of the machines). This dissymmetry is not explained by the mechanism proposed above. In this presentation we will study, using FEM modelling, how the ejection part of the compaction cycle could be responsible of this asymmetrical failure. Afterwards, influence of some process/product parameters on the capping tendency of biconvex tablet will be discussed, based on the phenomena found in the simulations. FEM simulations show that the ejection process can be separated into two phases. First, when the force applied by the lower punch is lower than the ejection force, the band of the tablet is fixed and the movement of the punch promotes a deformation of the tablet. At some point, the force needed to move the tablet is reached, and the tablet begins to move upward. During the first part of the unloading, the shear stress, that is responsible of the failure of the compact, increases on the upper side of the tablet and decreases on its lower side. The shear strength of the tablet may thus be reached because of the deformation of the tablet. This would promote capping only on the upper side of the tablet as sometimes observed during manufacturing. This mechanism makes it also possible to understand the influence of various process/product parameters on the capping tendency like lubrication or compaction speed.

1. Hiestand et al., J Pharm Sc., 1977, 66, 510-519.

Generating Statistically Equivalent Synthetic Microstructures of Additively Manufactured Stainless Steel

Kirubel Teferra^{*}, Lily Nguyen^{**}, David Rowenhorst^{***}

^{*}US Naval Research Laboratory, ^{**}US Naval Research Laboratory, ^{***}US Naval Research Laboratory

ABSTRACT

Additive manufacturing (AM) is a promising materials technology because of its ability to generate components according to prescribed CAD-based geometries with tight tolerances. The AM build process generates highly localized thermal cycles that induces rapid phase changes in the material. The frequency, localization, and speed of the thermally-driven phase changes is significantly different from the annealing processes associated with traditionally processed materials, often leading to different microstructural and constitutive properties. Since microstructure influences material properties, it is important to statistically characterize the features of these novel microstructures and develop models for their morphology. The three-dimensional microstructure of a material can be statistically characterized by reconstructing a specimen using electron backscatter diffraction (EBSD) coupled with mechanical serial sectioning. Since these datasets are extremely time consuming and costly to collect, synthetic microstructure models are trained to the data in order to generate statistically equivalent samples of the microstructure. Synthetic models for polycrystalline materials are usually variants of tessellation models. The microstructure of AM processed 316L is comprised of a highly chaotic morphology with very complex grain shapes that are not well characterized by only considering size and aspect ratio. This suggests that simple tessellation-based models are insufficient representations of the morphology, and novel models must be developed. This work studies the use of deep learning techniques to generate accurate representations of complex microstructures. Generative Adversarial Nets (GANs) is a methodology aimed at generating synthetic data that is indiscernible from real data. Two feed forward networks are simultaneously trained where one generates synthetic data, and the other builds a discriminator to distinguish the synthetic data from the real. The objective function is formulated to reach an equilibrium such that the discriminator returns an equal probability that the synthetic data is counterfeit or real. The efficacy of using GAN as a perturbation from an initial tessellation-based synthetic model in order to recover the error between the AM microstructure and the tessellation-based model will be studied. In addition, the Restricted Boltzman Machine, a generative model, will be employed to characterize the joint distribution of the model parameters such that statistically equivalent synthetic models can be simulated.

Machine Learning Materials Physics: Algorithms Predict Precipitate Morphology in an Alternative to Phase Field Dynamics

Gregory Teichert^{*}, Emmanuelle Marquis^{**}, Krishna Garikipati^{***}

^{*}University of Michigan, ^{**}University of Michigan, ^{***}University of Michigan

ABSTRACT

Machine learning has been effective at detecting patterns and predicting the response of systems that behave free of natural laws. Examples include learning crowd dynamics, recommender systems and autonomous mobility. There also have been applications to the search for new materials that bear relations to big data classification problems. However, when it comes to physical systems governed by conservation laws, the role of machine learning has been more limited. Here, we present our recent work in exploring the role of machine learning methods in discovering or aiding the search for physics. Specifically, this talk will focus on using machine learning algorithms to represent high-dimensional free energy surfaces with the goal of identifying precipitate morphologies in alloy systems. Traditionally, this problem is approached by combining phase field models, which impose first-order dynamics, with elasticity, to traverse a free energy landscape in search of minima. Equilibrium precipitate morphologies occur at these minima. Here, we exploit the ability of machine learning methods to represent high-dimensional data, combined with surrogate optimization, reduced order modeling, and sensitivity analysis as an alternate approach to finding minimum energy states. This combination of data-driven methods offers an alternative to the imposition of first-order dynamics via phase field methods, and represents one approach to learning materials physics with machine learning.

DNS and LES of Scalar Transfer across a Wind-driven Air-water Interface Characterized by Gravity-capillary Waves

Andres Tejada-Martinez*, Amine Hafsi**, Fabrice Veron***

*aetejada@usf.edu, **University of South Florida, ***University of Delaware

ABSTRACT

Direct numerical simulation (DNS) of an initially quiescent coupled air-water interface driven by an air-flow with free stream speed of 5 m/s generates gravity-capillary waves on the interface and Langmuir turbulence characterized by small-scale (centimeter-scale) Langmuir circulation (LC) beneath the interface. LC consists of counter-rotating vortices in the direction of the wind and waves. In addition to LC, the water side turbulence consists of smaller turbulent eddies similar to the shear-driven eddies associated with the classical wall streaks in wall-bounded turbulent flow. Large-eddy simulation (LES) with momentum equation augmented with the well-known Craik-Leibovich (C-L) vortex force is used to understand the roles of the wave and shear-driven LC (i.e. the Langmuir turbulence) and the smaller shear-driven eddies (i.e. the shear turbulence) in determining molecular diffusive scalar flux from the air side to the water side and vertical scalar transport beneath. The C-L force consists of the cross product between the Stokes drift velocity (induced by the interfacial waves) and the flow vorticity. It is observed that Stokes drift shear intensifies the smaller eddies (with respect to purely wind-driven flow, i.e. without wave effects) leading to enhanced diffusive scalar flux at the air-water interface. These intensified smaller eddies are interpreted as part of the overall wave and shear-driven Langmuir turbulence. Furthermore, it is also observed that the larger scales (i.e. the LC) lead to increased vertical scalar transport at depths below the interface and thus greater scalar transfer efficiency. Both DNS and LES show that transition to Langmuir turbulence leads to a spike in scalar flux characterized by an order of magnitude increase. In the field, these episodic flux increases, if linked to gusts and overall unsteadiness in the wind, are expected to be an important contributor in determining the long-term average of air-sea gas fluxes.

Advanced Geometry-based Mesh Generation and Adaptation for Complex Flow Problems at Large Scale

Saurabh Tendulkar^{*}, Mark Beall^{**}, Rocco Nastasia^{***}

^{*}Simmetrix Inc., ^{**}Simmetrix Inc., ^{***}Simmetrix Inc.

ABSTRACT

This presentation will describe state of the art developments in unstructured and semistructured meshing technologies driven by the needs of flow problems involving complex geometries and physics. Applications of these technologies to active research areas in aircraft and ballistics systems design will be presented. For aircraft systems, the focus will be on generating and adapting large scale high quality meshes where high anisotropy and semistructured nature are desirable to model boundary layers in high speed flow. For ballistics the focus will be on evolving domains and adaptive meshing with support for discontinuous solution fields in projectile motion and propellant burn simulations. The ability to generate and adapt these meshes in parallel while maintaining fidelity to model geometry will be discussed.

Coupling of Particle Blast Method (PBM) with Discrete Element Method for Buried Mine Blast Simulation

Hailong Teng*

*Livermore Software Technology Corp.

ABSTRACT

This paper presents two meshless methods: particles blast method (PBM) and discrete element method (DEM). Particle blast method (PBM) is intend to model the gaseous behavior of high velocity, high temperature detonation products. PBM is developed based on corpuscular method (CPM), which has been successfully applied to airbag deployment simulation where the gas flow is slow. For blast simulation where gas flow is extremely high, the equilibrium assumption in CPM is no long valid. By reformulating the particle interaction algorithm, we proposed the PBM that is capable of modelling thermally non-equilibrium system and applied this method for the simulation of blast loading. DEM focus on the modeling of granular media, which might exhibit complex behavior under different condition. Finally, the paper present the coupling of PBM with DEM for buried mine blast simulation.

Optimization of Structural Stiffness under Dependent Load

Xiaoyan Teng*, Bingkun Mao*, Dongri Li*, Xudong Jiang†

*Harbin Engineering University, Harbin, Heilongjiang Province, China,
tengxiaoyan@hrbeu.edu.com

†Harbin University of Science and Technology, Harbin, Heilongjiang Province, China,
xudongjiang@sina.com

Key words: Topology Optimization, Dependent Load, Structural Stiffness, Multi-load Structures

Abstract.

Dependent load is a kind of load which fixed on the existence of structure, accompanied with the topological optimization of the whole structure. Gravitational load is the most typical one of dependent load. It is of great importance to take dead weight into consideration for topological optimization especially when it comes to large-scaled civil engineering structure design. Based on the calculation formula of sensitivity of the structural compliance, aiming at the design of structural topological optimization under the collaboration of gravitational load and independent load, evolutionary structural optimization under multiple load is proposed after analyzing the relevance of load to element stiffness. In the presence of dead weight, the optimization model has non-convexity. The sensitivity of gravity loading to structural flexibility is no longer constant to a negative value, that is compliance is no longer a monotonically decreasing function. Hence, in this case, if the treatment method of flexibility of the past is still followed, the optimal solution may not be obtained and the iteration may be terminated. In this paper, RAMP model is used to solve the problem of topological optimization under volume constraint and multi-load respectively by using Hard-kill and Soft-kill techniques based on bidirectional evolutionary structural optimization. The optimal results of approximation theory are obtained through a stable optimization iteration process. Numerical examples show that the sensitivities remain negative for the Hard-kill mode; the positive and negative results of the sensitivity sign change of the Soft-kill mode, and the results obtained after the absolute sensitivities are very close to the Hard-kill mode. The correctness of the two cell deletion methods is verified. Finally, taking bridge structure as an example, optimized analysis is carried out under concentrated load and uniform load respectively. The optimization results are close to the actual engineering structure, which verifies the validity of this method.

1 INTRODUCTION

Multi-load mentioned in this paper refers to the existence of the load attached to the unit, which is accompanied by the unit of additions and deletions. In the past, multi-load refers to a collection of concentrated loads or surface loads. The characteristics of these loads do not disappear, and the size and direction of the acting point and force are invariable and will not change with the unit. Therefore, there are essential differences between these two kinds of multi-loads[1]. The multi-load problem studied in this paper is to consider gravity as a dependent load. It is necessary and

necessary to consider gravity in practical topology optimization problems, especially for large-scale civil engineering structures. Bruyneel and Duysinx^[2] have studied and improved the discontinuous SIMP model and obtained the stable optimal structure under the assumption of self-gravity, which also proves that considering the self-gravity in the optimization process can affect the final topology. Some scholars, such as Yang^[3] and Ansola^[4], studied and improved ESO methods and studied continuum topology optimization considering their own gravity. Taking into account the shortcomings of the ESO method, BESO method in this area will be fully developed, this article will be discussed. Therefore, this paper will carry out the structural topology optimization design under the combined action of gravity load and non-dependent load. In the process of structural topology optimization, this paper introduces the dependent load (gravity load), the gravity is distributed on the node of each unit, vertically downward, and attached to the unit exists, in the iterative process, with the unit Additions and deletions are added and deleted, and the gravity of the structure is constantly changing.

2 MATHEMATICAL DESCRIPTION OF DEPENDENT LOAD OPTIMIZATION PROBLEMS

For structural stiffness optimization problems, no matter whether it is a single load or multiple loads, the deformation of any node is a linear change under the volume constraints. Therefore, the effect of multiple loads is the superposition of the effects of all independent loads, and ultimately the structural stiffness can also be maximized. The mathematical description of the optimization problem is the same under both load conditions. The description is as shown in equation (1).

$$\begin{aligned}
 & \text{Find : } x = (x_1, x_2, \dots, x_n)^T \\
 & \text{Min : } C(x) = \frac{1}{2} \mathbf{f}^T \mathbf{u} \\
 & \text{Subject to : } \begin{cases} V^* - \sum_{i=1}^n V_i x_i = 0 \\ x_i = \{x_{\min}, 1\} (i = 1, 2, \dots, n) \end{cases} \quad (1)
 \end{aligned}$$

In the formula, C is the average compliance of the structure, and \mathbf{f} and \mathbf{u} are the force vector and displacement vector of the dependent load and the external load, respectively. V_i is the volume of a single unit and V^* is the set total volume of the structure. This binary design variable x_i indicates the density of the i -th element. Normally, x_{\min} is given a relatively small value of 0.001. This value close to zero indicates that the corresponding element is an empty element.

3 DEPENDENT LOAD OPTIMIZATION THEORIES

3.1 Sensitivity analysis

The difference between the load and the fixed external load in the text is whether to consider the dependent gravity load. In the finite element analysis, the expression of this applied force vector is shown in equation (2).

$$\mathbf{f} = \sum_{i=1}^k \mathbf{f}_i + \mathbf{f}_0 = \mathbf{K}\mathbf{u} + \mathbf{f}_0 \quad (2)$$

In the formula, \mathbf{f}_i represents the self-weight load vector of the i -th unit, and \mathbf{f}_0 represents the additional fixed load. By introducing the Lagrangian multiplier λ , the sensitivity of the displacement and the force vector can be determined, so the expression of the objective function is

shown in equation (3).

$$C = \frac{1}{2} \mathbf{f}^T \mathbf{u} + \lambda^T (\mathbf{f} - \mathbf{K} \mathbf{u}) \quad (3)$$

In the formula, $\lambda^T (\mathbf{f} - \mathbf{K} \mathbf{u})$ is equal to 0, so the new objective function is equal to the old one. The sensitivity of the modified objective function is derived as shown in equation (4).

$$\frac{dC}{dx_i} = \frac{1}{2} \frac{\partial \mathbf{f}^T}{\partial x_i} (\mathbf{u} + 2\lambda) + \left(\frac{1}{2} \mathbf{f}^T - \lambda^T \mathbf{K} \right) \frac{\partial \mathbf{u}}{\partial x_i} - \lambda^T \frac{\partial \mathbf{K}}{\partial x_i} \mathbf{u} \quad (4)$$

Since it is a stiffness optimization, it is necessary to remove $\frac{\partial u}{\partial x_i}$ from the sensitivity expression, because λ can take any value, so that

$$\lambda = \frac{1}{2} \mathbf{u} \quad (5)$$

Then, substituting equation (5) into equation (4), the simplified form of the sensitivity expression is shown in equation (6).

$$\frac{dC}{dx_i} = \frac{\partial \mathbf{f}^T}{\partial x_i} \mathbf{u} - \frac{1}{2} \mathbf{u}^T \frac{\partial \mathbf{K}}{\partial x_i} \mathbf{u} \quad (6)$$

The sensitivity expression under the fixed external load (without considering the gravity load) is shown in formula (7).

$$\frac{\partial C}{\partial x_i} = -\frac{1}{2} \mathbf{u}_i^T \mathbf{K}_i^0 \mathbf{u}_i \quad (7)$$

According to equation (6), the sensitivity value of the compliance degree is determined by the algebraic sum of the two terms on the right side of the equation. However, according to the comparison formula (7), if the self-weight exists, the sensitivity symbol cannot be determined and can be positive or negative. In other words, as the design variables change, the sign of the sensitivity value also changes, which indicates the non-monotonic characteristics of the degree of compliance. Therefore, in this case, if the processing method of the compliance is still used in the past, it may result in that an optimal solution or even an iterative suspension may not be obtained. The following content will explain the sensitivity processing methods under these two loading conditions.

3.2 Material interpolation schemes and sensitivity values

The material interpolation scheme with penalty factor is widely used in the SIMP method, so a high-quality 0-1 design can be obtained. In order to achieve this goal with the BESO method, the Young modulus of the intermediate material will be used as an interpolation function of the cell density, as shown in equation (8).

$$\begin{cases} E(x_i) = E_0 x_i^p \\ \mathbf{K} = \sum_i^n x_i^p \mathbf{K}_i^0 \end{cases} \quad (8)$$

In the formula, E_0 represents the Young modulus of the real unit, and \mathbf{K}_i^0 represents the stiffness matrix of the real unit. It is assumed here that Poisson's ratio is independent of design variables.

If the above material interpolation model is applied, for the soft element, although the stiffness matrix becomes smaller due to the existence of the penalty factor, the material density of the

element is not weakened correspondingly. Therefore, the gravity received by the element does not follow the stiffness matrix, This is illogical. This results in the unit's displacement vector being an indeterminate quantity. Therefore, the value of $(\mathbf{f}_i \mathbf{u})$ cannot be determined. The algebraic sum of the two terms on the right side of equation (6) will lose control. On the other hand, considering the self-weight condition, the objective function becomes a non-convex function. Because of this factor, it is impossible to obtain a better 0-1 design.

Here, a new interpolation scheme (RAMP) will be considered, which was proposed by Stolpe and Svanberg [5]. This interpolation model overcomes the disadvantages of the power-exponent function interpolation scheme described above. The density model and the Young's modulus of the material model are expressed by Equation (9).

$$\begin{cases} \rho_i = x_i \rho_0 \\ E_i = \frac{x_i}{1 + p(1 - x_i)} E_0 \end{cases} \quad (9)$$

In the formula, ρ_0 and E_0 represent the density and Young modulus of a solid material, respectively, and P is a penalty factor greater than zero. For a three-dimensional model, when the structure is subjected to finite element meshing, for the 8-node cubic element, the load (self-weight) of the element is uniformly distributed on 8 nodes, assuming that the direction of gravity is Y direction, such as the formula (10) Shown.

$$\mathbf{f}_i = V_i \rho_i \mathbf{g} \bar{\mathbf{f}} = V_i \rho_i \mathbf{g} \left\{ 0, -\frac{1}{8}, 0, 0, -\frac{1}{8}, 0 \right\}^T \quad (10)$$

Assume that a unit change only affects the dependent load, and therefore, the relative change in the external load is shown in Equation (11).

$$\frac{\partial f}{\partial x_i} = V_i \rho^0 \mathbf{g} \bar{\mathbf{f}}^T \mathbf{u}_i \quad (11)$$

The sensitivity of the average softness is shown in equation (12).

$$\frac{dC}{dx_i} = V_i \rho^0 \mathbf{g} \bar{\mathbf{f}}^T \mathbf{u}_i - \frac{1 + p}{2[1 + p(1 - x_i)]^2} \mathbf{u}_i^T \mathbf{K}_i^0 \mathbf{u}_i \quad (12)$$

It can be seen that the element sensitivity depends on the value of the penalty factor. The formula (12) can directly determine the sensitivity of the empty and real elements, respectively, as shown in equation (13).

$$\alpha_i = -\frac{1}{p + 1} \frac{dC}{dx_i} = \begin{cases} -\frac{V_i \rho^0 \mathbf{g} \bar{\mathbf{f}}^T \mathbf{u}_i}{p + 1} + \frac{1}{2} \mathbf{u}_i^T \mathbf{K}_i^0 \mathbf{u}_i & x_i = 1 \\ -\frac{V_i \rho^0 \mathbf{g} \bar{\mathbf{f}}^T \mathbf{u}_i}{p + 1} + \frac{1}{2[1 + p(1 - x_{\min})]^2} \mathbf{u}_i^T \mathbf{K}_i^0 \mathbf{u}_i & x_i = x_{\min} \end{cases} \quad (13)$$

For the purpose of minimizing the compliance, the sensitivity value should be updated, the design variable x_i of the cell corresponding to the low sensitivity value is changed to x_{\min} , and the value of the design variable x_i of the cell having the high sensitivity value is changed to 1. Similar to the exponential function interpolated material scheme, this scheme also needs to select a larger penalty factor. With discrete design variables, the scheme can achieve convergence and a stable 0-1 design.

It should be noted that for the new interpolation scheme, when the penalty factor tends to be infinitely large, the sensitivity value of the soft cell tends to zero, and the expression of the

sensitivity value at this time is expressed by Equation (14).

$$\alpha_i = \begin{cases} \frac{1}{2} \mathbf{u}_i^T \mathbf{K}_i^0 \mathbf{u}_i & x_i = 1 \\ 0 & x_i = x_{\min} \end{cases} \quad (14)$$

In the formula, $x_i = 0$ replaces $x_i = x_{\min}$ because soft cells are equivalent to empty cells. Therefore, the above sensitivity value will be used for hard killed BESO method. For the hard kill method, it can be seen from equation (14) that the sensitivity expression of the structure subjected to self-weighted self-weight and fixed external load is the same.

Sensitivity analysis shows that the non-monotonicity of the objective function depends on the value of the penalty factor. The larger the value of the penalty factor, the less obvious is the non-monotonicity. For extreme cases where the penalty factor is infinitely large, the non-monotonic characteristic is completely disappeared. Unlike the topological optimization problem of fixed loads, the choice of penalty factors does affect the ordering of the sensitivity of the solid elements. Therefore, for Hard-kill, the first term on the right side of the sensitivity formula completely disappears, and the Soft-kill in contrast, there may be differences in the optimization results. However, the high computational efficiency of Hard-kill methods has prompted a large number of scholars to conduct continuous research^[6].

4 NUMERICAL EXAMPLES

From the above, we can see that for the self-weight dependent load, if the soft killing method is used, the sensitivity expression shows that the objective function is non-monotonic, so it is not possible to perform the sensitivity update simply according to the magnitude of the strain energy, only according to the gradient and the energy method is optimized for calculation. Therefore, there are only Hard-kill and Soft-kill methods, but the Soft-kill method has too much calculation. Here is a simple example to compare the results of the two methods.

There are many types of dependent load optimization examples. The following examples are given by combining real objects: structures that are only subjected to gravity conditions, such as stone arch bridges; structures that are uniformly loaded, such as upper bearing arch bridges, middle bearing weights arch bridge and lower bearing arch bridge.

4.1 Stiffness optimization under concentrated loads

Example 1: The design domain size is 50mm x 20mm x 4mm. The four vertices of the bottom face are simply supported and restrained. The center of the top face is subjected to vertical downward force $F = 10\text{N}$, density $\rho = 1\text{g/mm}^3$, the elastic modulus of the material $E_1 = 1\text{GPa}$, and Poisson's ratio $\mu = 0.3$. The design domain is divided into $50 \times 20 \times 4$ mesh areas. The target volume is set to 50% of the total volume. The required parameter is: $ER = 0.02$, $r_{\min} = 3\text{mm}$.

Case1.1 Does not consider gravity ($G=0$, $F=10\text{N}$)

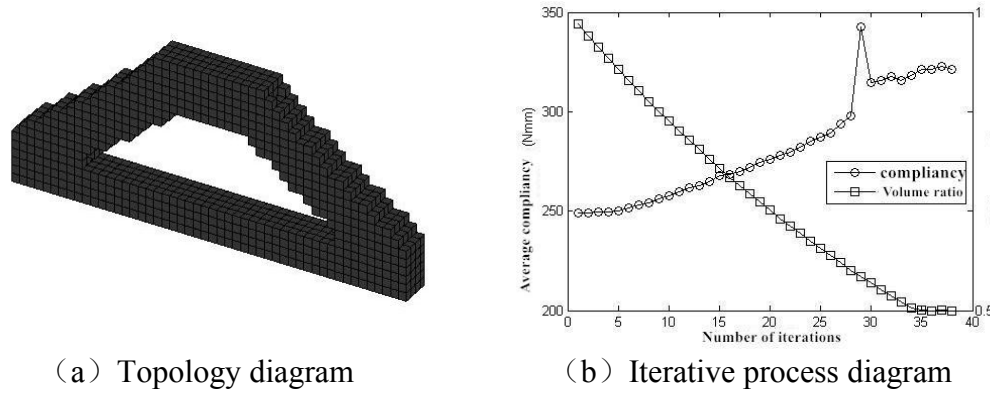


Fig. 1 Topological optimization results of simply supported beams under non-gravity

Case1.2 Under multiple loads ($G \neq 0$, $F=10N$)

For this example, Hard-kill and Soft-kill methods were used for comparison. The correctness of sensitivity treatment in Soft-kill was verified. The results are as follows:

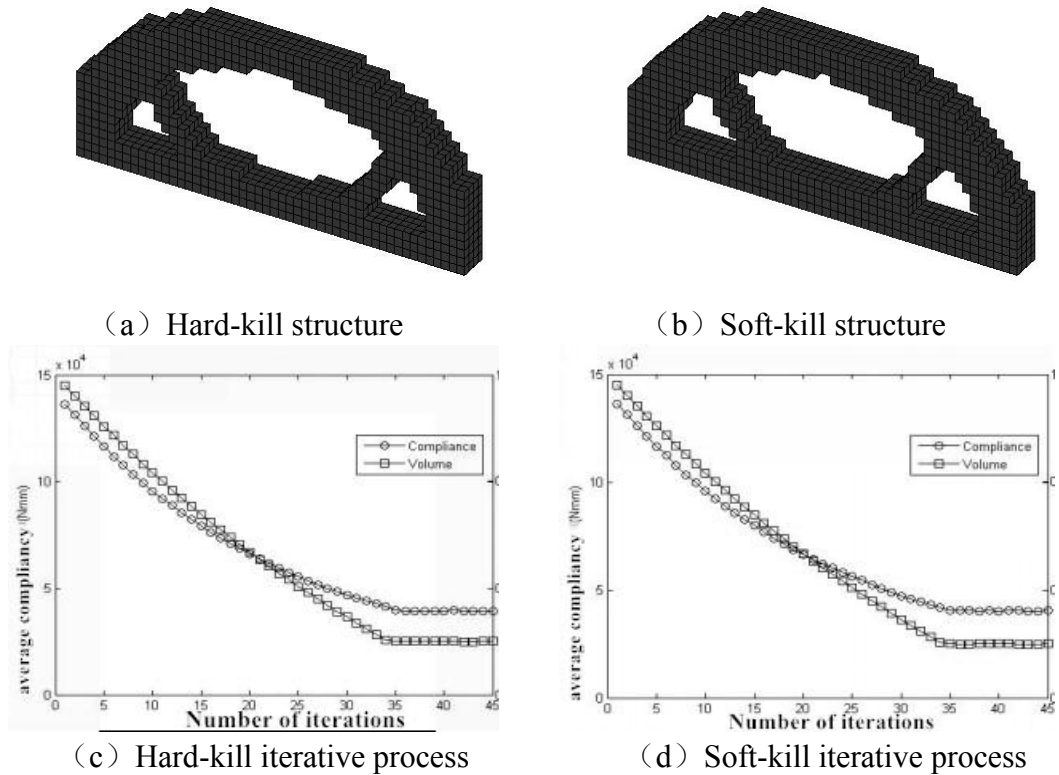


Fig. 2 Topological optimization results under gravity effect of simply supported beam (Hard-kill and Soft-kill)

Comparing Fig. 1(a) with Fig. 2(a)(b), it can be clearly seen that the structure undergoes a large change after the self-weight load is applied. The structure of Fig. 2 is more similar to the actual arch bridge structure. Comparing Fig. 2(a) with Fig. 2(b), the final structure of this method is very similar. Comparing Fig. 2(c) and Fig. 2(d), it can reach convergence smoothly, the convergence of the degree of flexibility makes the values: $C_1 = 39250 \text{ N}\cdot\text{mm}$ and $C_2 = 40390 \text{ N}\cdot\text{mm}$, respectively, and the difference is small. This verifies the correctness of the absolute value processing for Soft-

kill sensitivity values.

4.2 Stiffness optimization under uniform load

Through the example of the deck arch bridge, the half-through arch bridge and the through type arch bridge structure (as shown in Fig. 3), the initial design domain is established, and the structural topology optimization is performed under the joint action of the gravity load and the uniform load.

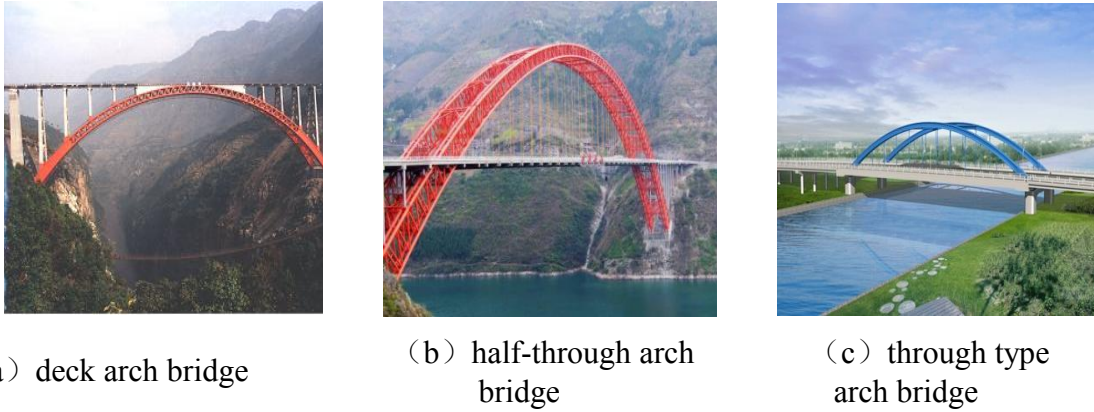


Fig. 3 Arch Bridge Engineering Structure

For the topology design of the bridge, the design domain will be divided into two categories: uniform load acting surfaces and non-active surfaces. In the iterative process, for the element corresponding to the action surface, not participating in the update of the variable, addition or deletion of the elements, is only used as a carrier of the external load, but the element corresponding to the Non-active surface is involved in updating the variable.

Example 2: Due to the different types of bridges, the design domain is also different: 1) Full design domain, the design domain size is $50\text{mm} \times 20\text{mm} \times 8\text{mm}$, the design domain is divided into $50 \times 20 \times 8$ mesh area; 2) The design domain is a U-shaped slot; 3) The design domain is an H-shaped slot. The four vertices of the bottom surface of the initial model corresponding to the three design domains are all clamped, and the top surface of the first design domain is uniformly distributed vertically downward; The inner surface of the bottom of the tank in the latter two design domains is subjected to vertical downward uniform load $F = 0.25\text{N/mm}^2$, density of material $\rho = 1\text{g/mm}^3$, elastic modulus $E_1 = 1\text{GPa}$, Poisson's ratio $\mu = 0.3$. The target volume is set to 40% of the total volume and the required parameter is: $ER=0.02$, $r_{\min} = 3\text{mm}$.

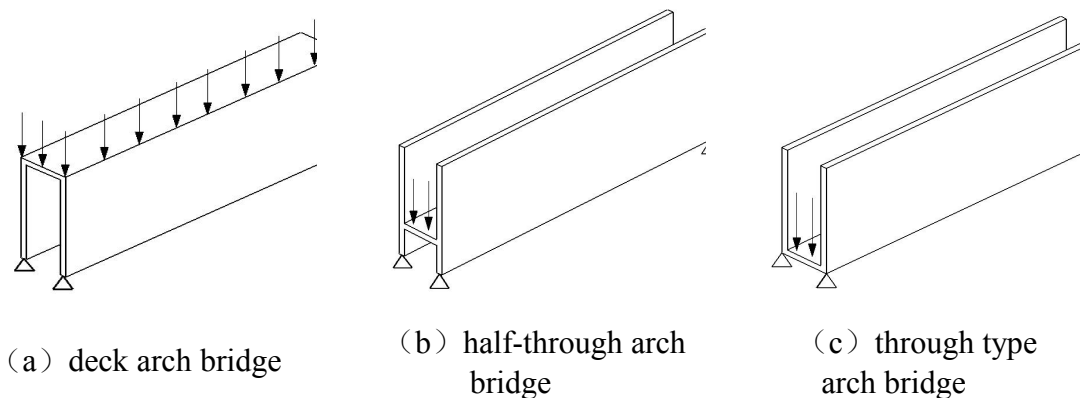
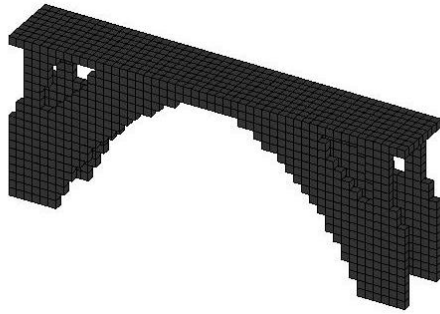
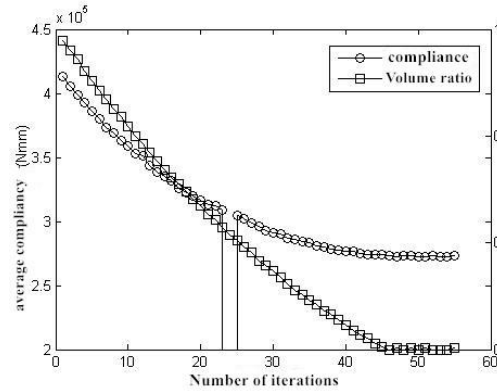


Fig. 4 Arch bridge design area

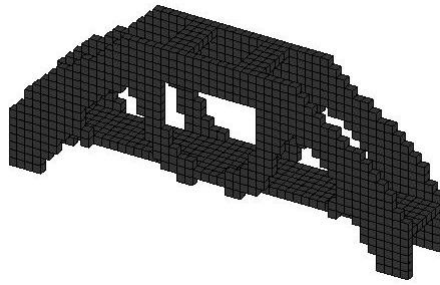
For the optimization of three arched bridges, the solution is as follows:



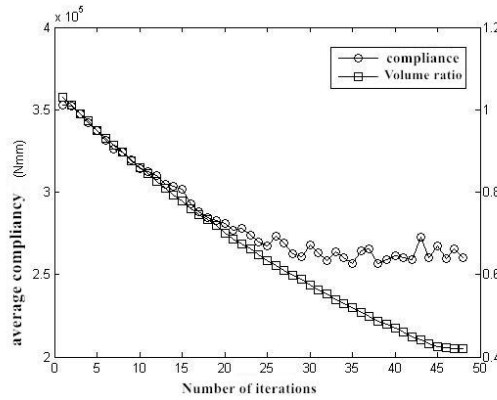
(a) Deck arch bridge topology



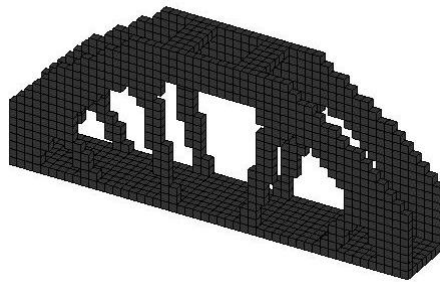
(b) Deck arch bridge iterative process chart



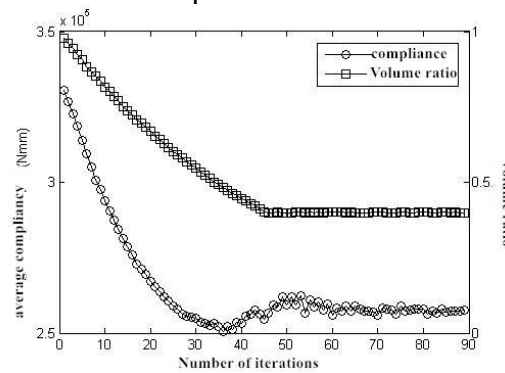
(c) half-through arch bridge topology



(d) half-through arch bridge iterative process chart



(e) through type arch bridge topology



(f) through type arch bridge iterative process chart

Fig. 5 Topology results of various bridges under uniform load conditions

For the above three results, it can be seen from the iterative process graph that the convergence value of flexibility are 2.734×10^5 N·mm, 2.601×10^5 N·mm and 2.575×10^5 N·mm, respectively, and the overall stiffness of the three structures is from small to large.

From the above listed optimization results, it can be seen that although there are some differences in the structure of various bridges in reality, the main structures are similar, and the

results obtained are calculated by algorithms and are similar to those of bridges built through experience. This verifies that this method has important guiding significance in the design of actual buildings.

5 CONCLUSION

This paper mainly focuses on the structural topology optimization design under the joint action of gravity and non-dependent loads. The design correlation of load and element stiffness is analyzed, a progressive topology optimization method for multi-load structures is proposed.

The paper theoretically illustrates the difference from fixed external loads, which is mainly manifested in the difference in sensitivity, which is highlighted by the difference in the sensitivity expressions of hard killing and soft killing, mainly because the objective function becomes Non-convex function. The symbol of the Hard-kill sensitivity value is unchanged, the compliance is monotonous, the sensitivity of the Soft-kill is variable, the compliance is non-monotonic, which is the most significant difference between the two methods in this case. The numerical example shows that for hard killing, the result is independent of the type of load. For soft killing, the result obtained after absolute processing of the sensitivity value is very close to the result obtained by hard killing. This treatment method is reasonable. At the same time, the numerical examples also prove the correctness of the application of the dependent load in engineering and the necessity of considering the gravity load in the design of large-scale civil engineering structures.

ACKNOWLEDGEMENTS

This research is supported by the National Natural Science Foundation, of China (Grant No.51505096),and National Natural Science Foundation of Heilongjiang Province of China (Grant No.QC2016056,E2016024). The authors are thankful to Harbin Engineering University for English correction of the manuscript and subsidies.

REFERENCES

- [1] Hui Zhang, Shu-Tian Liu, Xiong Zhang. Topology optimization of 3D structures with design-dependent loads. *Acta. Mech. Sin.*, 2010, 26: 767-775P
- [2] M. Bruyneel, P. Duysinx. Note on topology optimization of continuum structures including self-weight. *Struct. Multidiscip. Optim.* 2005, 29: 245-256P
- [3] X.Y. Yang, Y.M. Xie, G.P. Steven. Evolutionary methods for topology optimization of continuous structures with design dependent loads. *Comput. Struct.*, 2005, 83: 956-963P
- [4] R. Ansola, J. Canales, J.A. Tarrago. An efficient sensitivity computation strategy for the evolutionary structural optimization (ESO) of continuum structures subjected to self-weight loads. *Finite Elem. Anal. Des.*, 2006, 42: 1220-1230P
- [5] Stolpe M, Svanbergn K. An alternative interpolation scheme for minimum compliance topology optimization. *Structural and Multidisciplinary Optimization*, 2001, 22(2): 116-124P
- [6] O.M. Querin, V. Young, G.P. Steven, Y.M. Xie. Computational efficiency and validation of bi-directional evolutionary structural optimization. *Comput. Methods Appl. Mech. Eng.*, 2000, 189: 559-573

Characterization of Macroscopic Mechanical Behavior of Dry Woven-fabrics in Consideration of Mesoscopic Frictional-contact between Fiber Bundles

Kenjiro Terada^{*}, Shinnosuke Nishi^{**}, Ilker Temizer^{***}

^{*}Tohoku University, ^{**}Tohoku University, ^{***}Bilkent University

ABSTRACT

With a view to application to two-scale decoupled draping simulations of dry woven fabrics, we characterize the macroscopic in-plane and out-of-plane mechanical behavior by considering the mesoscopic frictional-contact phenomena between fiber bundles. The method of isogeometric analysis (IGA) is applied to the numerical plate/shell testing (NPT) for their in-plane periodic unit structures [1] involving frictional contact at mesoscale. To accommodate large strains and rotations for both macro- and mesostructures, the NPT is also re-formulated within the framework of finite strain theory as an extension of the small strain counterparts [2]. The mesostructure having periodicity only in in-plane directions, which is referred to as an in-plane unit cell or a virtual specimen in this study, is identified with a representative volume element (RVE) to characterize the macroscopic plate/shell behavior that reflects the interfacial frictional-contact and locking phenomena between twisted fiber bundles. NURBS basis functions are utilized to accurately solve meso-scale frictional-contact problems, and either knot-to-surface (KTS) or mortar-based KTS algorithm is employed to evaluate the contact- and friction-related variables [3]. A weaving process is simulated as a preliminary analysis to obtain the initial state of an in-plane unit cell that is subjected to both bending of adjacent fiber bundles contacting each other and in-plane tensile loading. Several numerical examples are presented to validate the formulation and demonstrate the performance and capability of the proposed method of IGA-based NPT for characterizing the macroscopic in-plane and out-of-plane nonlinear structural behavior of dry woven-fabrics especially in response to macroscopic shear deformations. [1] Matsubara, S., Nishi, S., Terada, K. On the treatments of heterogeneities and periodic boundary conditions for isogeometric homogenization analysis, *Internat. J. Numer. Methods Engrg.*, Vol. 109 (2017) pp. 1523-1548. [2] K. Terada, N. Hirayama, K. Yamamoto, M. Muramatsu, S. Matsubara, S. Nishi, Numerical plate testing for linear two-scale analyses of composite plates with in-plane periodicity, *Internat. J. Numer. Methods Engrg.*, Vol. 105, pp. 111–137, 2016. [3] Temizer, I., Wriggers, P., Hughes, T. J. R., Three-dimensional mortar-based frictional contact treatment in isogeometric analysis with NURBS, *Comput. Methods Appl. Mech. Engrg.*, Vol. 209-212, pp.115-128, 2012.

3-D FINITE ELEMENT IMPLEMENTATION OF HOUSNER FLUID-TANK DYNAMIC INTERACTION MODEL IN ELEVATED WATER TOWERS

GLORIA TERENZI and STEFANO SORACE[†]

* Department of Civil and Environmental Engineering, University of Florence
Via S. Marta 3, 50139
Florence, Italy
e-mail: terenzi@dicea.unifi.it

[†] Polytechnic Department of Engineering and Architecture, University of Udine
Via delle Scienze 206, 33100
Udine, Italy
e-mail: stefano.sorace@uniud.it

Key words: Fluid-Tank Dynamic Interaction, Water Tanks, Housner model.

Abstract. A 3-D multi-mass finite element model simulating the dynamic fluid-structure interaction in water tanks is presented in this paper. The spatial scheme is derived from the classical Housner analytical model, consisting in a two-mass (impulsive plus convective) representation of the phenomenon, which is being commonly used in most international Seismic Standards and Design Guidelines, and is still a reference also for finite element computation. However, it provides an oversimplified idealization of the interaction effects in time-history seismic analyses, and requires proper adaptations when the tank vessel includes an internal manhole. The 3-D finite element generalization of Housner basic model proposed here allows spreading the hydrodynamic pressure in sloshing conditions on the entire surface of the vessel, as well as correctly transmitting them to the supporting structure, in the case of elevated tanks.

1 INTRODUCTION

Pre-normative elevated water storage tanks are among the most seismically vulnerable structures. This is a consequence of the tall and slender geometry of staging, of the little redundancy and low ductility of the constituting members, as well as of an unfavourable structural configuration with respect to seismic action, i.e. with the highest portion of masses (vessel plus contained liquid) concentrated on top. An effective study of this class of structures via numerical time-history analysis necessarily starts from an accurate simulation of fluid-tank dynamic interaction. The classical Housner analytical model [^{1,2}], consisting in a two-mass (impulsive plus convective) representation of the phenomenon, is being commonly used in most international Seismic Standards and Design Guidelines [³⁻⁵], and is still

suggested as a reference also for finite element computation. However, its basic 2-D formulation allows obtaining only a oversimplified schematization of the structural problem. In view of this, a three-dimensional generalization of the model is proposed in this study, so as to properly spread the hydrodynamic pressure effects on the entire surface of the vessel walls. This is obtained by subdividing the water volume in n equal fractions, and calibrating the n choice to meet a satisfactorily smoothed reproduction of the analytical hydrodynamic pressure distribution with reasonable computational effort.

Detailed information on the practical implementation of the 3-D generalized model in time-history seismic analyses is offered in the next Section. Then, the model is demonstratively applied to the analysis of a typical case study, represented by a Intze-type elevated water tower with reinforced concrete (R/C) structure situated in a medium seismicity area.

2 FLUID-STRUCTURE DYNAMIC INTERACTION MODEL

The two-mass equivalent model formulated by Housner in [1] and updated in [2] splits the total liquid mass m_L into an impulsive mass m_i , which oscillates synchronously with the tank wall, and a convective mass m_c , which is subject to sloshing motion. As shown in Figure 1, in the basic 2-D schematization of the model, m_i is rigidly connected to the tank wall, whereas m_c is linked by two elastic springs with identical stiffness $k_c/2$. Both masses are rigidly joined to the vessel wall in the vertical direction.

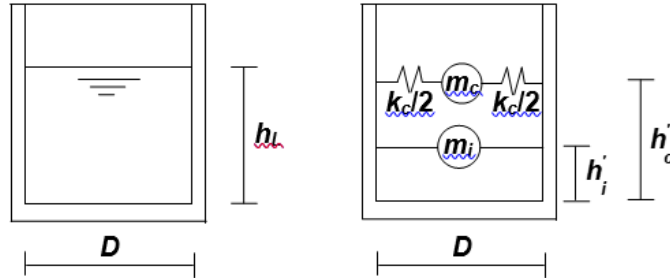


Figure 1. Two-mass model

Named h_i' , h_c' the heights of the two masses from the bottom of the tank wall, m_i , m_c , h_i' , h_c' and k_c are given by the following normative expressions for circular tanks with diameter D and maximum water free level h_L [3-5]:

$$\frac{m_i}{m_L} = \frac{\tanh\left(0.866 \frac{D}{h_L}\right)}{0.866 \frac{D}{h_L}} \quad (1)$$

$$\frac{m_c}{m_L} = 0.23 \frac{\tanh\left(3.68 \frac{h_L}{D}\right)}{\frac{h_L}{D}} \quad (2)$$

$$\frac{h_i'}{h_L} = 0.45 \quad \text{for} \quad \frac{D}{h_L} < 0.75 \quad (3a)$$

$$\frac{h_i'}{h_L} = \frac{0.866 \frac{D}{h_L}}{2 \tanh\left(0.866 \frac{D}{h_L}\right)} - 0.125 \quad \text{for} \quad \frac{D}{h_L} \geq 0.75 \quad (3b)$$

$$\frac{h_c'}{h_L} = 1 - \frac{\cosh\left(3.68 \frac{h_L}{D}\right) - 2.01}{3.68 \frac{h_L}{D} \cdot \sinh\left(3.68 \frac{h_L}{D}\right)} \quad (4)$$

$$k_c = 3.68 \frac{m_c \cdot g}{D} \tanh\left(3.68 \frac{h_L}{D}\right) \quad (5)$$

where g is the acceleration of gravity.

Expressions (1) through (5) are valid for tanks with rigid walls. This hypothesis is well suited for R/C containers, but is not always technically sound for steel ones. For cases where it cannot be accepted, in order to keep the hydrodynamic problem at a comparable level of simplification, a three-mass extension of Housner model including an additional mass linked to the tank wall by an elastic spring simulating wall flexibility can be adopted, as proposed in [2,6]. However, later studies [7] showed relatively little differences in m_i , m_c , h_i , h_c , h_i' , h_c' and k_c values obtained from rigid and flexible tank wall models; this motivates the assumption of the former as a reference for both R/C and steel tanks by the most important international Standards. Moreover, the two-mass model is identically adopted by all Standards for ground-supported and elevated tanks, where the latter additionally requires proper schematization of the supporting structure. As illustrated in Figure 2, this is basically idealized as a vertical cantilever with horizontal translation stiffness K_s and lumped structural mass m_s , including the mass of the container and a one-third portion of the mass of the staging [2,5], both in the normative seismic design of new tanks and the assessment of existing ones.

The vibration periods of the impulsive (i.e. m_i+m_s related) and convective modes of the resulting 2-degree-of-freedom (2-DOF) equivalent system, T_{i+s} and T_c , are

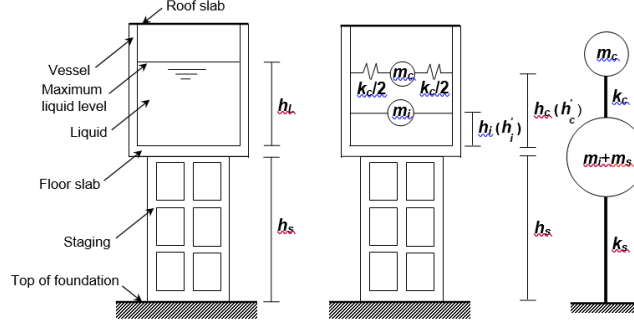


Figure 2. Two-mass idealization for elevated tanks

$$T_{i+s} = 2\pi \sqrt{\frac{m_i + m_s}{K_s}} \quad (6)$$

$$T_c = \frac{2\pi}{\sqrt{3.68 \tanh\left(3.68 \frac{h_L}{D}\right)}} \sqrt{\frac{D}{g}} \quad (7)$$

The 2-DOF model allows applying elementary dynamics relations to directly compute the maximum spectral response in terms of global parameters (base shear and moment, top drift, etc). These data are useful for a first-level quick evaluation of seismic performance of the structural system, as well as for checking the results of properly detailed finite element analyses, like the ones discussed in the next Sections. However, the 2-DOF model cannot be applied in its original schematization in the presence of an internal manhole.

In order to simulate the volumetric fluid-structure interaction, in the proposed model the water volume is subdivided in n equal fractions, each one being identified in plan with a circumferential angle Θ_n equal to $180^\circ/n$. Then, the alignments determined for half circumference are diametrically replicated for the other half, as shown in Figure 3, referred to tanks with a manhole.

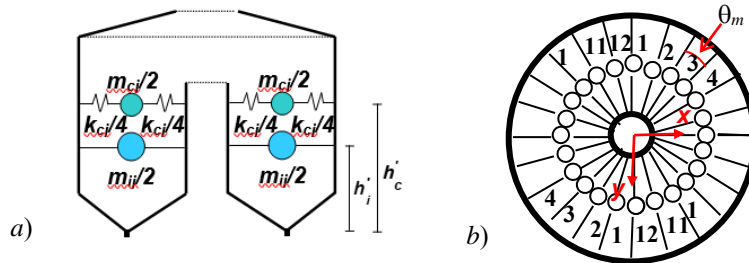


Figure 3. Reference parameters of the 3-D model for tanks with an internal manhole: section (a) and plan (b)

The influence of n on the finite element model response was evaluated by varying it from 6 (i.e. $\theta_n=30^\circ$) to 18 ($\theta_n=10^\circ$). The segmental reproduction of the analytical hydrodynamic pressure distribution on the vessel walls provided by the 3-D implementation of the two-mass model, progressively smoothing for increasing n values, was acceptable in all cases and totally satisfactory starting from $n=12$.

3 CASE STUDY WATER TOWER

The vertical cross section and the base plan of the water tower assumed as demonstrative case study for the application of the model are shown in the drawing on the left in Figure 4. The R/C vessel is Intze-type, constituted by two thin coaxial R/C cylindrical walls. The tank capacity and geometrical dimensions of the structure are as follows: maximum available water volume of 100 m^3 ; internal diameters of vessel and coaxial manhole equal to 6 m and 1 m, respectively; and external diameter of the staging base equal to 4.5 m.

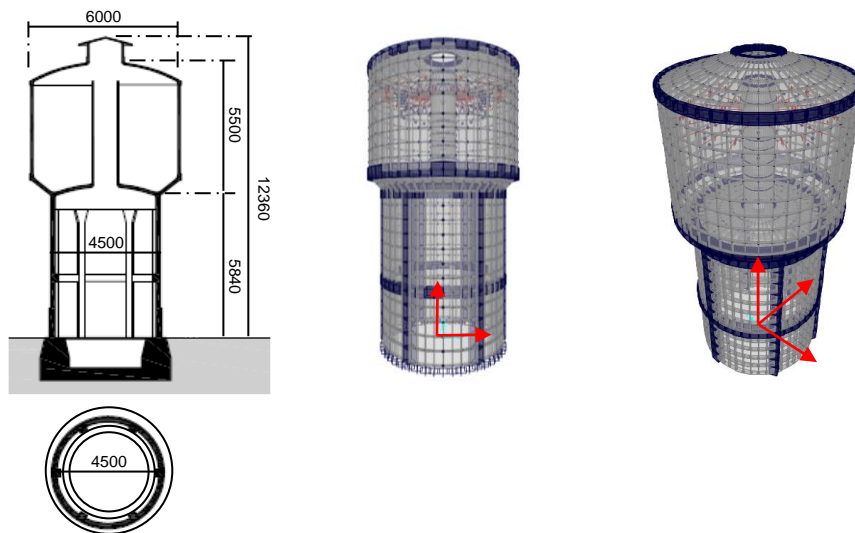


Figure 4. Cross section, base plan (dimensions in millimeters) and finite element model views of the water tower

The R/C shaft staging structure is constituted by a 150 mm-thick cylindrical wall ribbed by six columns with section of $(310 \times 310) \text{ mm} \times \text{mm}$, emerging on the internal side of the wall. The rib-columns are connected by a $(300 \times 300) \text{ mm} \times \text{mm}$ sized ring beam situated at their mid-height, and a $(150 \times 500) \text{ mm} \times \text{mm}$ sized top ring beam constituting the support of the vessel. The shaft wall has a 1200 mm-high thickening base of 50 mm, emerging on the external side. The external wall, manhole wall, bottom slab and floor slab of the vessel are 80, 80, 100 and 50 mm thick. The vessel is completed by an external inverted truncated cone

floor slabs and an internal cylindrical floor slab, bottom and top ring beams, a cylindrical roof slab, and a cylindrical lantern on top, with conical roof, for vessel aeration and natural illumination. The manhole is covered by a steel plug to prevent any fall of water in case of sloshing motion. The foundation consists of a 400 mm-thick base slab and a 1200 mm-high trapezoidal-shaped ring beam, with 1200 mm-wide lower base and 800 mm-wide upper base.

4 FINITE ELEMENT MODEL

The finite element model of the structure was generated by SAP2000NL calculus program [8]. Views of the model are displayed in Figure 4 too, along with the global reference coordinate systems, constituted by the Cartesian axes x , y and z . The mesh of the vessel and the shaft staging are made of shell-type elements. The upper small lantern was not expressly modelled, but its weight and the corresponding mass for the dynamic analyses were assigned to the underlying joints of the vessel.

The results of the modal and time-history analyses are presented in the following for $n=12$, to which $\theta_n=15^\circ$ corresponds. The horizontal and vertical cross sections of the finite element model, displayed in Figure 5, are referred to this choice.

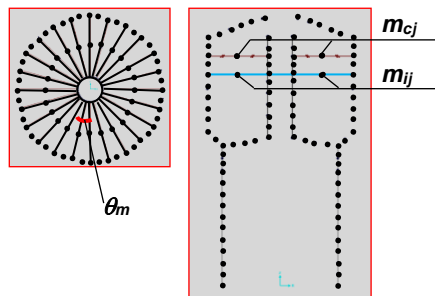


Figure 5. Horizontal and vertical sections of the finite element model of the tank

Concerning the 3-D implementation of the two-mass model, it should also be noted that, like in the 2-D scheme, the convective masses have only one relative DOF with respect to the tank walls to which they are connected, represented by the axial displacement of the associated springs (radial DOF in the 3-D layout). At the same time, the tangent and vertical relative displacements are null, since the convective masses are rigidly linked to the walls in these two directions. The former assumption corresponds to the fact that the horizontal hydrodynamic action of water is always exerted in radial direction. At the same time, the vertical rigid link compels the convective masses to respond jointly with the tank wall structure along this direction, similarly to the liquid impulsive masses, both in terms of modal analysis, for the “breathing” mode of the tank, and time-history analysis, for the response to the vertical ground motion component.

The m_i , m_c , h_i' , h_c' and k_c values calculated by means of Eqs. (1) through (5) are as follows: $m_i=71.800 \text{ kN}\cdot\text{s}^2/\text{m}$, $m_c=28.200 \text{ kN}\cdot\text{s}^2/\text{m}$, $h_i' = 2.41 \text{ m}$, $h_c' = 3.15 \text{ m}$ and $k_c=190 \text{ kN/m}$. For $n=12$, based on these values of the total water volume parameters, $m_{ij}=m_i/12=5.984 \text{ kN}\cdot\text{s}^2/\text{m}$, $m_{cj}=m_c/12=2.35 \text{ kN}\cdot\text{s}^2/\text{m}$, $k_{cj}=k_c/12=15.8 \text{ kN/m}$, for each water volume fraction, and $m_{ij}/2=2.992 \text{ kN}\cdot\text{s}^2/\text{m}$, $m_{cj}/2=1.175 \text{ kN}\cdot\text{s}^2/\text{m}$, $k_{cj}/4=3.95 \text{ kN/m}$, for the left and right portions of each volume fraction, are obtained. These data were introduced as input in the modal and time-history analyses of the structure.

A final observation about the 3-D finite element implementation of the two-mass model concerns the damping coefficients to be assigned to the two water masses for dynamic computations, which are fixed by all international Standards at 0.5% of the critical damping, for convective mass-governed modes, and at 5% for impulsive mass-governed modes. Consistently with these indications, a 0.5% value was associated in input to the translation DOF of each convective mass. At the same time, 5% was adopted for all the elements constituting the finite element meshes of the tank, impulsive water masses included, thus automatically involving all impulsive-related modal contributions.

Calculation of parameters m_c , m_i , k_c , as well as of h_i' and h_c' , was carried out by referring to an equivalent circular tank with a reduced diameter, D_r , instead of D , to obtain the same maximum water volume of 100 m^3 . As h_L is equal to 4 m , $D_r=5.62 \text{ m}$ results.

Figure 6 shows a graphical comparison of the maximum analytical (continuous line) and numerical (dotted line) hydrodynamic pressure distributions on the vessel wall, highlighting a satisfactory level of correlation for the $n=12$ value selected in this analysis. This confirms the results of previous numerical investigations [9] carried out with this n choice on water tanks with different structures.

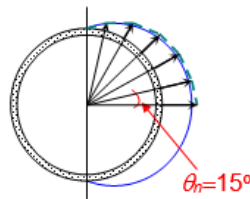


Figure 6. Maximum analytical (continuous line) and numerical (dotted line) hydrodynamic pressure distributions on the vessel wall

TIME-HISTOR PERFORMANCE ASSESSMENT ANAL SIS

The performance evaluation enquiry was carried out for the four reference seismic levels established by the Italian Standards [10], that is, Frequent Design Earthquake (FDE, with 81% probability of being exceeded over the reference time period V_R); Serviceability Design

Earthquake (SDE, with 50%/V_R probability); Basic Design Earthquake (BDE, with 10%/V_R probability); and Maximum Considered Earthquake (MCE, with 5%/V_R probability).

The V_R period is fixed at 75 years, which is obtained by multiplying the nominal structural life V_N of 50 years by a coefficient of use c_u equal to 1.5, imposed to structures whose seismic resistance is of importance in view of the consequences associated with their possible collapse. By referring to topographic category T1 (flat surface), and C-type soil (deep deposits of dense or medium-dense sand, gravel or stiff clay from several ten to several hundred meters thick), the resulting peak ground accelerations for the four seismic levels referred to the city of Florence, where the case study water tower is situated, are as follows: 0.082 g (FDE), 0.098 g (SDE), 0.223 g (BDE), and 0.27 g (MCE), for the horizontal motion components; and 0.017 g (FDE), 0.022 g (SDE), 0.079 g (BDE), and 0.111 g (MCE), for the vertical component.

The time-history analyses were developed by assuming artificial ground motions as inputs, generated by SIMQKE-II software [11] from the pseudo-acceleration elastic response spectra prescribed by the Italian Standards for Florence, graphed in Figure 7. The accelerograms were generated in families of seven both for the horizontal components (two families) and the vertical one (one family). As required by the Italian Standards, as well as by several other international seismic Codes and Regulations, in each time-history analysis the input motions were applied in groups of three simultaneous components, i.e. two horizontal components, with the first one selected from the first generated family of seven motions, and the second one selected from the second family, plus the vertical component.

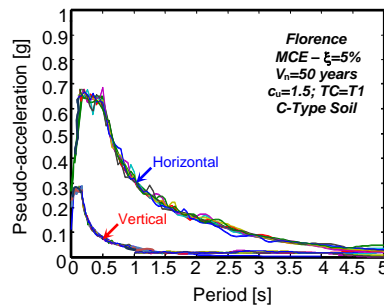


Figure 7. Normative pseudo-acceleration elastic response spectra for Florence — horizontal and vertical components

The results of the analyses carried out with the input motions scaled at the FDE and SDE levels show a completely elastic response, whereas the analyses at the BDE level highlight that an about 1.5 m-wide portion of the base section of the shaft staging is subjected to vertical tensile normal stresses greater than the strength of the vertical steel reinforcing bars situated in the same area (this portion is alternately generated on the opposite side, as a consequence of the alternate sign of seismic action). These data assess severely damaged

response conditions for the structure, but with residual margins towards structural collapse, which allows meeting the basic requirement of the Collapse Prevention (CP) performance level.

The analyses at the MCE level of seismic action represent the most significant step of the assessment study, owing to the importance class of the structure. Relevant results are synthesized in Figure 8, where the contour maps of the vertical normal stresses obtained from the most demanding among the seven groups of accelerograms are displayed on the finite element model of the structure.

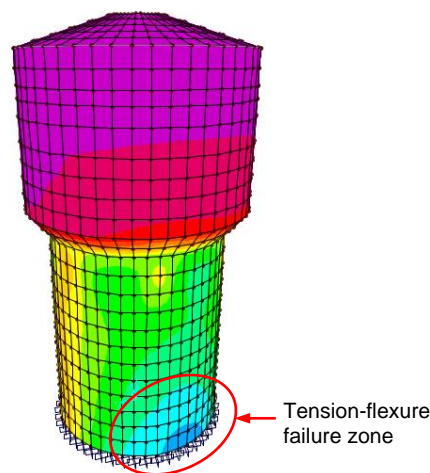


Figure 8. Contour maps of the vertical normal stresses obtained from the most demanding MCE-scaled group of input ground motions

This image shows that the portion of the base section subjected to vertical tensile normal stresses greater than the strength of the vertical reinforcing bars reaches about 4 meters. This wide tension-flexure failure zone is capable of causing overturning collapse mode of the shaft staging with respect to the foundation, similarly to the ones observed for the same type of elevated tanks in several earthquakes [12,13].

The foundation is not involved in the overturning mechanism thanks to the massive dimensions of the constituting ring beam and base slab. Indeed, the stress states transferred to the substrate are always compressive, with maximum values equal to 0.3 MPa, which are absorbed by the substrate with wide safety margins. In addition, also the response of the R/C vessel structure is within its safe domain. By summing up, the results of the assessment analysis in current conditions highlight the need for a substantial retrofit intervention of the shaft staging structure.

CONCLUSIONS

The 3-D generalized finite element model proposed in this study for the computational simulation of fluid-tank dynamic interaction problems showed a satisfactory correlation with the hydrodynamic pressure distributions calculated via numerical analysis, starting from relatively low values of the n number of water volume fractions.

This enhanced implementation of Housner two mass plan model allows also easily taking into account the presence of manholes in the tank vessels, as well as correctly transmitting the hydrodynamic pressure-related stress states to the staging structure, for elevated tanks.

The water tower examined as demonstrative case study highlighted the feasibility of the 3-D model in practical applications, offering details for its use in elevated tanks with different geometrical characteristics.

ACKNOWLEDGEMENTS

The study reported in this paper was sponsored by the Italian Department of Civil Protection within the ReLUIS-DPC Project 2014/2016, research Line 6: Isolation and Dissipation. The authors gratefully acknowledge this financial support.

REFERENCES

- [1] Housner, G.W. Dynamic behavior of water tanks. *Bulletin of the Seismological Society of America* (1963) 53: 381–387.
- [2] Haroun, M.A. and Housner, G.W. Seismic design of liquid storage tanks. *ASCE Journal of Technical Councils*, (1981) 107: 191–207.
- [3] ACI 350.3-06. *Seismic design of liquid-containing concrete structures*. Farmington Hills, MI (USA), ACI, American Concrete Institute, (2006).
- [4] 371R-08. *Guide for the analysis, design, and construction of elevated concrete and composite steel-concrete water storage tanks*. Farmington Hills, MI (USA): ACI, American Concrete Institute (2008).
- [5] IITK-GSDMA. *Guidelines for seismic design of liquid storage tanks*. Kanpur, India: National Information Center of Earthquake Engineering (2007).
- [6] Veletsos, A.S. Seismic response and design of liquid storage tanks. In: *Guidelines for the seismic design of oil and gas pipeline systems*. New York, NY (USA): ASCE Technical Council on Lifeline Earthquake Engineering, (1984): 255–370 and 443–461.
- [7] Jaiswal, O.R., Rai, D.C. and Jain, S.K. Review of code provisions on seismic analysis of liquid storage tanks. Document IITK-GSDMA-EQ04-V1.0. IITK-GSDMA. Kanpur, India: Indian Institute of Technology Kanpur (2004).

- [8] SAP2000NL. Theoretical and users' manual. Release 16.05. Berkeley (USA): Computers & Structures Inc. (2014).
- [9] Sorace, S., Terenzi, G. and Mori, C. Passive energy dissipation-based retrofit strategies for R/C frame water storage tanks. *Engineering Structures* (2016) 106:385-398.
- [10] Technical Standards on Constructions. Rome, Italy: Italian Council of Public Works (2008) [in Italian].
- [11] Vanmarcke, E.H., Fenton, G.A. and Heredia-Zavoni, E. SIMQKE-II – Conditioned earthquake ground motion simulator: User's manual, version 2.1. Princeton University. Princeton (NJ) (1999).
- [12] Rai, D.C. Elevated tanks. In Jain, Lettis, Bardet and Murty (Eds.). 2001 Bhuj, India earthquake reconnaissance report. *Earthquake Spectra* (2002) Supplement A to 18: 279–295.
- [13] Moslemi, M., Kianoush, M.R. and Pogorzelski, W. Seismic response of liquid-filled elevated tanks. *Engineering Structures* (2011) 33: 2074–2084.

A Hybridizable Discontinuous Galerkin Method for Nonlinear Elastostatics and Elastodynamics

Sebastien Terrana^{*}, Ngoc-Cuong Nguyen^{**}, Jaime Peraire^{***}

^{*}Massachusetts Institute of Technology, ^{**}Massachusetts Institute of Technology, ^{***}Massachusetts Institute of Technology

ABSTRACT

We present a hybridizable discontinuous Galerkin (HDG) method for solving large deformations problems of elastic bodies. The HDG method is developed for three-field formulations of both static and dynamic nonlinear elasticity problems. Our approach is endowed with several attractive features that make it worthwhile for computational solid dynamics. First, with regards to robustness, the method is not prone to a variety of locking phenomena such as volumetric locking for nearly incompressible materials, or shear and membrane locking for thin structures. Second, with regards to accuracy, the method yields optimal convergence for the approximate strain and stress tensors, whereas other finite element methods often give only suboptimal convergence. And third, with regard to efficiency, the method reduces the globally coupled unknowns to the degrees of freedom of the numerical trace on the interior faces only, leading to substantial savings in computational time and memory storage. This feature is particularly beneficial for thin structures because the number of interior faces can be even less than the number of boundary faces. In addition, we discuss some details of the HDG implementation, particularly the choice of the stabilization parameter, the parallel iterative solver and the preconditioner. Numerical results are presented to verify the convergence of the HDG method through some simple analytical problems and some popular benchmark problems in the literature. Results for large realistic simulations will also be presented and discussed.

Toward Efficient Real-time Reconstruction of Elastic Deformations and Stresses in Plate and Shell Structures

Alexander Tessler*

*Distinguished Research Associate, Structural Mechanics and Concepts Branch, NASA Langley Research Center, Hampton, VA 23681-2199

ABSTRACT

Since the inception of the inverse finite element method (iFEM) fifteen years ago [1], the field of structural health monitoring (SHM) has acquired a powerful computational tool for real-time reconstruction of full-field deformations and stress states in complex structures from in-situ strain measurements. The iFEM methodology is based on a weighted least-squares variational principle that provides the mathematical framework for formulating a wide range of finite elements similar to those used within the direct (forward) finite element method (FEM). The iFEM methodology can be readily implemented in any standard research or commercial finite element code. To date, iFEM-based models have been developed for shear-deformable beams, three-dimensional frames, flat plates and built-up shell structures. In recent years, iFEM has been explored further, validated experimentally, and applied to a variety of important industrial applications including aerospace, energy exploration, and marine applications. In this paper, theoretical fundamentals and new innovations in the iFEM technology will be discussed. The main focus will center around effective strategies that enhance iFEM from the standpoint of computational efficiency, accuracy, and robustness. To this end, several element-level regularization methods will be discussed that enable high-fidelity discretizations to be used in conjunction with relatively coarse distribution schemes of in-situ strain sensors, while ensuring the method's robustness and stability. Numerical examples will be presented that illustrate key features and advantages of this powerful enabling technology for structural health monitoring. [1] Tessler, A. and Spangler, J. L., A Variational Principle for Reconstruction of Elastic Deformations in Shear Deformable Plates and Shells. NASA/TM-2003-212445 (2003).

The Schwarz Alternating Method for Dynamic Multi-scale Coupling in Solid Mechanics

Irina Tezaur*, Alejandro Mota**

*Sandia National Laboratories, **Sandia National Laboratories

ABSTRACT

Concurrent multiscale methods for solid mechanics are essential for the understanding and prediction of behavior of engineering systems when a small-scale event will eventually determine the performance of the entire system. In [1], the domain-decomposition-based Schwarz alternating method was proposed as a means for concurrent multiscale coupling in finite deformation quasistatic solid mechanics. It was proven that the method converges to the single-domain solution provided each of the subdomain problems is well-posed, and that the convergence rate is geometric. The method was implemented in Sandia's Albany/LCM research code, and demonstrated to have a number of appealing features and advantages over completing multiscale coupling methods, most notably its concurrent nature (i.e., its ability to exchange information back and forth between small and large scales), its ability to couple non-conformal meshes with different element topologies, and its non-intrusive implementation into existing codes. Accuracy, convergence and scalability of the proposed method was demonstrated on several numerical examples. This talk will focus on some recent extensions of the Schwarz alternating formulation to dynamic solid mechanics problems. As with the quasi-static version of the method, the basic idea is to use the solution of a partial differential equation (PDE) on two or more regularly shaped domains comprising a more complex domain to iteratively build a solution for the more complex domain. Our dynamic Schwarz formulation is not based on a space-time discretization like other dynamic Schwarz-like methods; instead, it uses a governing time-stepping algorithm that controls time-integrators within each subdomain. As a result, the method is straight-forward to implement into existing codes (e.g, Albany/LCM), and allows the analyst to use different time-integrators with different time steps within each domain. We demonstrate on several test cases that coupling using the proposed method introduces no dynamic artifacts that are pervasive in other coupling methods (e.g., spurious wave reflections near domain boundaries), regardless of whether the coupling is done with different mesh resolutions, different element types like hexahedral or tetrahedral elements, or even different time integration schemes, like implicit and explicit. Furthermore, on dynamic problems where energy is conserved, we show that the method is able to preserve the property of energy conservation. REFERENCES [1] A. Mota, I. Tezaur, C. Alleman. "The alternating Schwarz method for concurrent multiscale coupling", *Comput. Meth. Appl. Mech. Engng.* 319 (2017) 19-51.

Stochastic Model Hyperreduction for Modeling and Quantifying Model-Form Uncertainties in Vibration Analysis

Radek Tezaur*, Charbel Farhat**, Todd Chapman***, Phil Avery****, Christian Soize*****

*Stanford University, **Stanford University, ***Stanford University, ****Stanford University, US Army Research Laboratory, *****Universite Paris-Est

ABSTRACT

A feasible, nonparametric, probabilistic approach for quantifying model-form uncertainties associated with a High-Dimensional computational Model (HDM) and/or a corresponding Hyperreduced Projection-based Reduced-Order Model (HPROM) [1,2] designed for the solution of generalized eigenvalue problems arising in vibration analysis, is presented. It is based on the construction of a Stochastic HPROM (SHPRM) associated with the HDM and its HPROM using three innovative ideas [3]: the substitution of the deterministic Reduced-Order Basis (ROB) with a Stochastic counterpart (SROB) that features a reduced number of hyperparameters; the construction of this SROB on a subset of a compact Stiefel manifold in order to guarantee the linear independence of its column vectors and the satisfaction of any applicable constraints; and the formulation and solution of a reduced-order inverse statistical problem to determine the hyperparameters so that the mean value and statistical fluctuations of the eigenvalues predicted in real time using the SHPRM match target values obtained from available data. If the data are experimental data, the proposed approach models and quantifies the model-form uncertainties associated with the HDM, while accounting for the modeling errors introduced by model reduction. If on the other hand the data are high-dimensional numerical data, the proposed approach models and quantifies the model-form uncertainties associated with the HPROM. Consequently, the proposed nonparametric, probabilistic approach for modeling and quantifying model-form uncertainties can also be interpreted as an effective means for extracting fundamental information or knowledge from data that is not captured by a deterministic computational model, and incorporating it in this model. Its potential for quantifying model-form uncertainties in eigenvalue computations is demonstrated for what-if? vibration analysis scenarios associated with shape changes for an engine nozzle. 1. C. Farhat, P. Avery, T. Chapman and J. Cortial, Dimensional Reduction of Nonlinear Finite Element Dynamic Models with Finite Rotations and Energy-Conserving Mesh Sampling and Weighting for Computational Efficiency, *International Journal for Numerical Methods in Engineering*, Vol. 98, pp. 625-662 (2014) 2. C. Farhat, T. Chapman and P. Avery, Structure-Preserving, Stability, and Accuracy Properties of the Energy-Conserving Sampling and Weighting (ECSW) Method for the Hyper Reduction of Nonlinear Finite Element Dynamic Models, *International Journal for Numerical Methods in Engineering*, Vol. 102, pp. 1077-1110 (2015) 3. C. Soize and C. Farhat, A Nonparametric Probabilistic Approach for Quantifying Uncertainties in Low- and High-Dimensional Nonlinear Models, *International Journal for Numerical Methods in Engineering*, Vol. 109, pp. 837-888 (2017)

A Novel Visco-hyper Elastic Constitutive Model for Elastomers to Capture Strain Rate Dependency

Rohan Thakkar*, Aleksander Czekanski**

*York University, **York University

ABSTRACT

Rubber-like materials undergo large deformations at relatively low stresses and recover their initial shape upon removal of the load. This exceptional ability makes them suitable and without doubt irreplaceable materials in vital engineering applications. This uncommon behavior of rubbers is caused by underlying coiled long chain polymer molecules. These chains straighten when the material is stretched and recoil upon removal of the load. As a result of molecular chains' rearrangement during loading process, they exhibit large strain elasticity and viscoelastic properties [1]. Generally, the framework of viscoelasticity can be classified into two distinct classes: a) Linear viscoelasticity & b) non-linear viscoelasticity. To summaries, linear viscoelasticity models are constituted by considering parallel and/or series arrangements of elastic springs and linear viscous dash-pots. These rheological analogies are superimposed by Boltzman's principle and the relaxation function is approximated with a prony series formulation. Whereas, non-linear viscoelastic constitutive relations are formulated by employing generalized integral based Kaye-BKZ theory. In this approach, numerous approximations of matrix stress functional defines the strain history on stresses. Rubber like materials involve highly non-linear deformation phenomena at finite strains and therefore, linear models are not adequate [2]. As a result, a quasi-linear viscoelastic frame work needs to be represented by 4-6 term prony series approximations. In contrast, the number of material constants can be reduced by articulating BKZ theory based nonlinear viscoelasticity [3]. Moreover, numerical implementation of such formulation is a straight forward and comparatively less time consuming process. For that reason, a novel power-exponential strain history functional has been proposed in nonlinear finite strain visco-hyperelastic framework to capture rate dependency in various types of elastomers. Derived constitutive relations are verified with respect to literature based high strain rate experimental data. Excellent agreement between numerical and experimental data have been achieved. The encouraging initial results leads to further expanding the scope of this work by implementing the newly developed model into commercial FE package.

Study of Turbulent Flows in an Air-filled Differentially-heated Cavity of Aspect Ratio 4: A Comparison between DNS, LES and Experimental Results

Nicolas Thiers^{*}, Olivier Skurtys^{**}, Romain Gers^{***}

^{*}Universidad Tecnica Federico Santa Maria, ^{**}Universidad Tecnica Federico Santa Maria, ^{***}Universidad Tecnica Federico Santa Maria

ABSTRACT

Natural convection in parallelepipedic enclosures of aspect ratio 4 (height / width) has been the subject of numerous studies over the past decades. Most of the numerical studies use simplified geometry considering a two dimensional case or an infinite depth assuming periodic conditions. In both cases, numerical results are significantly different of experimental data. In order to study the turbulent flows, three-dimensional Direct Numerical Simulation (DNS) and Large-Eddy Simulation (LES) were performed at $Ra_H = 10^{10}$, $Ra_H = 1.2 \times 10^{11}$ and $Ra_H = 10^{12}$. The aspect ratio width / depth was fixed to 1 and to be closer to experimental conditions, the non-slip boundary condition is imposed on the velocity at the six closing walls. To characterize the turbulent flows, stratification profile, the Nusselt number, Reynolds stress tensor, turbulent heat flux and PDF of the invariants for gradient velocity tensor were analyzed. Numerical results were compared with experimental data. The unsteady Boussinesq Navier-Stokes equations are solved using the high-order spectral element code Nek5000 for DNS and the Finite Volume Method (FVM) for LES where a OpenFoam solver was specially written. Simulations are performed at CCT-Val and NLHPC high performance clusters in Xeon X5675, 3.07GHz, 32GB RAM over 120 cores. The authors gratefully acknowledge financial support provided by Fondecyt research project n^o1171281.

Revisiting Screw-propelled Vehicles Utilizing Experimental and Computational Methods

Andrew Thoesen^{*}, Sierra Ramirez^{**}, Hamidreza Marvi^{***}

^{*}Arizona State University, ^{**}Arizona State University, ^{***}Arizona State University

ABSTRACT

Screw-Propelled Vehicles (SPV's) have been widely used for terrestrial applications such as transportation over mud, snow, and amphibious environments. Similar vehicles have also been applied to industrial processes such as dewatering. Typical designs rely on a large pontoon shaft and relatively small blades to prevent unwanted sinkage or blade damage. Studies have looked at the mobility of SPV's on the surface of granular media but there are not any computational and experimental studies on characterizing propulsive buried screws. We will examine this problem using Discrete Element Method (DEM), Resistive Force Theory (RFT) and experimental approaches. First, we must evaluate performance of the propelling screws in a well characterized media. For this study, we've chosen Earth gravity and spherical glass beads of relative uniform size to minimize additional variables. In doing so we can begin to build a framework for more extensive design evaluation of screw propelled vehicles in more exotic materials and different gravities. Understanding the role of screw design and its angular velocity on thrust force is also key to the advancement and control of SPV's. In particular, our study examines a submerged, double-helix Archimedes screw generating propulsive force against a bed of soda-lime glass beads. Thus, this research forms the basis for design of a future miniaturized exploration vehicle for space applications. In our study, we used three different screw designs of 10 cm length and 5 cm diameter. They had pitches of 4, 6, and 8cm. They were submerged in 2mm glass beads of 90% roundness with 0.1mm standard deviation. These screws were run between 30 RPM and 120 RPM. We used EDEM, a DEM software for computational studies of the screw interactions with granular media. We also analyzed this problem using RFT. There is small discrepancy between our DEM, RFT, and experimental results and we will discuss possible sources of error and the potential for using DEM and RFT as a design tool for SPV's.

Modelling of Brine Conversion in Antarctic Sea Ice within the Theory of Porous Media (TPM)

Andrea Thom^{*}, Tim Ricken^{**}

^{*}Stuttgart University, Germany, ^{**}Stuttgart University, Germany

ABSTRACT

According to NASA, Antarctic sea ice has reached its lowest extent ever recorded by satellites at the end of summer 2017 in the southern hemisphere after decades of moderate sea ice expansion. Besides a strong influence on the global climate linking the exchange of energy and gases between the atmosphere and the ocean, changes in sea ice have also a biological response concerning the ecosystem structure and function. These responses are strongly related to its physical and mechanical properties. Salt accumulations (brines) in growing sea ice are either rejected to the ocean, leading to a higher salinity of the upper ocean, or are trapped between ice crystals in pockets or channels, leading to a high salinity of the ice. Other inclusions like algae can serve as a food source for e.g. Antarctic krill in times of low resources in the water. A small-scale modelling of the porosity of the sea ice and its inclusions and the solid/brine multiphase microstructure, respectively, including thermodynamics of air-sea interactions as well as sea ice-biological linkages is a necessary tool to understand the heterogeneous sea ice nature better. Based on the Theory of Porous Media (TPM), cf. [1,2], the development of a thermodynamically consistent multiphase model which enables the continuum mechanical description of transport and phase transition phenomena in sea ice at a homogenized pore scale is presented. The model consists of a solid (ice), fluid and air phase including solvents and dissolved components in brine. The phase transition from water to ice is solved in each time step on the Gauss point scale as a coupled ODE system describing all dependencies of the thermodynamically un-equilibrium during phase transition. Its solution will be released to the upper scale via homogenization leading to an already established two-scale PDE-ODE approach for biomechanics applications [3]. [1] Ricken, Tim, and Joachim Bluhm. "Modeling of liquid and gas saturated porous solids under freezing and thawing cycles." *Aktuelle Forschung in der Bodenmechanik*, 2014. 23-42. [2] Ricken, Tim, et al. "Concentration driven phase transitions in multiphase porous media with application to methane oxidation in landfill cover layers." *ZAMM* 94.7?8 (2014): 609-622. [3] Ricken, Tim., et al. "Modeling function-perfusion behavior in liver lobules including tissue, blood, glucose, lactate and glycogen by use of a coupled two-scale PDE-ODE approach." *Biomechanics and modeling in mechanobiology* 14.3 (2015): 515-536.

Topological Optimization for Multi-Component Systems with Frequency and Stiffness Criteria

Simon Thomas*, Qing Li**, Grant Steven***

*University of Sydney, **University of Sydney, ***University of Sydney

ABSTRACT

Numerous engineering structures consist of multiple components for manufacturing, transport and economic reasons, which are assembled by various connection elements. This study aimed to develop a computational design framework for seeking optimal topologies of the patterns/configurations of connection elements as well as the structural components based upon the frequency and stiffness criteria. Building upon our earlier work, multi-objective optimization is first developed to optimize the connection elements for stiffness and frequency criteria simultaneously. Then the proposed multi-objective design is extended to topology optimization by incorporating both connection elements and component configurations. In this study, an evolutionary structural optimization (ESO) procedure is adopted, where a finite element based discrete sensitivity is derived to numerically evaluate the effect of presence and absence of a connection element and/or component element on the design criteria. A series of illustrative examples are presented to demonstrate the effectiveness of the proposed method, allowing maximizing, minimizing or targeting the individual natural frequencies or separation between them. It is noted that the methodology can be conceptually extended to many other multi-component structural systems connected by screws, rivets, welds and the like. Finally, a real-world example is considered through design of an electricity transmission tower, where natural frequency is adjusted to help mitigate potential damage from aeolian vibration. The application of this method to other component bonding types, such as adhesive sprays or 3D printing, is also explored by achieving up to 36% improvement in its multi-criteria objective function when compared with its classically screw-bonded counterpart.

Modal Stochastic Models of an Industrial Stator Vane : Comparison with Experimental Datas

Fabrice Thouverez*, Jonathan Philippe**

*Ecole Centrale de Lyon, **SAFRAN

ABSTRACT

In the context of aeronautic engines, some components have a spatial periodicity almost perfect like bladed disks or stator vanes. This periodicity comes from the fact that one sector (including blade and a part of the disk) are perfectly repeated. This property leads to a specific strategy of modelling called "cyclic symmetry" allowing a quick and efficient computation of the dynamic of such components. In fact, we always have a small loss of cyclic properties which may lead to very large variation in the estimation of the response of the system. Indeed, the energy which, for a tuned case, periodically spread over the structure could become concentrated only on few blades in the mistuned case. This phenomenon is associated, in most cases, to a mistuning of the sectors between them. If we have to manage this mistuning, we will need to take into account the complete system which can lead to very large computation time for industrial applications. To avoid this, we propose to carry out two approximations the first one will be associated to the stochastic properties of the system and the second will be a sub-structuring technic to reduce the initial size of the system. We choose to develop a stochastic modal analysis allowing to express the stochastic flexibility in a very easy way. This expression will be used to calculate the dynamic response of the structure in terms of statistic momentum or maximum of amplitude. To estimate this stochastic modal basis, we will develop several kind of approximation of the stochastic solution. The first one will be based on a polynomial chaos expansion and the second will use a Multivariate Adaptive Regression Splines (MARS) method. A comparison between these two procedures is presented in terms of efficiency and precision. These calculations are possible because the proposed method includes a sub-structuring technic based on a double modal synthesis combining a Craig-Bampton approach and the estimation of a reduced based of the interface. This strategy has been validated in view of the necessary precisions of our computations. In order to validate the complete numerical strategy an industrial stator vane has been modeled and also experimentally tested. The experimental data collected will allow to situate the real structure in relation to the stochastic simulations.

Advanced Immersed Boundary Methods and Their Applications in Biological Flows

Fang-Bao Tian^{*}, Joseph Lai^{**}, Lincheng Xu^{***}, John Young^{****}, Li Wang^{*****}

^{*}School of Engineering and Information Technology University of New South Wales, Canberra, ACT 2600, Australian, ^{**}School of Engineering and Information Technology University of New South Wales, Canberra, ACT 2600, Australian, ^{***}School of Engineering and Information Technology University of New South Wales, Canberra, ACT 2600, Australian, ^{****}School of Engineering and Information Technology University of New South Wales, Canberra, ACT 2600, Australian, ^{*****}School of Engineering and Information Technology University of New South Wales, Canberra, ACT 2600, Australian

ABSTRACT

This talk first introduces our recent progresses on developing immersed boundary methods, including sharp-interface immersed boundary-finite difference method for fluid-structure interactions involving large deformations, adaptive immersed boundary-lattice Boltzmann method for fluid-structure interactions at moderate and high Reynolds numbers, and feedback immersed boundary method based on high-order finite difference method for fluid-structure interactions involving acoustics and shock waves. Several benchmark cases are then presented to validate the accurate and efficiency of these solvers. Finally, several applications of these methods in biological are briefly introduced to demonstrate their capabilities in complex flow computations.

Level-Set-Based Topology Optimization for Nonlinear Problems

Jiawei Tian*, Shikui Chen**

*Department of Mechanical Engineering, State University of New York at Stony Brook, **Department of Mechanical Engineering, State University of New York at Stony Brook

ABSTRACT

Most structural topology optimization studies are limited to problems involving in linear elastic behaviors with small deformation. However, for some compliant mechanisms with soft rubber-like material undergoing large deformation, it is necessary to consider nonlinear elastic analysis into topology optimization, and hyperelastic model can accurately predict this mechanical behavior. In this paper, we model the mechanics of structures utilizing the compressible Neo-Hookean hyperelastic formulation and employ the level-set-based topology optimization method to get the optimized structure for nonlinear responses. In addition, the nonlinear global governing equation based on the residual form can be solved by using the Newton-Raphson algorithm. Shape sensitivity analysis is derived by using the adjoint variable method, and the design velocity field is calculated according to the gradient-based method. In order to verify the feasibility and the effectiveness of the above-presented method, several two-dimensional examples, including a cantilever beam, an MMB beam, and a stent are implemented and studied. The optimized result shows that the optimized structures can achieve the desired nonlinear large deformation.

Improved XFEM: Recent Advances

Rong Tian*

*Software center for high performance numerical simulation, Institute of Applied Physics and Computational Mathematics

ABSTRACT

The direct extension of singular tip enrichment of XFEM, the core of the method, to crack growth simulation has long been a difficulty due to: (a) elevated bad conditioning as crack propagating, (b) extra-dof dynamics and energy inconsistency, and (c) “null” critical time step size and mass lumping at crack tip. Based on an extra-dof-free partition of unity enrichment technique (Rong Tian. *Comput. Methods Appl. Mech. Engrg.* 266 (2013) 1–22), we have improved XFEM through a crack tip enrichment without extra dof (Rong Tian, Longfei Wen. *Comput. Methods Appl. Mech. Engrg.* 285 (2015) 639-658; Longfei Wen, Rong Tian. *Comput. Methods Appl. Mech. Engrg.* 308 (2015) 256-285). This paper will present a detailed introduction to the recent advances of the improved version of XFEM in both 2D and 3D as well as their parallel implementation. The improved XFEM’s excellent stability, accuracy, and straightforwardness in implementation will be demonstrated.

Consistent Traction Boundary Conditions for Nonlocal Models

Xiaochuan Tian^{*}, Jianfeng Lu^{**}, Qiang Du^{***}, Xingjie Li^{****}

^{*}University of Texas at Austin, ^{**}Duke University, ^{***}Columbia University, ^{****}UNC Charlotte

ABSTRACT

It is a recurring problem in scientific computing to design efficient numerical algorithms for a problem imposed on unbounded domains. Such problem is multiscale in its nature since the fundamental difficulty usually roots in the existence of two widely separated spatial scales. The first is a large spatial scale representing the size of the space or the material body. The second is much smaller spatial scale of interest, for example, the part of the material body where crack or fracture actually happens or the the part of the body on which non-zero external forces exert. In this talk, we introduce a consistent nonlocal traction boundary condition for static nonlocal problems so that the computation limited to a finite domain still approximates the correct result for an unbounded domain. Such a traction boundary condition is also important in the engineering practice since it eliminates the surface effect of using nonlocal models on bounded domains. This is a joint work with Qiang Du, Xingjie Helen Li and Jianfeng Lu.

Bridging Between EMMS and Nonequilibrium Thermodynamics: Structure-Dependent Analysis of Energy Dissipation and CFD Validation

Yujie Tian*, Wei Wang**

*State Key Laboratory of Multiphase Complex Systems, Institute of Process Engineering, Chinese Academy of Sciences, **State Key Laboratory of Multiphase Complex Systems, Institute of Process Engineering, Chinese Academy of Sciences

ABSTRACT

Gas-solid fluidized bed is a typical nonlinear nonequilibrium dissipative system, featuring meso-scale structures with bimodal distribution of solid concentration and velocity. The energy-minimization multi-scale (EMMS) model focuses on such dissipative characteristics by decomposing the system into the dense-dilute two-phase structures which is inherently consistent with such bimodal distribution of parameters in gas-solid fluidized bed. However, the stability condition of EMMS model has not been fully understood, especially for its relationship with those extremum principles in nonequilibrium thermodynamic, for example, the Minimum Entropy Production Principle (Prigogine, 1967). In previous work, a structure-dependent multi-fluid model (SFM) (Hong et al., 2013) was proposed, the mass, momentum balance equations of which could be reduced to the hydrodynamic equations of two-fluid model (TFM) and those of the EMMS model under certain simplifications. In this work, SFM is further refined by applying the volume average method on a control volume considering the dense-dilute two-phase structures. Then, the structure-dependent energy dissipation rate is formulated, and extends to the extremum behavior of dissipation processes (Tian et al., 2017). It reveals that the results based on the minimum energy dissipation rate applies only to homogeneous, dilute flow states, but fails in the particle-fluid compromising fluidization regime, in particular, fails to predict choking transition. In contrast, the EMMS stability condition based on the principle of compromise in competition between dominant mechanisms well predicts the regime transition of fluidization. This work unfolds a fresh viewpoint to understand the relation between EMMS stability condition and nonequilibrium thermodynamics. Two-fluid model based CFD simulation is further performed, validating the advantage of EMMS approach for characterizing dissipative structure in fluidized beds. References: Prigogine, I., 1967. Introduction to Thermodynamics of irreversible processes, Interscience Publisher. New York. Hong, K., Shi, Z., Wang, W., Li, J., 2013. A structure-dependent multi-fluid model (SFM) for heterogeneous gas-solid flow. Chem. Eng. Sci. 99, 191–202. Tian, Y., Geng, J., Wang, W., 2017. Structure-dependent analysis of energy dissipation in gas-solid flows: Beyond nonequilibrium thermodynamics. Chem. Eng. Sci. 171, 271–281.

SPH ANALYSIS OF INKJET DROPLET IMPACT DYNAMICS

T. TILFORD*, J. BRAUN†, J. C. JANHSEN†, M. BURGARD†, C. BAILEY*

*Computational Mechanics and Reliability Group, University of Greenwich, UK
Email T.Tilford@gre.ac.uk

† Fraunhofer-Institut für Produktionstechnik und Automatisierung, Germany

Key words: SPH, Additive Manufacturing, Microelectronics, Microfluidic Analysis

Abstract. This paper presents a novel Smoothed Particle Hydrodynamics (SPH) framework for analysis of droplet impact dynamics in a 3D inkjet printing process. Results obtained are validated against experimentally derived high-speed imaging data. The numerical framework is based on the Smoothed Particle Hydrodynamics approach of Monaghan et al [1] which has been proven to be efficient and effective for analysis of dynamic fluid flow problems involving free surface interfaces. The SPH approach has been augmented through addition of the kernel gradient correction scheme proposed by Belytschko et al [2] and stabilization terms of Marrone et al [3]. This correction provides a more accurate approximation of the boundary forces including surface tension which dominate at typical inkjet droplet lengthscales ($<100\ \mu\text{m}$). Analysis is expedited through adoption of the OpenACC programming paradigm to enable GPU based computation.

Numerical analyses have been validated against analytical solutions, reference macroscale problems and through comparison with experimental high speed imaging data of the inkjet printing process. The experimental setup consisted of a Fuji Dimatix SL-128 inkjet printhead jetting an acrylate based 3D printing build material onto a glass substrate. Images of a single inkjet droplet impacting onto the glass slide were captured at a rate of 100,000 frames per second, with droplet diameter assessed using a weight test approach.

Qualitative comparison of the numerical and experimental results showed a good agreement, indicating that the implemented framework is effective for analysis of the fluidic aspects of the printing process. The model is able to assist in tackling manufacturing issues that can detrimentally influence the quality of manufactured parts through provision of insight into the process.

1 INTRODUCTION

Additive manufacturing is becoming widely adopted across a range of industrial sectors and being applied to increasingly high value and high complexity products. Piezoelectric drop-on-demand inkjet printing systems can be used to form truly three dimensional, multi material objects with very high dimensional accuracy. The development of conductive pastes that can be dispensed using inkjet printers has enabled the approach to be utilised for development of microelectronics components.

The large number of academic research 3D printing systems targeting the electronics packaging sector [4-6] are now augmented by a number of commercially available systems intended for production of saleable products such as the Nano Dimension Dragonfly [7] and the Optomec [8] systems. The EU funded NextFactory [9-11] project has developed a 3D printing, micro-deposition, micro-assembly, and curing system, illustrated in Figure 1a, that can accurately deposit and cure both functional and structural materials and place/embed components in an integrated manner within a single platform. The system uses a hybrid approach in order to increase its flexibility, with an inkjet system augmented by microdeposition tools that enable conductive adhesive materials to be used alongside silver nano-inks for conductive features.

The system enables producers of micro-mechatronic systems to manufacture complete products on a single machine with the manufacturing process from CAD design to finished product taking a number of hours rather than more lengthy timescales typically associated with traditional manufacturing methods. The three-dimensional nature of the build process enables manufacture of complex 3D microsystems as readily as 2D and 2.5D devices.

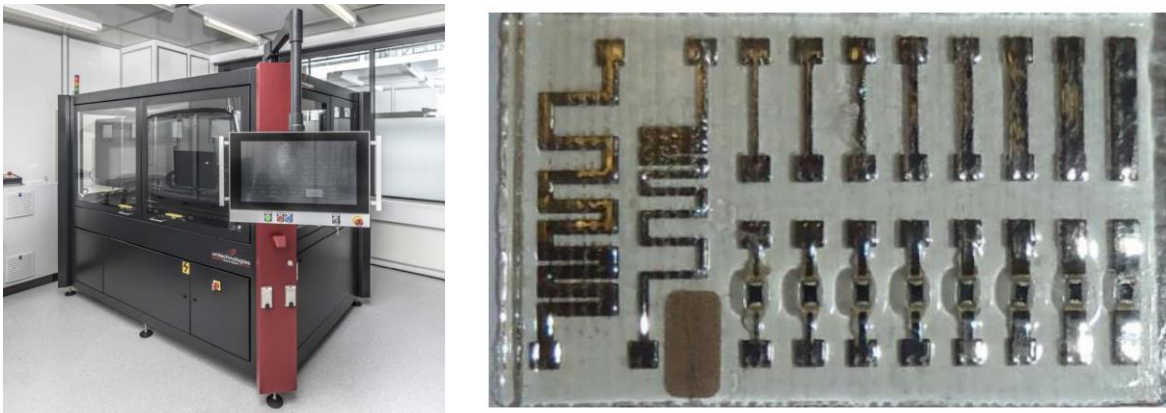


Figure 1(a): NextFactory 3-D additive manufacturing system and 1(b) 3-D printed microelectronics test structure

As is the norm for the electronics sector, new manufacturing approaches need to be considered in terms of the long term reliability of the final product. In addition to commonplace reliability qualification approaches such as JEDEC tests, there is an increasing drive to assess component quality during the manufacturing process. Condition based monitoring approaches measure key parameters associated with component quality during manufacture and continually optimise process parameters in real time to increase final quality and reliability of formed components [12, 13]. Such condition based monitoring systems need to be trained as to how variation of process parameters influences product quality. A numerical model, capable of detailed analysis of the process, can be used to underpin such an approach.

The primary requirement of the numerical model for inkjet deposition is to capture the complex physics involved when an inkjet droplet impacts a printed surface. There are a number of significant challenges in such an analysis. The primary challenge is that analysis of droplet impact upon an idealised flat surface is insufficient. Only the first layer of an inkjet printed structure will be deposited on the flat baseplate. The following layers will be deposited onto a layer of partially cured polymer droplets which form an uneven surface and will deform on impact. The material is not a simple Newtonian fluid such as water but a complex multi-component polymer which exhibits shear dependent viscous behaviour – a complex non-Newtonian material. Additionally, the impact is very severe with a droplet of diameter in the order of 40 microns impacting at approx. 5 metres per second.

Traditional computational fluid dynamics (CFD) approaches such as the Finite Volume Method [14] would be readily capable of modelling the impact dynamics of a small number of droplets. However, in order to consider prediction of the development of defects over a number of layers it is necessary to take advantage of a more efficient approach such as GPU enabled SPH. This approach has a number of advantages over traditional methods in that interfaces are explicitly captured rather than needing to be approximated but, more critically, incorporates a finite support distance enabling the problem domain to be subdivided into a large number of overlapping subdomains which can be assessed on a single core of a graphical processor unit.

2 Numerical Approach

The Smoothed Particle Hydrodynamics (SPH) approach was developed by Lucy [15] and by Gingold and Monaghan in 1977 [1]. It is a versatile discrete particle method for solution of a number of differing physical phenomena. It is a computationally highly effective method for solution of complex fluid flows, particularly in cases with interfaces and large deformations. The SPH approach considers the fluid as a collection of particles, each associated to a number of physical properties such as position, velocity, mass, density, etc. At the heart of the SPH approach is a means of evaluating spatial derivatives through integral interpolants which use kernels to approximate a delta function. The integral interpolant of any quantity function $A(r)$ is defined by:

$$A(r) = \int_{\Omega} A(r')W(r - r', h)dx \quad (1)$$

This relates the value of parameter A , a scalar variable such as pressure, at location r , through integration of the value of A over surrounding space Ω with a smoothing kernel W . This smoothing kernel essentially acts as a weighting factor which, critically, enables the variation of A at distances greater than a defined value to be ignored. This finite support radius enables the physical domain to be subdivided into a number of overlapping subdomains which greatly enhances the computational efficiency of the approach. In the standard SPH formulation, this can be written as:

$$A_i(r) = \sum_j A_j \frac{m}{\rho} W(r_i - r_j, h) \quad (2)$$

In which the value of A of particle i is evaluated by summing the values of A at all particles within the support radius as a function of their mass, m , density, ρ and kernel, W . This can be extended to spatial derivatives through the following functions:

$$\nabla A_i(r) = \sum_j A_j \frac{m}{\rho} \nabla W(r_i - r_j, h) \quad (3)$$

$$\nabla^2 A_i(r) = \sum_j A_j \frac{m}{\rho} \nabla^2 W(r_i - r_j, h) \quad (4)$$

A number of different kernels have been proposed in SPH literature, each with differing behaviour benefits and drawbacks. The cubic spline kernel has been adopted for this analysis as it is the most widely used and understood. The Cubic spline is given by the following function, with normalisation factors, σ , of $1/h$, $10/(7\pi h^2)$, and $1/(\pi h^3)$ in one, two and three dimensions respectively.

$$W(r, h) = \sigma \begin{cases} 1 - \frac{3}{2}q^2 + \frac{3}{4}q^3 & 0 \leq q \leq 1 \\ \frac{1}{2}(2 - q)^3 & 1 \leq q \leq 2 \\ 0 & q > 2 \end{cases} \quad (5)$$

This limited support radius enables the solution domain to be subdivided into cell each with dimension equal to the support radius. When each cell is linked with the 26 surrounding cells to form a sub-region, the domain is separated into a number of overlapping subdomains in that a particle inside the subregion will only have a valid interaction with particles in the same region as particles in other regions will be more than the support radius away. This is a key advantage of the SPH approach in that the computational cost of solving a number of small problems is significantly lower than solving one very large problem. Additionally, the numerical processing can be performed on a graphical processing unit (GPU) which comprises a relatively large number of relatively small cores which is ideally suited to such problems.

Within each subdomain it is necessary to determine the movement of each particle as a function of the acceleration due to interaction forces from surrounding particles. The fluid flow forces are governed by the Navier Stokes Equations, which can be written as:

$$\frac{\delta}{\delta t}(\rho u) + (\rho u \cdot \nabla) = -\nabla p + \mu \nabla^2 u + g \quad (6)$$

In the SPH approach these can be reformulated as a smoothed interaction force between each pair of particles. The acceleration of a particle can therefore be derived through summation of these forces over all particles within the support radius. The total acceleration force can be written as:

$$\frac{\delta \rho_i}{\delta t} = -\rho_i \sum_j (u_j - u_i) \cdot \nabla W(r_i - r_j, h) \frac{m_i}{\rho_i} \quad (7)$$

$$\begin{aligned} \frac{\delta}{\delta t}(\rho u_i) = & - \sum_j m_j \left[\left(\frac{p_i}{\rho_i^2} + \frac{p_j}{\rho_j^2} \right) \right. \\ & \left. - \frac{\varepsilon}{\rho_i \rho_j (\mu_i + \mu_j)} \frac{4\mu_i \mu_j}{r_{ij}^2 + \eta^2} \frac{u_{ij} \cdot r_{ij}}{r_{ij}^2 + \eta^2} \right] \nabla W(r_i - r_j, h) \end{aligned} \quad (8)$$

In addition to the standard SPH formulation, a number of additional functions needed to be implemented in order to address specific challenges of the inkjet droplet impact problem. The first of these is to implement the dissipative SPH framework of Marrone et al [3] in order to better deal with the violent impact events. This framework involves modification of the interaction forces to incorporate additional stabilisation terms such that:

$$\begin{aligned} \frac{\delta \rho_i}{\delta t} = & -\rho_i \sum_i (u_j - u_i) \cdot \nabla W(r_i - r_j, h) \frac{m_j}{\rho_j} \\ & + \delta h c_0 \sum_j \psi_{ij} \cdot \nabla W(r_i - r_j, h) \frac{m_j}{\rho_j} \end{aligned} \quad (9)$$

where:

$$\psi_{ij} = 2(\rho_j - \rho_i) \frac{r_{ji}}{|r_{ij}|^2} - [(\nabla\rho_i) + (\nabla\rho_j)] \quad (10)$$

$$\pi_{ij} = \frac{(-u_i) \cdot r_{ji}}{|r_{ij}|^2} \quad (11)$$

The XSPH correction of Monaghan [16] has been implemented to stabilise the analysis, which modifies the particle velocity based on the velocity of the surrounding particles in a manner given by:

$$\frac{\delta r_i}{\delta t} = u_i + \varepsilon \sum_j \frac{m_{bj}}{\bar{\rho}_{ij}} u_{ji} W(r_i - r_j, h) \quad (12)$$

Furthermore, the kernel gradient correction approach of Belytschko [2] is implemented to correct the evaluation of the kernel and gradient values at interfaces. In these regions the support radius covers a region of liquid, represented by particles, and a region of air which, in this implementation, is represented by an absence of particles. The approach of Belytschko requires a 4x4 matrix to be inverted in order to determine the correction factors however this increases the accuracy of the analysis in the critical impact phase of the process. Time integration has been handled through use of a velocity Verlet scheme [17] while material cure behaviour has been handled through a viscosity modification term. A more detailed analysis of the cure kinetics and the non-Newtonian rheometry of the jetted fluids are required to improve the accuracy of the model.

$$\mathbf{A} = \sum_j W_i^s \begin{bmatrix} 1 & \delta x & \delta y & \delta z \\ \delta x & \delta x \delta x & \delta y \delta x & \delta z \delta x \\ \delta y & \delta x \delta y & \delta y \delta y & \delta z \delta y \\ \delta z & \delta x \delta z & \delta y \delta z & \delta z \delta z \end{bmatrix} \quad (13)$$

$$\mathbf{A}\alpha = \mathbf{I} \quad (14)$$

$$W_i^s = \frac{W_i}{\sum_j \left(\frac{m_j}{\rho_j} W_j \right)} \quad (15)$$

$$W = \alpha_{11} + \alpha_{12}\delta x + \alpha_{13}\delta y + \alpha_{14}\delta z \quad (16)$$

$$\nabla W_x = \alpha_{21} + \alpha_{22}\delta x + \alpha_{23}\delta y + \alpha_{24}\delta z \quad (17)$$

$$\nabla W_y = \alpha_{31} + \alpha_{32}\delta x + \alpha_{33}\delta y + \alpha_{34}\delta z \quad (18)$$

$$\nabla W_z = \alpha_{41} + \alpha_{42}\delta x + \alpha_{43}\delta y + \alpha_{44}\delta z \quad (19)$$

3 Droplet Impact Analysis

Analysis of a single droplet of uncured polymer has been performed using the model. The analysis has considered an initial state of a perfectly spherical droplet of diameter $23\mu\text{M}$ travelling toward a flat plane at 5 Ms^{-1} . The fluid is considered to have constant viscosity of $0.015\text{ Pa}\cdot\text{S}$ and density 1000.0 KgM^{-3} . Surface energy values for the fluid-air interface and fluid surface interface were taken as 72 mJM^{-2} . Polymer materials typically exhibit non-Newtonian behavior and the surface energy behavior is more complex than considered in the model and as such the accuracy of the analysis will be limited until the model is extended to capture these phenomena.

The development of the droplet shape during the impact, as predicted by the numerical model, is illustrated in Figure 2. The six images show the droplet at $1, 10, 20, 86, 200$ and $400\ \mu\text{s}$ after impact. The high impact speed causes relatively localized deformation in the immediate post impact phase before the kinetic energy is transferred into transverse momentum and significant viscous energy dissipation. The point at which the droplet has greatest transverse radius occurs at $86\ \mu\text{s}$, where momentum forces have been balanced by the surface tension forces resulting in zero velocity at the outermost extents of the droplet. Beyond this time, the surface tension forces draw the droplet back into a more spherical shape as shown in in the 200 and $400\ \mu\text{s}$ plots.

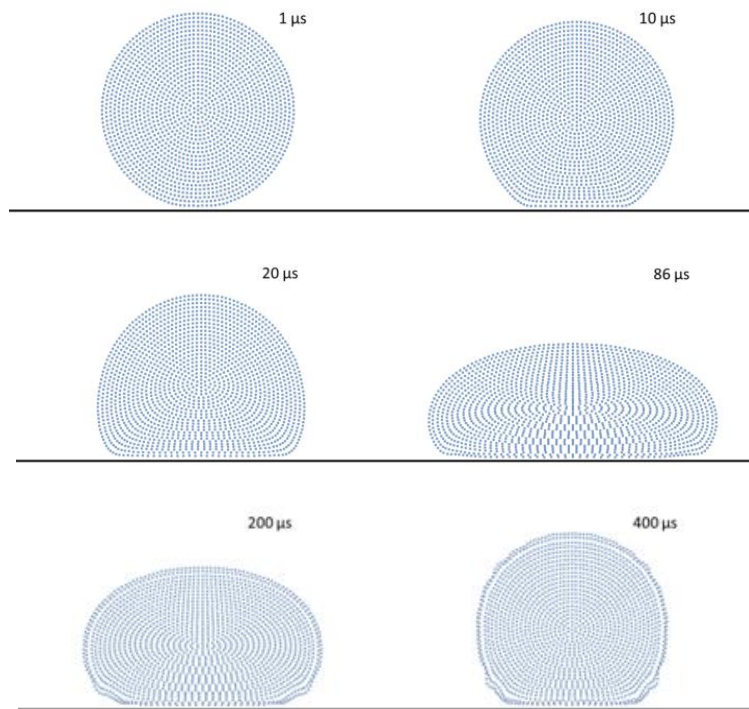


Figure 2: Single droplet impact sequence

These numerical results can be validated through qualitative comparison with high speed imaging data. The experimental setup consisted of a Fuji Dimatix SL-128 inkjet printhead jetting an acrylate based 3D printing build material onto a glass substrate. Images of a single inkjet droplet impacting onto the glass slide were captured at a rate of 100,000 frames per second, with droplet diameter being accurately assessed using a weight test approach. Figure 3 illustrates a droplet impact sequence showing one in every three images for conciseness. Comparison of these images with numerically derived results would suggest a discrepancy between the actual surface tension values and those considered in the model.

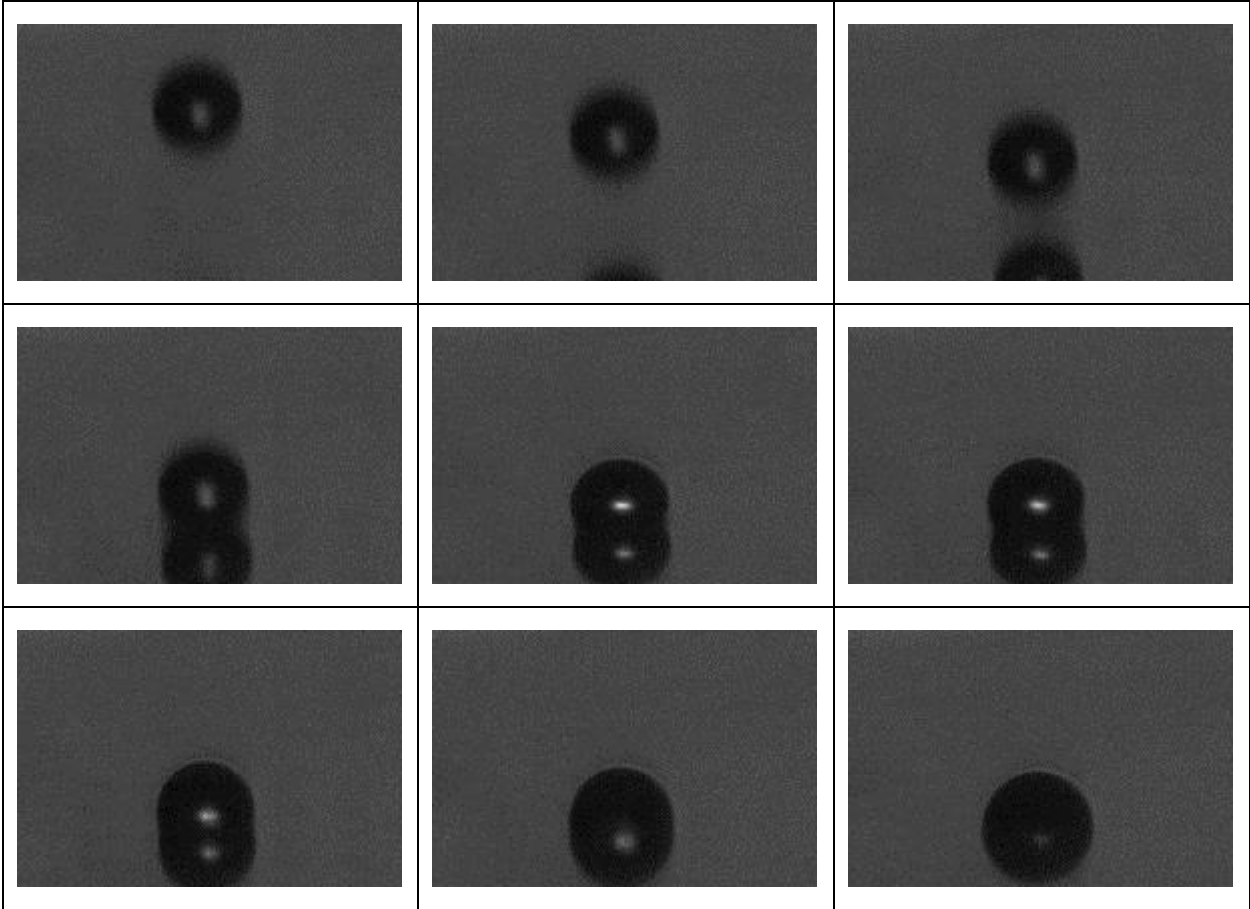


Figure 3: High-speed imaging droplet impact sequence

Conclusions

A new, effective approach for analysis of droplet impact dynamics associated with piezoelectric drop-on-demand inkjet printing systems was presented. The SPH formulation of Lucy and Gingold and Monaghan has been used as the basis for the model, with the δ -SPH terms of Marrone et al and gradient correction terms of Belytschko used to improve the accuracy and stability.

Qualitative comparison of results obtained from the numerical framework with experimentally derived high speed imaging data show the applicability of the approach. The approach could be further enhanced by implementation of an iterative incompressible approach such as that proposed by Ihmsen et al [18] and through integration of an appropriate cure kinetics model to capture post impact UV cure processes.

Acknowledgements

This paper is based on work supported by the NextFactory research project funded under the European Community's 7th Framework Programme (FP7/2007-2013) under grant agreement No. 608985 and through University of Greenwich REF/PP funding

REFERENCES

- [1] Monaghan, J. J., "On the Problem of Penetration in Particle Methods". *Journal Computational Physics*, Vol. 82, pp. 1-15, 1989
- [2] Belytschko, T., Krongauz, Y., Organ, D., Fleming, M., "Meshless methods: an overview and recent developments", *Computer Methods in Applied Mechanics and Engineering*, Vol. 139, Issues 1-4, pp. 3-47, 1996
- [3] Marrone, S., Antuono, M., Colagrossi, A., Le Touzé, D., Graziani, G., "δ-SPH Model for Simulating Violent Impact Flows", *Computer Methods in Applied Mechanics and Engineering*. Vol. 200, pp. 1526-1542, 2011
- [4] Kawahara, Y., Hodges, S., Cook, B. S., Zhang, C., Abowd, G. D., "Instant inkjet circuits: lab-based inkjet printing to support rapid prototyping of UbiComp devices", *Proc UbiComp'13*, September 8-12, 2013, Zurich, Switzerland, pp. 363-372
- [5] B. Khorramdel, J. Liljeholm, M. Laurila, T. Lammi, G. Mårtensson, T. Ebefors, F. Niklaus, M. Mäntysalo, Inkjet printing technology for increasing the I/O density of 3D TSV interposers, *Microsystems and Nanoengineering*, Vol. 3, 10.04.2017, p. 17002.
- [6] Integration of inkjet and RF SoC technologies to fabricate wireless physiological monitoring system, H Sillanpää, A Vehkaoja, D Vorobiev S Nurmentaus, J Lekkala, M Mäntysalo, *Proc. 5th Electronics System-integration Technology Conference (ESTC)*, Helsinki, 2014, doi:10.1109/ESTC.2014.6962739

- [7] <http://www.nano-di.com> [Accessed: 31 May 2018].
- [8] M O'Reilly and Jeff Leal, Jetting your way to fine pitch 3D interconnects, *Chip Scale Review*, Sept/Oct 2010
- [9] NextFactory, <http://www.nextfactory-project.eu> [Accessed: 31 May 2018].
- [10] Guentheil, J., Holzinger, D., Birch, R., Refle, O., "Process & Machine Development for the Integration of Conductive Paths Inside a 3D Printed Microsystem", Proc. Direct Digital Manufacturing Conference, Berlin, Germany, 2016
- [11] Tilford, Timothy, Stoyanov, Stoyan, Braun, Jessica, Janhsen, Jan Cristophe, Burgard, Matthias, Birch, Richard and Bailey, Christopher (2018) Design, manufacture and test for reliable 3D printed electronics packaging. *Microelectronics Reliability*, 85. pp. 109-117. ISSN 0026-2714 (doi:10.1016/j.microrel.2018.04.008)
- [12] Turloukis, G., Stoyanov, S., Tilford, T., Bailey, C., "Data driven approach to quality assessment of 3D printed electronic products", Proc. 38th International Spring Seminar on Electronics Technology, 2015, pp. 300 – 305
- [13] S. Stoyanov, C. Bailey, Machine learning for additive manufacturing of electronics, 40th International Spring Seminar on Electronics Technology (ISSE), 2017
- [14] Patankar, Suhas V., *Numerical Heat Transfer and Fluid Flow*, McGraw-Hill, 1980
- [15] Lucy, L., "A numerical approach to testing the fission hypothesis", *Journal Astronomical.*, Vol. 82, pp. 1013-1924, 1977
- [16] Gingold, R. A., Monaghan, J. J., "Smoothed Particle Hydrodynamics: Theory and Application to non-Spherical Stars" *Mon. Not. R. Astr. Soc.*, Vol. 181, pp. 375-389, 1977
- [17] L. Verlet, "Computer Experiments on Classical Fluids, I: Thermodynamical Properties of Lennard-Jones Molecules. *Phys Rev*, Vol. 159, pp. 98–103, 1967
- [18] M. Ihmsen, J. Cornelis, B. Solenthaler, C. Horvath, M. Teschner, Implicit Incompressible SPH, *IEEE Transactions on Visualization and Computer Graphics*, July 2013.

Multiscale Modelling of Transport Processes and ASR Induced Damage in Concrete

Jithender Jaswant Timothy*, Tagir Iskhakov**, Günther Meschke***

*Ruhr University Bochum, **Ruhr University Bochum, ***Ruhr University Bochum

ABSTRACT

Heterogeneous porous materials, such as concrete are often characterized by a pore-space spanning multiple length scales and a distributed network of microcracks, which either exists a priori, e.g. caused by the production process (shrinkage etc.), or which is later induced by the loading process. As a consequence, molecular transport, fluid flow and the load carrying capacity is strongly influenced specifically by the density and the topology (geometry, distribution, connectivity) of the pores and microcracks. In the first part of the presentation, using a combination of a recursive analytical micromechanics model [1] and direct numerical simulations, the effective transport properties for various isotropic and anisotropic damage configurations and pore-size distributions are computed. In the second part of the presentation, the effective transport properties are incorporated into a multiscale model for describing damage and deterioration in concrete due to Alkali-Silica Reaction (ASR) [2] while simultaneously being subject to combined mechanical, hygral and chemical loads. While microcrack propagation and evolution due to ASR gel pressure at the microscale is modelled within the framework of microporomechanics [3] and upscaled using mean-field homogenization, the kinetics of ASR is described at the aggregate scale using a finite element model. The overall capabilities of the model are shown using select examples and comparison with experimental data. References [1] Timothy, J. J. and Meschke, G. Cascade lattice micromechanics model for the effective permeability of materials with microcracks. *Journal of Nanomechanics and Micromechanics (ASCE)*, 6(4):04016009, 2016. [2] Bangert, F., Kuhl, D. and Meschke, G.,'Chemo-hygro-mechanical modelling and numerical simulation of concrete deterioration caused by alkali-silica reaction';, *International Journal for Numerical and Analytical Methods in Geomechanics* 28 (2004) 689-714. [3] Dormieux, L., Kondo, D. and Ulm, F.J. 'Microporomechanics';, (2006) Wiley & Sons.

Fast Simulation of Columnar Grain Growth During Laser Powder Bed Additive Manufacturing

Albert To^{*}, Jian Liu^{**}, Qian Chen^{***}, Yunhao Zhao^{****}, Wei Xiong^{*****}

^{*}University of Pittsburgh, ^{**}University of Pittsburgh, ^{***}University of Pittsburgh, ^{****}University of Pittsburgh,
^{*****}University of Pittsburgh

ABSTRACT

The goal of this work is to establish the link between process parameters and grain morphology and texture of laser power bed additive manufacturing (AM) processes. A quantitative method is proposed to predict the epitaxial growth of columnar grains within and across melt pools and texture formation during a metal AM process. Finite element simulation is used to predict the geometry and thermal profile of the melt pool. The thermal gradient distribution within the 3D melt pool determines the crystallography direction and growth direction of the columnar grains within each deposited single and multiple tracks. The multiple tracks with the predicted geometry are amalgamated together to represent the bulk part, and the epitaxial growth of grains across the boundary of neighboring tracks are quantitatively simulated. The proposed method will be validated by experimental studies of metal AM processed Inconel 718. The effects of process parameters and scan strategy on the grain texture will also be explored.

AFLOW: Integrated Infrastructure for Automated Computational Materials Design

Cormac Toher^{*}, Corey Oses^{**}, David Hicks^{***}, Frisco Rose^{****}, Eric Gossett^{*****}, Ohad Levy^{*****}, Marco Fornari^{*****}, Marco Buongiorno Nardelli^{*****}, Stefano Curtarolo^{*****}

^{*}Duke University, ^{**}Duke University, ^{***}Duke University, ^{****}Duke University, ^{*****}Duke University, ^{*****}Duke University, ^{*****}Central Michigan University, ^{*****}University of North Texas, ^{*****}Duke University

ABSTRACT

The AFLOW infrastructure for computational materials design [1] accelerates the development and the deployment of new technologies by automating high-throughput first principles calculations. AFLOW includes modules to analyze crystal symmetry, generate hypothetical materials structures by decorating crystallographic prototypes, model substitutional disorder, determine thermodynamic stability, as well as to calculate phonon dispersions, electronic structure and thermo-mechanical properties [2]. The results for more than 1.7 million materials entries are publicly accessible via the AFLOW data repository, which is available online at aflow.org. AFLOW data is being used to train machine-learning models, and to predict the synthesizability of disordered materials. Additional tools, such as the AFLUX Search-API [3] are available to programmatically search and process the data, and are integrated with the AFLOW framework. [1] C. Toher et al., The AFLOW Fleet for Materials Discovery, submitted arXiv:1712.00422 (2017). [2] C. Toher, C. Oses, J. J. Plata, D. Hicks, F. Rose, O. Levy, M. de Jong, M. D. Asta, M. Fornari, M. Buongiorno Nardelli, and S. Curtarolo, Combining the AFLOW GIBBS and Elastic Libraries to efficiently and robustly screen thermomechanical properties of solids, *Phys. Rev. Materials* 1, 015401 (2017). [3] F. Rose, C. Toher, E. Gossett, C. Oses, M. Buongiorno Nardelli, M. Fornari, and S. Curtarolo, AFLUX: The LUX materials search API for the AFLOW data repositories, *Comput. Mater. Sci.* 137, 362-370 (2017).

High-order Residual Distribution Scheme for the Euler Equations of Fluid Dynamics

Svetlana Tokareva^{*}, Remi Abgrall^{**}, Paola Bacigaluppi^{***}

^{*}University of Zurich, ^{**}University of Zurich, ^{***}University of Zurich

ABSTRACT

In the present work, a high order finite element type residual distribution scheme is designed in the framework of multidimensional compressible Euler equations of gas dynamics. The strengths of the proposed approximation rely on the generic spatial discretization of the model equations using a continuous finite element type approximation technique, while avoiding the solution of a large linear system with a sparse mass matrix which would come along with any standard ODE solver in a classical finite element approach to advance the solution in time. In this work, we propose a new Residual Distribution (RD) scheme, which provides an arbitrary explicit high order approximation of the smooth solutions of the Euler equations both in space and time. The design of the scheme allows for an efficient diagonalization of the mass matrix without any loss of accuracy. This is achieved by coupling the RD formulation [1] with a Deferred Correction (DeC) type method [2] for the discretization in time and choosing Bernstein polynomials as shape functions. This work is the extension of [3] to multidimensional systems. We have assessed our method on several challenging benchmark problems for one- and two-dimensional Euler equations and the scheme has proven to be robust and to achieve the theoretically predicted high order of accuracy on smooth solutions. As the second contribution, we show how to compute a relevant weak solution from a pressure-based formulation of the Euler equations of fluid mechanics using our high order RD approach. The pressure-based formulation is in particular useful when dealing with nonlinear equations of state since it is easier to compute the internal energy from the pressure than the opposite. This makes it possible to get oscillation-free solutions, contrarily to classical conservative methods. Finally, we present the extensions of the proposed RD scheme to some models of multiphase flow as well as Lagrangian hydrodynamics. [1] R. Abgrall, Residual distribution schemes: Current status and future trends, *Computers and Fluids* 35 (2006) 641--669. [2] Y. Liu, C.-W. Shu, M. Zhang, Strong stability preserving property of the deferred correction time discretisation, *Journal of Computational Mathematics* 26 (2008) 633-656. [3] R. Abgrall, High order schemes for hyperbolic problems using globally continuous approximation and avoiding mass matrices, *Journal of Scientific Computing* 73 (2017) 461-494

Exponential Integrators: Methods and Software

Mayya Tokman*

*University of California, Merced

ABSTRACT

Over the past decades, exponential integration emerged as a numerical technique that carries significant computational savings compared to current state-of-the-art approaches for certain classes of stiff problems. In this talk we will explain advantages exponential methods offer and discuss theoretical and practical aspects of designing and implementing different classes of efficient exponential integrators. We focus on Exponential Propagation Iterative Methods of Runge-Kutta type (EPIRK) that provide a general framework that can be adapted to construct exponential schemes based on the properties of the problem of interest. In particular, we will discuss the new class of implicit-exponential (IMEXP) methods. These time integrators provide an efficient alternative to implicit-explicit (IMEX) schemes for problems where both the linear and nonlinear forcing in the equations introduce stiffness. We will describe a software package EPIC that contains implementation of efficient exponential methods for serial and parallel computational platforms and illustrate performance gains these schemes provide using test problems and concrete applications.

Cerebrospinal Fluid-Brain Simulations Subject To Loading Conditions

Milan Toma*, Paul Nguyen**

*New York Institute of Technology, **Emory University

ABSTRACT

A fluid-structure interaction (FSI) analysis is used to simulate the interaction between the brain and the cerebrospinal fluid in which the brain is submerged within the skull. Smoothed-particle hydrodynamics is used to represent the fluid flow within the head and its interaction with all the brain and skull structures. These simulations show the fluid particles moving and interacting with the brain gyri and sulci. Thus, the FSI model and its computational analysis have the capability to locate areas (down to the exact gyri and sulci) of the brain the most affected under given loading conditions and therefore assess the possible damage to the brain and consequently predict the symptoms. Closed brain injuries are a common danger in contact sports and motorized vehicular collisions. Mild closed brain injuries, such concussions, are not easily visualized by computed imaging or scans. Having a comprehensive head/brain model and using fluid-structure interaction simulations enable us to see the exact movement of the cerebrospinal fluid under such conditions and to identify the areas of brain most affected.

Meshless RBF-based Biomechanical Simulation of Human Respiratory Muscles

Igor Tominec^{*}, Nicola Cacciani^{**}, Pierre-Frédéric Villard^{***}, Elisabeth Larsson^{****}

^{*}Uppsala University, ^{**}Karolinska Institutet, ^{***}Université de Lorraine, ^{****}Uppsala University

ABSTRACT

The main objective of our research is to understand the functionality of a human diaphragm, the main muscle of the respiratory system. Its action affects the volume of the thorax cavity, such that the lungs can inflate and deflate, enabling a human to breathe. The aim is to enable medical researchers to perform studies on ventilator induced diaphragm dysfunction (VIDD). The diaphragm models in existing simulation tools are not advanced enough to capture the processes that lead to VIDD. Our approach is based on a continuum mechanics model that arises from nonlinear elasticity. The equations are solved on a 3D diaphragm geometry obtained from images of real patients. We aim to include the viscoelastic memory effect of the material, together with the anisotropic layout of the fibre bundles that form the muscle. The model is simulated using localized radial basis function methods in space and a quasistatic approach in time. Many numerical challenges are addressed, such as how to use anisotropic basis functions in order to treat the non-trivial high-aspect ratio geometry, convergence and computational speed of the nonlinear iterations, and the stability in time.

DNS of Plane Couette Flow with Roughness in the Transitional Region

Takeru Tomioka*, Takahiro Tsukahara**

*Tokyo University of Science, **Tokyo University of Science

ABSTRACT

There are many investigations of wall-bounded turbulence, but few studies consider the influence of wall roughness on the transition process. From practical perspective, it is important to consider the roughness effect on the wall turbulence and its subcritical transition to turbulence. An earlier work by direct numerical simulation (DNS) of plane Couette flow (pCf) with roughened walls [1], reported a decrease in the lower critical Reynolds number (below which any disturbance decays) on roughened walls. It was also shown that turbulent intermittent structures arising in the transitional region were changed significantly due to the roughness given only on one wall. Details of such structure changes are still unknown. In this study, we focused on the intermittent structure observed in the transitional region of the roughened pCf. We analyzed the pCf driven by the top wall with adding the roughness to the bottom static wall. The roughness is mimicked by the body force rather than actually creating the roughness element [2]. This model term consists of roughness density, shape function, and average roughness height h . With fixing the former two parameters, we focused on the change of the intermittent structure through a parametric study with respect to h . In the absence of roughness, turbulent stripes (i.e., localized turbulence bands) form obliquely to the main stream direction, but non-oblique turbulence stripes (hereinafter called "vertical turbulent stripes") were confirmed when h was high. We examined further how the structure would be changed by changing the Reynolds number and h in the parameter range where the vertical turbulence stripe was detected. The streamwise width of each band of the vertical turbulent stripes was found to decrease as the Reynolds number and/or h decrease, and when turbulent fraction falls below a certain value, the laminar flow occurs. Moreover, by expanding the calculation area in the streamwise direction, we observed a split of the vertical turbulence band into two bands. In the full paper, we will investigate the onset condition and mechanism of the vertical turbulent stripes. Reference [1] Ishida, T., Brethouwer, G., Duguet, Y., and Tsukahara, T., Laminar-turbulent patterns with rough walls. *Phys. Rev. Fluids*, 2, 073901 (2017) [2] Busse, A. and Sandham, N. D., Parametric forcing approach to rough-wall turbulent channel flow, *J. Fluid Mech.* 712, 169 (2012).

Structural Topology Optimization Considering Geometrical and Material Nonlinearities

Liyong Tong*, Quantian Luo**

*The University of Sydney, **The University of Sydney

ABSTRACT

Multi-objective structural topology design optimization considering geometrical and material nonlinearities and multiple constraints is a challenging problem. Unlike linear structural topology optimization, it may involve repeated analyses of highly nonlinear structural systems and repetitive sensitivity analyses of topological designs if a gradient method is adopted. There exist several difficult issues in both nonlinear structural and sensitivity analyses. For example, how to represent an arbitrary topology of an element in nonlinear finite element formulations to ensure successful completion of each nonlinear analyses? How to use full nonlinear solutions, instead of approximate linear ones, in the updates of topological designs? In this study, the moving iso-surface threshold method is used to address this challenging optimization problem. A generalized mathematical formulation for nonlinear output displacement is derived. In this formulation, the displacement is expressed in terms of total mutual strain energy density calculated using virtual stresses and real strains of all incremental load steps in a nonlinear finite element analysis. This is different from the formulation where only the solution at the final load step is used in sensitivity analysis. This generalized formulation can easily fit in the formulation used in the moving iso-surface threshold method. Two optimization problems involving geometrical and material nonlinearities are considered. The first optimization problem is concerned with the topological design of nonlinear compliant mechanism with multi-objectives and multi-constraints. By using the problem formulation based on moving iso-surface threshold method, an effective algorithm is developed to maximize chosen displacements at multiple outputs for a compliant mechanism with displacement and volume constraints and nonlinear effects. Numerical results of the present algorithm for linear and nonlinear compliant mechanisms are obtained and compared with those linear ones available in the literature. The second optimization problem is about optimal topology design of pressurized cellular structures for potential application in morphing aircraft structures, in particular morphing aircraft wing camber variation using topology optimization to increase lift coefficient. First of all, optimal topology design of a pressurized unit cell is obtained. In the design iteration, super-elements are used to model pressure loading on structural boundaries with fluid-structure interaction and to obtain the optimal solution via a developed algorithm. Thereafter this pressurized unit cell is used as a building block to form integrated pressurized multi-cell wing rib structural component for wing camber morphing.

Comparison of Accuracy and Computational Cost of Different Numerical Boltzmann Solvers

Erik Torres^{*}, Jeff Haack^{**}, Irene Gamba^{***}, Thierry Magin^{****}

^{*}University of Minnesota, ^{**}Los Alamos National Laboratories, ^{***}University of Texas at Austin, ^{****}Von Karman Institute for Fluid Dynamics

ABSTRACT

In this work we compare two numerical methods for solving the Boltzmann Equation for neutral gas mixtures: a deterministic kinetic solver based on the Spectral-Lagrangian method [1] and the stochastic, particle-based Direct Simulation Monte Carlo (DSMC) method [2]. We measure the relative computational cost, both in terms of memory use and CPU run-times, to obtain a pre-set level of accuracy in the macroscopic moments. In order to perform a fair comparison, we will define clear metrics for assessing solution accuracy, given the differences inherent to the two numerical techniques (deterministic vs. stochastic). Three test cases are chosen to for this comparison, each one to stress-test a specific part of the two distinct methods. The first involves the time-unsteady, space-homogeneous relaxation of a mixture of mono-atomic gases, initially at different Maxwell-Boltzmann distributions. This allows us to directly compare the cost of solving the non-linear collision term for the two methods, without worrying about particle advection. The second test case is flow of a mono-atomic gas across a normal shock wave. We obtain the solution as a time-steady problem in the shock's frame of reference. The pre- and post-shock states, specified in terms of macroscopic moments are imposed as boundary conditions at the limits of a 1-D physical domain, whereas velocity space remains 3-D. The third test case involves heat transfer across a mono-atomic gas between two diffusely reflecting walls. Both the initial transient and final steady-state profiles of macroscopic moments are used for our comparison. For the Spectral-Lagrangian solver, the main factor in obtaining accurate solutions lies in sizing the velocity mesh to fully capture and resolve the velocity distribution function(s) of all components in the gas mixture. The computational cost increases with the 6th power of the number of velocity nodes used, and becomes the limiting factor for this method. In case of the DSMC method, statistical noise in the macroscopic moments is caused by the finite particle number used to approximate the velocity distributions in each physical location. This noise is of special concern at high gas temperatures and low stream velocities.

REFERENCES [1] I. M. Gamba and S. H. Tharkabhushanam, Spectral-Lagrangian methods for collisional models of non-equilibrium statistical states, *J. Comp. Phys.*, 228(6), 2012-2036. [2] G.A. Bird, *Molecular Gas Dynamics and the Direct Simulation of Gas Flows*, Oxford Science Publications, 1994.

A Unified Framework for the Modeling and Simulation of Fluid Surfaces

Alejandro Torres-Sánchez*, Marino Arroyo**, Daniel Millán***

*Universitat Politècnica de Catalunya, **Universitat Politècnica de Catalunya, ***CONICET, Universidad Nacional de Cuyo

ABSTRACT

We develop a novel framework for the three-dimensional modeling and simulation of fluid surfaces from a continuum mechanics viewpoint. Fluid surfaces are ubiquitous in cell and tissue biology, with examples including lipid bilayers, the acto-myosin cortex, or epithelial monolayers. These surfaces usually involve a non-linear coupling between mechanical and chemical signals, which play a key role in important biophysical processes such as cell division, migration or morphogenesis. Thus, there is a growing interest in modeling and simulating these fluid interfaces. This, however, requires of a general framework that tackles the chemo-mechanical coupling transparently and deals with the geometric aspects of a time-evolving surface. To handle the multi-physics aspects of these surfaces, we base our approach on Onsager's variational principle, which provides a variational formulation for the dissipative dynamics of soft-matter systems. In addition to coupling different physical ingredients, modeling fluid surfaces inevitably requires the tools and language of differential geometry to describe a deforming surface evolving in Euclidean space. For instance, the classical rate-of-deformation tensor couples interfacial flows with shape changes in the presence of curvature. Furthermore, the fluid nature of these surfaces challenges classical Lagrangian or Eulerian descriptions of deforming bodies. Indeed, due to the fluid nature of the surface, Lagrangian parametrizations generate very large distortions that require a large amount of remeshing. On the other hand, since we need to track the position of the interface in Euclidean space, the meaning of an Eulerian description is unclear. Arbitrary Lagrangian-Eulerian formulations, well established for bulk media, appear as a natural choice but such a formulation for a deforming surface needs careful consideration. Finally, the three-dimensional simulation of lipid bilayers requires unconventional numerical methods since the resulting equations involve higher-order derivatives of the parametrization, lead to a mixed system of elliptic and hyperbolic partial differential equations and are stiff and difficult to integrate in time. Indeed, surface shape enters into the energy and dissipation expressions through curvature, which involves second-order derivatives of the parametrization. From a finite element method perspective, this implies that the basis functions used to represent the parametrization need to be smooth. Here, we propose a discretization based on subdivision surfaces. While the Galerkin FEM deals naturally with elliptic equations, hyperbolic systems such as the continuity equation modeling fluid transport require special treatment.

Hierarchical Boltzmann Simulations and M(odel)-refinement

Manuel Torrilhon*

*RWTH Aachen University

ABSTRACT

(to be announced)

Isogeometric Analysis on Meshes with Polar Singularities: Applications to High-order PDEs and Structure-preserving Discretizations

Deepesh Toshniwal^{*}, Hendrik Speleers^{**}, Thomas J R Hughes^{***}

^{*}University of Texas at Austin, ^{**}University of Rome Tor Vergata, ^{***}University of Texas at Austin

ABSTRACT

Representing arbitrary surfaces with a finite number of polynomial patches requires the introduction of polar points for high-valence neighborhoods in quadrilateral meshes. Such holes can be filled by means of polar spline surfaces, where the basic idea is to use periodic spline patches with one collapsed boundary. Building splines over such singularities requires special rules to ensure smoothness; ensuring suitability for design and analysis imposes further constraints. A general framework for building C^k polar spline parametric patches of arbitrary degree and with arbitrary number of elements at the hole boundary was presented in [1]. Apart from a simple, geometric construction of smooth basis functions, it was shown that it is possible to endow upon the spline basis interesting properties such as non-negativity and partition of unity. Numerical experiments indicating optimal approximation behavior, even at the singular point, were presented in [1]. In this talk, we will present applications of the technology developed in [1] to high-order PDEs, such as the Cahn-Hilliard equations, where the smoothness afforded by the spline basis allows straightforward numerical discretization and implementation. Moreover, using smooth polar splines as a basis for zero forms, we will construct basis functions for higher-order differential forms and present a pointwise divergence free discretization of the Stokes equation. [1] D. Toshniwal, H. Speleers, R.R. Hiemstra, and T.J.R. Hughes. "Multi-degree smooth polar splines: A framework for geometric modeling and isogeometric analysis", *Comput. Methods Appl. Mech. Engrg.* 316, 1005-1061, 2017.

Numerical Modeling of Nucleation Mechanisms for 3D Heterogeneous Microstructures

Thomas Toulorge^{*}, Marc Bernacki^{**}, Pierre-Olivier Bouchard^{***}, Modesa Shakoor^{****}, Victor Trejo Navas^{*****}

^{*}Mines ParisTech, ^{**}Mines Paris Tech, ^{***}Mines ParisTech, ^{****}Mines ParisTech, ^{*****}Mines ParisTech

ABSTRACT

Ductile fracture of metallic materials is known to be based on the mechanisms of voids nucleation, growth and coalescence. Voids nucleation is usually due either to failure of particles (fragmentation) or to failure at the interface between particles and the matrix (debonding). Coalescence is characterized by the initiation and propagation of micro-cracks between voids leading to final fracture. The most observed coalescence mode is due to internal necking between neighbouring voids with plastic localization in the intervoid ligaments. For lower stress triaxiality ratios, a shear driven localization mode can also be observed. This mode, often called void-sheet coalescence, is not yet perfectly understood. This work focuses on the development of an efficient finite element approach for the modeling of failure mechanisms of complex 3D microstructures under large plastic strain and multi-axial loading conditions. Heterogeneous microstructures are represented by a matrix containing particles and voids defined by level-set functions and mesh adaption techniques [1]. A finite element analysis of 3D heterogeneous microstructures with randomly distributed particles is carried out so as to study the influence of particles debonding and fragmentation on void coalescence by internal necking [2]. Micromechanical simulations of a microstructure with 20% particle volume fraction show that voids nucleation leads to an early plastic strain localization mechanism that favors void coalescence and reduces ductility. This work was performed within the COMINSIDE project funded by the French Agence Nationale de la Recherche (ANR-14-CE07-0034-02 grant). REFERENCES [1] M. Shakoor, M. Bernacki and P.-O. Bouchard, A new body-fitted immersed volume method for the modeling of ductile fracture: analysis of void clusters and stress state effects on coalescence, *Engineering Fracture Mechanics*, 147, 398–417 (2015). [2] M. Shakoor, M. Bernacki and P.-O. Bouchard, Ductile fracture of a metal matrix composite studied using 3D numerical modeling of void nucleation and coalescence, *Engineering Fracture Mechanics*, in Press

Development of Augmented Reality Experience System of Indoor Damage due to Earthquake

Takuya Toyoshi^{*}, Daigoro Isobe^{**}, Takuzo Yamashita^{***}, Kazutoshi Matsuzaki^{****}, Hiromitsu Tomozawa^{*****}

^{*}National Research Institute for Earth Science and Disaster Resilience, ^{**}University of Tsukuba, ^{***}National Research Institute for Earth Science and Disaster Resilience, ^{****}Mizuho Information & Research Institute, Inc., ^{*****}Mizuho Information & Research Institute, Inc.

ABSTRACT

Utilization of virtual reality (VR) and augmented reality (AR) technique is useful for education of disaster. The objective of this research is to develop a fusion technique to generate AR experience video for indoor damage using three-dimensional images with calculated results. National Research Institute for Earth Science and Disaster Resilience (NIED) is developing a virtual experience system of indoor disaster damage. This system consists of a data acquisition part and a data processing and playback part. The data acquisition part can measure and provide synchronized three-dimensional images, sound and acceleration. The system was applied to the E-Defense shake table test of the 10-story reinforced concrete (RC) building and a VR experience video of indoor damage was successfully generated. This video visualized on head mounted display (HMD) can provide a virtual experience of indoor disaster under seismic excitation [1]. A numerical analysis system called E-Simulator, which is under construction by NIED, can analyze motions and falls of indoor furniture and fixture under seismic excitation. A finite element method based on the adaptively shifted integration (ASI) – Gauss technique is used for this analysis. This method can simulate various indoor situations which are difficult to reproduce in actual experiments with high accuracy and low calculation cost using fewer elements [2]. To achieve the objective of this research, the data of indoor damages on the 10th floor of the 10-story RC building specimen excited on the shake-table test of the E-Defense was used. The acceleration data measured on the 10th floor was used for the motion analysis of furniture placed at various locations. A system to paste the texture from several furniture images was developed, and more realistic visualized data was produced. Furthermore, a fusion technique between numerical results and three-dimensional images was developed, in which the data are synchronized by linear interpolation. The generated images are to be shown in the presentation. References [1] Takuzo Yamashita, Mahendra Kumar Pal, Kazutoshi Matsuzaki and Hiromitsu Tomozawa, Development of Virtual Reality Experience System of Interior Damage due to Earthquake Utilizing E-Defense Shake Table Test, Journal of Disaster Research, pp. 882-890, 2017. [2] Daigoro Isobe, Takuzo Yamashita, Hiroyuki Tagawa, Mika Kaneko, Toru Takahashi and Shojiro Motoyui, Motion Analysis of Furniture under Seismic Excitation Using the Finite Element Method, Japan Architectural Review, doi: 10.1002/2475-8876.1015, 2017.

A Parametric Class of Composites with a Large Achievable Range of Effective Elastic Properties

Davi Colli Tozoni^{*}, Denis Zorin^{**}, Igor Ostanin^{***}, George Ovchinnikov^{****}

^{*}Courant Institute, New York University, ^{**}Courant Institute, New York University; Skolkovo Institute of Science and Technology, ^{***}Skolkovo Institute of Science and Technology, ^{****}Skolkovo Institute of Science and Technology

ABSTRACT

We investigate computationally an instance of the problem of G-closure for periodic metamaterials, i.e, the problem of determining what homogenized material properties can be achieved. We consider composites with isotropic homogenized elasticity tensor, obtained as a mixture of two isotropic materials, focusing on the case of a single material with voids. This problem is important, in particular, in the context of designing small-scale structures for metamaterials in the context of additive fabrication, making possible to obtain a range of material properties using a single base material. We demonstrate that two closely related simple parametric families based on the structure proposed by O. Sigmund attain good coverage of the space of isotropic properties satisfying Hashin-Shtrikman bounds. In particular, for positive Poisson ratio, we demonstrate that Hashin-Shtrikman bound can be approximated arbitrarily well, within limits imposed by numerical approximation: a strong evidence that these bounds are achievable in this case. For negative Poisson ratios, we numerically obtain a bound which we hypothesize to be close to optimal, at least for metamaterials with rotational symmetries of a regular triangle tiling.

A Comparison of Fluid-Structure-Interaction Approaches to Blood Flow Modeling with Vessel Prestress

Justin Tran^{*}, Vijay Vedula^{**}, Kathrin Baeumler^{***}, Alison Marsden^{****}

^{*}Stanford University, ^{**}Stanford University, ^{***}Stanford University, ^{****}Stanford University

ABSTRACT

Recent advances in computational modeling of blood flow include modeling the fluid-structure-interaction (FSI) effects between the vessel wall and the blood flow. These effects are crucial as the rigid wall assumption overestimates predictions of wall shear stress, disregards pressure wave propagation, and neglects the mechanical stresses experienced by the wall. Several methods were proposed to model vessel wall deformability. The Coupled Momentum Method (CMM) [1] approximates the vessel wall as a thin membrane where the interface traction is modeled as a body force in the linear elastodynamics equations. As the fluid mesh remains fixed, CMM incurs only a small increase in cost compared to rigid wall approximation, but is generally reliable for modest deformations of less than 10% of the vessel radius. The Arbitrary Lagrangian-Eulerian (ALE) [2] is a general framework for FSI that solves the fully coupled equations for fluid flow, nonlinear wall deformation, and time evolution of the computational mesh. A grid velocity is introduced into the convective term of the Navier-Stokes equations through a space-time Piola transform from an arbitrary mesh to a reference mesh, while satisfying the kinematic and dynamic constraints at the fluid-solid interface. ALE can accommodate large deformations on generic geometries, at a relatively higher cost. In this study, we compare the performance and computational results between using CMM and ALE for modeling blood flow in both idealized and patient-specific models. Additionally, we consider the effect of prestress in the vessel walls for both approaches [3]. Typically, when patient-specific models are constructed from image data, the walls are stressed and in equilibrium with the pressure and viscous forces from the fluid. This phenomenon is commonly neglected, but can lead to large differences when comparing simulation results to time-resolved clinical imaging data. This is especially true for CMM, where initialization requires inflation of the model so the displacements depart from a state of equilibrium with the fluid forces. This can lead to over-inflation which may not be correct. The main contributions of this work are a quantitative comparison of two common methods for FSI in cardiovascular applications both implemented in the same solver, and an analysis of including the effect of prestress for various idealized and patient-specific anatomic models. [1] Figueroa, C. Alberto, et al. Computer methods in applied mechanics and engineering. 2006. [2] Bazilevs, Yuri, et al. Computational Mechanics. 2006. [3] Hsu, Ming-Chen, and Yuri Bazilevs. Finite Elements in Analysis and Design. 2011.

ANALYTIC METHOD TO IDENTIFY TRAIN LOAD FROM INTEGRATED SLEEPER IN-SITU

L-H. TRAN^{*†}, T. HOANG^{*}, D. DUHAMEL^{*}, G. FORET^{*},
S. MESSAD[†] AND A. LOAËC[†]

^{*}Laboratoire Navier, UMR 8205, Ecole des Ponts ParisTech,
IFSTTAR, CNRS, UPE, Champs-sur-Marne, France
le-hung.tran@enpc.fr, tien.hoang@enpc.fr, denis.duhamel@enpc.fr, gilles.foret@enpc.fr

[†]SATEBA, 33 places des Corolles, 92400 Courbevoie, France
s.messad@sateba.com, a.loaec@sateba.com

Key words: Railway Dynamics, Instrumented Sleeper, Fiber Bragg gratings, Green’s function, Computation methods.

Abstract. The degradation of railway tracks can be observed through several measurement techniques. Recently, a method to diagnose the railway track using Fiber Bragg gratings (FBG) has been proposed. FBG are integrated inside the railway sleeper and is named a “Smart Sleeper”. To study the sleeper behavior, an analytical model for the dynamics of railway sleepers has been developed, which can calculate rapidly the sleeper responses. In this model, by using the relation between the rail forces and displacements of a periodically supported beam, the dynamic equation of the sleeper is written with the help of the Euler-Bernoulli beam equation and Dirac’s functions. Subsequently, thanks to the Green’s function of this system, the sleeper dynamic response is calculated analytically. A linear relation between the train loads and the sleeper strains is shown in the frequency domain. This article presents an application of this model to calculate the train loads from the strains measured by the FBG. Based on the analytical model, we obtain a matrix which presents the link between the loads and the sleeper responses. By integrating this matrix and the Fourier transform of the measurements recorded by the FBG at the middle and at the two rail-seats, the train loads can be quickly calculated by using the solver `mldivide` of MATLAB. The numerical application shows that the identified train loads are different for different wheels and different rails. This highlights the irregularity of the wheel-rail contact forces which can be used to detect the defaults in the rolling stock in future works.

1 INTRODUCTION

Generally, defective materials can be detected by several different methods. The easiest is the correlation by image analysis but it is slow and not exact. Measurement of elastic waves, electrical resistance or acoustic emission focus on a variation of the propagation time of waves and electrical resistance to detect the internal cracks of objects. The study of the dynamic properties of systems in the frequency domain (modal analysis) is then applied [1, 2, 3]. Material

damage would have abnormal resonant frequencies.

In recent years, a novel technology using the Fiber Bragg Grating (FBG) to diagnose the railway track has been developed. In 2010, Filograno et al. [12] posed the FBG sensors on the rail in different directions (vertical, horizontal and inclined at an angle 45°) for monitoring the high speed line from Madrid to Barcelona in real time. They could detect the train parameters: train speed and acceleration, the distance between the wheel and wheel number. Moreover, the dynamic charge can be calculated in a precise way. Wei et al. [13, 14] presented two methods: X-Crossing and D-Crossing to avoid the area where signals are noisy. Buggy et al. [15] has used the FBG to monitor the fishplate (junction of two rails). In the same year, Tam et al. [16] presented the system ‘‘Smart Railways’’ which has been developed by KCRS’s East Rail in Hong Kong. The FBG sensor has been demonstrated to be able to detect the rail imperfection [17, 18]. A railway sleeper ‘‘Smart Sleeper’’ [19] which has been developed by Sateba with 6 sensors allows us to measure the sleeper strain when the train is passing.

Substantial research using analytical and numerical methods for rail track has been carried out. Analytical models of the rail track have been developed by considering the model of an infinite beam placed on a continuous foundation [8, 9, 10] or a periodically supported beam [4, 5, 6, 7]. Some research focus on the pre-stressed concrete sleeper using FEM in 2D and in 3D [20, 21]. In 2017, Tran et al. [11] has developed an analytical model of the railway sleeper which allows us to rapidly calculate the sleeper response.

In this paper, based on the analytical model of the railway sleeper, an ‘‘inverse problem’’ has been developed to determine the train loads. By considering a beam resting on a Kelvin-Voigt foundation and by assuming a periodic charge, the sleeper strain and the train loads can be written as a linear relation in the frequency domain with the help of the Green’s function. The charges can be determined by using the MATLAB solver `mldivide`. We verified this problem to a good precision by back-calculating the train loads from a signal. That is a combination of imposed loads and random noise. Another application has been shown in this paper with the real measurements recorded by the ‘‘Smart Sleeper’’. The results of this application shows the different charges applied on each rail which corresponds to different strain level recorded by the FGB of the sleeper.

2 GORVERNING EQUATIONS

2.1 Analytical model of the sleeper

A railway track can be modeled as shown in Fig. 1. In this track, the sleeper together with the ballast and foundation are modeled by an Euler-Bernoulli beam resting on a Kelvin-Voigt foundation. The sleeper length is $2L$ (from $-L$ to L) and the rail positions are at $x = \pm a$. The sleeper displacement $w_s(x, t)$ under a force $F(x, t)$ is driven by the dynamic equation of the Euler-Bernoulli pre-stressed beam as follows:

$$E_s I_s \frac{\partial^4 w_s(x, t)}{\partial x^4} + \rho_s S_s \frac{\partial^2 w_s(x, t)}{\partial t^2} - T \frac{\partial^2 w_s(x, t)}{\partial x^2} + k_f w_s(x, t) + \zeta_f \frac{\partial w_s(x, t)}{\partial t} = F(x, t) \quad (1)$$

where ρ_s , E_s , S_s and I_s are the density, the Young’s modulus, the section and the cross-sectional moment inertia of the sleeper respectively; k_f and ζ_f are the stiffness and damping coefficients

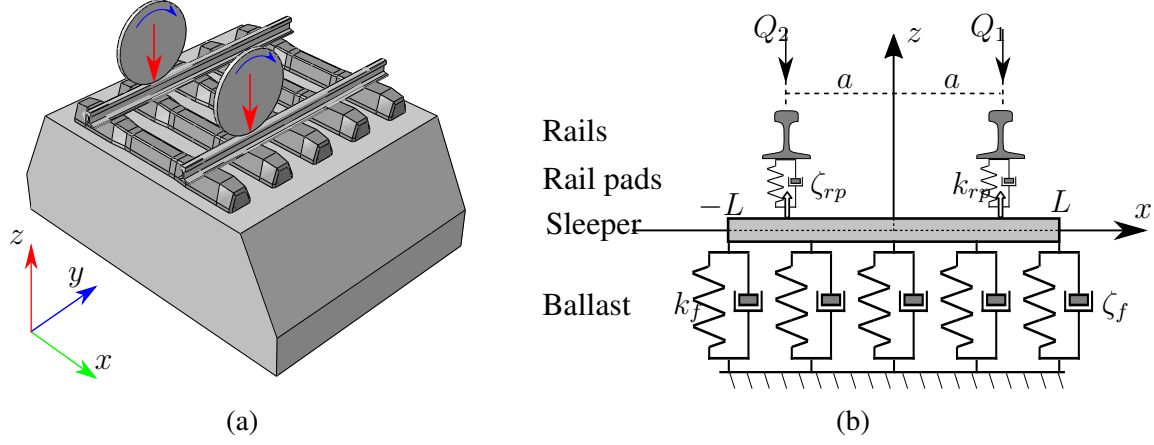


Figure 1: Railway track (a) and the analytical model representation (b)

of the foundation and T is the sleeper pre-stress. The force applied by the rails on the sleeper $F(x, t)$ can be written with the help of the Dirac's functions as follows :

$$F(x, t) = -R_1(t)\delta(x - a) - R_2\delta(x + a) \quad (2)$$

where R_1 and R_2 are the reaction forces applied on the rail positions ($x = \pm a$). For a free-free beam posed on the foundation, the moment (3a) and the shear force (3b) are vanishing at two extremities, thus these boundary conditions can be imposed by the 2nd and 3rd partial derivative with regard to x set to zero respectively:

$$\begin{cases} \frac{\partial^2 w_s}{\partial x^2}(-L, t) = \frac{\partial^2 w_s}{\partial x^2}(L, t) = 0 \\ \frac{\partial^3 w_s}{\partial x^3}(-L, t) = \frac{\partial^3 w_s}{\partial x^3}(L, t) = 0 \end{cases} \quad (3a)$$

$$\begin{cases} \frac{\partial^2 w_s}{\partial x^2}(-L, t) = \frac{\partial^2 w_s}{\partial x^2}(L, t) = 0 \\ \frac{\partial^3 w_s}{\partial x^3}(-L, t) = \frac{\partial^3 w_s}{\partial x^3}(L, t) = 0 \end{cases} \quad (3b)$$

Eq. (1) together with the boundary conditions (3) is a 4th order linear differential equation in the frequency domain which can be solved with help of the Green's function. (The calculation of the Green's function is shown in Appendix B). Hence, the sleeper response in the frequency domain $\hat{w}_s(x, \omega)$ can be written as follow:

$$\hat{w}_s(x, \omega) = \frac{-\hat{R}_1}{E_s I_s} G_a(x, \omega) + \frac{-\hat{R}_2}{E_s I_s} G_{-a}(x, \omega) \quad (4)$$

By substituting $x = a$ and $x = -a$ into the aforementioned equation, we obtain respectively the sleeper displacement at the rail positions:

$$\begin{aligned} \hat{w}_s(a, \omega) &= \frac{-\hat{R}_1}{E_s I_s} G_a(a, \omega) + \frac{-\hat{R}_2}{E_s I_s} G_{-a}(a, \omega) \\ \hat{w}_s(-a, \omega) &= \frac{-\hat{R}_1}{E_s I_s} G_a(-a, \omega) + \frac{-\hat{R}_2}{E_s I_s} G_{-a}(-a, \omega) \end{aligned} \quad (5)$$

The model of the periodically supported beam and together with the consecutive law of the rail pads shows the expression of the reaction force (see Appendix A). The combination at Eqs. (17) and (5) gives us the result of the reaction force of the sleeper on the two rails:

$$\begin{aligned}\hat{R}_1 &= \frac{E_s I_s}{\mathcal{K}} \frac{\mathcal{Q}_1 [G_{-a}(-a, \omega) + \chi] - \mathcal{Q}_2 G_{-a}(a, \omega)}{[\chi + G_a(a, \omega)] [\chi + G_{-a}(-a, \omega)] - G_a(-a, \omega) G_{-a}(a, \omega)} \\ \hat{R}_2 &= \frac{E_s I_s}{\mathcal{K}} \frac{\mathcal{Q}_2 [G_a(a, \omega) + \chi] - \mathcal{Q}_1 G_a(-a, \omega)}{[\chi + G_a(a, \omega)] [\chi + G_{-a}(-a, \omega)] - G_a(-a, \omega) G_{-a}(a, \omega)}\end{aligned}\quad (6)$$

where $\chi = E_s I_s \frac{k_p + \mathcal{K}}{k_p \mathcal{K}}$. Then, the sleeper displacement in the frequency domain can be obtained by replacing \hat{R}_1 and \hat{R}_2 in Eq. (4). The sleeper strain can be calculated using the beam theory and together with the equation of the sleeper response (4):

$$\hat{\varepsilon}_x(x, z, \omega) = z_s \left(\frac{\hat{R}_1}{E_s I_s} G_a''(x, \omega) + \frac{\hat{R}_2}{E_s I_s} G_{-a}''(x, \omega) \right) \quad (7)$$

where z_s is the distance to the beam's neutral axis. By using the inverse Fourier transform of Eqs. (4) and (7), we can get the sleeper response and the sleeper strain in the time domain.

2.2 Identification of the train load

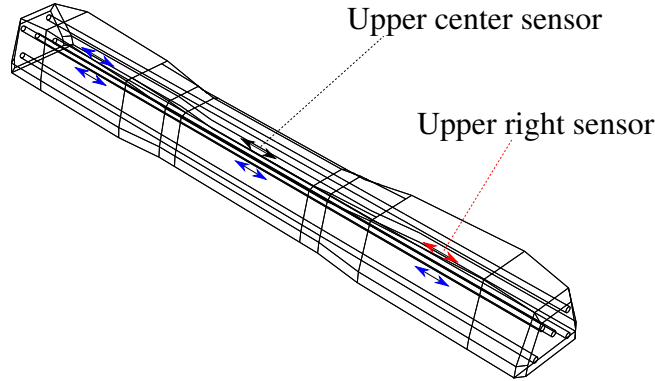


Figure 2: Instrumented sleeper: upper right sensor (red), and upper center sensor (black)

We will apply this analytical model to identify the train load from the sleeper strain. A ‘‘Smart Sleeper’’ which has been developed by Sateba with 6 Fibre Bragg Grating sensors (FBG) integrated in the longitudinal direction allow us to obtain the sleeper strain as the train passes. These sensors are situated at the two rail seats and at the middle of the sleeper. The signals are recorded by these sensors in the time domain and by using the Fourier transform, we can obtain these signals in the frequency domain. We can rewrite Eq. (7) as follows:

$$\hat{\varepsilon}_i(x_i, z_{s_i}, \omega) = \mathbf{A}_{i1}(x_i, z_{s_i}, \omega) \hat{R}_1(\omega) + \mathbf{A}_{i2}(x_i, z_{s_i}, \omega) \hat{R}_2(\omega) \quad (8)$$

where (x_i, z_{s_i}) are the positions of the sensors, $\mathbf{A}_{i1} = \left(\frac{z_{s_i}}{E_s I_s} G''_a(x_i, \omega) \right)$ and $\mathbf{A}_{i2} = \left(\frac{z_{s_i}}{E_s I_s} G''_{-a}(x_i, \omega) \right)$.

This equation can be also rewritten as:

$$[\hat{\varepsilon}(\omega)] = [\mathbf{A}_{i1}(\omega) \quad \mathbf{A}_{i2}(\omega)] \begin{bmatrix} \hat{R}_1(\omega) \\ \hat{R}_2(\omega) \end{bmatrix} \quad (9)$$

where $[\hat{\varepsilon}(\omega)]$ represents the vector signals in the frequency domain and has a dimension n_f that depends on the number of signals.

The reaction forces of the sleeper on the rail can be calculated by the equivalent charges Q_k where $k = 1, 2$ which corresponds to right and left rails. From Eq. (6), we obtain:

$$\begin{bmatrix} \hat{R}_1(\omega) \\ \hat{R}_2(\omega) \end{bmatrix} = \begin{bmatrix} \mathbf{B}_{11}(\omega) & \mathbf{B}_{12}(\omega) \\ \mathbf{B}_{21}(\omega) & \mathbf{B}_{22}(\omega) \end{bmatrix} \begin{bmatrix} Q_1(\omega) \\ Q_2(\omega) \end{bmatrix} \quad (10)$$

where these 4 components \mathbf{B}_{ik} are 4 known constants. The equivalent charges Q_k are calculated on each rail k (see Appendix A) as follows:

$$Q_k(\omega) = \frac{\mathcal{K}(\omega)}{v E_r I_r \left[\left(\frac{\omega}{v} \right)^4 - \lambda_r^4 \right]} \sum_{j=1}^K Q_{kj} e^{-i\omega \frac{D_j}{v}} = [\mathbf{C}(\omega)] \mathbf{Q}_k \quad (11)$$

where $\mathbf{Q}_k = [Q_{kj}]_j$ is a column vector of all moving loads on the rail k . The matrix $[\mathbf{C}(\omega)]$ has dimensions $[n_f \times K]$ with n_f and K represent the length of the vector $[\hat{\varepsilon}(\omega)]$ and the wheel number respectively. Eq. (11) can be rewritten as follows:

$$\begin{bmatrix} Q_1(\omega) \\ Q_2(\omega) \end{bmatrix} = [\mathbf{C}(\omega)] \begin{bmatrix} \mathbf{Q}_1 \\ \mathbf{Q}_2 \end{bmatrix} \quad (12)$$

The combination of Eqs. (9), (10), and (12) allows us to deduce the relation between the sleeper strains and the train loads as follows:

$$[\hat{\varepsilon}(\omega)] = [\mathbf{A}_{i1}(\omega) \quad \mathbf{A}_{i2}(\omega)] \begin{bmatrix} \mathbf{B}_{11}(\omega) & \mathbf{B}_{22}(\omega) \\ \mathbf{B}_{21}(\omega) & \mathbf{B}_{22}(\omega) \end{bmatrix} [\mathbf{C}(\omega)] \begin{bmatrix} \mathbf{Q}_1 \\ \mathbf{Q}_2 \end{bmatrix} \quad (13)$$

And we can also rewritten the Eq. (13) as a linear equation:

$$[\hat{\varepsilon}(\omega)] = [\mathbf{F}_{i1}(\omega) \quad \mathbf{F}_{i2}(\omega)] \begin{bmatrix} \mathbf{Q}_1 \\ \mathbf{Q}_2 \end{bmatrix} = [\mathbf{F}(\omega)] [\mathbf{Q}] \quad (14)$$

Eq. (14) is a linear relation between the sleeper strains and train loads. Hence, we can use function `mldivide`¹ in MATLAB to solve this linear equation.

¹This solver has many methods of factorization to solve a system linear equation which depend on the dimension of the matrices (for example: Cholesky factorization for a matrix symmetric with real, positive diagonal element; Gaussian elimination to reduce the system to a triangular matrix if the matrix is upper Hessenberg etc.). In this case, the matrix $\mathbf{F}(\omega)$ is rectangular, thus method of QR factorization will be used in the `mldivide` solver

3 NUMERICAL APPLICATION

3.1 Verification

The objective of this section is to verify the precision of the inverse problem. By using the analytical signals generated by the analytical model, we apply it on the inverse problem to identify the train loads. The test will be done with the analytical signal and noise signal. The parameters of the railway track is shown in Table 1. These parameters allows us to generate the analytical signals for identifying the train loads.

Content	Unit	Notation	Value
Young's modulus of rail	GPa	E_r	210
Cross-sectional moment inertia of rail	m^4	I_r	3E-05
Rail density	kgm^{-3}	ρ_r	7850
Rail section area	m^2	S_r	7.69E-3
Young's modulus of sleeper	GPa	E_s	48
Cross-sectional moment inertia of sleeper	m^4	I_s	4.32E-4
Density of sleeper	kgm^{-3}	ρ_s	2475
Sleeper section area	m^2	S_s	54.9E-3
Length of sleeper	m	$2L$	2.41
Track gauge	m	$2a$	1.435
Stiffness of ballast	MNm^{-1}	k_f	240
Damping coefficient of ballast	$kNsm^{-1}$	ζ_f	58.8
Stiffness of rail pad	MNm^{-1}	k_{rp}	192
Damping coefficient of rail pad	$MNsm^{-1}$	ζ_{rp}	1.97
Train speed	ms^{-1}	v	50
Pre-stress of sleeper	kN	T	300
Sleeper spacing	m	l	0.6

Table 1: Parameters of the railway track

The charge per wheel on each rail has been generated randomly. Fig. 3 shows the superposition of the charges introduced and identified (blue line and red column respectively) on the left rail (a) and right rail(b). In the two figures, the blue line has the same value as the red columns in this figure because we found the same train loads. The relative error is about $3.7 \times 10^{-4} \%$. We can conclude that the inverse problem is verified with a good precision. The difference is due to small errors introduced during the numerical calculations.

Now, we add a random noise to the sleeper response to simulate the real measurements. Fig. 4 shows the sleeper strain as a red line and the noise signal as a blue line on the left rail (a) and right rail (b) in a time interval which corresponds to the time for the passing of a train. By using the inverse problem, the superposition of the train loads introduced and identified is shown in Fig. 5.

With the noise, the train loads have been found with a small difference. In this figure, the red column and blue line corresponding to trains loads introduced and identified don't have the same value. The table 2 shows the relative error with different levels of noise in the signal.

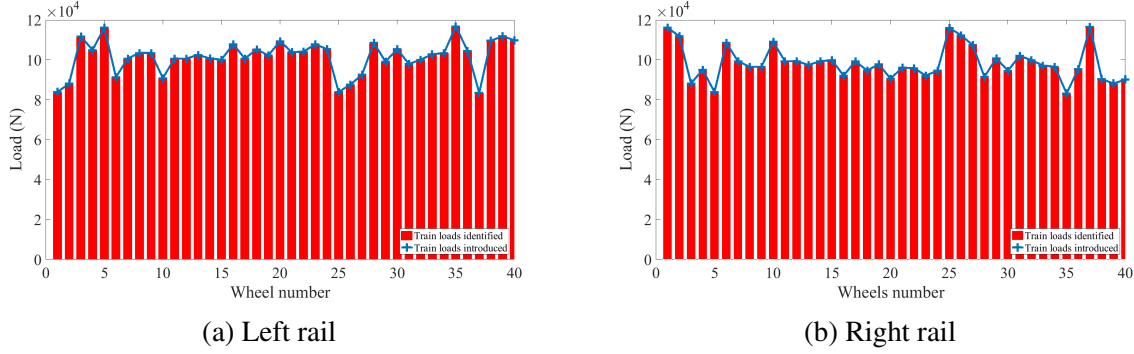


Figure 3: Superposition of the train loads introduced and identified on the left rail (a) and right rail (b)

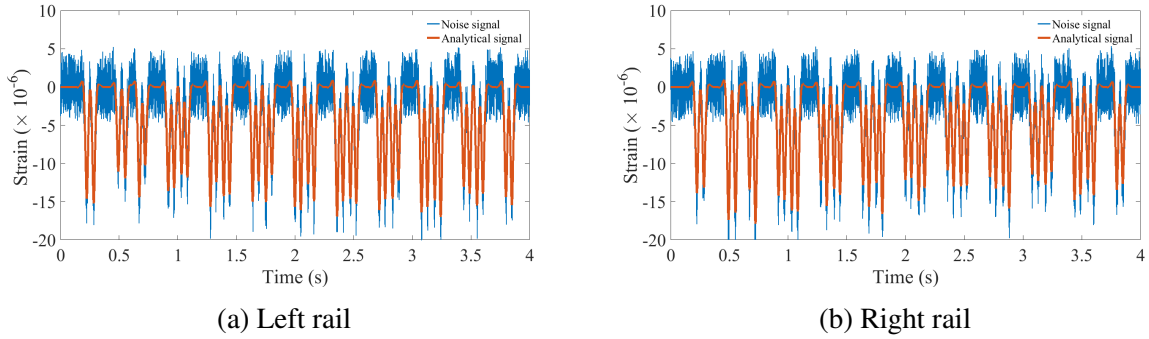


Figure 4: Analytical and noise signals on the left rail (a) and right rail (b)

Amplitude of noise	Left rail	Right rail	Average
Slightly noisy	0.281 %	0.285 %	0.283 %
Noisy	0.585 %	0.597 %	0.592 %
Very noisy	1.186 %	1.159 %	1.172 %
Strongly noisy	2.541 %	2.634 %	2.588 %

Table 2: Relative error between the train loads introduced and identified fore different noise levels

Fig. 4 shows the case of large amount of introduced noise which the relative error is 1.17 %. With the strongly noisy signal, the relative error is about 2.6 %. Thus, we can conclude that the train loads identified have been found with a good precision.

3.2 Real signal

We will use the measurements recorded in-situ with the help of the “Smart Sleeper”. The measurement has been performed at Creil, France, on the 6th of May 2017. Fig. 7 shows the signal recorded by the “Smart Sleeper” during the passing of a train which contains 10 wagons

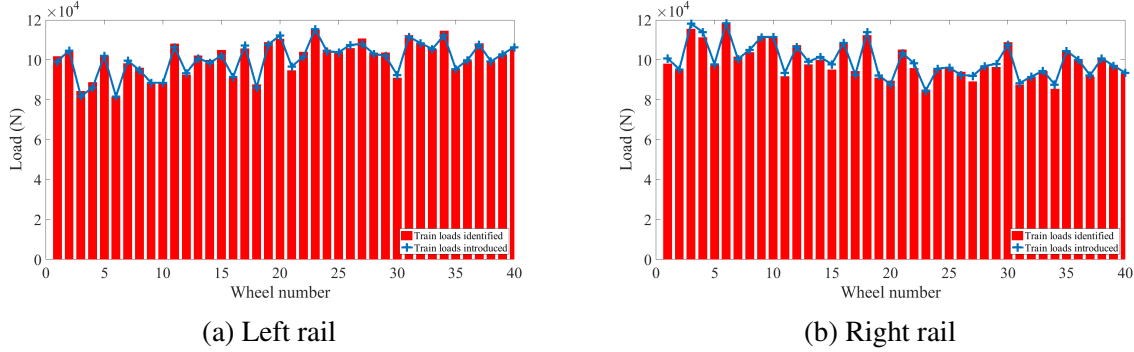


Figure 5: Superposition of the train loads introduced and identified on the left rail (a) and right rail (b)

including the locomotive. The green and red line represent the measurements on the left (a) and right (b) upper sensor respectively. The train loads on the two rails are shown in Fig. 6. The black in Fig. 7 represents the analytical sleeper response by using the identified train loads.

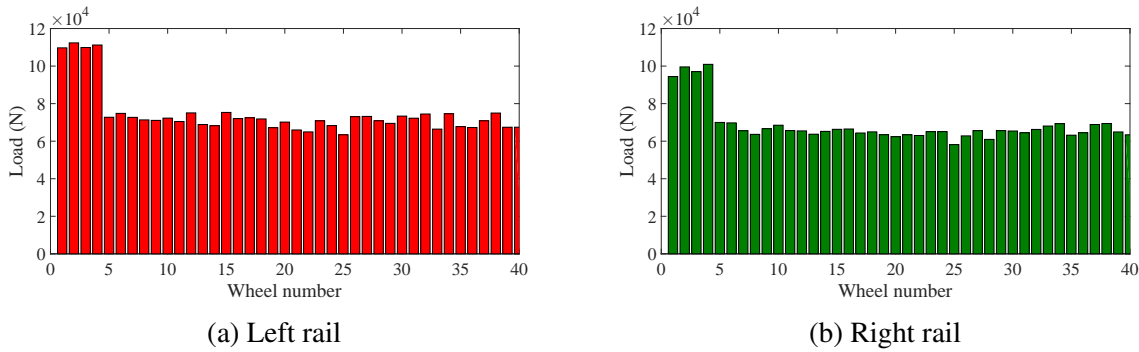


Figure 6: Train loads identified by using the measurements on the left rail (a) and right rail (b)

We note that the value of the first four loads on the two rails are bigger than the rest, corresponding to the locomotive of the train, which is normally heavier than the wagons. In the Fig. 7, the first four peaks are also superior to the rest.

Moreover, we note that the train loads on the two rails are not the same (in Fig 7, the sleeper strains on the left rail are superior to the right rail). By identifying the train loads, this phenomenon is demonstrated by the different charges on the two rails. The charges applied on the left rail are bigger than the right rail. This could be explained by the non-homogenous foundation or by the unbalanced of rolling stock.

4 CONCLUSION

Based on an analytical model of the railway sleeper the inverse problem has been developed to identify the train loads. In the frequency domain, the sleeper strain and the train loads can be linked by a linear relation. The train loads identified from the measurements in-situ demonstrate

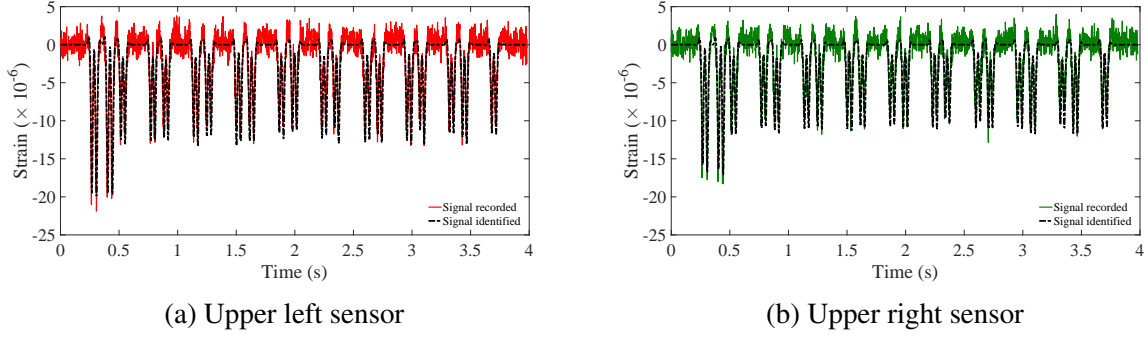


Figure 7: Sleeper response on the left rail (a) and right rail (b)

different values for each wheel of the train. Thus, this technique can detect the imperfection of the wheel-rail contact when the train load on one rail is much higher than the other. In future works, the model should be developed to identify other parameters of the railway track.

Acknowledgement

This work has been developed in the context of a partnership between Sateba (Consolis Group) and Ecole des Ponts ParisTech. The authors would like to thank the personnel of Sateba for their support.

A Periodically supported beam model

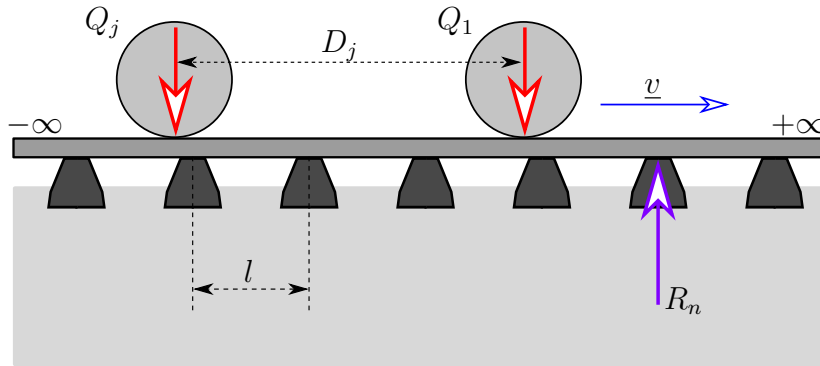


Figure 8

The periodically supported beam is shown in Fig. 8. When the rails are modeled by periodically supported beams [7], the forces R_k on each rail k in the frequency domain can be calculated as follows:

$$\hat{R}_k(\omega) = \mathcal{K}\hat{w}_r^{(k)}(\omega) + Q_k(\omega) \quad (15)$$

where \mathcal{K} is the equivalent stiffness, Q_k are the equivalent charges of the two rails which are determined. Let $w_r^{(k)}$ be the rail k displacements at the sleeper position respectively and $w_s(x, t)$

is the sleeper displacement where $x = \pm a$ corresponds to the positions of the rail seats. The forces \hat{R}_k can be expressed by the constitutive law of the rail pads in the frequency domain as follows:

$$\hat{R}_k(\omega) = -k_p (\hat{w}_r^{(k)}(\omega) - \hat{w}_s(a, \omega)) \quad (16)$$

where $k_p = k_{rp} + i\omega\zeta_{rp}$ is the dynamic stiffness of the rail pad and k_{rp} , ζ_{rp} are the stiffness and damping coefficients of the rail pads. By substituting Eq. (15) into Eq. (16), we obtain:

$$\hat{R}_k(\omega) = \frac{k_p \mathcal{K}}{k_p + \mathcal{K}} \hat{w}_s(a, \omega) + \frac{k_p}{k_p + \mathcal{K}} \mathcal{Q}_k(\omega) \quad (17)$$

B Green's function

By using the Fourier transform and combining equations (1), (2) and (3), this system dynamics equation can be rewritten in the frequency domain :

$$\begin{cases} \hat{w}_s''''(x, \omega) - \frac{T}{E_s I_s} \hat{w}_s''(x, \omega) - \frac{\rho_s S_s \omega^2 - k_b}{E_s I_s} \hat{w}_s(x, \omega) = -\frac{\hat{R}_1}{E_s I_s} \delta(x - a) - \frac{\hat{R}_2}{E_s I_s} \delta(x + a) \\ \hat{w}_s''(-L, \omega) = \hat{w}_s''(L, \omega) = 0 \\ \hat{w}_s'''(-L, \omega) = \hat{w}_s'''(L, \omega) = 0 \end{cases} \quad (18)$$

where (\square') stands for the partial derivative with regard to x and $k_b = k_f + i\omega\zeta_f$ is the foundation dynamic stiffness. The Green's function $G_a(x, \omega)$ of Eq. (18) is defined by :

$$\frac{\partial^4 G_a(x, \omega)}{\partial x^4} - \alpha_s^2 \frac{\partial^2 G_a(x, \omega)}{\partial x^2} - \lambda_s^4 G_a(x, \omega) = \delta(x - a) \quad (19)$$

where $\alpha_s = \sqrt{\frac{T}{E_s I_s}}$ and $\lambda_s = \sqrt[4]{\frac{\rho_s S_s \omega^2 - k_b}{E_s I_s}}$. This is a 4th order linear differential equation and its Green's function [22] can be written as follows:

$$G_a(x, \omega) = \begin{cases} A_1 e^{\lambda_1 x} + A_2 e^{\lambda_2 x} + A_3 e^{\lambda_3 x} + A_4 e^{\lambda_4 x} & \text{for } x \in [-L, a] \\ B_1 e^{\lambda_1 x} + B_2 e^{\lambda_2 x} + B_3 e^{\lambda_3 x} + B_4 e^{\lambda_4 x} & \text{for } x \in [a, L] \end{cases} \quad (20)$$

where A_i , B_i , and λ_i (with $1 \leq i \leq 4$) are parameters to be determined. λ_i is the 4 complex roots of the characteristic equation:

$$\mathcal{P}(\lambda) = \lambda^4 - \alpha_s^2 \lambda^2 - \lambda_s^4 \quad (21)$$

By using the boundary conditions of the free-free beam (continuity condition for displacement, slope and moments, discontinuity of magnitude one at the point force), we can obtain analytical expressions for A_i , B_i .

REFERENCES

- [1] H. F. Lam, Q. Hu and M. T. Wong, The Bayesian methodology for the detection of railway ballast damage under a concrete sleeper, *Engineering Structures* 81 (2005) 289–301.
- [2] A. Remennikov, S. Kaewunruen, Experimental Investigation on dynamic railway sleeper/ballast interaction, *Experimental Mechanics* 46 (1) (2006) 57–66.
- [3] M. Kodai, W. Tsutomu and S. Masamichi, Damage detection method for sleepers based on vibration properties, *EDP Sciences* 24 (2015).
- [4] D.J. Mead, Free wave propagation in periodically supported, infinite beams, *Journal of Sound and Vibration* 11 (2) (1970) 181–197.
- [5] D.J. Mead, Wave propagation in continuous periodic structures: research contributions from Southampton, *Journal of Sound and Vibration* 190 (3) (1996) 495–524.
- [6] X. Sheng, C. Jones and D. Thompson, Responses of infinite periodic structures to moving or stationary harmonic loads, *Journal of Sound and Vibration* 303 (3-5) (2007) 873–894.
- [7] T. Hoang, D. Duhamel, G. Foret, H. Yin, P. Joyez and R. Caby, Calculation of force distribution for a periodically supported beam subjected to moving loads, *Journal of Sound and Vibration* 388 (2017) 327–338.
- [8] H. Ding, L. Q. Chen, S. P. Yang, Convergence of Galerkin truncation for dynamic response of finite beams on nonlinear foundations under a moving load, *Journal of Sound and Vibration* 331 (10) (2012) 2426-2442.
- [9] V. H. Nguyen, D. Duhamel, Finite element procedures for nonlinear structures in moving coordinate. Part 1: Infinite bar under moving axial loads, *Computer & Structures* 84(21) (2006) 1368–1380.
- [10] V. H. Nguyen, D. Duhamel, Finite element procedures for nonlinear structures in moving coordinate. Part 2: Infinite beam under moving harmonic loads, *Computer & Structures* 86(21) 2056–2063.
- [11] L. H. Tran, T. Hoang, D. Duhamel, G. Foret, S. Messad, A. Loaïc, Analytical model of the dynamics of railway sleeper, 6th International Conference on Computational Methods in Structural Dynamics and Earthquake Engineering 2 (2017) 3937–3948.
- [12] M. L. Filograno et al., Real time monitoring of railway traffic using Fiber Bragg Grating sensors, *IEEE Sensors Journal* 12(1) (2012) 85–92.
- [13] C. Wei et al., A Fiber Bragg Grating sensor system for train axle counting, *IEEE Sensors Journal* 12(10) (2010) 1905–1912.
- [14] C. Wei et al., Real-Time train wheel condition monitoring by Fiber Bragg Grating sensors, *International Journal of Distributed Sensor Networks* 10 (2012).

- [15] S. J. Buggy et al., Railway track component condition monitoring using optical fibre Bragg Grating sensors, *Measurements Science and Technology* 27(5) (2016) 1–15.
- [16] H. Y. Tam et al., Utilization of fiber optic Bragg Grating sensing systems for health monitoring in railway applications, *6th International Workshop on Structural Health Monitoring*, Stanford University, Stanford, CA, September 11-13, (2007) 1824.
- [17] R. Pimentel et al., Hybrid Fiber-Optic/Electrical measurement system for characterization of railway traffic and its effects on a short span bridge, *IEEE Sensors Journal* 8(7) (2008) 1243–1249.
- [18] S. L. Ho et al., Real time monitoring of railway traffic using Fiber Bragg Grating sensors, *IEEE Sensors Journal* (2006) 125–129.
- [19] L. Arnaud, P. Charles, Smart Sleeper : Measurement of bending moments in concrete sleepers laid on ballast tracks, *Transport Research Arena (TRA) 5th Conference: Transport Solutions from Research to Deployment*, (2014).
- [20] G. Kumaran, D. Menon and K. Krishnan Nair, Dynamic studies of railtrack sleepers in a track structure system, *Journal of Sound and Vibration*, 268(3) (2003) 485–501
- [21] A. A. Arab, S. S. Badie and M. T. Manzari, A methodological approach for finite element modeling of pretensioned concrete members at the release of pretensioning, *Engineering Structures*, 33(6) (2011) 1918–1929
- [22] E. Zauderer, *Partial differential equations of applied mathematics*, John Wiley Sons (1989).

An Engineering-oriented Simplified Methodology for Analysing Non-linear Behavior of Reinforced Concrete Structures

Nhu Cuong Tran*

*EDF R&D;

ABSTRACT

Modelling the non-linear behavior of damaged concrete structure is always a complex challenge for civil engineer. On one hand, application of non-linear damage models developed in the litterature for civil engineering structures is still difficult because of their complexity and their limited capacity. On the other hand, the elastic modelling approach used by many engineering services can overestimate stress inside structure especially in the case of displacement loading. In this work, we present a new structural modelling approach which is able to take into account the damage level of concrete without applying non-linear damage models. This approach is particularly suitable to the structures which mainly work in bending mode as beam or shell. The philosophy here is to do some iterative computations. The computation at current step uses a reduced Young modulu of damaged concrete which is determined as a function of strain computed in the previous step. The results obtained after three iterative computations using this approach are compared with the ones obtained in a real non-linear damage modelling. The difference between them which is lower than 10% is considered good for a civil engineering application. This simple, rapide and performant computation approach could be an alternative method to integrate into commercial software for engineering applications.

Simple Numerical Model for a Pipe-Lay on Uneven Seabed

Pavel Trapper*

*Ben-Gurion University of the Negev

ABSTRACT

Submarine pipeline installation process involves the pipe being laid from a barge into the water all the way to the bottom where it comes into contact with a seabed. The possible unevenness of the seabed, such as inclined plane, pits and hills may substantially affect pipeline configuration and lead to severe stress concentrations. In order to perform a proper design of the pipeline, one has to account for the pipe-seabed interaction. In the present study, a simple numerical model to analyze static pipeline configurations during the pipe-lay process on uneven seabed is presented. The technique also accounts for nonlinear stiffness of soil, and other environmental loading such as drag forces applied by the sea water. The solution technique is based on a finite difference discretization of nonlinear beam equation, which accounts for large deformations of the pipe. The whole pipeline is treated as single continuous segment. The solution is carried out in an incremental/iterative way, where the pipe is being gradually released from the barge into the water and laid on a seabed. During this process, pipe nodes are laid down and, one by one, come into a contact with the seabed. Active set of nodes beyond the touchdown point is updated iteratively, allowing for the separation due to irreversible plastic deformation of the seabed and emerging free spans. To demonstrate the method, several pipe-lay scenarios with different seabed topographies are presented. It is shown how on-bottom unevenness, including pits and hills, can affect pipeline configuration, formation of free spans, tension forces, shear forces, bending moments within the pipe, and its embedment into the seabed. The role of a top tension force applied by the laying barge is emphasized. The approach presents simple and computationally efficient way to analyze the pipe-lay on a seabed with complex geometry and nonlinear stiffness. The proposed model, contrary to time-consuming commercial packages, allows for performing the analysis in reasonable time on standard engineering computers.

A New Family of Hybrid Particle-mesh Methods for Conservation Laws

Nathaniel Trask^{*}, Pavel Bochev^{**}, Mauro Perego^{***}

^{*}Sandia National Laboratories, ^{**}Sandia National Laboratories, ^{***}Sandia National Laboratories

ABSTRACT

A key challenge in the practical application of traditional mesh-based methods is the dependence of the approximation upon the quality of an underlying mesh. This poses a bottleneck for engineering workflows, in which time to solution may be dominated by mesh-generation in preprocessing. Meshfree discretizations, on the other hand, possess a rich approximation theory that is by definition independent of any underlying mesh. Though accurate, pure meshfree schemes face their own challenges in developing notions of either discrete conservation or a stability theory; both properties taken for granted in mesh-based methods. In this talk, we present recent work using generalized moving least squares (GMLS) to address these issues and obtain the favorable properties of both worlds. By incorporating both meshfree approximation and an underlying mesh, we develop a family of hybrid particle/mesh schemes that may either be used in an Eulerian setting to enhance the accuracy and robustness of classical finite volume methods, or may be used in a Lagrangian setting to develop particle discretizations with notions of conservation and consistency.

Aeroelastic Analysis of an Inverted Wing Operating in Ground Effect Using Fluid-Structure Interaction

Ian Travell*, Rishi Abhyankar**

*Cranfield University / Multimatic Inc., **Cranfield University

ABSTRACT

A fluid-structure interaction model with strong coupling was developed for an inverted swept wing operating in ground effect. This model offered an improvement over traditional CFD models due to its ability to capture aeroelastic effects and provided the ability to investigate aeroelastic tailoring. A structural finite element model was used to determine a composite laminate structures for a simplified Formula 1 wing such that it would be sufficiently stiff to pass FIA rules mandated stiffness criteria. A 2D fluid model was used to validate the CFD solution using published experimental data for a Tyrrell 026 front wing aerofoil. The lift coefficient calculated in CFD correlated to experimental data to within 3 %. The fluid and structural models were then combined into a FSI model with strong two-way coupling. Causes of numerical instabilities from combining the two models were identified, discussed, addressed. Steady state solutions were attained for both a CFD model and a FSI model using the same 3D wing geometry, with the FSI model predicting an additional 2.19 % downforce over the CFD case. Aeroelastic tailoring was investigated by varying the laminate ply orientations and thicknesses and by changing the core material construction. A novel laminate structure was employed to couple the wing bending and torsion modes together. This resulted in the wing angle decreasing under fluid loading and provided a modest reduction in drag. A similar drag reduction effect was achieved by reducing the laminate thickness at the trailing edge to decrease the effective aerofoil camber when subjected to fluid loading. The laminate thickness at the leading edge was increased to maintain spanwise bending stiffness.

The Utility of Rapid Prototyping and 3D Virtual Modeling in Procedural Planning and Surgical Simulation for Congenital Heart Disease

Hannah Tredway*, Puneet Bhatla**, Michael Argilla***, Ralph Mosca****

*NYU School of Medicine, **Division of Pediatric Cardiology, Department of Radiology, NYU Langone Medical Center, ***Division of Pediatric Cardiology, NYU Langone Medical Center, ****Department of Cardiac Surgery, NYU Langone Medical Center

ABSTRACT

Background: Accurate characterization of cardiac anatomy is critical for the understanding and management of congenital heart disease (CHD). While traditional imaging methods allow for visualization of cardiac structures and depiction of morphologic defects, adequate understanding of the spatial relationships and complex cardiac connections remains a challenge. Rapid prototyping and three-dimensional (3D) models are gaining utility in the understanding and management of complex CHD as they allow for detailed portrayal of cardiac anatomy and visualization from multiple viewpoints. Here, we discuss our experience in creating patient-specific models and their utility in procedural simulation and planning. Methods: For each case, a virtual or physical 3D model was generated using computed tomography source data imported into an image post-processing workstation. Commercially available software was used to segment the blood pool and build a patient-specific heart replica. The models were cropped to highlight the anatomy of interest from various planes. When indicated, flexible models were printed using a polyjet printer. Cases: First, is an 11-month-old with numerous cardiac anomalies including multiple large muscular ventricular septal defects (VSD's). Following several failed attempts at closure with operative and interventional techniques, a virtual 3D model was requested to better characterize the complex interventricular communications. The model demonstrated a large residual VSD located adjacent to the initial closure device and another that was restricted by prominent muscular trabeculations. This depiction illuminated the potential challenge of traversing the in situ device with a catheter, allowing the interventionalist to elicit an optimal approach for device closure. The model also guided the echocardiographer in obtaining appropriate imaging angles to detect the success of the procedure. Next, is a 12-month-old with total anomalous pulmonary venous return that was surgically corrected via an anastomosis between the pulmonary veins and the right atrium. After one year, the patient presented in heart failure with significant left to right shunting across the residual interatrial communication. A model was requested to better elucidate the intracardiac anomalies. This physical model allowed the surgeon to manipulate the structures and elicit the feasibility of placing a baffle between the pulmonary veins and the left atrium, thereby redirecting blood flow and reducing intracardiac shunting. Conclusion: Virtual and printed 3D cardiac models can be invaluable in depicting the anatomy and complex spatial relationships of CHD. These models provide the means to visualize and manipulate the anatomy in any desired plane and thereby play a crucial role in guiding surgical and interventional strategies.

Flow Simulation in Heterogeneous Porous Media with the Moving Least-Squares Method

Dimitar Trenev^{*}, Laurent White^{**}, Rohan Panchadhara^{***}

^{*}ExxonMobil Research & Engineering, ^{**}ExxonMobil Research & Engineering, ^{***}ExxonMobil Research & Engineering

ABSTRACT

For historical reasons, as well as its speed of execution and simplicity, the two-point-flux finite-volume method is still the preferred technique for discretizing Darcy's law in most commercial reservoir simulators today. It is well known, however, that this method suffers from inaccuracies when applied to grids that are not K-orthogonal, which tends to occur more frequently as reservoir engineers rely on increasingly complex reservoir models. As reservoir simulations are used to guide the decisions during the development planning and production optimization of oil and gas fields, it is important to develop improved numerical methods for a more accurate and reliable prediction of the flow streams. In this talk, we present some novel enhancements of the moving least-squares method designed to specifically handle discontinuous and anisotropic permeability fields. This approach is an attractive alternative to the traditional discretization scheme based on the two-point-flux approximation for Darcy's law and a first-order finite-volume scheme for transport for two main reasons. First, the proposed cell-centered reconstruction scheme does not directly rely on mesh topology or whether the mesh is K-orthogonal. Second, increasing the number of neighboring points involved in the reconstruction results in a higher-order approximation of sharp flow fronts, offering an increased resolution when compared to the first-order approximation. We will present a set of numerical results – from solving Poisson's equation with discontinuous tensors on a non-K-orthogonal mesh, to a complete oil-water flow simulation in a complex, anisotropic reservoir – in support of these claims.

ON CONTROLLING, MONITORING AND HARVESTING ENERGY FROM STRUCTURAL VIBRATION USING NETWORKS OF DISTRIBUTED PIEZOELECTRIC PATCHES

M.A. TRINDADE, J.Q. VELÁSQUEZ, A.H. SHIGUEOKA,
H.J. CRUZ NETO, F.M. HORIY

Department of Mechanical Engineering,
São Carlos School of Engineering, University of São Paulo,
São Carlos, SP 13566-590, Brazil,
trindade@sc.usp.br, <http://www.eesc.usp.br/labdin>

Keywords: Vibration control, Piezoelectric materials, Sensors networks, Spatial modal filters.

Abstract. Piezoelectric materials are widely employed as thin layers or patches bonded on thin flexible structures forming multilayer composite structures, which may be used in automotive, aeronautical, aerospace, microelectronics and micromechanics applications, for sensing, vibration control, structural health monitoring, energy harvesting, among others. The search for performance improvement of these piezoelectric patches involves the optimization of the electromechanical coupling between piezoelectric patches and structural vibration modes. For that, there are several important aspects to account for, including the bonding effectiveness between patches and host structure, the location of each patch alone and the relative distribution of the patches. This work presents some recent advances on the optimization of networks of piezoelectric patches for applications in active structural vibration control and energy harvesting from structural vibrations.

1 INTRODUCTION

Piezoelectric materials are widely employed as thin layers or patches adhesively bonded on thin flexible structures forming multilayer composite structures, which may be used in automotive, aeronautical, aerospace or even microelectronics and micromechanics applications, for sensing, vibration control, structural health monitoring, energy harvesting, among others [1, 2, 3].

In vibration control applications, the piezoelectric patches may be used as sensors and/or actuators that enable the development of passive, active, semi-passive or active-passive vibration control solutions [1]. The performance and interest of active solutions are always limited by relatively weak actuation power of piezoelectric patches and cumbersome power electronics. One advantage of active-passive solutions is that they may combine the adaptivity of active control with the robustness of passive control. This could be achieved using an optimized combination of viscoelastic treatments for passive damping and piezoelectric actuators for active control [4, 5]. To

tackle the issue of required power for active control, some authors considered the use of resonant shunt circuits in series with the voltage source to improve the control authority [6, 7, 8, 9].

In this case, the advantage of a network of piezoelectric patches is that it allows targeting either a selected small number of vibration modes or even a specific single one. Thus, some authors proposed the use of adaptive/reconfigurable arrays or networks of sensors and actuators with the main objective of minimizing the power spilled to control non-interesting dynamics. Most methodologies proposed in these studies are based on the concept of modal, semi-modal or quasi-modal control using, for instance, spatial modal filters [10, 11, 12, 13, 14, 15]. These are particularly interesting for the attenuation of specific low-frequency vibration or sound radiation modes. In this case, the signals of the sensors in a network are combined to approximate the response of a selected mode-equivalent system, in which the contribution of undesired modes is excluded. By doing this, a feedback of such combined (or filtered) signal could lead to a focus of the control effort on the modes of interest and also would not affect the undesired modes.

Another way of profiting from a network of sensors for a focused active control is by considering a methodology so-called incomplete state feedback (ISF), also known as partial state feedback or optimal output feedback, as proposed by [16]. Its main advantage is to start from well-known LQR optimal control which provides good frequency properties, such as gain and phase margins. Instead of using a state observer, which increases system complexity, real-time computational effort and time delays, this technique considers only measured outputs for feedback. However, unlike LQR, the performance of ISF is dependent on system initial conditions. Therefore, some technique must be considered to guarantee robustness of the control performance for realistic unknown initial conditions [16, 17]. It is also important to consider the output matrix design, which includes the number, type and position of sensors. In analogy to the LQR control problem, a quadratic cost function may also be used to optimize ISF sensors locations [18, 17].

Presented results show that the active vibration control performance can be substantially increased with the use of such strategies. In addition, the adaptivity of solution is preserved in the sense that it can be modified in real time according to the operation and/or performance criteria.

In structural health monitoring (SHM) applications, networks of piezoelectric patches working as sensors may be used to detect damage by means of changes in the structural response signature [2]. This typically includes permanent mounted or embedded elements for sensing or data acquisition, signal processing and wireless communication [19]. Fortunately, piezoelectric materials high electromechanical coupling characteristic allows their use as sensor but also for micro power generation or energy harvesting [3]. In energy harvesting applications, networks of piezoelectric patches working in sensor mode connected to a harvester electric circuit are bonded onto flexible structures subjected to a vibration source, such that the vibration energy may be converted into usable electric energy. However, to improve the performance of piezoelectric energy harvesting of a sensors network, it is required to increase the electromechanical coupling between host structure and piezoelectric patches. For that, there are several important aspects to account for, including the bonding effectiveness between each patch and host structure, the location of each patch alone and the relative distribution of the patches. Besides, these important properties to be optimized may also be subjected to uncertainties [20, 21]. In this case, the advantage of a network of sensors is to facilitate localization of potential damages and also it may improve the amount of harvested energy with little added complexity. Therefore, once again, the use of a properly designed network of sensors may improve the overall multifunctional performance of system.

This work presents some recent results on the design of networks of sensors aiming at improving

active vibration control and energy harvesting performances based on a plate type host structure.

2 ACTIVE VIBRATION CONTROL USING PIEZOELECTRIC NETWORKS AND DISCRETE MODAL FILTERS

In this section, some results on the active vibration control of a plate type structure using a network of piezoelectric sensors and actuators are presented. The general design criteria is to allow using the very simple and practical direct output feedback control law. In the present study, for a given network of piezoelectric sensors and actuators bonded onto the host structure, three strategies to evaluate the optimal output feedback control gains are considered: i) using the network as a spatial modal filter to obtain an equivalent modal sensor which signal can be fed back as control voltage applied to piezoelectric actuators; ii) using a genetic algorithm optimization to evaluate control gains for each piezoelectric sensor output; and iii) using incomplete state feedback technique to evaluate control gains for each piezoelectric sensor output.

2.1 Problem description

An aluminum plate with dimensions $545 \times 400 \times 3$ mm, density of 2700 kg/m^3 , Young module of 69 GPa, Poisson's ratio 0.33, and clamped at all edges is considered as the host structure. 20 piezoelectric patches with dimensions $24 \times 25 \times 0.5$ mm and made of piezoceramic PZT5H are distributed over the host structure, such that a regular network of four by four sensors and another of two by two actuators are considered as shown in Figure 1. The finite element mesh together with the positions of sensors and actuators and input and output locations considered for the simulations are shown in Figure 2. The mobility of the first input/output (In1/Out1) will be considered for performance evaluation.

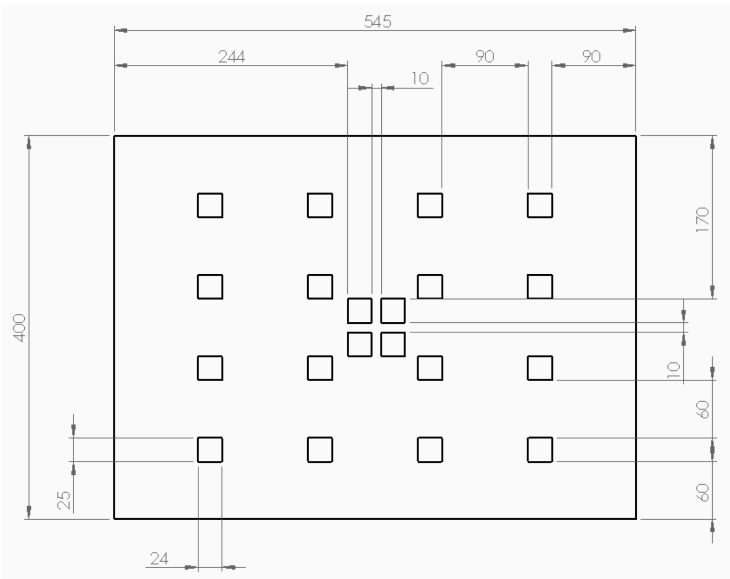


Figure 1: Regular network of piezoelectric patches, four by four sensors and four actuators in the center, 24×25 mm, bonded onto a clamped aluminum plate, $545 \times 400 \times 3$ mm.

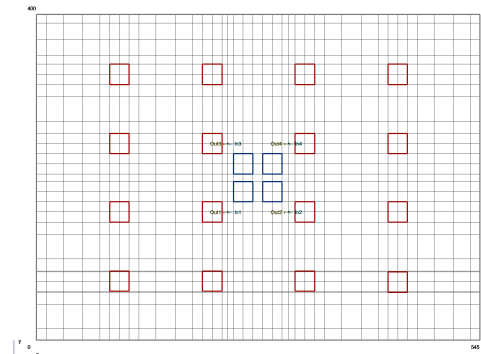


Figure 2: Finite element mesh, sensors/actuators positions and input/output locations.

Starting from a finite element model for the structure with piezoelectric patches with mechanical displacements and electric charges at patches as degrees of freedom, it is possible to write

electromechanical coupled equations of motion. A reduced-order model is then obtained, by projecting onto a reduced undamped modal basis, where the first m vibration modes are retained. This leads to the following equations of motion written in terms of modal coordinates, voltages induced in sensors and voltages applied to actuators,

$$\ddot{\boldsymbol{\eta}} + \Lambda \dot{\boldsymbol{\eta}} + \Omega^2 \boldsymbol{\eta} = \Phi^T \mathbf{f}(t) + \Phi^T \mathbf{K}_{uva} V_a \quad (1)$$

$$\mathbf{V}_s = -\mathbf{K}_{uqs}^T \Phi \boldsymbol{\eta}, \quad (2)$$

where Λ is a matrix of modal damping; Ω^2 is a diagonal matrix whose elements are the square of the natural frequencies; Φ is a matrix whose columns are the eigenvectors associated to the m first vibration modes normalized such that $\Phi^T \mathbf{M} \Phi = \mathbf{I}$, where \mathbf{I} is the identity matrix. The vector $\boldsymbol{\eta}$ is obtained from the transformation $\mathbf{u} = \Phi \boldsymbol{\eta}$. By defining the state vector as $\mathbf{z} = [\boldsymbol{\eta} \quad \dot{\boldsymbol{\eta}}]^T$, it is possible to rewrite the system equations as

$$\dot{\mathbf{z}} = \mathbf{A} \mathbf{z} + \mathbf{B}_f \mathbf{f} + \mathbf{B}_a V_a, \quad (3)$$

$$y = \dot{u}_p = \mathbf{C}_y \mathbf{z}, \quad \mathbf{C}_y = [\mathbf{0} \quad \mathbf{C}_u \Phi], \quad (4)$$

$$\dot{\mathbf{V}}_s = \mathbf{C} \mathbf{z}, \quad \mathbf{C} = [\mathbf{0} \quad \mathbf{K}_{uqs}^T \Phi], \quad (5)$$

The output of the modal filter is, according to its definition,

$$V_f = \boldsymbol{\alpha}^T \mathbf{V}_s. \quad (6)$$

The control law of the form

$$V_a(t) = -K_f \dot{V}_f = -\mathbf{K} \dot{\mathbf{V}}_s = -\mathbf{K}_z \mathbf{z}, \quad \text{with } \mathbf{K} = K_f \boldsymbol{\alpha}^T, \quad \mathbf{K}_z = \mathbf{K} \mathbf{C}. \quad (7)$$

Thus, the control law can be either seen as the direct feedback of a single output \dot{V}_f with control gain K_f or as the direct feedback of multiple outputs $\dot{\mathbf{V}}_s$ with control gains \mathbf{K} . One way or another, given \mathbf{K} it is possible to factor out K_f to obtain a vector $\boldsymbol{\alpha}$ that establishes the relative gain distribution for each sensor.

By using Eqs. (3), (5), (6) and (7), it is possible to arrive at the state-space formulation of the closed-loop system. Then, by taking its Laplace Transform and isolating \mathbf{z} , the closed-loop displacement velocity measured at a given point and the control effort may then be calculated by combining to Eqs. (4), (5) and (7), resulting in

$$y(s) = \mathbf{C}_y (\mathbf{I}s - \mathbf{A} + K_f \mathbf{B}_a \boldsymbol{\alpha}^T \mathbf{C})^{-1} \mathbf{B}_f f(s) = H_{yf}(s) f(s) \quad (8)$$

$$V_a(s) = -K_f \boldsymbol{\alpha}^T \mathbf{C} (\mathbf{I}s - \mathbf{A} + K_f \mathbf{B}_a \boldsymbol{\alpha}^T \mathbf{C})^{-1} \mathbf{B}_f f(s) = H_{vaf}(s) f(s). \quad (9)$$

Thus the FRF with force input $f(\omega)$ and displacement velocity output $y(\omega)$, hereinafter denominated H_{yf} , may be found by evaluating Eq. (8) after applying the transformation $s = i\omega$ over the desired frequency range. Likewise, the FRF of the force input $f(s)$ and control effort output $V_a(s)$, henceforth denominated H_{vaf} , may be found after following the same procedure with Eq. (9).

2.2 Control design

2.2.1 Design of control gains based on spatial modal filters (LSQ)

The first method for designing the feedback control is based on the concept of spatial modal filters. It consists on first determining the optimal weighting coefficients $\boldsymbol{\alpha}$ based on the FRF of

each sensor in the network and the natural frequencies of the target vibration modes. Hence, the resulting filtered response (weighted sum of sensors outputs) can be designed to approximate a desired FRF. For instance, a desired FRF may be defined as the response of an equivalent system of one degree of freedom with natural frequency ω_j and damping factor ξ_j such that

$$g_j(\omega) = \frac{2\xi_j\omega_j^2}{\omega_j^2 - \omega^2 + 2i\xi_j\omega_j\omega} \quad (10)$$

Considering \mathbf{Y} as the discretized FRF matrix, with one column for each sensor in the network and one row for each frequency $\omega \in [\omega_1, \dots, \omega_m]$ and \mathbf{G}_j as the discretized target FRF, with one row for each frequency ω according to $g_j(\omega)$, one then searches for a vector of coefficients α_j such that

$$\mathbf{Y}\alpha_j = \mathbf{G}_j. \quad (11)$$

According to [14], the linear system defined by Eq. (11) in general admits only approximate solutions, which will be denoted α_j^* . The vector of weighting coefficients α_j^* represents the best solution, in the least-squares sense, for the design of a modal filter which isolates the j -th vibration mode response. The approximation of Eq. (11) can be obtained by traditional Moore-Penrose pseudo-inverse. Since \mathbf{Y} may be decomposed through QR decomposition, where \mathbf{Q}_Y is an orthonormal matrix and \mathbf{R}_Y is upper triangular, such that $\mathbf{Y} = \mathbf{Q}_Y\mathbf{R}_Y$, α_j^* can be written as

$$\alpha_j^* = \mathbf{R}_Y^{-1}\mathbf{Q}_Y^H\mathbf{G}_j \quad (12)$$

Alternatively, one may design a multi-modal target FRF by combining different mono-modal ones, such as $\mathbf{G}_c = \sum_j w_j \mathbf{G}_j$. w_j may be defined depending on the relative importance of each vibration mode to the feedback control performance criteria. The QR decomposition method was one of the methods employed in this work being convenient for the cases in which the FRF matrix has had full column rank. Besides, it can be shown that the pseudo-inverse method provides the least squares solution. Therefore, from now on, this method for evaluating the weighting coefficients will be denoted LSQ.

This technique may be effective for a given frequency range. However, [12] stated that the number of sensors required in the network should be at least the number of modes present in the frequency band of interest. Then, [14], have shown that is possible to decrease the number of required sensors by optimizing their locations. In any case, however, for practical applications in which the modal filter is not perfect, some further digital filtering could be required [15].

Then, with weighting coefficients α defined, the output feedback control gain K_f is evaluated using an dichotomy search algorithm so as to minimize the following cost function

$$J = \begin{cases} \sum_j W_j |H_{yf}(\omega_{r,j})|, & \text{if } \xi_j > 0.25\% \text{ and } \max_{\omega_{r,j}} |H_{vaf}(\omega_{r,j})| \leq 200 \text{ V/N} \\ 10^6, & \text{otherwise} \end{cases} \quad (13)$$

where W_j are weighting coefficients and $\omega_{r,j}$ is the resonance frequency of the j -th vibration mode. Thus J is a weighted sum of all the peaks of the FRF H_{yf} provided all modal damping are above a given threshold (0.25%) and control voltage is below a stipulated limit (200 V/N). In practice, the control gain K_f is increased until either modal damping or control effort (or both) criteria is violated. If at least one is violated, a high value is set to the cost function to penalize the solution.

2.2.2 Design of control gains using Genetic Algorithm (GA)

Another strategy is to search for sensors signal weights that optimize the closed-loop response according to a given cost function [22]. Using this approach, the corresponding combined signal may not be related to that of a modal filter but its response is such that when fed back through the control actuators, the closed-loop response is improved. This is done through a direct search using genetic algorithm, which is an evolutive computation method based on a population that undergoes successive applications of mainly two operations, crossover and mutation, that will search the best individual. Each individual in a population is an instance of the design parameters. In the present case, one individual is a set of weighting coefficients α , whose probability of survival in the population depends on how well it scores with the objective function. For each individual, the control gain K_f is calculated according to the procedure described in the previous section. The fitness of each individual is then set to the performance index J used to find the optimal K_f .

2.2.3 Design of control gains using optimal output feedback (ISF)

The third method for evaluating the control gains is based on a technique put forward by Levine and Athans [16] that consists on solving an optimization problem considering a quadratic performance criterion, similar to LQR method, but for which the control input is proportional to a vector of outputs, unlike LQR for which the control input is proportional to the full state vector.

Considering the state space system defined in (3), (4) and (5), the control gain vector $\mathbf{K} = K_f \alpha^T$ is to be determined in order to minimize the following cost function

$$J = \int_0^{\infty} (\mathbf{z}^T \mathbf{Q} \mathbf{z} + R V_a^2) dt, \quad (14)$$

that represents a trade-off between control effort and performance. Considering that the system is stabilizable, it is possible to rewrite this function in the form

$$J = \text{tr} \{ \mathbf{P} \mathbf{Z} \} + \text{tr} \{ \mathbf{S} (\mathbf{A}_c^T \mathbf{P} + \mathbf{P} \mathbf{A}_c + \mathbf{Q} + \mathbf{K}^T \mathbf{R} \mathbf{K}) \} \quad (15)$$

in which \mathbf{Z} is a matrix given by the product $\mathbf{z}(0) \mathbf{z}^T(0)$, $\mathbf{S} \in \mathbb{R}^{2n \times 2n}$ is a symmetric matrix of Lagrange multipliers and \mathbf{A}_c is the closed loop matrix ($\mathbf{A}_c = \mathbf{A} - \mathbf{B}_a \mathbf{K} \mathbf{C}$). The first order necessary conditions for optimality are given by the partial derivatives of J with respect to the independent variables

$$\frac{\partial J}{\partial \mathbf{S}} = \mathbf{A}_c^T \mathbf{P} + \mathbf{P} \mathbf{A}_c + \mathbf{Q} + \mathbf{C}^T \mathbf{K}^T \mathbf{R} \mathbf{K} \mathbf{C} = 0, \quad (16)$$

$$\frac{\partial J}{\partial \mathbf{P}} = \mathbf{A}_c \mathbf{S} + \mathbf{S} \mathbf{A}_c^T + \mathbf{X} = 0, \quad (17)$$

$$\frac{1}{2} \frac{\partial J}{\partial \mathbf{K}} = \mathbf{R} \mathbf{K} \mathbf{C} \mathbf{S} \mathbf{C}^T - \mathbf{B}_a^T \mathbf{P} \mathbf{S} \mathbf{C}^T = 0. \quad (18)$$

Equations (16), (17) and (18) are the necessary conditions given by [16]. Differently from the case of full state feedback, it is not possible to manipulate these equations in order to obtain one equation in function of a single variable, which means that they must be solved simultaneously. With this purpose, two algorithms are proposed to obtain a solution. In the first one, it is used a least squares method with the Levenberg-Marquardt algorithm. Like the algorithms proposed for

the problem of optimal output feedback, only (18) is used in the least squares method, so that in the i -th iteration, given the value of K_i , (16) and (17) are solved for P_i and S_i using an algorithm to solve Sylvester equations.

The existence of an optimal output feedback control is related to the existence of a static output feedback that stabilizes the system. This investigation about stability can be done using control Lyapunov functions, which allows to determine not only which control law stabilizes flexible structures, but also an optimal control law. It can be shown [17] that, for a structure with low damping, a cost function given by the velocity squared of one of its points plus the control squared is minimized by the collocated control with negative velocity feedback of the same point. Another interesting aspect of this result is that it is a solution of the LQR problem with only one sensor.

One important issue of the methodology proposed is the dependence of the cost function and the optimal solution on system initial conditions. The method proposed here to overcome this difficulty is based on a robust formulation, which consists in optimizing the cost function for the worst case of the uncertainty. To present the methodology, the cost function is first rewritten using the fact that for every control gain \mathbf{K} that makes the closed loop system stable, the second term of the cost function vanishes, such that

$$J = \text{tr}\{\mathbf{P}\mathbf{Z}\}, \quad (19)$$

then, it is possible to specify a set that may represent well the possible system initial conditions, in which \mathbf{z}_0 is a central value, such that the initial condition belongs to a box of dimension $2n$ centered at \mathbf{z}_0 with width Δ . Thus, the cost function for the worst case (\bar{J}) is

$$\bar{J} = \text{tr}\{\mathbf{P}(\mathbf{z}_0\mathbf{z}_0^T + \mathbf{z}_0\Delta^T + \Delta\mathbf{z}_0^T + \Delta\Delta^T)\}. \quad (20)$$

2.3 Comparison between the optimum from LSQ, GA and ISF

First, a modal analysis of the plate was performed to determine the vibration modes that could contribute the most to acoustic radiation and evaluate their natural frequencies and electric potential induced in the patches. Based on this analysis, the first, fourth and eighth vibration modes were selected as target for the active vibration control. Then, an assessment of the closed-loop performance when considering the three control design strategies presented in the previous section (LSQ, GA and ISF) is performed.

For LSQ, a target FRF is defined as $\mathbf{G}_c = \sum_j w_j \mathbf{G}_j$, with $w_j = 1$ for $j = 1, 4, 8$ and $w_j = 0$ for all other modes. Then, the control gain K_f is evaluated according to the cost function J , with $W_j = 1$ for $j = 1, 4, 8$, $W_j = 0.1$ for $j = 2, 3, 5, 6, 7, 9, 10$ and $W_j = 0.01$ for $j > 10$. The same cost function is used for GA strategy, where both weighing coefficients and control gain are evaluated simultaneously. For ISF, matrix \mathbf{Q} is defined based on the total energy of the system, $\mathbf{Q} = \text{diag}(\omega_1^2, \dots, \omega_N^2, 1 \dots, 1)$, and effort weighting is defined by trial and error to guarantee a maximum of 200 V/N in the actuators, such that $R = 10^{-8}$. In all cases, the frequency range considered for control design is [0, 1500] Hz. These parameters lead to the control gains and weighting coefficients shown in Table 1.

Figure 3 shows the closed-loop mobility using LSQ, GA and ISF strategies. Also, as reference, the open-loop mobility is also shown. It is noticeable that all strategies allow to reduce the peak amplitudes of the target modes (1, 4 and 8). However, LSQ performance is much smaller than GA and ISF ones. The amplitude reductions for the first, fourth and eighth modes are, respectively, 4, 4 and 0.5 dB for LSQ, 30, 23 and 8 dB for GA, and 31, 19 and 10 dB for ISF. The largest amplitude amplification is 3 dB for LSQ, 0.7 dB for GA, and 0.9 dB for ISF, within the design

Table 1: Control gains obtained with LSQ, GA and ISF strategies.

Sensor	K_f V/(V/s)	1	2	3	4	5	6	7	8
		9	10	11	12	13	14	15	16
LSQ	0.0064	-0.8631	-0.5785	0.6065	1.0000	0.1944	0.2146	0.1166	-0.0271
		0.5428	0.4526	-0.2706	-0.4946	-0.4883	-0.0748	0.2504	0.5630
GA	0.0418	-0.1081	-0.1127	-0.0844	0.1416	0.2727	1.0000	0.7536	0.3876
		0.1163	0.8014	0.7584	0.2967	-0.1715	-0.0756	-0.1199	-0.0104
ISF	0.0413	0.1184	0.3269	0.3559	0.1584	0.3414	0.9492	0.9274	0.4286
		0.3705	1.0000	0.9685	0.4383	0.1596	0.3971	0.4237	0.1852

frequency range. The closed-loop modal damping factors for the first, fourth and eighth modes are, respectively, 0.8, 0.8 and 0.8% for LSQ, 15, 4 and 56% for GA, and 18, 5 and 8% for ISF.

Figure 4 shows the voltage control response for the LSQ, GA and ISF strategies in order to obtain the closed-loop performance shown in Figure 3. It is noticeable that the control effort frequency spectrum is quite different for the three strategies. Indeed, the resonance peak that limits the control effort and, thus, the closed-loop performance corresponds to the 9th, 3rd and 7th modes for LSQ, GA and ISF strategies, respectively.

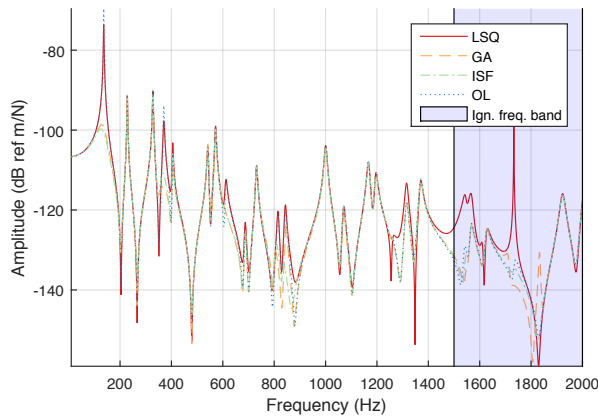


Figure 3: Comparison between open-loop and closed-loop mobility using LSQ, GA and ISF strategies.

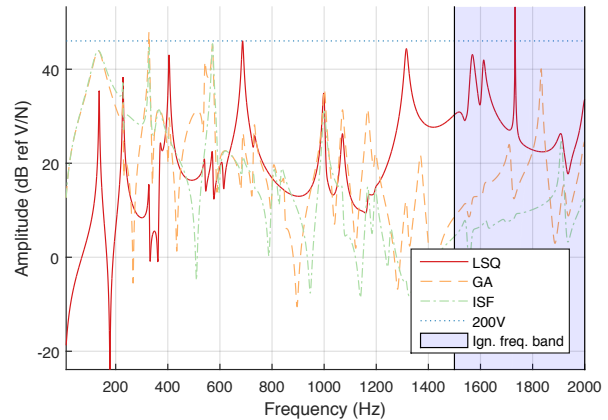


Figure 4: Comparison between control effort using LSQ, GA and ISF strategies.

3 DISTRIBUTION OPTIMIZATION FOR ELECTROMECHANICAL COUPLING PERFORMANCE

In the literature, few works focused on the optimization of distributed networks of piezoelectric sensors to maximize their energy harvesting capabilities. Thus, some aspects affecting the electromechanical coupling of a piezoelectric sensors network, such as patches positioning, are studied here. This is done by, first, analyzing the effect on the electromechanical coupling of successive segmentation of piezoelectric material and the number of piezoelectric patches covering the host structure. Then, a genetic algorithm optimization is used to determine the optimal distribution of a fixed number of patches to maximize the electromechanical coupling. Results are obtained using a custom finite element model that accounts for adhesive layer properties.

3.1 Problem description

In the present work, it is considered that the potentially harvestable energy of a given piezoelectric element depends strongly on the effective electromechanical coupling coefficient (EMCCe) it provides to the structure. This represents the energy fraction that could be stored in the piezoelectric element when the structure vibrates in a given mode. The EMCCe of the structure depends on the electromechanical coupling coefficient (EMCC ou k_{ij}^2) of the material and on the mechanical coupling between the piezoelectric element and the host structure, consequently it can be expected that the EMCCe will be smaller than the material EMCC [23].

On the other hand, previous works indicate a potential reduction on the mechanical coupling between host structure and piezoelectric element due to the presence of an adhesive layer between them [20]. To evaluate the effect of the adhesive layer on the performance of surface-bonded piezoelectric patches working as energy harvesting devices, two analyses were proposed. In the first one, the effect of successive segmentation is investigated, once it is expected that segmentation could have a positive effect of mitigating electric charge cancellation but also a negative one due to an increase of border effects in the adhesive layer. In the second analysis, an optimization procedure is proposed to find a distribution of mechanically and electrically uncoupled piezoelectric patches that maximizes the EMCCe of the first five vibration modes.

3.2 Evaluation of effective electromechanical coupling (EMCCe)

For a generic flexible structure with a discrete distribution of piezoelectric patches, it is possible to evaluate the structure's EMCCe provided by each piezoelectric patch. A general procedure to calculate the EMCCe based on modeling has been proposed [23]. The i -th modal parameters, mode and natural frequency, of a structure with a discrete distribution of piezoelectric elements for SC and OC electric boundary conditions respectively can be found and, thus, the EMCCe of the structure, provided by a piezoelectric element, when it is vibrating in the i -th mode shape is defined as

$$k_i^2 = \frac{\omega_{OC}^i{}^2 - \omega_{SC}^i{}^2}{\omega_{OC}^i{}^2}. \quad (21)$$

3.3 Description of the proposed analyses

A network of piezoelectric patches is bonded onto a rectangular clamped plate aiming at harvesting energy from structural vibrations within a frequency-range that contains the first five resonant frequencies. The plate has dimensions $420 \times 320 \times 1 \text{ mm}^3$ and is made of aluminum with properties: Young modulus 70 GPa, Poisson's ratio 0.34 and mass density 2700 kg/m^3 . The piezoelectric patches have thickness 0.5 mm and are made of PZT-5H piezoceramic with properties taken from [20]. The patches are bonded to the structure using an adhesive layer with thickness 0.1 mm and properties: Young modulus 2.7 GPa, Poisson's ratio 0.4 and mass density 1140 kg/m^3 .

A uniform mesh of 42×32 elements was used to discretize aluminum plate, adhesive layer and piezoelectric patches. A modal analysis was performed and the first five mode shapes and natural frequencies of the clamped plate (without piezoelectric patches) are shown in Figure 5.

3.4 Analysis of a rectangular grid of piezoelectric patches

First, considering a patch size of $40 \times 40 \text{ mm}^2$, an analysis of the effective EMCC for varying number of patches in a rectangular grid is performed. In Table 2, the modal, average and specific

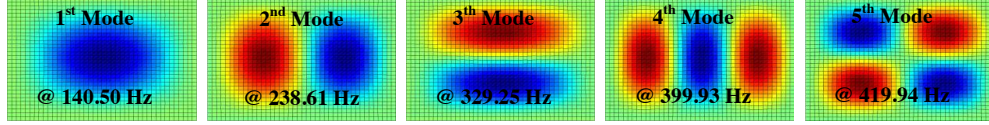


Figure 5: First five mode shapes of vibration and its natural frequencies for the clamped aluminum plate.

EMCCe by percentage of covered area are shown. Additionally, in the last one row, the ratio of average EMCCe per patch is also shown.

The biggest value of average EMCCe (9.2 %) found is for a configuration area with 48 patches (8x6). In terms of efficiency, 24 patches (6x4), 20 patches (5x4) and 16 patches (4x4) have similar values of specific EMCCe.

Table 2: Average and specific by percentage of covered area EMCCe values for all configurations of tested areas holding constant the patch size (40x40 mm²).

Patches in y-direction	Patches in x-direction									
	8		7		6		5		4	
	k_g^2	k_g^{2*}	k_g^2	k_g^{2*}	k_g^2	k_g^{2*}	k_g^2	k_g^{2*}	k_g^2	k_g^{2*}
7	8.8	13.2	8.3	14.2	7.3	14.6	6.1	14.6	4.9	14.6
6	9.2	16.2	8.7	17.4	7.7	17.9	6.4	17.9	5.1	17.8
5	9.0	18.8	8.5	20.3	7.4	20.8	6.2	20.8	4.9	20.7
4	7.7	20.3	7.3	21.8	6.4	22.4	5.3	22.3	4.2	22.1
3	5.8	20.4	5.5	21.9	4.8	22.3	3.9	22.0	3.1	21.9
2	3.8	19.7	3.5	21.1	3.0	21.2	2.5	20.8	2.0	20.7

3.5 Optimization of network distribution

Next, an optimization is performed to find the optimal distribution of a network of piezoelectric patches, which maximizes the average EMCCe for the first five modes of the structure. This is done using a genetic algorithm (GA) based optimization method. The objective is to find the vector x_{Np} , that represent the positions of N_p piezoelectric patches, which maximizes the cost function

$$J(x_{Np}) = \sum_{i=1}^{N_m=5} k_i (x_{Np})^2. \quad (25)$$

Results obtained in the previous parametric analyses were used as initial data to search for optimal distributions of a network of piezoelectric patches that maximize the average EMCCe of the structure and, consequently, its expected harvesting performance when working in a frequency-range that contains the first five natural frequencies. Thus, it has been chosen to find the optimal distribution of a network with 16, 20 and 24 piezoelectric patches of 40 × 40 mm². Network distributions found with GA are shown in Figure 6. Modal and average EMCCe values are presented in Table 3. They are also compared with values found from a rectangular centered network distribution with the same number of patches.

For 16 patches, a slight improve on the average EMCCe is obtained, compared to the corresponding rectangular grid, but it is also worthwhile to notice a reduction on the difference between maximum and minimum modal values which could be valuable to improve the global efficiency of a multimodal device. A similar conclusion could be drawn for the network with 20 patches. On

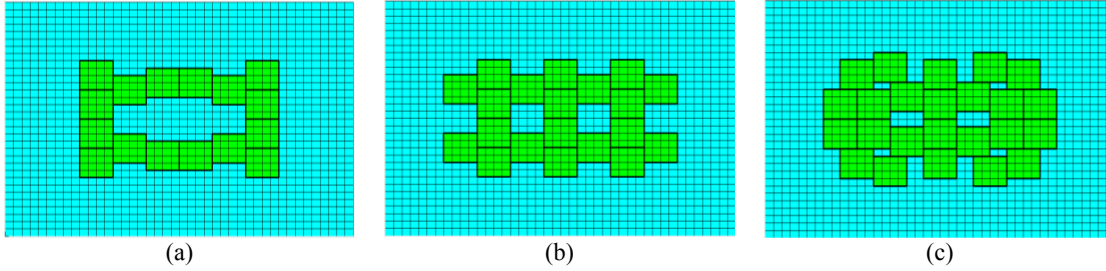


Figure 6: Optimized network configuration, with (a) sixteen, (b) twenty, and (c) twenty four patches.

the other hand, for the network with 24 patches, it was not possible to improve the global EMCCe, but the difference between maximum and minimum modal values are reduced.

Table 3: Comparison between modal and average EMCCe values obtained from optimized location of the piezoelectric patch network and from a rectangular distribution of the network.

	16 Patches		20 Patches		24 Patches	
	Optimized	Rectangular	Optimized	Rectangular	Optimized	Rectangular
Mode 1	4.2	7.1	6.4	8.1	7.3	8.6
Mode 2	5.7	3.3	6.5	5.4	7.9	7.4
Mode 3	3.9	4.7	4.6	5.2	5.2	5.5
Mode 4	4.0	3.7	5.3	4.1	6.1	5.4
Mode 5	4.4	2.3	4.6	3.7	5.2	5.0
EMCCeg	4.4	4.2	5.5	5.3	6.4	6.4
EMCCeg*	23.2	22.1	23.0	22.3	22.2	22.4
EMCCeg/P	0.28	0.26	0.27	0.26	0.26	0.27

4 CONCLUDING REMARKS

This work presented recent advances on the optimization of networks of piezoelectric patches for active structural vibration control and energy harvesting from structural vibrations. Results show that it is possible to profit from a network of sensors to improve and focus active vibration control strategies provided their gains is properly optimized. Three strategies to design the control gains are presented and analyzed. Aiming at energy harvesting from structural vibrations, another study was performed showing that by optimizing the distribution of sensors, it possible to improve the effective electromechanical coupling coefficient along a given frequency range.

ACKNOWLEDGEMENTS

Financial support of the National Council for Scientific and Technological Development (CNPq), through grants 574001/2008-5 and 309193/2014-1, is acknowledged.

REFERENCES

- [1] Ahmadian, M. and DeGuilio, A.P. Recent advances in the use of piezoceramics for vibration suppression. *Shock and Vibration Digest* (2001) **33**(1):15–22.
- [2] Gilbert, J.M., and Balouchi, F., Comparison of energy harvesting systems for wireless sensor networks, *International Journal of Automation and Computing* (2008) **5**(4):334–347.
- [3] Sodano, H.A., Inman, D.J., and Park, G., A review of power harvesting from vibration using piezoelectric materials, *Shock and Vibration Digest* (2004) **36**(3):197–206.

- [4] Trindade, M.A., Benjeddou, A. and Ohayon, R. Finite element modelling of hybrid active-passive vibration damping of multilayer piezoelectric sandwich beams – Part II: System analysis. *International Journal for Numerical Methods in Engineering* (2001) **51**(7):855–864.
- [5] Trindade, M.A. and Benjeddou, A. Hybrid active-passive damping treatments using viscoelastic and piezoelectric materials: review and assessment. *Journal of Vibration and Control* (2002) **8**:699–746.
- [6] Tang, J., Liu, Y. and Wang, K.-W. Semiactive and active-passive hybrid structural damping treatments via piezoelectric materials. *Shock and Vibration Digest* (2000) **32**(3):189–200.
- [7] Sirohi, J. and Chopra, I. Actuator power reduction using L-C oscillator circuits. *Journal of Intelligent Material Systems and Structures* (2001) **12**(12):867–877.
- [8] Godoy, T.C. and Trindade, M.A. Modeling and analysis of laminate composite plates with embedded active-passive piezoelectric networks. *Journal of Sound and Vibration* (2011) **330**:194–216.
- [9] Santos, H.F.L. and Trindade, M.A. Structural vibration control using extension and shear active-passive piezoelectric networks including sensitivity to electrical uncertainties. *Journal of the Brazilian Society of Mechanical Sciences and Engineering* (2011) **33**:287–301.
- [10] Meirovitch, L. and Baruh, H. Control of self-adjoint distributed-parameter systems. *Journal of Guidance, Control, and Dynamics* (1982) **5**(1):60–66.
- [11] Fripp, M.L. and Atalla, M.J. Review of modal sensing and actuation techniques. *Shock and Vibration Digest* (2001) **33**(1):3–14.
- [12] Preumont, A., François, A., De Man, P. and Piefort, V. Spatial filters in structural control. *Journal of Sound and Vibration* (2003) **265**(1):61–79.
- [13] Tanaka, N. and Sanada, T. Modal control of a rectangular plate using smart sensors and smart actuators. *Smart Materials and Structures* (2007) **16**(1):36–46.
- [14] Pagani Jr., C.C. and Trindade, M.A. Optimization of modal filters based on arrays of piezoelectric sensors. *Smart Materials and Structures* (2009) **18**(9):095046.
- [15] Trindade, M.A., Pagani Jr., C.C. and Oliveira, L.P.R., Semi-modal active vibration control of plates using discrete piezoelectric modal filters, *Journal of Sound and Vibration* (2015) **351**:17–28.
- [16] Levine, W. and Athans, M. On the determination of the optimal constant output feedback gains for linear multi-variable systems. *IEEE Transactions on Automatic Control* (1970) **15**(1):44–48.
- [17] Cruz Neto, H.J. and Trindade, M.A. Optimal placement of sensors for the output feedback control of structures using quadratic performance criterion. In *Proceedings of the 24th ABCM International Congress of Mechanical Engineering*, December 3-8, (2017), Curitiba, PR, Brazil.
- [18] Cai, G.P. and Lim, C. Continuous suboptimal control with partial state feedback. *Journal of Vibration and Control* (2005) **11**(4):561–578.
- [19] Le, M.Q., Capsal, J.F., Lallart, M., Hebrard, Y., Van Der Ham, A., Reffe, N., Geynet, L., and Cottinet, P.J. Review on energy harvesting for structural health monitoring in aeronautical applications. *Progress in Aerospace Sciences* (2015) **79**:147–157.
- [20] Trindade, M.A., Santos, H.F.L. and Godoy, T.C. Effect of bonding layer uncertainties on the performance of surface-mounted piezoelectric sensors and actuators. *XIV International Symposium on Dynamic Problems of Mechanics (DINAME)* (2013), Buzios, RJ, Brazil.
- [21] Velasquez, J.Q. and Trindade, M.A. Effect of adhesive layer properties on the performance of surface-mounted piezoelectric sensors and actuators. *Meeting on Aeronautical Composite Materials and Structures (MACMS)* (2015), São Carlos, SP, Brazil.
- [22] Horiy, F.M., Shigueoka, A.H., Trindade, M.A. Analysis of piezoelectric sensor networks for spatial modal filters and active vibration control. In *24th ABCM International Congress of Mechanical Engineering (COBEM)* (2017), Curitiba, PR, Brazil.
- [23] Trindade, M.A., and Benjeddou, A. Effective electromechanical coupling coefficients of piezoelectric adaptive structures: critical evaluation and optimization. *Mechanics of Advanced Materials and Structures* (2009) **16**(3):210–223.

Multi-fidelity Information Fusion Using Deep Neural Networks

Rohit Tripathy*, Ilias Bilonis**

*Purdue University, **Purdue University

ABSTRACT

A common scenario in computational science is the availability of a suite of simulators solving the same physical problem, such that the simulators are at varying levels of cost/fidelity. High fidelity simulators are more accurate but are computationally expensive, whereas low fidelity models can be evaluated cheaply while suffering from reduced accuracy. Additionally, many engineering applications are characterized by model parameters / boundary conditions / initial conditions etc. which are not known exactly. The surrogate-based approach to uncertainty quantification requires one to evaluate the forward model enough times such that one can construct a cheap (but accurate) approximation to the numerical solver. If the outputs from the simulators of varying fidelities are correlated, one can leverage information from low-fidelity simulators to augment information from a small number of evaluations of the high-fidelity simulator to construct an accurate surrogate model. In this work, we demonstrate a deep neural network (DNN) approach for constructing accurate surrogate models for uncertainty quantification by fusing information from multifidelity sources. DNNs are naturally suited for multi-fidelity information fusion because of the hierarchical representation of information. Our approach is validated on a synthetic example as well as an example from advanced manufacturing.

A Fast Statistical Homogenization Procedure (FSHP) for Random Composite

Patrizia Trovalusci*, Marco Pingaro**, Maria Laura De Bellis***, Emanuele Reccia****

*Sapienza University of Rome, **Sapienza University of Rome, ***University of Salento, ****Sapienza University of Rome

ABSTRACT

Composites materials are used in many engineering applications and typically exhibit a micro-structure made of randomly distributed inclusions (particles) embedded into a dissimilar matrix. A key aspect, recently investigated by many researchers, is the evaluation of appropriate mechanical properties to be adopted for the study of their behaviour. Homogenization procedures may be adopted for the definition of equivalent moduli able to take into account at the macroscale the material properties emerging from the internal micro-structure. In the case of materials with random micro-structure it is not possible to a priori define a Representative Volume Element (RVE), this being an unknown of the problem in contrast to the classical homogenization approach. A possible way to solve this problem is to approach the RVE using finite-size scaling of intermediate control volume elements, named Statistical Volume Elements (SVEs), and proceed to homogenization. Here a homogenization procedure, consistent with a generalized Hill-Mandel condition, is adopted in conjunction with a statistical procedure, by which scale-dependent bounds on classical moduli are obtained using Dirichlet and Neumann boundary conditions for solving Boundary Value Problems (BVPs) [1]. The outlined procedure has provided significant results, also extended to non-classical continuum formulations, but with high computational cost which prevents the possibility to perform series of parametric analyses. We here propose a so-called Fast Statistical Homogenization Procedure (FSHP) developed within an integrated framework that automates all the steps to perform: from the simulations of each random realization of the microstructure to the solutions of the boundary value problems for the SVEs, up to the evaluation of the final size of the RVE for the homogenization of the random medium. Within the FSHP the BVPs has been solved numerically adopting a mixed Virtual-Finite Element Method (VEM-FEM), with a single Virtual Element for the inclusions and triangular Finite Elements for the matrix, determined using random mesh generators. The computational strategies and the discretization adopted allow us to very efficiently solve the series (hundred) of BVPs and to rapidly converge to the RVE size detection. Several simulations are then performed by modifying the material contrast (ratio between the moduli of the materials components) deriving the size of the RVE for performing homogenization on various kinds of two-phases random composites. References Trovalusci, P., Ostoja-Starzewski, M., De Bellis, M.L., Murralli, A., "Scale-dependent homogenization of random composites as micropolar continua," *Eur. J. Mech. A-Solid*, 49, 396-407 (2015).

From Spinodal to Critical Fracture

Lev Truskinovsky*, Hudson Borja da Rocha**

*ESPCI, **ESPCI

ABSTRACT

Fracture in disordered solids is known to be intermittent across a vast range of scales from earthquakes to micro-peeling. The observed power law avalanche behavior has been previously linked to either spinodal or critical points. We use the simplest mean field model to show that both associations are relevant. The realization of a particular scenario in a quasi-statically driven system with over-damped athermal dynamics depends on the two parameters representing disorder and rigidity.

Creep Life Prediction of Ferritic-Martensitic Steels at High and Low Stresses Through Crystal Plasticity and Grain Boundary Modeling

Timothy Truster^{*}, Kristine Cochran^{**}, Mark Messner^{***}, Omar Nassif^{****}, David Parks^{*****}, Sam Sham^{*****}

^{*}University of Tennessee, ^{**}DR&C, Inc., ^{***}Argonne National Laboratory, ^{****}University of Tennessee, ^{*****}DR&C, Inc., ^{*****}Argonne National Laboratory

ABSTRACT

Advanced reactors designed to operate at higher temperatures than current light water reactors require structural materials with high creep strength and creep-fatigue resistance to achieve long design lives. Grade 91 is a ferritic/martensitic steel designed for long creep life at elevated temperatures. The time required to complete an experiment limits the availability of long-life creep data for Grade 91 and other structural materials. Design methods often extrapolate the available shorter-term experimental data to longer design lives. However, extrapolation methods tacitly assume the underlying material mechanisms causing creep for long-life/low-stress conditions are the same as the mechanisms controlling creep in the short-life/high-stress experiments. A change in mechanism for long-term creep could cause design methods based on extrapolation to be non-conservative. The goal for physically-based microstructural models is to accurately predict material response in experimentally-inaccessible regions of design space. Ideally, the individual mechanism models adhere to the material physics and not an empirical calibration to experimental data and so the model remains predictive for a wider range of loading conditions. This paper describes such a physically-based microstructural model for Grade 91 at 600° C. The model explicitly represents competing dislocation and diffusional mechanisms in both the grain bulk and grain boundaries using the crystal plasticity finite element method and cavity growth-based interface elements, respectively. The model accurately recovers the available experimental creep curves at higher stresses and the limited experimental data at lower stresses, predominately primary creep rates. The model predicts a mechanism shift for 600° C at approximately 100 MPa from a dislocation-dominated regime at higher stress to a diffusion-dominated regime at lower stress. This mechanism shift impacts the creep life, notch-sensitivity, and creep ductility of Grade 91. In particular, the model predicts existing extrapolation methods for creep life may be non-conservative when attempting to extrapolate data for higher stress creep tests to low stress, long-life conditions.

Modeling and Simulations of Fused Deposition Modeling

Gretar Tryggvason^{*}, Huanxiong Xia^{**}, Jiakai Lu^{***}

^{*}Johns Hopkins University, ^{**}Johns Hopkins University, ^{***}Johns Hopkins University

ABSTRACT

Additive manufacturing processes generally include complex multiphysics and multiscale processes, and an evaluation of suitable material/process models require accurate solutions of the governing equations, so that solutions can be compared with experimental results. Here, a fully resolved computational model is developed for the FDM (Fused Deposition Modeling) process, where objects are built by depositing filaments of hot polymers that fuse together when they solidify. The process is embedded in a hexahedral computational domain, where both the polymer and the ambient air are included. A finite volume/front tracking method and the one-fluid formulation are used to model the fluid flow, heat transfer, volume shrinkage, residual stress, as well as the moving immiscible interface. The extrusion of the polymer is modeled by using a volume source inside a rigid body with an open outlet, which is moving along a specific path. A temperature and shear-rate depend viscosity and a modified neo-Hooke stress model are used for the polymer to describe its viscoelastic behavior and find the solid stress. The model is solved by an implicit projection scheme with second-order accuracy both for time integration and space discretization. The accuracy and convergence properties are tested by grid refinement studies for a simple setup involving two short filaments, one on top of the other. The effect of the various injection parameters, such as nozzle speed, cooling condition, depositing and bridging space are briefly examined and the applicability of the approach to simulate the construction of simple multilayer objects is shown. In addition to helping evaluate the accuracy and fidelity of material models, fully resolved simulations also provide the "ground truth" for the simplified/reduced order model that are suitable for part-scale simulations.

Directly Aerodynamics Characteristics Simulation in Upper Airway by Medical Image

Tzu-I Tseng*, Fang-An Kuo**

*National Center for High-performance Computing, **National Center for High-performance Computing

ABSTRACT

The study predicts the flow characteristics in upper airway by using computational fluid dynamics (CFD) method to solve the flow governing Navier-Stokes equations. CFD simulations should be performed after image segmentation, geometry reconstruction and computing mesh generation. However, it requires a large amount of resources to reconstruct a suitable geometry for upper airway and generate the mesh. Because every medical image implied a two-dimensional mesh in Cartesian coordinate system, this study demonstrated a directly CFD technique based on the image-base grid calculates the flow characteristics in upper airway. The marked and cell (MAC) for structure mesh method is a popular and commonly used algorithm in computer graphics to discretize functions for fluid and other simulations. In addition, it is very simple to use and do the embarrassingly parallel computation by using the single instruction multiple data (SIMD) on the graphics processing unit (GPU) device. However, the MAC method was hard to trend the solid object with complex geometry especially applied in bio-mechanics simulation. The direct-forcing immersed boundary method (IBM) can correct the boundary effect from the interaction of the solid boundary and fluid flow and improve the accuracy the of flow simulation. In this study we employ the MAC method with direct-forcing IBM applied to solve the upper airway, by using massive floating-points-operation parallel computation on the GPU device. By using this technique compare to traditional procedure, the total processed time from an hour reduce to couple minutes.

Phase-field Simulation of the Effect of Temperature and Yield Stress Conditions on the Martensitic Transformation in Low-carbon Steel

Yuhki Tsukada^{*}, Emi Harata^{**}, Toshiyuki Koyama^{***}

^{*}Nagoya University, ^{**}Nagoya University, ^{***}Nagoya University

ABSTRACT

Microstructure evolution during the martensitic transformation (MT) in steels is strongly influenced by alloy composition and transformation temperature. The elastic strain energy derived from the MT influences the size and morphology of the martensite phase. A phase-field simulation study has shown that in low-carbon steels, the slip deformation during the MT plays an important role in the formation of habit plane between the parent and martensite phases [1]. Most recently, a phase-field model was developed which considered the elastic strain energy associated with the fcc-to-bct lattice deformation and slip deformation during the MT [2]. In the phase-field model, slip deformations of parent and martensite phases were calculated in the regions where the von Mises yield criterion was exceeded. In this study, the MTs in Fe-0.1mass%C were simulated at 600 K, 650 K and 700 K; at each temperature, the value of yield stress was varied for elucidating its effect on the martensite microstructure. Simulation results show that the MT progresses with forming the cluster composed of three tetragonal variants of the martensite phase. The equivalent plastic strain caused by the slip deformation is large in the interior of the martensite variant domains. However, the slip deformation of the parent phase is also confirmed to occur near the martensite phase. At 600 K and 650 K, the variant domain size decreases with increasing the value of yield stress. It is assumed that when the yield stress is high and the slip deformation is difficult to occur, the formation of minute multi-variant structure is effective for relaxing the elastic strain energy during the MT. On the other hand, at 700 K, the variant domain size is not influenced by the value of yield stress. It is presumed that at 700 K, the driving force for the MT is small and the transformation is slowed down; this leads to the increase in the slip deformation of the martensite phase and hence the formation of minute multi-variant structure is not an important factor for relaxing the elastic strain energy during the MT. References: [1] Y. Tsukada et al., ISIJ Int. 55 (2015) 2455-2462. [2] Y. Tsukada et al., Proc. of the 5th International Symposium on Steel Science (ISSS 2017), in press.

CFD Analysis in an Oil Hydraulic Vane Pump

Tetsuhiro Tsukiji^{*}, Shunsuke Akiyoshi^{**}, Yoshinari Nakamura^{***}, Kazunari Suzuki^{****}

^{*}Sophia University, ^{**}Sophia University, ^{***}KYB Corporation, ^{****}KYB Corporation

ABSTRACT

Abstract With the development of technology, hydraulic machinery, including hydraulic vane pumps, has recently become smaller, faster, and more durable against pressure. However, these trends make cavitation occur more easily, and cavitation causes problems with the performance of hydraulic machines because of the resulting vibration, noise, and erosion. Based on the experimental result of the outlet pressure measured using an actual vane pump, cavitation causes pressure fluctuation when the rotational speed exceeds a certain value. Pressure fluctuations make it difficult to control the pump and hydraulic system. Therefore, suppression of cavitation in the high-speed rotation region is important, and finally it is necessary to change the shape of the vane pump for operation at high speed. In this study, we aim to evaluate the accuracy of CFD analysis by conducting three-dimensional flow analysis of hydraulic vane pump and to improve pump performance by improving design of vane pump. We conducted a CFD analysis with consideration of internal leakage using the Zwart-Gerber-Belamri cavitation model[1]. Experimental values obtained by experiments were compared with CFD results to examine the accuracy of analysis. We also attempted to increase the volumetric flow rate and decrease the cavitation by changing the shape of the cam ring, using CFD analysis considering leakage. ANSYS Fluent 16.1 solver was used. The standard $k-\epsilon$ turbulent model was adopted to solve flow field. To solve Multi phase flow, the primary phase was set to "oil" and the secondary phase to "oil vapor". Main conclusions are as follows. 1. The CFD calculation of vane pump has sufficient accuracy to estimate the volumetric flow rate not only in the low speed rotation region but also in the high-speed rotation region where the cavitation is dominant by considering the internal leakage. 2. Changing the shape of the cam ring is effective for suppressing the cavitation phenomenon and the discharge flow rate also increased. Reference [1] P. J. Zwart, A. G. Gerber, T. Belamri, 2004, "A Two-Phase Flow Model for Predicting Cavitation Dynamics," ICMF International Conference on Multiphase Flow, Paper No. 152

Frictionless Contact Analysis in Finite Cover Method Using Nitsche's Method

Makoto Tsukino*, Takahiro Yamada**

*Quint Corporation, **Yokohama National University

ABSTRACT

The voxel-based analysis is used for not only structural analyses of mechanical parts but analyses in bioengineering or of microstructure of materials as an effective method for complex structure analyses because of its facility of mesh generation. In the voxel modeling, the surfaces of objects are represented as stepwise shape even if the original surfaces are smooth and hence it is difficult to analyze models that contain contact conditions. The finite cover method (FCM) [1], which is introduced the manifold method concept in which the mathematical cover and the physical domain are defined independently from each other, has capability to manage contact problems easier for its capability of geometry representation, although it holds an advantage in mesh generation. To apply the FCM to practical problems, a contact algorithm needs to be adopted. In general finite element analyses of contact problems, the penalty method is widely used thanks to its simple implementation. In the penalty method, a significant large penalty parameter needs to be employed to assure accuracy. However, such a penalty parameter may cause numerical instability since it makes the stiffness matrix ill-conditioned. Moreover, in the FCM formulation, the nodal points for displacements are located independently from the geometry representation and hence it is difficult to manage the positions of integration points for contact constraint, which may cause inaccurate distribution of the contact pressure due to the over-constraint with concentration of the integration points. To circumvent such difficulties, we apply the Nitsche's method for the contact algorithm in frictionless contact analyses formulated in [2] to FCM. In the Nitsche's approach, constraints for both the non-penetration condition and the equilibrium of stresses on the contacting surfaces are taken into account with a smaller penalty parameter for the stabilization term and that improve in problems associated with the penalty method. To show effectiveness of our approach, we calculate some 2D frictionless contact problems such as a Hertz contact problem. References [1] Jin C., Suzuki K., Ohtsubo H.: Linear Structural Analysis Using Cover Least Square Approximation, J. Appl. Mech., Vol.3, pp167-176, 2000. [2] Wriggers P., Zavarise G.: A formulation for frictionless contact problems using a weak form introduced by Nitsche, Comput. Mech., Vol.41, pp.407-420, 2008.

Modeling and Prediction of Particle Size Distribution in Milling Process using Discrete Element Method

Yuki Tsunazawa*, Chiharu Tokoro**

*National Institute of Advanced Industrial Science and Technology (AIST), Geological survey of Japan (GSJ),

**Waseda University

ABSTRACT

A milling process in mineral processing is the first and important process which determines the efficiency of the overall processes. To achieve the high efficiency of the later separation process, the particle size and its distribution should be appropriately controlled. The control of particle size distribution in the milling process is often difficult because the milling process is strongly affected by not only physical properties of raw ore but also operation conditions in the milling system. Numerical studies have been examined in order to investigate the optimal operation parameters and apparatus design of the milling system. Since these numerical studies were mostly concerned with the behavior of grinding media in the milling system, it has not been well-established that the prediction of particle size distribution during the milling process. The objective of this study was to develop a new method to predict particle size distribution during the milling process using the discrete element method (DEM). To develop the prediction method, we investigated a correlation between the experiments and the DEM simulations. In the experiments, copper ore, whose size was less than 2 mm, was grinded with a tumbling mill under various kinds of operation conditions. Based on the experimental results and the population balance model, we determined the grinding rate coefficient. In the DEM simulations, we only calculated grinding media in the tumbling mill and considered the effect of grinding samples. The DEM simulations were performed to calculate collision energy under the same operation conditions in the tumbling mill. As a result, we obtained a good correlation between collision energy obtained from the DEM simulations and the grinding rate coefficient obtained from the experiments. Therefore, this study proposed the prediction method of the particle size distribution in the milling systems using the DEM and the DEM simulations would contribute to determine milling conditions for appropriate control of particle size distribution during the milling process.

Accelerated Exploration and Learning of Complex Free Energy Landscapes

Mark Tuckerman*

*New York University

ABSTRACT

Theory, computation, machine-learning, and high-performance computers are playing an increasingly important role in helping us understand, design, and characterize a wide range of functional materials, chemical processes, biomolecular/biomimetic structure. The synergy of computation and experiment is fueling a powerful approach to address some of the most challenging scientific problems. In this talk, I will describe the efforts we are making in my group to develop new computational methodologies that address specific challenges in free energy exploration and generation. In particular, I will describe our recent development of enhanced free energy based methodologies for determining conformational preferences of bound and free oligopeptides, for predicting structure, polymorphism, and defects in molecular crystals, for studying crystal growth mechanisms, and for aiding in the understanding of first-order phase transitions. The strategies we are pursuing include large time-step molecular dynamics algorithms, heterogeneous multiscale modeling and learning techniques, which allow “landmark” locations (minima and saddles) on a high-dimensional free energy surface to be mapped out, and enhanced-sampling methods, which allow relative free energies of the landmarks to be generated efficiently and reliably. I will then discuss new schemes for using machine learning techniques to represent and perform computations using multidimensional free energy surfaces.

Monolithic Multigrid for Multiphysics Applications Arising from Resistive MHD

Raymond Tuminaro*, Eric Cyr**, Tobias Wiesner***, John Shadid****

*Sandia, **Sandia, ***Leica Geosystems AG, ****Sandia

ABSTRACT

We consider a resistive iso-thermal MHD formulation that includes dissipative terms for the momentum and magnetic induction equations. This model provides a base-level continuum description of charged fluids in the presence of electromagnetic fields (e.g. for understanding basic plasma physics mechanisms or for investigating magnetic confinement fusion systems). While multigrid methods are efficient for many single-field applications, the design of multigrid preconditioners for multiphysics systems is challenging when the coupling between different fields is strong. Multiphysics systems frequently give rise to matrices that are far from M-matrices, which are easily addressed by standard algebraic multigrid (AMG) methods. Often, standard relaxation algorithms do not smooth errors appropriately while AMG grid transfer procedures also have difficulties as these procedures often rely on positive-definite matrix properties. In this talk, we propose a multigrid strategy that takes advantage of the block structure associated with multiphysics systems. Here, blocks are defined by different physical quantities (or fields) and different equation types. Block diagonal prolongators are developed such that the Navier-Stokes and the Maxwell sub-pieces are interpolated separately. By using the same aggregates to build the prolongator blocks for the Navier-Stokes and Maxwell part, the co-location of unknowns at each mesh vertex is preserved throughout the multigrid hierarchy. Additionally, the proposed multigrid smoother is again based on a block idea (e.g., block Gauss-Seidel). While the talk focuses on a specific MHD context, we emphasize our more general purpose block framework. Specifically, the framework allows one to devise a wide variety of monolithic multigrid preconditioners. Different multigrid kernels (e.g., aggregation schemes, grid transfer strategies, smoothing algorithms) can be applied to different matrix sub-blocks and the results of these kernels can be combined in fairly flexible ways via an xml input deck. This flexible multigrid framework, provided by the MueLu package within Trilinos, drastically simplifies the implementation of block multigrid preconditioners for new types of applications. Additionally, the framework facilitates the definition of simple user interfaces to the resulting application-specific preconditioners. These simple interfaces reduce the number of exposed parameters for end users who want to apply the preconditioners in a production environment. We demonstrate the algorithms and framework for MHD multiphysics problems in the Drekar Finite Element MHD code and compare the performance of the resulting multigrid preconditioners with alternative preconditioning methods.

Variational Peridynamic Fracture: A Phase-field Inspired Framework for Peridynamic Damage Modeling

Michael Tupek*, David Littlewood**

*Sandia National Laboratories, **Sandia National Laboratories

ABSTRACT

A framework for deriving peridynamic bond-damage models which establishes a direct link to phase-field fracture methods [1] is proposed. In recent years, two approaches for modeling crack propagation in brittle materials have received significant attention: phase-field fracture and peridynamics. However, despite their obvious qualitative similarities, a direct relationship between them has yet to be established. By formulating peridynamics as an integral regularization of variational fracture, we introduce a unifying framework that: 1) can be used to derive both the well-known bond-breaking criterion [3] as well as newly proposed smoothly evolving bond-damage models, 2) provides a rigorous approach for extending brittle peridynamic damage models to non-bond-based peridynamic theories, and 3) enables the development of both Griffith and cohesive peridynamic damage models in the small peridynamic length scale limit. These improvements are both novel and important as they promise to address several outstanding issues in peridynamic failure modeling, including: 1) that the use of an instantaneous bond-breaking criteria can lead to abrupt energy releases leading to excessive numerical noise, poor accuracy, and lack of solver convergence, 2) computational convergence results for brittle state-based peridynamic damage models are relatively lacking, and 3) existing peridynamic fracture models are Griffith in the limit of the horizon going to zero, necessarily implying an unjustified and unnecessary relation between the peridynamic horizon and fracture process zone size. The proposed damage models are demonstrated using the open source peridynamics code Peridigm. REFERENCES [1] B. Bourdin, G.A. Francfort, and J.-J. Marigo. Numerical experiments in revisited brittle fracture. *J. Mech. Phys. Solids*, 48:797–826, 2000. [2] C. Miehe, F. Welschinger, and M. Hofacker. Thermodynamically consistent phase-field models of fracture: Variational principles and multi-field fe implementations. *International Journal for Numerical Methods in Engineering*, 83:1273–1311, 2010. [3] S.A. Silling, and E. Askari. A meshfree method based on the peridynamic model of solid mechanics. *Computers and Structures*, 83:1526–1535, 2005.

An Implicit Generalized Finite-Difference Method for Solving a Generalized Dual-Phase Lag Equation

Lukasz Turchan*

*Silesian University of Technology

ABSTRACT

Numerical solution of the bioheat transfer problem is discussed. The heat conduction in the domain considered is described by the generalized dual-phase lag model (GDPL) [1]. Such a model is created by a single partial differential equation and an additional formula concerning the dependence between blood and tissue temperatures. The model is supplemented by the appropriate boundary and initial conditions. At the stage of numerical computations an implicit scheme of generalized finite difference method (GFDM) is used [2]. In the first step of this method application, the time discretization is introduced using the differential quotients. In the next step, the cloud of nodes covering the interior and the boundary of domain considered is generated. Then the temperature function is expanded into the Taylor series. The approximation of the local values of the first and second spatial derivatives results from the least squares criterion. Introduction of this derivatives into differential equation produces a set of coupled linear equations which are valid for a given time step. In this way the nodal temperatures for the successive time steps are calculated [3]. The examples of computations, the comparison with the classical FDM solution and the conclusions will be presented in the final part of presentation. [1] Y. Zhang, Generalized dual-phase lag bioheat equations based on nonequilibrium heat transfer in living biological tissues, *International Journal of Heat and Mass Transfer*, 52 (21-22), 4829-4834, 2009. [2] B. Mochnecki, E. Majchrzak, Numerical modeling of casting solidification using generalized finite difference method, *THERMEC 2009, Materials Science Forum*, 638, 2676-2681, Trans. Tech. Publications, 2010. [3] L. Turchan, Solving the dual-phase lag bioheat transfer equation by the generalized finite difference method, *Archives of Mechanics*, 69 (4-5), 389-407, 2017.

Real-time High-Performance Robust Surgical Cutting Simulations

George Turkiyyah^{*}, Julien Abinahed^{**}, Ahmad Al-Ansari^{***}, Nicolas Haddad^{****}, Dinesh Manocha^{*****}, Nikhil Navkar^{*****}, Gorune Ohannessian^{*****}, Zherong Pan^{*****}, Georges Younes^{*****}

^{*}American University of Beirut, ^{**}Hamad Medical Corporation, ^{***}Hamad Medical Corporation, ^{****}American University of Beirut, ^{*****}University of North Carolina, ^{*****}Hamad Medical Corporation, ^{*****}American University of Beirut, ^{*****}University of North Carolina, ^{*****}Hamad Medical Corporation

ABSTRACT

Surgical simulation represents an extremely challenging class of computational science simulations where both high performance and absolute robustness are essential requisites for effectiveness. To be used as tools for planning personalized care or for rehearsing patient-specific procedures, surgical simulators must provide support for realistic and consistent geometric and mechanical behavior suitable for real-time interactions. Even a single contact that is not correctly detected and resolved, anywhere in space and at any time step, can result in completely erroneous and visually distracting simulation. The challenges of these simulations come from the need for: (1) interaction with non-linear deformable materials that undergo topological changes due to incisions and resections; (2) geometrically rich tool-tissue contact and interaction; and (3) dynamically changing tissue-tissue contact interactions. To ensure robustness in this environment, geometric computations and algorithms must interact at a fine-grained level with a finite element model of non-linear elastic deformations to resolve the dynamic contact conditions and update model deformations accordingly. Vertex-face and edge-edge contacts are identified and used to constrain the space of allowable deformations. These computations must be performed in real-time at several frames per second on models involving several tens of thousands of elements, pushing the limits of robust simulation in a high-performance computational simulation. In this work, we present incremental data structures and solution algorithms to support nonlinear elastic simulations in the dynamically changing environment of surgical cutting. Our geometric collision detection algorithms and finite element solution algorithms exploit hierarchical representations and incremental fast updates to the model, contact conditions, and solution. We perform continuous collision detection between discrete time steps so as not to miss any collision. This reduces to performing a high number of elementary tests corresponding to vertex-face and edge-edge combinations from triangle meshes, using efficient methods to accelerate the collision computation. The combination of these techniques result in simulation methods that exhibit only log-linear complexity allowing us to demonstrate robust real-time three-dimensional surgical cutting procedures at scale.

Leveraging Exascale Computational Resources to Accelerate Qualification of Additively Manufactured Parts

John Turner*, James Belak**

*Oak Ridge National Laboratory, **Lawrence Livermore National Laboratory

ABSTRACT

Additive manufacturing (AM), or 3D printing, of metals is transforming the fabrication of parts by reducing the weight of final parts, reducing waste (and hence energy) in the manufacturing process, and dramatically expanding the design space, allowing optimization of shape and topology. However, although the physical processes involved in AM are similar to those of welding, a field with a wealth of experimental, modeling, simulation, and characterization research over the past decades, qualification of AM parts remains a challenge. While modeling approaches and simulation tools for welding and similar processes are quite mature, they are proving inadequate for AM processes. We believe this is in part due to the fact that the process-structure-property-performance relationship is typically treated in an uncoupled manner, relying on tabular databases and hence unable to adequately capture the rapid dynamics and non-equilibrium nature of AM processes. The Exascale Additive Manufacturing Project (ExaAM) is a collaboration between U.S. Dept. of Energy laboratories as part of the Exascale Computing Project (ECP, <https://exascaleproject.org/>). ECP is a broad program including research efforts in hardware component and system design, system software, and science application development to deploy a computational ecosystem capable of delivering at least fifty times the performance of today's largest systems. ExaAM is one of the applications selected for the development and implementation of models that would not be possible on even the largest of today's computational systems. With the prospect of Exascale computing resources in mind, one of the goals of ExaAM is to remove some of the limitations noted above by coupling high-fidelity sub-grid simulations within continuum process simulations to determine microstructure, properties, and hence performance using local conditions. We briefly describe the approach being taken in ExaAM, which involves integrating and extending existing physics components for microstructure evolution, melt pool dynamics, polycrystalline properties, and part scale performance, most of which were not developed specifically for AM but which include the relevant high-fidelity physics capabilities. We also discuss plans for verification and validation of this new integrated simulation environment through collaboration with efforts such as AM-Bench (<https://www.nist.gov/ambench>), a set of benchmark test problems under development by a team led by NIST.

Influence of Sub-ply Voids in the Fracture Behavior of Fiber-reinforced Composites Using a Multiscale Analysis

Sergio Turteltaub*, Gijs de Jong**

*Delft University of Technology, **Delft University of Technology

ABSTRACT

The effective fracture behavior of a fiber-reinforced composite laminate depends on a series of design and manufacturing factors that include the material properties of the fiber and the matrix as well as the ply configuration (e.g., fiber volume fraction). An additional factor that influences the onset and propagation of micro-cracks at the sub-ply length scale are defects that appear during manufacturing. At that scale, defects may appear as micro-voids inside the matrix or as gaps between closely-spaced fibers that prevent filling. To study the influence of these micro-defects on the effective traction-separation response of a composite, a multiscale analysis is conducted where the defects are explicitly accounted for in finite element simulations. A recently-developed multiscale theory is expanded to account for voids in the computational domain. It is shown that the Hill-Mandel condition may be separated into two terms, one accounting for the actual crack and one for the voids that contribute to the crack process. The simulations are carried out using a separate traction-separation relation for each constituent (matrix, fiber and matrix-fiber interface) and for distinct mixed mode loading conditions until complete fracture is achieved. A convergence analysis is carried out to establish the existence of a representative volume element that includes voids of each type (matrix voids and fiber-gaps). Through a parametric analysis of configurations with a given void type and volume fraction, the influence of the void content on the effective fracture strength and the effective fracture energy of a composite can be quantified. Results show that for a mode II loading condition, both the effective fracture energy and strength decrease with increasing void content, while for mode I only the effective energy decreases. These effects only become significant when the void content exceeds a critical value, which depends on the type of voids evaluated.

Field Monte Carlo Potts-based Modeling of Discontinuous Dynamic Recrystallization under Finite Deformation

Abbas Tutcuoglu^{*}, Dennis Kochmann^{**}, Kaushik Bhattacharya^{***}

^{*}California Institute of Technology, ^{**}ETH Zurich, ^{***}California Institute of Technology

ABSTRACT

Discontinuous dynamic recrystallization (DDRX) describes the process observed predominantly in low-to-medium stacking fault energy metals by which pristine grains with a new orientation nucleate at high energy sites and subsequently migrate to consume the surrounding plastically more severely distorted grains. In previous attempts to simulate DDRX, stochastic models such as the Monte Carlo Potts model (MCP) provided popular means by which the random nature of grain boundary migration and nucleation could be incorporated. Despite invaluable insights into the mathematical aspect of recrystallization, the underlying physical models were generally of simplified nature and thus failed to capture the full complexity inherent in the inelastic phenomena occurring on the microscale, including anisotropy, finite deformation or alternative strain accommodating processes such as twinning. A vertical homogenization approach is pursued to account for the multiscale nature of DDRX by introducing a representative volume element (RVE) on the mesoscale. The associated initial boundary value problem is solved using an improved spectral solver which allows for the presence of discontinuities inherent in high-angle grain boundaries without the occurrence of severe ringing artifacts. A crystal plasticity model is employed to capture the deformation state on the microscale based on a set of elastic and inelastic state variables, for the latter of which the temporal evolution is governed by the principle of minimum dissipation potential. Following the MCP ansatz, we formulate misorientation switches to model both grain boundary migration as well as nucleation, with the latter replacing ad-hoc nucleation models incorporating a hard threshold as employed in numerous previous attempts to simulate DDRX. An integral modification to classic MCP models consists in the amendment of the two aforementioned state switches by simultaneous changes of both elastic and inelastic states in the idea of a Field Monte Carlo Potts model (FMCP). The state changes, for which the respective definitions are motivated by experimental observations, are conducted in a novel time-continuous fashion. Using data on the microstructural evolution and the stress-strain response for copper during torsion experiments, we assess the performance of our FMCP model.

Relative Entropy and Applications to the Convergence of Thermomechanical Theories

Athanasios Tzavaras*

*King Abdullah University of Science and Technology

ABSTRACT

The relative entropy is a calculation originally developed for hyperbolic systems of conservation laws which exploits the entropy structure of hyperbolic systems in order to compare two appropriate solutions of the same or related thermomechanical systems. The method provides an appropriate metric in order to assess stability and convergence of numerical schemes. In this talk I will survey this method in two directions: (a) First, for general entropy dissipating hyperbolic-parabolic systems where the hyperbolic part is symmetrizable. This provides convergence for solutions from the system of thermoviscoelasticity to the system of adiabatic thermoelasticity in the limit as the viscosity and heat conduction tend to zero. (b) Second, for a class of dispersive systems that can be written as Euler flows generated by a variational structure induced by an energy functional. This class admits as examples the Euler-Korteweg system, the quantum hydrodynamics system, and various models of multi-component flows.

A Machine Learning Approach for Plastic Deformation History Using Spatial Strain Correlations

Michail Tzimas^{*}, Stefanos Papanikolaou^{**}, Stephen Langer^{***}, Andrew Reid^{****}, Hengxu Song^{*****}

^{*}West Virginia University, ^{**}West Virginia University, ^{***}National Institute of Standards and Technology,
^{****}National Institute of Standards and Technology, ^{*****}West Virginia University

ABSTRACT

We demonstrate a machine learning (ML) approach to quantify the deformation history of a specimen based on spatially resolved information that can be derived from a small-strain, non destructive mechanical test. The deformation history is encoded in the microstructure through the inhomogeneity of dislocation ensembles, and in the spatial correlations of dislocation patterns. Our playground consists of uni-axially compressed crystalline thin films of various widths generated by a discrete dislocation plasticity simulation. We explore the range of applicability of ML for typical protocols that are being used in mechanical testing, and as a function of possible size effects and stochasticity. While strain information is traditionally thought to not be a proper state variable for crystal plasticity, we find that spatially-resolved strain correlations contain much richer information that may be used to classify plastically predeformed samples in most cases. However, we also find that size effects and uncertainty may render unsupervised techniques unable to distinguish different plasticity regimes. Furthermore, we explore the applicability of this approach on quantifying source strength, recognizing statistical variations in source strength and recognizing the number of active slip systems in a sample.